R-08-09

Numerical modelling of surface hydrology and near-surface hydrogeology at Forsmark

Site descriptive modelling

SDM-Site Forsmark

Emma Bosson, Svensk Kärnbränslehantering AB

Lars-Göran Gustafsson, Mona Sassner
DHI Sverige AB

September 2008

Svensk Kärnbränslehantering AB
Swedish Nuclear Fuel
and Waste Management Co
Box 250, SE-101 24 Stockholm
Tel +46 8 459 84 00

ISSN 1402-3091
SKB Rapport R-08-09

Numerical modelling of surface hydrology and near-surface hydrogeology at Forsmark

Site descriptive modelling SDM-Site Forsmark

Emma Bosson, Svensk Kärnbränslehantering AB

Lars-Göran Gustafsson, Mona Sassner
DHI Sverige AB

September 2008

Summary

The Swedish Nuclear Fuel and Waste Management Company (SKB) is currently performing site investigations at two potential sites for a final repository for spent nuclear fuel. This report presents results of water flow and solute transport modelling of the Forsmark site. The modelling reported in this document focused on the near-surface groundwater, i.e. groundwater in Quaternary deposits and shallow rock, and surface water systems, and was performed using the MIKE SHE tool. The most recent site data used in the modelling were delivered in the Forsmark 2.3 dataset, which had its "data freeze" on March 31, 2007. The present modelling is performed in support of the final version of the Forsmark site description that is produced during the site investigation phase. This model version is referred to as SDM-Site Forsmark.

In this work, the hydrological modelling system MIKE SHE has been used to describe near-surface groundwater flow and the contact between groundwater and surface water at the Forsmark site. The surface water system at Forsmark is described with the one-dimensional "channel flow" modelling tool MIKE 11, which is fully and dynamically integrated with MIKE SHE.

The MIKE SHE model presented in /Aneljung and Gustafsson 2007/ was updated with data from the F2.3 data freeze. The main updates concerned the geological description of the saturated zone and the time series data on water levels and surface water discharges. The time series data used as input data and for calibration and validation was extended until the Forsmark 2.3 data freeze (March 31, 2007).

The present work can be subdivided into the following four parts:

1. Update of the numerical flow model (with the previous model presented in /Aneljung and Gustafsson 2007/ as the starting point).
2. Sensitivity analysis and calibration of the model parameters.
3. Validation of the calibrated model, followed by evaluation and identification of discrepancies between measurements and model results.
4. Additional sensitivity analysis and calibration in order to resolve the problems identified in point three above.

The Forsmark area has a small-scale topography; the study area is almost entirely below 20 m.a.s.l. No major water courses flow through the studied catchments. The brooks connecting the lakes with the sea are small. The lakes are shallow, with mean depths ranging from 0.1 m to 1m. Wetlands are frequent in the area. Till is the dominating type of Quaternary deposit. The Quaternary deposits are often shallow; their mean depth is approximately 5 m and the maximum depth observed is 16 m (south-east of Lake Fiskarfjärden). Most of the lakes are underlain by fine-grained sediments. The typical sediment stratigraphy is from down and up: glacial and/or post glacial clay, sand and gravel, and gyttja.

The bedrock hydrogeological conditions in Forsmark are characterised by a hydraulic anisotropy. The upper c. 200 m of the bedrock contains high-transmissive horizontal fractures/sheet joints. Results from the site investigations indicate that these sheet joints interconnect hydraulically across large distances. The bedrock between the sheet joints is less conductive. Below c. 200 m no sheet joints occur and the fracture frequency is very low. The pattern of local small-scale recharge and discharge areas in the Quaternary deposits overlays the more large scale flow system in the bedrock. The groundwater recharge from the QD to the upper bedrock is easily transmitted in the upper bedrock even at low gradients due to the high transmissive sheet joints. The groundwater level in the upper bedrock is very flat and at c. 0.5 meter above sea level, m.a.s.l.

The calibrated model showed good agreement between measured and calculated surface water discharges and surface water levels. Also the calculated groundwater elevations in the Quaternary deposits showed a good agreement with the observed values. However, the calculated groundwater elevations in the bedrock were in general above the observed levels.
The main actions taken during the calibration can be summarised as follows:

1. The potential evapotranspiration was reduced in order to reach the observed accumulated discharge.
2. The uppermost layer of Quaternary deposits in Forsmark is very high-conductive. A drainage function was activated in the model to describe the fast transport of water in the upper soil layer to the water courses.
3. Anisotropy in the hydraulic conductivity of the till was applied in the model.
4. The model was extended to a depth of 600 m (from 150 m), where a no flow boundary condition was applied.

When validating the model, the model was run for an independent data period. The validation period comprises weather conditions not present during the calibration period. In 2006 there was a very fast and distinct snow melt in the spring followed by a very dry summer. The model was not able to reproduce these events/periods properly. There was a lack of discharge in all the surface water stations during the snow melt and the pattern of the time series for some groundwater observation points deviated from the measured during the summer. Also, the response to the autumn rains was too slow in the model.

The groundwater elevations in the bedrock were consistently above the observed levels; however this was identified already after the calibration. It was found that this deviation between measurements and calculated levels in the bedrock was very important for the evaluation of the conceptual model. The difference between measurements and calculated values was much smaller in the Quaternary deposits than in the bedrock. Since the levels in the rock were consistently overestimated, this lead to erroneous vertical head gradients between the Quaternary deposits and the bedrock in some areas. The calculated gradient was always directed upwards from the bedrock to the Quaternary deposits, whereas the measurements showed downward gradients within the so-called target area.

After the validation and evaluation of the model results, it was decided to run an additional sensitivity analysis, including simulations of a pumping test, in order to further investigate possible reasons for the high calculated heads in the bedrock and the problems related to the surface water discharge during the validation period. Also, the influence of the drainage of the SFR repository was analysed.

The results from the additional sensitivity analysis showed that the bedrock properties had to be modified to lower the calculated heads in the bedrock and to improve the agreement with the responses observed during the pumping test. The vertical conductivity was reduced by a factor of ten, and the horizontal conductivity of the sheet joints was increased by a factor of ten. The storage coefficient of the rock was reduced by several orders of magnitude to achieve fast responses similar to those observed in the pumping test.

To reach a good agreement between measurements and the calculated heads in the bedrock an activation of the drainage at the SFR repository was needed. When implementing the SFR drainage, the calculated groundwater levels in the bedrock were lowered and the difference between calculations and measurements was reduced. The final mean absolute error between observed and calculated groundwater elevation in the Quaternary deposits was 0.28 m, and the corresponding value for the bedrock was 0.41 m. However, the mean errors were very small implying that the mean groundwater situation in both the Quaternary deposits and the bedrock was properly described by the model.

The solute transport modelling presented in this report included particle tracking, PT, and advection-dispersion, AD, simulations. The studied particle and AD solute sources were placed in the bedrock as well as on the ground surface. When modelling transport from solute sources in the rock these were located at 140 m.b.s.l. In the PT simulations particles were entered both all over the model area and only inside the area for the planned repository. The pattern of recharge and discharge areas at the surface were studied, but also the flow paths in the bedrock. The PT simulations were run for 300 years and 5,000 years. The AD simulations were run for 200 years.

The particle tracking results indicated a relative slow transport from the bedrock up to the ground surface. The horizontal fractures/sheet joints short-circuited the upward transport paths of the particles released in the area where these structures were represented. The particles reaching ground surface when introducing particles all over the model area were concentrated to lake areas, the depressions around the streams, and the sea. When introducing particles inside the planned repository area only, all exit points were found in the sea; no particles discharged in the land part of the model area. The overall pattern of exit points after 300 years did not change when running the model for 5,000 years. However, the exit points moved further out in the sea.

The AD results from the case where the solute was introduced at 140 m.b.s.l. showed that the transport was directed both upwards and downwards. The upward transport in the bedrock was mainly directed towards the sea and the lake areas. When the transported solute reached a layer where the sheet joints were represented in the model, the horizontal component of the transport dominated. As a result, only a minor fraction of the injected solute appeared above the areas with high hydraulic conductivity. Discharge from the bedrock to the Quaternary deposits was limited. Only in areas above the Eckarfjärden regional fracture zone the Quaternary deposits could receive groundwater and solutes from the bedrock.

In summary, an extensive sensitivity analysis and calibration process is the basis for the results of the MIKE SHE model presented in this report. The general impression is that the model shows good agreement with field measurements, and hence confirms the conceptual model of the Forsmark site.

Sammanfattning

Svensk Kärnbränslehantering AB (SKB) genomför för närvarande platsundersökningar inom två potentiella områden för lokalisering av ett slutförvar för utbränt kärnbränsle. Denna rapport presenterar resultat av vattenflödes– och transportmodelleringar av Forsmarksområdet. Modelleringen som redovisas i denna rapport är fokuserad på det ytnära grundvattnet, dvs grundvattnet i jordlagren och i den övre delen av berget, och ytvattensystemet. Modelleringen har utförts med modellverktyget MIKE SHE. De senaste platsspecifika data som använts ingick i datamängden F2.3 med s k datafrys den 31 mars 2007. Modelleringen ingår i den sista versionen av platsbeskrivande modell som tas fram under platsundersökningsskedet. Denna modellversion kallas SDM-Site Forsmark.

Modellsystemet MIKE SHE har använts för att beräkna och beskriva den ytnära hydrogeologin i Forsmark och kontakten mellan yt– och grundvatten. Ytvattensystemen har beskrivits i det endimensionella modellverktyget MIKE 11 vilket är helt integrerat med grundvattenmodellen i MIKE SHE.

Den MIKE SHE-modell som presenterades i /Aneljung och Gustafsson 2007/ har uppdaterats med data från datafrys 2.3. De huvudsakliga uppdateringarna har gjorts i den geologiska modellen och de parametrar som beskriver de hydrogeologiska egenskaperna i den mättade zonen. Tidsseriedata som har använts för kalibrering och validering av modellen har utökats fram till datumet för datafrysen, den 31 mars 2007.

De genomförda modelleringsarbetena kan delas in i följande 4 delar:

1. Den numeriska flödesmodellen som presenterades i /Aneljung och Gustafsson 2007/ uppdaterades med nya data.
2. Känslighetsanalys och kalibrering av den uppdaterade flödesmodellen.
3. Validering av den kalibrerade modellen samt utvärdering av avvikelser mellan mätta värden modellresultat.
4. Kompletterande känslighetsanalys och kalibrering för att komma till rätta med de avvikelser som identifierats i punkt 3.

Forsmark karakteriseras av små höjdskillnader och en småskalig topografi. Hela modellområdet ligger under 20 meter över havet. Det finns inga större vattendrag som rinner genom området; istället är det små bäckar som sammanbinder sjöarna och rinner ut i havet. Alla sjöar är grunda och det finns många våtmarker i området. Medeldjupen för samtliga sjöar ligger mellan 0.1 m och 1 m. Den dominerande jordarten i området är morän. Det är tunna jordlager med ett medeldjup på ca 5 m. Det största jorddjup som observerats i borrningar på land är 16 m, vilket uppmättes i områdets sydöstra del i närheten av Fiskarfjärden. Sjöarna underlagras av finkorniga sediment. Den typiska lagerföljden är, nerifrån och upp; glacial och/eller postglacial lera, sand och grus, och gyttja.

De hydrogeologiska förhållandena i Forsmark karakteriseras av en hydraulisk anisotropi i berggrunden. De övre ca 200 m av berget består av hydrauliskt högkonduktiva horisontella sprickzoner, bankningsplan. Undersökningar visar att dessa bankningsplan står i hydraulisk kontakt över stora områden. Bergmassan mellan bankningsplanen är emellertid mycket tätare, vilket gör att den vertikala hydrauliska konduktiviteten är låg inom dessa områden. Under 200 m djup upphör bankningsplanen och sprickfrekvensen är mycket låg. De lokala in– och utströmningsområdena i jordlagren överlagrar det mer storskaliga flödessystem som återfinns i berget. De högkonduktiva bankningsplanen medverkar till att den grundvattenbildningen som sker från jordlagren till den övre delen av berget enkelt transporteras ut i bergmassan även vid låga gradienter.

Grundvattennivån i den övre delen av berget följer inte topografin på samma sätt som den i jordlagren utan är relativt platt. De flesta nivåobservationer i bergets övre del ligger kring 0,5 meter över havet.

Den kalibrerade modellen visar på bra överensstämmelse mellan mätta och beräknade ytvattenflöden, ytvattennivåer och grundvattennivåer i jordlagren. De beräknade grundvattennivåerna i berget låg dock konstant över de observerade nivåerna. De åtgärder som utfördes under kalibreringen kan sammanfattas som följer:

1. Den potentiella evapotranspirationen reducerades för att modellen skulle uppvisa rätt ackumulerad avrinning.
2. Det översta jordlagret i Forsmark har en mycket hög hydraulisk kapacitet. För att efterlikna detta i modellen aktiverades en dräneringsfunkion. Detta medför att det sker en snabb transport av vattnet i jordlagren och ut i vattendragen vid ett regntillfälle.
3. Anisotropi i moränens hydrauliska egenskaper ansattes i modellen.
4. Modellens nedre rand flyttades från 150 meter under havet till 600 meter under havet och en tät rand ansattes i botten av modellen.

Valideringsperioden som modellen testades mot innehåller vädersituationer som inte täcktes in under kalibreringsperioden. Under 2006 var det en mycket snabb och kraftig snösmältning på våren som följdes av en extremt torr sommar. Modellen klarade inte av att reproducera dessa två händelser tillräckligt väl. Snösmältningstoppen återskapades inte korrekt i modellen; den beräknade avrinningen var ca 20 % lägre än den observerade. De beräknade tidsserierna för grundvattennivåerna i jordlagren fick ett avvikande mönster i vissa observationspunkter. Efter den torra sommaren 2006 hade modellen dessutom svårt att svara på de första höstregnen. Responsen var något sen och den beräknade avrinningen på hösten 2006 blev således för låg.

Grundvattennivåerna i berget var generellt högre än de observerade nivåerna, vilket hade observerats redan under kalibreringsperioden. Eftersom grundvattennivåerna i berget stadigt låg över nivåerna i jordlagren, medan nivåerna i jordlagren överensstämde relativt väl med de observerade, uppkom i vissa områden i modellen hydrauliska gradienter mellan jord och berg som inte stämde med de uppmätta. I modellen skapades en uppåtriktad gradient mellan jord och berg i hela området, medan fältobservationerna visar på en nedåtriktad gradient inom det delområde för det planerade förvaret.

Efter att modellen validerats beslutades det att utföra en kompletterande känslighetsanalys och kalibrering, inklusive modellering av ett pumptest, för att försöka komma till rätta med de frågor som identifierats då modellen testades mot oberoende data. I detta skede undersöktes också eventuell hydraulisk inverkan från SFR, slutförvaret för låg– och medelaktivt avfall, som ligger inom modellområdet.

Resultaten från den kompletterande känslighetsanalysen visade att de hydrauliska parametrarna för berget måste modifieras för att det höga beräknade grundvattentrycket i berget reduceras. Den vertikala hydrauliska konduktiviteten reducerades med en faktor 10 och den horisontella hydrauliska konduktiviteten i bankningsplanen ökades med en faktor 10. Dessutom reducerades magasinstalet för att rätt respons skulle uppnås vid modelleringen av pumptestet.

För att uppnå en bra överensstämmelse mellan mätta och modellerade värden för grundvattennivåerna i berget var det tvunget att aktivera ett vattenuttag i SFR. När SFR implementerades i modellen sjönk grundvattennivåerna i berget och felet mellan observerade och beräknade värden minskades betydligt. Medelvärdet för alla absolutfel mellan mätta och modellerade grundvattennivåer i jordlagren hamnade på 0,28 m och motsvarande värde för berget låg på 0,41 m. Medelfelet är emellertid nära noll vilket innebär att medelgrundvattenytan i modellen är bra beskriven.

Transportmodelleringen som redovisas i denna rappart inkluderar partikelspårningsberäkningar (PT) och advektionsdispersionsberäkningar (AD). Partiklar eller källor med löst ämne (AD-beräkningarna) placerades såväl i berget som på markytan i modellen. När källan placerades i berget gjordes detta på nivån 140 meter under havet. I PT beräkningarna ansattes källan både över hela modellområdet och enbart inom det planerade förvarsområdet. Mönstret av in– och utströmningsområden studerades såväl som flödesvägarna i berget. PT-simuleringarna kördes för 300 år och 5 000 år, medan AD-simuleringarna kördes för 200 år.

PT-beräkningarna visar på en långsam transport från berget och upp mot ytan. Bankningsplanen kortsluter många av flödesvägarna och när partiklarna väl når områden med bankningsplan sker det en horisontell transport ut mot havet. I det fall då partiklar introduceras inom hela modellområdet på nivån 140 meter under havet är de partiklar som når ytan koncentrerade till sjöar, lågpunkter utmed vattendrag och havet. Då partiklar introduceras inom det planerade förvarsområdet hamnar alla s k utsläppspunkter i havet. Det mönster av utsläppspunkter som noteras efter 300 års simulering ändras inte mycket då modellen körs i 5 000 år; utsläppspunkterna förflyttar sig dock längre ut i havet.

Resultaten från AD-beräkningar då källan placerades 140 meter under havet visar att det lösta ämnet sprider sig såväl uppåt som nedåt i modellen. Den uppåtriktade transporten koncentreras mot sjöar och vattendrag; när föroreningen stöter på ett beräkningslager som innehåller bankningsplan domineras transporten av den horisontella komponenten. Som en följd av detta är det endast en mindre del av den tillförda mängden som når upp över områden med höga horisontella konduktiviteter. Utströmningen från berget till jordlagren är begränsad. I modellen är det enbart jordlagren ovanför Eckarfjärdszonen som nås av grundvatten och tillhörande löst ämne från berget.

Sammanfattningsvis kan konstateras att en omfattande känslighetsanalys och kalibreringsprocess ligger till grund för de resultat som presensteras i denna rapport. Det övergripande intrycket är att modellen visar på god överensstämmelse med de mätningar som utförts på platsen och att resultaten bekräftar den konceptuella modell som byggts upp över hydrologin och den ytnära hydrogeologin i Forsmark.

Contents

1 Introduction

1.1 Background

The Swedish Nuclear Fuel and Waste Management Company (SKB) is performing site investigations at two different locations in Sweden, referred to as the Forsmark and Laxemar areas, with the objective of siting a final repository for high-level radioactive waste. Data from the site investigations are used in a variety of modelling activities; the results are presented within the frameworks of Site Descriptive Models (SDM), Safety Assessment (SA), and Environmental Impact Assessment (EIA). The SDM provides a description of the present conditions at the site, which is used as a basis for developing models intended to describe the future conditions in the area.

This report presents model development and results of numerical flow and transport modelling of surface water and near-surface groundwater at the Forsmark site. Data from the Forsmark 2.3 data freeze (March 31, 2007) constitute the most recent input to the modelling. The numerical modelling was performed using the modelling tool MIKE SHE and is based on the site data and conceptual model of the Forsmark areas described in /Johansson 2008, Johansson and Öhman 2008/. The present work is a part of the modelling performed for the final version of the Forsmark SDM to be produced during the site investigation stage. This SDM version is referred to as SDM-Site Forsmark and is reported in /SKB 2008/.

Modelling of radionuclide transport is an important part of the analyses performed in order to support the safety assessments. This report presents solute transport applications based on both particle tracking simulations and advection-dispersion calculations. Scenarios relevant for the transport from a deep geological repository have been studied, but also the pattern of recharge and discharge areas.

1.2 Objective and scope

The general objectives of the site descriptive modelling of the Forsmark area and the specific objectives of the SDM-Site Forsmark modelling are presented in /SKB 2008/. The present report is a background report describing the numerical modelling of surface hydrology and near-surface hydrogeology in Forsmark.

The objectives of the modelling reported in this document are to:

1 Update the previous MIKE SHE model described in /Aneljung and Gustafsson 2007/ with new data from the F2.3 data freeze and present the input data used in the model.

2 Present the methodology and results from the sensitivity analysis of the flow model.

3 Calibrate the MIKE SHE water flow model to site data in the form of groundwater levels, surface water discharges and surface water levels.

4 Validate the calibrated flow model using an independent data and present the results from the validation calculation. The results are evaluated in terms of surface water discharges and levels, groundwater levels in Quaternary deposits, groundwater head elevations in the bedrock, the pattern of recharge and discharge areas, and the overall water balance of the area.

5 Analysis of solute transport from potential sources at large depth in the rock into the near-surface system, and from sources on the ground surface into the rock system.

1.3 Setting

The Forsmark area is located approximately 120 km north of Stockholm, in northern Uppland within the municipality of Östhammar. Figure 1-1 shows the regional model area and the so-called candidate area considered by the site investigation and within the site descriptive modelling. Also some lakes and other objects of importance for the hydrological modelling are shown in the figure.

The candidate area is the area initially prioritised for potentially hosting the geological repository. This means that the repository possibly could be built somewhere within this area, not that it would occupy the whole area. This implies that more detailed investigations have been performed inside the candidate area than in the rest of the regional model area, at least for that some of the site investigation disciplines (see /SKB 2008/ for details). The candidate area is situated in the immediate vicinity of the Forsmark nuclear power plant and the underground repository for low– and medium-active nuclear waste, SFR. It is located along the shoreline of Öregrundsgrepen (a part of the Baltic), and extends from the nuclear power plant and the access road to the SFR facility in the northwest to the Kallrigafjärden bay in the southeast.
The candidate area is approximately 6 km long and 2 km wide.

A description of the meteorological, hydrological and hydrogeological conditions in the Forsmark area is presented in /Johansson 2008/. /Lindborg (ed.) 2008/ gives a description of the whole surface and near-surface system, including the most recent models of, e.g. the topography and the Quaternary deposits. The site characteristics and parameters considered in the present work are summarised and described in Chapter 2.

In this report, the reference system for altitude levels is RHB70. Depending on type of data presented, levels will be given in metre above sea level, m.a.s.l., or metre below sea level, m.b.s.l. according to RHB70.

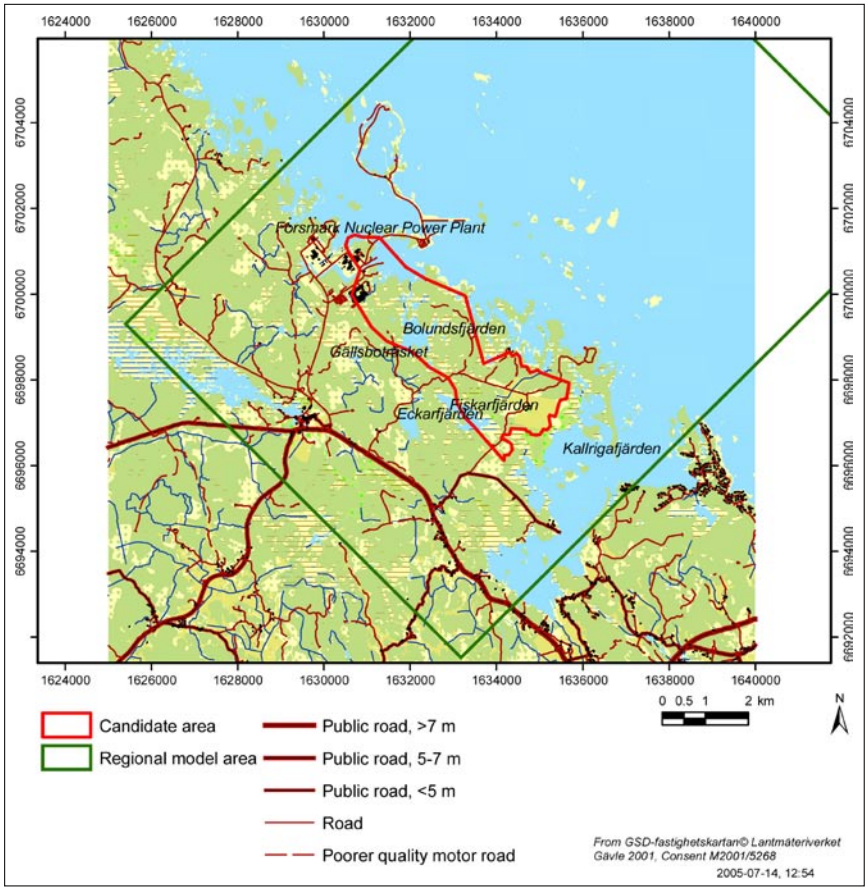

Figure 1-1. *Map of the land part of the regional model area and some objects of particular interest for the hydrological modelling.*

1.4 Related modelling activities

Several modelling activities have provided the various external input data and models required for the present modelling and the preceding SDM site modelling. Whereas most of these inputs are described in some detail in Chapter 2 and in /Johansson 2008/, we discuss here briefly the interactions with the hydrogeological activities that consider flow modelling of the integrated rock-Quaternary deposits system.

The work described in this report is focused on the surface systems, i.e. the Quaternary deposits and the upper part of the bedrock. The numerical model was developed using the MIKE SHE tool. The ground surface, as obtained from the topographic model of the site, is the upper model boundary. During the modelling process, the vertical extent of the model varied; the bottom boundary was initially located at 150 m.b.s.l. (metres below sea level), and then moved to 600 m.b.s.l. The modelling activities that provided inputs to the various parts of this work can be summarised as follows:

- The SDM Forsmark 2.2 hydrogeological modelling preformed with the ConnectFlow modelling tool /Follin et al. 2007/ delivered the hydrogeological properties of the rock and the bottom boundary condition used in the basic setup of the model and in the sensitivity analysis.
- The Forsmark version 2.2 and 2.3 geological models of the Quaternary deposits /Hedenström et al. 2008, Hedenström and Sohlenius 2008/ provided the geological-geometrical framework for the stratigraphical description used in the MIKE SHE model.
- The SDM-Site conceptual modelling of the hydrology and near-surface hydrogeology at the Forsmark site /Johansson 2008/ provided a basic hydrogeological parameterisation and a hydrological-hydrogeological description to be tested in the numerical modelling.

The relations between the near-surface and bedrock hydrogeological models are discussed in /Follin et al. 2008/ and /SKB 2008/.

1.5 This report

This report provides an integrated presentation of the modelling activities listed as parts 1–5 in Section 1.2. Chapter 2 describes the input data (part 1). Chapter 3 describes the modelling tool and the numerical flow model. In Chapter 4, the calibration and sensitivity analysis (part 2 and 3) is presented, whereas Chapter 5 presents the validation and evaluation of the model (part 4). Chapter 6 contains a description of an additional calibration process and sensitivity analysis performed due to discrepancies between measurements and the model results presented in Chapter 5. Results of solute transport modelling (part 5) are presented in Chapters 5 and 6. In Chapter 7, the conclusions of the work are presented.

The modelling process was divided into 4 main steps. First, the numerical flow model (with the previous model presented in /Aneljung and Gustafsson 2007/ as the starting point) was updated with data as presented in Chapter 2. Then, an initial sensitivity analysis and calibration of the model parameters was performed. During this initial calibration an updated version of the bedrock model was delivered and implemented in the MIKE SHE model. In the third part of the modelling work, the calibrated model was tested using independent time series data, and after that a complementary calibration and sensitivity analysis was performed. At the time for this complementary modelling, the QD-model was updated from the 2.2 to the 2.3 version /Hedenström et al. 2008/.

2 Site hydrology and input data

2.1 Site hydrology

The Forsmark area has a flat, small-scale topography. The study area is almost entirely below 20 m.a.s.l. (see Figure 2-1). In the hydrological characterisation of the site, 25 “lake-centred” catchments and sub-catchments have been delineated; catchments and lakes are described in /Brunberg et al. 2004/. No major water courses flow through the catchments shown in Figure 2-1. Small brooks connect the lakes with the sea. The brooks downstream Lake Gunnarsboträsket, Lake Eckarfjärden and Lake Gällsboträsket carry water most of the year, but can be dry during dry years /Johansson 2008/. The main lakes in the area are Lake Eckarfjärden, Lake Fiskarfjärden, Lake Gällsboträsket and Lake Bolundsfjärden. The lakes are shallow, with mean depths ranging from 0.1 m to 1 m.

Approximately 70% of the total catchments area is covered with forest; agricultural land is only present in the south-eastern part. Wetlands are frequent in the area and covers more than 25% in some sub-catchments. Till is the dominating type of Quaternary deposit (QD) and bedrock outcrops is frequent. The Quaternary deposits are often shallow, the mean depth is approximately 5 m and the maximum depth observed is 16 m and is found south-east of Lake Fiskarfjärden. Most of the lakes are underlain by fine-grained sediments. The typical sediment stratigraphy from down and up is; glacial and/or post glacial clay, sand and gravel, clay-gyttja and gyttja.

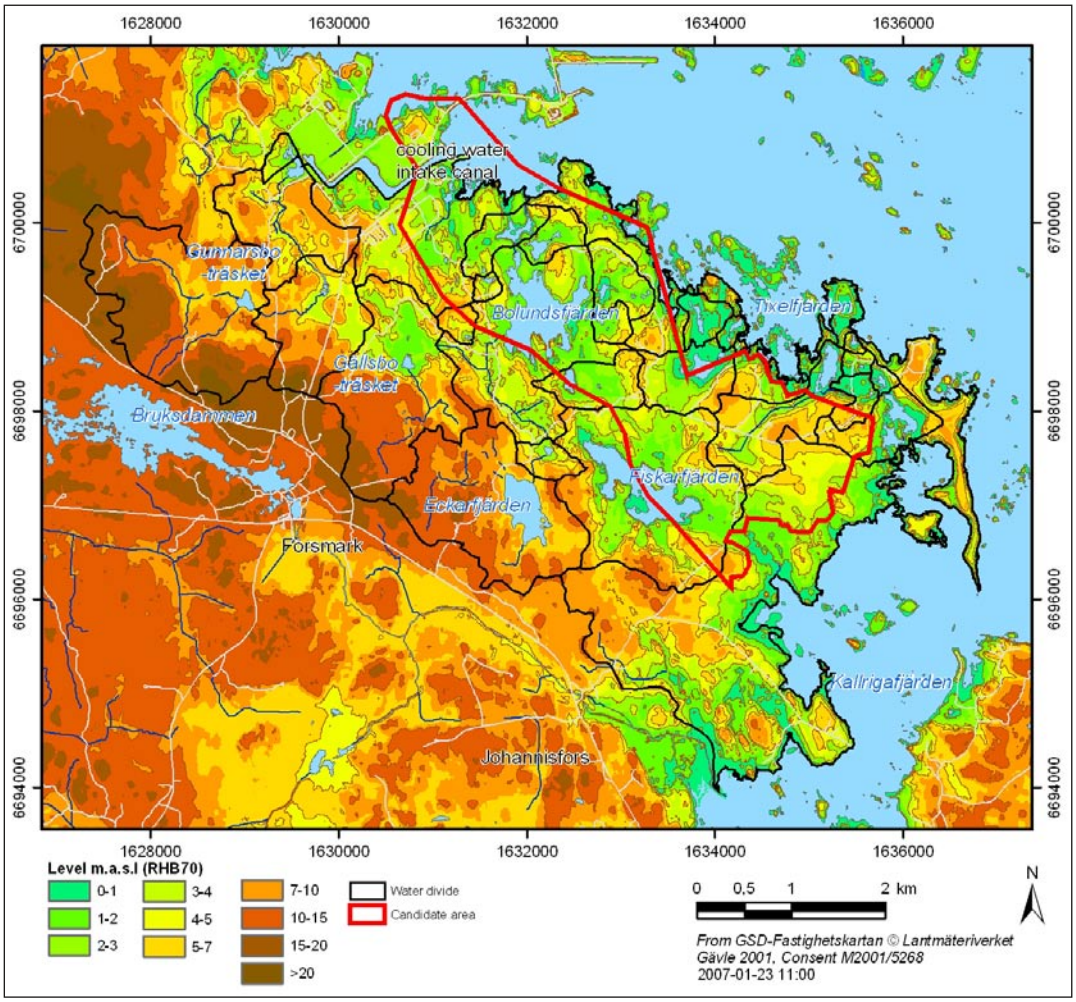

Figure 2-1. *Topographical map of the Forsmark area. Surface water divides are indicated in the figure.*

In Figure 2-2 the overall conceptual model of the near-surface hydrogeology is illustrated. The outer and internal surface water and near-surface groundwater divides of the model area are assumed to coincide. The small-scale topography implies that many small catchments are formed with local, shallow groundwater flow systems in the QD. Combined with the decreasing hydraulic conductivity with depth and the anisotropy of the tills dominating in the area (implying higher horizontal than vertical hydraulic conductivities), it is obvious that a dominating part of the groundwater will move along very shallow flow paths. Groundwater levels in QD are very shallow with mean levels within a depth of less than a metre in most of the area. The groundwater level is highly correlated with the topography of the ground surface.
The conceptual model is further discussed in /Johansson 2008/.

The bedrock hydrogeological conditions in Forsmark are characterised by a hydraulic anisotropy within the north-western part of the candidate area indicated in Figure 2-1. Within this area, often referred to as the "target area" (see /SKB 2008/ for a definition) the upper c. 200 m of the bedrock contains high-transmissive horizontal fractures/sheet joints. Results from the site investigations indicate that these sheet joints interconnect hydraulically across large distances /Follin et al. 2008, Johansson 2008/. The bedrock between the sheet joints is less conductive. Below there are no fractures/sheet joints of this type, and the overall fracture frequency is very low.

Groundwater recharge from precipitation is the dominating source of recharge. Under normal weather conditions the lakes act as discharge areas for groundwater in the QD. Due to the transpiration, the groundwater levels are lowered around the lakes during dry summers, and the lakes may become recharge areas. The local small-scale recharge and discharge areas in the Quaternary deposits overlay the more large scale flow system in the bedrock. The groundwater recharge from the QD to the upper bedrock is easily transmitted in the upper bedrock even at low gradients due to the high-transmissive sheet joints and other structures there. The groundwater level in the upper bedrock is very flat and at c. 0.5 m.a.s.l.

2.2 Input data

The input data to the MIKE SHE model include data on topography, land use, vegetation, geology, hydrogeology and meteorology. A new geological model was implemented in the present MIKE SHE model. Both the description of the bedrock geology and that of the Quaternary deposits have been updated since the Forsmark 1.2 model version of MIKE SHE /Johansson et al. 2005/. The geological models of the QD and the bedrock are further described in Sections 2.2.2 and 2.2.3. Data on land use and topography are the same as in the 1.2 model version.

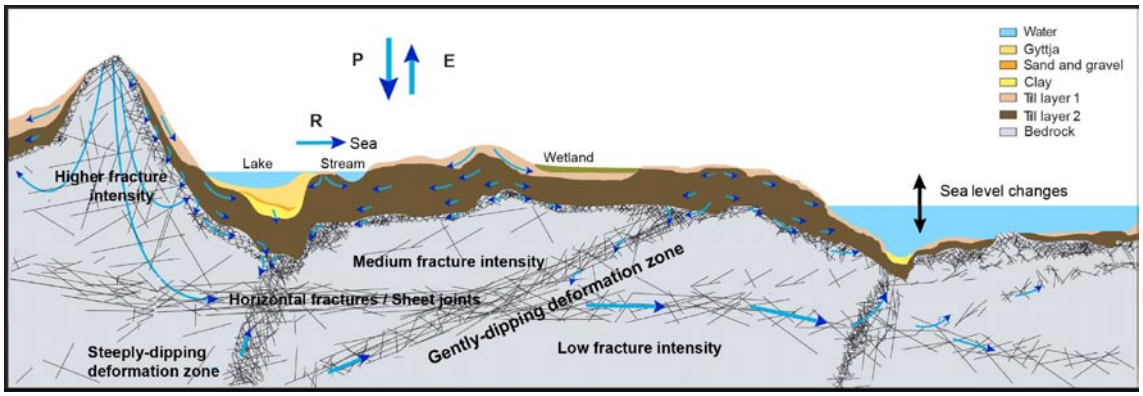

Figure 2-2. *Conceptual model of the hydrology and near-surface hydrogeology at Forsmark /Follin et al. 2007/.*

The time series of meteorological data, groundwater levels, and surface water levels and discharges have been extended until the Forsmark 2.3 data freeze (March 31, 2007). The model has been calibrated to data for the period from May 15, 2003, to July 31, 2005, and the model was validated using data from between August 1, 2005, and March 31, 2007.

2.2.1 Meteorology

The MIKE SHE model uses data on temperature, precipitation and potential evapotranspiration. Locally measured data are available for the period between 15th of May, 2003, and 31st of March, 2007. The meteorological input data are taken from two meteorological stations within the candidate area, the Högmasten and Storskäret stations (see Figure 2-3).

The precipitation used in the model is calculated as the mean value of the two meteorological stations and is corrected for wind losses according to the method described in /Johansson 2008/. In the first set of simulations, it is described as precipitation including snow melt. When data are missing from one station, they are replaced by data from the other. When data are missing for both stations, multiple regression analysis on overlapping data periods with the meteorological stations at Lövsta, Örskär and Östhammar has been used to calculate a theoretical precipitation for the area.

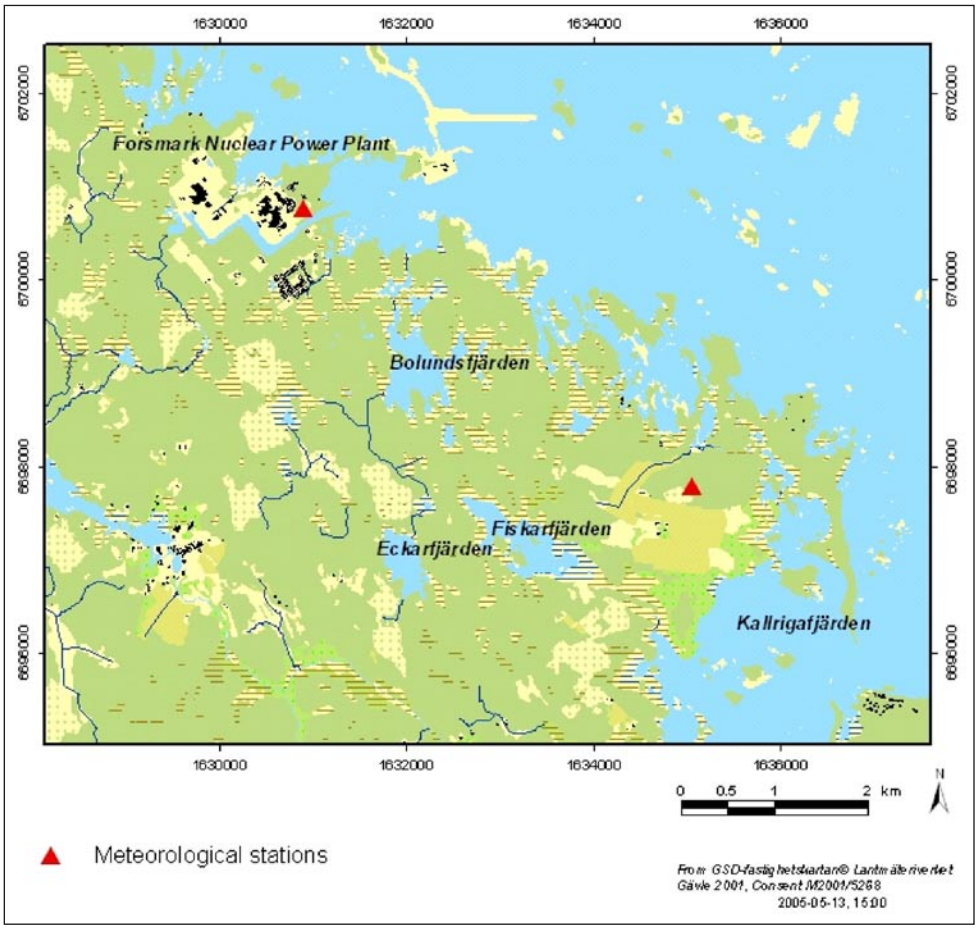

Figure 2-3. *Positions of the two meteorological stations Högmasten and Storskäret. The Högmasten station is situated in the north-west close to the nuclear power plant, and the Storskäret station is situated east of Lake Fiskarfjärden.*

The corrected precipitation data have been combined with results from an air-temperature dependent snow routine. The content of the snow storage melts at a rate defined by the degree-day coefficient, multiplied with the temperature from the meteorological stations. The degree-day coefficient has been calibrated against measurements of snow cover and snow water content, and is set to 1.23 mm/day/°C /Juston et al. 2007/. The result is a daily time series of estimated site-average ground surface inflow, see Figure 2-4. The precipitation shows a similar pattern over the period. However, the spring and summer of 2006 shows a different pattern. A momentary and distinct snow melt is followed by a very dry period. The intense snow melt is reflected in the discharge in the water courses and the dry period is observable in the groundwater levels in the area. Table 2-1 summarises the monthly sum of the net precipitation for each year 2004–2006.

The potential evapotranspiration, PET, was calculated with the Penman equation according to /Eriksson 1981/, using data from the local station Högmasten. The original dataset from the Sicada database contains some negative values of PET that reflect condensation, especially during cold winter periods. MIKE SHE cannot handle negative input data on PET; therefore, the time series was corrected as described below.

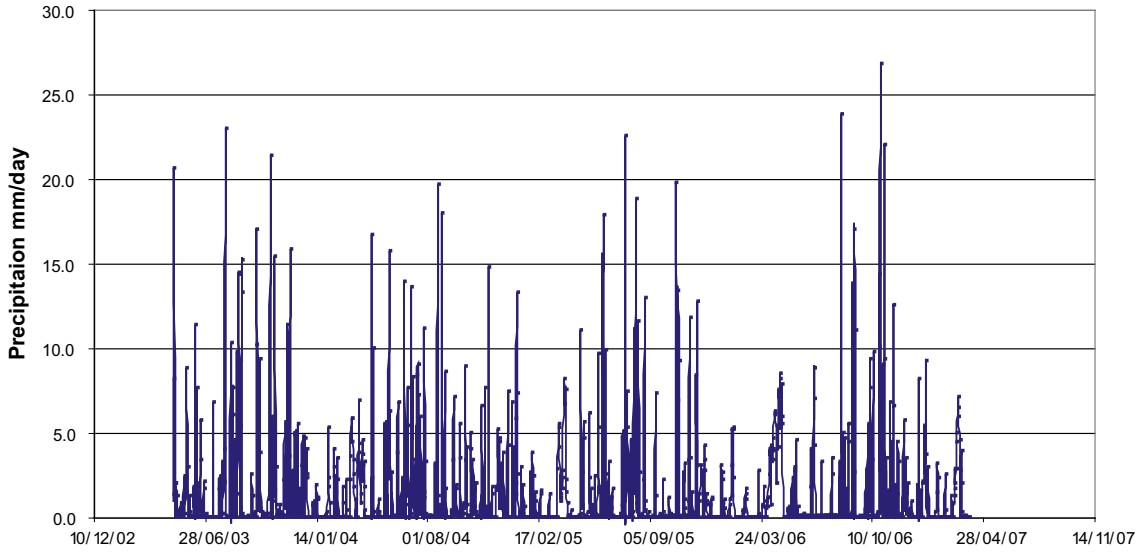

Figure 2-4. *Site average precipitation including snow melt.*

Table 2-1. Monthly sum of the precipitation including snow melt for the period 2004–2006.

	2004	2005	2006
January	6.68	44.91	26.29
February	29.44	17.21	13.14
March	57.61	29.27	7.60
April	50.45	38.13	129.50
May	43.95	40.48	22.76
June	45.98	80.66	30.53
July	83.82	59.92	10.29
August	54.73	85.37	59.40
September	28.82	11.83	50.93
October	39.93	51.15	134.59
November	35.33	55.33	58.00
December	55.15	30.35	20.27
Total	531.88	544.61	563.29

As raw data are given in 30 minutes intervals, whereas daily sums are more relevant as input to MIKE SHE, the first step was to calculate the daily sums including negative values. In this way negative values during night and morning hours were transferred as a reduction to daytime hours with positive PET values. In the second step, all daily values where checked in a chronological order. During winter time, when the total daily sum could be negative, these negative daily values were moved backwards in time, reducing originally positive values. In other words, when negative values were detected, this value was applied as a reduction of the previous positive value, and the negative value was set to zero. This method ensures that the total volume in the time series used as model input is the same as in the raw data, but negative values are moved backwards in time. The result after correction is shown in Figure 2-5.

The temperature input to MIKE SHE is used to calculate the effect of snow melt and snow cover. When applying the site-average ground surface inflow as precipitation input to the model, the snow melt is included in the input data. The measured temperature has therefore only been used when calculating the applied ground surface inflow and the PET.

The total precipitation for the data period, 15th of May 2003–31st of March 2007, is 2,224 mm, and the potential evaporation 1,954 mm. Table 2-2 shows the sums for the calibration period, May 2003–July 2005, and the validation period, August 2005–March 2007. The annual sums for 2004–2006 are also presented in the table. The precipitation and the potential evapotranspiration Figure 2-5. Potential evapotranspiration from the local station at Högmasten.

are almost equally distributed over the data period. A slight increase in the precipitation can be noticed; the precipitation is increased by 6% from 2004 to 2006. The potential evapotranspiration increases by 5% during the same period.

The reason why precipitation is somewhat larger than the PET volume when the validation period is included is that data are only available until March 2007. This means that the data only include months of very low PET during the year 2007.

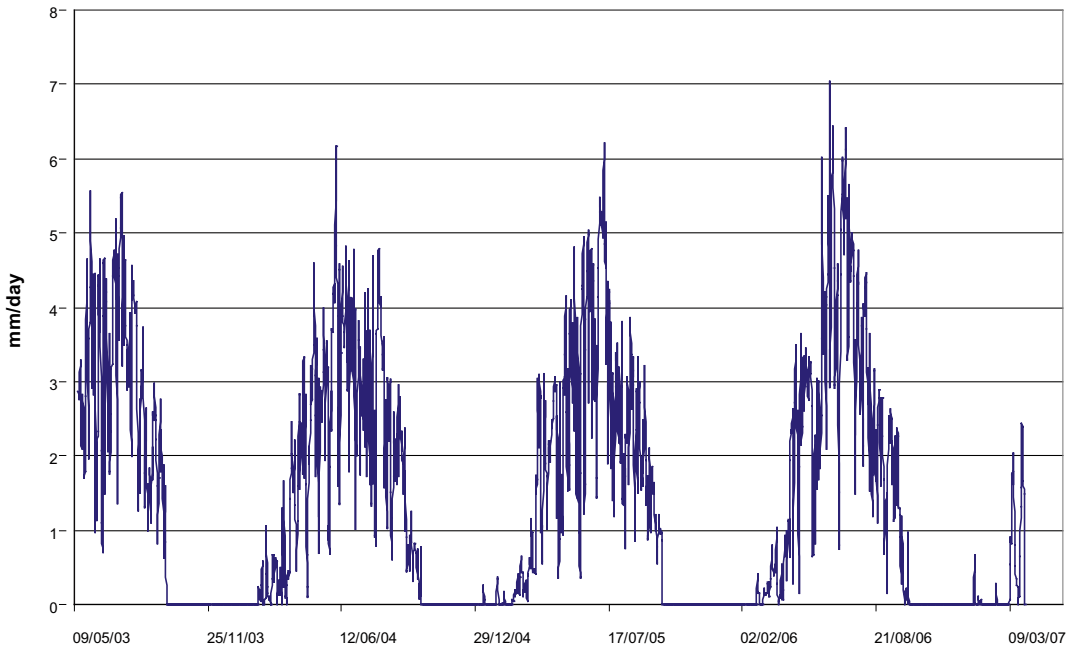

Figure 2-5. *Potential evapotranspiration from the local station at Högmasten.*

Table 2-2. Precipitation including snow melt, in mm, for the data period. The sums for the calibration period, the validation period and each year within the data period covering a whole year are also listed in the table.

Period	Net precipitation, mm	Potential evapotranspiration, mm
Total data period, 15 May 2003–31 March 2007	2,224	1,954
Calibration period, 15 May 2003–31 July 2005	1,278	1,274
Validation period, 1 August 2005–31 March 2007	909	680
Yearly sum 2004	532	500
Yearly sum 2005	545	508
Yearly sum 2006	563	525

2.2.2 Bedrock hydrogeology

Input to the geological description of the bedrock is obtained from the ConnectFlow groundwater flow model /Follin et al. 2007, Follin et al. 2008/. The horizontal and vertical resolutions of the data on the hydraulic conductivity and porosity of the bedrock are 20 m. Data representing the horizontal properties are introduced to the MIKE SHE model as geological layers every 20 m. The model is based on the Forsmark 2.2 geological model. In general, the hydraulic conductivity in this model is higher than in the F1.2 model. Especially the upper c. 200 m of the bedrock are highly fractured and water conductive. Horizontal sheet joints are present in the upper bedrock and are interconnected hydraulically.

According to hydraulic tests performed in percussion-drilled boreholes, the horizontal hydraulic conductivity of the fractures/sheet joints in the upper rock is very high, and the groundwater flow in the areas is dominated by the horizontal component. In Figures 2-6 and 2-7, the horizontal hydraulic and vertical conductivities at 70 m.b.s.l., respectively, are shown. There is a distinct difference in the conductivity fields between the horizontal and vertical conductivities, the sheet joints dominate the pattern in Figure 2-6. In general the hydraulic conductivities of the non-fractured bedrock are in the range 10^{-9} to 10^{-8} m/s, whereas the hydraulic conductivities of the fractured parts vary from 10^{-6} to 10^{-4} m/s. Two deliveries of ConnectFlow data from HydroNet were made during the modelling process; Figures 2-6 and 2-7 illustrate the data from the second delivery.

The ID-numbers of the two sets are listed below:

- SDM22_HCD7Ec_HRD5_phi2F_HSD4_BC9_IC3
- SDM23_HCD2h100A2b_HRD5r1_phi4F_HSD5d_IC3Mat_MD2_MOW18

The specific yield of the bedrock is assumed to be equal to the effective porosity, which is given from the ConnectFlow modelling. The storage coefficient, S_s [m^{-1}], is calculated according to an empirical relationship between the hydraulic conductivity and the storage coefficient:

$$S_s = a \cdot K^b$$

where K is the hydraulic conductivity [m/s], and the dimensionless parameters a and b are assigned the values $a = 6.037 \cdot 10^{-5}$ and $b = 0.2312$ based on experimental data from earlier studies at Äspö /Rhén et al. 1997/.

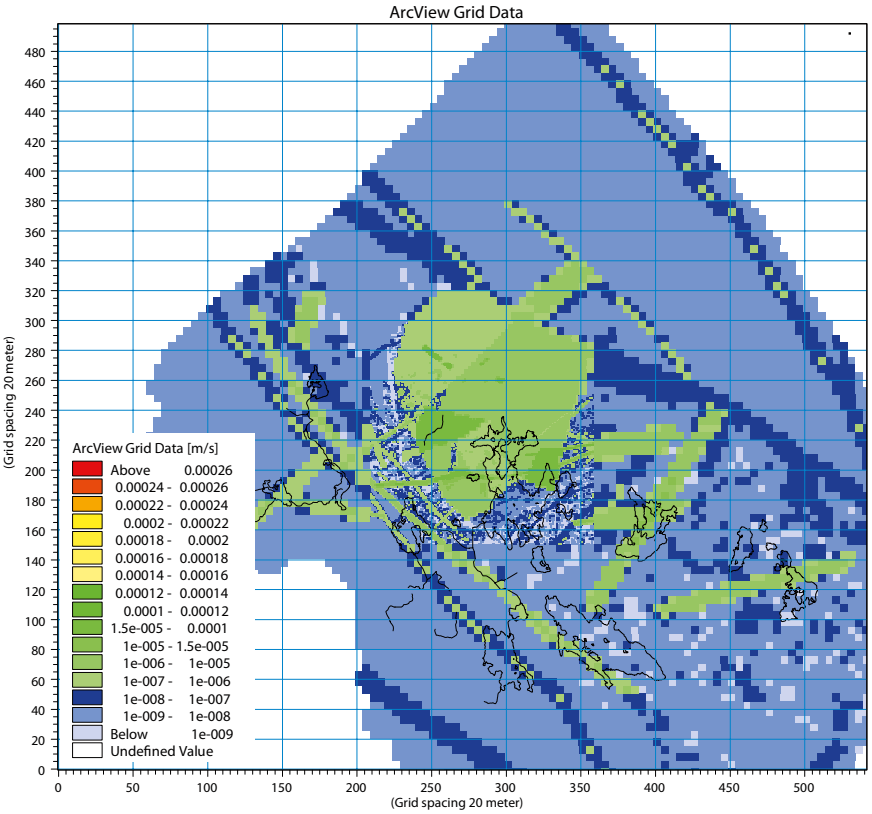

Figure 2-6. *Horizontal hydraulic conductivity at 60-70 m.b.s.l. The lakes and the streams in the area are marked in the figure.*

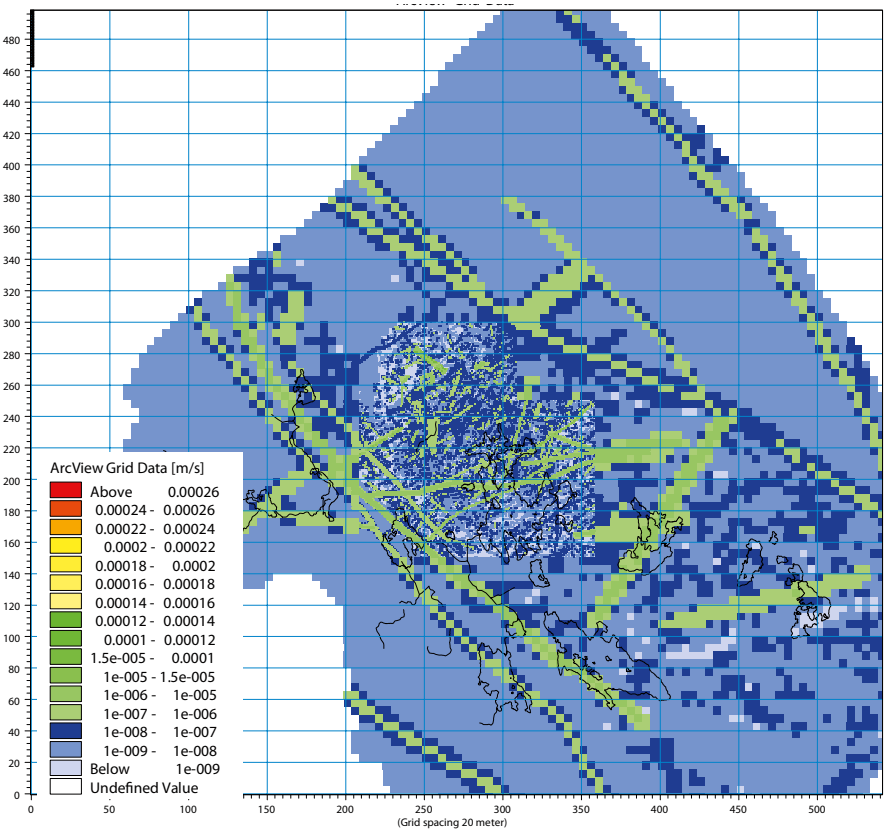

Figure 2-7. *Vertical hydraulic conductivity at 60-70 m.b.s.l. The lakes and the streams in the area are marked in the figure.*

2.2.3 Quaternary deposits

The geological model for the Quaternary deposits is developed in the modelling tool MIKE Geomodel /DHI Software 2007/. The conceptual model is presented in Figure 2-8. The model consists of nine units referred to as layers or lenses. The model is geometrical and presents the total regolith depth and the bedrock topography. The conceptual model for the construction of the different layers is based on knowledge from the site as well as general geological knowledge on similar formations. The layers are denoted Z1–Z6 and L1–L3. All layers and lenses may have zero thickness in parts of the model area. The lower level of each layer is specified and the layers are used as direct input to the MIKE SHE model. Each layer in the geological model of the Quaternary deposits represents a geological layer in MIKE SHE.

The model presents the geometry of the lower level of each layer in terms of elevation above sea level (RHB 70). The model has a spatial resolution of 20×20 m^2. The lower level of Z5 is interpolated from the dataset of information on the total depth of the Quaternary deposits, as well as the bedrock outcrops. Thus, the lower level of Z5 represents the bedrock surface regardless of whether it is covered by deposits or not. The bottom layer, Z6, is characterized by fractured bedrock. This layer is included in the model because a high-conductive layer has been recorded in the contact zone between bedrock and QD, see e.g. /Werner and Johansson 2003/, which implies that it may be of interest to vary the properties of this layer in the flow modelling. The geological model is described in detail in /Hedenström et al. 2008/. Each layer consists of one or several types of Quaternary deposits; the layers are described in Table 2-3. The layers L1–L3 describe the extension of the lake sediments.

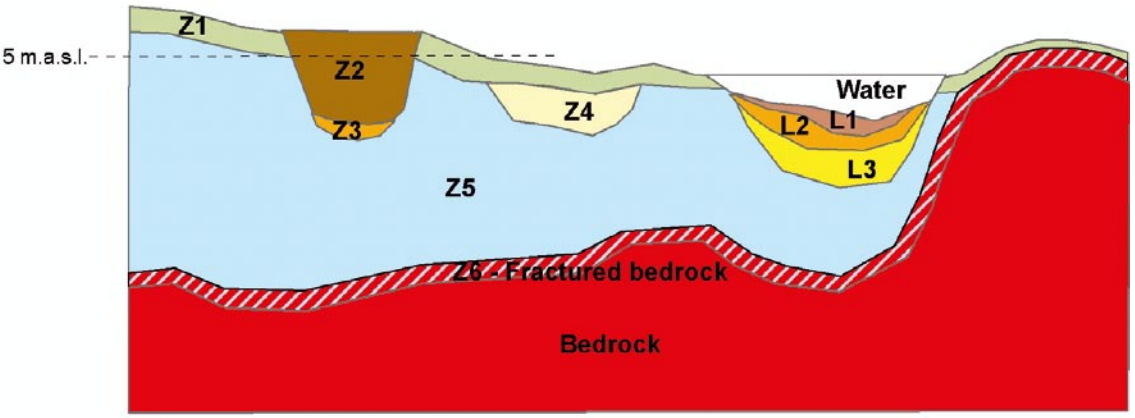

Figure 2-8. *Conceptual model for the geometry of Quaternary deposits.*

Table 2-3. Deposits, simplified codes and occurrence for the six layers and three lenses.

Description of layer/lens	Simplified code	Description/Occurrence
Gyttja (algal gyttja, calcareous gyttja, clay gyttja-gyttja clay)	L1	When peat is present as surface layer in the vicinity of a lake area, this is included in the L1 lens.
Postglacial and sand and/or gravel	L2	
Clay (glacial and postglacial)	L3	
Surface layer	Z1	The layer is affected by soil forming processes and is present within the entire modelled area, except where the surface is covered by peat or where the model has a lens (under lakes). On bedrock outcrops, the layer is 0.1 m and 0.6 m in other areas. If the total modelled regolith depth is less than 0.6 m, Z1 will be the only layer. The layer can be connected to the map of Quaternary deposits and assigned properties in accordance to the properties of the deposits.
Peat	Z2	This layer is only present where peat is presented on the QD-map.
Postglacial sand/gravel, glaciofluvial sediment and artificial fill	Z3	The layer is only present where the surface layer consists of postglacial sand/gravel, glaciofluvial sediment or artificial fill .
Postglacial clay	Z4a	
Glacial clay	Z4b	
Till	Z5	This layer is present in a major part of the model area. The lower limitation of Z5 represents the bedrock surface, i.e. Z5 represents a Digital Elevation Model for the bedrock surface.
Fractured bedrock	Z6	This layer has a constant depth of 0.5 m and represents the bedrock upper part, calculated from the interpolated Z5.The layer represents a high conductive zone that have been observed in many of the hydraulic tests within Forsmark.

Hydraulic properties were assigned to each layer in the geological model. The values are based on site data and other knowledge of the site. A detailed description of the hydraulic properties of the QD is given in /Johansson 2008, Johansson and Öhman 2008/. Table 2-4 presents the base setup of hydraulic properties in the MIKE SHE model. This set of parameters was used as a starting point for the calibration process. Note that isotropy is assumed in the hydraulic conductivities of all the Quaternary deposits. The values presented in Table 2-4 were updated during the calibration process.

2.2.4 Unsaturated zone description

Coarse till is the dominating type of Quaternary deposit in the area, and accordingly also in the unsaturated zone description. Figure 2-9 shows the distribution of Quaternary deposits in the unsaturated zone, as described in the Forsmark 1.2 model /Bosson and Berglund 2006/. The description of the unsaturated zone has not been updated in the present version of the MIKE SHE model.

Field studies indicate that the coarse till in the area has different properties at different depths /Lundin et al. 2005/. The uppermost c. 50 cm of the soil profile has a higher total porosity, but also a lower capacity of retaining water than the underlying soil (a higher specific yield). The

Table 2-4. Hydraulic properties for each layer in the geological model of the Quaternary deposits.

Layer	K (m/s)	Total porosity	Specific yield
L1	Gyttja: $3 \cdot 10^{-7}$	Gyttja: 0.5	0.03
	Peat, upper 0.6 m: $1 \cdot 10^{-6}$ Peat, depth > 0.6 m: $3 \cdot 10^{-7}$	Peat, upper 0.6 m: 0.6	0.20
		Peat, depth > 0.6 m: 0.40	0.05
L2	$1.5 \cdot 10^{-4}$	0.35	0.20
L3	$1.5 \cdot 10^{-8}$	0.55	0.05
Z1	Till (fine and coarse): $3 \cdot 10^{-5}$	0.35	0.15
	Clay: $1 \cdot 10^{-6}$	0.55	0.05
	Sand: $1.5 \cdot 10^{-4}$	0.35	0.20
Z2	$3 \cdot 10^{-7}$	0.40	0.05
Z4a	$1.5 \cdot 10^{-8}$	0.45	0.03
Z4b	$1.5 \cdot 10^{-8}$	0.45	0.03
Z5	Coarse: $1.5 \cdot 10^{-6}$	0.25	0.05
	Fine grained: $1 \cdot 10^{-7}$	0.25	0.03
Z6	$1.5 \cdot 10^{-5}$ (from slug tests)	0.35	0.15

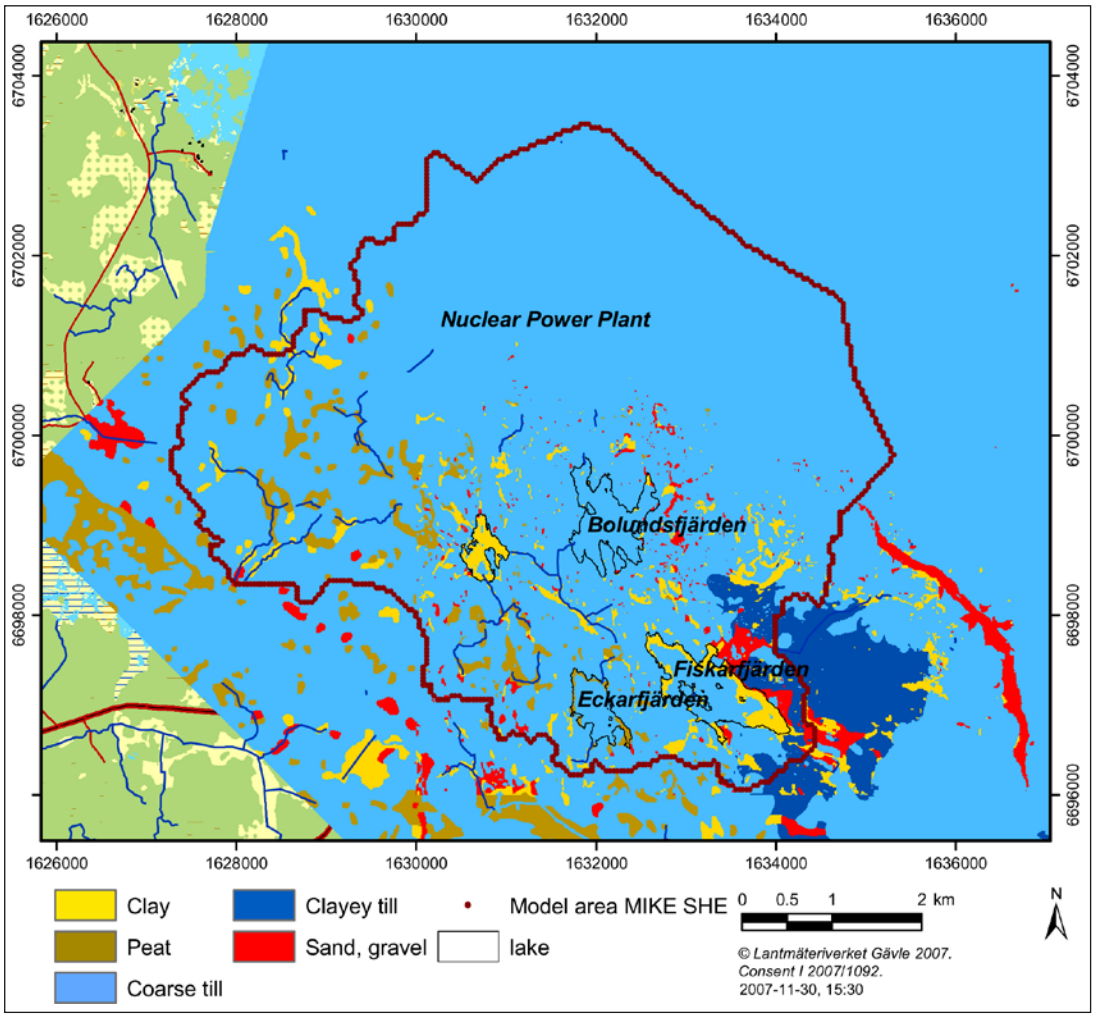

Figure 2-9. *Distribution of Quaternary deposits in the model. The dark red line indicates the boundary of the MIKE SHE model area.*

variations in the pF-curves used in the model update are based on data from /Lundin et al. 2005/, site specific data on the saturated hydraulic conductivity /Juston et al.2007/, and generic data from the same type of till /Knutsson and Morfeldt 2002/ . The uppermost 50 cm of the coarse till applied in the model has a total porosity of 0.38, and a hydraulic conductivity at full saturation of $3 \cdot 10^{-5}$ m/s. The relation between the moisture potential, pF, and the moisture content is shown in Figure 2-10.

In the model description, the underlying till in the depth interval from 0.5 to 2 m below ground surface has a total porosity of 0.22 and a hydraulic conductivity of $1.5 \cdot 10^{-6}$ m/s. The air entry level is at 30 cm (corresponding to pF 1.5). The relation between the moisture potential, pF, and moisture content is shown in Figure 2-11.

The description of the fine till included in the soil profile under the Quaternary deposits type "clayey till" is also described with an air entry level of 30 cm (corresponding to pF 1.5). The total porosity is 0.275 and the saturated hydraulic conductivity is $1.5 \cdot 10^{-7}$ m/s. The relation between the moisture potential, pF, and the moisture content for this QD type is shown in Figure 2-12.

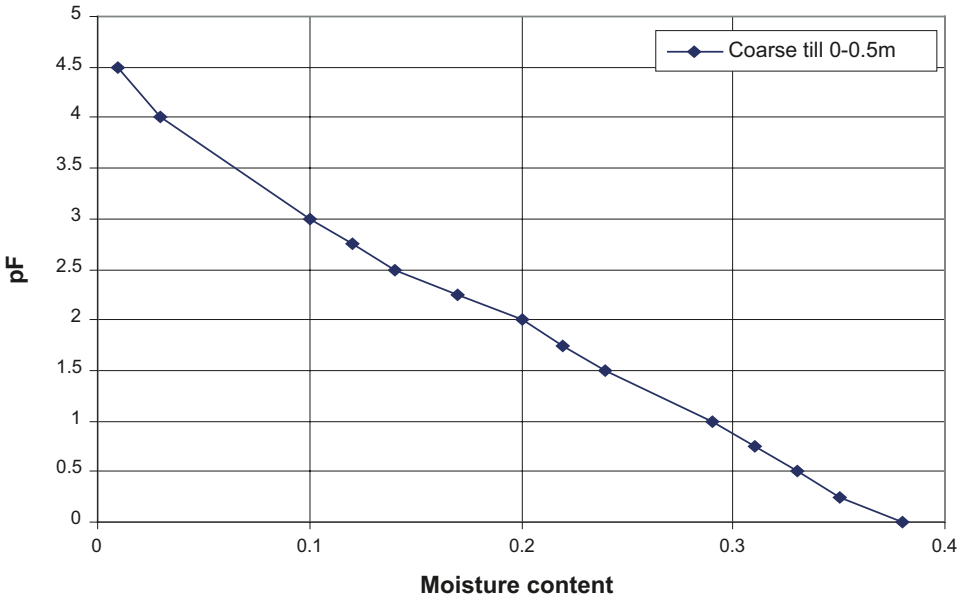

Figure 2-10. *Relation between moisture potential, pF, and moisture content for the uppermost 50 cm of a coarse till soil profile.*

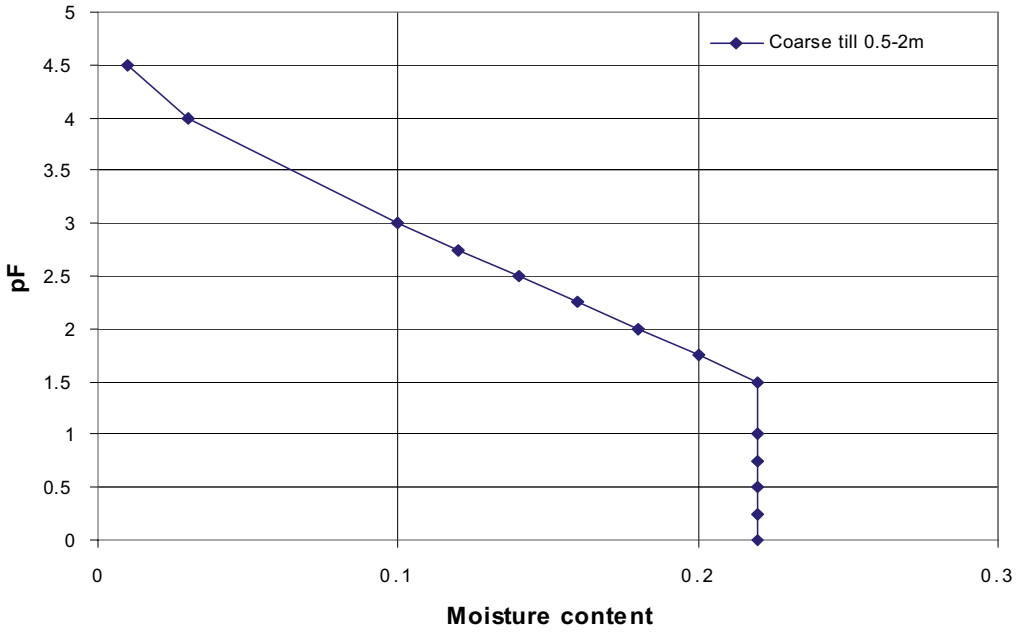

Figure 2-11. *Relation between moisture potential, pF, and moisture content for coarse till 50 to 200 cm below the ground surface.*

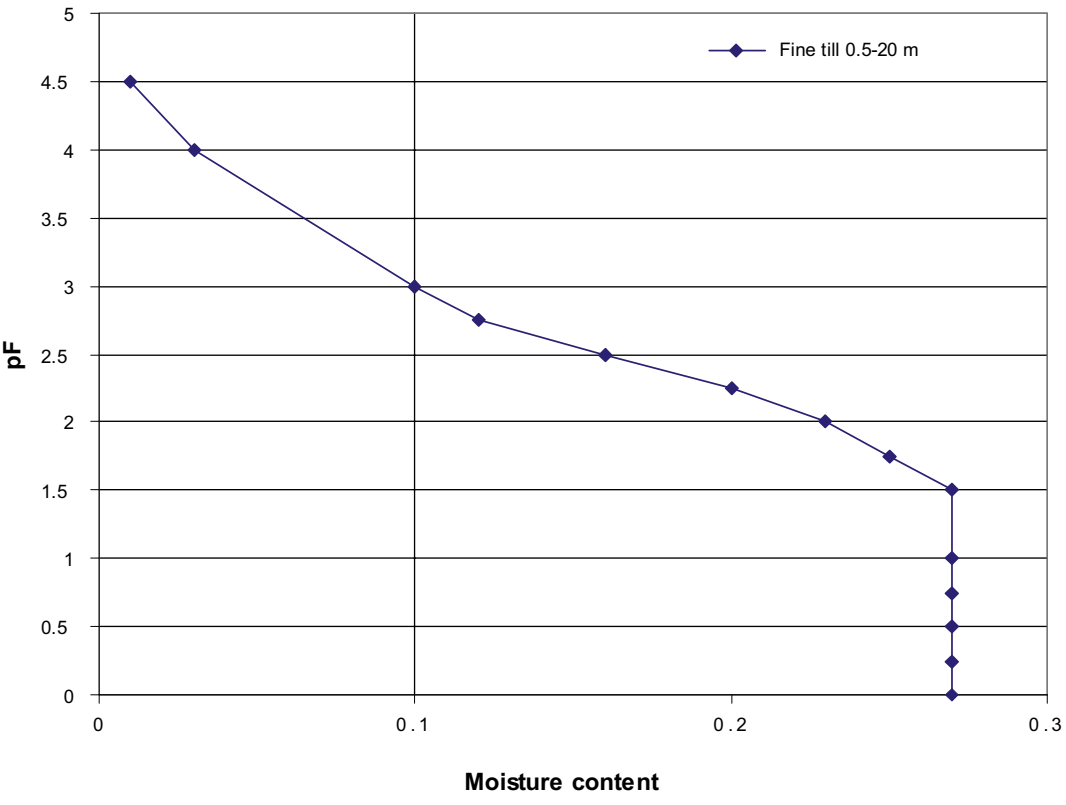

Figure 2-12. *Relation between moisture potential, pF, and moisture content for fine till 0.5 to 20 m below the surface for the Quaternary deposit clayey till.*

2.2.5 Stream and lake data

Data on lake threshold levels and bathymetry from the Forsmark data freeze 1.2 have been used as input to the description of the surface water system in MIKE 11. With one exception, the MIKE 11 model has not been updated since the latest version of the MIKE SHE/MIKE 11 model reported in /Aneljung and Gustafsson 2007/. An additional inlet to Lake Eckarfjärden was found during the site investigations, and this branch was added to the MIKE 11 model. Figure 2-13 shows the water courses described in the MIKE 11 model and points where bottom elevations and cross sections of the water courses have been measured.

Cross sections and bottom elevations have been measured every ten meters along the water course. X and Y coordinates for the stretch of the water course, data on the cross sections and data for the lake thresholds are used in the MIKE 11 model. Figure 2-14 shows an example of a cross section in the water course downstream Lake Eckarfjärden. The lake thresholds used as input data to the MIKE 11 model are also marked in Figure 2-13. Table 2-5 shows data on the lake thresholds marked in Figure 2-13.

The parameter describing the bed resistance, the Manning number (M), has not been changed since the previous version of the MIKE 11 model reported in /Aneljung and Gustafsson 2007/. Thus, the Manning number is 10 $m^{1/3}s^{-1}$ in the whole model area except from the branch downstream Eckarfjärden where a value of 3 $m^{1/3}s^{-1}$ is used. The leakage coefficient, which affects the conductance used in the calculation of the water flow exchange between the stream network and the saturated zone in MIKE SHE, is not changed either; the value is set to 10^{-5} s^{-1}. This means that the leakage coefficient is not limiting the contact between the groundwater and the surface water

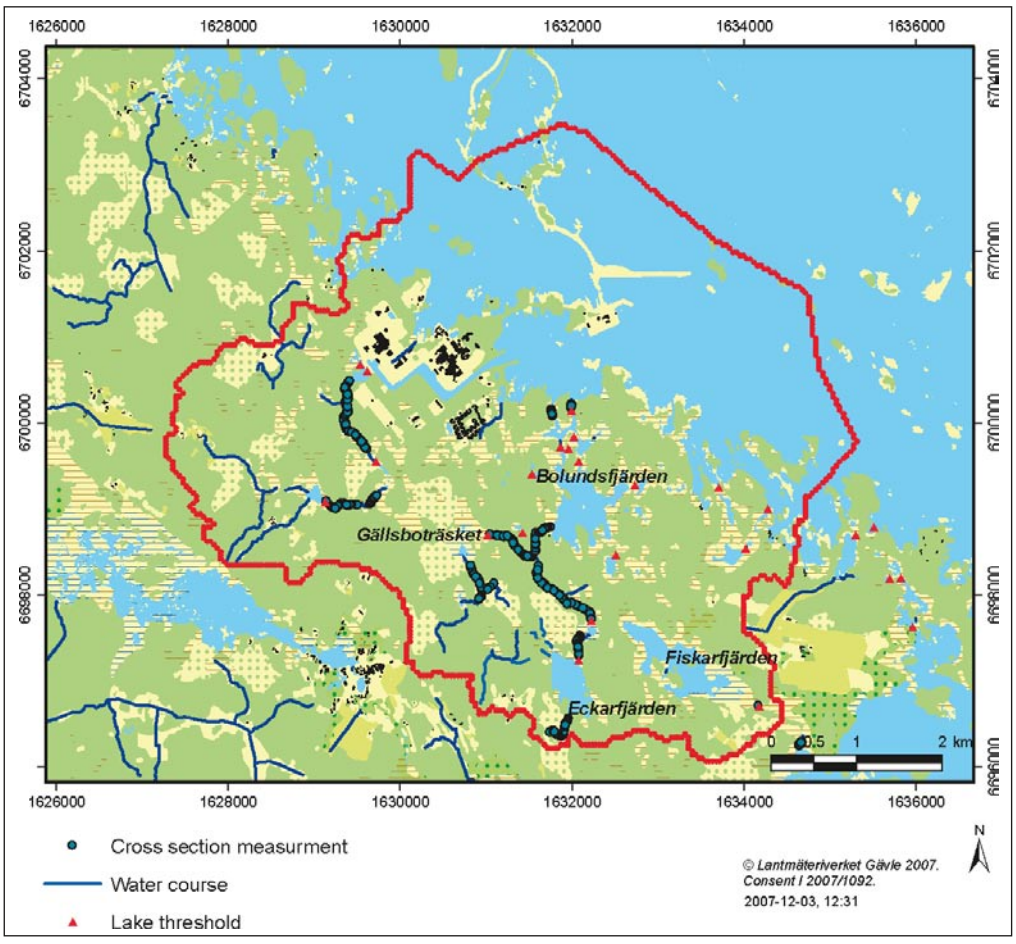

Figure 2-13. *Field controlled water courses, measured cross sections in water courses and measured lake thresholds used in the MIKE 11 model. The red line indicates the boundary of the MIKE SHE model area.*

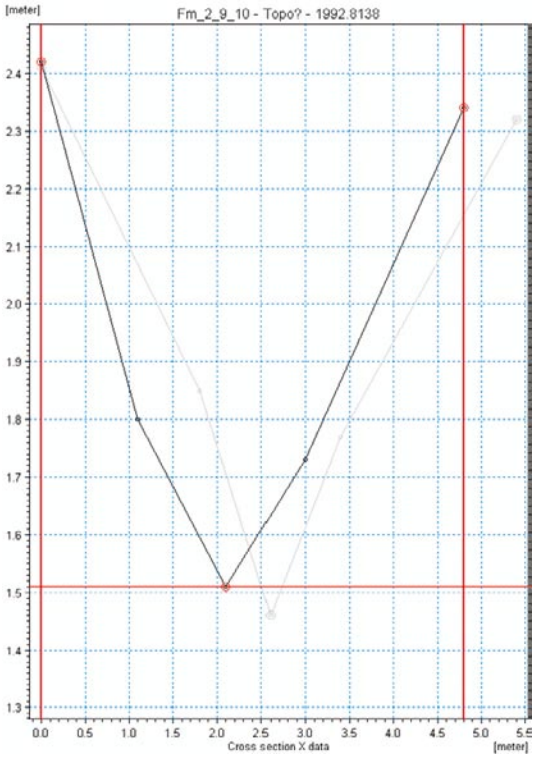

Figure 2-14. *A cross section, black line, of the water course downstream Lake Eckarfjärden. The grey line indicates the cross section 10 m downstream the actual cross section.*

Table 2-5. Data on lake thresholds in the area.

ID code	Name	Threshold level (m.a.s.l.)
AFM000010	Eckarfjärden	5.15
AFM000048	Labboträsket	2.65
AFM000049	Lillfjärden	–0.35
AFM000050	Bolundsfjärden	0.28
AFM000051	Fiskarfjärden	0.28
AFM000052	Bredviken	–0.26
AFM000073	Gunnarsbo-Lillfjärden (south)	1.92
AFM000074	Norra Bassängen	0.19
AFM000081	Märrbadet	–0.29
AFM000084	Simpviken	–0.32
AFM000086	Tallsundet	–0.23
AFM000087	Graven	0.44
AFM000089	Vambörsfjärden	1.02
AFM000090	Stocksjön	2.7
AFM000091	Puttan	0.48
AFM000093	Kungsträsket	2.31
AFM000094	Gällsboträsket	1.47
AFM000095	Gunnarsboträsket	5.68
AFM000096	Gunnarsbo-Lillfjärden (north)	1.07

2.2.6 Calibration data

Data from five surface water level monitoring stations and four surface water discharge monitoring stations have been used for calibration and evaluation of the surface water discharge and surface water levels. Four surface water level stations are placed in the lakes in the model area and one station measures the sea water level. 34 groundwater monitoring wells in Quaternary deposits and 39 observation points (sections) in percussion-drilled boreholes in bedrock have been used for calibration and evaluation of the groundwater heads in the area.

The time series of groundwater head in the bedrock are disturbed by drilling and pumping during long periods. A screened data set has been used for the heads in the percussion drilled bore holes to avoid calibration to disturbed periods. The observations are mainly located within the candidate area, with no or only a few points in the north-western part of the model catchment. Figure 2-15 shows the locations of the surface water discharge stations and boreholes where monitoring data used in the present analysis have been obtained.

Data from a pumping test in HFM14, see Figure 2-16, have been used in the calibration of the bedrock parameters. The interference test was performed in July 2006; the pumping started on the 4th of July and stopped on the 19th of July. A time series of the pumping rate in HFM14 was used as input to the simulations. When evaluating the results, data on the drawdown in the HFM-wells in the area were used. The simulation of the pumping test is described in Section 6.1.2.

Figure 2-15. *Positions of monitoring points used for model calibration and evaluation; SFM points are groundwater monitoring wells in QD and HFM points percussion-drilled boreholes in rock. PFM points are surface water discharge measurements. The red line indicates the boundary of the MIKE SHE model area.*

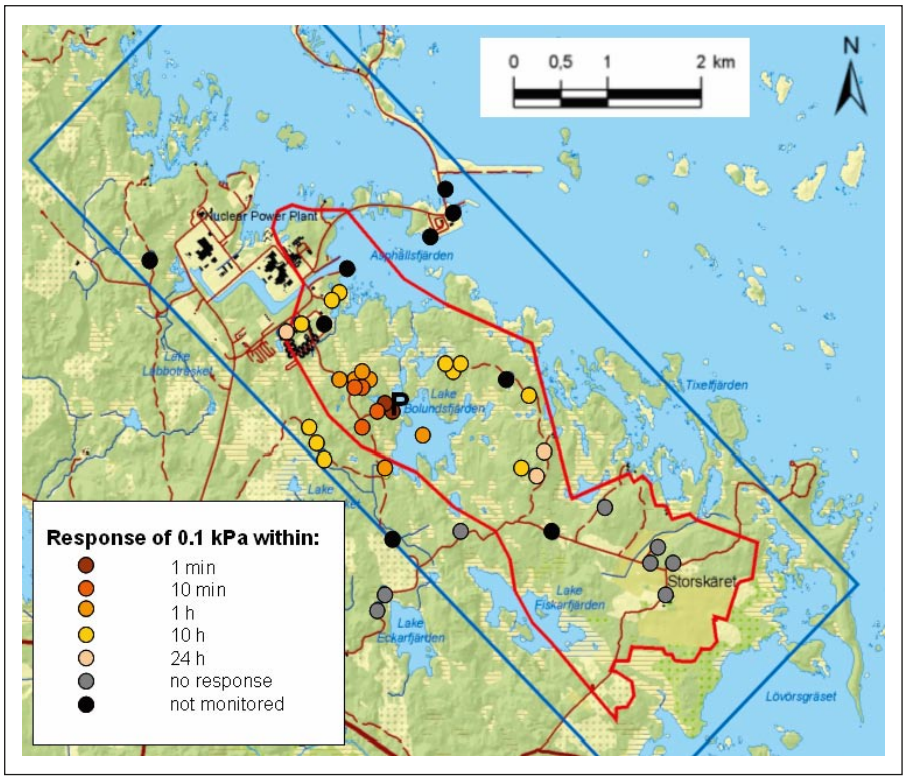

Figure 2-16. *HFM14 (P), where the interference test was performed in July 2006. The map is showing response times in the bedrock. The maximum radius of influence was about 1.8 km. Reproduced from /Follin et al. 2007/.*

2.2.7 Vegetation and overland flow properties

Vegetation parameters are used to specify vegetation data for the evapotranspiration calculations. The vegetation parameters are time varying vegetation characteristics for each type of vegetation that is specified in the model domain. In the following section, a short summary of the vegetation parameters used in the model is presented.

Calculations with the overland flow module are required when MIKE 11 is used in a MIKE SHE model. This is because the overland flow module provides lateral runoff to the water courses in MIKE 11. The properties used in the overland flow module are briefly described below.

Vegetation

Interception is defined as the process whereby precipitation is retained on the leaves, branches, and stems of the vegetation. The amount of precipitation that can be intercepted by the vegetation canopy is determined by multiplying the interception capacity, C_{int}, by the leaf area index, LAI. The coefficient C_{int} defines the interception storage capacity of the vegetation and depends on the surface characteristics of the vegetation type. The leaf area index, LAI, is the area of leaves divided by the area of the ground. It may vary between 0 and 7 depending of the vegetation type. The intercepted water evaporates without adding to the moisture storage in the soil.

The root distribution in the soil is expressed by the A_{root} parameter. The value of A_{root} may depend on soil bulk density with higher values for soils with high bulk density where root development may be more restricted than for soils with low bulk density. A typical value is 1, which implies that 60% of the root mass is located in the upper 20 cm of the soil with a root depth of 1 m. Lower A_{root} values decrease this fraction and give a more even root distribution.

The crop coefficient, K_c, is used to adjust the reference evapotranspiration relative to the actual evapotranspiration of the specific crop. A K_c value of 1 means that the maximum evapotranspiration rate will equal the reference evapotranspiration rate (e.g. PET). Because of seasonal changes, the vegetation may have different crop stages. For each crop stage, the vegetation parameters LAI and K_c need to be specified. Figure 2-17 shows the vegetation field in the SDM-Site Forsmark model. The main vegetation type of the land part of the model area is coniferous forest, but also areas classified as deciduous forest and "open land" (mainly grass) are present.

Table 2-6 shows the parameter values used in the simulations. They are based on values obtained from the vegetation database files that follows with the installation of the MIKE SHE software programme /DHI Software 2008/ and on the values given in /Kristensen and Jensen 1975/. For deciduous forest and open land the LAI values depend on the crop season.

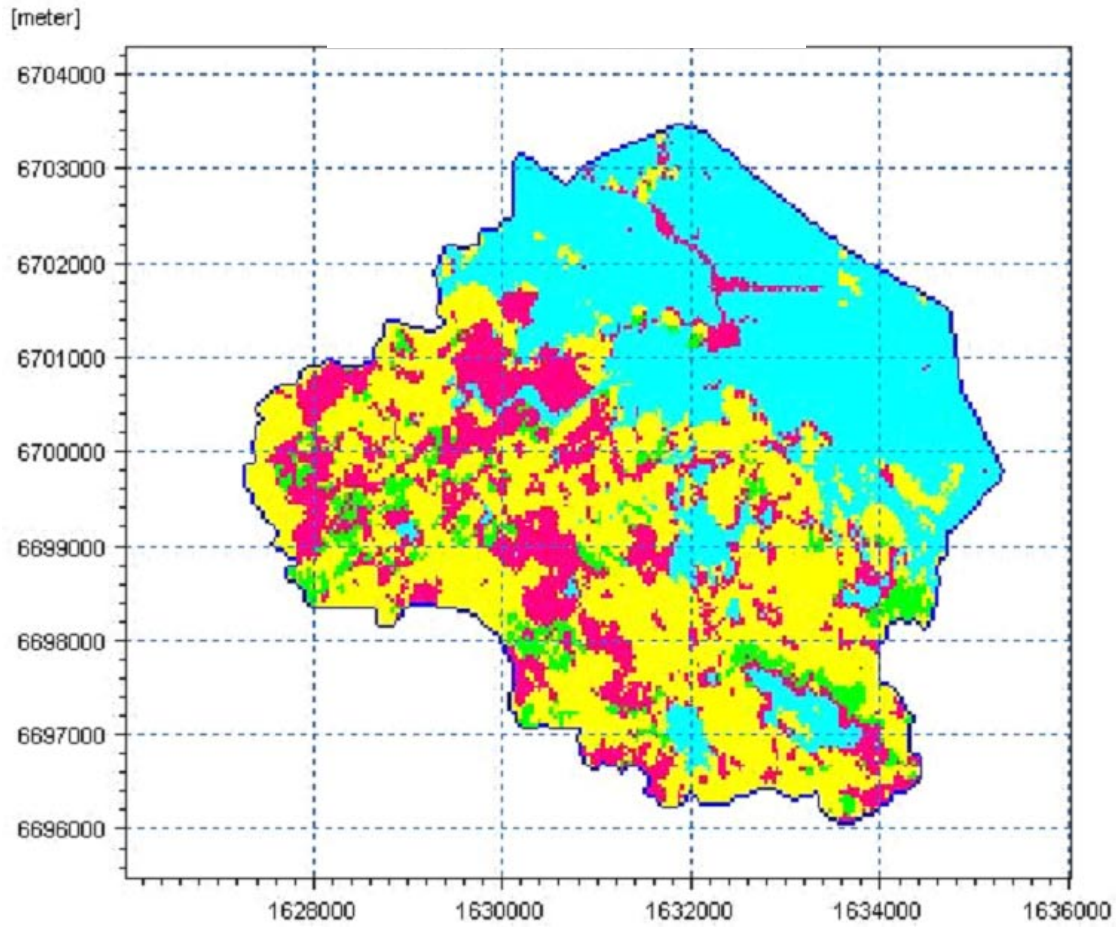

Figure 2-17. *Vegetation map of the Forsmark area. For orientation, the lakes and streams are marked in the figure. Grid code colours are: blue=surface water, green=deciduous forest, yellow=coniferous forest, and pink=open land.*

Table 2-6. Vegetation parameters used in the Forsmark 2.3 model.

	Vegetation parameter			
	Cint	LAI	Aroot	Kc
Vegetation code	(mm)	(–)	(m^{-1})	(–)
Water	0	0	1	1
Deciduous forest	0.2	0–6	1	1
Coniferous forest	0.5	7	1	1
Open land	0.1	4–7	1	1

Overland flow

The overland flow module is necessary when using the MIKE11 model in MIKE SHE, since the overland flow module provides lateral runoff to the rivers. The basic parameters that needs to be specified for the calculation of overland flow are

- the Manning number, M,
- the Detention storage parameter,
- the initial water depth on the ground surface (ponded water).

The Manning number, M, typically has values between 100 (smooth channels) and 10 (thickly vegetated channels). Generally, lower values of M are used for overland flow compared to channel flow. In the present model, the M value for overland flow is set to 5 $m^{1/3}/s$.

Detention storage parameter is used to limit the amount of water that can flow on the ground surface. The depth of ponded water must exceed the detention storage before water will flow as sheet flow to the adjacent cell. In the present model, the detention storage was set uniformly over the area to a value of 2 mm.

The intial water depth is the initial condition for the overland flow calculations, i.e. the initial depth of water on the ground surface. The initial water depth in the present model was based on an earlier calculation and chosen so that lakes already were filled up by water.

2.2.8 Drainage of the SFR repository

For drainage of the SFR repository located below the sea at Forsmark Harbour, Figure 2-18, a pumping of approximately 6 l/s is necessary. The pumping is conducted from two sumps at two different levels, 88 m and 140 m below the sea level. The pumping rates from the upper and lower levels are approximately 1.2 and 4.8 L/s, respectively /Jakob Levén, pers. comm./. When evaluating the influence of the SFR repository on the hydrogeological conditions in model area a pumping rate of 6 L/s was applied to a well placed at location of the SFR-repository. The simulations with the SFR repository included in the model are described in Section 6.1.3.

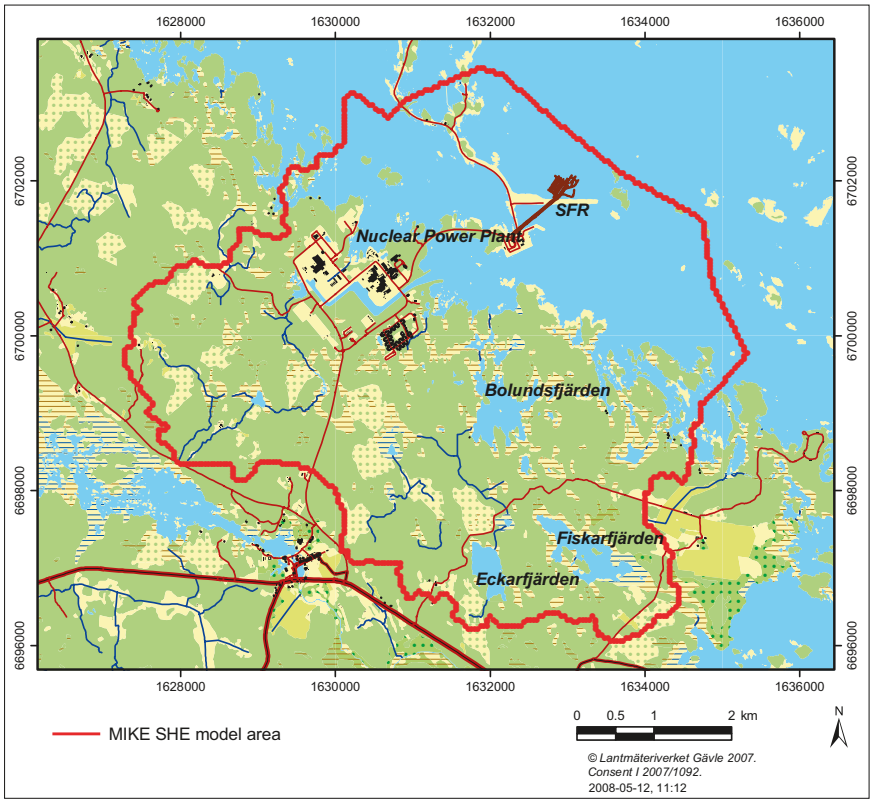

Figure 2-18. *Location of the SFR repository.*

3 Modelling tool and numerical flow model

3.1 The MIKE SHE modelling tool

3.1.1 The Water movement module

The modelling tool used in the analysis is MIKE SHE. MIKE SHE is a dynamic, physically based modelling tool that describes the main processes in the land phase of the hydrological cycle. The code used in this project is software release version 2007 SP2 /DHI Software 2007/ and version 2008 SP1 /DHI Software 2008/.

The precipitation can either be intercepted by leaves or fall to the ground. The water on the ground surface can infiltrate, evaporate or form overland flow. Once the water has infiltrated the soil, it enters the unsaturated zone. In the unsaturated zone, it can either be extracted by roots and leave the system as transpiration, or it can percolate down to the saturated zone. MIKE SHE is fully integrated with a channel-flow code, MIKE 11. The exchange of water between the two modelling tools takes place during the whole simulation, i.e. the two programs run simultaneously. The modelling processes are summarised in Figure 3-1.

MIKE SHE is developed primarily for modelling of groundwater flow in porous media. However, in the present modelling the bedrock is also included. The bedrock is parameterised by use of data from the Forsmark 2.2 groundwater flow model developed using the ConnectFlow code /Follin et al. 2007/. Hydrogeological parameters can be imported directly to the corresponding elements in the MIKE SHE model.

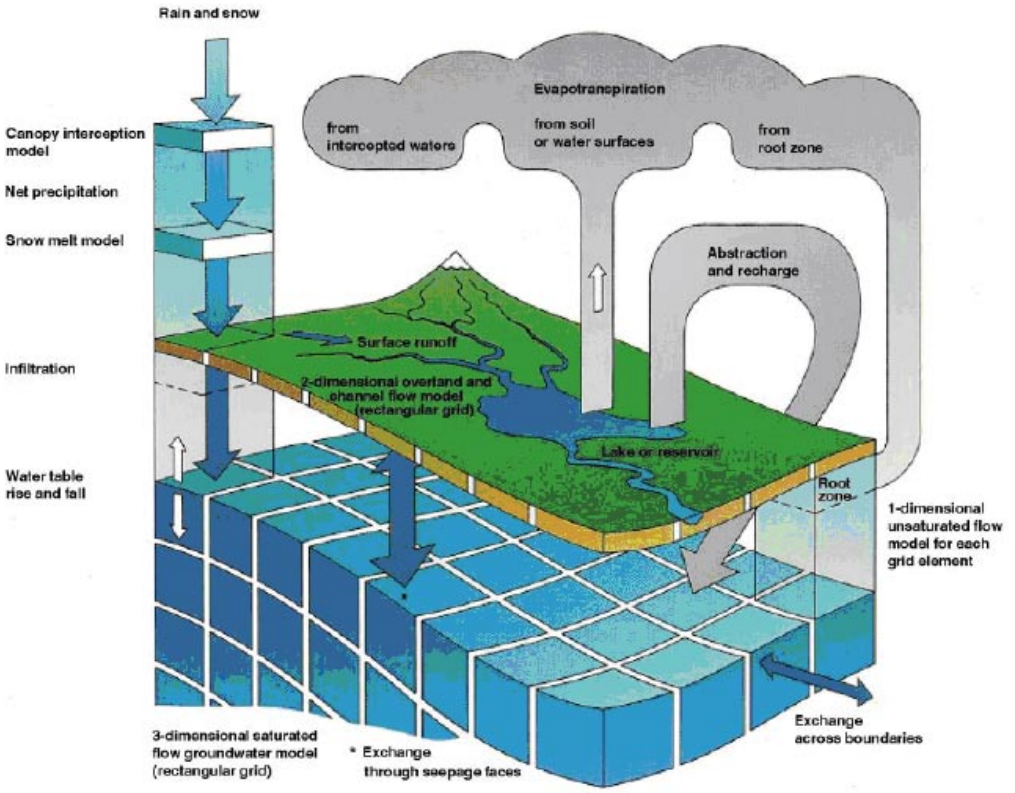

Figure 3-1. *Overview of the model structure and the processes included in MIKE SHE /DHI Software 2007/.*

MIKE SHE consists of the following model components:

- Precipitation (rain or snow).
- Evapotranspiration, including canopy interception, which is calculated according to the principles of /Kristensen and Jensen 1975/.
- Overland flow, which is calculated with a 2D finite difference diffusive wave approximation of the Saint-Venant equations, using the same 2D mesh as the groundwater component. Overland flow interacts with water courses, the unsaturated zone, and the saturated (groundwater) zone.
- Channel flow, which is described through the river modelling component, MIKE 11, which is a modelling system for river hydraulics. MIKE 11 is a dynamic, 1D modelling tool for the design, management and operation of river and channel systems. MIKE 11 supports any level of complexity and offers simulation tools that cover the entire range from simple Muskingum routing to high-order dynamic wave formulations of the Saint-Venant equations.
- Unsaturated water flow, which in MIKE SHE is described as a vertical soil profile model that interacts with both the overland flow (through ponding) and the groundwater model (the groundwater table is the lower boundary of the unsaturated zone). MIKE SHE offers three different modelling approaches, including a simple 2-layer root-zone mass balance approach, a gravity flow model, and a full Richards's equation model.
- Saturated (groundwater) flow, which allows 3D modelling of flow in a heterogeneous aquifer, with aquifer conditions shifting between unconfined and confined. The spatial and temporal variations of the dependent variable (the hydraulic head) are described mathematically by the 3D Darcy equation and solved numerically by an iterative implicit finite difference technique.

For a detailed description of the processes included in MIKE SHE and MIKE 11, see /Werner et al. 2005/ and /DHI Software 2007/.

The communication between the river network in MIKE 11 and the overland component in MIKE SHE can be defined in two different ways:

- using so called flood codes, where water levels from MIKE 11 simply are transferred to MIKE SHE, or
- using a two-way communication based on a so called overbank spilling option.

In this version of the Forsmark model, the two-way overbank spilling option is applied. This option allows river water to spill onto the MIKE SHE model as overland flow. The overbank spilling option treats the river bank as a weir. When the overland flow water level or the river water level is above the left or right bank elevation, water will spill across the bank based on the weir formula:

$$Q = \Delta x \cdot C \cdot (H_{us} - H_w)^k \cdot \left[1 - \left(\frac{H_{ds} - H_w}{H_{us} - H_w}\right)^k\right]^{0.385}$$

where Q is the flow across the weir, Δx is the cell width, C is the weir coefficient, H_{us} and H_{ds} refer to the height of water on the upstream and downstream side of the weir, respectively, H_w is the height of the weir, and k is a head exponent.

If water levels are such that water is flowing to the river, overland flow to the river is added to MIKE 11 as lateral inflow. If the water level in the river is higher than the level of ponded water, river water will spill onto the MIKE SHE cell and become part of the overland flow. If the upstream water depth over the weir approaches zero, the flow over the weir becomes undefined. Therefore, the calculated flow is reduced to zero linearly when the upstream height goes below a threshold.

The communication between the river network and the groundwater aquifer is calculated in the same way as in previous versions of the code. The exchange flow between a saturated zone grid cell and a river link is calculated as a conductance multiplied by the head difference between the

river and the grid cell. The conductance between the grid cell and the river link depends on the conductivity of both the river bed and the aquifer material /DHI Software 2007/.

3.1.2 The transport module

This section presents the principles behind the solute transport analyses performed in MIKE SHE. Transport modelling can be performed either with the Particle tracking module or the Advection-dispersion module. A detailed description of the governing equations is given in /Gustafsson et al. 2008/.

Particle tracking is here modelled as purely advective transport, i.e. transport with the flowing groundwater only. This means that the substance is moved by the Darcy flow vectors, whereas other mechanisms (such as transport governed by concentration gradients) do not affect the transport of the particles. The particles can have any locations in the water movement grid net, i.e. their movement is in this sense completely independent of the numerical resolution. However, they are of course affected by the velocity field, the accuracy of which is affected by the resolution. This gives a very distinct result, which is usually easy to evaluate regarding transport paths and discharge locations.

Advection-dispersion modelling includes, except advective transport, also dispersion, which allows the substance to move in other directions than the modelled velocity field. The strength of the solute transport through dispersion is controlled by given dispersivities in different directions. The physical interpretation of the dispersion is diffusion and velocity variations related to small scale heterogeneities that are not included in the model description but affect solute spreading. This means that the more accurately the spatial variability in the hydrogeological properties is described (and hence the spatial variations in the groundwater velocity), the smaller the dispersivities applied in the model should be.

3.2 The numerical flow model

3.2.1 Model domain and grid

Most of the on-shore part of the Forsmark regional model area is included in the MIKE SHE model area considered in the present work. However, the upstream (inland) boundary follows the water divide towards the river Forsmarksån catchment, rather than the boundary of the regional model area. The MIKE SHE model area, which has a size of 37 km^2, is shown in Figure 3-2. It can be seen that the south-western part of the regional model area is excluded. Furthermore, the MIKE SHE model area extends some distance into the sea, although the offshore part of the MIKE SHE area is much smaller than that of the regional model area (cf. Figure 1-1).

When defining the horizontal extent of the model area, the candidate area, the surface water divides and the regional fracture zones were taken into consideration. The surface water divide towards the river Forsmarksån catchment is a natural boundary for the south western part of the model area. In addition, the field-controlled catchment area boundaries identified in the surface-hydrological modelling were used to determine the position of the on-shore part of the north-western boundary.

Previous particle tracking simulations where particles have been released inside the area of the planned repository indicate that the near-shore bays might be discharge areas for the repository. Therefore it was desirable to include parts of the sea into the model. The Singö deformation zone is a natural boundary in the sea. Therefore, the MIKE SHE model area was extended with some margin outside the Singö deformation zone. The main deformation zones, Eckarfjärdszonen (in the south-east) and Singözonen (at the sea) are also shown in Figure 3-2.

Figure 3-2. *Map showing the MIKE SHE model area, the candidate area, and parts of the regional model area boundary. The regional fracture zones are also marked in the figure.*

The reason for using the bedrock geology as the main input to defining the model boundaries is that the major deformation zones also constitute major hydrogeological structures, see, e.g. /Follin et al. 2007/ that may act as boundaries for horizontal flow and transport. The vertical extent of the initial (base) setup of the MIKE SHE model was from the ground surface down to 150 m.b.s.l. The effects of the position of the bottom boundary and the bottom boundary condition applied were analysed in a sensitivity analysis during the calibration process. Based on the results of this analysis the final calibrated model was extended down to 600 m.b.s.l. (see Section 4.5).

The horizontal resolution of the calculation grid is 40 m by 40 m in the whole model area, and is applied on all of the flow components in MIKE SHE, i.e. the overland flow, the unsaturated zone (including evapotranspiration), and the saturated zone. The unsaturated zone, which is a 1D vertical model description, is however treated in a semi-distributed manner, see below. Hydrogeological input data for the bedrock and the Quaternary deposits and geometrical data for the bedrock and QD layers are given on a 20 m × 20 m grid. An arithmetic mean of four data points was used in the pre-processing of data when converting the 20 m × 20 m grid to the 40 m × 40 m model grid.

The vertical resolution varies with depth, both for the unsaturated and the saturated zone, according to the description below. The vertical geologic distribution is interpolated to the vertical grid in the following manner: In each horizontal model grid cell, the vertical geologic model is scanned downwards and the properties from the geological model are assigned to the cell.

The properties are based on the average of the values found in the cell weighted by the thickness of each of geological layer /DHI Software 2007/. For example, if there are three different geological layers in a model grid cell each with a different value for the specific yield, then the specific yield for the model grid cell is calculated as:

$$S_y = \frac{S_{y1} \cdot z_1 + S_{y2} \cdot z_2 + S_{y3} \cdot z_3}{z_1 + z_2 + z_3}$$, where z_i is the thickness of geological layer *i*.

The vertical hydraulic conductivity is not calculated as described above. Vertical flow depends mostly on the lowest hydraulic conductivity in the geological layers presented. A harmonic weighted mean value is therefore used instead. The vertical hydraulic conductivity for the three geological layers described above will be calculated as follows:

$$K_v = \frac{z_1 + z_2 + z_3}{\frac{z_1}{K_{v1}} + \frac{z_2}{K_{v2}} \frac{z_3}{K_{v3}}}$$

In the Quaternary deposits, several geological layers may be included in the same calculation layer. The calculation layers in the bedrock follow the geological layers given by the ConnectFlow modelling team, see Section 3.2.4.

3.2.2 The surface stream network

The length of the surface stream network described in MIKE 11 is approximately 20 km, which is divided into 96 calculation nodes for discharge and 119 calculation nodes for the water level. This gives an average length between calculation nodes for flow of 208 m and for water level 168 m. A cross-section is given at the majority of the head calculation nodes. The surface stream network in MIKE11 is laterally communicating with the overland flow and saturated zone components in MIKE SHE.

3.2.3 The unsaturated zone

In order to speed up the simulation, only a limited number of grid cells are simulated in the unsaturated zone modelling. The selection of which cells to consider in the simulation is made through a classification system where those unsaturated zone columns that have the same conditions (i.e. the same soil profile, land use, meteorology and groundwater depth) are grouped together. From each group only one column, randomly selected, is simulated.

In the Forsmark model, an exception from this is made in areas with ponding water on the surface, i.e. lakes and wetland areas, excluding the sea. In these areas, the unsaturated zone simulation is executed in all grid cells. This has been found important in order to ensure a proper simulation of the evapotranspiration /Aneljung and Gustafsson 2007/. The vertical discretisation is the same for all soil profiles, see Table 3-1, starting with a resolution of a few centimetres in the top soil and increasing to a few decimetres at the depth where the groundwater table is typically reached in Forsmark.

Table 3-1. The vertical discretisation of the unsaturated zone.

Depth interval	Cell height (m)	Number of cells
0–1 m	0.1	10
1–5 m	0.5	8
5–10 m	1	5
10–20 m	2	5

3.2.4 The saturated zone

The ground surface, as given by the topographic model, is the upper model boundary. The bottom boundary in the base setup of the model is at 150 m.b.s.l., whereas in the final model version it is at 600 m.b.s.l. MIKE SHE distinguishes between geological layers and calculation layers. The geological layers (cf. Sections 2.2.2 and 2.2.3) are the basis for the model parameterisation, which means that the hydrogeological parameters are assigned to the different geological layers. The calculation layers are the units considered in the numerical flow model. In cases where several geological layers are included in one calculations layer, the properties of the latter are obtained by averaging of the properties of the former. The base setup of the present model consists of 10 calculation layers. During the calibration process the vertical extent of the model was extended and the final calibrated model consists of 14 calculation layers.

In general, the calculation layers follow the geological layers. However, one exception is the calculation layers in the Quaternary deposits. The lake sediments and other Quaternary deposits are included in the two uppermost calculation layers. In the initial model setup, the uppermost calculation layer has a minimum thickness of 2 m and the other calculation layers have a minimum thickness of 1 m. The lake sediments are included in the uppermost calculation layer. If the depth of the lake sediments is larger than 2 m, the lower level of calculation layer 1 follows the lower level of the lake sediments. The coupling between geological layers and calculation layers in the QD is illustrated in Figure 3-3.

In the sea, the lower boundary of the uppermost calculation layer follows the sea bottom. Modelling large volumes of overland water is very time-consuming in MIKE SHE and may cause numerical instabilities. Therefore, the sea is described as a geological layer filled with gravel of high hydraulic conductivity. The “sea-gravel” is present from the sea bottom up to the level of the lowest measured sea-level during the simulation period.

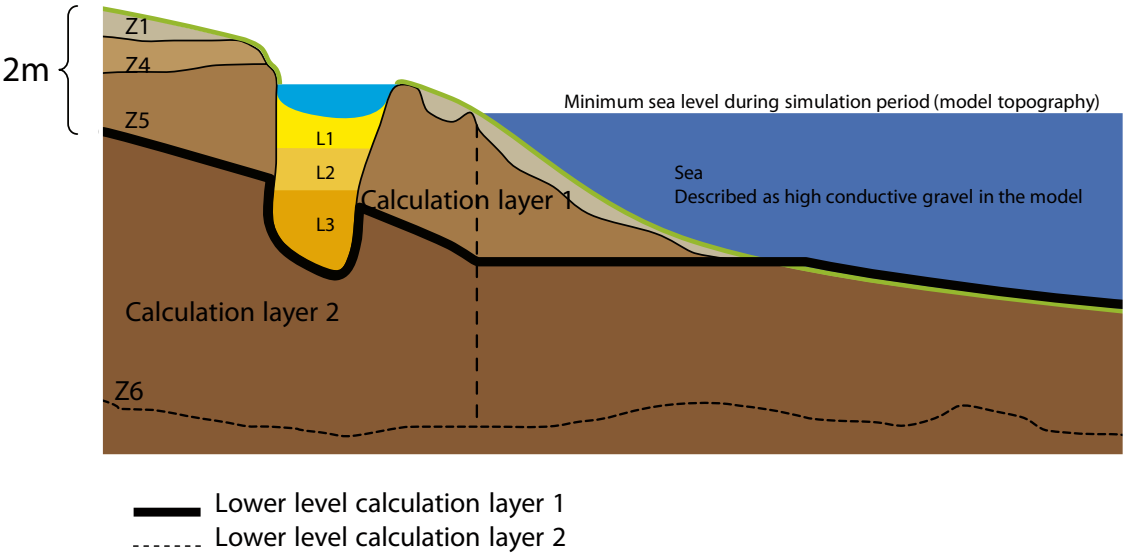

Figure 3-3. *Illustration of the calculation layers in the QD.*

The "sea-gravel" is included in the uppermost calculation layer; therefore, the model topography is flat at the sea. The reason why the minimum sea level is chosen as the upper limit for the "sea gravel" is that the littoral zone in the model should be able to vary with time. When the measured sea level rises above the minimum sea level, overland water is built up in the littoral zone and the water level/the sea can rise and move towards land during periods of high water levels.

The model topography (i.e the upper boundary of the uppermost calculation layer) is defined as follows:

If DEM (Digital elevation model) > minimum sea level → Topography = DEM
If DEM < minimum sea level → Topography = minimum sea level

The part of calculation layer 1 containing the sea has an internal boundary condition with a prescribed time-varying head given by the measured sea-level. Since the internal boundary is set from the sea bottom up to the minimum sea-level, the littoral zone may vary during the simulation. The lower layer of calculation layer one is calculated in six steps:

1. If lake sediment is present → Lower level = Lower level of L3.
2. If *Topography* > minimum sea level → Lower level = Topography – 2 m.
3. If *Topography* < minimum sea level → Lower level = Sea bottom (DEM).
4. Calculate the thickness, T, of calculation layer one based on step 1 and 2.
5. Correct for the littoral zone: If T < 2 m → set T to 2 m.
6. Lower level of calculation layer 1 = *Topography* – T

The lower layer of calculation layer 2 follows the lower level of Z6, with the condition that the minimum thickness of the layer has to be 1 m. In areas where the thickness is smaller than 1 m, calculation layer 2 enters the uppermost geological bedrock layer (with a maximum of one meter). Since all the geological bedrock layers are 20 m or thicker the impact from calculation layer 2 is only affecting the uppermost bedrock layer. For all the other bedrock layers geological layers and the calculation layers coincide.

3.2.5 Initial and boundary conditions and time stepping

The groundwater divides are assumed to coincide with the surface water divides; the latter are reported in /Brunberg et al. 2004/. Thus, a no-flow boundary condition is used for the on-shore part of the model boundary. The sea forms the uppermost calculation layer in the off-shore parts of the model. As described above, the sea is represented by a geological layer consisting of highly permeable material. The hydraulic conductivity of this material is set to 0.001 m/s. The sea part of the uppermost calculation layer has a time-varying head boundary condition. The measured time-varying sea level is used as input data.

The top boundary condition is expressed in terms of the precipitation and potential evapotranspiration (PET). The precipitation and PET are assumed to be uniformly distributed over the model area, and are given as time series. The actual evapotranspiration is calculated during the simulation.

The bottom boundary condition in the base setup of the model is a fixed-head condition. Model results from the Forsmark 2.2 ConnectFlow groundwater flow modelling /Follin et al. 2007/ are used as input data when setting the head bottom boundary condition in MIKE SHE. The calculated hydraulic head at 150 m.b.s.l. is imported to the MIKE SHE model. The time step used in the ConnectFlow simulations is much longer than that in the MIKE SHE modelling, which implies that short-term temporal variations cannot be captured. Thus, the bottom boundary condition in the MIKE SHE model is assumed to be constant with time. A no-flow boundary was analysed in the sensitivity analysis, see Section 4.5, and the bottom boundary condition in the final calibrated model is a no-flow condition.

The calibration period is from May, 2003, through July, 2005. The simulations use a so called hot start, which constitutes the initial conditions. Hot start data are stored monthly, and data representing the 4th of May 2005 were used as initial conditions. These conditions were created by running the model until semi steady-state conditions were reached. This means that the model was run, with the time-dependent boundary conditions given by the meteorological data, until the variations during the year had stabilised (e.g. the pressure at a certain point shows more or less the same variation from one year to the next). The results from this simulation were used as initial conditions. The initial conditions were updated before the final version of the model was run. In MIKE SHE a maximum time step is defined for each compartment of the model. During the simulation the time step may be reduced. The maximum time step for each compartment is listed in Table 3-2.

Table 3.2. Maximum time steps for the different compartments of the MIKE SHE-MIKE 11 model.

Compartment	Maximum timestep
Overland	1 h
Unsaturated zone	1 h
Saturated zone	3 h
MIKE 11 (water courses)	5 s

4 Model development and calibration

The calibration procedure is an iterative process since each action taken results in changed conditions for many processes in the model. Section 4.2 gives an overview of the calibration steps taken in order to obtain a calibrated model. In Section 4.3, the results from the surface water calibration are presented. Section 4.4 illustrates the results from the calibration of the groundwater head elevations in the Quaternary deposits and Section 4.5 presents results from the calibration of the head elevations in the bedrock as well as the analysis of the bottom boundary condition. In Section 4.6, the calibration process and sensitivity analysis is concluded.

4.1 Calibration targets

The calibration of a model is a process that may be driven very far. There are, however, a number of arguments against extensive so-called curve fitting. For example, a field observation only represents the conditions in a certain point, while the model represents the value in the centre point of a grid element (in this case covering 40 m × 40 m in the horizontal plane), and therefore a perfect fit does not necessarily mean a better model.

Once the model is calibrated, a model validation shows the capability of the model to extrapolate results beyond the calibration time series. If the validation results are significantly worse than the calibration results, the model is unbalanced in the sense that the model has been forced to fit observations. As a consequence, the physical model parameters for an unbalanced model are often outside the ranges that may be justified physically. Therefore, an objective of the calibration is to enable validation results that are in the same order of magnitude as the calibration results by keeping physical model parameters within ranges that can be justified by the actual site conditions.

Another important objective is to reach a correct water balance, including both the temporal and spatial variations. Furthermore, it is important that the gradients between different model compartments are represented correctly by the model, including their temporal variation. This means that the model distributes the water and its flow paths in a proper way under different hydrological conditions during the year.

The error may be described in several ways. Different definitions are often used for discharges and head elevations. Errors in discharges are typically described in terms of peak errors, total volume errors, mean absolute error or some kind of correlation coefficient (i.e. the Nash Sutcliffe correlation coefficient, R2). The choice depends on the purpose of the model. In the present case, the water balance is the far most important result. This means that total volume errors are important, but also their temporal variations. This motivates the use of mean absolute errors. Since few flow meters have an accuracy higher than 10–15%, volume errors of less then 10–15% are often considered satisfactory.

Errors in head elevations are often described in terms of mean error (ME) or mean absolute error (MAE). Mean errors are more relevant when the temporal variation is small, while mean absolute errors are applicable when the amplitude is higher. Depending on the gradients of the model, the required maximum mean errors could differ. In a very flat area, an error of a few decimetres may be a poor result. Conversely, an error of that magnitude could be seen as

an excellent result in a more hilly area or in an area where gradients between different layers are high. Since the Forsmark area is relatively flat with small vertical gradients, small errors are required for the model to be considered acceptable. However, mean errors less then 20 cm should be satisfactory.

The mean absolute errors on the other hand should, as for discharge errors, be compared with the amplitudes. For the Forsmark area, where groundwater elevation amplitudes typically vary between 1 and 2 meter, mean absolute errors of between 20 and 40 cm would be a good result. The following performance criteria are used in this report:

Mean error, ME

$$ME = \frac{1}{n}\sum_t (q_{obs_t} - q_{sim_t})$$

Mean absolute error, MAE

$$MAE = \frac{1}{n}\sum_t \left|(q_{obs_t} - q_{sim_t})\right|$$

Correlation coefficient, R

$$R = \sqrt{\frac{\sum_t (q_{sim_t} - \overline{q_{sim}})(q_{obs_t} - \overline{q_{obs}})}{\sum_t (q_{sim_t} - \overline{q_{sim}})^2 \sum_t (q_{obs_t} - \overline{q_{obs}})^2}}$$

Nash Sutcliffe correlation coefficient, R2

$$R2 = 1 - \frac{\sum_t (q_{obs_t} - q_{sim_t})^2}{\sum_t (q_{obs_t} - \overline{q_{obs}})^2}$$

Where q_{obs_t} and q_{sim_t} are the observed and simulated values at a certain time *t* and location *i*, and *n* is the number of observations at this location.

4.2 Calibration methodology

4.2.1 Verifying the numerical solution

The first requirement is that the model provides a stable numerical solution. There is no meaning to start adjusting physical parameters before the model gives a sound numerical solution that has a physical meaning. Therefore, the first step in the calibration process must always be to check for numerical instabilities and to validate the physical meaning of the first model results. The numerical accuracy is controlled by the numerical iteration criteria and the time step. In time step optimization, a reasonable compromise between actual simulation times and numerical stability must be reached.

A background concerning time steps of different model components and model control parameters is given in /DHI Software 2007/. A few updates have been made to the model in order to improve the numerical solution. The resulting time steps and model control parameters are shown in Table 4-1.

Table 4-1. Time steps and model control parameters; OL = overland flow, SZ = saturated zone, UZ = unsaturated zone, and ET = evapotranspiration.

Parameter	Value
Initial timestep	1 h
Maximum allowed OL, UZ, ET time step	1 h
Maximum allowed SZ timestep	3 h
MIKE 11 time step	5 s
Maximum courant number OL	0.75
Maximum profile water balance error, UZ/SZ coupling	0.001 m
Maximum allowed UZ iterations	50
Iteration stop criteria	0.002
Timestep reduction control: Maximum water balance error in one node (fraction)	0.03
Maximum allowed SZ iterations	80
Maximum head change per SZ iteration	0.05 m
Maximum SZ residual error	0.005 m/d
Saturated thickness threshold	0.05 m

4.2.2 The surface stream network

In the previous model version reported in /Aneljung and Gustafsson 2007/, the Manning number in MIKE 11 was roughly calibrated against measured data for a part of the system upstream of Lake Bolundsfjärden. The Manning number was calibrated to be as low as 3 $m^{1/3}s^{-1}$ in the upper parts of the water course branch just downstream of Lake Eckarfjärden. For the remaining branches in MIKE 11, the calibrated Manning number of 3 $m^{1/3}s^{-1}$ resulted in too high water levels. Therefore, a Manning number of 10 $m^{1/3}s^{-1}$ was used for the remaining branches. These values are kept throughout the calibration process reported here.

The leakage coefficient in MIKE 11, which affects the conductance used in the calculation of the water exchange between the stream network and the saturated zone, is set to a high value ($1 \cdot 10^{-5}$ m/s). This value is selected so that the leakage coefficient is not limiting the hydraulic interaction between groundwater and surface water. Thus, the hydraulic conductivities in the saturated zone will limit the water exchange.

4.2.3 Calibration procedure – from top to bottom

Once the obvious input errors in the new model were corrected, an initial calibration of model parameters and model input was made in order to define a base case. The initial part of the model calibration was primarily focused on the surface water system. The reason is that in order to obtain a correct description of the amount of water available for infiltration it is important to describe the surface water system as correctly as possible.

Once the model surface water system is roughly in agreement with the measurements, the calibration procedure switches focus to the groundwater head elevations in the Quaternary deposits, and once they are calibrated the accuracy between measured and calculated groundwater head in the bedrock monitoring points were analysed. Table 4-2 lists the main steps taken in the calibration procedure. Each step is further described in the following text. The calibration procedure is also illustrated in Figure 4-1, where the connections between the different steps are shown.

Table 4-2. Description of calibration steps.

Step no	Action
1	Sensitivity simulation with overland Manning number = 1.
2	Sensitivity simulation with overland Manning number = 0.001.
3	Sensitivity simulation of the saturated hydraulic conductivity, Ks, in the unsaturated zone reduced by a factor of 10.
4	Simulation with extension of the surface stream network in Lake Eckarfjärden.
5	Simulation including subsurface drainage, with option “drainage routed downhill based on adjacent drain levels”. (based on step 4)
6	Sensitivity simulation of the root mass distribution, Aroot, increased by a factor of 2. (based on step 5)
7	Sensitivity simulation of the root mass distribution, Aroot, reduced by a factor of 2. (based on step 5)
8	Sensitivity simulation of the specific yield, S_y, in the unsaturated zone, increased by a factor of 1.5. (based on step 5)
9	Sensitivity simulation of the specific yield, S_y, in the unsaturated zone, reduced by a factor of 2. (based on step 5)
10	Simulation with “drainage routing based on grid codes” in all grid cells. (based on step 5)
11	Simulation with “drainage routing based on grid codes” upstream Lake Eckarfjärden and “drainage routed downhill based on adjacent drain levels” elsewhere. (based on step 5)
12	Simulation with an updated potential evapotranspiration value, PET. (based on step 11)
13	Sensitivity simulation of the interception coefficient, C_{int}, reduced by a factor of 2. (based on step 12)
14	Sensitivity simulation of the leaf area index, LAI, reduced by a factor of 2. (based on step 12)
15	Sensitivity simulation of the drainage time constant, TC, increased by a factor of 5. (based on step 12)
16	Sensitivity simulation of the drainage time constant, TC, reduced by a factor of 5. (based on step 12)
17	Simulation with reduction of the potential evapotranspiration by 5%. (based on step 12)
18	Simulation with reduction of the potential evapotranspiration by 10%. (based on step 12)
19	Simulation with reduction of the potential evapotranspiration by 7.5%. (based on step 12)
20	Sensitivity simulation of hydraulic conductivity in the till, Ktill, vertical hydraulic conductivity reduced by a factor 10. (based on step 19)
21	Sensitivity simulation of hydraulic conductivity in the till, Ktill, horisontal hydraulic conductivity increased by a factor 10. (based on step 19)
22	Sensitivity simulation of hydraulic conductivity in the till, Ktill, horisontal hydraulic conductivity increased by a factor 5; vertical hydraulic conductivity reduced by a factor 2. (based on step 19)
23	Sensitivity simulation of hydraulic conductivity in the till, Ktill, horisontal hydraulic conductivity reduced by a factor 5; vertical hydraulic conductivity reduced by a factor 50. (based on step 19)
24	Sensitivity simulation of hydraulic conductivity in the till, Ktill, horisontal hydraulic conductivity reduced by a factor 10; vertical hydraulic conductivity reduced by a factor 100. (based on step 19)
25	Simulation with introduction of a new geological layer, surface bedrock layer, for areas with no or very thin soil layer upon the underlying bedrock. (based on step 22)
26	Simulation with hydraulic conductivity values of $1 \cdot 10^{-6}$ m/s in the new surface bedrock layer and with freshwater heads in the bottom boundary. (based on step 25)
27	Simulation with hydraulic conductivity values of $1 \cdot 10^{-6}$ m/s in the new surface bedrock layer and with environmental water heads in the bottom boundary.(based on step 25)
28	Simulation with hydraulic conductivity values of $1 \cdot 10^{-7}$ m/s in the new surface bedrock layer and with freshwater heads in the bottom boundary. (based on step 25)
29	Simulation with hydraulic conductivity values of $1 \cdot 10^{-7}$ m/s in the new surface bedrock layer and with environmental water heads in the bottom boundary. (based on step 25)
30	Simulation with division of subareas with different properties of horisontal hydraulic conductivity and unsaturated zone specific yield, S_y. (based on step 29)
31	Simulation with a new data set of bedrock properties (based on step 30)
32	Simulation with reduced potential evapotranspiration of 15% (based on step 31)
33	Sensitivity analysis with bottom boundary condition of environmental water heads reduced by 1 meter and a lower level of bottom boundary at 150 m.b.s.l. (based on step 32)
34	Sensitivity analysis with a no-flow bottom boundary condition and a lower level of bottom boundary at 150 m.b.s.l. (based on step 32)
35	Sensitivity analysis with bottom boundary condition of environmental water heads and a lower level of bottom boundary at 250 m.b.s.l. (based on step 32)
36	Sensitivity analysis with a no-flow bottom boundary condition and a lower level of bottom boundary at 600 m.b.s.l. (based on step 32)

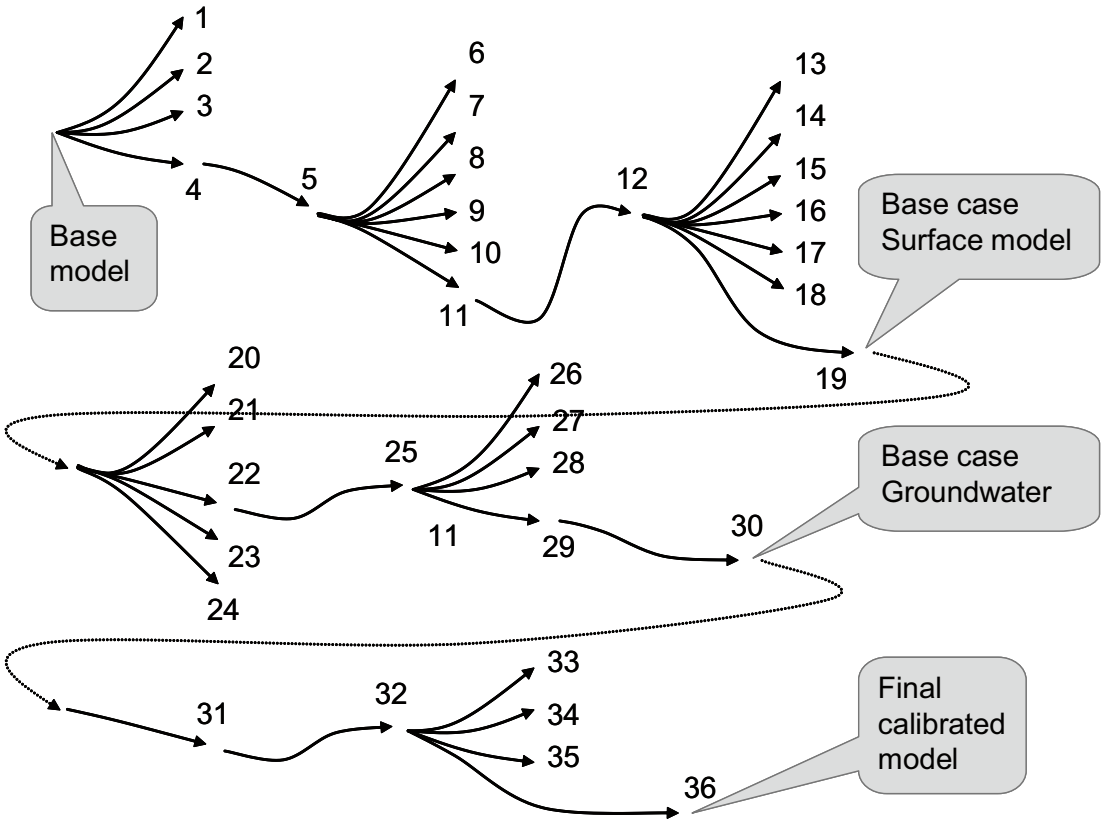

Figure 4-1*. Illustration of the calibration steps and sensitivity analysis.*

4.2.4 The surface water system (step 1 to 19)

Initial simulations showed a lack of runoff from the overland component to the surface water system, specifically for the surface discharge station at the outlet of Lake Eckarfjärden. Also, the discharge peaks were too narrow, i.e. the model response was too quick. Therefore, initial calibration steps focused primarily on the surface discharges.

The overland Manning number (step 1 and 2)

The Manning number, M, for overland flow was initially set to 5 $m^{1/3}s^{-1}$. In the previous model version, the overland M was decreased from 10 $m^{1/3}s^{-1}$ to 5 $m^{1/3}s^{-1}$, which was regarded as more realistic for this particular type of flow. In the present modelling, two additional simulations were performed, with values of M = 1 $m^{1/3}s^{-1}$ and M = 0.001 $m^{1/3}s^{-1}$, respectively (steps 1 and 2 in Table 4-2). These additional simulations were carried out to check whether the changed Manning number would lead to a better agreement with measured surface water discharges, as well as to see whether computational times would decrease since the main part of the computational time is due to the overland component.

The simulation with the lower overland M, i.e. M = 0.001 $m^{1/3}s^{-1}$, showed too slow hydraulic responses during peaks, and also resulted in less discharge (and more infiltration and evaporation). The simulation with an overland M = 1 $m^{1/3}s^{-1}$ resulted in very small changes in discharge patterns, but it also caused instabilities in some of the lakes in the area. Therefore, the original overland Manning number was kept unchanged at M=5 $m^{1/3}s^{-1}$ in the rest of the calibration procedure.

Surface stream network upstream Lake Eckarfjärden (step 4)

Although the simulated surface discharges were too small compared to measured discharges in all four measurement stations, the difference between measured and calculated discharge was much larger for Lake Eckarfjärden than for the other stations. The main reason for this was found to be that the catchment area of Lake Eckarfjärden described by the 40 m × 40 m topography in MIKE SHE did not fully agree with the field controlled water divide of Lake Eckarfjärden. The details of the topography were not captured by the 40 m model grid.

The effect of the discrepancy between the modelled and the field-controlled (real) water divides was that water that in reality went to the discharge station downstream Lake Eckarfjärden was directed towards Lake Gällsboträsket in the model. This resulted in a too small calculated discharge at the station downstream Lake Eckarfjärden. In an attempt to lead the water towards Lake Eckarfjärden, the MIKE 11 stream network was extended with a number of additional branches to Lake Eckarfjärden, see Figure 4-2 (step 4 in Table 4-2). However, it was found that the additional MIKE 11 branches were not enough to lead all water towards the lake.

Different measures could be taken to force the water within the area of the Eckarfjärden catchment to Lake Eckarfjärden in the model. Specifically, it is either possible to extend the surface stream network further or to include the MIKE SHE subsurface drainage option. Saturated zone drainage is a special boundary condition in MIKE SHE used to define natural and artificial drainage systems. Water is removed from the saturated zone by surface drainage and routed to local surface water bodies. The extension of the stream network, described in Figure 4-2, did not generate enough water to the stream, therefore different drainage options were analysed and will be described below.

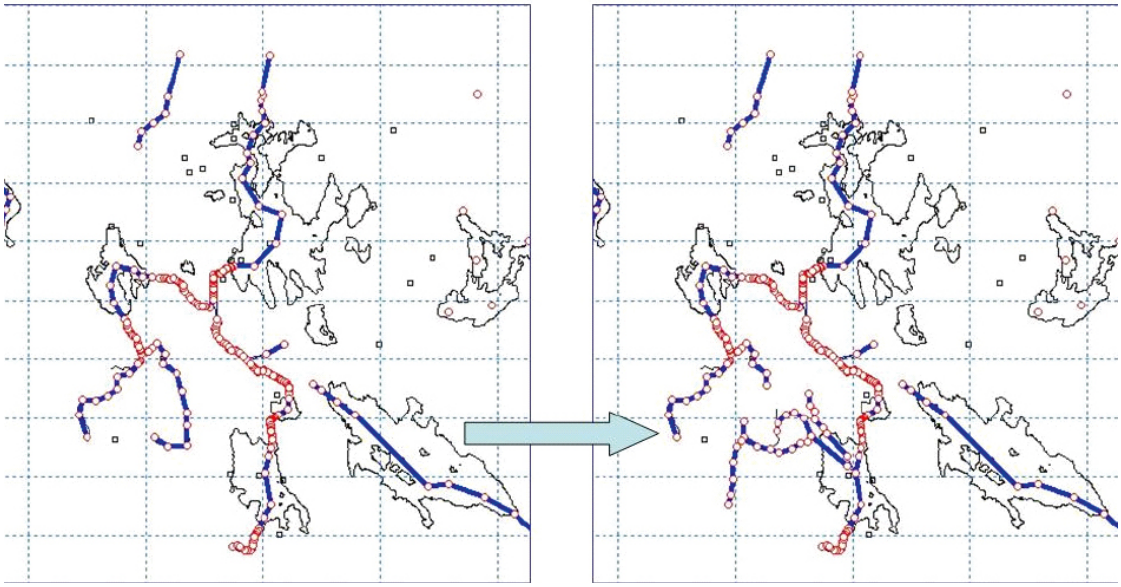

Figure 4-2. *Changes in the MIKE 11 surface water network. The blue lines indicate the extension of the M11 network, red dots indicate a defined cross section.*

Subsurface drainage describing high conductive top soil layer (step 5, 10–11, 15–16)

Since the simulations indicated that the model runoff was too fast in comparison to measurements, it seemed more likely that parts of the runoff occurs in the uppermost part of the Quaternary deposits, being more high conductive, rather than only on the ground surface. The groundwater table variations also indicated that this may be the situation at hand. The approach to model this would be to include a thinner (e.g. 0.5 m) top calculation layer in the saturated zone. In the present version of MIKE SHE, however, the transpiration process can only be activated in the top calculation layer. This is a notable disadvantage, because the transpiration is an important process when describing the temporal variation of both groundwater heads and runoff, the modelling of which should not be limited in depth for model capability reasons.

Instead, the extra runoff capacity in the high conductive top soil layers was described in an alternative way, by activating subsurface drainage. The drainage function is normally applied to describe physical drains or presence of ditches and surface stream networks not included in the stream network in MIKE 11. The hypothesis in this case was that the highly conductive top layer also works as a drain for the upper groundwater.

As an initial approach the model option “drainage routed downhill based on adjacent drain levels” (step 5 in Table 4-2) was selected. The reference system is created automatically using the slope of the drains calculated from the drainage levels in each cell. Thus, as long as a downward slope is found, the drain flow will continue until crossing a river or the model boundary.

Input parameters to the drainage option is the level at which the drainage is activated, which was set to 0.5 m below ground because this is the typical thickness of the high conductive top soil layer, and a time constant that is mathematically equivalent to a leakage coefficient. This means that it simply is a linear coefficient used to regulate how quickly the water will drain.

The drainage time constant was estimated based on the “extra hydraulic conductivity” in the top soil (geological layer Z1) compared to the deeper Quaternary deposits (below Z1). In order not to double-count this extra top soil hydraulic capacity, the geological layer Z1 was given the same hydraulic conductivities as the layer just below Z1. Z1 is only 0.5 thick where a QD-layer is present. Thus, the high conducitivty values that are present in Z1 are transferred from Z1 to the drainage function since the calculation layers must be thicker than 0.5 m. When including the properties of Z1 in a calculation layer that contains several geological layers with lower hydraulic conducitivty values, the transport capacity of Z1 is not properly decribed by the model since the thickness of Z1 is much less than the thickness of the calulation layer.

Results from the first simulation with the drainage option (step 5) indicated that not all water removed by drainage was routed to the surface stream network. The reason is that if local depressions in the drainage levels exist, the saturated zone nodes in these depressions may become the recipients for a number of drain flow producing nodes. This often results in the creation of a small lake at such local depressions. When the topography is flat, local depression are often artificial depressions, and to avoid the water to be directed to local depressions, drainage routing based on grid codes may be used, which forces the drain flow to the river links in MIKE 11.

Two more alternatives, with different drainage routing principles, were simulated. The first alternative used drainage routing based on grid codes (step 10 in Table 4-2), which forces all of the drain flow to the river links in MIKE 11. This alternative gave too large runoff volumes to all of the discharge stations, except the one downstream of Lake Eckarfjärden. Consequently, the second alternative (step 11 in Table 4-2) used the same grid code option for the catchment of Lake Eckarfjärden and the option “drainage routed downhill based on adjacent drain levels” elsewhere in the model area.

A sensitivity analysis of the drainage time constant, T_c, was also performed (steps 15 and 16 in Table 4-2). An increased value gave a slightly larger runoff volume, but on the other hand too narrow peaks. The original values were kept unchanged.

The unsaturated zone and evapotranspiration (step 3, 6–9, 12–14, 17–19)

Since a lower saturated hydraulic conductivity in the unsaturated zone (K_s) generally increases the surface stream flow, a sensitivity simulation with the conductivity reduced by a factor of 10 was performed (step 3 in Table 4-2). The results, however, indicated that the difference was small and therefore no change of K_s was made in the model setup.

With drainage option 1 included in the model, sensitivity analysis with regard to the root mass distribution, A_{root}, and the unsaturated zone specific yield, S_y, were made (steps 6 to 9 in Table 4-2). Results showed that changes in the A_{root} parameter has a negligible effect on both surface water levels and surface discharges in the area and no changes were made in the existing model. The changes in the specific yield, S_y, had a somewhat larger effect on the results. However, the effect was still too small to lead to a general change of S_y in the model setup.

At this point in the calibration process it was discovered that the potential evapotranspiration values used so far were not consistent with the latest dataset in the database. The time series used in the pre-modelling /Aneljung and Gustafsson 2007/ had been used. The model was therefore updated with new values taken from the Sicada database (step 12 in Table 4-2), see Section 2.2.2. The new values of the potential evapotranspiration were higher than the previous ones, which lead to decreased runoff again. In order to obtain a better agreement with measured values, sensitivity analyses were made of the vegetation parameters C_{int} and LAI (steps 13 to 14 in Table 4-2). LAI is the leaf area index and C_{int} is the interception coefficient that defines the interception storage capacity of the vegetation per unit of LAI.

None of the sensitivity analysis indicated that it was possible to reach a satisfying agreement between measured and calculated values with physically realistic values of the vegetation parameters. Therefore, it was concluded that a sensitivity analysis with reductions of the new potential evapotranspiration values should be performed (steps 17–19 in Table 4-2). It was estimated that a reduction by approximately 5–10% was reasonable. After the sensitivity analysis, a reduction of 7.5% was made, which is further discussed in section 5.2.

With all the simulation steps discussed above (steps 1 to 19 in Table 4-2), the calibration of the surface water part of the model was concluded. Major results from these steps are shown in section 4.2. The calibrated surface water base case contains the original set-up of vegetation and unsaturated zone parameters. The changes compared to the original setup included:

- extension of the surface stream network upstream Lake Eckarfjärden,
- reduction of the potential evapotranspiration rates with 7.5%,
- inclusion of subsurface drainage as a representation of a highly conductive top soil layer.

The groundwater levels in the Quaternary deposits (step 20 to 30)

The calibration procedure then proceeded to the calibration of the groundwater levels in the Quaternary deposits against measurements in the groundwater monitoring wells (see Section 4.3). Most of the area is covered by a layer of till and, consequently, a sensitivity analysis of the conductivity of the till is an important step in the groundwater modelling. Steps 20 to 24 in Table 4-2 are all different sensitivity simulations of the till hydraulic conductivity. In the original model setup the vertical and horizontal conductivities were equal (i.e. isotropic conditions). In all five sensitivity cases, anisotropic conditions were considered. Specifically, all cases were characterised by an anisotropy ratio of 10, with the horizontal conductivity being 10 times larger than the vertical.

When evaluating the results from the simulations, it was noted that in areas with bedrock outcrops or in areas with a thin soil layer the present model was not describing the dynamics of the groundwater correctly. In these areas, properties from the uppermost geological layer describing the bedrock were used. According to the ConnectFlow model results, this layer describes the bedrock in an appropriate way from approximately 20 m below ground surface up to 4 m below ground surface. Bedrock close to the ground surface is often more fractured and more hydraulically conductive than deeper layers. A new geological layer was created to describe the uppermost bedrock, i.e. areas with no or a very thin soil layer. This layer described

the uppermost four meters of the bedrock (step 25 in Table 4-2), and is only present in areas where the soil depth is less than 4 meters.

The head values at the bottom boundary in the original model were so-called freshwater head values (FWH). This means that no account is taken to the fact that water at lower levels has a higher density because of the higher salt content. To account for the increasing density at depths, environmental heads (EWH) were calculated and tested in the model. To investigate the impact of using freshwater heads or environmental heads on the simulation results, simulations were made with both types of heads on the model boundaries. Four simulations were made in order to evaluate the sensitivity to the different bottom boundary heads and the hydraulic conductivity of the new surface bedrock layer (steps 26 to 29 in Table 4-2) on the groundwater heads in the monitoring points.

Based on the sensitivity analysis of till conductivity and the unsaturated zone specific yield it was found that different monitoring points react differently in the sensitivity analysis. In some areas the results in the groundwater monitoring points were better with higher hydraulic conductivity values, and for some areas it was indicated that a higher specific yield gave better results. In step 30 in Table 4-2, the area was divided into subareas with different parameter values. At the local heights close to SFM0004, SFM0005 and SFM0009, and in the catchment of Lake Eckarfjärden, the horizontal hydraulic conductivity in the till was increased by a factor 10, and the unsaturated zone specific yield was increased by a factor 1.5.

After the simulation steps 20 to 30 in Table 4-2, the calibration of the head elevations in the Quaternary deposits was concluded. Major results from these steps are shown in section 4.3. The main differences between the calibrated surface water base case and the calibrated groundwater base case are:

- introduction of anisotropy in till saturated zone layers,
- vertical hydraulic conductivities in the till reduced by a factor 2 and horizontal conductivities increased by a factor 5,
- introduction of a new surface bedrock geological layer for areas with no or a very thin soil layer,
- division into subareas with different values of till conductivities and unsaturated specific yield,
- introduction of environmental heads at the bottom boundary.

The groundwater heads in the bedrock (step 31 to 36)

The calibration procedure then proceeded to the calibration of the groundwater head elevations in the bedrock and the bottom boundary conditions, see Section 4.4. At this time, a new version of the dataset of the bedrock hydraulic conductivities, porosities and calculated heads was delivered and implemented in the model (step 31 in Table 4-2). The new lower vertical hydraulic conductivities resulted in a reduced vertical flow in the bedrock and in a reduced discharge in the water courses. The reduction of the discharge was not acceptable with regard to measurements and a calculation with a potential evapotranspiration reduced with 15% (previously 7.5%) compared to the original data was performed (step 32 in Table 4-2).

Finally, a sensitivity analysis of the model bottom boundary conditions and the bedrock properties was made (steps 33 to 36 in Table 4-2). Step 36, which produced the best results, concluded the calibration of the bedrock head elevations, and consequently also the whole calibration procedure. This model version not only produced the best results in the bedrock, but also in the Quaternary deposits and in the surface stream network.

To summarise the calibration, the main differences between the groundwater base case and the final calibrated model are:

- a new version of the data set for hydraulic conductivities, porosities and calculated heads was implemented,
- the potential evapotranspiration was reduced by 15% compared to original data,
- the model was extended to a depth of 600 m.b.s.l. and the bottom boundary was changed to a no-flow boundary.

The next step in the model development was to validate it against an independent dataset, which had not been used in the calibration process. The results of this validation step are shown in Chapter 5.

4.3 Surface water system

Following the calibration procedure presented in Section 4.1, some of the results are presented in the remainder of this chapter. Some of the sensitivity simulations were made with a model that still was not fully calibrated with regard to the surface water. As a consequence, the water levels or surface discharges presented in this section may differ between figures showing the same measurement station. Besides the model changes discussed in Section 4.2, changes were also made with regard to initial values. Therefore, the figures in this chapter should be studied in terms of differences between the curves in each figure and not the differences between the different figures.

4.3.1 Results from early simulations

The initial simulations showed a lack of surface water in comparison to discharge measurements. Figures 4-3 to 4-6 show results in the form of surface water discharges from one of the early simulations compared to the discharge measurements. All figures show lower calculated discharge than measured.

To estimate how much water is missing at each station the accumulated discharge was calculated. Figures 4-7 to 4-10 show the accumulated calculated discharges in comparison to accumulated measured discharges. At the station at the outlet of Lake Eckarfjärden, the initial calculations resulted in a discharge corresponding to less than 50% of the measured discharge. Also, at the stations downstream of Lake Gunnarsboträsket and Lake Stocksjön the calculated discharges are much lower than measured. The station with the best agreement is that at Lake Bolundsfjärden, where the calculated discharge is almost 80% of the measured. Figures 4-11 to 4-14 show the surface water levels from the same early model simulation as in Figures 4-3 to 4-10.

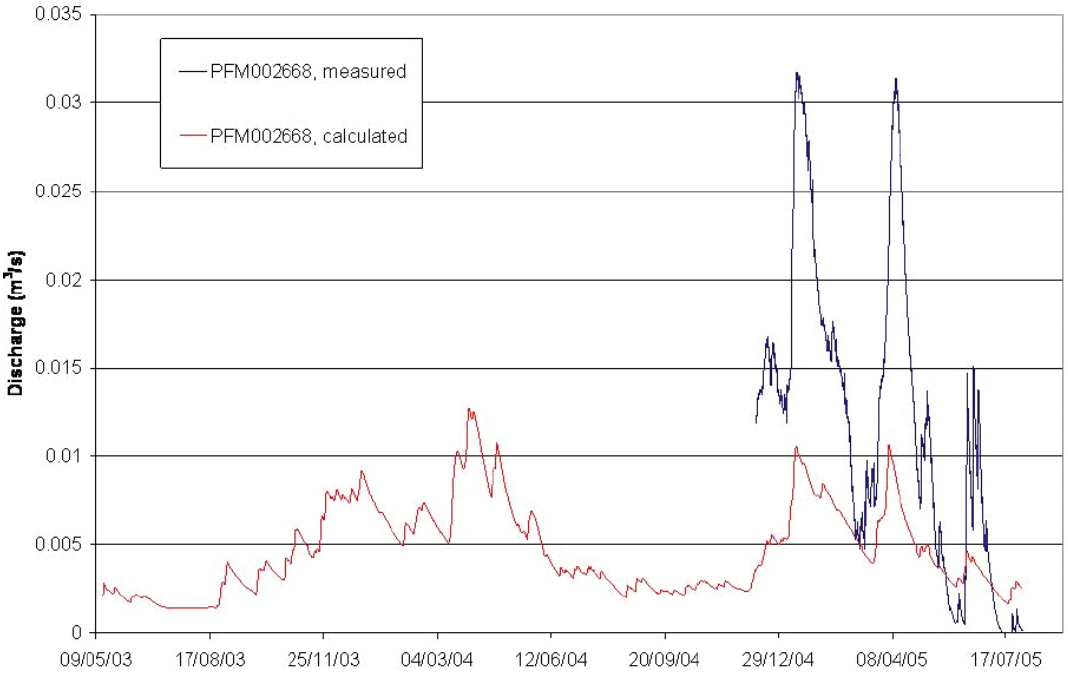

Figure 4-3. *Calculated surface water discharge compared to measurements at station PFM002668 (Lake Eckarfjärden) from an early simulation.*

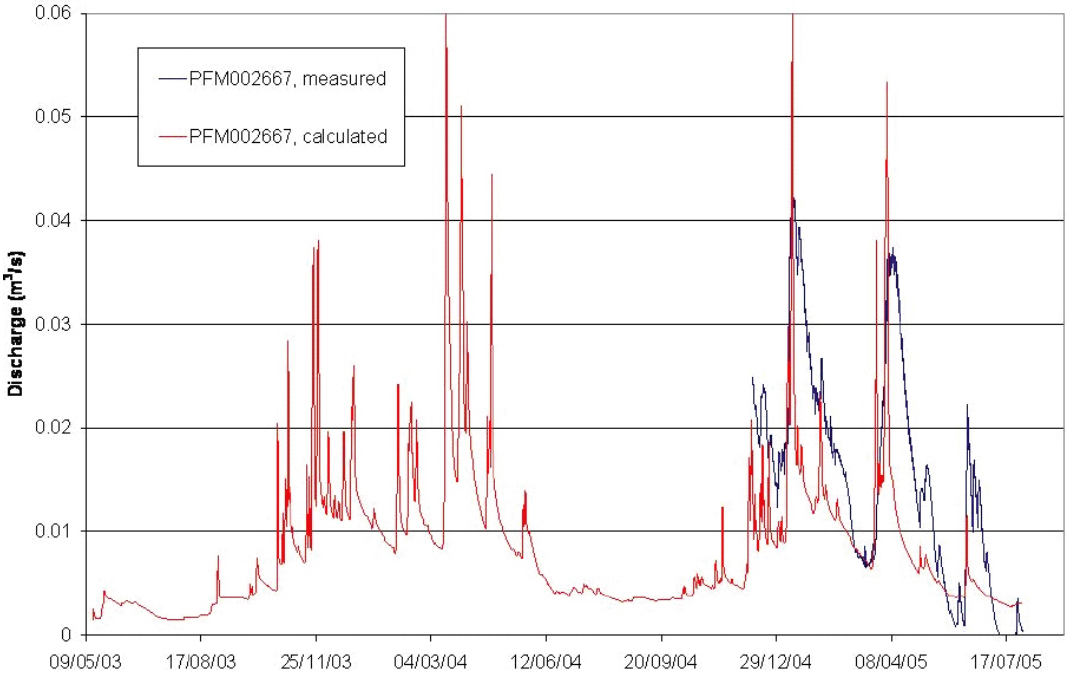

Figure 4-4. *Calculated surface water discharge compared to measurements at station PFM002667 (Lake Stocksjön) from an early simulation.*

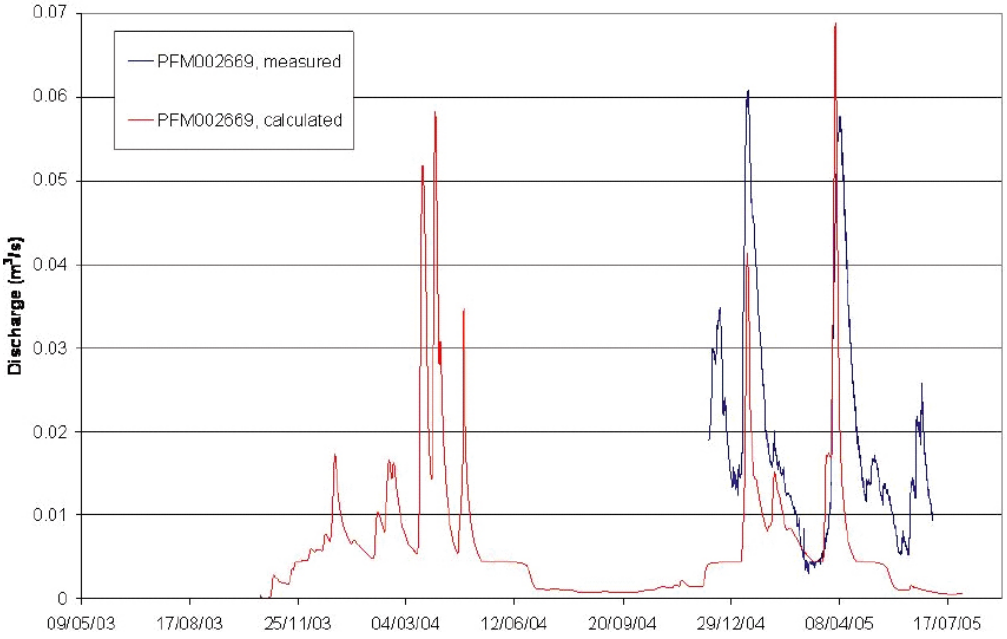

Figure 4-5. *Calculated surface water discharge compared to measurements at station PFM002669 (Lake Gunnarsboträsket) from an early simulation.*

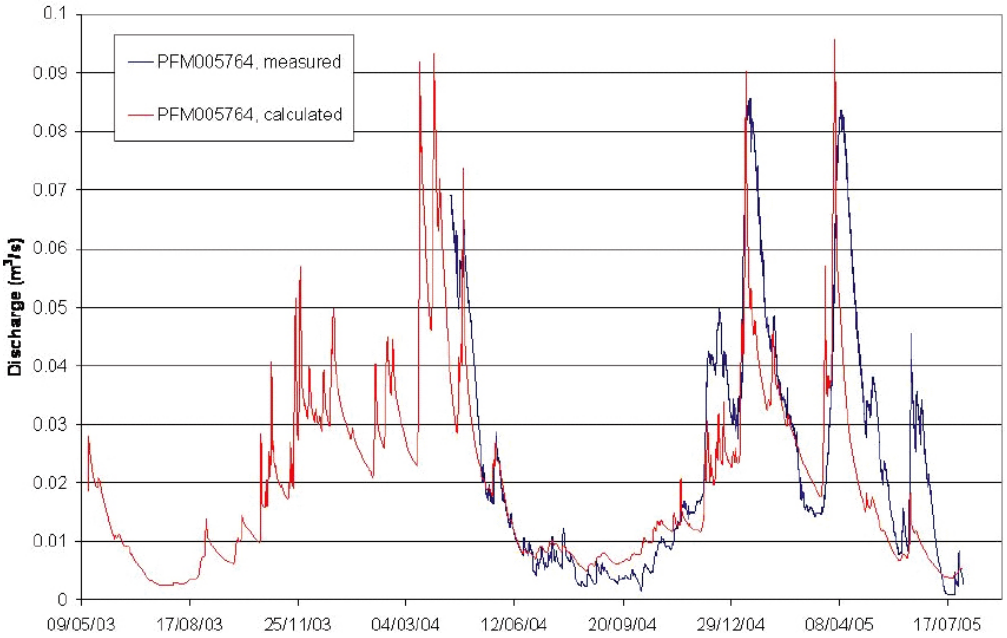

Figure 4-6. *Calculated surface water discharge compared to measurements at station PFM005764 (Lake Bolundsfjärden) from an early simulation.*

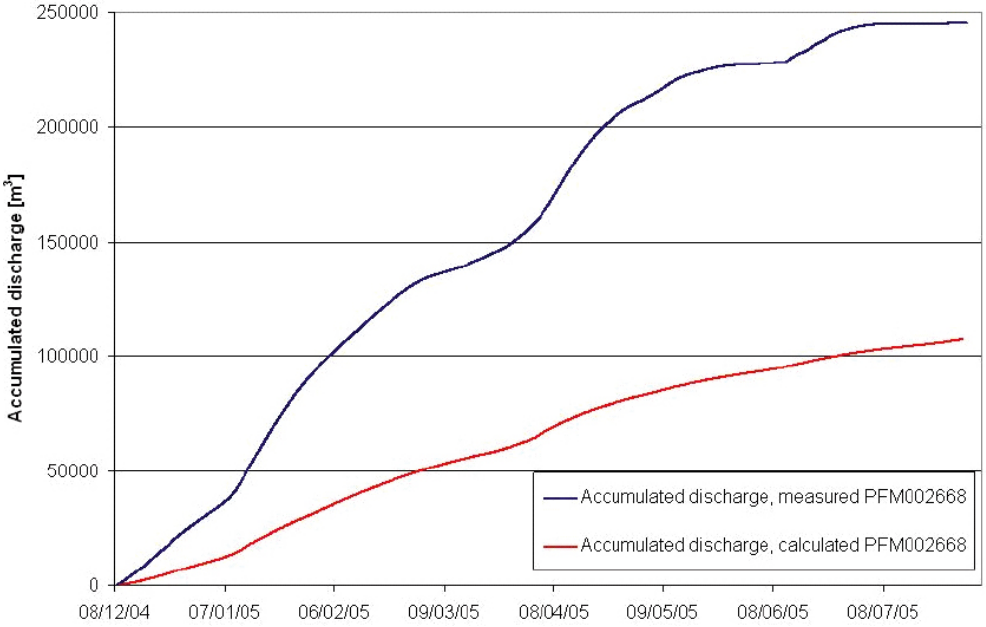

Figure 4-7. *Calculated accumulated discharge compared to measurements at station PFM002668 (Lake Eckarfjärden) from an early simulation.*

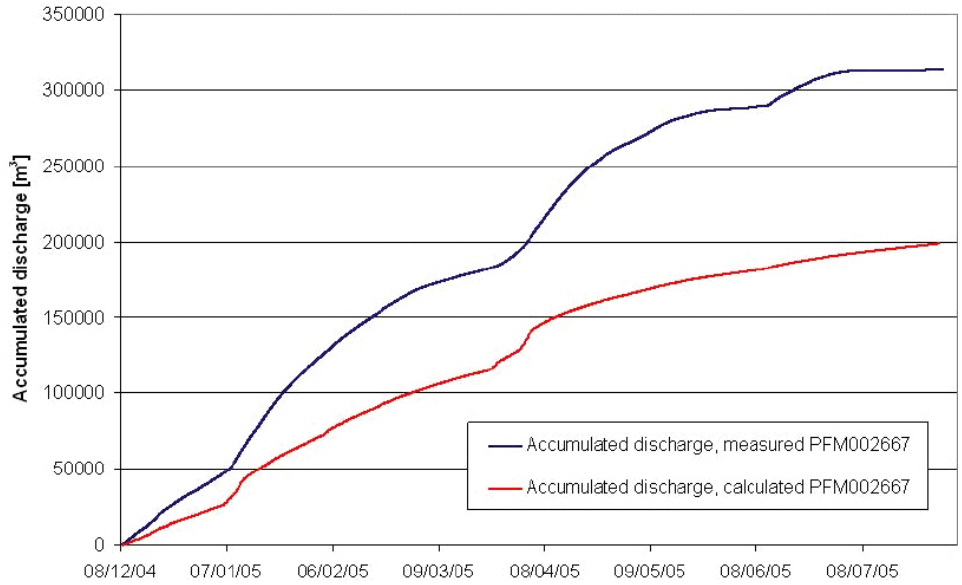

Figure 4-8. *Calculated accumulated discharge compared to measurements at station PFM002667 (Lake Stocksjön) from an early simulation.*

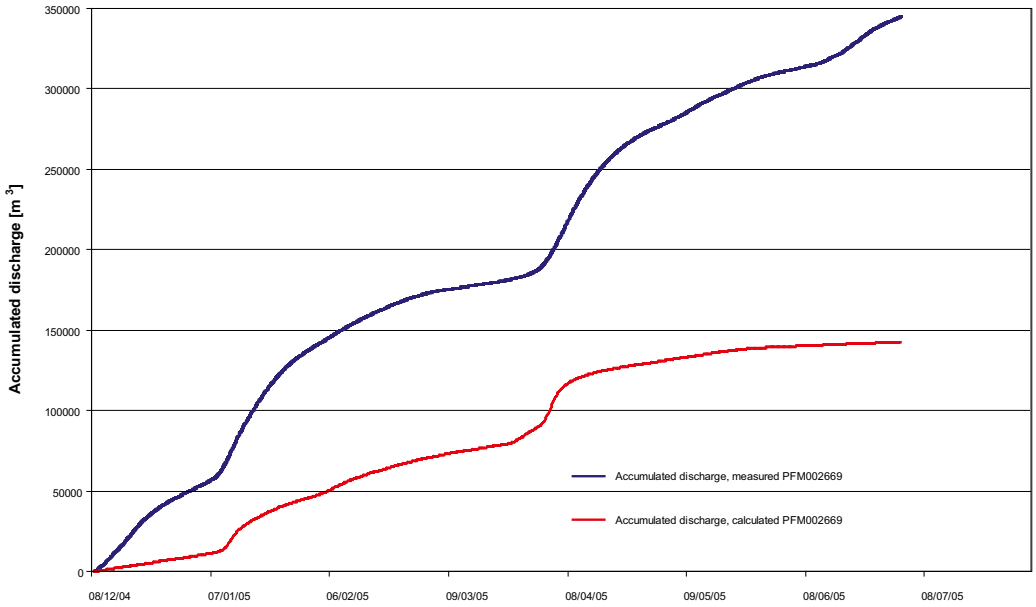

Figure 4-9. *Calculated accumulated discharge compared to measurements at station PFM002669 (Lake Gunnarsboträsket) from an early simulation. Measurements of the discharge were only available until 2005-07-02, while the model simulation ended 2005-07-31.*

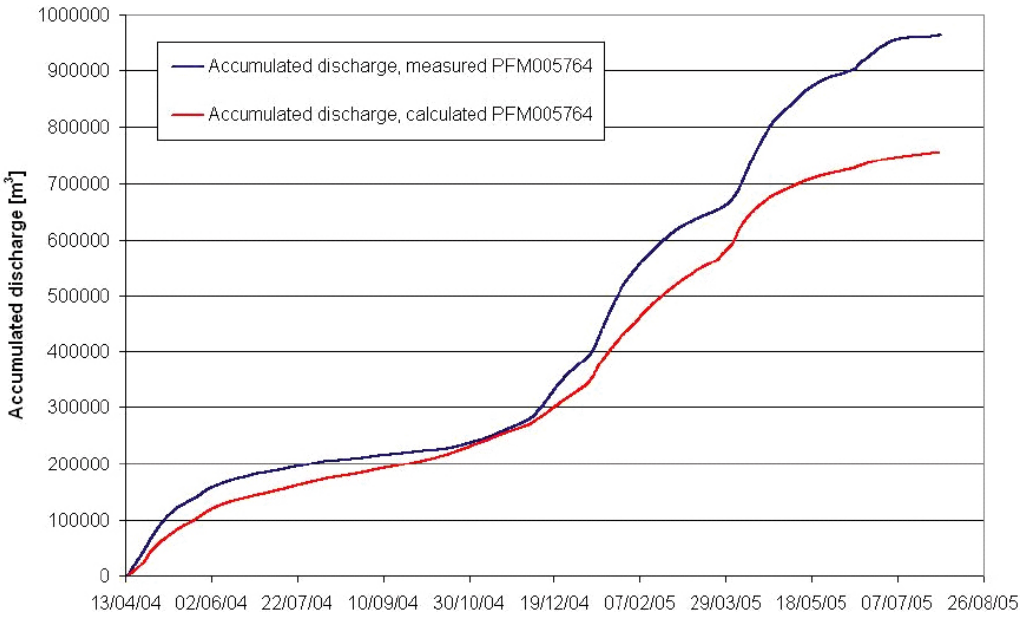

Figure 4-10. *Calculated accumulated discharge compared to measurements at station PFM005764 (Lake Bolundsfjärden) from an early simulation.*

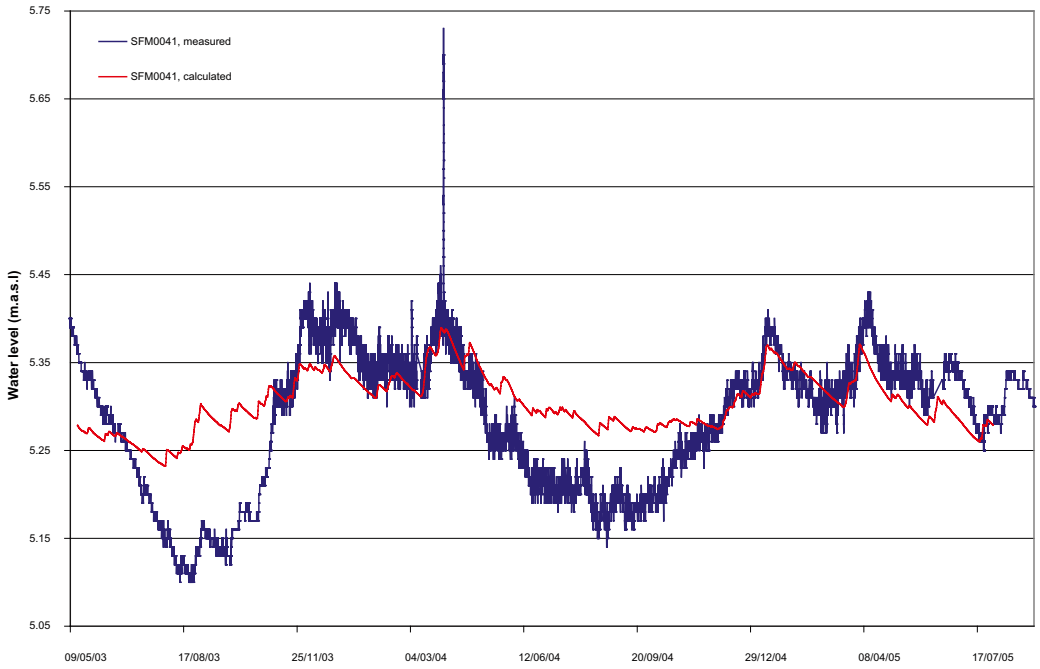

Figure 4-11. *Calculated surface water level compared to measurements at station SFM0041 (Lake Eckarfjärden) from an early simulation.*

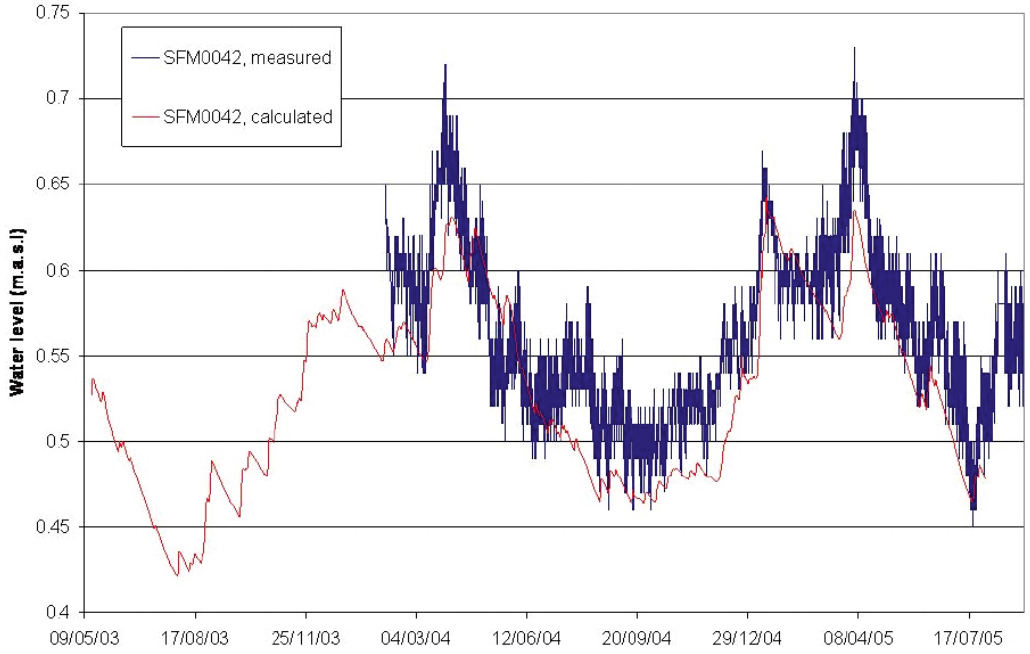

Figure 4-12. *Calculated surface water level compared to measurements at station SFM0042 (Lake Fiskarfjärden) from an early simulation.*

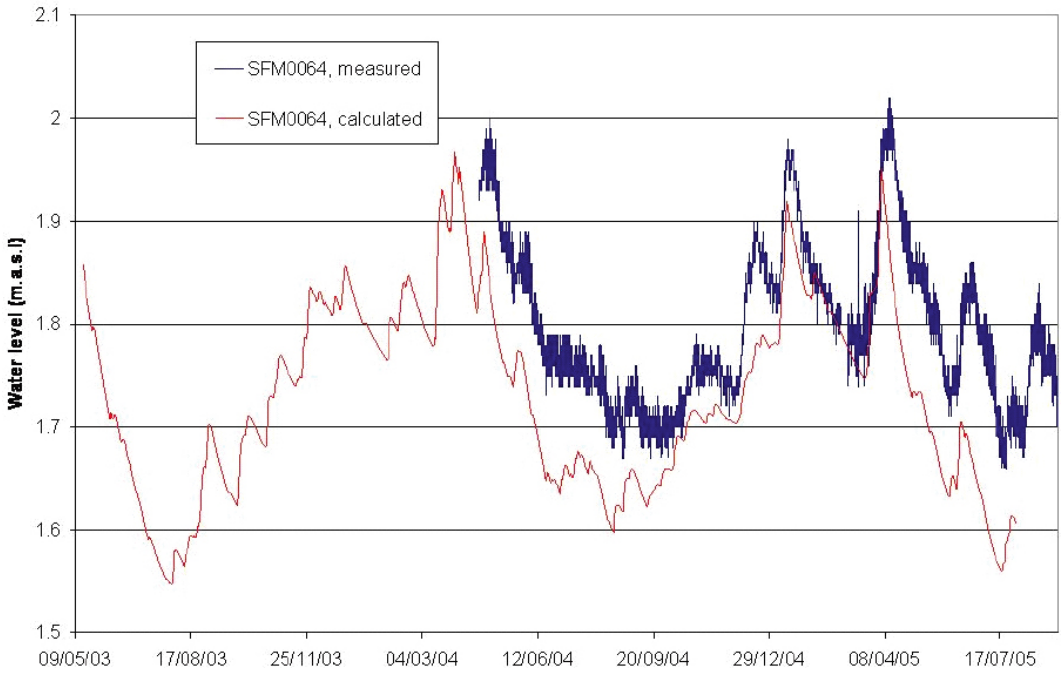

Figure 4-13. *Calculated surface water level compared to measurements at station SFM0064 (Lake Gällsboträsket) from an early simulation.*

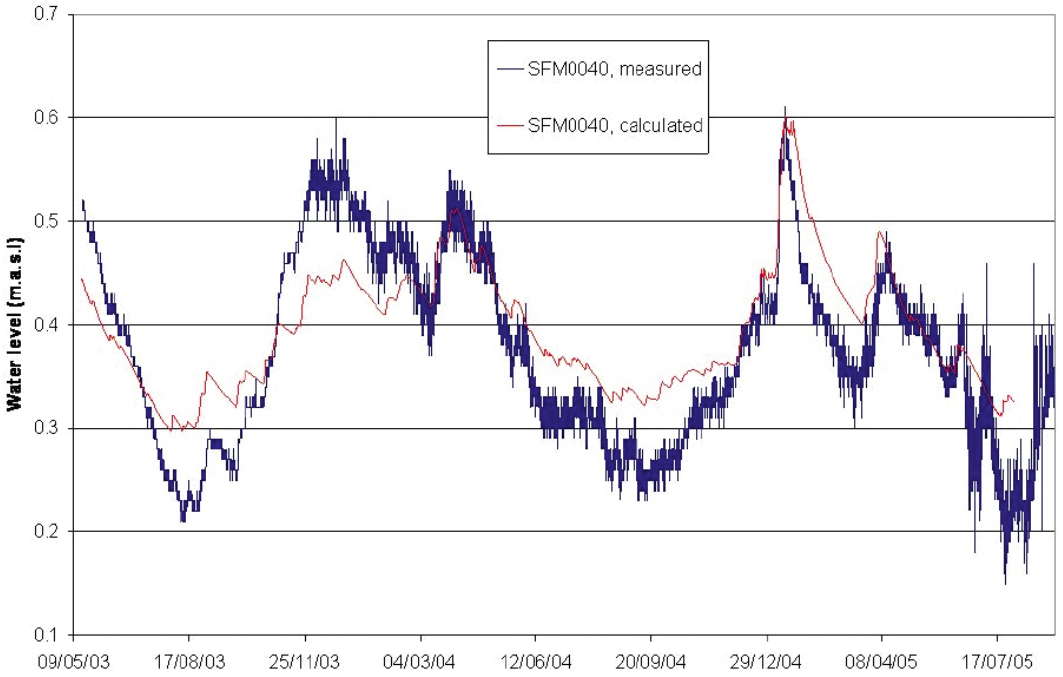

Figure 4-14. *Calculated surface water level compared to measurements at station SFM0040 (Lake Bolundsfjärden) from an early simulation.*

4.3.2 Sensitivity analysis of the saturated hydraulic conductivity

Generally, a lower saturated hydraulic conductivity in the unsaturated zone results in larger surface runoff. Because of the low simulated surface discharges, a simulation was made with the saturated hydraulic conductivity in the unsaturated zone, K_s, reduced by a factor of 10. However, the simulation showed that the effect of reducing K_s was negligible. Therefore, the K_s values were not changed in the model. Figures 4-15 and 4-16 show examples of results from the K_s sensitivity simulations in terms of water levels for Lake Fiskarfjärden and surface discharges for Lake Eckarfjärden. The other stations showed similar small effects.

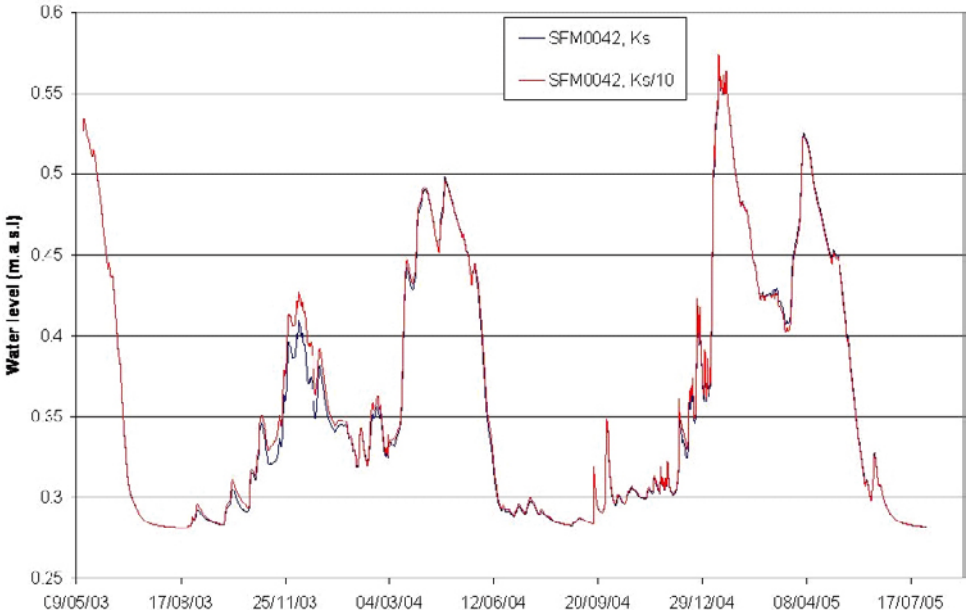

Figure 4-15. *Surface water levels in Lake Fiskarfjärden from sensitivity analysis of the saturated hydraulic conductivity, K_s, in the unsaturated zone. The blue line shows results with the original K_s and the red line results from simulation with K_s reduced by a factor of 10.*

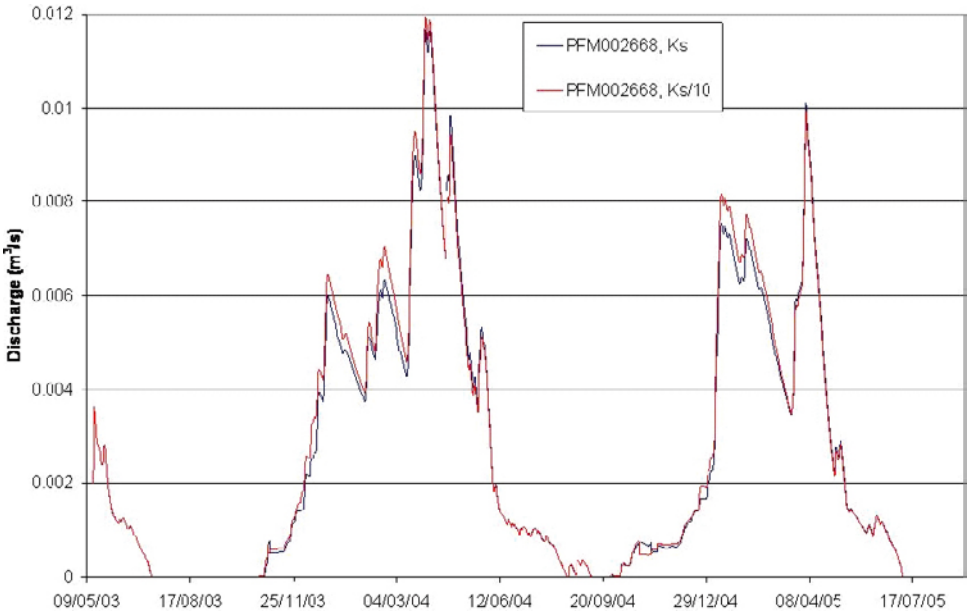

Figure 4-16. *Discharges downstream of Lake Eckarfjärden from sensitivity analysis of the saturated hydraulic conductivity, K_s, in the unsaturated zone. The blue line shows results with the original K_s and the red line shows results from simulation with K_s reduced by a factor of 10.*

4.3.3 Implemetation of sub-surface drainage

The surface river network was extended with some additional branches to Lake Eckarfjärden, see Figure 4-2. Although the extended network branches add some extra runoff, there is still a lack of discharge at the station. Figure 4-17 compares the measured discharge and the calculated surface water runoff at station PFM002668 in the outlet of Lake Eckarfjärden for the original case and for the case with the extended MIKE 11 stream network.

Since the simulations indicated that the model runoff was too fast in comparison to measurements, it seemed more likely that parts of the runoff occurs in the uppermost part of the soil layer, being more high conductive. Subsurface drainage was introduced in order to describe this phenomenon (see Section 4.2 for more details).

Figure 4-18 illustrates the surface discharge at Eckarfjärden when subsurface drains with "drainage routed downhill based on adjacent drain levels" (see Section 4.2), was added to the model (option 1). Although the subsurface drains gave some additional flow it is still far from the measurement results. One of the reasons for this is that parts of the drainage flow ends up in local depressions, which are not in direct contact with the surface stream network. On the other hand, when forcing all of the drain flow directly to the stream links in MIKE 11 by using drainage routing based on grid codes (option 2), too large runoff volumes were produced in all of the discharge stations, except the one downstream of Lake Eckarfjärden.

One explanation for the lack of runoff to Lake Eckarfjärden is that the model catchment is somewhat smaller than the actual catchment. The water divides according to the 40 m-resulution model topography contributes to a smaller catchment area for Lake Eckarfjärden than the field controlled catchment area. The calculated catchment area is approximetely 5% smaller than the real catchment area. When mixing these two alternatives (option 3), with direct routing to Lake Eckarfjärden and drainage routed downhill elsewhere, the simulated discharge is much closer to measured values. These results are shown in Figure 4-19 as hydrographs and in Figure 4-20 as accumulated discharges. The mixed drainage alternative (option 3) produces an accumulated discharge of about 86% of the accumulated measured discharge for Lake Eckarfjärden.

One of the input parameters in all simulations where drainage is included is the time constant, T_c. The time constant is equivalent to a leakage coefficient; it is simply a factor that is used to regulate how quickly the water can drain. In the present case, the subsurface drainage is interpreted as additional runoff capacity in the top soil layer, and the time constant is consequently estimated based on this interpretation (see Section 4.1). In order to analyze the impact of changes in this drainage time constant, two sensitivity simulations were run, changing the constant in two directions with a factor of 5. Figures 4-21 and 4-22 show examples of results. Neither of the two sensitivity simulations had any important effect on the surface water discharge volume. The only effect is seen on the maximum peak flows.

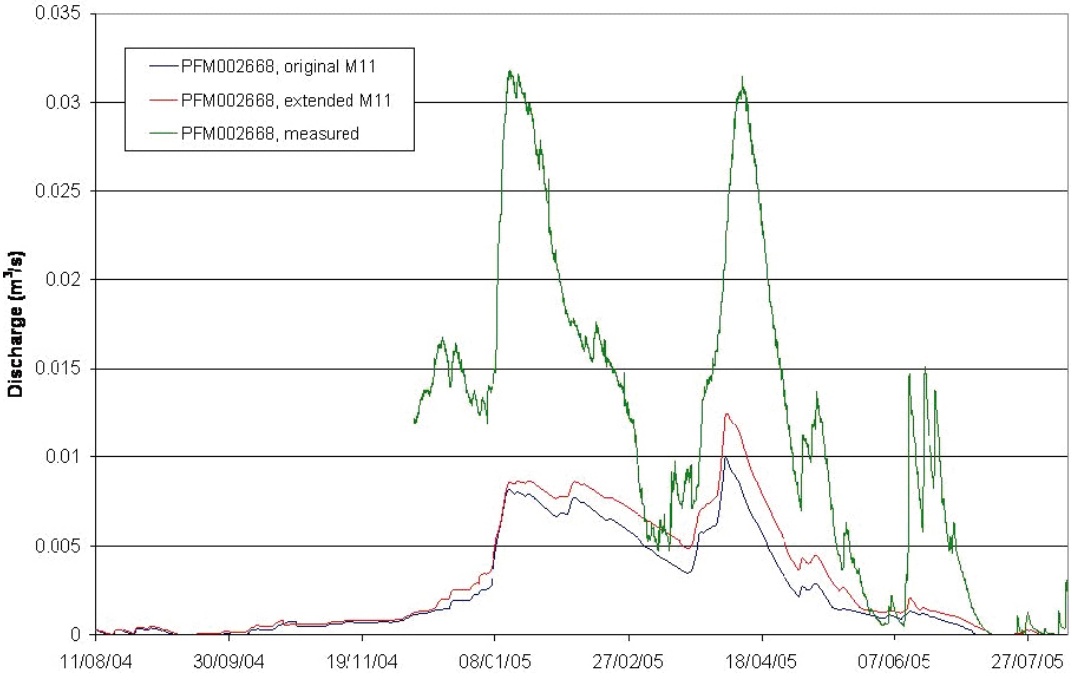

Figure 4-17. *Comparison between measured and calculated surface discharges at station PFM002668 (Lake Eckarfjärden) with and without the additional MIKE 11 branches in the model.*

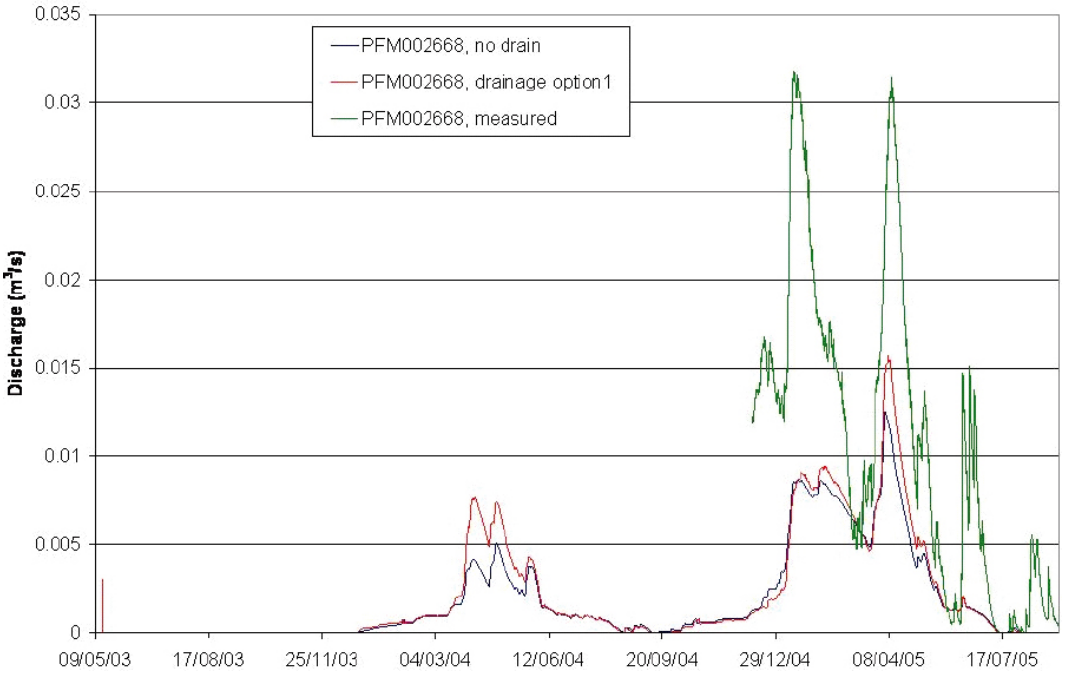

Figure 4-18. *Comparison between measured and calculated surface discharges at station PFM002668 (Lake Eckarfjärden) with no drainage included and with drainage option 1 activated in the model.*

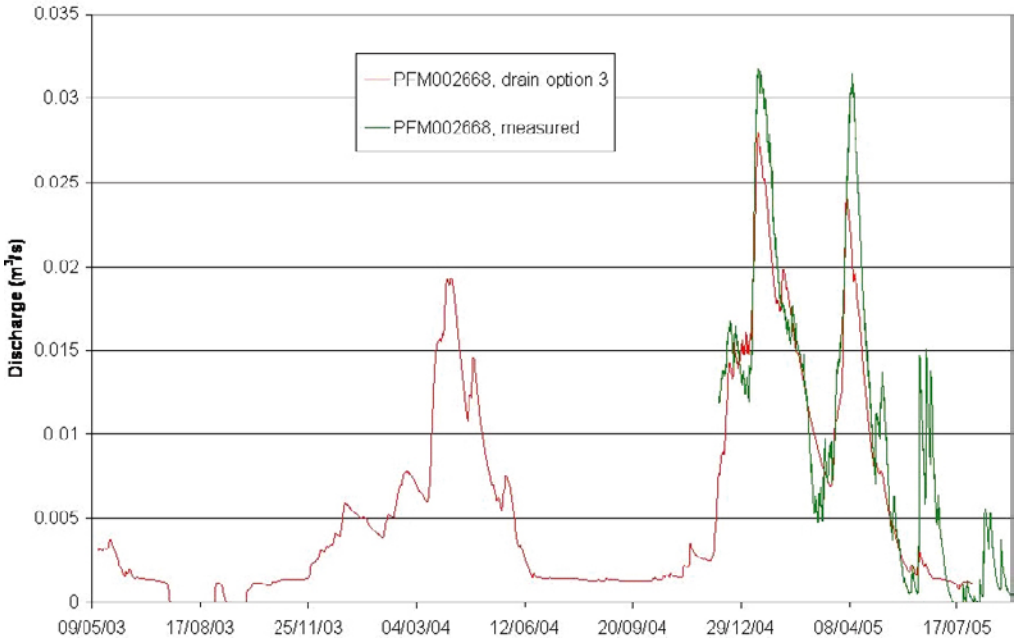

Figure 4-19. *Comparison between measured and calculated surface discharges at station PFM002668 (Lake Eckarfjärden) with drainage option 3 activated in the model.*

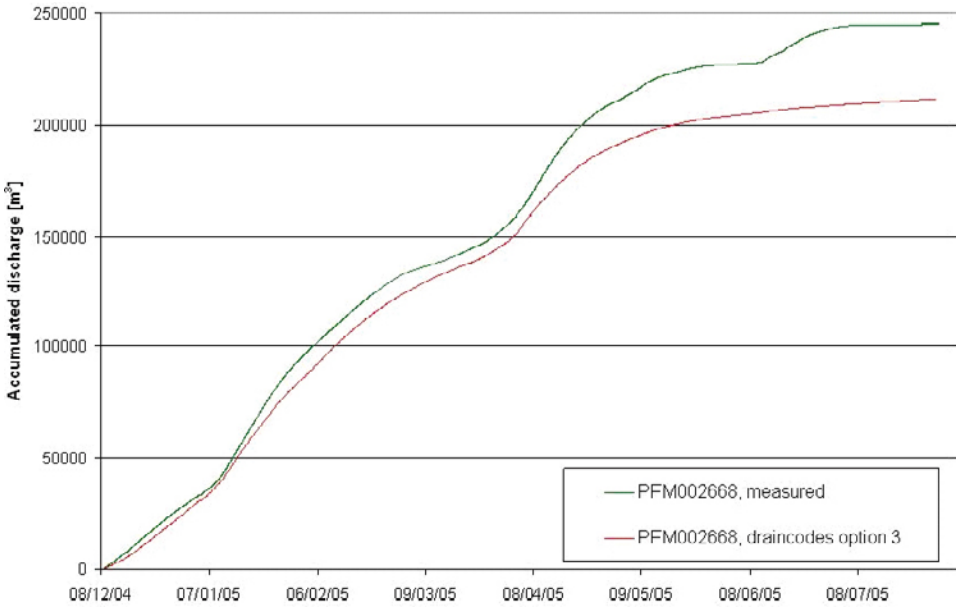

Figure 4-20. *Comparison between measured and calculated accumulated surface discharges at station PFM002668 (Lake Eckarfjärden) with drainage option 3 activated in the model.*

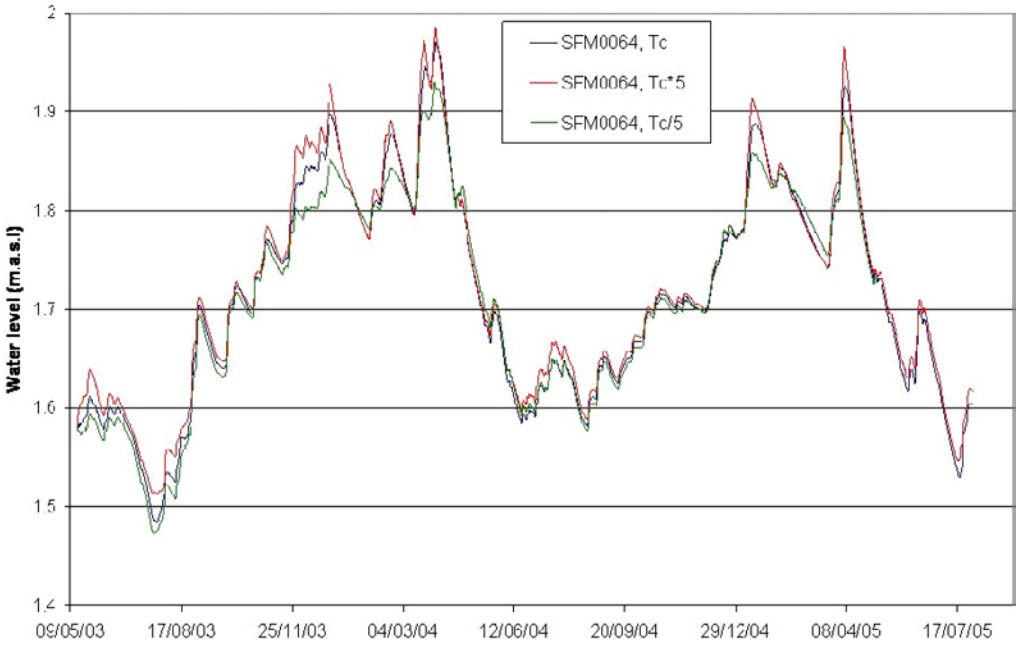

Figure 4-21. *Calculated surface water levels from sensitivity analysis of the drainage time constant, T_c, in the unsaturated zone. Results are from Lake Gällsboträsket; the blue line shows results with the original T_c, the red line results for T_c increased by a factor of 5, and the green line results for T_c reduced by a factor of 5.*

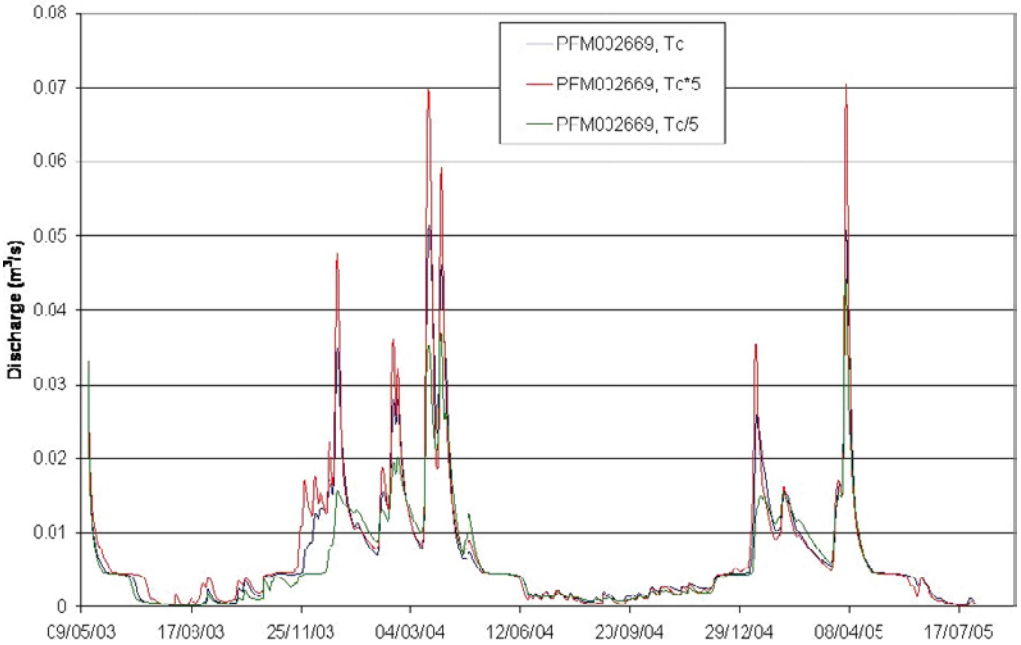

Figure 4-22. *Calculated surface water discharges from sensitivity analysis of the drainage time constant, T_c, in the unsaturated zone. Results are from Lake Gunnarsboträsket; the blue line shows results with the original T_c, the red line results for T_c increased by a factor 5, and the green line results for T_c reduced by a factor of 5.*

4.3.4 Sensitivity analysis of the unsaturated zone specific yield

The specific yield of the unsaturated zone, i.e. the available pore volume in the pF-curve between the porosity at field capacity and the total porosity, affects the groundwater level fluctuations. A higher value of the specific yield generates smaller fluctuations in the groundwater head elevation, while a smaller specific yield means a smaller storage capacity with larger fluctuations in the groundwater head.

In the sensitivity analysis, the specific yield in the unsaturated zone was increased by a factor of 1.5 or decreased by a factor of 2. The field capacity equals that of the base case. The effect of the changes of the specific yield was very small both on the surface water levels and the surface water discharges.

The changes in the unsaturated zone specific yield obviously cause changes in the groundwater monitoring points as well. However, comparing the calculated groundwater heads with measurements indicated that different areas in the model reacted differently to the changes. At this stage of the calibration, no changes were made to the model with regard to the specific yield (see further analysis of groundwater head elevation in Section 4.4).

4.3.5 Sensitivity analysis of the vegetation parameters

The vertical distribution of the water extraction by transpiration (i.e. by water uptake in the vegetation) depends on the A_{root} parameter. As A_{root} approaches zero the root distribution, and hence the transpiration, becomes more uniformly distributed with depth in the soil profile. The sensitivity analysis considered evaluation of a root mass distribution quantified as $A_{root} = 0.5$, corresponding to a higher root mass density deeper down the soil profile (a more even root distribution over depth than in the original model), and a root mass distribution given by $A_{root} = 2$, corresponding to a higher root mass density in the uppermost part of the soil profile. The original A_{root} value was set to 1.

Interception is defined as the process whereby precipitation is retained on the leaves, needles, branches, and stems of vegetation. The amount of precipitation, which can be intercepted by the vegetation canopy is determined by multiplying the interception capacity, C_{int}, by the leaf area index, LAI. The intercepted water evaporates without adding to the moisture storage in the soil. For the interception coefficient, C_{int}, a sensitivity analysis was made, in which the values were reduced by a factor 2. The effects of this change were very small and no changes were made to the model setup. In the same way, a sensitivity analysis was made of the leaf area index LAI, in which the values were reduced by a factor 2. Also in this case the effects were very small and did not lead to changes in the model.

4.3.6 Reduction of the potential evapotranspiration

During the calibration procedure it was discovered that the potential evapotranspiration (PET) values used so far were not in accordance with the latest data delivery. The model was therefore updated with the new values. The new PET values were higher than the previous ones, which lead to a decrease in the runoff.

Since none of the sensitivity analyses of the vegetation or soil parameters indicated that it was possible to reach a satisfying agreement between measured and calculated values just by changing these parameters (within physically realistic intervals), it was concluded that a sensitivity analysis with reductions of the new potential evapotranspiration values should be performed. It was estimated that a reduction by approximately 5–10% was reasonable.

The sensitivity was investigated in three simulations with 5%, 7.5% and 10% PET reductions, respectively. Figures 4-23 and 4-24 show examples of surface water discharges with the different reductions. The difference between the simulation cases with 7.5% and 10% reductions is not very large, whereas the case with the 5% reduction still showed too small discharges. Therefore, the model was updated with the new PET values reduced by 7.5%.

With the changes discussed above introduced to the model, the base case resulting from the surface water calibration was set. Figures 4-25 to 4-36 show results from the calibrated surface water model; in the following this model is referred to as *Basecase surface water*.

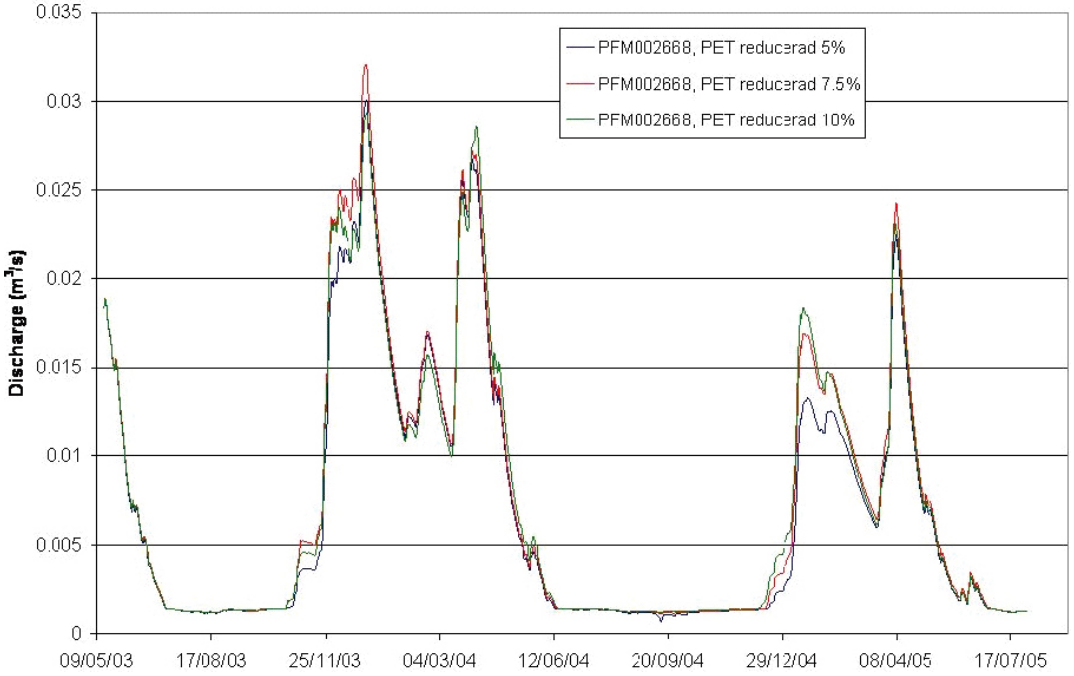

Figure 4-23. *Surface water discharges at PFM002668 (Lake Eckarfjärden) for different PET reductions (blue line: 5% reduction, red line 7.5% reduction, green line: 10% reduction).*

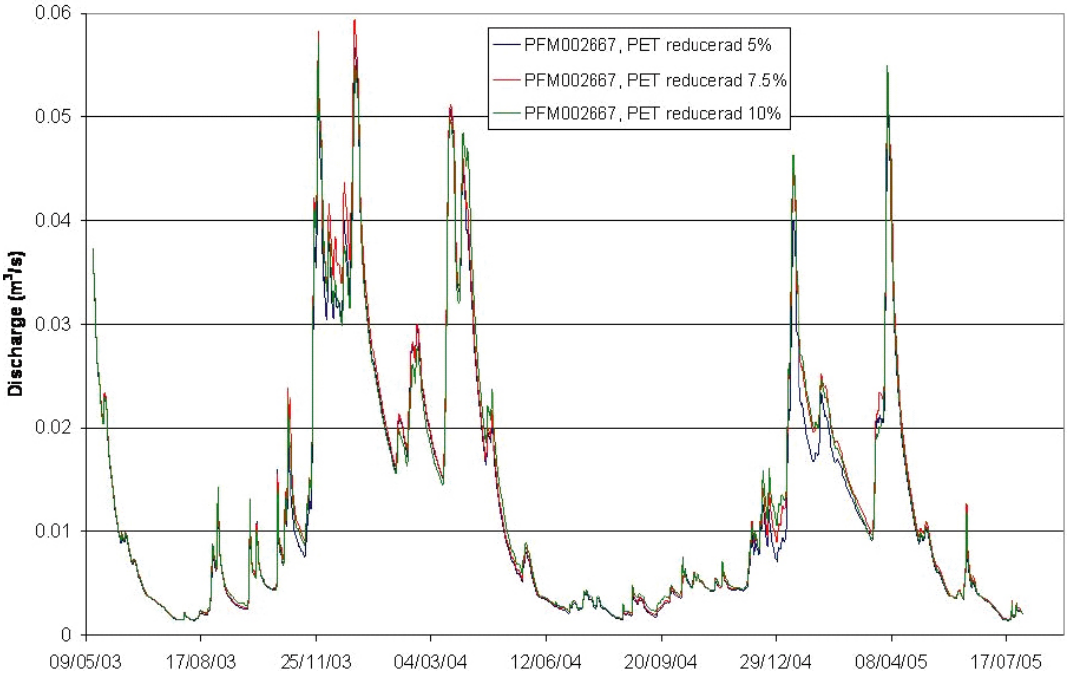

Figure 4-24. *Surface water discharges at PFM002667 (Lake Stocksjön) for different PET reductions (blue line: 5% reduction, red line 7.5% reduction, green line: 10% reduction).*

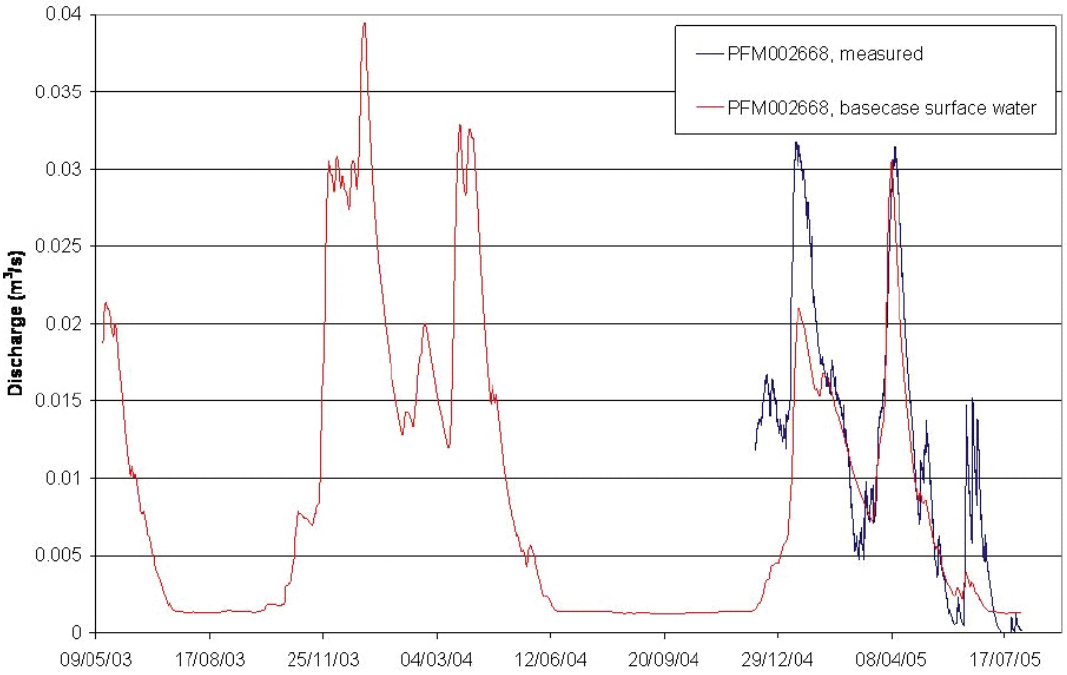

Figure 4-25. *Calculated surface water discharges from Basecase surface water compared to measurements at station PFM002668 (Lake Eckarfjärden).*

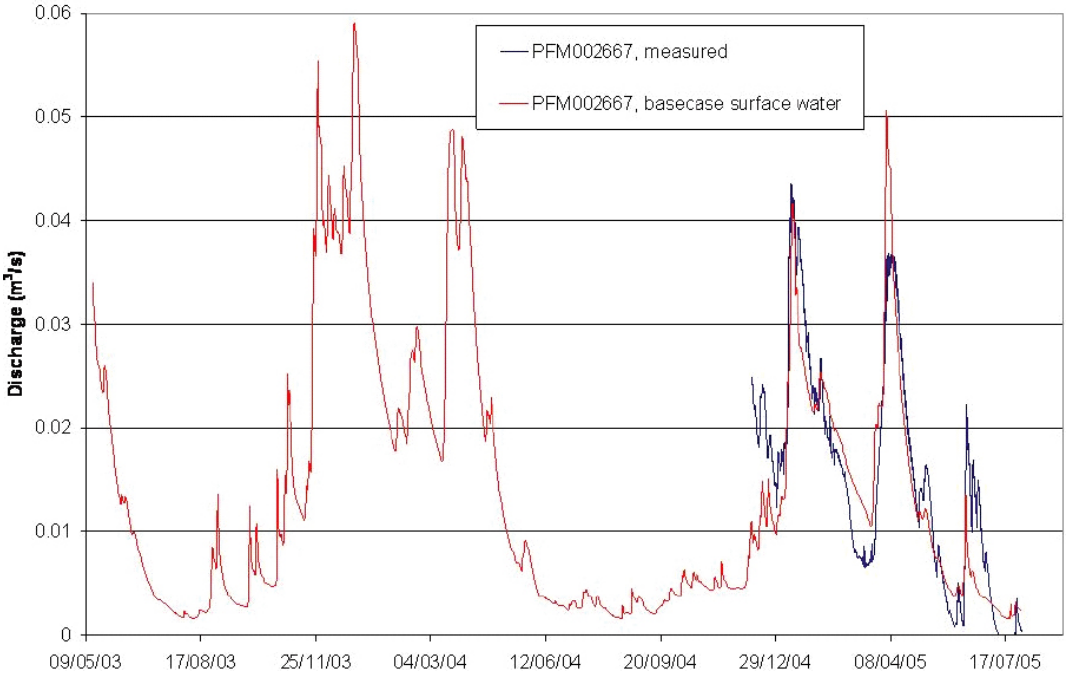

Figure 4-26. *Calculated surface water discharges from Basecase surface water compared to measurements at station PFM002667 (Lake Stocksjön).*

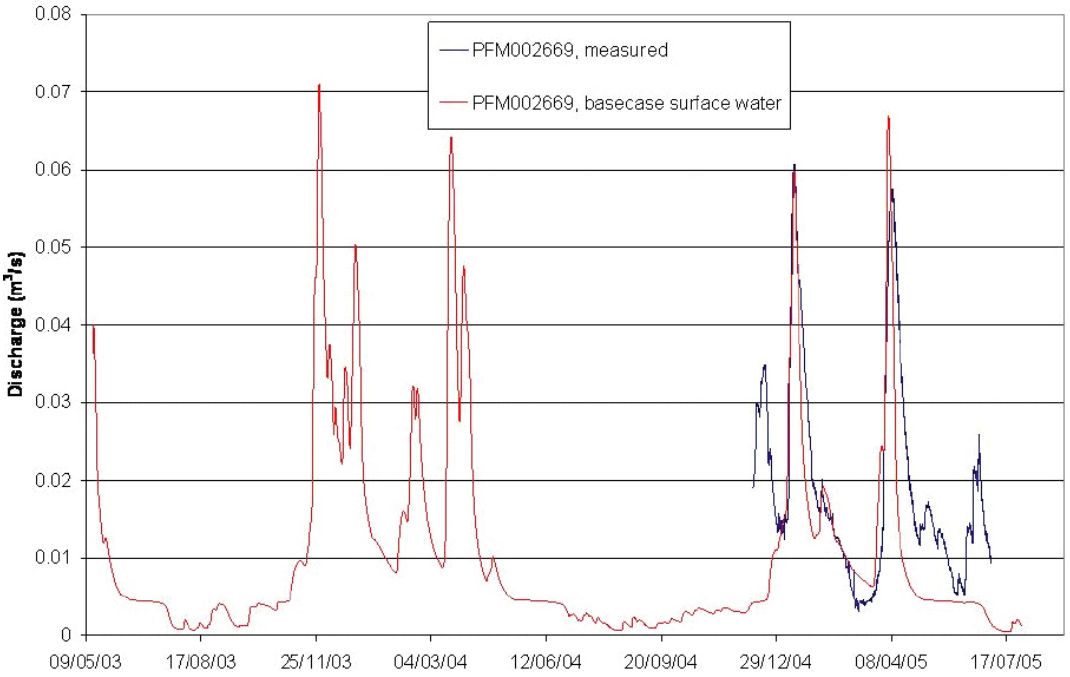

Figure 4-27. *Calculated surface water discharges from Basecase surface water compared to measurements at station PFM002669 (Lake Gunnarsboträsket).*

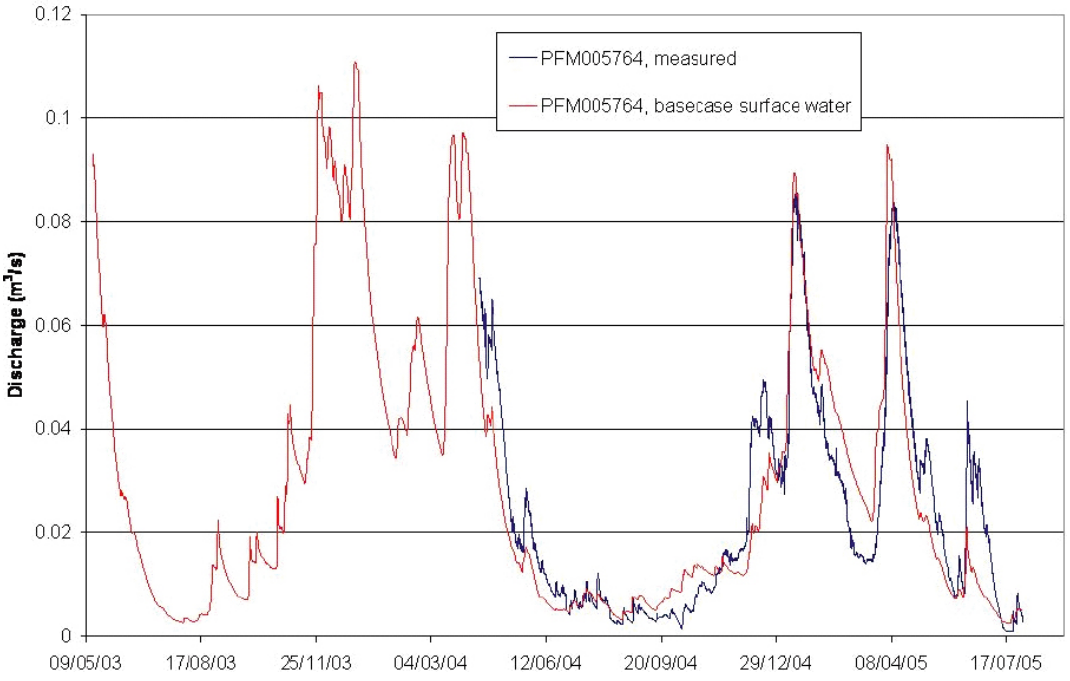

Figure 4-28. *Calculated surface water discharges from Basecase surface water compared to measurements at station PFM005764 (Lake Bolundsfjärden).*

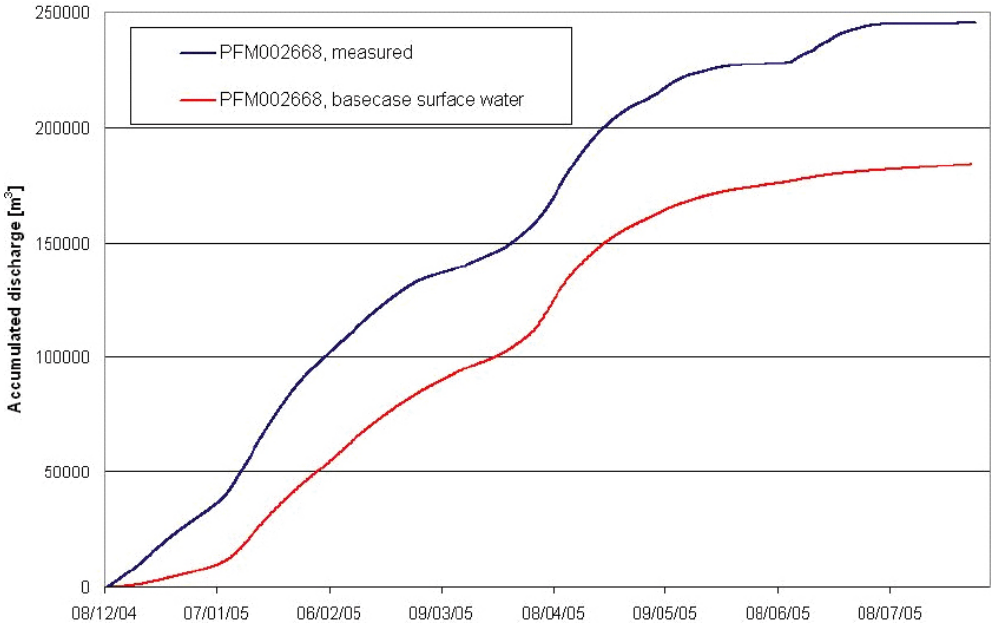

Figure 4-29. *Calculated accumulated discharges from Basecase surface water compared to measurements at station PFM002668 (Lake Eckarfjärden). At the end of the simulation, the calculated accumulated discharge is approximately 75% of the measured.*

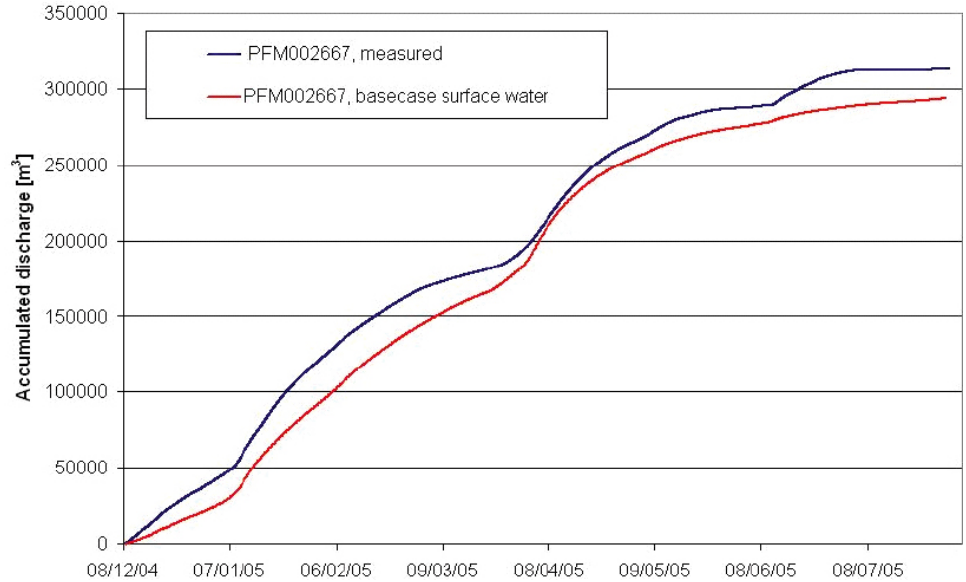

Figure 4-30. *Calculated accumulated discharges from Basecase surface water compared to measurements at station PFM002667 (Lake Stocksjön). At the end of the simulation, the calculated accumulated discharge is approximately 94% of the measured.*

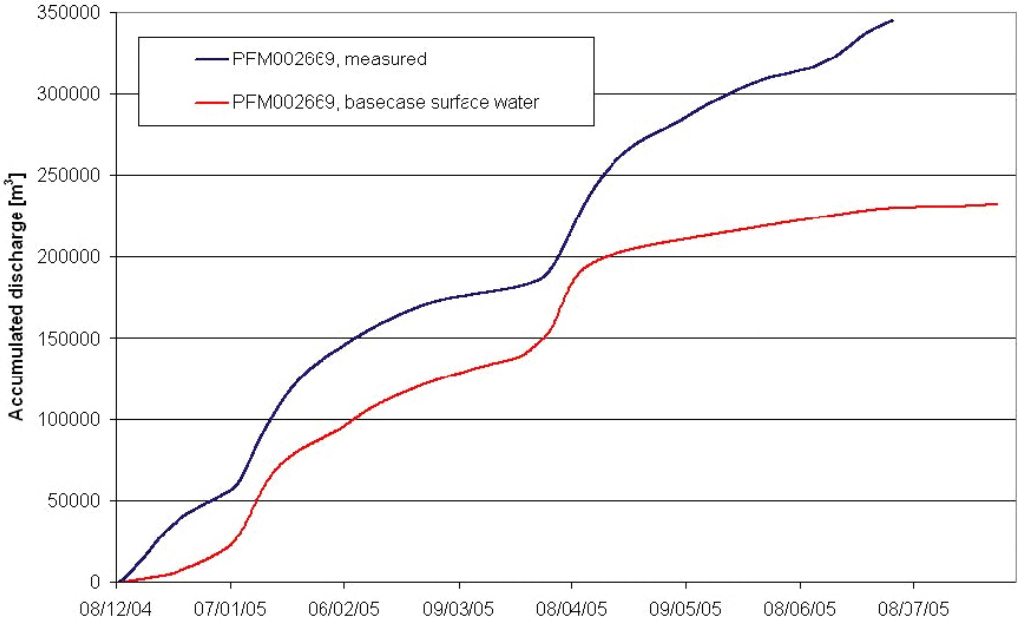

Figure 4-31. *Calculated accumulated discharges from Basecase surface water compared to measurements at station PFM002669 (Lake Gunnarsboträsket). At the end of the simulation, the calculated accumulated discharge is approximately 67% of the measured (measurements were only available until July 2, 2005, whereas the simulation ended July 31, 2005).*

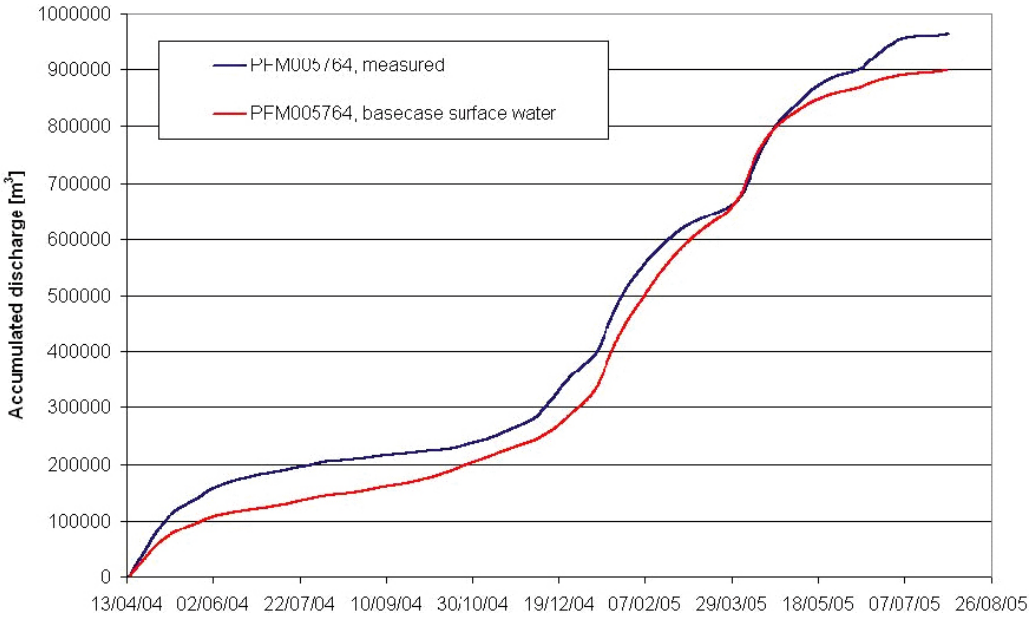

Figure 4-32. *Calculated accumulated discharges from Basecase surface water compared to measurements at station PFM005764 (Lake Bolundsfjärden). At the end of the simulation, the calculated accumulated discharge is approximately 93% of the measured.*

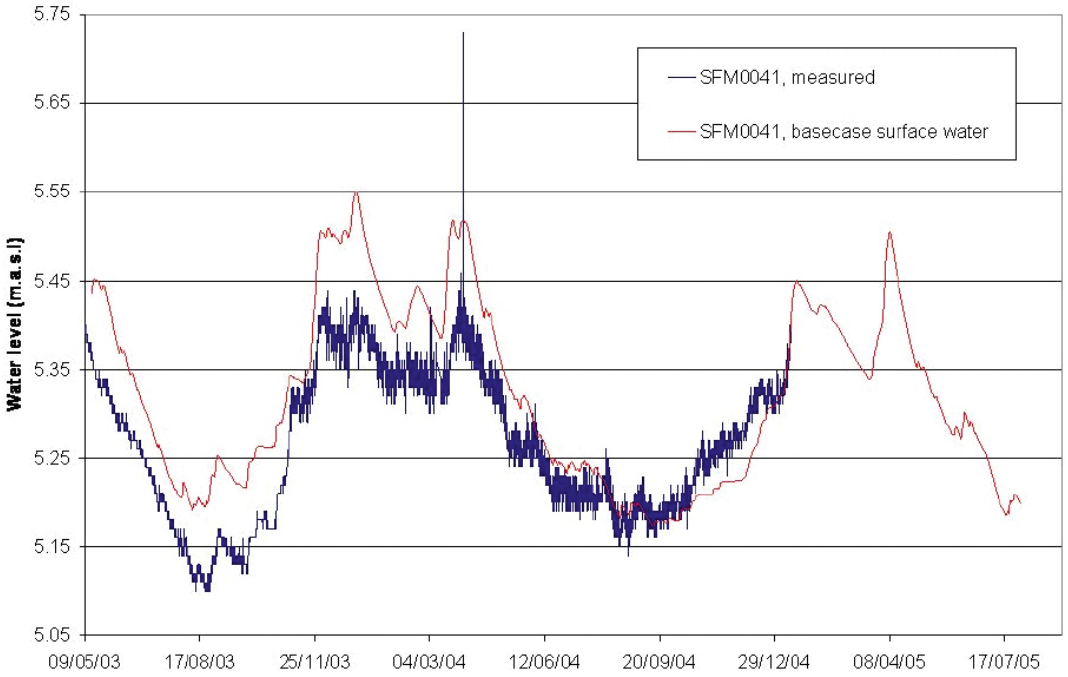

Figure 4-33. *Calculated surface water level from Basecase surface water compared to measurements at station SFM0041 (Lake Eckarfjärden).*

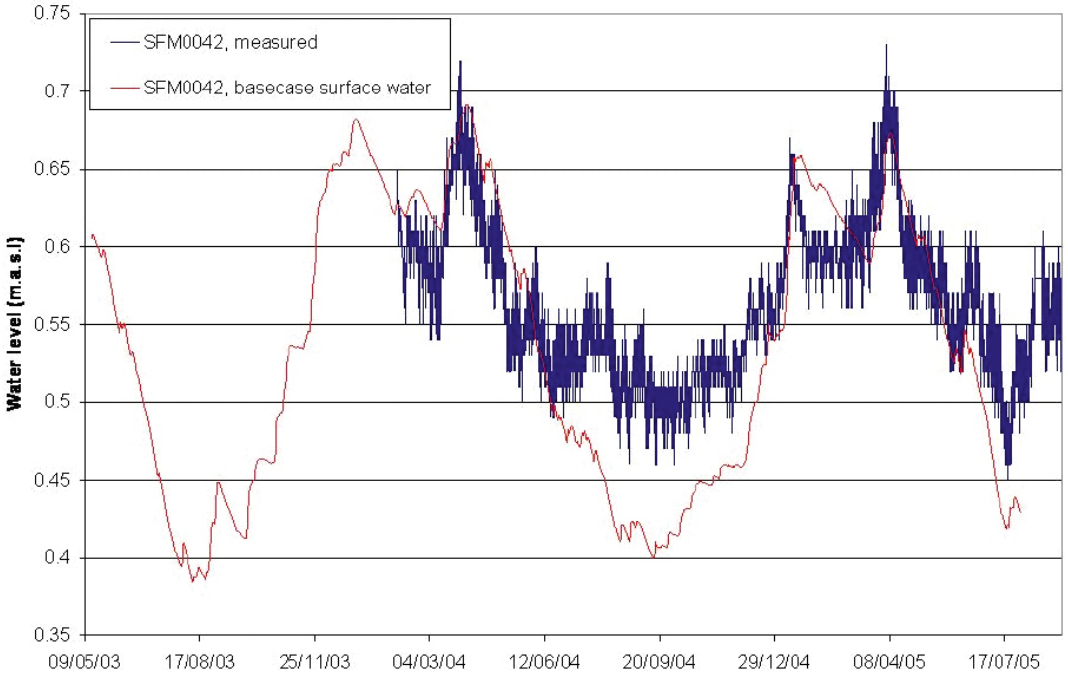

Figure 4-34. *Calculated surface water level from Basecase surface water compared to measurements at station SFM0042 (Lake Fiskarfjärden).*

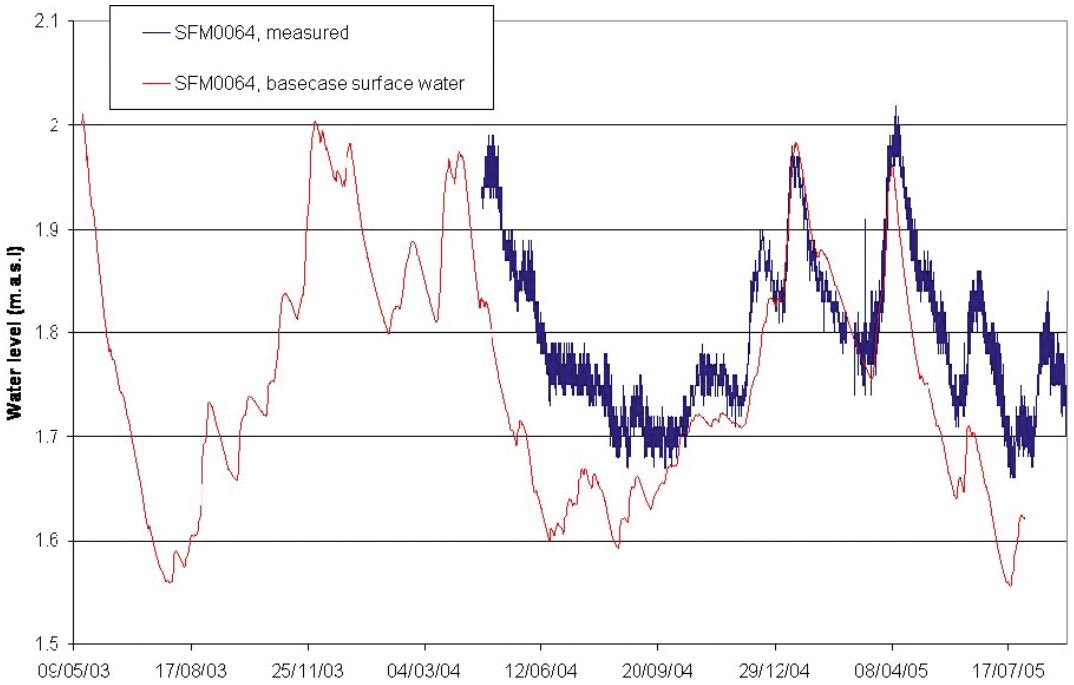

Figure 4-35. *Calculated surface water level from Basecase surface water compared to measurements at station SFM0064 (Lake Gällsboträsket).*

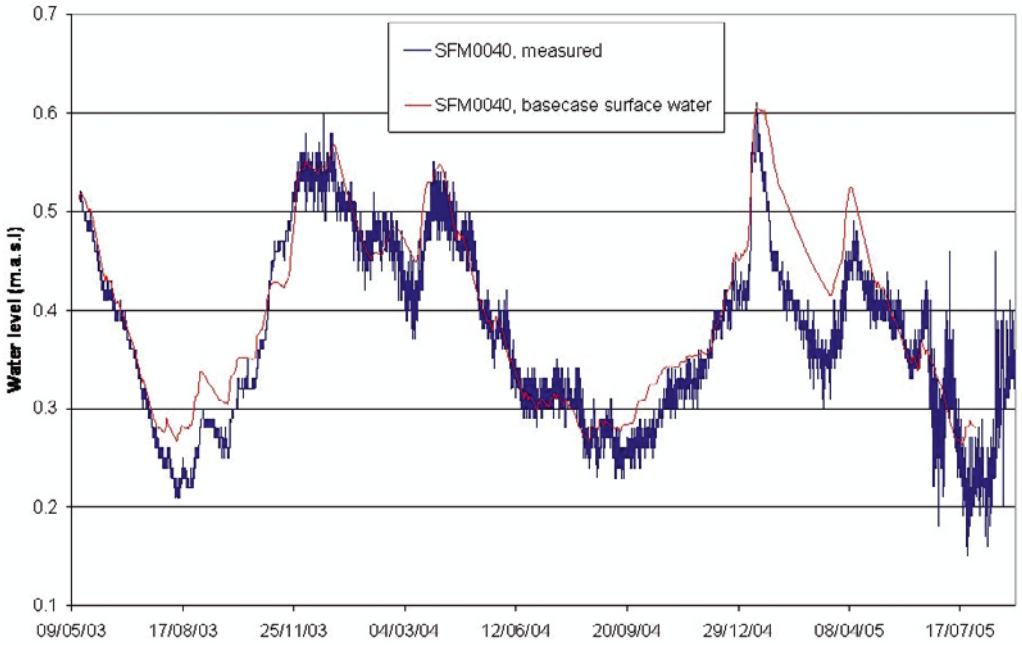

Figure 4-36. *Calculated surface water level from Basecase surface water compared to measurements at station SFM0040 (Lake Bolundsfjärden).*

4.3.7 Results from “Basecase surface water”

Figures 4-25 to 4-28 show the modelled and measured surface water discharges in all the four measurement stations. The model does not capture all the flow peaks in the measurements, but in general the agreement between simulation and measurements is good. Figures 4-29 to 4-32 show the accumulated discharges for the four stations. There is still some lack of discharge in the Eckarfjärden and Gunnarsboträsket stations, although smaller than with the initial model setup. Figures 4-33 to 4-36 compare the modelled and measured surface water levels in the four monitored lakes.

Table 4-3 shows the mean absolute errors (MAE) and mean errors (ME) for each of the surface water monitoring points, and their improvement from the initial setup to *Basecase surface water*. For SFM0041 and SFM0042 the MAE values are higher for *Basecase surface water* than they were for the initial simulation. However, a comparison between Figure 4-11 and Figure 4-33 shows that *Basecase surface water* appears to give a better fit to the measurements although the MAE value is higher.

The errors in the surface water levels are generally very small. When comparing with the water level amplitude however, the relative errors are not negligible at all sites, e.g. at Lake Eckarfjärden (SFM0041).

The errors in the discharge are of the same magnitude when comparing to the monitored amplitudes. The relative errors are possibly even smaller for the discharges. Both levels and discharge at Lake Bolundsfjärden, which is the most downstream monitoring station, present excellent agreement.

Table 4-3. Mean errors compared to measurements for an initial simulation compared to Basecase surface water.

Monitoring point	Initial simulation		Basecase surface water	
Surface water level	MAE (m)	ME (m)	MAE (m)	ME (m)
SFM0041	0.045	–0.008	0.074	–0.067
SFM0042	0.032	0.025	0.046	0.021
SFM0040	0.047	0.005	0.027	–0.019
SFM0064	0.090	0.089	0.088	0.082
Surface discharge				
PFM002668	0.0073	0.0066	0.0043	0.0032
PFM002667	0.0071	0.0054	0.0042	0.0011
PFM002669	0.0122	0.0112	0.0086	0.0064
PFM005764	0.0084	0.0053	0.0072	0.0020

4.4 Groundwater head elevations in Quaternary deposits

4.4.1 Sensitivity analysis of the till hydraulic conductivity

Because most of the area is covered by a till layer, it is important to perform a sensitivity analysis of the conductivity of the till layer and this was the first step taken in the calibration process of the groundwater head elevations in the Quaternary deposits. In the original model set-up the till was described isotropically. In all five sensitivity cases an anisotropic relation is introduced because it is more realistic to believe that the vertical conductivity is smaller than the horizontal. Results from sensitivity analyses during the pre-modeling phase also indicate the necessity of anisotropic hydraulic conditions /Aneljung and Gustafsson 2007/.

In all simulated cases the anisotropic ratio is 10, where the horizontal conductivity is 10 times larger than the vertical. Table 4-4 summarizes the till conductivity sensitivity cases. The hydraulic conductivity variations are described relative to the conductivities used in *Basecase surface water*.

Figures 4-37 to 4-42 show results from the sensitivity cases K_{till}·5 and K_{till}/5 compared to results from the *Basecase surface water* simulation, and from measurements in six of the groundwater monitoring points. The results are illustrated for the points in which the differences between *Basecase surface water* and the sensitivity simulations were noticeable. In many points the differences were very small.

In five of the six figures shown below, the sensitivity simulation K_{till}·5 gave the best results. When evaluating the mean absolute error (MAE) with regard to all groundwater monitoring points in Quaternary deposits and all surface water measurement points, it was also shown that the simulation K_{till}·5 resulted in the lowest mean errors. As a result, the hydraulic conducitivies in the till were changed in accordance with simulation case K_{till}·5, i.e. the horisontal conductivities were increased by a factor of 5 and the vertical conductivities were reduced by a factor of 2.

Table 4-4. Description of sensitivity cases; K_h and K_v are the horizontal and vertical hydraulic conductivities in *Basecase surface water*, respectively.

Simulation name	Horisontal hydraulic conductivity	Vertical hydraulic conductivity
$K_{till} \cdot 10$	$K_h \cdot 10$	K_v
$K_{till} \cdot 5$	$K_h \cdot 5$	$K_v/2$
K_{till}	K_h	$K_v/10$
$K_{till}/5$	$K_h/5$	$K_v/50$
$K_{till}/10$	$K_h/10$	$K_v/100$

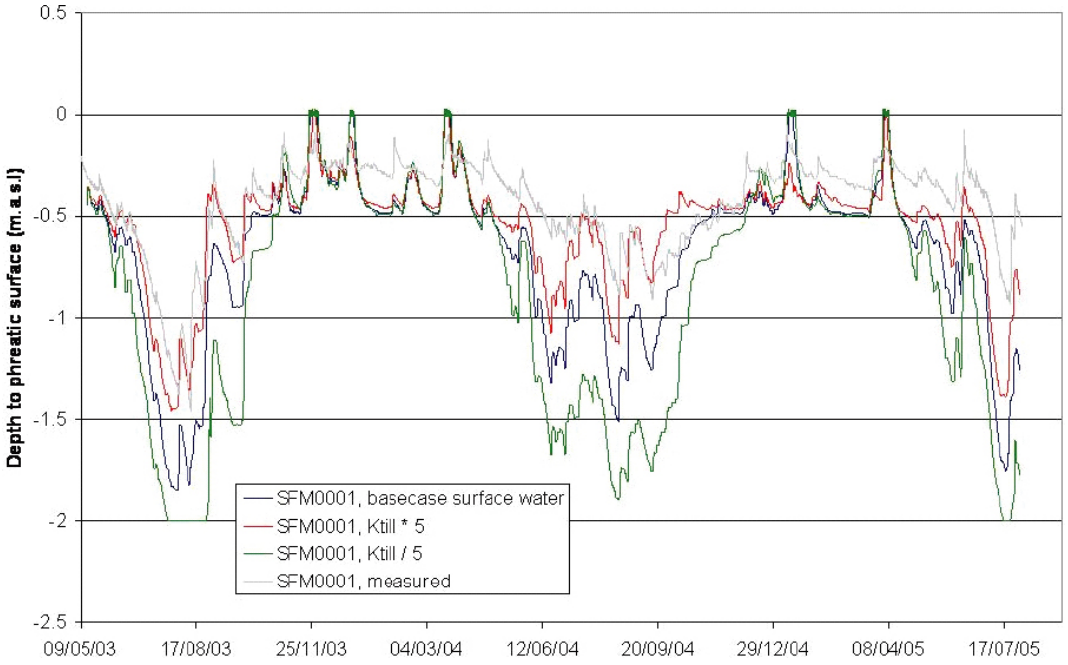

Figure 4-37. *Measured and calculated head elevations in SFM0001; results for Basecase surface water and sensitivity cases $K_{till} \cdot 5$ and $K_{till}/5$ are shown in the figure.*

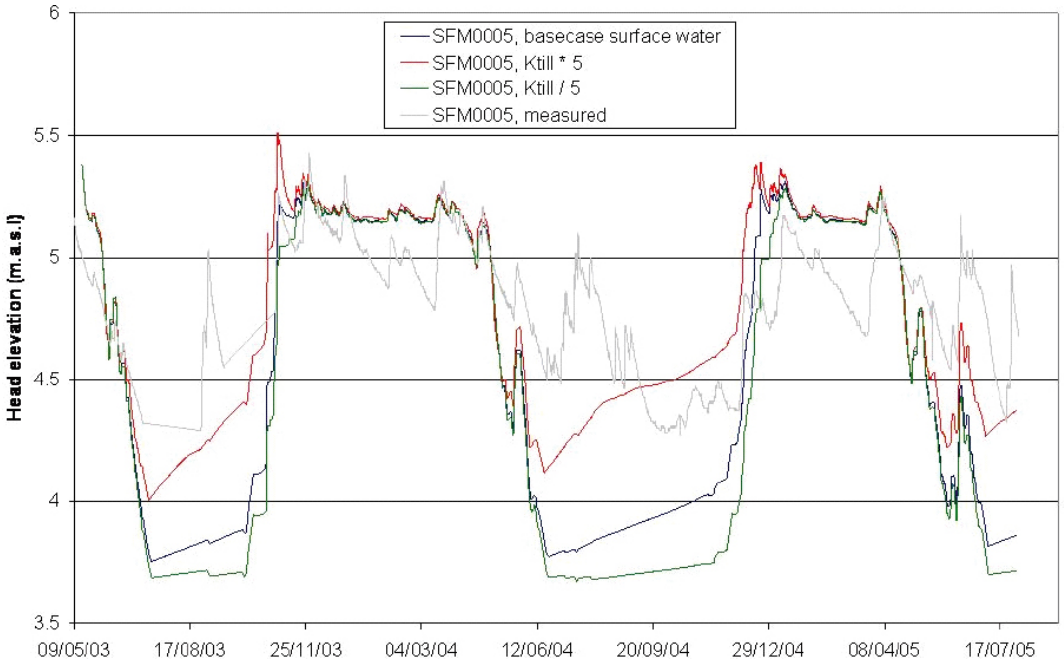

Figure 4-38. *Measured and calculated head elevations in SFM0005; results for Basecase surface water and sensitivity cases $K_{till} \cdot 5$ and $K_{till}/5$ are shown in the figure.*

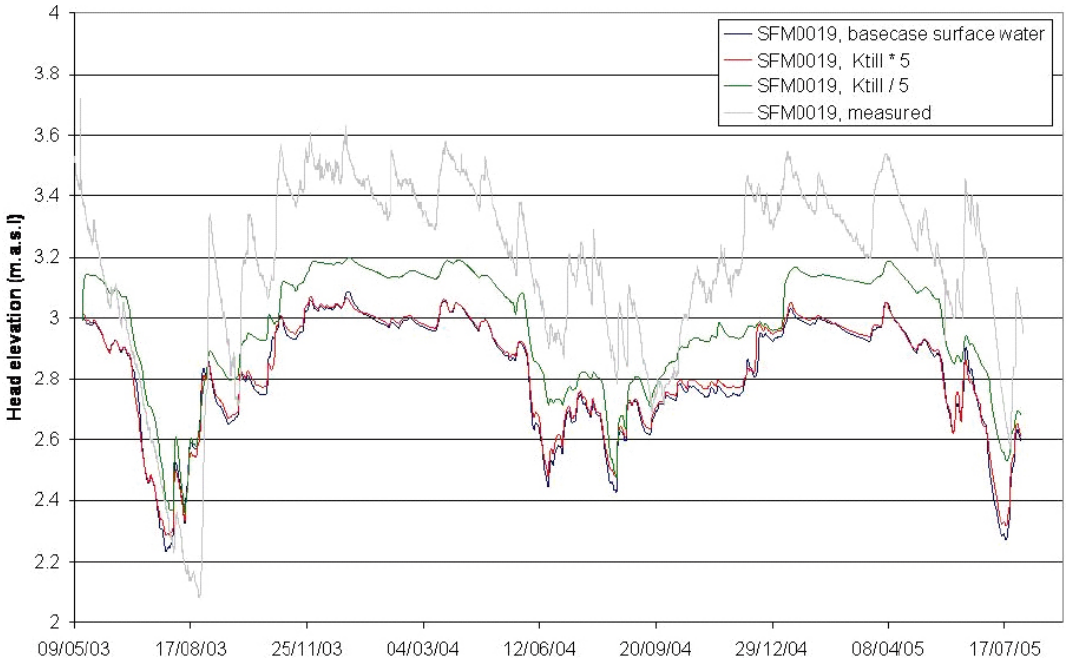

Figure 4-39. *Measured and calculated head elevations in SFM0019; results for Basecase surface water and sensitivity cases $K_{till} \cdot 5$ and $K_{till}/5$ are shown in the figure.*

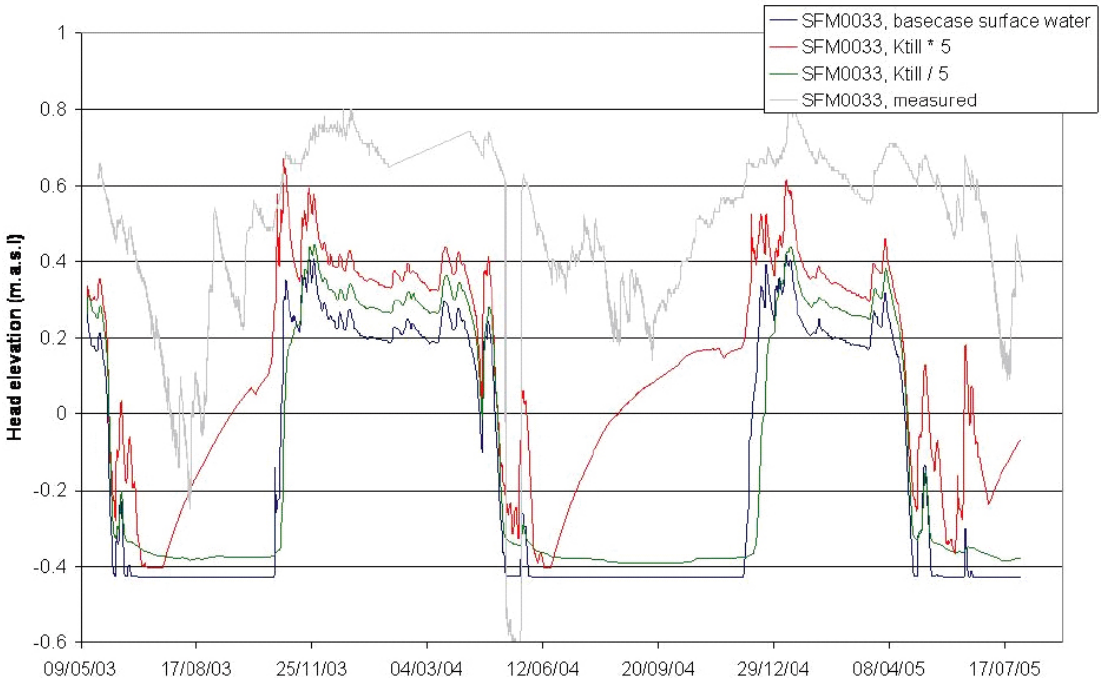

Figure 4-40. *Measured and calculated head elevations in SFM0033; results for Basecase surface water and sensitivity cases $K_{till} \cdot 5$ and $K_{till}/5$ are shown in the figure.*

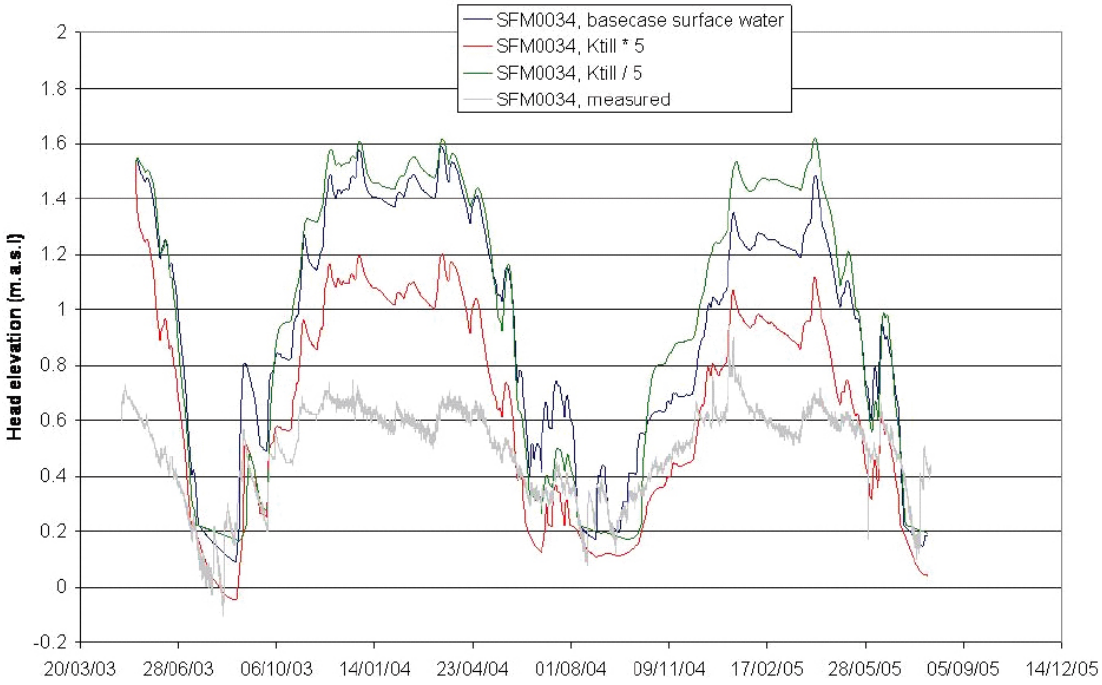

Figure 4-41. *Measured and calculated head elevations in SFM0034; results for Basecase surface water and sensitivity cases $K_{till} \cdot 5$ and $K_{till}/5$ are shown in the figure.*

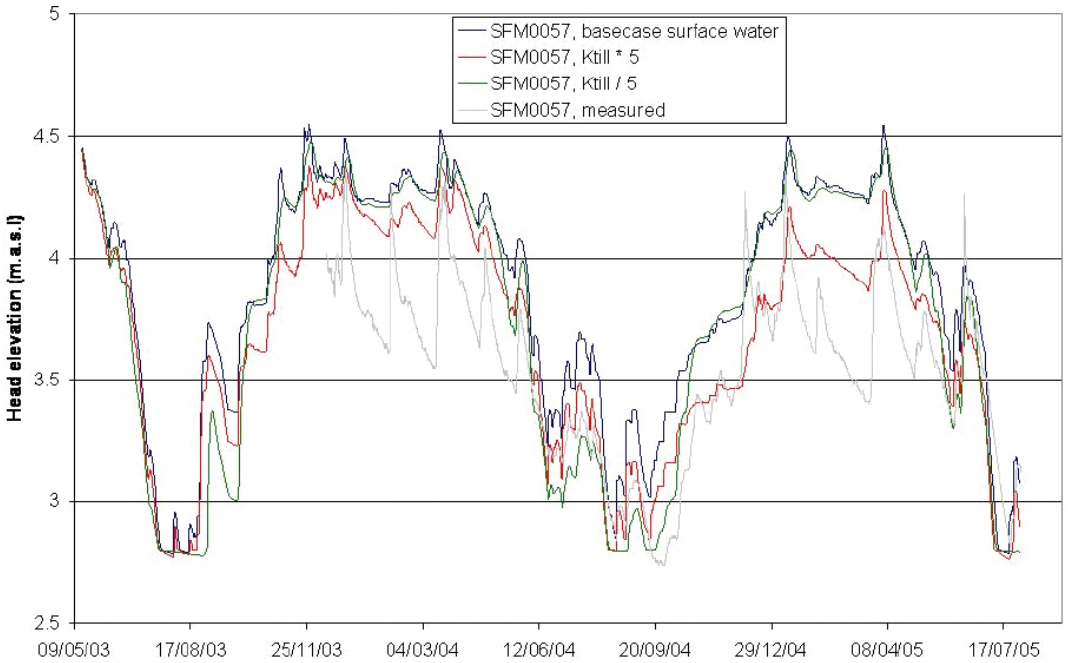

Figure 4-42. *Measured and calculated head elevations in SFM0057; results for Basecase surface water and sensitivity cases $K_{till} \cdot 5$ and $K_{till}/5$ are shown in the figure.*

4.4.2 Sensitvity analysis of the properties of the upper rock

When evaluating results from the simulations, some problems were noted in areas located at local heights with no or a thin soil layer. Since the calculation layers differ from the geological layers, the parameters in each calculation layer are calculated as mean values of the values associated with the geological layers included. Because the evapotranspiration processes only takes place in the uppermost calculation layer, this layer must not be too thin.

For areas with a thin soil layer on the bedrock, the result of the averaging performed to obtain calculation layer parameters is that the mean conductivity values become too low. This is because the conductivity values of the bedrock layer dominate. The bedrock model obtained from ConnectFlow describes the bedrock up to 4 m below ground only. Thus, there is no layer describing the bedrock outcrops or areas with a thin QD layer in the ConnectFlow parameterisation. So far, the upper bedrock layer from the ConnectFlow model has been used for parameterisation in these areas. The lower level of this bedrock layer is 20 m.b.s.l.

Model results showed that the very low hydraulic conducitivty values, on the order of 10^{-10} m/s in some areas, in this upper bedrock layer generated incorrect groundwater levels in the cells very close to cells with bedrock outcrops. In reality, bedrock situated close to the soil surface is often more hydraulically conductive than deeper layers. To account for this in the model, a new geological layer was introduced in the model. Homogenous properties were assigned to this layer, which describes the uppermost bedrock. The lower level of this layer was set to 4 m.b.g.s. Thus, this geological layer is present from the ground surface down to 4 m.b.g.s. in areas with bedrock outcrops or a QD layer thinner than 4 m. The subdivision into calculation layers was not changed when introducing the new geological rock layer.

A sensitivity analysis of the hydraulic conductivities in the newly created surface bedrock layer was also performed. Two simulations were conducted with values of the hydraulic conductivity of $1{\cdot}10^{-6}$ m/s and $1{\cdot}10^{-7}$ m/s, respectively. The effects of changing the conductivity values in the surface bedrock layers were found to be small. Figures 4-43 to 4-45 show results from the monitoring boreholes where the most significant changes occurred. The mean absolute errors in the simulations differed very little. After these tests, the hydraulic conductivity of the upper bedrock was set to $1{\cdot}10^{-7}$ m/s in the model.

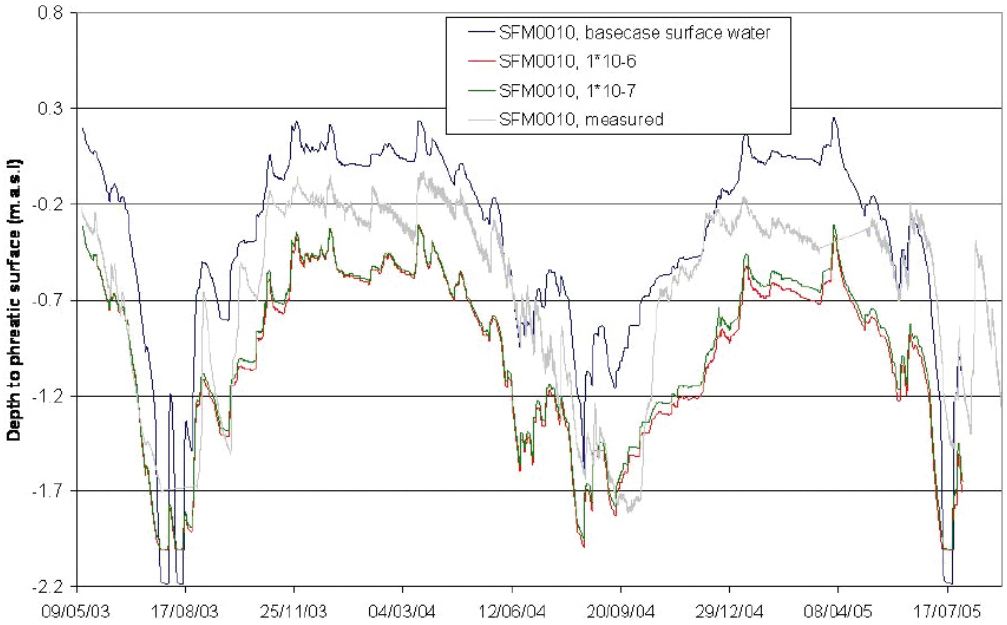

Figure 4-43. *Measured and calculated head elevations in SFM0010 showing the effects of implementing a surface bedrock layer and the sensitivity to its properties (the Basecase surface water model contains no such layer).*

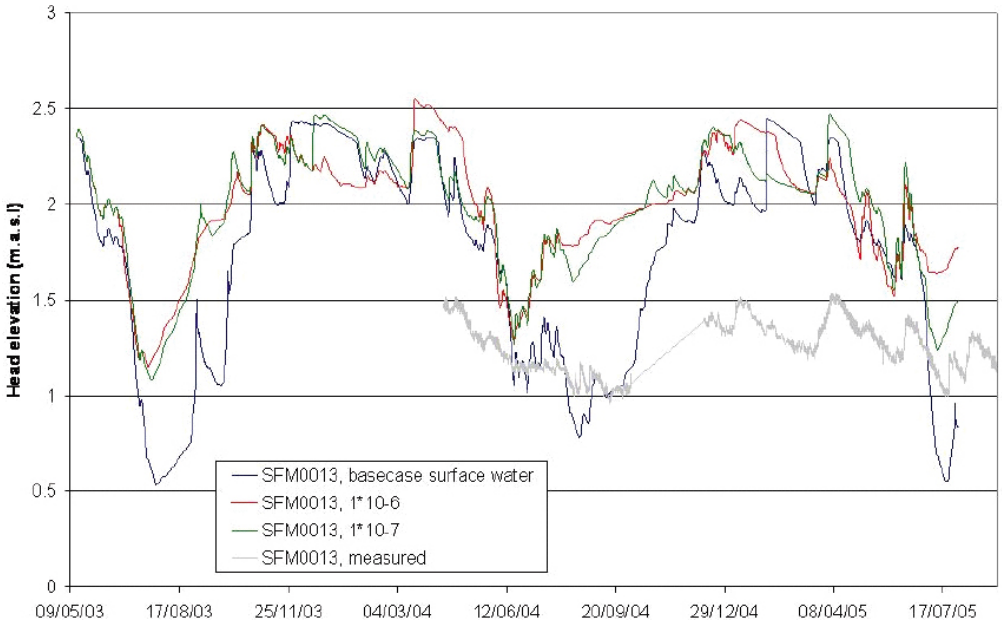

Figure 4-44. *Measured and calculated head elevations in SFM0013 showing the effects of implementing a surface bedrock layer and the sensitivity to its properties (the Basecase surface water model contains no such layer).*

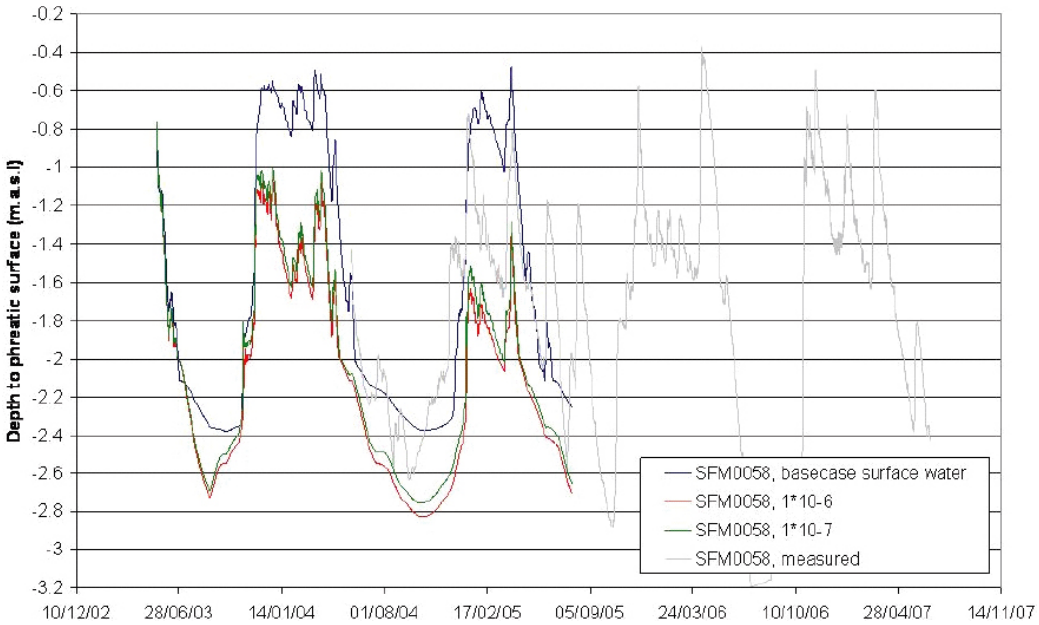

Figure 4-45. *Measured and calculated head elevations in SFM0058 showing the effects of implementing a surface bedrock layer and the sensitivity to its properties (the Basecase surface water model contains no such layer).*

4.4.3 Use of sub-domains in the hydraulic parametrisation

The sensitivity analysis of the till hydraulicconductivity and the unsaturated zone specific yield indicated that different monitoring points reacted differently on the tested parameter variations. In some areas, the results in the groundwater monitoring points were better with higher hydraulic conductivity values, and in some areas it was found that a higher specific yield gave better results. As a consequence, a subdivision of the model area was made in which the horizontal hydraulic conductivity was increased by a factor of 10 in the catchment of Lake Eckarfjärden and in the local height close to SFM0004, SFM0005 and SFM0009 (see Figure 4-46).

Since the K_h-values had already been increased by a factor of 5 based on the sensitivity analysis discussed in Section 4.4.1, this means that the original values were multiplied by a factor of 50 in these areas. In the same areas the unsaturated zone specific yield was increased with a factor 1.5. No parameter changes were made in other areas.

After the introduction of the surface bedrock layer and the division of the model area into sub-areas with different parameter setups, several groundwater monitoring points showed improved results. Figures 4-47 to 4-49 show examples of points for which the difference between calculated and measured values was reduced. Also, looking at the MAE-values quantifying the differences between calculated and measured heads, it is noted that the mean MAE for all monitoring wells in Quaternary deposits was reduced.

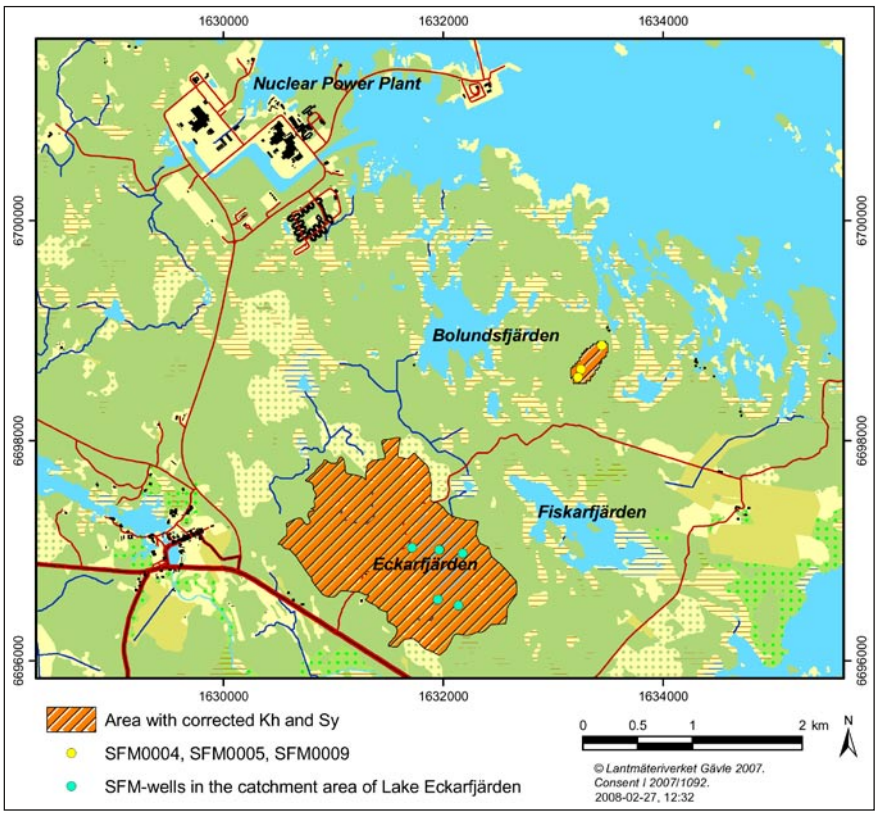

Figure 4-46. *Areas where K_h was multiplied by 10 and the specific yield in the unsaturated zone was increased by a factor of 1.5.*

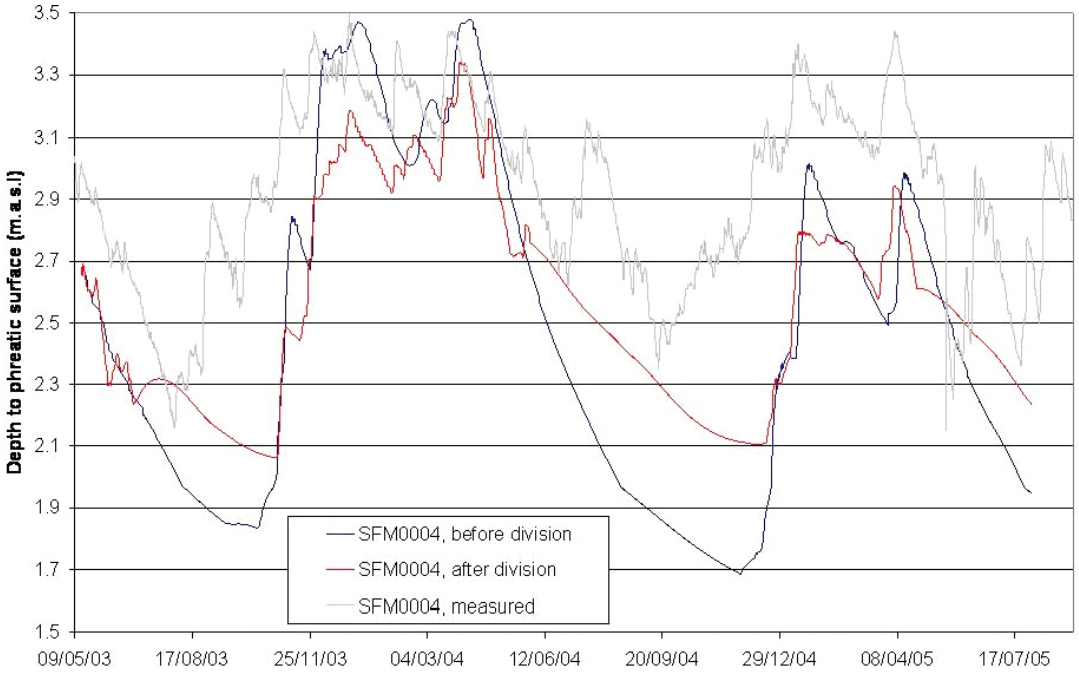

Figure 4-47. *Measured and calculated head elevations in SFM0004 showing effect of dividing the model area into sub-areas; in the sensitivity case, the K_h values in the catchment area of Lake Eckarfjärden were increased.*

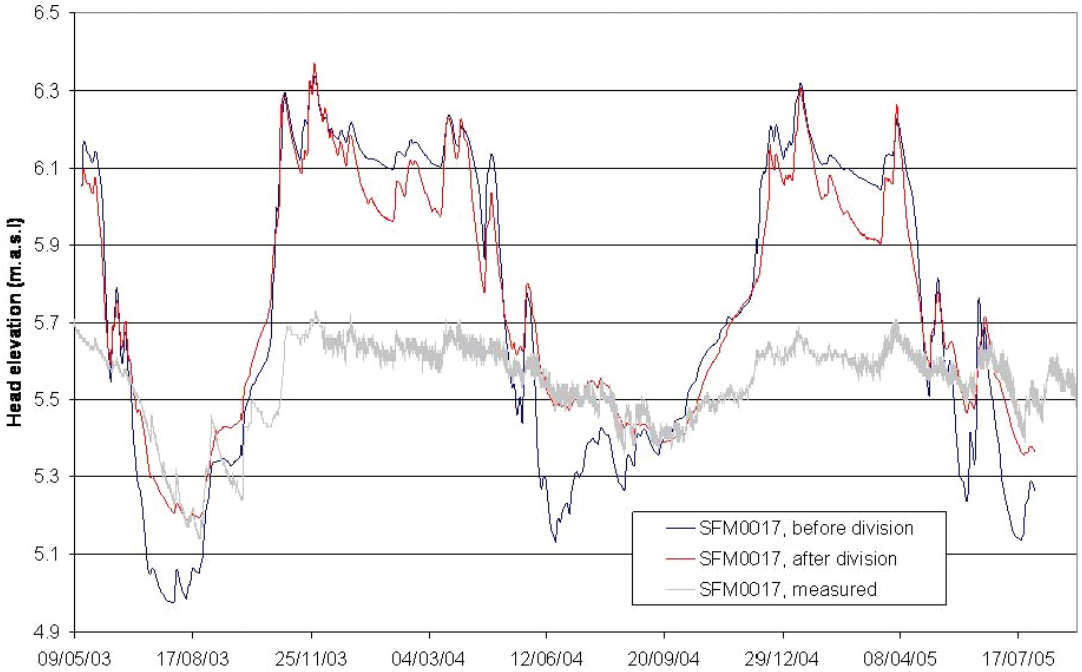

Figure 4-48. *Measured and calculated head elevations in SFM0017 showing effect of dividing the model area into sub-areas; in the sensitivity case, the K_h values in the catchment area of Lake Eckarfjärden were increased.*

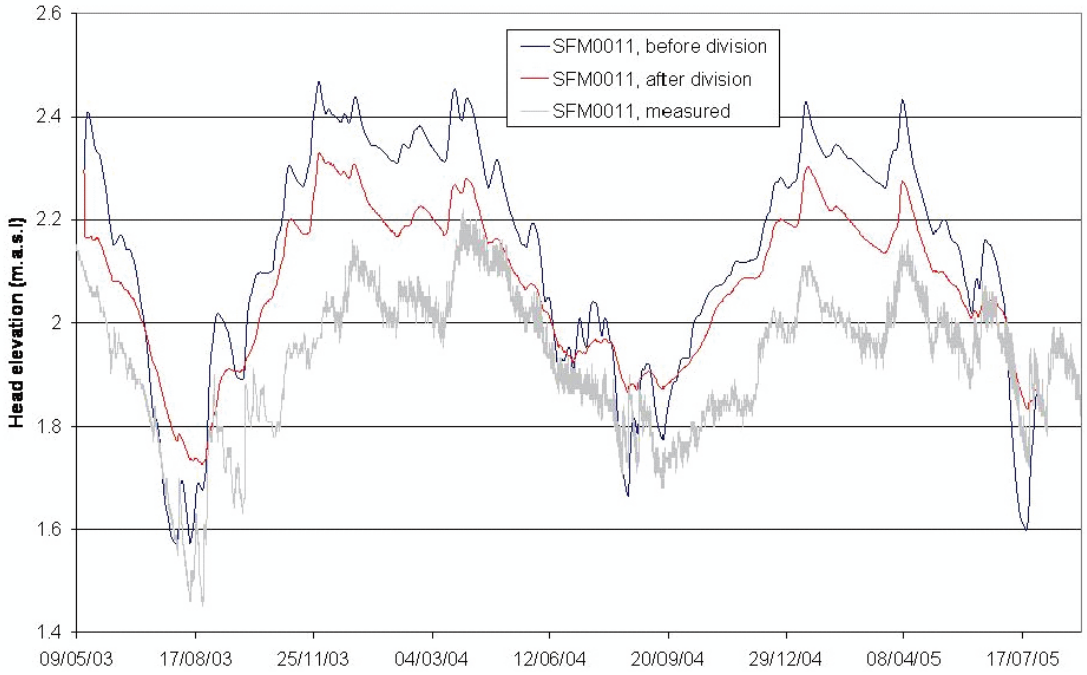

Figure 4-49. *Measured and calculated head elevations in SFM0011 showing effect of dividing the model area into sub-areas; in the sensitivity case, the K_h values in the catchment area of Lake Eckarfjärden were increased.*

4.4.4 Influence of using environmental head on the bottom boundary

At the bottom boundary of the model, head values obtained from the ConnectFlow modelling are used as boundary condition. In the original MIKE SHE model setup, the head values at the bottom boundary were so-called freshwater head values (FWH). This means that the fact that the water at lower levels has a higher density because of the increasing salt content with depth is not taken into account. In order to include the effects of the varying density in the modelling, environmental heads (EWH) have been calculated, see /Johansson 2008/ of these calculations, and used in the MIKE SHE model. The significance of the density effects was evaluated by compaing simulation results with these two types of head bottom boundary conditions.

The simulation results show that the effect of using environmental heads instead of freshwater heads is very small. For most groundwater monitoring points the resulting mean absolute errors differs only one or two centimeters. Only one of the boreholes (SFM0021) showed a slightly larger difference, which is illustrated in Figure 4-50.

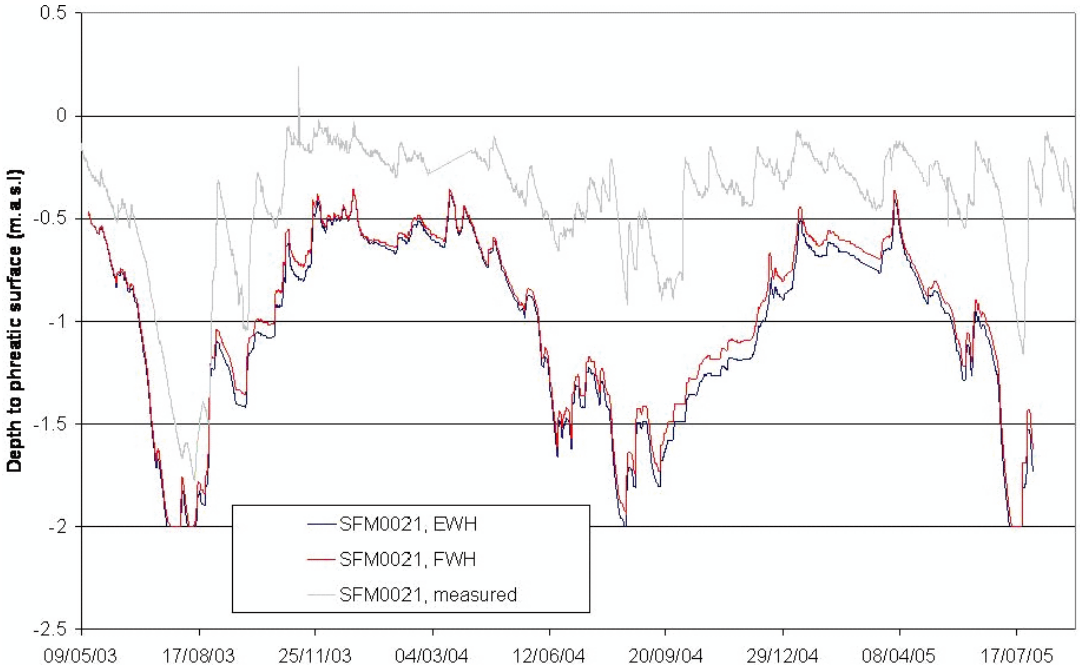

Figure 4-50. *Comparison of measured groundwater head in SFM0021 and simulation results for models using environmental water head (EWH) and freshwater head (FWH) at the bottom boundary.*

4.4.5 Definition of "Basecase groundwater"

After these sensitivity studies, the calibration of the head elevations in the Quaternary deposits was concluded. The main differences between *Basecase surface water* and the updated base case resulting from the groundwater level calibration are:

- introduction of anisotropy in the hydraulic conductivity of the till layers,
- vertical hydraulic conductivities in the till were reduced by a factor of 2 and horizontal conductivities increased by a factor of 5,
- introduction of a new surface bedrock geological layer with a higher hydraulic conductivity than the rock mass below it,
- division of the Quaternary deposits into subareas where different values of till conductivities and unsaturated specific yield were used in the model,
- introduction of environmental head values at the bottom boundary.

In the following, this updated model is referred to as *Basecase groundwater.*

4.5 Bedrock properties and bottom boundary conditions

Sensitivity analyses of the bottom boundary conditions in previous versions of the MIKE SHE model showed that the surface water dynamics and the near surface groundwater levels are more or less independent of the bedrock properties and the bottom boundary conditions, provided the model is deeper than approximately 100 m /Bosson and Berglund 2006/. With this in mind, the sensitivity analysis of the bottom boundary condition in the present modelling was performed late in the calibration process. The Forsmark 1.2 bedrock model was sparsely fractured and the conductivity values generally very low. The bottom boundary in the Forsmark 1.2 MIKE SHE model was located at 150 m.b.s.l., and a prescribed head calculated with the DarcyTools model /SKB 2005/ was set as bottom boundary condition in the MIKE SHE model.

The Forsmark 2.2 bedrock hydrogeology modelling was performed using ConnectFlow only /Follin et al. 2007/ (in the version 1.2 modelling both DarcyTools and ConnectFlow were used).

Based on the experience from the preceding modelling step, the bottom boundary condition in the present version of the MIKE SHE model was initially a prescribed head at 150 m.b.s.l. calculated with the ConnectFlow model. The original dataset of conductivity and porosity values and calculated heads from ConnectFlow delivered in August 2007 was based on preliminary modelling results. A new dataset was delivered at the time for the start of the calibration and sensitivity analysis of the bedrock properties and bottom boundary condition.

When processing this new dataset, some errors were found in the original data (delivered in August 2007). During the processing of the original data set, i.e. when implementing the ConnectFlow data to the MIKE SHE model, the vertical conductivity values in the upper bedrock became too high. This was probably due to errors in the calculation from the 20 m grid in Connect Flow to the 40 m grid used in MIKE SHE. No difference was found between the original and new calculated groundwater heads and porosities. Thus, the new data set used from this stage in the modelling process has in general a lower vertical conductivity, not only due to the updated data but also due to errors in the processing of the first data set which generated too high conductivity values. However, the Forsmark 2.2 bedrock model has considerably higher hydraulic conductivity values in the upper bedrock than the version 1.2 model and there are more fractures and high-conductive volumes in the model.

4.5.1 Effects of using the updated bedrock description

When implementing the new lower values of the vertical bedrock conductivity in the model, the vertical flow in the bedrock and the discharge in the water courses were reduced. The reduction of the discharge was not acceptable; the divergence between measured data and modelled values was too large. The lower conductivity values reduced the vertical flow in the bedrock and the transport from the bedrock system up to the surface was also reduced. In the base setup of the model, the high head at the bottom boundary, in combination with the relatively high vertical conductivity values, "pushed water up" to the surface water system. Since previous sensitivity calculations showed that the only way to generate a notably higher discharge in the water courses was to reduce the potential evapotranspiration, a calculation with a potential evapotranspiration reduced with 15% compared to the original data was performed. This calculation resulted in good results for the surface runoff. The following calculations were therefore executed with the new reduced potential evapotranspiration as input data.

The groundwater head elevation in the Quaternary deposits was not very sensitive to the new conductivity values in the bedrock, thus a new calibration of the SFM-wells was not needed. Table 4-5 presents the MAE and ME for each groundwater well in the Quaternary deposits. The mean error, ME, is defined such that a negative value means that the calculated values are higher than the simulated ones. There is an insignificant reduction of the average MAE for all the wells with 0.02 m. However, some wells are affected by the new lower bedrock conductivity values, but the majority in a positive way. The most distinct reduction of the MAE is seen in SFM0012 below Lake Gällsboträsket. Lake Gällsboträsket is underlain by a fracture zone. In the original model the conductivity values of this fracture zone were very high, up to 10^{-4} m/s, and the head at the bottom boundary was propagated through the bedrock system all the way up to the till. This resulted in a too high calculated head in SFM0012.

In Table 4-5, all the SFM-wells where the reduction of the MAE was 0.05 m or more are marked with green colour. The wells where the MAE values increased with 0.05 m or more are marked with red. It can be seen in the table that MAE decreased with more at least 0.05 m in eight wells and increased with 0.05 m or more in three wells.

Whereas the effects on the monitoring wells in QD are small, the lower vertical rock conductivity values have an impact on the groundwater head elevations in the bedrock. The flow resistance between the head bottom boundary and the surface is increased with the lower conductivity values and the head in the upper bedrock also increases. The calculated head in the bedrock was too high already with the original model, but the effect is reinforced by the new lower vertical conductivity values.

The mean absolute errors (MAE) for the monitoring wells in the bedrock (HFM-wells) are listed in Table 4-6. The HFM-wells are divided into sections with packers at different depths. The sections are numbered from the bottom of the borehole, i.e. HFM02_1 is situated below HFM02_2. The mean errors (ME) are not listed since all the calculated values for the HFM-wells are larger than the measured heads; this means that each ME value is equal to corresponding MAE, with a change of sign such that all ME are negative. The summary in Table 4-6 shows that the average MAE for all the HFM-monitoring wells increases with 0.17 m when implementing the new vertical conductivity values in the bedrock description.

Table 4-5. Mean absolute errors (MAE) and mean errors (ME) for the SFM-wells. MAE and ME are reported for *Basecase groundwater* and for a case with updated K-values in the bedrock (otherwise similar to *Basecase groundwater*). In green-marked wells MAE decreased with 0.05 m or more, and in red-marked ones MAE increased with 0.05 m or more.

SFM-well ID	Basecase groundwater		*Basecase groundwater* with updated bedrock K-values	
	MAE	ME	MAE	ME
Calculated heads				
SFM0003	0.20	–0.20	0.22	–0.21
SFM0004	0.37	0.37	0.23	–0.14
SFM0005	0.25	–0.01	0.22	–0.13
SFM0011	0.16	–0.16	0.18	–0.18
SFM0012	0.39	0.39	0.10	–0.10
SFM0013	0.65	–0.65	0.58	–0.58
SFM0014	0.24	–0.24	0.26	–0.25
SFM0015	0.09	–0.08	0.10	–0.09
SFM0016	0.14	–0.14	0.16	–0.16
SFM0017	0.31	–0.30	0.38	–0.37
SFM0022	0.03	–0.02	0.04	–0.02
SFM0023	0.05	–0.04	0.05	–0.04
SFM0026	0.35	–0.26	0.33	–0.05
SFM0033	0.33	0.28	0.31	0.26
SFM0034	0.29	–0.26	0.34	–0.33
SFM0036	0.24	–0.21	0.27	–0.26
SFM0039	0.05	–0.04	0.05	–0.04
SFM0057	0.23	–0.18	0.29	–0.27
SFM0062	0.07	0.06	0.07	0.06
SFM0065	0.19	–0.03	0.19	–0.05
SFM0066	0.12	0.03	0.12	0.04
Depths to phreatic surface				
SFM0001	0.13	0.09	0.13	0.07
SFM0002	0.31	0.31	0.26	0.25
SFM0009	0.43	0.43	0.36	0.34
SFM0010	0.33	0.31	0.34	0.32
SFM0018	0.19	–0.01	0.18	–0.07
SFM0019	0.41	–0.41	0.38	–0.38
SFM0020	0.16	–0.14	0.23	–0.22
SFM0021	0.60	0.60	0.45	0.45
SFM0028	0.14	–0.05	0.14	–0.05
SFM0030	0.62	0.56	0.54	0.46
SFM0049	0.20	–0.11	0.19	–0.07
SMF0058	0.46	0.46	0.34	0.34
Mean	**0.26**	**0.01**	**0.24**	**–0.04**

Table 4-6. Mean absolute errors (MAE) for the HFM-wells. MAE are reported for Basecase groundwater and for a case with updated K-values in the bedrock (otherwise similar to Basecase groundwater).

HFM-well ID	Basecase groundwater	*Basecase groundwater* with updated bedrock K-values
HFM02_1	1.57	1.66
HFM02_2	0.98	1.25
HFM02_3	0.97	1.24
HFM03_1	1.02	1.20
HFM03_2	1.01	1.91
HFM04_1	0.80	0.87
HFM04_2	0.67	0.88
HFM04_3	0.55	0.63
HFM10_1	1.31	1.50
HFM10_2	0.82	1.00
HFM11_1	0.61	0.31
HFM11_2	0.29	0.56
HFM15_1	1.34	1.41
HFM15_2	1.33	1.39
HFM20_2	0.98	1.16
HFM20_3	0.65	1.04
HFM20_4	1.47	1.27
Mean	**0.96**	**1.13**

The model resulting from the calibration to the heads measured in SFM-wells, *Basecase groundwater,* showed too high calculated heads in the bedrock independently of which set of vertical hydraulic conductivity values that was used as input. In the following text, *Basecase groundwater 2* refers to the model calibrated to the SFM-well heads, but with the updated version of the conductivity values in the bedrock.

4.5.2 Sensitivity analysis of the bottom boundary condition

A number of sensitivity cases were defined to analyse the effect of the bottom boundary condition on the heads in the HFM monitoring sections. Table 4-7 summarises the different sensitivity cases simulated in the analysis performed to investigate the effects of changing the bottom boundary condition. Since the rock in the upper 200 m of the bedrock is highly fractured, one case was defined where the bottom boundary was located at 250 m.b.s.l. At this depth the fracture frequency, and hence the hydraulic conductivity values, are lower.

Since the original bottom boundary condition generated higher calculated groundwater heads than those in the observed data, one case was defined where the calculated heads from the ConnectFlow model were lowered by 1 m. This was done for the land parts of the model area only. The calculated head below the sea was kept unchanged. Finally, two cases with no-flow bottom boundary conditions were also defined, one case where the model bottom boundary was located at 150 m.b.s.l. and one case where the model was extended to a level of 600 m.b.s.l.

Table 4-7. Sensitivity cases in the investigation of the bottom boundary condition. EWH stands for environmental water head; "EWH-1 m" denotes the case with calculated boundary EWH reduced by 1 m.

Sensitivity case	Bottom boundary condition	Lower level of bottom boundary (m.b.s.l.)
Sens_Boundary1	EWH-1 m	150
Sens_Boundary2	No-flow	150
Sens_Boundary3	EWH	250
Sens_Boundary4	No-flow	600

The results from the sensitivity analysis showed that the bottom boundary condition affects both the discharge in the water courses and the groundwater head elevation in the bedrock. The boundary condition mainly has an influence on the groundwater fluxes in the bedrock. The accumulated calculated and measured discharges for each discharge station are shown in Figures 4-51 to 4-54. The accumulated discharges for all sensitivity cases and stations are summarised in Table 4-8.

The groundwater head elevation in the bedrock is strongly affected by the bottom boundary condition, see Table 4-9. When the head is reduced (*Sens_Boundary1*), or when a no-flow boundary condition is used (*Sens_Boundary2* and *-4*), the groundwater head elevation in the bedrock decreases. The case where the bottom boundary is set at 250 m.b.s.l. (*Sens_Boundary3*) results in too high calculated groundwater heads.

The effect of the bottom boundary condition on the vertical flow is shown in Figure 4-55. The percolation from the unsaturated zone to the saturated zone is not influenced by the bottom boundary condition. The groundwater situation in the Quaternary deposits seems to be independent on the bottom boundary condition of the model. However, the vertical flow in the bedrock is strongly dependent on whether there is a no-flow or head boundary at the bottom of the model. The vertical groundwater flux in mm/year at the depth 150 m.b.s.l. is presented in Figure 4-55. In the calibrated model *Basecase groundwater 2*, the net vertical flow is 11 mm/year directed upwards. The corresponding net calculated flow at the same depth in ConnectFlow is almost zero, c. 1 mm up and c. 1 mm down. The result that is most similar to the calculated flux in ConnectFlow is obtained in the case where the model is extended to a depth of 600 m (*Sens_Boundary4*).

When all the results from the sensitivity analysis of the bottom boundary are summarized, the best results are achieved with the deep model with a no-flow boundary condition at 600 m.b.s.l. For the surface water discharge, *Sens_boundary1* generates the largest differences between model and measurements for all the discharge stations except from the station downstream Lake Stocksjön. *Sens_boundary2, -3 and -4* show acceptable accumulated discharges for all the stations. The groundwater head elevation in the HFM-wells shows the best agreement with measured data for *Sens_Boundary2*. However, for obvious reasons *Sens_Boundary2*, which has a no-flow boundary at 150 m.b.s.l., does not generate any flow at the –150 m level in the bedrock.

The vertical flow is of interest for the transport modelling, therefore a deep model with a no-flow boundary is preferable. According to the groundwater heads, *Sens_Boundary1* (EWH–1m) also shows better agreement with measured data than *Sens_Boundary4* (no-flow at 600 m.b.s.l.), but this case generates a too large vertical groundwater flux in the bedrock. The MAE for all the

HFM-wells is reduced from 1.13 m to 0.79 m for case *Sens_Boundary4*. Thus, *Sens_Boundary4* is considered to give acceptable results for the groundwater head elevation in the bedrock.

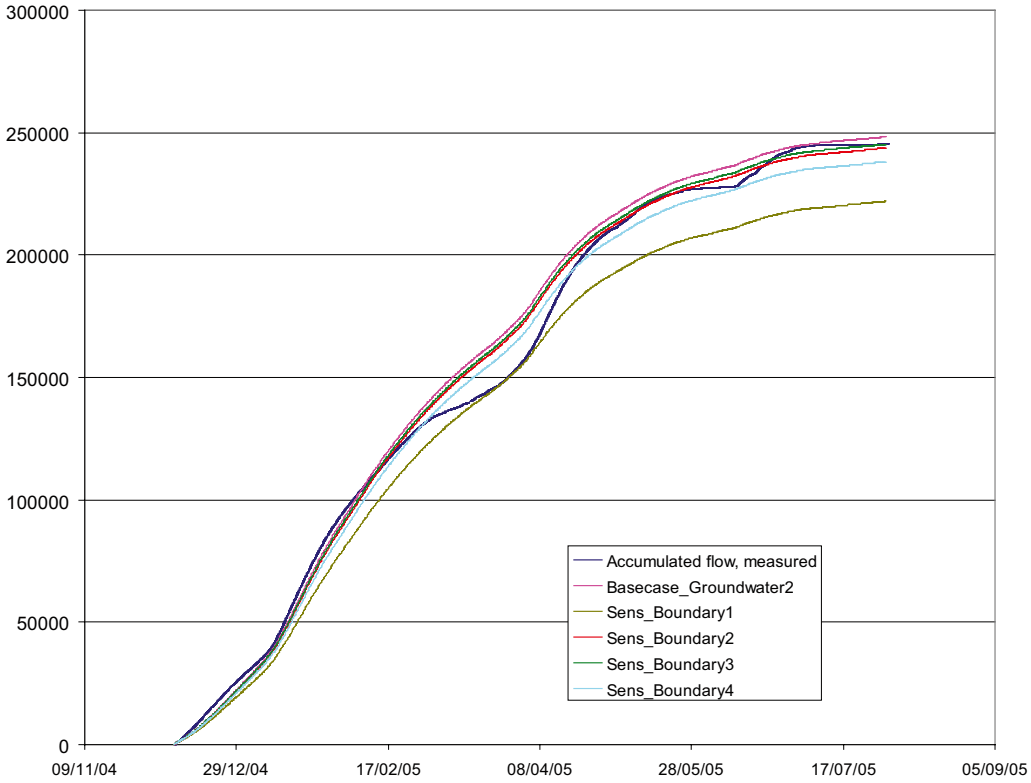

Figure 4-51. *Accumulated discharge (m^3) downstream Lake Eckarfjärden; measured data, Basecase groundwater 2 results, and the four bottom boundary sensitivity cases are shown.*

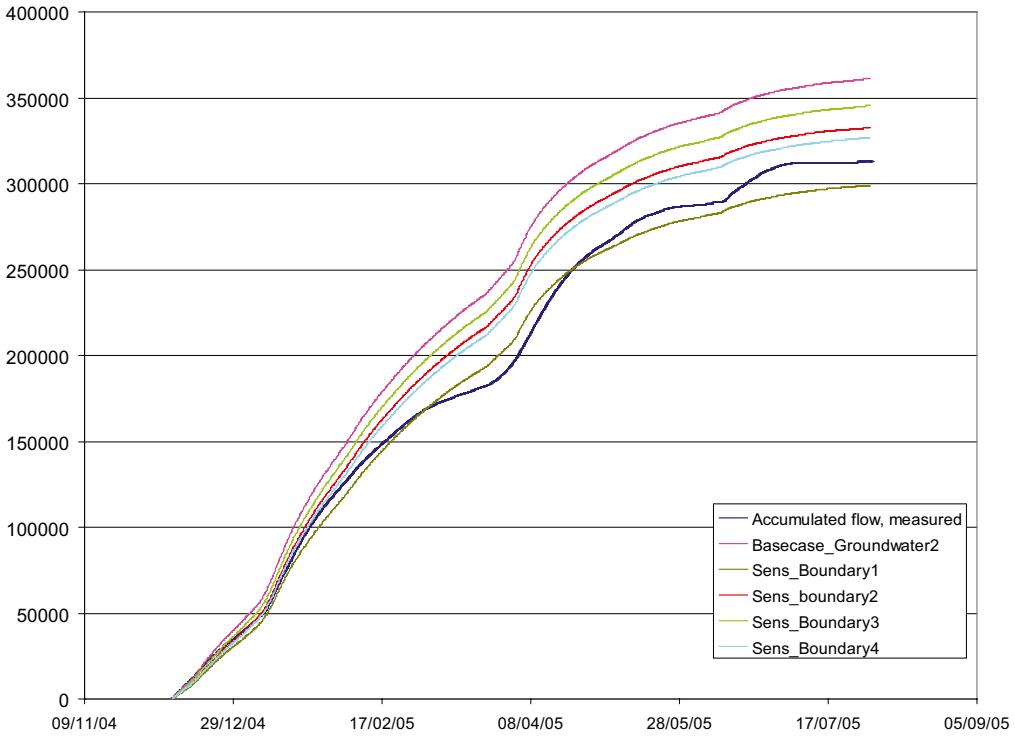

Figure 4-52. *Accumulated discharge (m^3) downstream Lake Stocksjön; measured data, Basecase groundwater 2 results, and the four bottom boundary sensitivity cases are shown.*

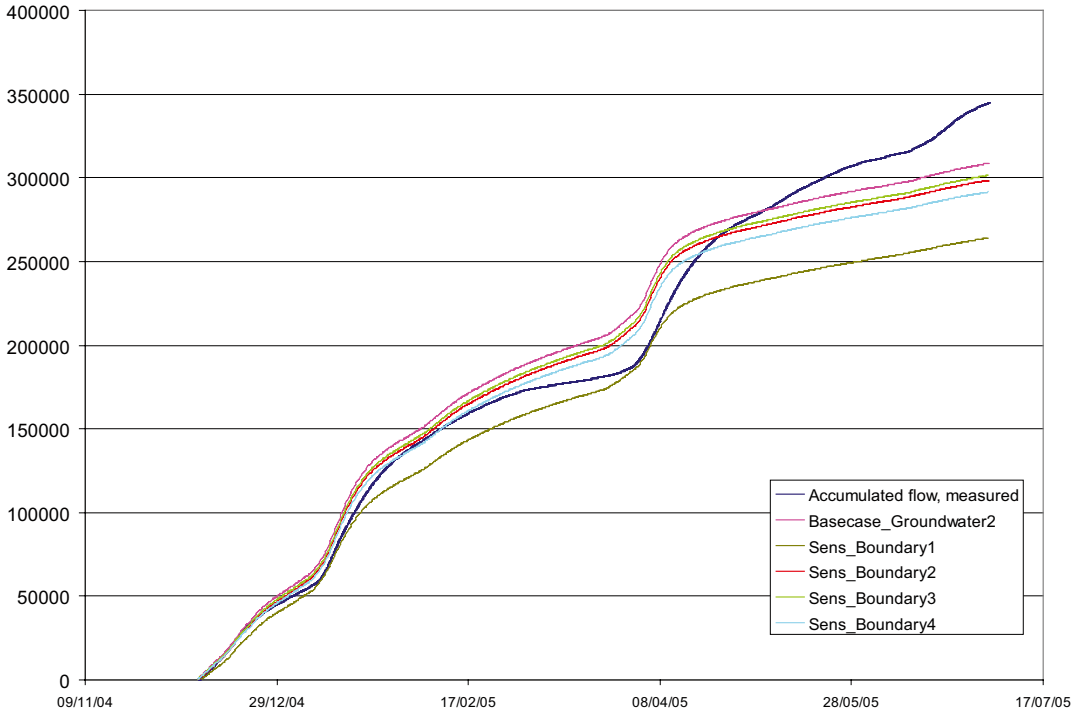

Figure 4-53. *Accumulated discharge (m^3) downstream Lake Gunnarsboträsket; measured data, Basecase groundwater 2 results, and the four bottom boundary sensitivity cases are shown.*

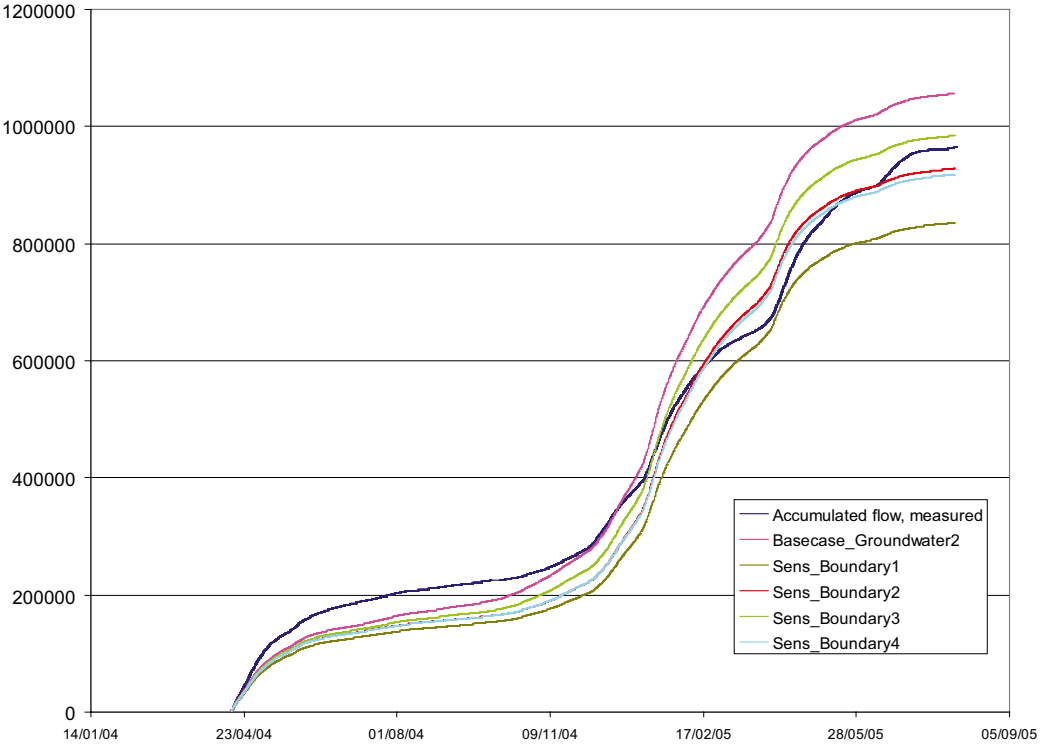

Figure 4-54. *Accumulated discharge (m^3) upstream Lake Bolundsfjärden; measured data, Basecase groundwater 2 results, and the four bottom boundary sensitivity cases are shown.*

Table 4-8. The differences between measured and calculated accumulated discharge for all sensitivity cases and discharge stations; the differences are expressed in %.

	PFM002668 L. Eckarfjärden	PFM002667 L. Stocksjön	PFM002669 L. Gunnarsboträsket	PFM005764 L. Bolundsfjärden
Basecase groundwater 2	+1	+13	–12	+9
Sens_Boundary1	–11	–5	–31	–15
Sens_Boundary2	0	+6	–15	+4
Sens_Boundary3	0	+10	–14	+3
Sens_Boundary4	–3	+5	–18	–5

Table 4-9. Mean absolute errors (MAE) in metres for SFM monitoring wells and HFM monitoring sections (with numbering starting from the bottom of the borehole) for the sensitivity cases testing the bottom boundary condition.

	Basecase_Groundwater, New K-values in the bedrock.	Sens_Boundary1	Sens_Boundary2	Sens_Boundary3	Sens_boundary4
Heads, SFM					
SFM0003	0.22	0.17	0.14	0.21	0.19
SFM0004	0.23	0.20	0.55	0.22	0.21
SFM0005	0.22	0.21	0.25	0.22	0.22
SFM0011	0.18	0.16	0.13	0.17	0.17
SFM0012	0.10	0.06	0.18	0.09	0.08
SFM0013	0.21	0.14	0.13	0.19	0.16
SFM0014	0.26	0.25	0.24	0.25	0.25
SFM0015	0.10	0.08	0.08	0.10	0.10
SFM0016	0.16	0.14	0.13	0.15	0.15
SFM0017	0.38	0.37	0.31	0.37	0.37
SFM0022	0.04	0.04	0.04	0.04	0.04
SFM0023	0.05	0.05	0.05	0.05	0.05
SFM0026	0.33	0.34	0.32	0.33	0.33
SFM0033	0.31	0.32	0.33	0.31	0.32
SFM0034	0.34	0.31	0.27	0.33	0.32
SFM0036	0.27	0.27	0.24	0.27	0.27
SFM0039	0.05	0.04	0.03	0.04	0.04
SFM0057	0.29	0.27	0.11	0.28	0.28
SFM0062	0.07	0.09	0.10	0.08	0.08
SFM0065	0.19	0.19	0.19	0.19	0.19
SFM0066	0.12	0.12	0.12	0.12	0.12
Depths to phreatic surface, SFM					
SFM0001	0.13	0.14	0.15	0.13	0.14
SFM0002	0.26	0.32	0.41	0.27	0.29
SFM0009	0.36	0.37	0.44	0.36	0.36
SFM0010	0.34	0.37	0.33	0.35	0.35
SFM0018	0.18	0.17	0.18	0.18	0.18
SFM0019	0.38	0.32	0.30	0.36	0.34
SFM0020	0.23	0.22	0.15	0.22	0.22
SFM0021	0.45	0.53	0.87	0.47	0.49
SFM0028	0.14	0.13	0.13	0.13	0.13

SFM0030	0.54	0.56	0.64	0.55	0.55
SFM0049	0.19	0.19	0.19	0.19	0.19
SFM0058	0.34	0.41	0.50	0.36	0.38
Mean, SFM	**0.23**	**0.23**	**0.25**	**0.23**	**0.23**
Heads, HFM					
HFM02_1	1.66	0.91	1.09	1.39	1.24
HFM02_2	1.25	0.97	0.75	1.17	1.11
HFM02_3	1.24	0.96	0.75	1.16	1.10
HFM03_1	1.20	1.01	0.84	1.14	1.10
HFM03_2	1.91	1.00	0.83	1.14	1.10
HFM04_1	0.87	0.54	0.17	0.56	0.37
HFM04_2	0.88	0.08	0.13	0.61	0.47
HFM04_3	0.63	0.38	0.39	0.32	0.18
HFM10_1	1.50	0.39	0.59	1.24	0.91
HFM10_2	1.00	0.20	0.33	0.74	0.45
HFM11_1	0.31	0.37	0.11	0.12	0.07
HFM11_2	0.56	0.14	0.19	0.40	0.31
HFM15_1	1.41	0.75	0.87	1.28	1.14
HFM15_2	1.39	0.68	0.88	1.26	1.12
HFM20_2	1.16	0.28	0.43	0.89	0.75
HFM20_3	1.04	0.48	0.31	0.87	0.78
HFM20_4	1.27	1.10	1.41	1.22	1.20
Mean, HFM	**1.13**	**0.60**	**0.59**	**0.91**	**0.79**

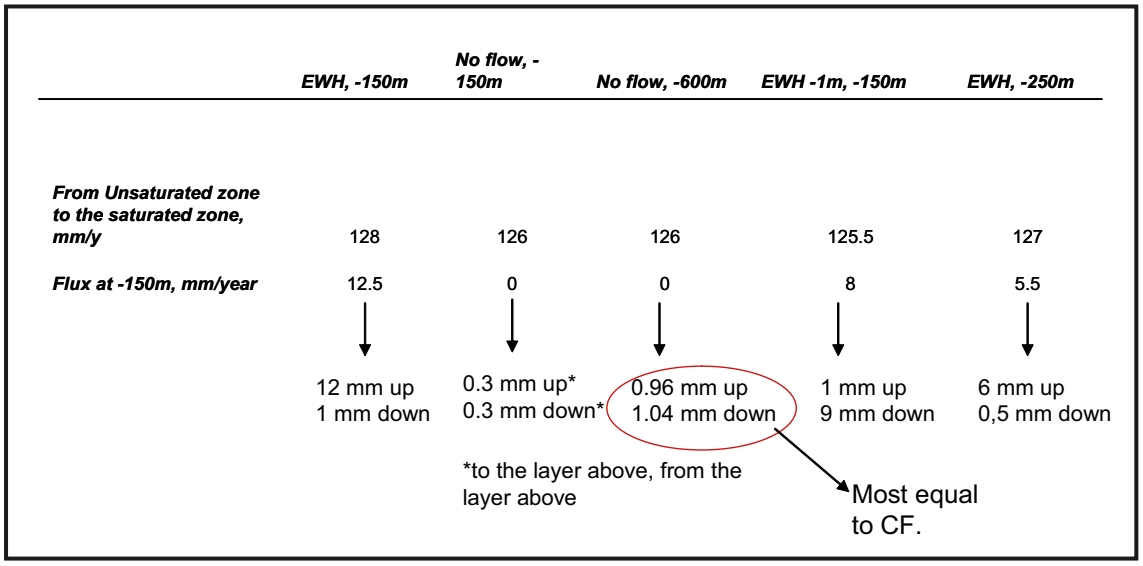

Figure 4-55. *Vertical fluxes (mm/year) at the depth of 150 m in the MIKE SHE model for different bottom boundary sensitivity cases.*

The outcome of this analysis is that the original approach to achieve a coupling between the deep rock hydrogeological model (ConnectFlow) and the near-surface groundwater model (MIKE SHE) by using a prescribed head at the bottom boundary of the latter is abandoned. Instead, the coupling is achieved by comparing the calculated vertical groundwater fluxes in the bedrock. The prescribed head imported from ConnectFlow leads to overestimated groundwater fluxes in the bedrock part of the MIKE SHE model; a no-flow boundary appears to describe the groundwater fluxes more accurately.

Since *Sens_Boundary4* gave the same vertical fluxes as ConnectFlow model, this case was selected for use in the continued modelling. The parameter setup in *Sens_Boundary4* was considered as the final product of the calibration. In the following text, this model version is referred to as the *Final calibrated model.* A validation simulation using the *Final calibrated model* was run for the period August 1, 2005, to March 31, 2007. The results of the validation simulation are presented in Chapter 5.

4.5.3 Sensitivty analysis of the bedrock properties

A final sensitivity analysis testing the effects of the hydraulic parameters of the bedrock was performed. However, the results from this last sensitivity analysis were not used to modify the input to the model in order to improve the MIKE SHE results. Thus, the bedrock description was not changed relative to that in ConnectFlow at this stage. The outcome of the analysis is discussed in this chapter and also served as an input to the hydrogeological modelling of the bedrock.

Five bedrock properties sensitivity cases were defined, two cases where all the geological layers in the bedrock part of the MIKE SHE model were modified and three cases where the hydraulic properties of the upper 200 m of the bedrock were modified. The sensitivity cases are listed in Table 4-10.

The SFM-wells are almost independent of the changes in the hydraulic conductivities of the bedrock. Minor changes of the MAE were noticed in some wells. However, the average MAE value did not change in the different sensitivity cases.

Table 4-10. Sensitivity cases testing the effects of the hydraulic properties of the bedrock.

Sensitivity case	Parameter changes
Sens_Bedrock1	Vertical hydraulic conductivity in all bedrock divided by 10
Sens_Bedrock2	Horizontal hydraulic conductivity in all bedrock multiplied by 10
Sens_Bedrock3	Horizontal hydraulic conductivity in the upper 200 m of the bedrock multiplied by 10
Sens_Bedrock4	Horizontal hydraulic conductivity in the upper 200 m of the bedrock multiplied by 50
Sens_Bedrock5	Horizontal hydraulic conductivity in the upper 200 m of the bedrock multiplied by 100

In the bedrock, however, there are noticeable effects on the groundwater head elevations in all sensitivity cases. The best results for the HFM-wells are achieved in the case *Sens_Bedrock4*. The groundwater head elevation in the bedrock decreases already when the horizontal conductivities are multiplied by a factor of 10, *Sens_Bedrock3*, but the best results are achieved when the horizontal conductivity was multiplied by 50. Multiplying the horizontal conductivity by a factor of 10 still results in too high calculated heads for all the HFM-wells but when the conductivity is multiplied by the 50 the calculated head in some of the wells becomes lower than the measured values. In *Sens_Bedrock5*, where the horizontal conductivity was multiplied by 100, the calculated heads fall much below the measured values, and the mean MAE increases again.

The case *Sens_Bedrock3,* where the horizontal hydraulic conductivity in the upper 200 m of the bedrock is multiplied by ten, results in the same positive change of the MAE as the case *Sens_Bedrock2*, where the hydraulic conductivity of all the geological layers in the bedrock have been modified. The MAE is reduced from 0.79 m to 0.49 m in *Sens_Bedrock2* and to 0.50 m in case *Sens_Bedrock3*, i.e. the two cases result in the same MAE for the HFM-wells. Thus, the lower bedrock with low fracture frequency does not need to be modified to reach better results for the HFM-wells.

Table 4-11 lists all the MAE and the ME for the *Final calibrated model* and the five sensitivity cases. In the *Final calibrated model* the calculated head in the bedrock was too high in all HFM-wells. When the horizontal hydraulic conductivity is increased by a factor of 50 or 100, the calculated values in some wells become too low. These values have a positive ME in Table 4-11. Figures 4-56 and 4-57 show time series of measured and calculated heads in some of the HFM-wells for the five sensitivity cases.

The main differences between Basecase groundwater and the Final calibrated model can be summarised as follows:

- An updated dataset for the bedrock was implemented in the model.
- The PET was reduced with 15% compared to the original values (7.5% in *Basecase groundwater*).
- The vertical extent of the model was increased to 600 m.b.s.l. A no-flow boundary condition was applied at the bottom boundary.
- The results from the bedrock properties sensitivity analysis were not taken into account when defining the *Final calibrated model*; however, they indicate that further improvement of the model would be possible by modifying the hydraulic parameters of the bedrock.

Table 4-11. Mean absolute errors (MAE) and mean errors (ME) for each HFM borehole section in the bedrock properties sensitivity cases.

	Final calibrated model		Sens_Bedrock1: Kv/10		Sens_bedrock2: Kh*10		Sens_Bedrock3: Kh upper bedrock times 10		Sens_Bedrock4: Kh upper bedrock times 50		Sens_Bedrock5: Kh upper bedrock-times 100	
HFM-well	**MAE**	**ME**	**MAE**	**ME**	**MAE**	**ME**	**MAE**	**ME**	**MAE**	**ME**	**MAE**	**ME**
HFM02_1	1.24	-1.24	1.32	-1.32	0.89	-0.89	0.89	-0.89	0.74	-0.74	0.74	-0.74
HFM02_2	1.11	-1.10	1.01	-1.01	0.69	-0.69	0.69	-0.69	0.56	-0.56	0.56	-0.56
HFM02_3	1.10	-1.10	1.00	-1.00	0.68	-0.69	0.69	-0.69	0.55	-0.55	0.55	-0.55
HFM03_1	1.10	-1.10	1.01	-1.00	0.74	-0.74	0.74	-0.74	0.57	-0.57	0.54	-0.54
HFM03_2	1.10	-1.10	1.00	-1.00	0.73	-0.73	0.73	-0.73	0.57	-0.57	0.53	-0.53
HFM04_1	0.37	-0.37	0.11	0.02	0.13	0.13	0.14	0.14	0.23	0.23	0.19	0.19
HFM04_2	0.47	-0.47	0.15	-0.12	0.09	0.08	0.1	0.09	0.27	0.27	0.29	0.29
HFM04_3	0.18	-0.17	0.16	0.16	0.36	0.36	0.36	0.36	0.55	0.55	0.57	0.57
HFM10_1	0.91	-0.91	0.51	-0.51	0.18	-0.18	0.22	-0.22	0.12	0.10	0.20	0.19
HFM10_2	0.45	-0.45	0.33	-0.33	0.15	0.02	0.14	0.00	0.41	0.41	0.52	0.52
HFM11_1	0.07	0.01	0.59	-0.58	0.40	-0.39	0.46	-0.46	0.12	-0.08	0.49	0.49
HFM11_2	0.31	-0.31	0.45	-0.45	0.28	-0.28	0.31	-0.31	0.13	-0.11	0.18	0.17
HFM15_1	1.14	-1.13	1.12	-1.12	0.72	-0.72	0.73	-0.73	0.44	-0.44	0.37	-0.37
HFM15_2	1.12	-1.12	1.05	-1.05	0.68	-0.68	0.68	-0.68	0.39	-0.39	0.32	-0.32
HFM20_2	0.75	-0.75	0.71	-0.71	0.37	-0.37	0.37	-0.37	0.21	-0.21	0.22	-0.22
HFM20_3	0.78	-0.78	0.69	-0.69	0.34	-0.34	0.34	-0.34	0.16	-0.16	0.16	-0.16
HFM20_4	1.20	-1.20	1.29	-1.29	0.86	-0.86	0.86	-0.86	0.67	-0.67	0.63	-0.63
Mean	**0.79**	**-0.78**	**0.74**	**-0.71**	**0.49**	**-0.41**	**0.50**	**-0.42**	**0.39**	**-0.21**	**0.42**	**-0.13**

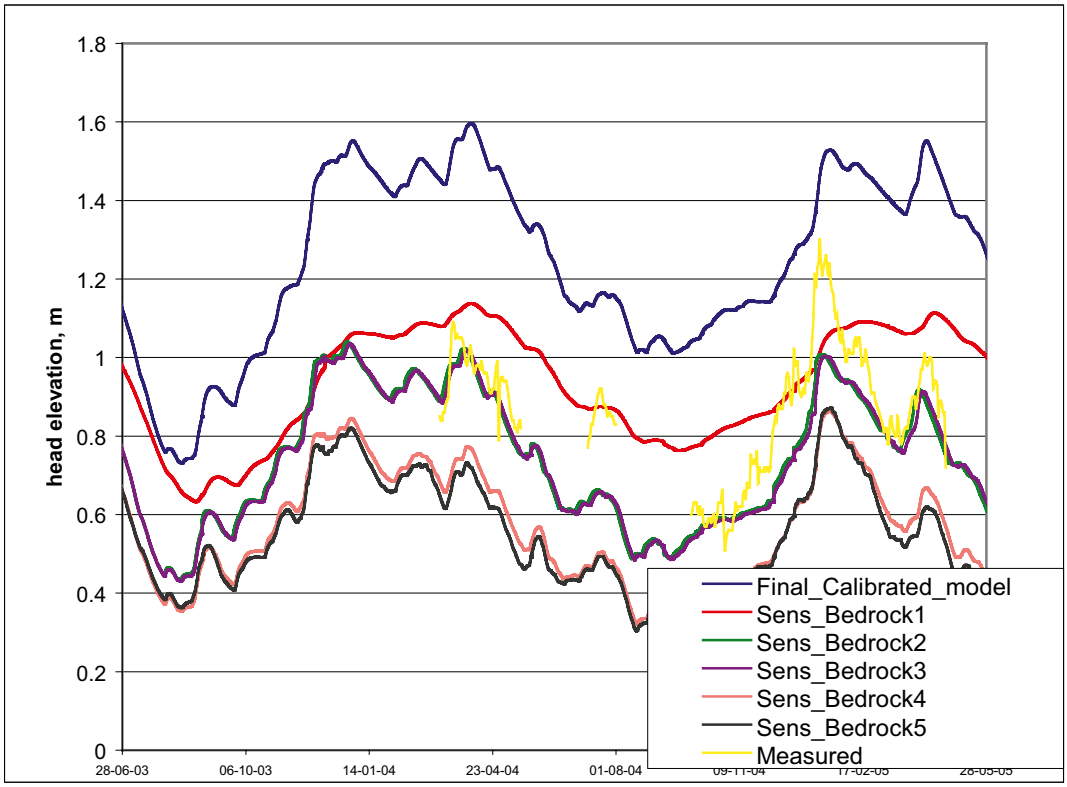

Figure 4-56. *Measured and calculated head time series for the borehole section HFM4_2; results are shown for the cases considered in the bedrock properties sensitivity analysis.*

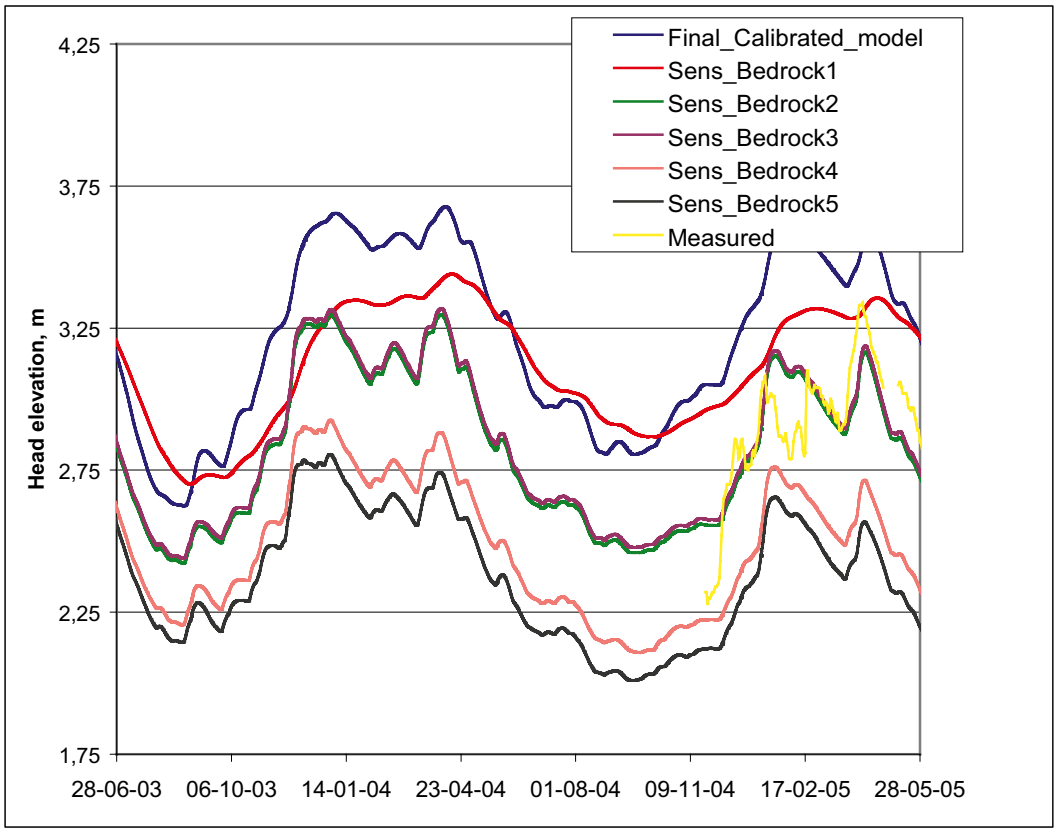

Figure 4-57. *Measured and calculated head time series for the borehole section HFM10_2; results are shown for the cases considered in the bedrock properties sensitivity analysis.*

4.6 Summary of the calibration and the sensitivity analyses

Figure 4-58 summarises the calibration process and all the steps taken to reach the *Final calibrated model*. The figure illustrates the main sub-versions of the model, main actions taken in each step and the target of each calibration step. In total, 36 modelling steps were taken. An extensive sensitivity analysis has been made in order to analyse the model and its sensitivity to different parameters.

Since the focus of the MIKE SHE modelling is the describing the dynamics of the surface waters, the groundwater-surface water interactions and the near-surface groundwater dynamics, the sensitivity analyses were focused to the hydraulic properties of the Quaternary deposits and the unsaturated zone parameters. However, a few sensitivity simulations were performed in order to analyse the hydraulic properties of the bedrock. The model was not calibrated to the results of these bedrock analyses, i.e. the hydraulic properties of the bedrock were not updated even if some sensitivity cases generated better results for the groundwater monitoring points in the bedrock than the original model setup. The results from the sensitivity analysis of the bedrock properties are just used to support a discussion about the groundwater elevations in the bedrock.

In the middle of the calibration process, a new version of the hydraulic parameterisation of the bedrock was delivered. The new conductivity values were lower and the vertical flow generated by the calculated head used as bottom boundary condition was reduced. The vertical flow through the bedrock had so far in the modelling process caused an upward flow to the surface and contributed to the discharge in the water courses. Once the new conductivity values were implemented, the surface water discharge was reduced. Previous analyses had shown that the only way to obtain a considerable increase of the surface water discharge was to decrease the potential evapotranspiration. The main reason for this is the fact that wetlands dominate the area, where the actual evaporation is very much controlled by the potential evaporation. Thus, the potential evapotranspiration was reduced by 15% compared to the original values, i.e. the first reduction by 7.5% in *Basecase groundwater* was doubled. This is illustrated by the dotted arrows in Figure 4-58.

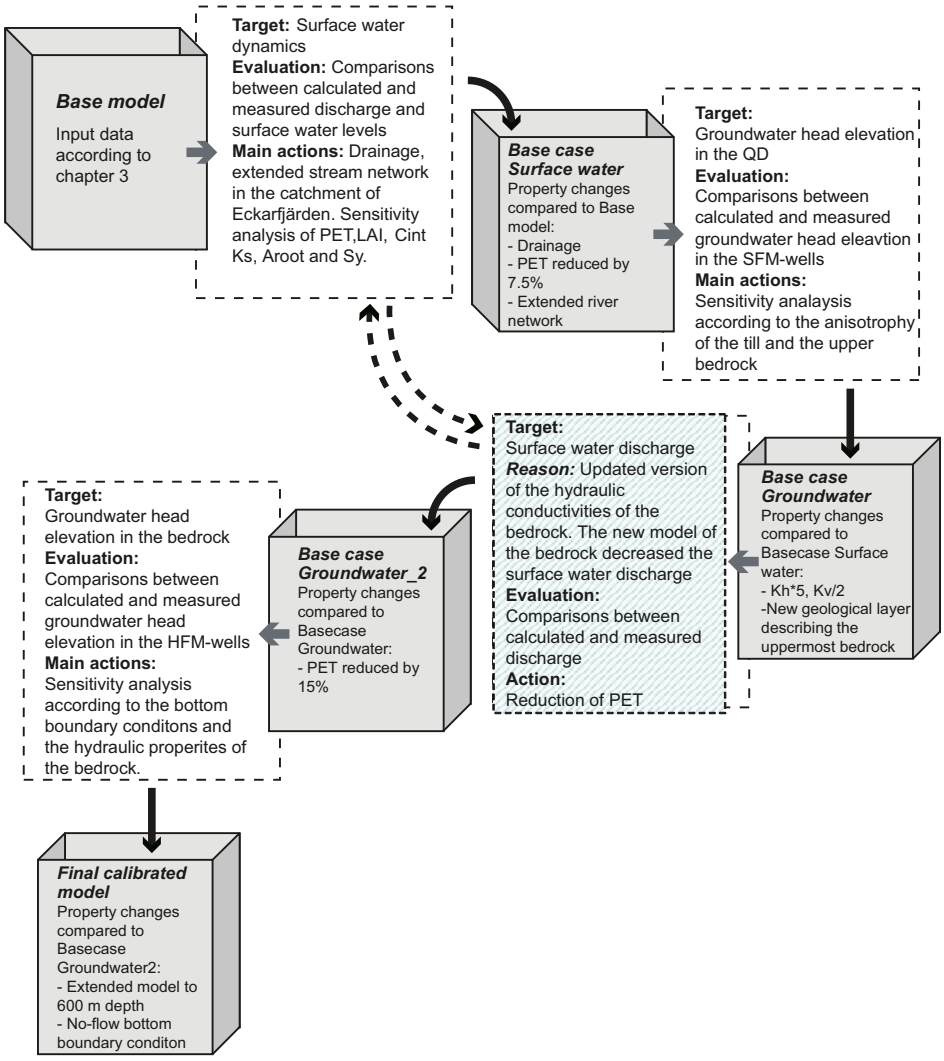

Figure 4-58. *Summary of the calibration steps and sensitivity analyses performed in the development of the Final calibrated model.*

One important finding in the calibration process was the outcome of the analysis of the bottom boundary condition. This analysis showed that the bottom boundary condition used in the base set up of the model generated water to the model, resulting in too high vertical groundwater fluxes, compared to the ConnectFlow model, and too high groundwater elevations in the bedrock. After this analysis the model was extended to 600 m depth and a no-flow boundary was used at the bottom of the model.

Five main sub models were defined during the calibration process. The *Base model,* containing the input data described in Chapter 3, *Basecase surface water* with updated parameters as a result of the analysis of the surface water dynamics. The model version *Basecase surface water* was evaluated using the measured discharges in the water courses and the lake water levels. *Basecase groundwater* contains updated properties of the till and the surface bedrock. This model was evaluated using data from the groundwater monitoring wells in the Quaternary deposits. *Basecase groundwater 2* contains the updated version of the bedrock properties and the potential evapotranspiration has been reduced by 15%.

The *Final calibrated model* is the resulting model after all the sensitivity analyses and calibration steps described in this chapter. This model was validated using data measured during the time period following the calibration period. The results from the validation of the *Final calibrated model* are presented in Chapter 5.

5 Testing the flow model using independent data

In this chapter, results are presented for both the calibration period and a validation period providing data not used in the calibration. As described in Chapter 4, the model was calibrated for the period from the 15th of May, 2003, to the 31th of July 2005. The validation period used for testing the model was from the 1st of August, 2005, to the Forsmark 2.3 data freeze, which was on the 31th of March, 2007. The differences between the two periods will be highlighted and discussed in this chapter.

5.1 Surface water levels and surface water discharge

Four surface water level stations and four surface water discharge stations are located within the model area (Figure 5-1). The surface water level stations are situated in Lake Eckarfjärden, Lake Bolundsfjärden, Lake Gällsboträsket and Lake Fiskarfjärden. Three of the discharge stations are located in the catchment area of Norra Bassängen, AFM000074, and one discharge station is placed in the catchment area of Gunnarsboträsket-Lillfjärden, AFM000073. All stations have been used in the calibration of the surface water model (i.e. the MIKE 11 model).

In general, there is a good agreement between measured and calculated water levels over the calibration and validation period. The average mean absolute error, MAE, between measured and calculated water levels for all the lakes during the combined calibration and validation period was 6.3 cm. The mean error, ME, was 1.4 cm. In Table 5-1 the MAE and ME for each lake are listed. Time series showing calculated and observed water levels for each lake are shown in Figures 5-2 to 5-5. The calibration and validation periods are marked in the figures. The agreement between measured and calculated water levels during the calibration period continues during the independent validation period. The dry period during spring and summer 2006 is reflected in the model results as low calculated water levels in the lakes. The drought during the spring and summer of 2006 is an “extreme” event not represented during the calibration period; thus, the agreement is an indication of a stable model.

The calculated water level in Lake Gällsboträsket is in general lower than the measured water level. The high water levels are better captured by the model than the low water levels. During periods of low water levels, the calculated levels are 10–20 cm below the observed water levels. The opposite is shown for Lake Eckarfjärden. The calculated water levels in Eckarfjärden are in general 10 cm higher than observed data. However, the MAE for the whole period is only 7 cm which can be regarded as a good agreement.

Figure 5-1. *Locations of monitoring points for surface water levels and surface water discharges.*

Table 5-1. Mean absolute error and mean error for the water levels in the lakes in the model area. The errors are based on the combined calibration and validation period.

	MAE	ME
Lake Eckarfjärden, SFM0041	0.072	–0.026
Lake Fiskarfjärden, SFM0042	0.048	0.014
Lake Bolundsfjärden, SFM0040	0.034	–0.025
Lake Gällsboträsket, SFM0064	0.099	0.091
Mean, all lakes	0.063	0.014

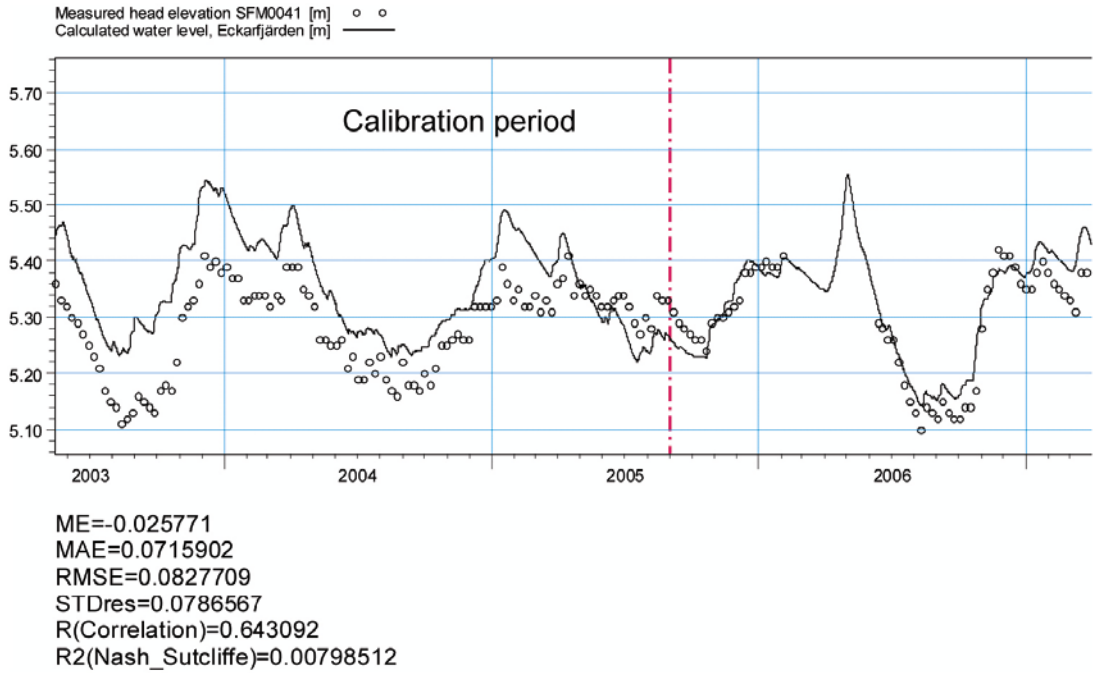

ME=-0.025771
MAE=0.0715902
RMSE=0.0827709
STDres=0.0786567
R(Correlation)=0.643092
R2(Nash_Sutcliffe)=0.00798512

Figure 5-2. *Calculated and measured water levels in Lake Eckarfjärden.*

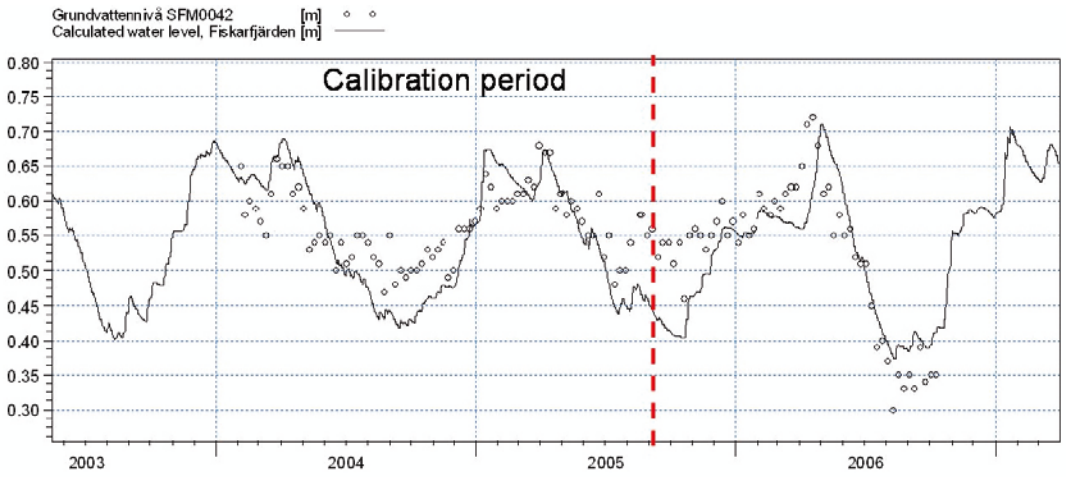

ME=0.0141171
MAE=0.0477504
RMSE=0.0577437
STDres=0.0559914
R(Correlation)=0.783531
R2(Nash_Sutcliffe)=0.48088

Figure 5-3. *Calculated and measured water levels in Lake Fiskarfjärden.*

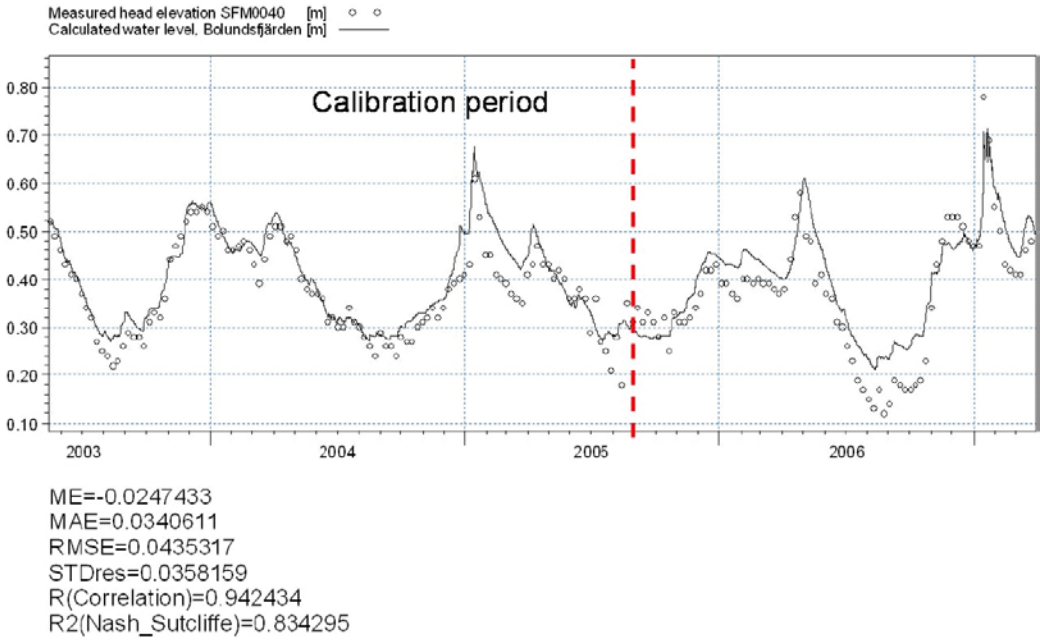

Figure 5-4. *Calculated and measured water levels in Lake Bolundsfjärden.*

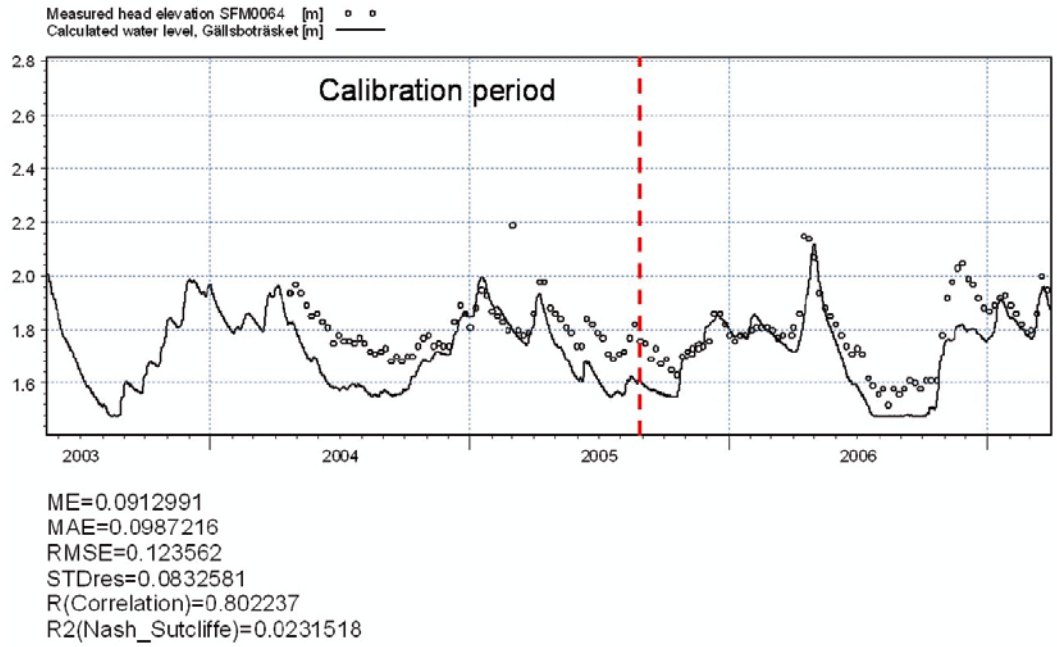

Figure 5-5. *Calculated and measured water levels in Lake Gällsboträsket.*

Figure 5-6 to 5-9 shows a comparison between measured and calculated discharges in PFM002667 (downstream Lake Stocksjön), PFM002668 (downstream Lake Eckarfjärden), PFM002669 (downstream Lake Gunnarsboträsket) and PFM005764 (upstream Lake Bolundsfjärden). The model shows a better agreement both in terms of the size of the peak discharges and the response compared to the pre-modelling reported in /Aneljung and Gustafsson 2007/.

The discharge peaks in November and December 2006 are not fully captured by the model; the calculated peaks for all discharge stations show too low values. The first peak in November 2006 is not reflected in the model. The agreement is better during the second peak in December 2006.

The model reflects the momentary run-off, due to a quick snow melt in April 2006, but the peaks are too small. A large volume of water is therefore missing in the accumulated discharge, cf. Figures 5-10 to 5-13. The response during the second run-off, in spring 2005, in PFM000069 downstream Lake Gunnarsboträsket, is too quick. The peak is too narrow and a large volume of water is missing. Before this run-off event, the accumulated calculated discharge is almost the same as the observed values (Figure 5-12).

In general, the results for the accumulated discharge show better agreement for the calibration period than for the validation period. Due to the models disability to reflect the run-off in

November and December 2006 and the high peak discharges during the snowmelt in April 2006, the accumulated calculated discharge for the validation period shows somewhat poorer agreement with the measured accumulated discharge. The difference between calculated and measured accumulated discharges during the calibration period for PFM000067 is +5%, for PFM000068 –3%, for PFM000069 –18% and for PFM005764 +5%. The corresponding numbers for the whole period is –16%, –20%, –26% and –12%.

The accumulated discharge is best described by the model for PFM005764, with an accumulated difference of –12%. This station is placed most downstream in the system. The catchment of Norra Bassängen is the largest catchment within the model area. The internal distribution of the run-off within the catchment is not always fully captured by the model, but the total accumulated run-off at the outlet of the catchment is well described in the model. The calculated peak discharge in April 2006 is, however, still too small, also in PFM005764.

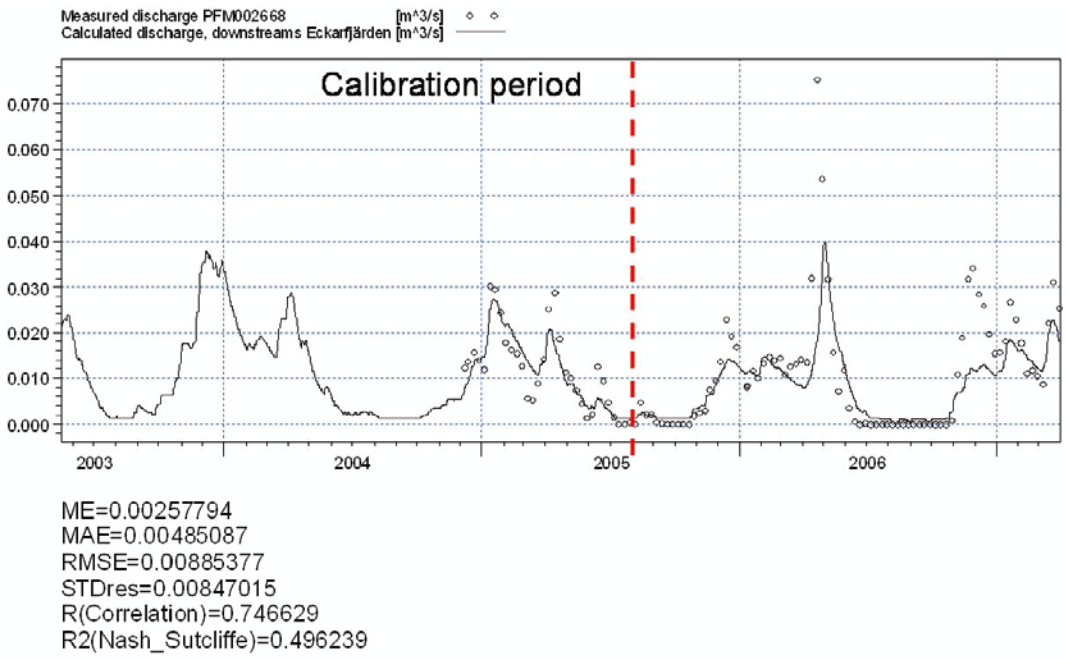

Figure 5-6. *Comparison between measured and calculated discharges in PFM002668 downstream Lake Eckarfjärden.*

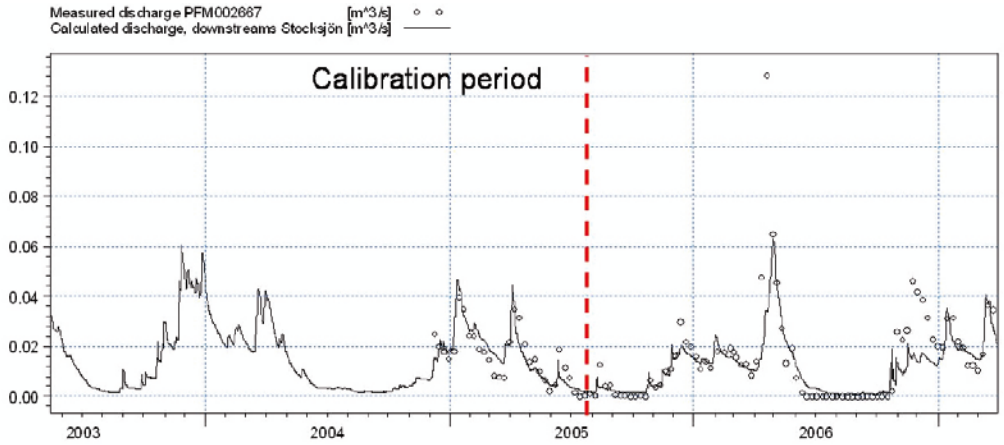

ME=0.00142599
MAE=0.00496656
RMSE=0.00776875
STDres=0.00763676
R(Correlation)=0.793024
R2(Nash_Sutcliffe)=0.613916

Figure 5-7. *Comparison between measured and calculated discharges in PFM002667 downstream Lake Stocksjön.*

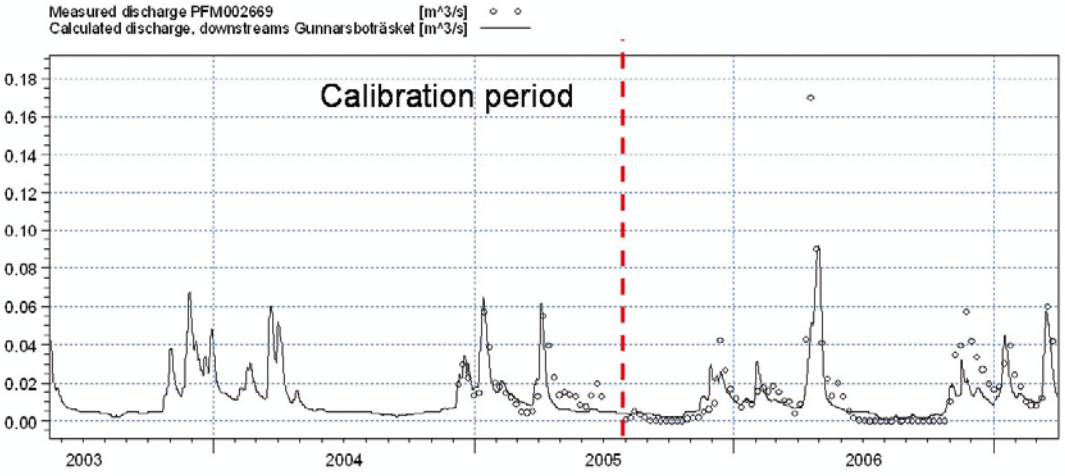

ME=0.00435092
MAE=0.00856621
RMSE=0.0169421
STDres=0.0163738
R(Correlation)=0.718775
R2(Nash_Sutcliffe)=0.474478

Figure 5-8. *Comparison between measured and calculated discharges in PFM00269 downstream Lake Gunnarsboträsket.*

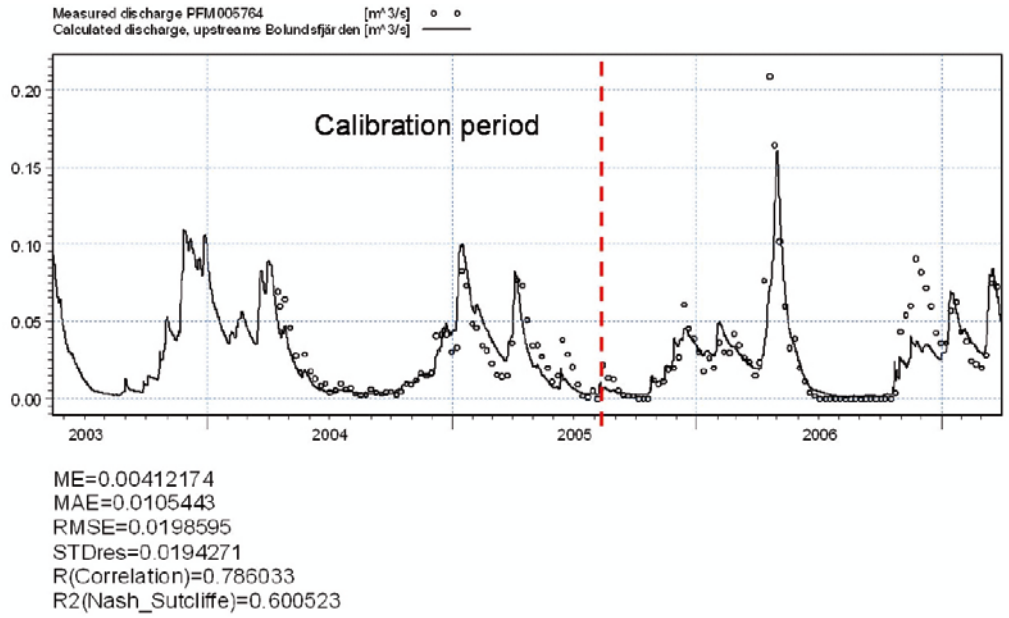

Figure 5-9. *Comparison between measured and calculated discharges in PFM005764 downstream Lake Bolundsfärden.*

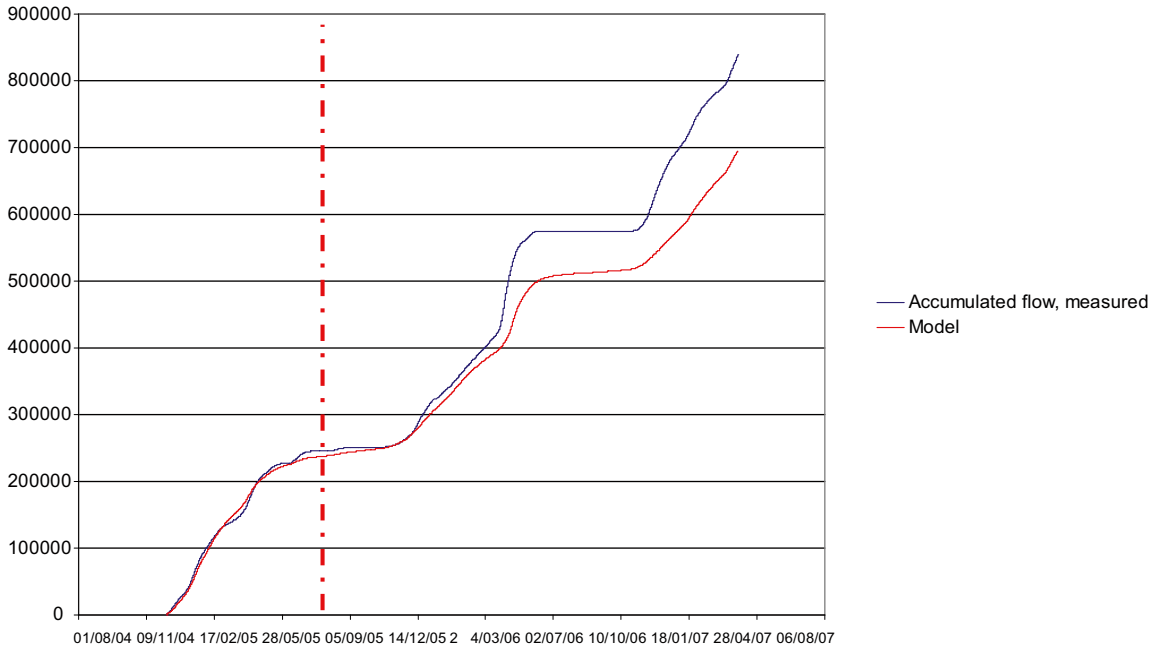

Figure 5-10. *Accumulated discharge (m^3) in PFM002668 downstream Lake Eckarfjärden. The red dotted line marks the end of the calibration period and the start of the validation period.*

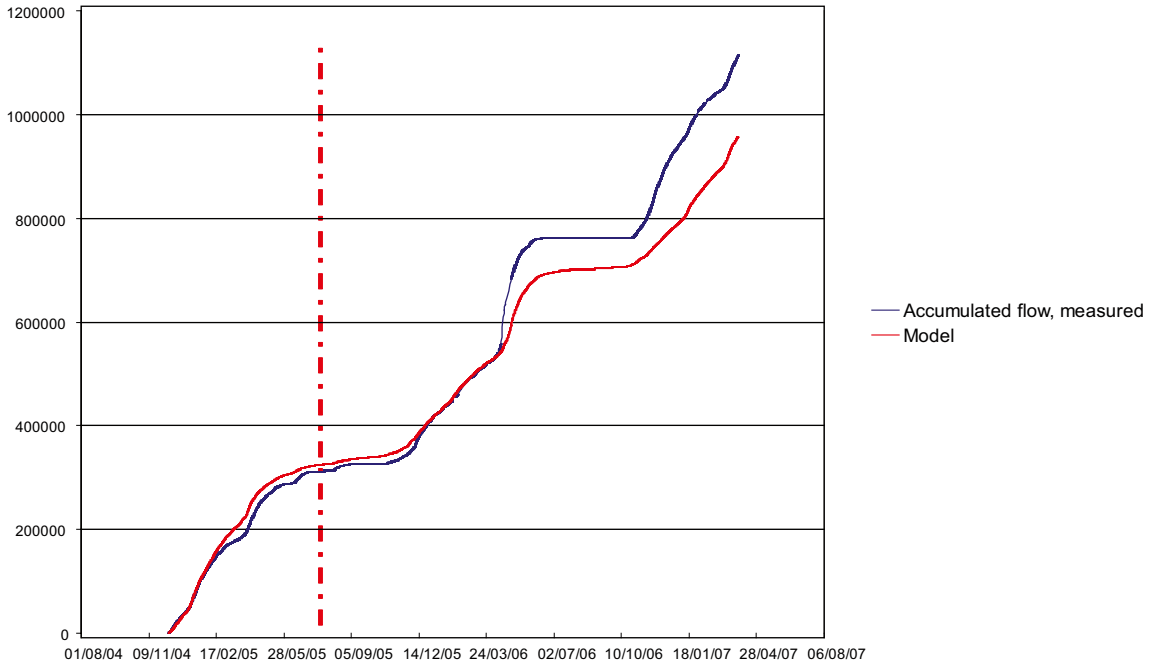

Figure 5-11. *Accumulated discharge (m^3) in PFM002667 downstream Lake Stocksjön. The red dotted line marks the end of the calibration period and the start of the validation period.*

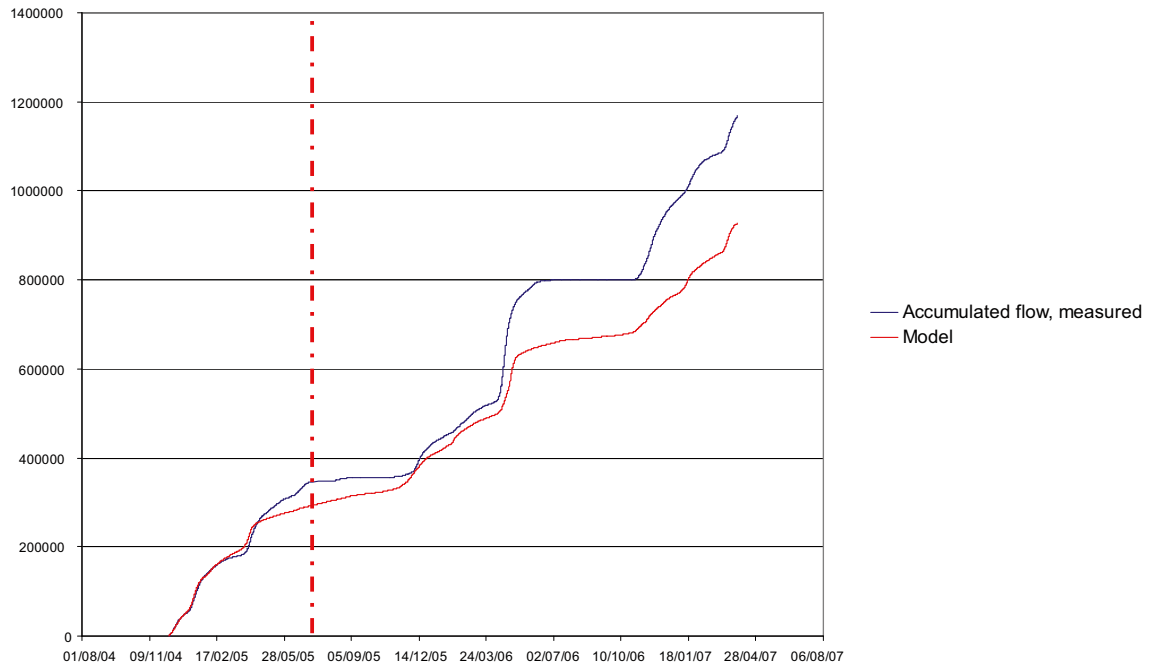

Figure 5-12. *Accumulated discharge (m^3) in PFM002669 downstream Lake Gunnarsboträsket. The red dotted line marks the end of the calibration period and the start of the validation period.*

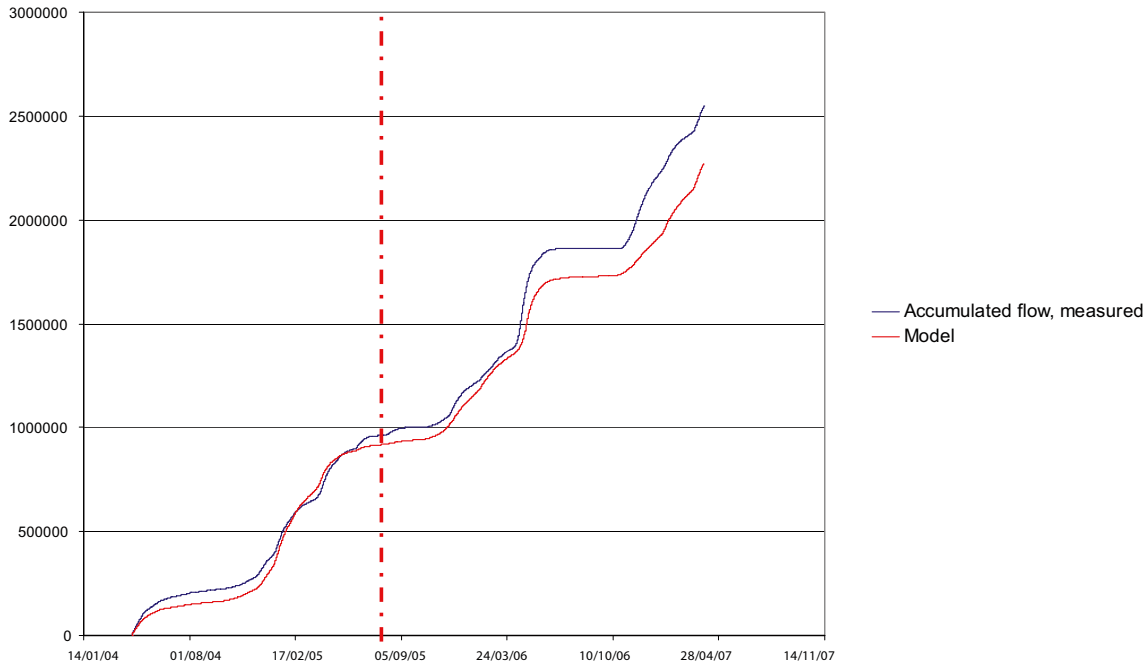

Figure 5-13. *Accumulated discharge (m^3) in PFM005764 downstream Lake Bolundsfjärden. The red dotted line marks the end of the calibration period and the start of the validation period.*

The underestimation of the discharge during the April 2006 event might also influence the too slow response in the model during autumn 2006. Because earlier peaks, not as dominated by snow melt as April 2006, are relatively well described, a possible reason is that the snow precipitation not has been properly implemented in the model. This will be further discussed in Chapter 6.

The specific discharge for the whole model area and during the calibration period is 4.7 L/(s km^2) and for the validation period 4.6 L/(s km^2). The internal distribution of the discharge between the different discharge stations vary between 4.2 and 5.1 L/(s km^2) depending on which period is analysed (Table 5-2). The largest mean specific discharge for all stations is calculated during the calibration period. The highest calculated specific discharge for a single station is found in PFM005764 upstream Lake Bolundsfjärden and is obtained for the validation period. The specific discharge for this station is 5.1 L/(s km^2). The lowest specific discharge, 4.2 L/(s km^2), is calculated for the station downstream Lake Eckarfjärden for the validation period. In general, the calculated specific discharge is lower than the measured. The fast and distinct discharge in April 2006 is underestimated for all discharge stations, which is the major reason for the small calculated specific discharge.

Table 5-2. Specific discharge, L/(s km²), for each discharge station for the calibration period and the validation period. Calculated values for the same period as the measured values are also listed in the table.

Discharge station	Specific discharge			
	Calculated specific discharge for the calibration period,15/3-03–31/7-05 (L/(s km²)).	Calculated specific discharge for the validation period, 1/8-05–31/3-07 (L/(s km²)).	Calculated specific discharge for measured period* (L/(s km²)).	Measured specific discharge (L/(s km²)).
PFM002667, Stocksjön	4.75	4.37	4.38	5.13
PFM002668. Eckarfjärden	4.72	4.19	4.21	5.07
PFM002669, Gunnarsboträsket	4.38	4.56	4.51	5.61
PFM005764, Bolundsfjärden	5.00	5.07	4.29	4.88
Mean	**4.71**	**4.55**	**4.35**	**5.17**

* Measured period for PFM005764: April 15, 2004-March 31, 2007

Measured period for PFM002667, PFM2668 and PFM2669: December 8, 2004-March 31, 2007

5.2 Groundwater head elevation

The groundwater monitoring wells used in the calibration and evaluation of results are shown in Figure 2-15 (Section 2.2.6). The majority of the SFM-wells have continuous time series covering the whole simulation period. The times series of the HFM-wells are disturbed due to pumping and drilling. Undisturbed time series are only available for relatively short periods of time.

In general, the agreement between the simulated and calculated values is good. The MIKE SHE model describes the groundwater head elevation in the Quaternary deposits at in a proper way, but there is a larger discrepancy between measured and simulated values in the bedrock. The correlation between the simulated and calculated mean head elevations in the Quaternary deposits are shown in Figure 5-14, and the correlation between the simulated and calculated values in the bedrock is presented in Figure 5-15. The correlations are better in the Quaternary deposits than in the bedrock; in the bedrock the calculated head elevations are generally above the observed values.

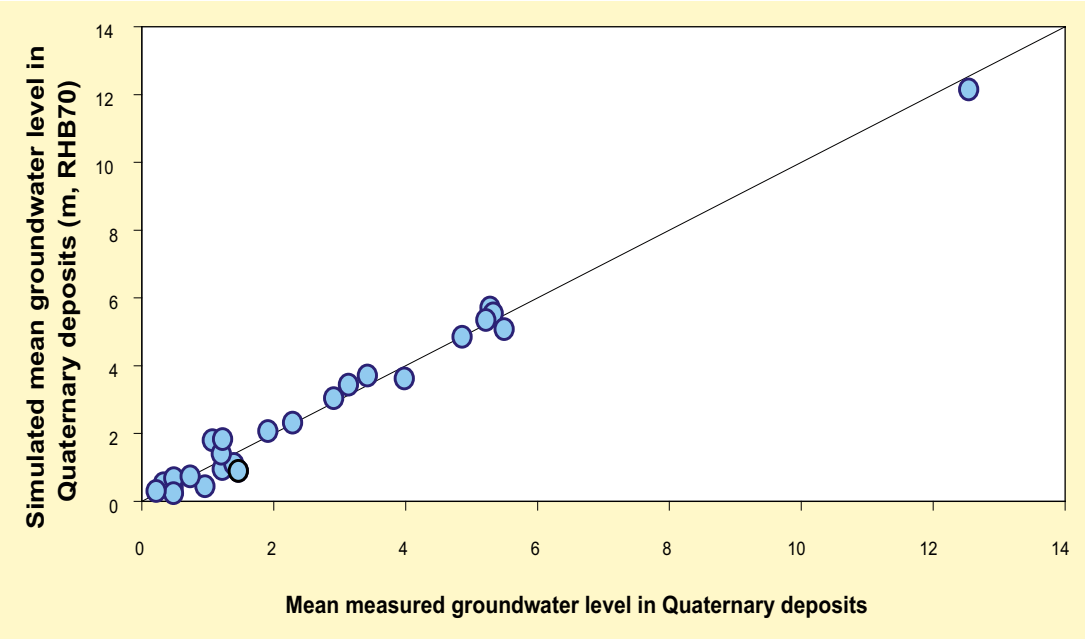

Figure 5-14. Correlation between measured and calculated mean head elevations (based on the period May 15th, 2003 – March 31st, 2007).

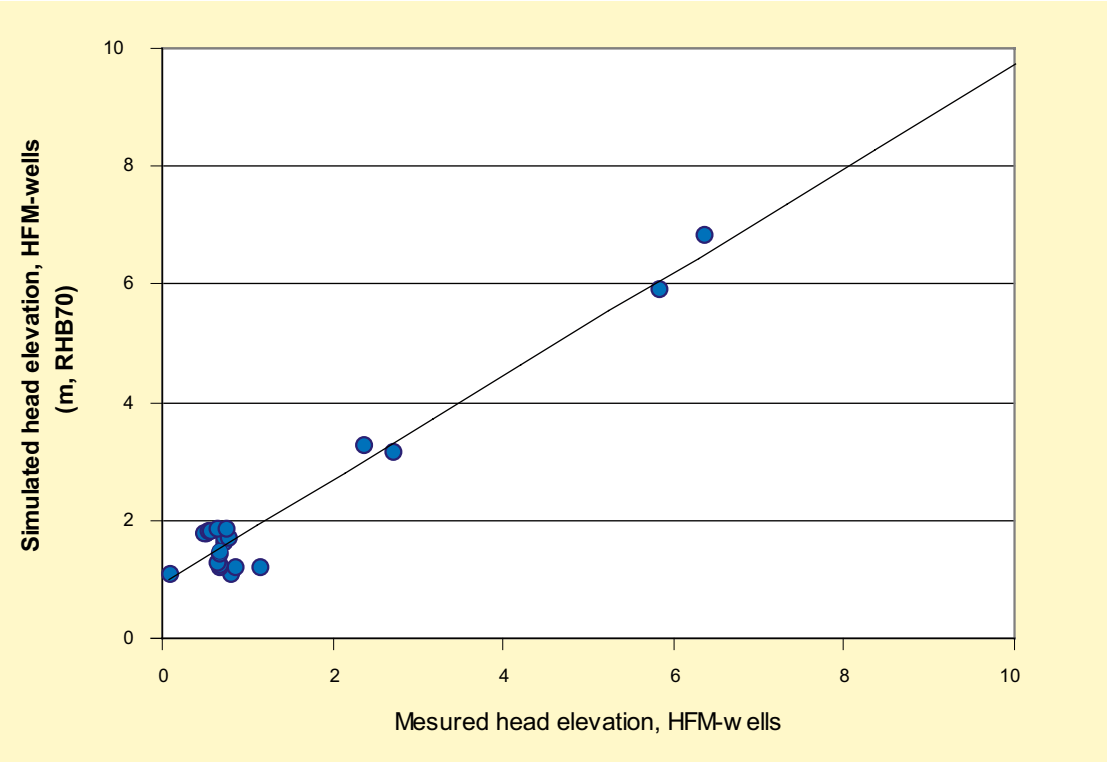

Figure 5-15. *Correlation between measured and calculated mean head elevations in percussion drilled boreholes (based on the period May 15th, 2003 – March 31st, 2007).*

5.2.1 Groundwater head elevation in the Quaternary deposits, SFM-wells

Figures 5-16 to 5-21 show a comparison between calculated and measured groundwater head elevations for some of the SFM-wells. Results from all the SFM-wells are presented in Appendix 1.

Some boreholes are located in local depressions or slopes, where the interpolated model topography deviates from the real ground level at the borehole. While the transpiration processes often is of large importance for the groundwater level variation, and this process is depth dependent, it may be more representative to use the calculated and measured depth to the phreatic surface, rather then the elevation, as a basis for comparison. This is done in Figures 5-20 and 5-21. The following wells are evaluated according to the depth to phreatic surface: SFM0001, SFM0002, SFM0009, SFM0010, SFM0018, SFM0019, SFM0020, SFM0021, SFM0028, SFM0030, SFM0049 and SFM0058.

There is a good agreement between the measured and the calculated values for the SFM-wells. The average of all mean absolute errors over the combined validation and calibration period is 0.24 m, and the average of all mean errors (measured – calculated) is as low as 0.02 m. The low mean error indicates that the mean groundwater table in the model area is very well described by the model. Also the mean absolute error is rather low, indicating that also the temporal variations are resolved by the model. The mean absolute error and the mean error for each SFM-well are listed in Table 5-3.

In general, the calculated heads are somewhat higher than the measured ones, with two exceptions (SFM0033 and SFM0066), which have mean calculated heads below the measured values. The overall pattern and accordance between the measured and calculated head elevations during the calibration period continue during the validation period. The draught during the spring and summer of 2006 is clearly seen in most of the SFM-wells.

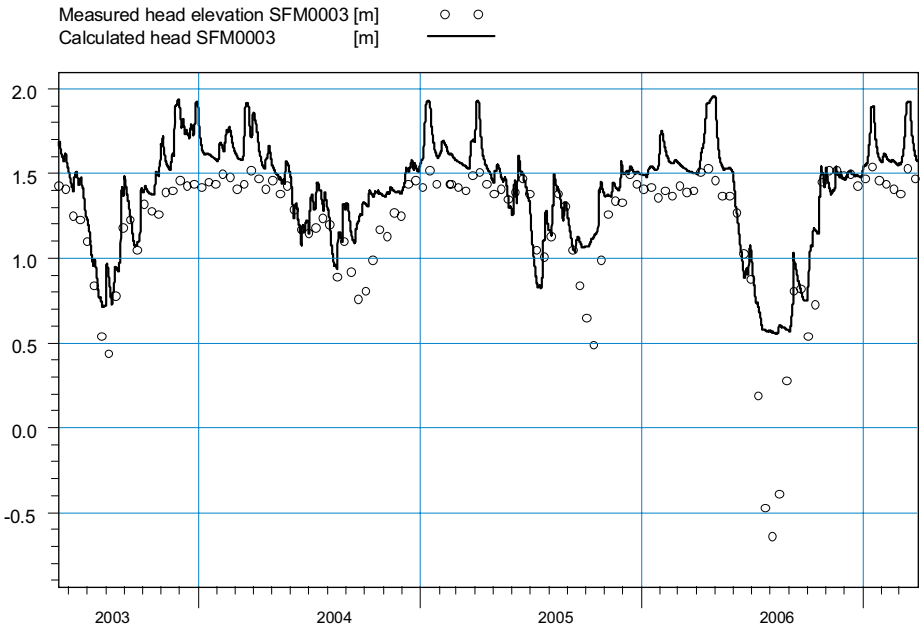

ME=-0.199446
MAE=0.207565
RMSE=0.282936
STDres=0.200684
R(Correlation)=0.86546
R2(Nash_Sutcliffe)=0.487323

Figure 5-16. *Measured and calculated head elevations in SFM0003.*

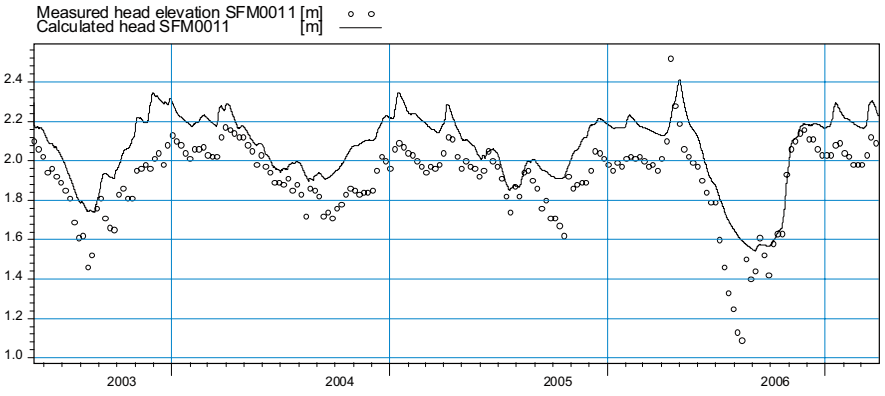

ME=-0.162495
MAE=0.165149
RMSE=0.182602
STDres=0.0833013
R(Correlation)=0.896632
R2(Nash_Sutcliffe)=0.031702

Figure 5-17. *Measured and calculated head elevations in SFM00011.*

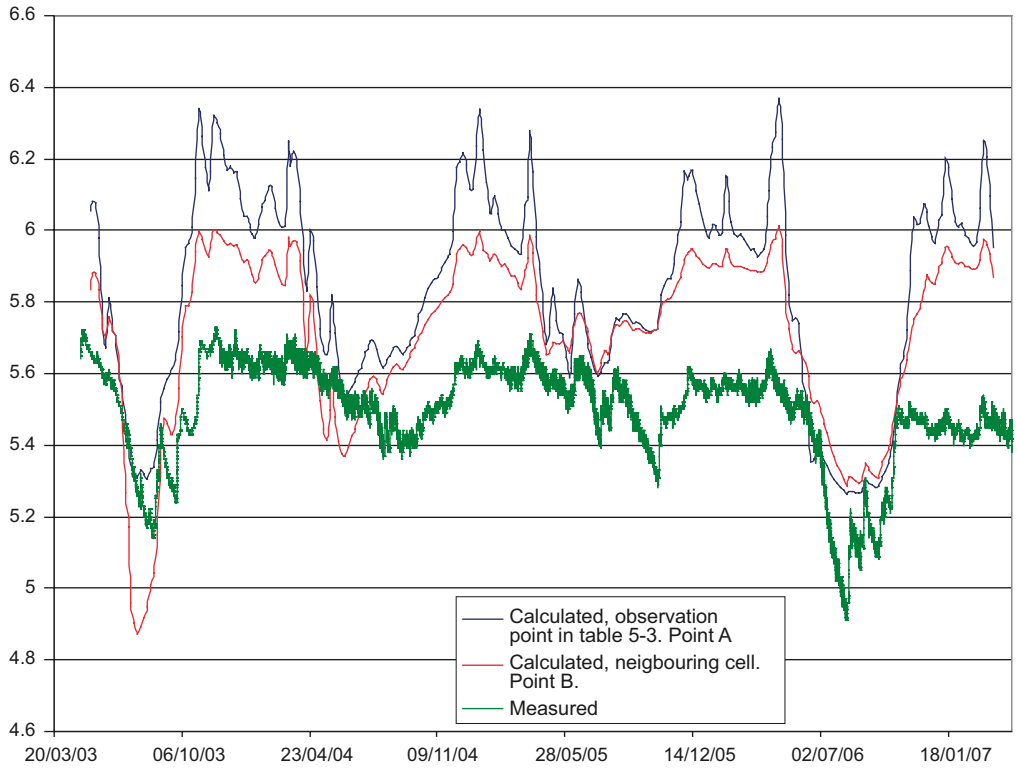

Figure 5-18. *Measured and calculated head elevations in SFM0017, which in the model is situated on the boundary between two cells. The calculated groundwater elevations for both cells are shown in the figure. The elevation of the ground surface at SFM0017 is 5.65 m.a.s.l. and the well is situated in a wetland. It is seen in the measured values that the groundwater reaches the ground surface. In the model, due to the grid resolution, the topography is set to 6.33 m.a.s.l. in point A and 5.82 m.a.s.l. in point B. Therefore, the calculated groundwater elevation is too high in both points.*

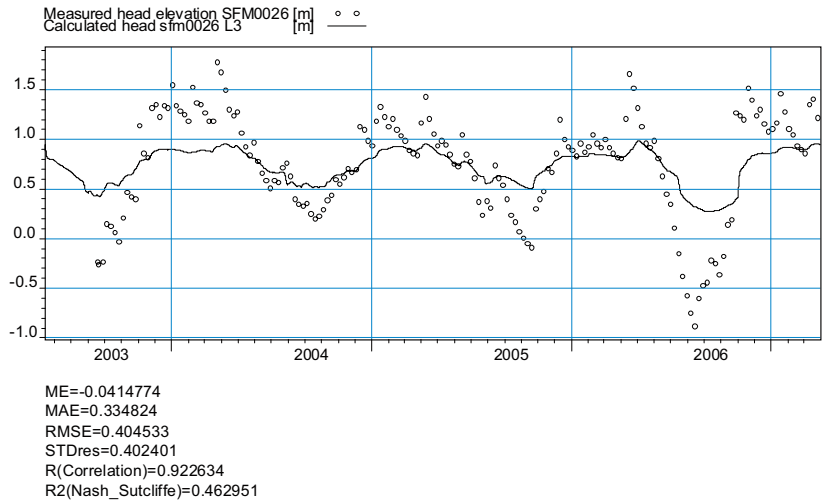

Figure 5-19. *Measured and calculated head elevations in SFM0026. The measured elevation of the ground surface is 0.7 m and in the model 0.75m; thus, artesian conditions are reached both in reality and in the model.*

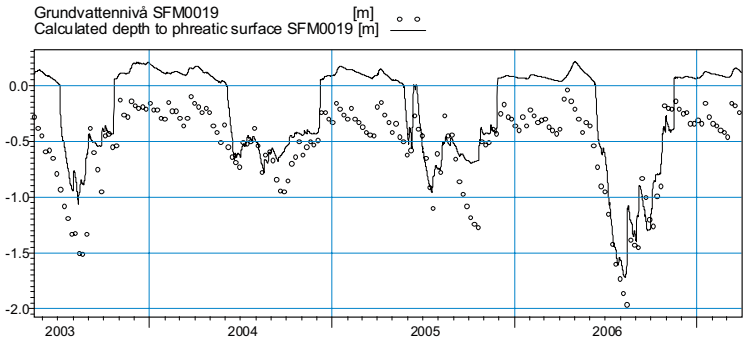

ME=-0.309941
MAE=0.324969
RMSE=0.366982
STDres=0.1965
R(Correlation)=0.887692
R2(Nash_Sutcliffe)=0.0578039

Figure 5-20. *Measured and calculated groundwater depths in SFM0019.*

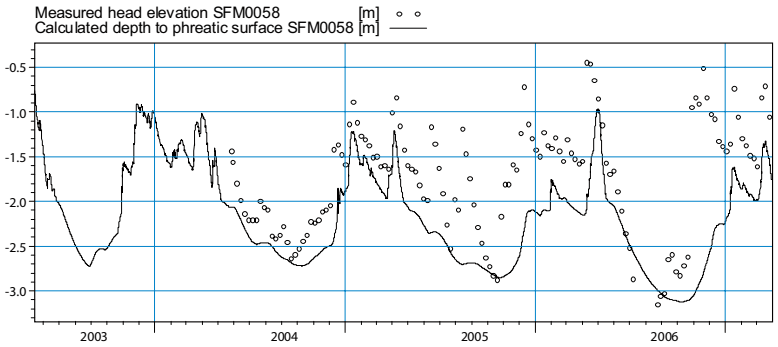

ME=0.557082
MAE=0.566843
RMSE=0.71889
STDres=0.454381
R(Correlation)=0.674601
R2(Nash_Sutcliffe)=-0.389444

Figure 5-21. *Measured and calculated groundwater depths in SFM0058.*

Table 5-3. Mean absolute errors and mean errors for the SFM-wells. Results are listed both for the calibration period and the combined calibration and validation period.

ID code, SFM-well	Calibration period		Calibration and validation period	
	MAE	ME	MAE	ME
Calculated head				
SFM0003	0.19	–0.19	0.21	–0.20
SFM0004	0.21	–0.11	0.23	–0.12
SFM0005	0.22	–0.12	0.21	–0.11
SFM0011	0.17	–0.17	0.17	–0.16
SFM0012	0.08	–0.04	0.08	–0.05
SFM0013	0.21	–0.09	0.23	–0.07
SFM0014	0.25	–0.25	0.24	–0.24
SFM0015	0.10	–0.09	0.09	–0.08
SFM0016	0.15	–0.15	0.15	–0.15
SFM0017	0.37	–0.37	0.37	0.37
SFM0022	0.04	–0.01	0.05	–0.02
SFM0023	0.05	–0.04	0.07	–0.06
SFM0026	0.33	–0.04	0.34	–0.04
SFM0033	0.32	0.26	0.32	0.24
SFM0034	0.32	–0.31	0.28	–0.25
SFM0036	0.27	–0.22	0.26	–0.22
SFM0039	0.04	–0.03	0.04	–0.03
SFM0057	0.28	–0.26	0.31	–0.27
SFM0062	0.08	0.08	0.11	0.04
SFM0065	0.19	–0.03	0.20	–0.07
SFM0066	0.12	0.05	0.11	0.02
Depth to phreatic surface				
SFM0001	0.14	0.08	0.16	0.08
SFM0002	0.29	0.29	0.28	0.27
SFM0009	0.36	0.35	0.38	0.36
SFM0010	0.35	0.34	0.39	0.37
SFM0018	0.18	–0.07	0.17	–0.05
SFM0019	0.34	–0.33	0.32	–0.31
SFM0020	0.22	–0.22	0.22	–0.22
SFM0021	0.49	0.49	0.53	0.53
SFM0028	0.13	–0.04	0.16	–0.05
SFM0030	0.55	0.48	0.61	0.52
SFM0049	0.19	–0.05	0.19	–0.03
SMF0058	0.38	0.38	0.57	0.58
Mean, all SFM-wells	**0.23**	**–0.01**	**0.24**	**0.02**

The calculated head elevations during summer 2006 drop to levels well below the lowest levels calculated for the calibration period, but the observed levels during summer 2006 are even lower than the calculated ones in some boreholes. This shows that the effects of the extremely dry summer are not fully described by the model. A reason for this might be the fact that the transpiration cannot reach deeper than to the bottom of the uppermost saturated zone calculation layer, which is often only 2 m deep. Another reason might be overestimated hydraulic conductivities, which then could override the transpiration capacity.

The contact between the lakes and the underlying till is well described by the model. Figures 5-22 to 5-25 show the calculated surface water level and the head elevation in the till under each lake. In the model, all lakes have gyttja, sand and clay sediments between the lake bottom and the till. The extension of the clay is much smaller in Lake Bolundsfjärden than in the other lakes. However, a low conductive layer of gyttja reduces the contact with the underlying till. Results from pumping tests during the site investigation indicate that there is very limited contact through the lake sediments, and the hydraulic conductivity for the clay is therefore set to 10^{-8} m/s and the hydraulic conductivity for the gyttja to 10^{-7} m/s. It was not needed to correct the conductivity values for the lake sediments during the calibration process. The initial low values have been kept.

Figures 5-26 and 5-27 show the groundwater levels in the SFM-wells in the Quaternary deposits in terms of means and ranges of observed and calculated data. In Figure 5-26 the depths to the groundwater are co-plotted with the bedrock depth. The data are ordered according to bedrock depth. In Figure 5-27 the calculated and observed groundwater elevations are co-plotted with the ground elevation and the bedrock elevation at each well location. The data are ordered according to the bedrock elevation. Of all the wells included in the modelling, none has a mean groundwater elevation below 0 m. Four wells exhibit calculated minimum values below 0 m. The lowest calculated mean value is calculated for SFM0036, 0.56 m.b.s.l. It is also clearly seen in Figure 5-27 that the groundwater table follows the topography.

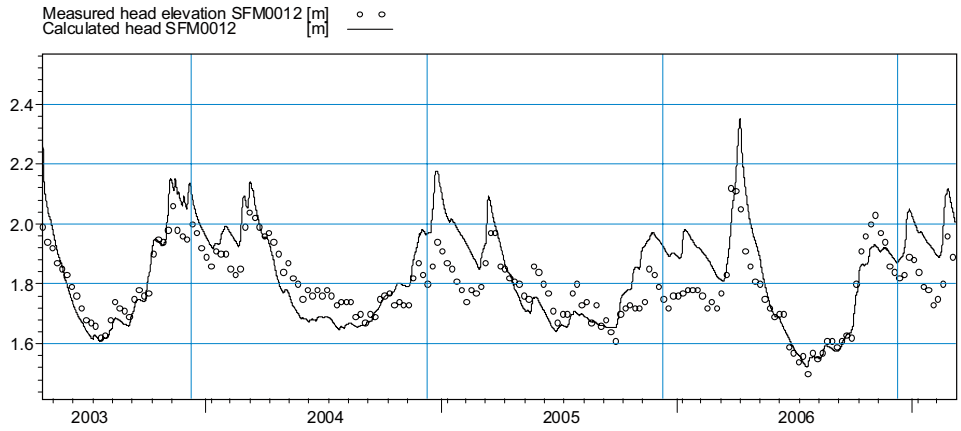

ME=-0.0476403
MAE=0.0783763
RMSE=0.0948149
STDres=0.0819772
R(Correlation)=0.877628
R2(Nash_Sutcliffe)=0.384091

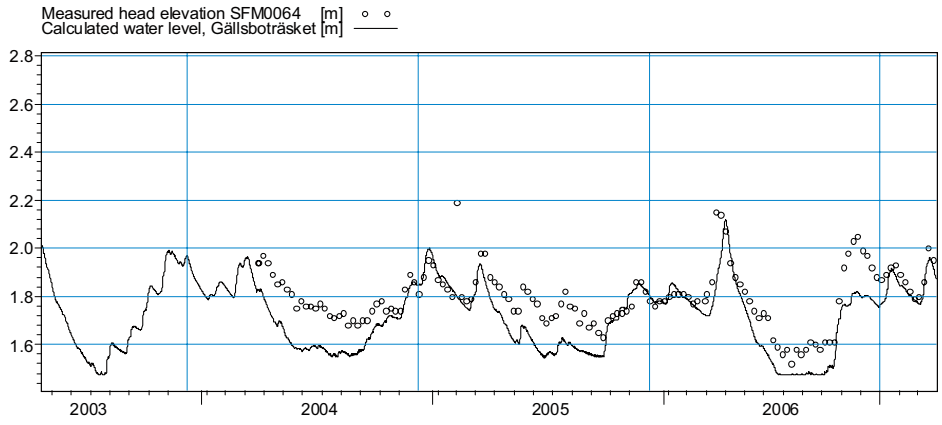

ME=0.0912991
MAE=0.0987216
RMSE=0.123562
STDres=0.0832581
R(Correlation)=0.802237
R2(Nash_Sutcliffe)=0.0231518

Figure 5-22. *Comparison between measured and calculated surface water levels and head elevations in the till under Lake Gällsboträsket. The lower figure shows a comparison between the measured and calculated surface water level in the lake, and the upper figure shows a comparison between the measured and calculated groundwater head in the till below the lake.*

ME=-0.0792843
MAE=0.0877464
RMSE=0.0992607
STDres=0.0597218
R(Correlation)=0.770746
R2(Nash_Sutcliffe)=-0.453664

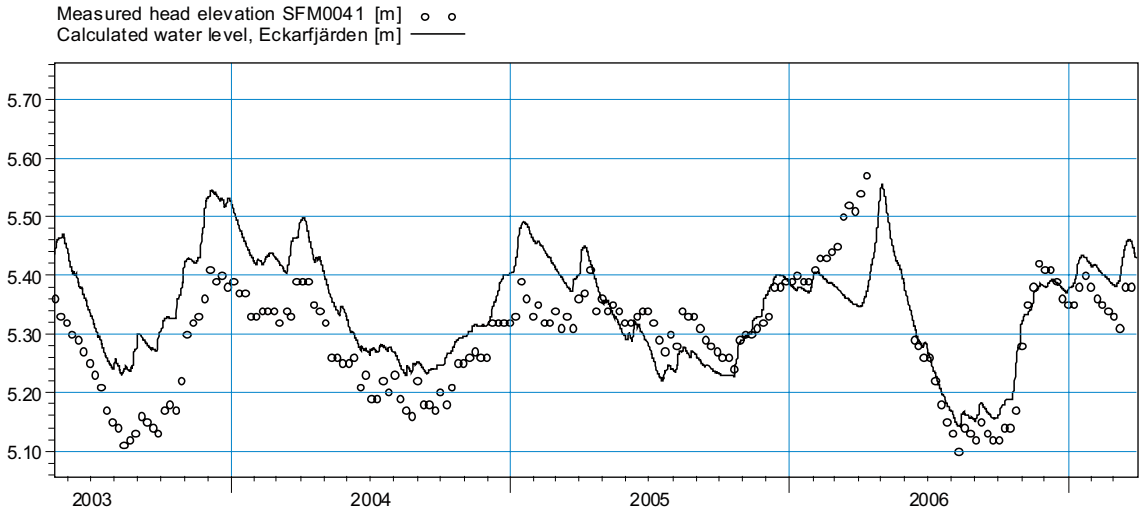

ME=-0.025771
MAE=0.0715902
RMSE=0.0827709
STDres=0.0786567
R(Correlation)=0.643092
R2(Nash_Sutcliffe)=0.00798512

Figure 5-23. *Comparison between measured and calculated surface water levels and head elevations in the till under Lake Eckarfjärden. The lower figure shows a comparison between the measured and calculated surface water level in the lake, and the upper figure shows a comparison between the measured and calculated groundwater head in the till below the lake.*

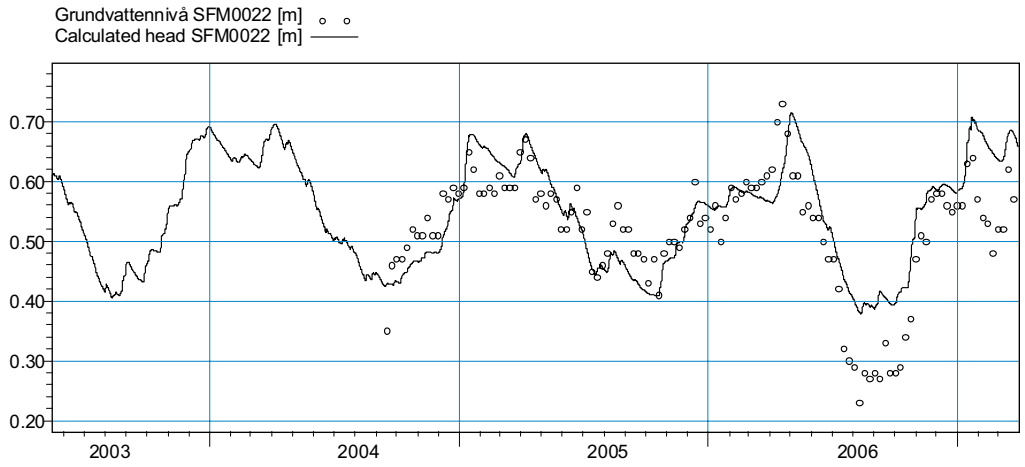

ME=-0.0241239
MAE=0.0536042
RMSE=0.0663902
STDres=0.0618522
R(Correlation)=0.785439
R2(Nash_Sutcliffe)=0.538296

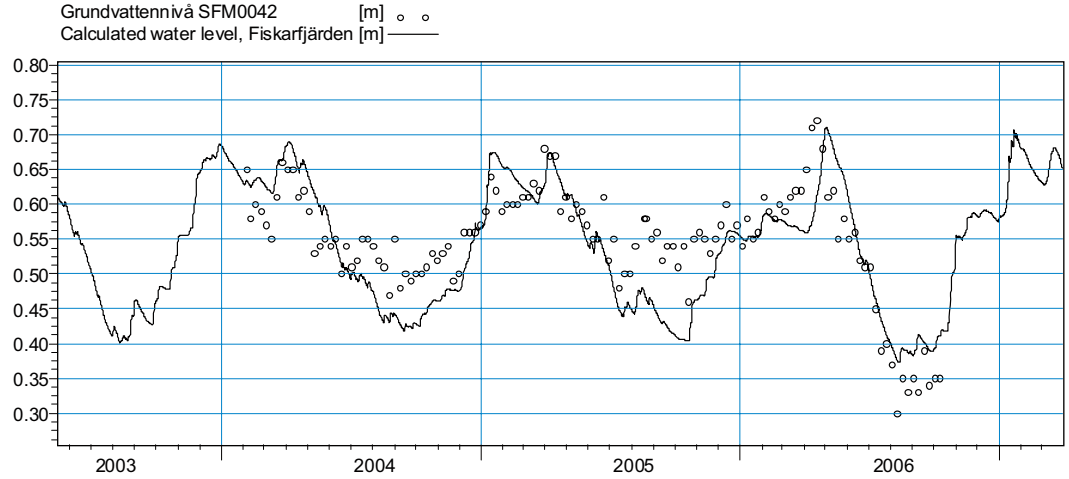

ME=0.0141171
MAE=0.0477504
RMSE=0.0577437
STDres=0.0559914
R(Correlation)=0.783531
R2(Nash_Sutcliffe)=0.48088

Figure 5-24. *Comparison between measured and calculated surface water levels and head elevations in the till under Lake Fiskarfjärden. The lower figure shows a comparison between the measured and calculated surface water level in the lake, and the upper figure shows a comparison between the measured and calculated groundwater head in the till below the lake.*

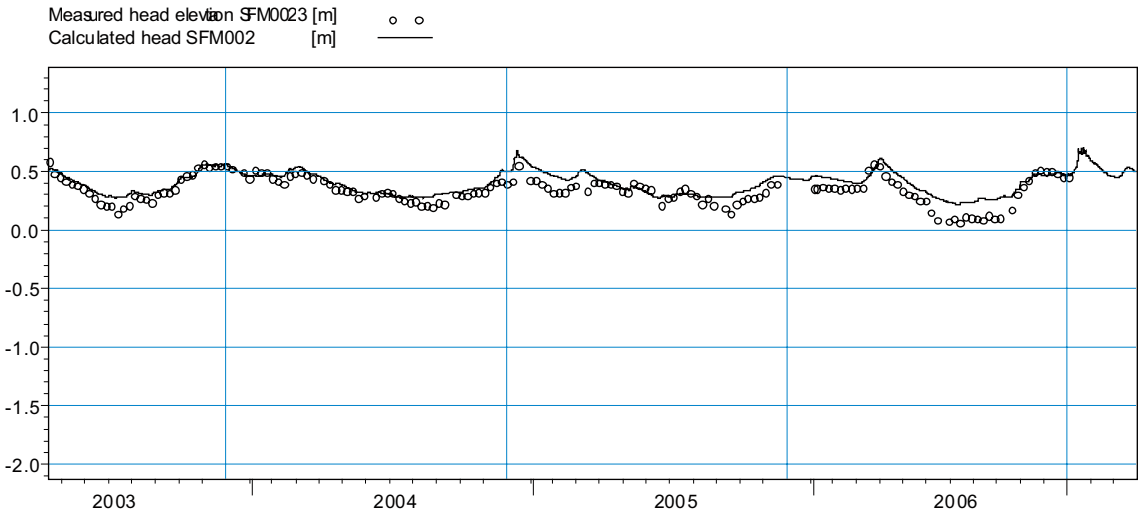

ME=-0.0593063
MAE=0.0722972
RMSE=0.192031
STDres=0.182644
R(Correlation)=0.61371
R2(Nash_Sutcliffe)=0.25892

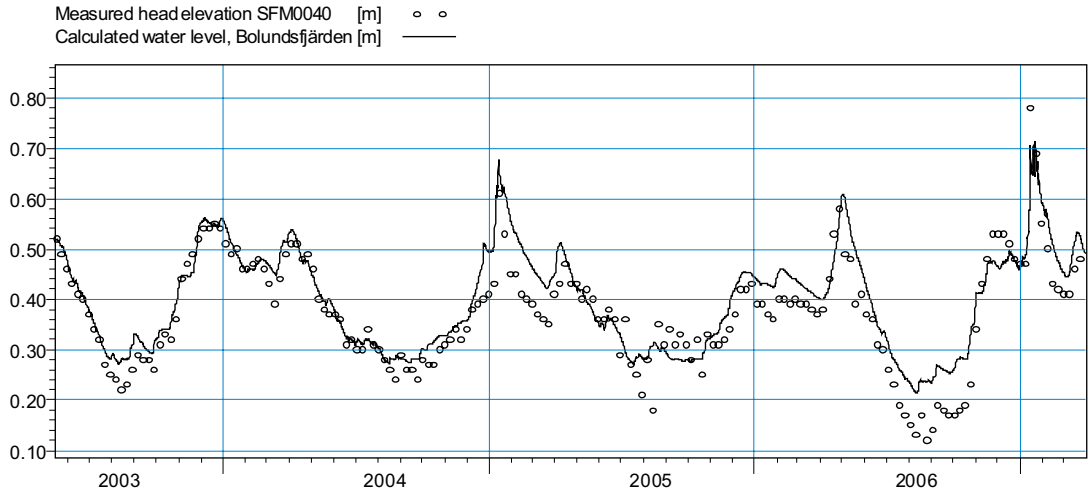

ME=-0.0247433
MAE=0.03406 11
RMSE=0.0435 317
STDres=0.0358 159
R(Correlation)=0.942434
R2(Nash_Sutcliffe)=0.834295

Figure 5-25. *Comparison between measured and calculated surface water levels and head elevations in the till under Lake Bolundsfjärden. The lower figure shows a comparison between the measured and calculated surface water level in the lake, and the upper figure shows a comparison between the measured and calculated groundwater head in the till below the lake.*

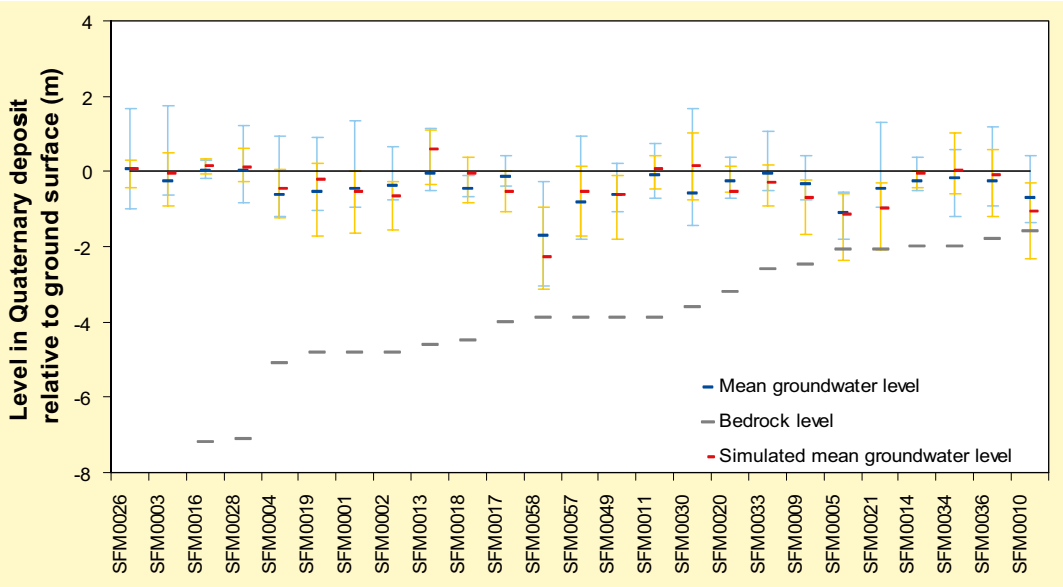

Figure 5-26. *Simulated and measured groundwater depths in the SFM-wells. The ranges of measured data are marked with blue colour and the ranges of simulated values with yellow colour. Data are ordered from left to right according to the bedrock depth.*

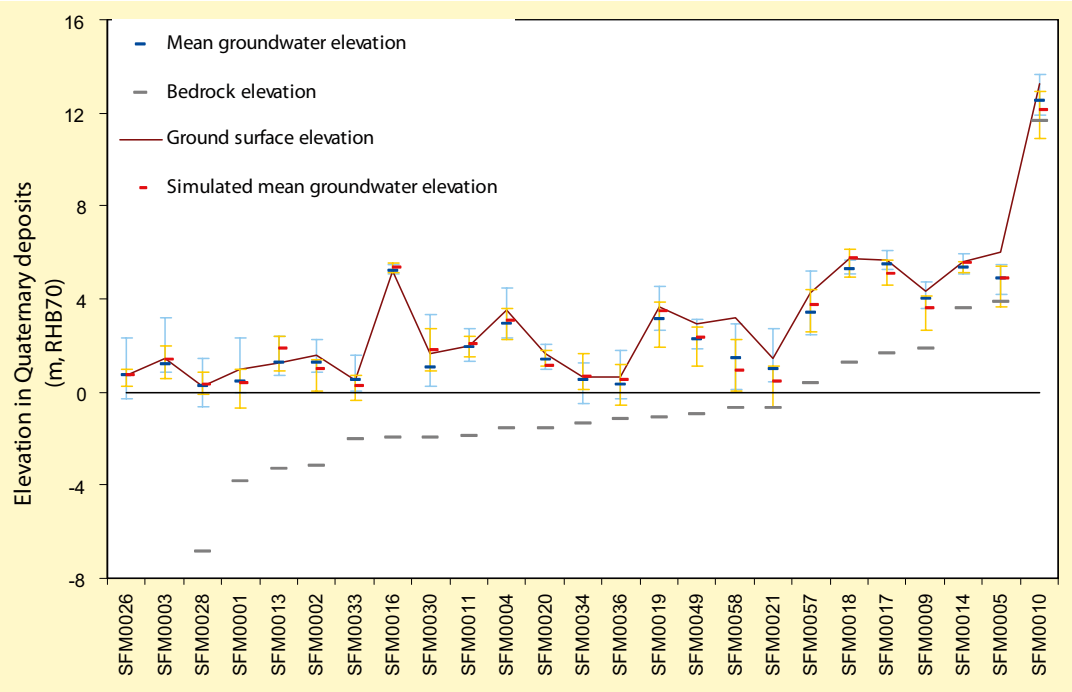

Figure 5-27. *Simulated and measured groundwater elevation in the SFM-wells. The ranges of measured data are marked with blue colour and the ranges of simulated values with yellow colour. Data are ordered from left to right according to the bedrock elevation.*

5.2.2 Groundwater head elevation in the bedrock

The calculated head elevation in the bedrock is in general higher than the measured head elevation in the HFM-wells. The mean absolute error for all the boreholes is 0.75 m. The monitoring of some HFM-wells had not started before the end of the calibration period; thus, the comparison has for these wells only been done for the validation period. The best agreement between measured and calculated heads is achieved for HFM11 where the MAE is 10–30 cm depending on which level of the borehole that is evaluated. A comparison between measured and calculated groundwater elevations in HFM11 is shown in Figures 5-28 and 5-29.

Some wells, namely HFM04, HFM10, HFM11, HFM16 and HFM20, have mean absolute errors in the calculated heads equal to or smaller than 0.5 m. The rest of the boreholes have errors of approximately 1 m. The mean absolute error for each well is listed in Table 5-4; an X in the table indicates that no measurements were available for the calibration period. It can be seen that the mean error decreases for most wells when adding the validation period.

Time series for some of the HFM boreholes are presented in Figures 5-30 to 5-34. The pattern of the calculated curves follows the measured data even though the calculated values are too high. The draught during the summer of 2006 is reflected by low head elevations even in the upper bedrock, both in measurements and in the model. The time series with undisturbed data are very short, which is a problem when evaluating the results for the head elevations in the bedrock.

Another problem with this evaluation is the differences in the salt content of the groundwater. MIKE SHE does not handle density driven groundwater flow, which means that the salt content and its effects on the density of the water are not taken into consideration when the head is calculated. In the HFM boreholes the point water head is measured. MIKE SHE calculates heads based on homogeneous density, so called fresh water heads; see /Johansson 2008/ for a discussion on density effects and head definitions. Since the gradients in Forsmark are very low, the density likely has a certain effect on the groundwater flow.

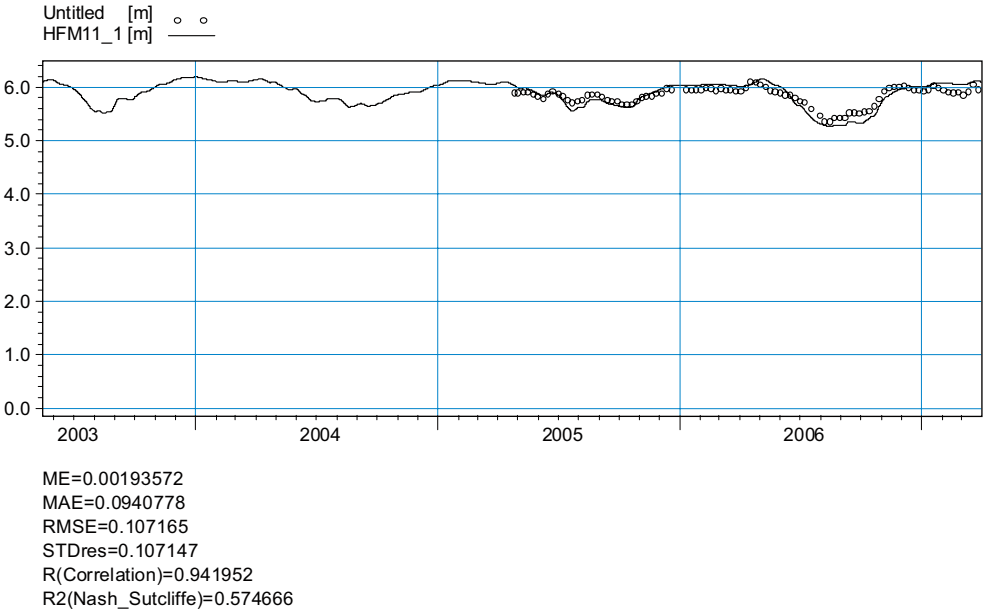

Figure 5-28. *Comparison between measured and calculated head elevations in HFM11_1, the lowest section of HFM11. The observation point in the model is placed in the middle of the section, approximately 80 m.b.s.l.*

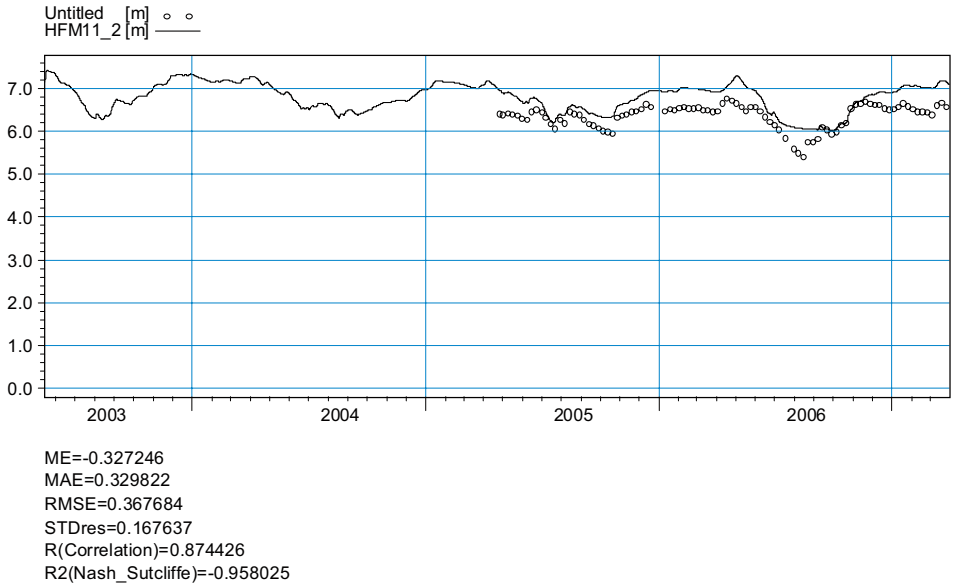

Figure 5-29. *Comparison between measured and calculated head elevations in HFM11_2, the upper section of HFM11. The observation point is placed in the middle of the section, approximately 40 m.b.s.l.*

Table 5-4. Mean errors for the HFM boreholes; "X" indicates that no measurement were available for the evaluated simulation period.

HFM section ID	Mean error, calibration period	Mean error, combined calibration and validation period	Number of days with available data for the combined calibration and validation period
HFM01_1	X	0.80	20
HFM01_2	X	0.95	20
HFM02_1	1.24	1.12	478
HFM02_2	1.11	1.10	462
HFM02_3	1.09	1.12	478
HFM03_1	1.10	1.06	464
HFM03_2	1.10	1.05	464
HFM04_1	0.37	0.30	702
HFM04_2	0.47	0.41	710
HFM04_3	0.18	0.16	706
HFM10_1	0.91	0.87	940
HFM10_2	0.45	0.44	940
HFM11_1	0.07	0.09	789
HFM11_2	0.31	0.33	789
HFM15_1	1.14	1.00	525
HFM15_2	1.12	0.97	569
HFM16_1	X	0.44	454
HFM16_2	X	0.47	454
HFM16_3	X	0.50	454
HFM20_2	0.75	0.54	343
HFM20_3	0.78	0.58	320
HFM20_4	1.20	0.98	345
HFM32_1	X	1.10	446
HFM32_2	X	1.10	446
HFM32_3	X	0.96	349
HFM32_4	X	0.92	495
HFM34_3	X	0.81	358
Mean	**0.79**	**0.75**	**501**

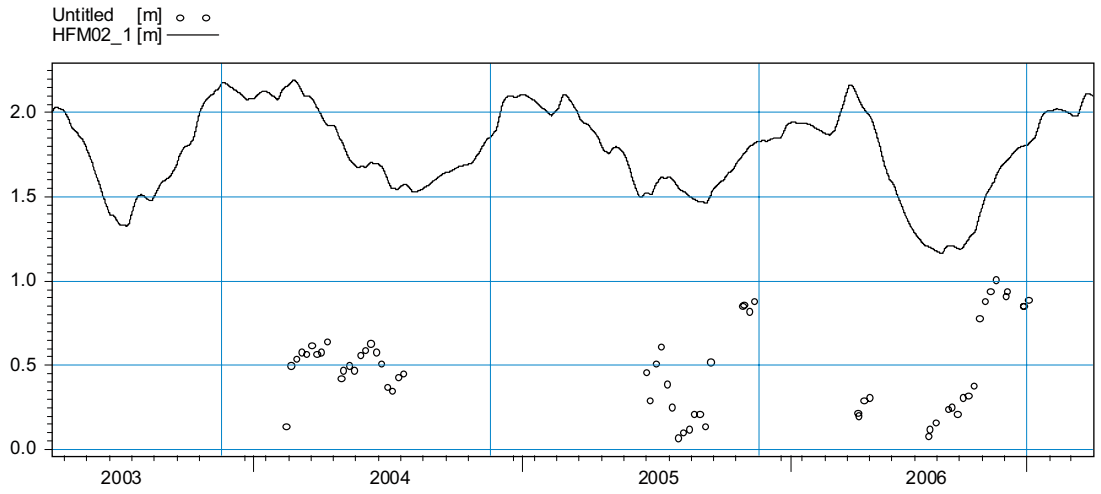

ME=-1.12082
MAE=1.12082
RMSE=1.15474
STDres=0.277823
R(Correlation)=0.351084
R2(Nash_Sutcliffe)=-18.8848

Figure 5-30. *Comparison between measured and calculated head elevations in HFM2_1, the lowest section of HFM2. The observation point in the model is placed in the middle of the section, approximately 75 m.b.s.l.*

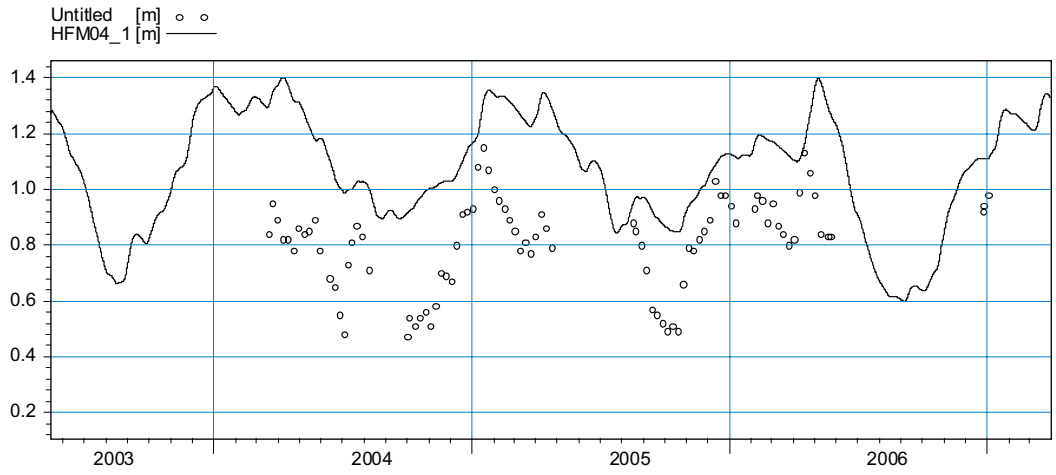

ME=-0.312032
MAE=0.312032
RMSE=0.338507
STDres=0.131237
R(Correlation)=0.65538
R2(Nash_Sutcliffe)=-3.4438

Figure 5-31. *Comparison between measured and calculated head elevations in HFM4_1, the lowest section of HFM4. The observation point in the model is placed in the middle of the section, approximately 140 m.b.s.l.*

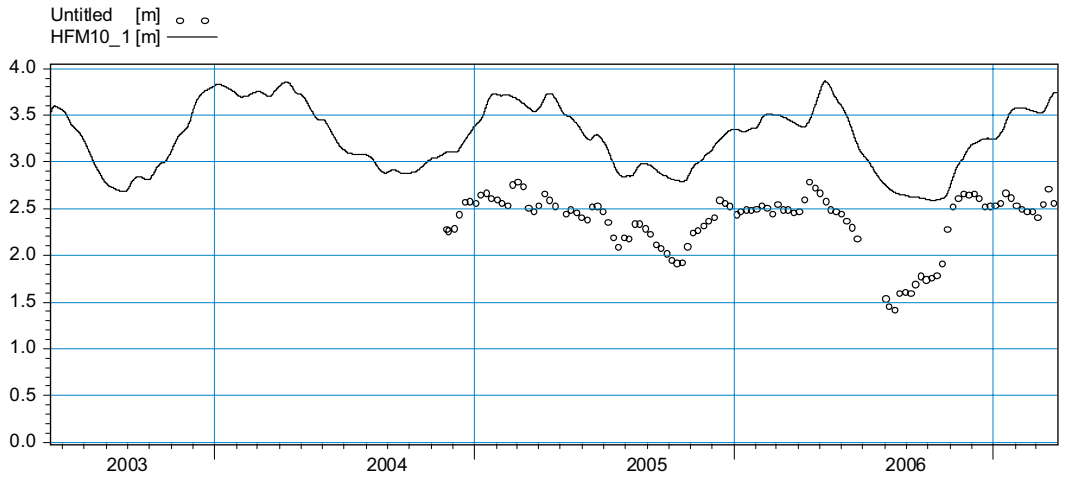

ME=-0.874197
MAE=0.874197
RMSE=0.896766
STDres=0.199922
R(Correlation)=0.81717
R2(Nash_Sutcliffe)=-7.80035

Figure 5-32. *Comparison between measured and calculated head elevations in HFM10_1, the lowest section in HFM10. The observation point in the model is placed in the middle of the section, approximately 115 m.b.s.l.*

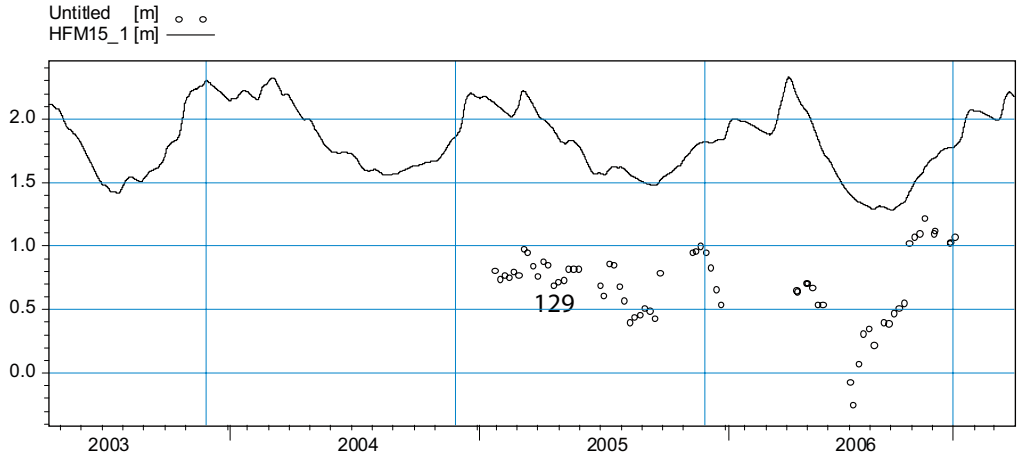

ME=-0.995586
MAE=0.995586
RMSE=1.03239
STDres=0.273182
R(Correlation)=0.460475
R2(Nash_Sutcliffe)=-12.6662

Figure 5-33. *Comparison between measured and calculated head elevations in HFM15_1, the lowest section in HFM1. The observation point in the model is placed in the middle of the section, approximately 65 m.b.s.l.*

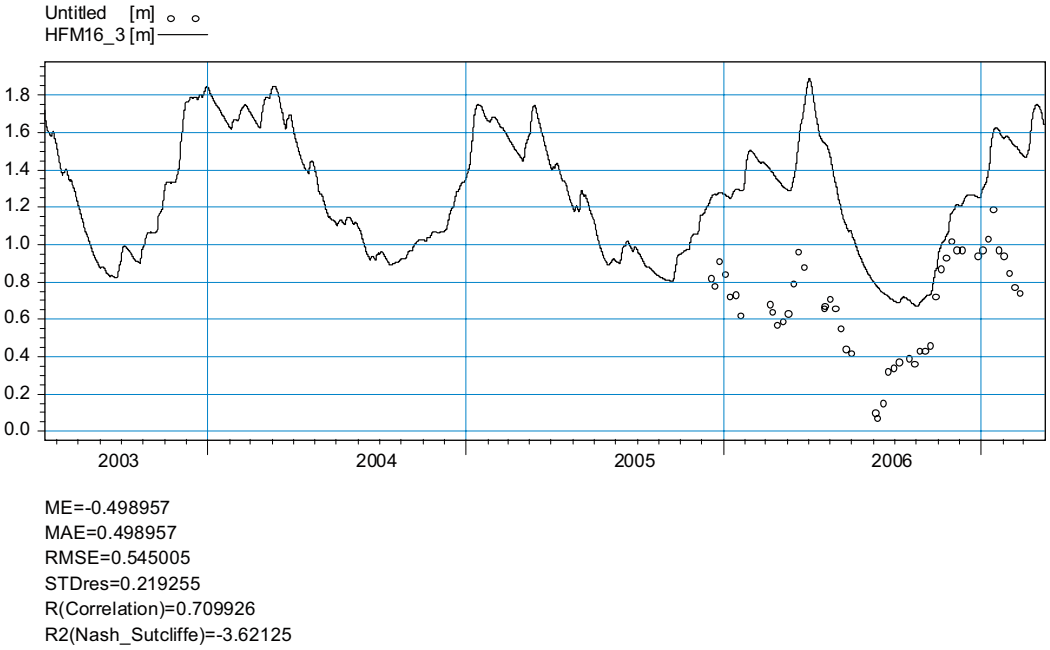

Figure 5-34. *Comparison between measured and calculated head elevations in HFM16_3, the uppermost section in HFM16. The observation point in the model is placed in the middle of the section, approximately 50 m.b.s.l.*

5.2.3 Groundwater table

Generally, the calculated groundwater level within the model area was found to be close to the ground surface, see Figure 5-35. This is also seen in the results for the SFM-boreholes, see Section 5.2.1. The mean groundwater level during a three-year period September 2003 – September 2006, i.e. spatially averaged over the model area and temporally averaged over the simulation period, was calculated to 0.93 m below the ground surface. Groundwater depths of up to 6 m below ground surface were obtained in the area of relatively higher elevation in the south-western part of the model area.

The contours of mapped lakes and water courses in the model area are indicated in Figure 5-35. Areas where the model results show ponded water on the ground surface are indicated by different blue colours. In the areas with ponded water, i.e modelled lakes and wetlands, the different shades of blue indicate the calculated hydraulic head in the uppermost calculation layer. The "positive depths" can be translated to the calculated water depths in the lakes within the model area. The calculated ponded areas, i.e calculated lakes and wetlands, do coincide with the field controlled wetlands and lakes. As described above, the groundwater table follows the topography. This is confirmed by the strong correlation between the mean calculated ground water elevation and the topography (Figure 5-36). SFM0058 is an outlier. This well is situated in till in a locally elevated area. The average groundwater table in the Quaternary deposits seems to be determined by the local ground surface elevation. The measured data show that the majority of the boreholes have a mean groundwater level between 0.5 m and 1 m below the ground surface /Johansson 2008/.

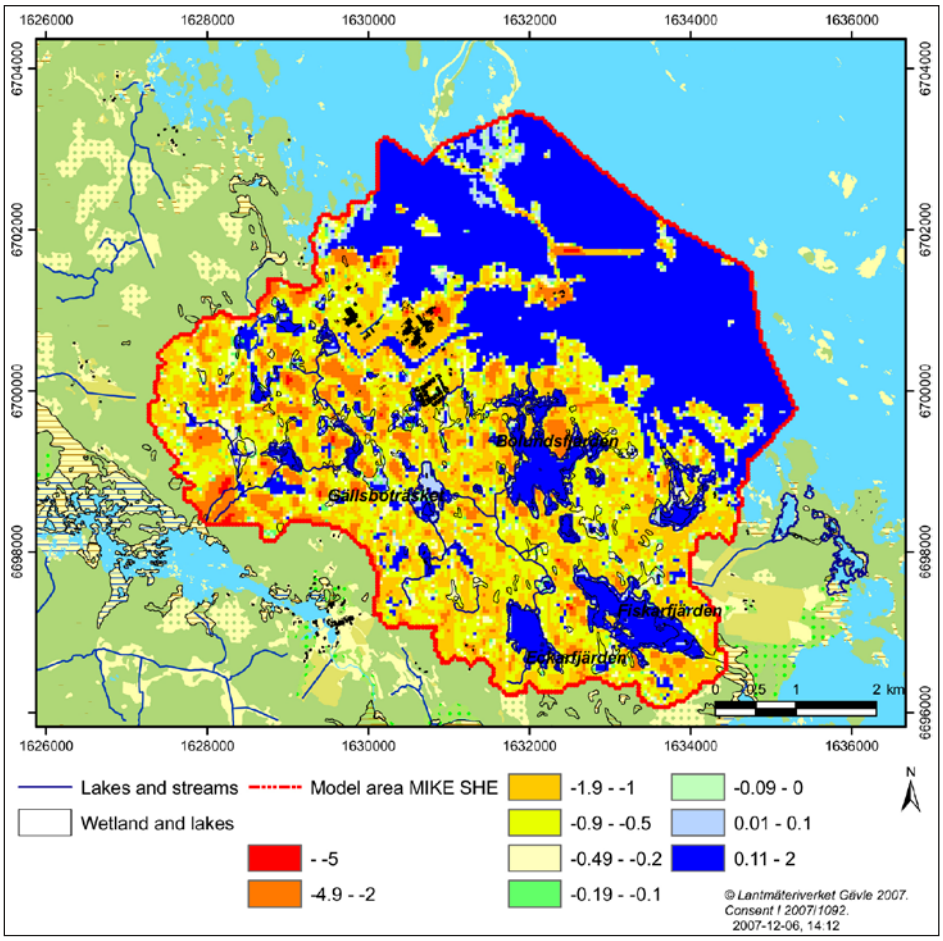

Figure 5-35. *Calculated mean depth to the groundwater table (metres) for the period September 2003 – September 2006.*

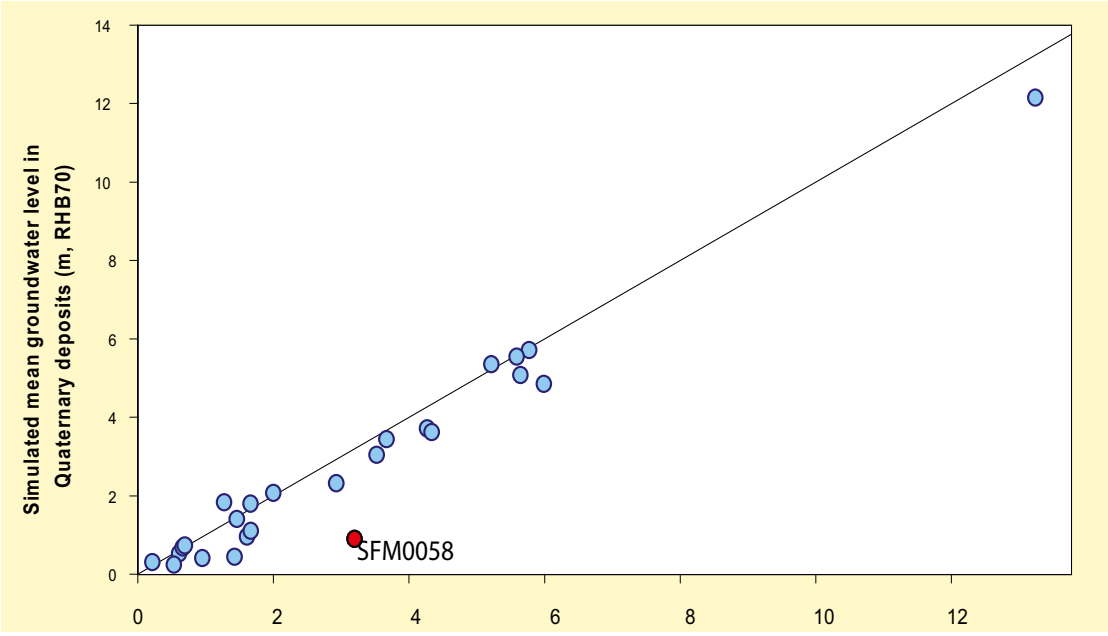

Figure 5-36. *Correlation between the calculated mean groundwater elevation and the ground surface elevation at the monitoring well location. The red-marked well, SFM0058, is an outlier (see text).*

5.3 Transport modelling

This chapter presents the particle tracking simulations performed using the flow model discussed above. Scenarios relevant for the transport from a deep geological repository are studied, but also the pattern of recharge and discharge areas associated with near-surface groundwater flow. The positions where the particles exit the model volume on the ground surface, so called exit points, represent an important type of information for the safety assessment. In the safety assessment biosphere modelling, the areas where the exit points are located will be analysed and described. Thus, the biosphere modellers need to know when and to what extents the exit points show up in, for example, future agricultural areas or lakes, or in the sea.

Particle sources located both at depth in the bedrock and at the top of the model are considered. The modelling activities described below consist of particle tracking simulations only. Advection-dispersion simulations have also been performed, but will not be discussed here. All the simulations performed with the MIKE SHE Advection-Dispersion module are presented in /Gustafsson et al. 2008/. In all transport modelling, advective transport is modelled based on the *Final calibrated model*, which is described in Chapter 5. In the particle tracking scenarios reported here, particles (one in each grid cell) are initially introduced in the top layer or in a deeper bedrock layer at a level of approximately 140 m.b.s.l.

5.3.1 Input data and simulation specification

In particle tracking simulations, hypothetical inert particles or "water parcels" are traced as they are transported by the groundwater flow field in the model volume. The resulting flow paths provide important information as such; they connect the selected starting points with groundwater discharge points or other exit points on the model boundaries. Furthermore, travel or residence times and travel distances along the flow paths can be calculated.

The calculated, three-dimensional flow field described in Chapter 5 is the basis for the advective transport of the particles. In addition to the input required for the flow modelling, the particle tracking simulations require input data on the kinematic porosity, the number of particles introduced, and the starting point of each particle. The kinematic porosity of the bedrock is imported from the ConnectFlow model /Follin et al. 2007/. This is the same dataset as that used to describe the specific yield in the water movement calculations (see Chapter 3); the specific yield and the kinematic porosity are assumed to be equal. Similarly, the kinematic porosity of each Quaternary deposit material is assumed to be equal to the specific yield of that material (see Chapter 3).

The particle tracking calculations are carried out for the saturated zone only. When a particle moves from the saturated zone to another compartment of the model, that particle is not traced further. It is registered to which sink/compartment the particle moves. Quantities such as the travel time and travel distance and the position of the particle are also registered. Thus, it is possible to get information on where the particle leaves the saturated zone and where it goes. A more detailed description of the methodology of the particle tracking calculations is given in /Bosson and Berglund 2006/ and /DHI Software 2007/.

Two cases, referred to as *PT0-bedrock* and *PT0-top*, were studied in the particle tracking simulations:

- *PT0-bedrock*: One particle is introduced in each cell at c. 140 m.b.s.l. in the whole model area.
- *PT0-top*: One particle is introduced in each cell in the uppermost calculation layer in the whole land part of the model area.

The simulation time was 300 years in all *PT0-bedrock* and *PT0-top* simulations, using the calculated transient flow modelling results obtained for the simulated one-year period October 2003 to October 2004 as input. This means that the model results from the MIKE SHE Water movement calculation for this one-year period were cycled 300 times.

5.3.2 Particle tracking results

In total, 22,867 particles (one in each cell in the whole model area) were introduced in case *PT0-bedrock*. The overall results, expressed in terms of where the particles left the saturated zone, i.e. to which other model compartments or boundaries they went, are summarised in Table 5-5. The dominating sink is the combined Overland flow-Unsaturated zone compartment; it is not possible to separate these two sinks. The results also show that 40% of the particles were still left in the model volume at the end of the simulation; this implies that it takes less than 300 years for 60% of the flow paths to reach the ground surface or other model boundaries from a depth of c. 140 m.

An illustration of the numbers in Table 5-5 is shown in Figure 5-37. The figure shows the position of each particle where it has left the saturated zone and moved to a specific sink. The different sinks are marked with different colours. The green dots represent the particles that moved to the combined Overland flow-Unsaturated zone sink. Since the majority of the green dots are situated in the lakes or close to water courses, i.e. in saturated areas, it can be concluded that the majority of the 37% registered in this sink in fact moved to the Overland flow compartment.

Figure 5-37 above is also an illustration of the discharge areas of particles in the uppermost calculation layer. The majority of the particles discharge in lakes and stream valleys. Among the particles that move to the sea, the majority discharges in the littoral zone. Figures 5-38 to 5-41 show the accumulated particle count in each cell in calculation layer 2, 4, 6 and 9. Calculation layer 2 contains the lower part of the Quaternary deposits. The lower level of calculation layer 4 is placed at 30 m.b.s.l., the lower level of calculation layer 6 is at 70 m.b.s.l., and calculation layer 9 is at 130 m.b.s.l.

The accumulated particle count is the total number of times a cell has been hit by a particle. A particle is registered, and the accumulated particle count is increased, each time it passes that specific cell. If the accumulated particle count is zero, no particles have moved through that cell. Thus the figures illustrate the discharge and recharge areas in each layer. By studying the accumulated particle count from layer 9 to 2 it is possible to see how the particles move to high-conductive areas in the bedrock and further towards discharge areas at the surface.

There is a clear concentration of particles in the horizontal sheet joints represented in layer 6. This high conductive area short-circuits the water flow and many particles move out to the sea in this layer. Figure 5-41 shows the accumulated particle count in layer 2, i.e. the discharge from the bedrock to the Quaternary deposits. Lakes, stream valleys and low bathymetric points on the sea bottom are the main discharge areas for flow from the bedrock to the Quaternary deposits on land and the sea bottom sediments.

Table 5-5. Distribution of particles on different sinks for a case with injection at c. 140 m.b.s.l. in the whole model (PT0-bedrock).

Sink	Number of particles	%
Particles removed to OL-UZ*	8,571	37
Particles removed directly to streams	907	4
Particles removed by drain to streams	798	3
Particles gone to the sea	3,514	16
Particles left in the model	9,077	40
Sum	22,867	100

*OL-UZ is the combined Overland flow-Unsaturated zone sink

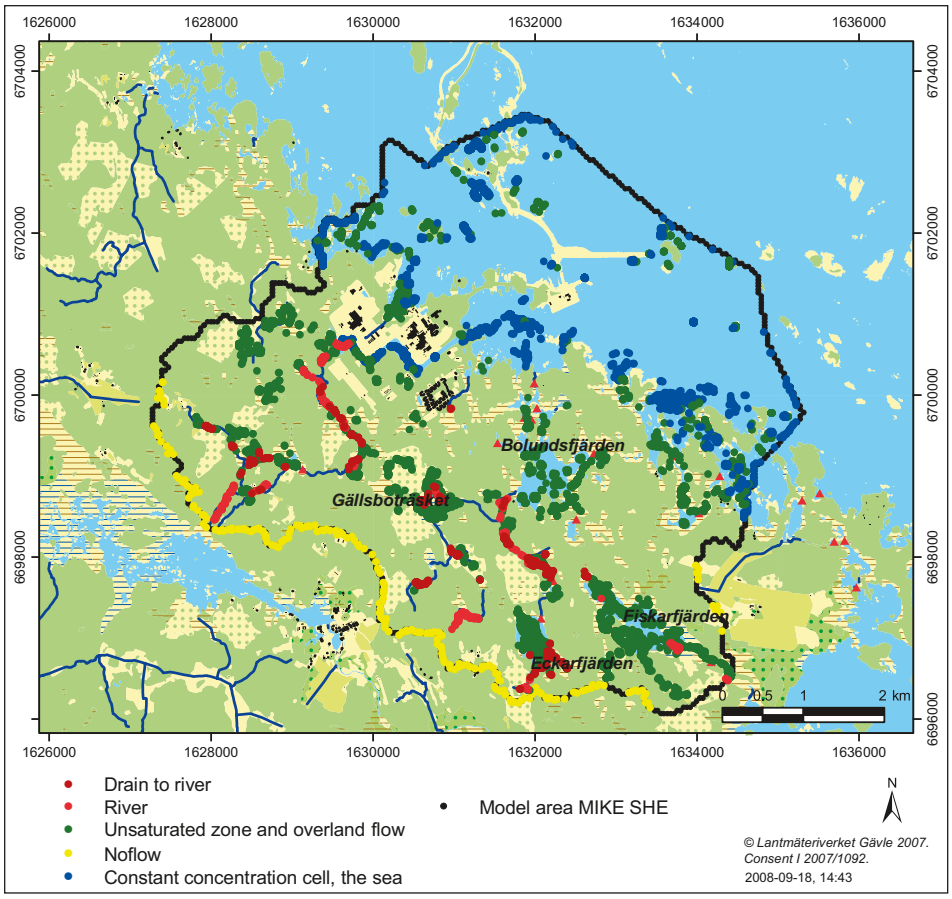

Figure 5-37. *Positions of the particles where they left the saturated zone. The different types of sinks the particles moved to are marked in the figure.*

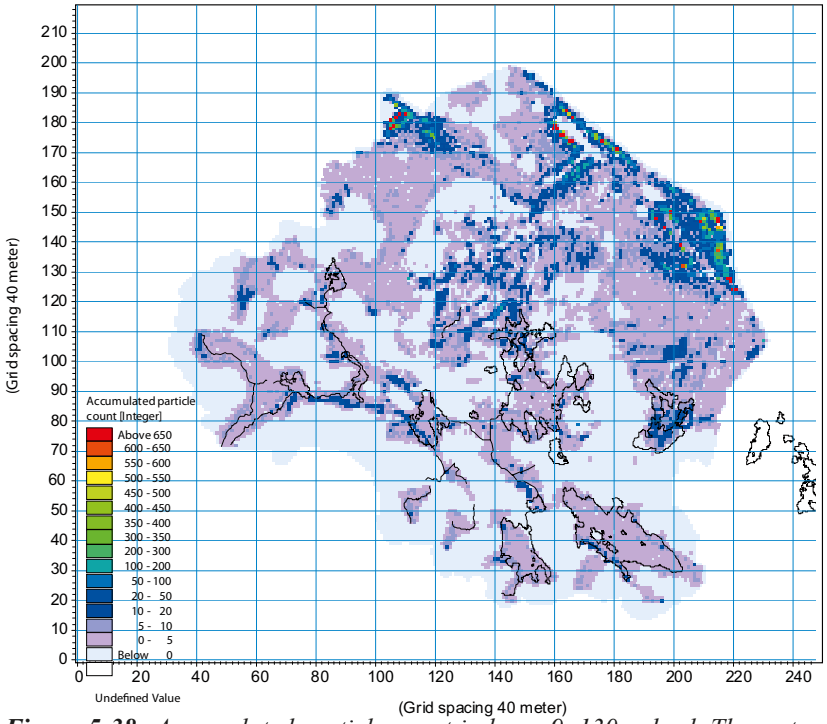

Figure 5-38. *Accumulated particle count in layer 9, 130 m.b.s.l. The water courses and the shorelines of the lakes are marked by black lines in the figure.*

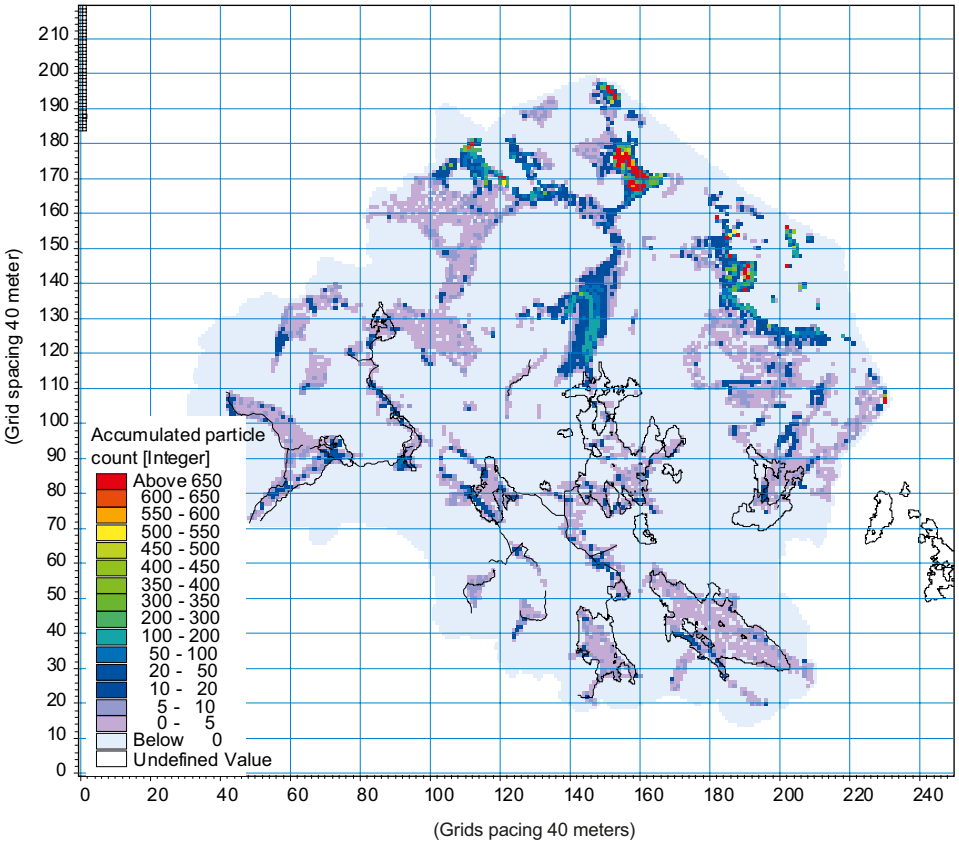

Figure 5-39. *Accumulated particle count in layer 6, 70 m.b.s.l. The water courses and the shorelines of the lakes are marked by black lines in the figure.*

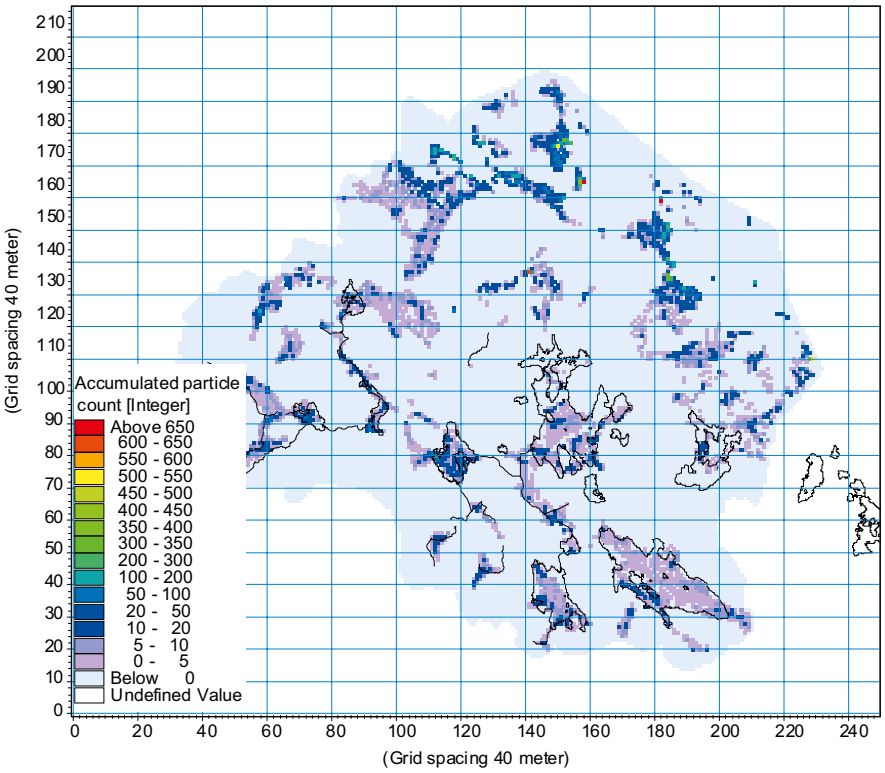

Figure 5-40. *Accumulated particle count in layer 4, 30 m.b.s.l. The water courses and the shorelines of the lakes are marked by black lines in the figure.*

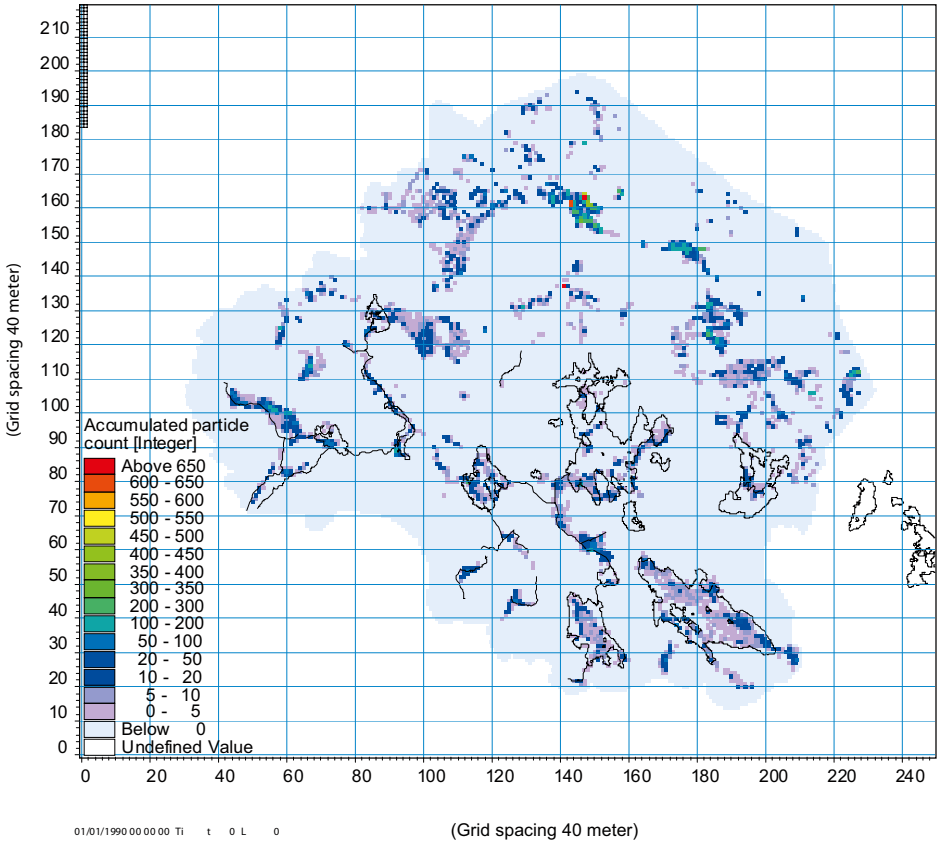

Figure 5-41. *Accumulated particle count in layer 2, which mainly consists of QD. The water courses and the shorelines of the lakes are marked by black lines in the figure.*

Figures 5-42 and 5-43 illustrate particle release areas for different discharge areas corresponding to different registration zones in the MIKE SHE model. A registration zone can be a catchment area, a lake or some other sub-volume of interest for the analysis of the results. In Figure 5-42 each of the four lakes, Lake Bolundsfjärden, Lake Eckarfjärden, Lake Gällsboträsket and Lake Fiskarfjärden represent a registration zone. Thus, the figure illustrates where the particles registered in each registration zone were released at c. 140 m.b.s.l. It is seen that the particles move towards the lakes. The particles registered in each lake originate from their surroundings. No evidence for long-range transport can be found. Most of the particles released at 140 m.b.s.l. remain within the catchment where they were released.

In Figure 5-43 the sea is a registration zone, i.e. the figure shows the starting points for the particles registered in the sea. Most of the particles registered in the sea are also released below the sea. In the figure, the area with high horizontal hydraulic conductivity in the bedrock, at 70 m.b.s.l., is marked with a dotted line. Almost all the particles released in the land part of this high-conductive area are registered in the sea. There is a horizontal transport of particles towards the sea inside this area. Particles released in the blue area close to the model boundary have gone to the model boundary. This is the reason for the empty areas at the sea in the figure. The cooling water intake canal to the nuclear power plant is also a discharge area for particles. The canal is a part of the sea and it is seen in Figure 5-43 that particles released around the canal has been registered in the sea.

Accumulated particle counts for cells in the profile through Lake Eckarfjärden shown in Figure 5-44 are presented in Figure 5-45. The accumulated particle counts, i.e. the total numbers of particles moved through each cell, are shown for five different times (T), T=0, T= 4 month, T= 1 year, T= 10 years and T= 100 years. The figure illustrates how the particles move towards the lake; there is a concentration of particles under the lake. The topographical slope towards the lake and the littoral zone act as a recharge area. There is an accumulation of particles under the level where the particles were introduced. This phenomenon, with a littoral zone acting as a recharge area is also seen in the results when studying the gradient between different model compartments in Section 6.2.5.

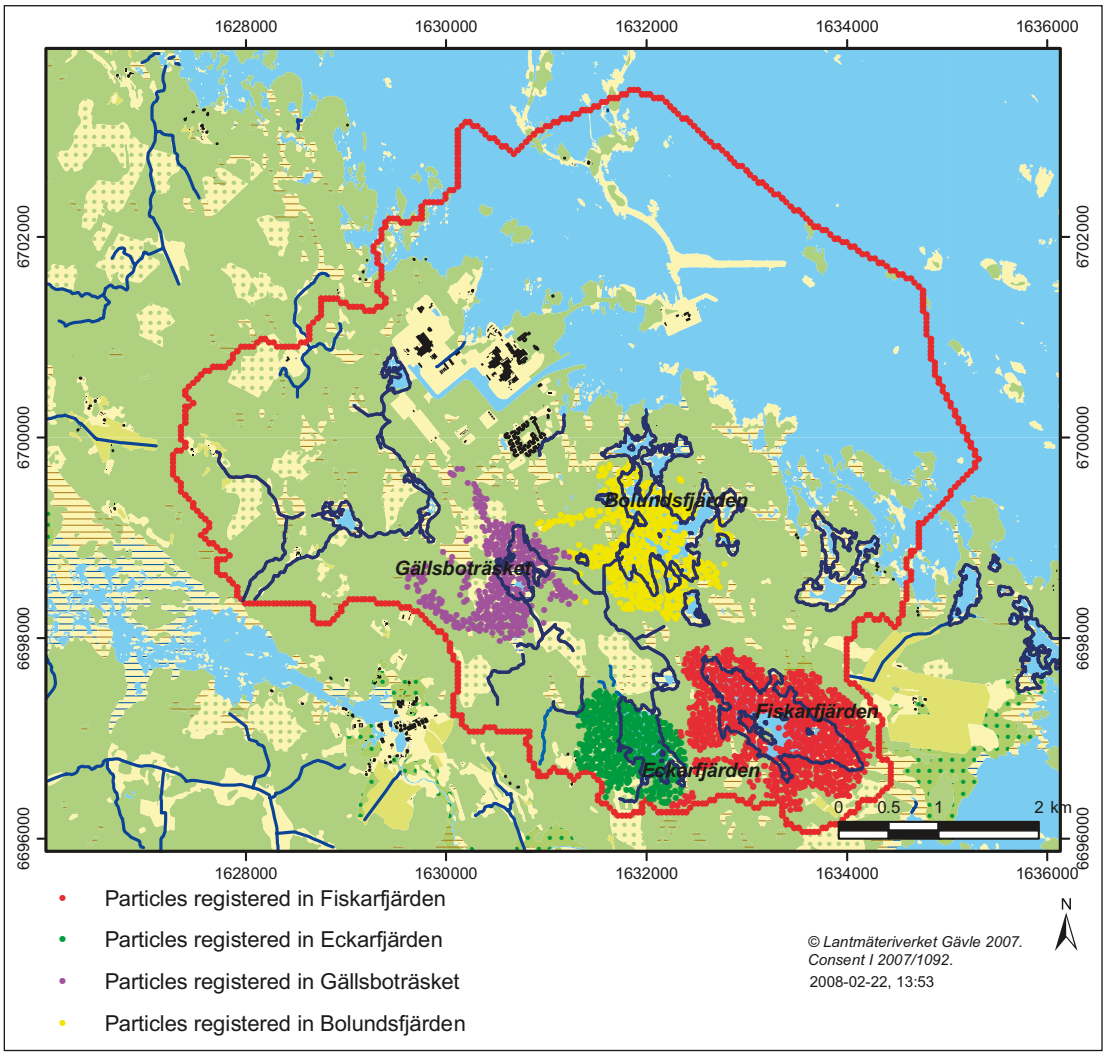

Figure 5-42. *Release areas for particles registered in Lake Gällsboträsket, Lake Eckarfjärden, Lake Bolundsfjärden and Lake Fiskarfjärden.*

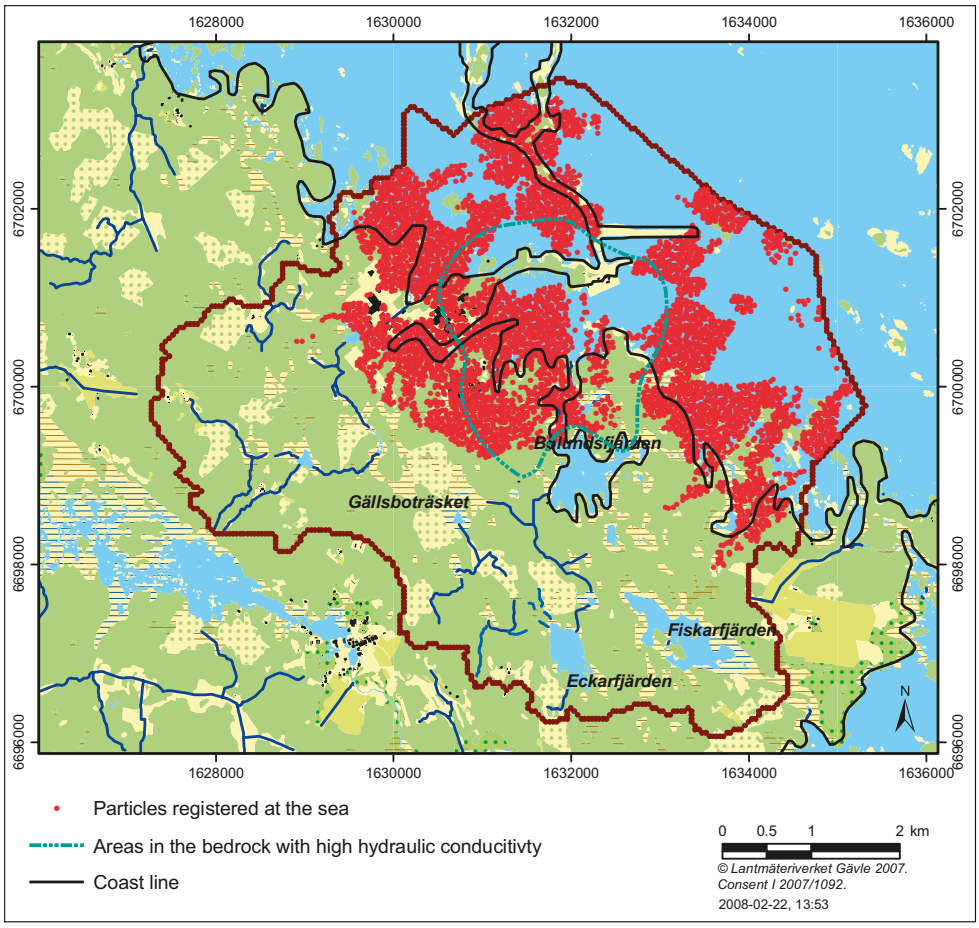

Figure 5-43. *Release areas for particles registered in the sea. The area with high horizontal hydraulic conductivity at 70 m.b.s.l. is also marked in the figure.*

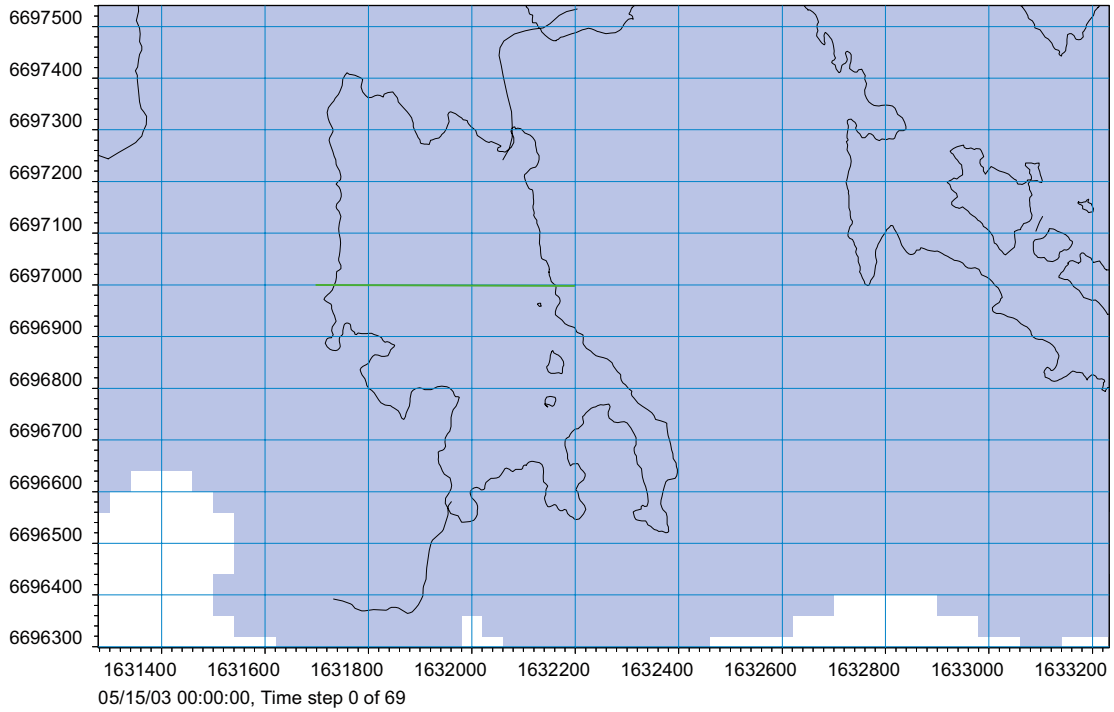

Figure 5-44. *Lake Eckarfjärden with green line indicating profile for which accumulated particle counts in Figure 5-45 are calculated.*

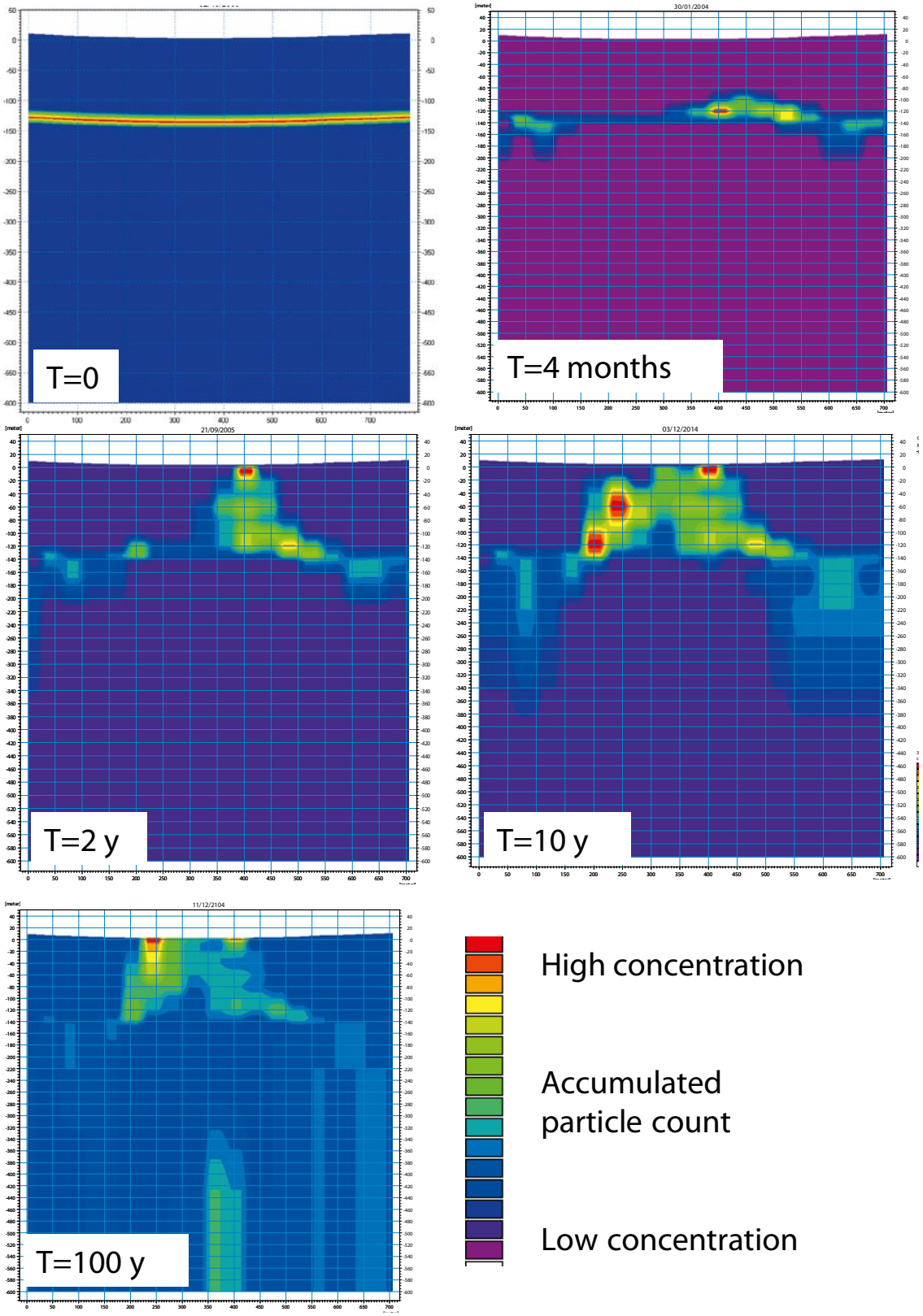

Figure 5-45. *Accumulated particle counts at the start of the simulation and after 4 months, 2 years, 10 years and 100 years in a profile through Lake Eckarfjärden (Figure 5-44).*

In case *PT0-top*, one particle in each cell was introduced in the uppermost layer of the model. The overall results, expressed in terms of where the particles left the saturated zone, i.e. to which other model compartments or boundaries they went, are summarised in Table 5-6. In total, 16,703 particles were introduced to the model. Particles placed in an unsaturated cell or in a cell in contact with a river link are directly excluded from the simulation. In the sea, the uppermost calculation layer has a prescribed head describing the varying sea water level; no particles were introduced in the sea. This is the reason for the reduced number of particles introduced in case *PT0-top* compared to *PT0-bedrock*. The dominating sink is the combined Overland flow-Unsaturated zone compartment; 78% of the particles discharged to either the Unsaturated zone or the Overland flow compartment.

The accumulated particle counts in layers 2, 3, 6 and 9 are presented in Figures 5-46 to 5-49. The areas with an accumulated particle count higher than zero in layer 2 can be interpreted as recharge areas in the Quaternary deposits. The accumulated particle count in the lakes is almost zero. Figure 5-47, showing the accumulated particle count in layer 3 illustrates the recharge areas between the QD and the uppermost bedrock. Still, there are no clear patterns of recharge and discharge areas, except from the lakes. The areas under the lakes have not received any particles. Deeper in the bedrock, in layer 6 and 9 the pattern of the fracture zones is clearer. Many particles reach layer 6 and move towards the areas with high horizontal conductivity. Only a few percent of the particles reach calculation layer 9. Fracture zones with gradients directed downwards receive in total 966 particles.

An additional case was simulated where particles were released only in the area of the planned repository. Since the vertical resolution of the MIKE SHE model is very low below 200 m.b.s.l., the particles were released at the same level as in case *PT0-bedrock*, (c. 140 m.b.s.l.) even though the repository is planned to be build at a depth of approximately 500 m. One particle in each cell in an area corresponding to the horizontal extent of the planned repository was released; the release area is shown in Figure 5-50.

The exit points are shown in Figure 5-51. The majority of the particles released inside the repository area discharged to the sea. The particles showed up in the sea basin near the nuclear power plant and the SFR facility. Some particles also went to the combined Overland flow-Unsaturated zone sink. Among the particles gone to the combined OL-UZ sink, almost all went to Lake Bolundsfjärden or the vicinity of this lake.

Table 5-6. Distribution of particles on different sinks for a case with injection at the upper model boundary (PT0-top).

Sink	Number of particles	%
Particles removed to OL-UZ*	13,024	78
Particles removed directly to streams	861	5
Particles removed by drain to streams	1,173	7
Particles gone to model boundary	497	3
Particles gone to the sea	601	4
Particles left in the model	547	3
Sum	16,703	100

*OL-UZ is the combined Overland flow-Unsaturated zone sink

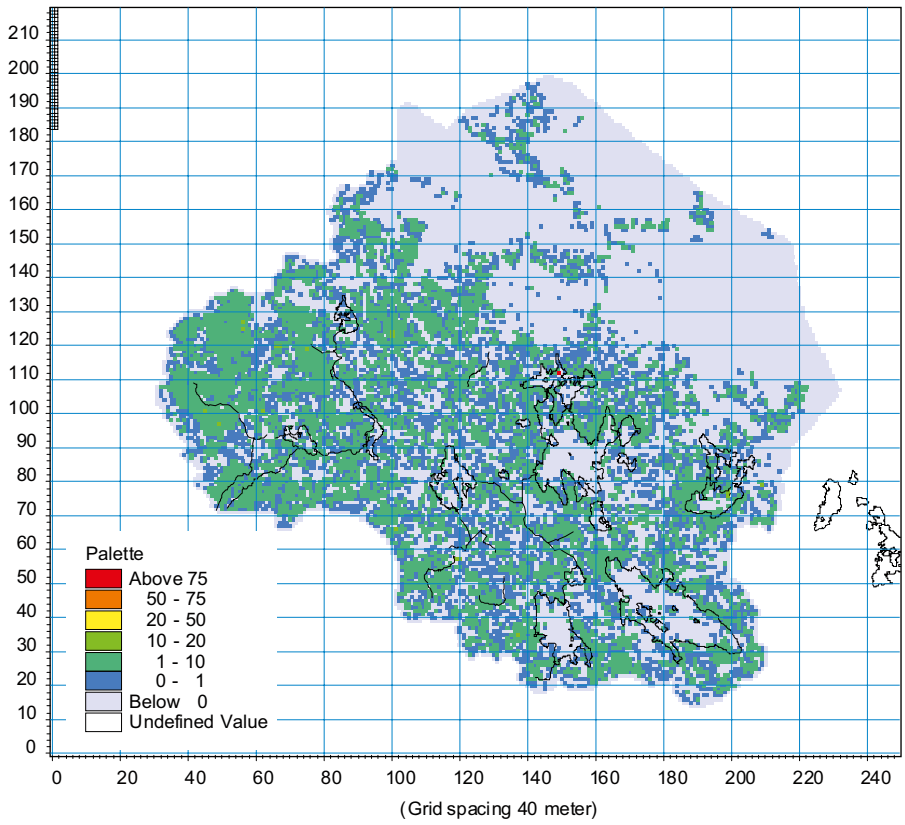

Figure 5-46. *Accumulated particle count in layer 2 (the lower QD layer). The water courses and the shorelines of the lakes are marked by black lines in the figure.*

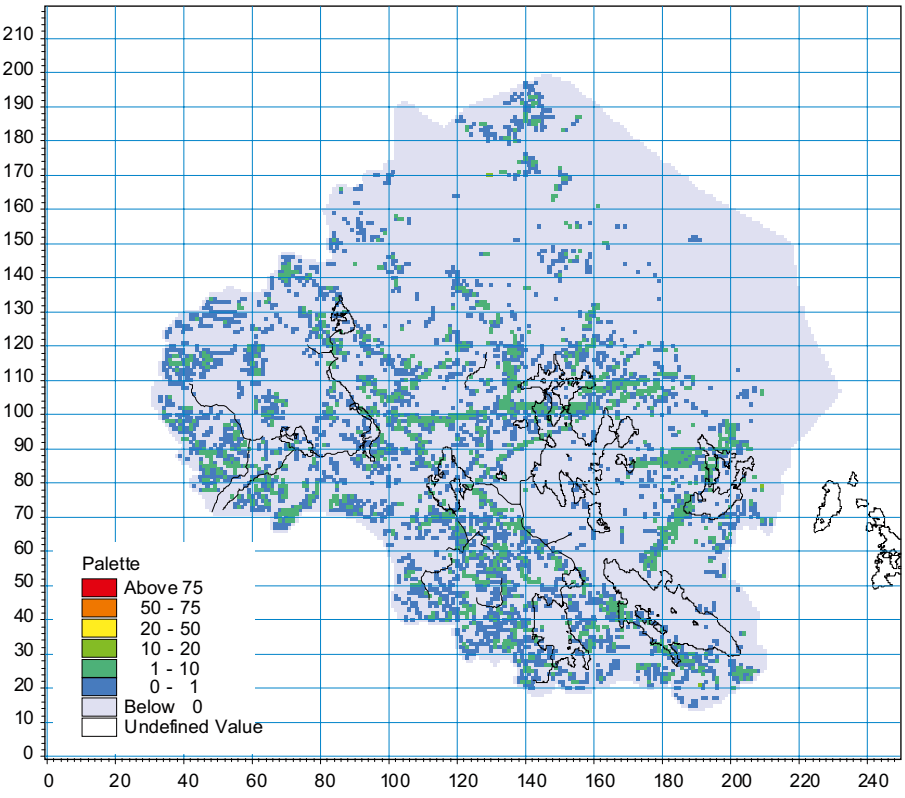

Figure 5-47. *Accumulated particle count in layer 3, the uppermost bedrock layer at c. 10 m.b.s.l. The water courses and the shorelines of the lakes are marked by black lines in the figure.*

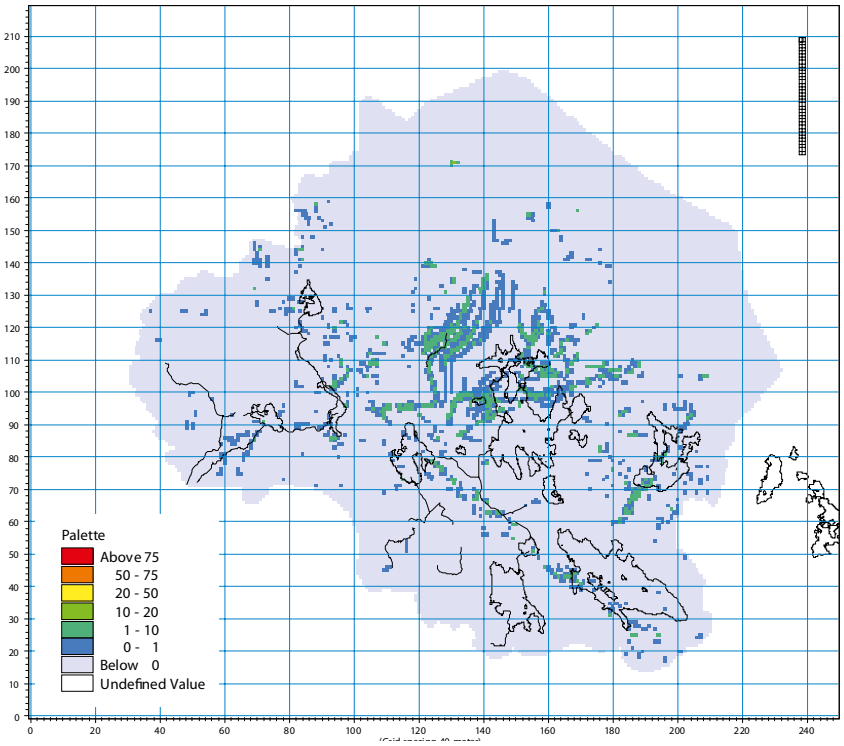

Figure 5-48. *Accumulated particle count in layer 6 at c. 70 m.b.s.l. The water courses and the shorelines of the lakes are marked by black lines in the figure.*

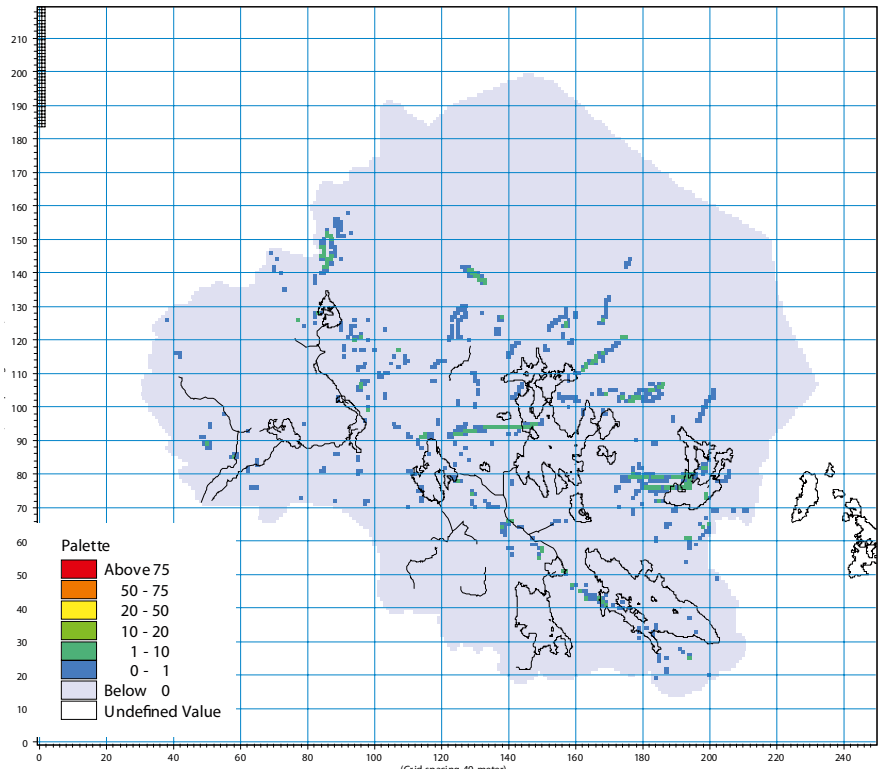

Figure 5-49. *Accumulated particle count in layer 9 at c. 130 m.b.s.l. The water courses and the shorelines of the lakes are marked by black lines in the figure.*

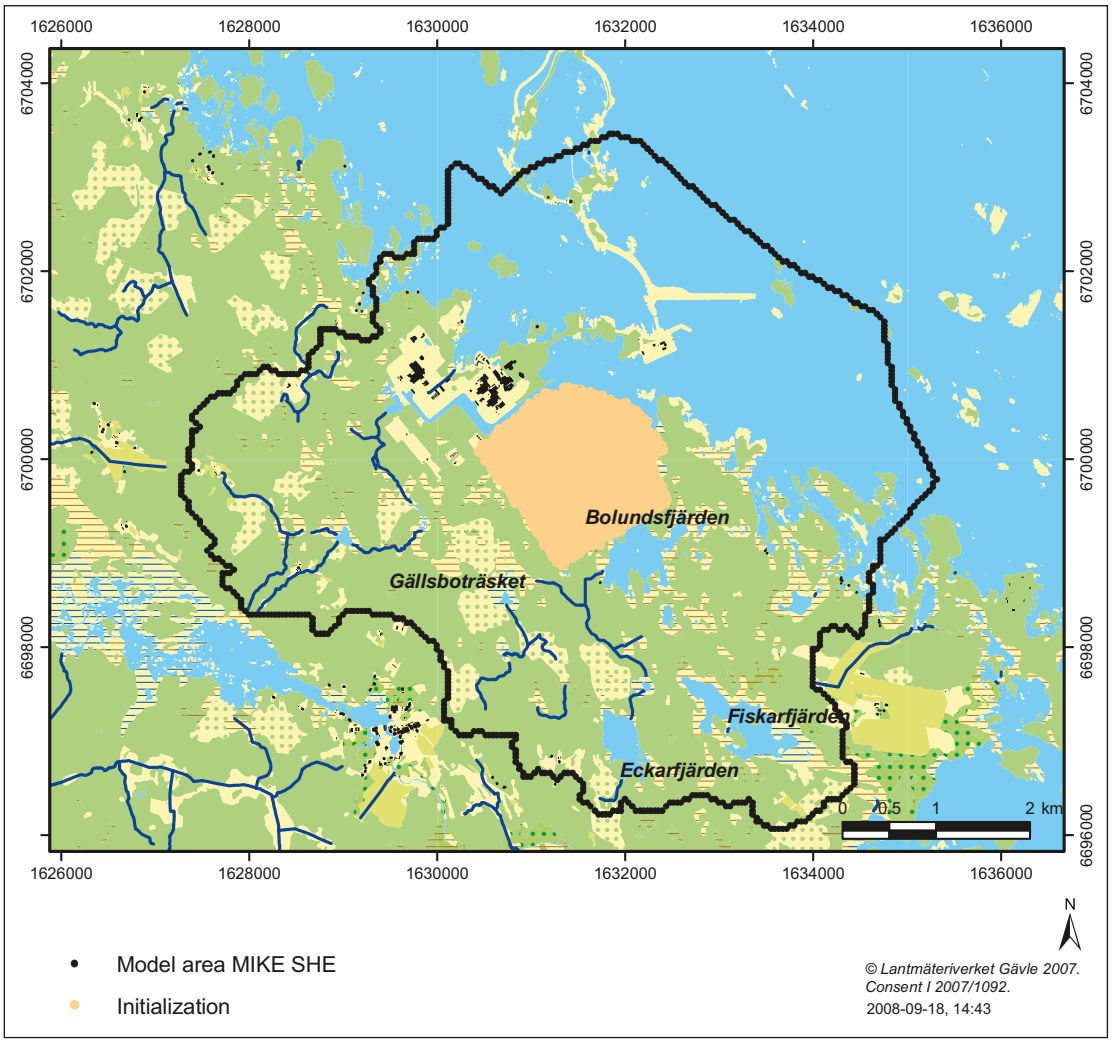

Figure 5-50. *The horizontal extent of the area corresponding to the planned repository. One particle was released in each cell at c. 150 m depth inside this area.*

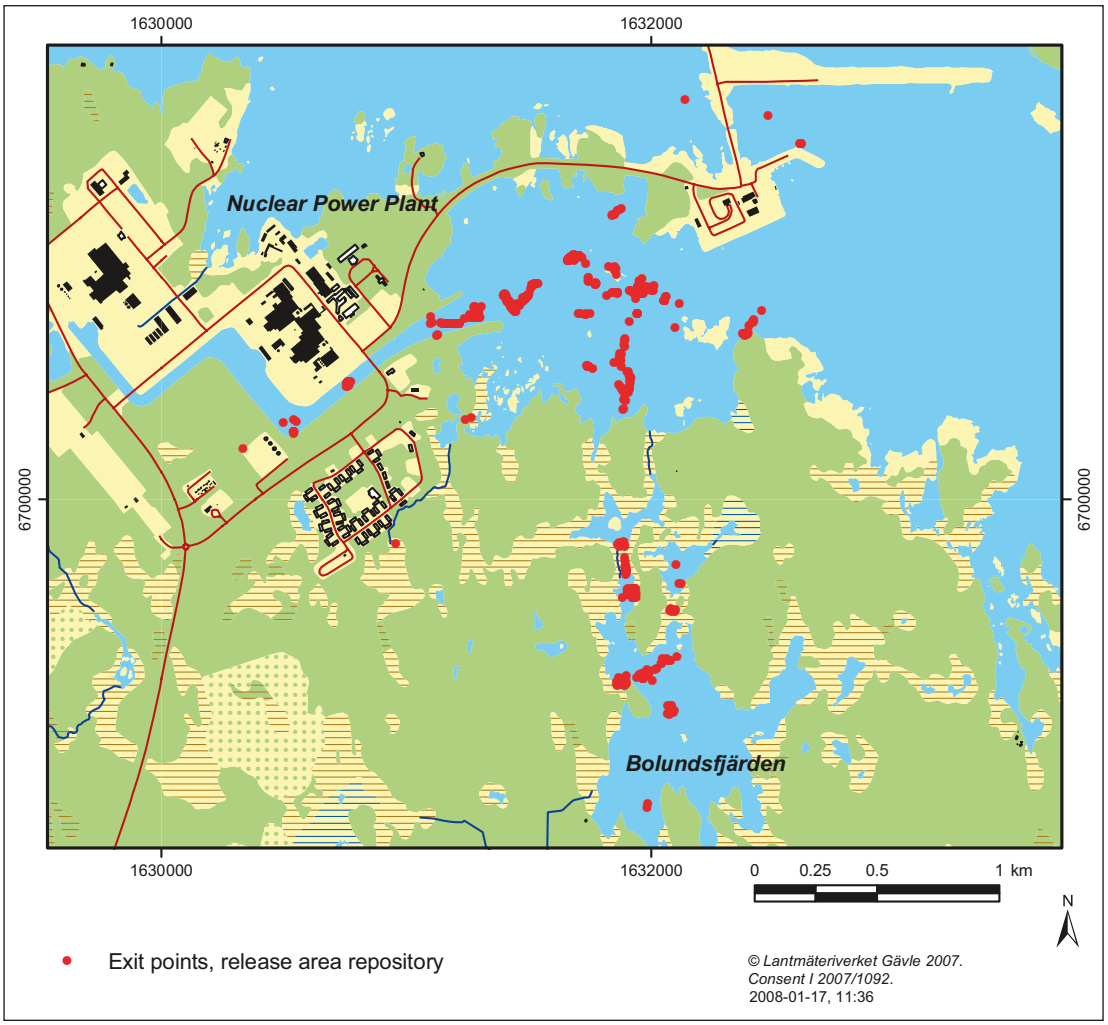

Figure 5-51. *Exit points for the case where particles were released inside an area corresponding to the planned repository.*

5.3.3 Summary of the particle tracking simulations

The particle tracking results indicates local flow cells with short flow paths and a relative fast transport from the bedrock up to the ground surface. The areas with horizontal structures of high horizontal hydraulic conductivities, the so-called sheet joints, short circuit the flow paths of particles released in the area where these structures are found.

The overall pattern of recharge and discharge areas shown in the particle tracking results are not always verified by the observed measurements at the site. The observed downward gradient between the QD and the bedrock in the area around Lake Bolundsfjärden is not reflected in the model results. In the model, all the lakes and the areas close to the lakes act as discharge areas. Due to the model's overestimation of the groundwater elevation in the bedrock, the gradient between the QD and the bedrock is always directed upwards in the major part of the model area. The pattern of recharge and discharge areas of particles in the model is therefore somewhat doubtful. The importance of the hydraulic gradient between different model compartments is further discussed in Chapter 6.

5.4 Calculations with new QD-model

When the calibration process described in Chapter 4 was finalised and the MIKE SHE model was validated, a new version of the geometric model of the Quaternary deposits was delivered. The effects of the changes in the QD model were analysed by implementing the new geological layers in the calibrated MIKE SHE model. Both flow modelling and transport calculation were performed. The results of this modelling are presented in the following.

5.4.1 Main differences between the two QD-models

The differences between the version 2.2 and 2.3 QD models are described in /Hedenström et al. 2008/. The helicopter-borne geophysics data used as input to the first (version 2.2) QD model used in the MIKE SHE modelling overestimated the depth to the bedrock. Therefore, the modelled total depth of Quaternary deposits in some areas became too large. A new QD model, in /Hedenström et al. 2008/ referred to as the 2.3 model, was produced without the geophysical data as input.

Figure 5-52 shows the difference between the total QD depths in the two models. The largest differences are obtained for areas below the sea, where the difference between the two models is up to 22 m. In the inland part of the QD model, the largest differences are up to ten meters. The thickness and extent of the lake sediments have not been changed. Inside the MIKE SHE model area, the largest difference is found in the western part and close to the nuclear power plant. The conceptual model, the number of geological layers and the hydraulic properties of each layer were not changed. Thus, it was only the geometrical model of the QD that was updated.

5.4.2 Results of flow modelling

The new QD model did not cause any larger effects on the groundwater table in the model area. The changes in the mean absolute errors for the majority the SFM- and HFM-wells were very small. No effects on the water levels and surface water discharges could be observed. The MAE and ME of all the SFM- and HFM-wells and the surface water stations are listed in Appendix 2. There are three SFM-wells that are affected by the change of QD model: SFM0033, SFM0057 and SFM0058. The pattern and seasonal variation is improved in SFM0033, even though the MAE is somewhat increased. A comparison of the time series for SFM0033 with the old and the new QD models is shown in Figure 5-53.

The change of QD model has a negative influence on SFM0057; the MAE increases from 0.31 m to 0.58 m. In SFM0058, MAE is decreased from 0.57 m to 0.45 m. Comparison of the time series for SFM0057 and SFM0058 obtained with old and new models are shown in Figures 5-54 and 5-55. There is a reduction of 2 cm in the mean of all MAE for the HFM-wells. A reduction of the mean absolute error can be noticed in almost all HFM-wells, although the reductions are small.

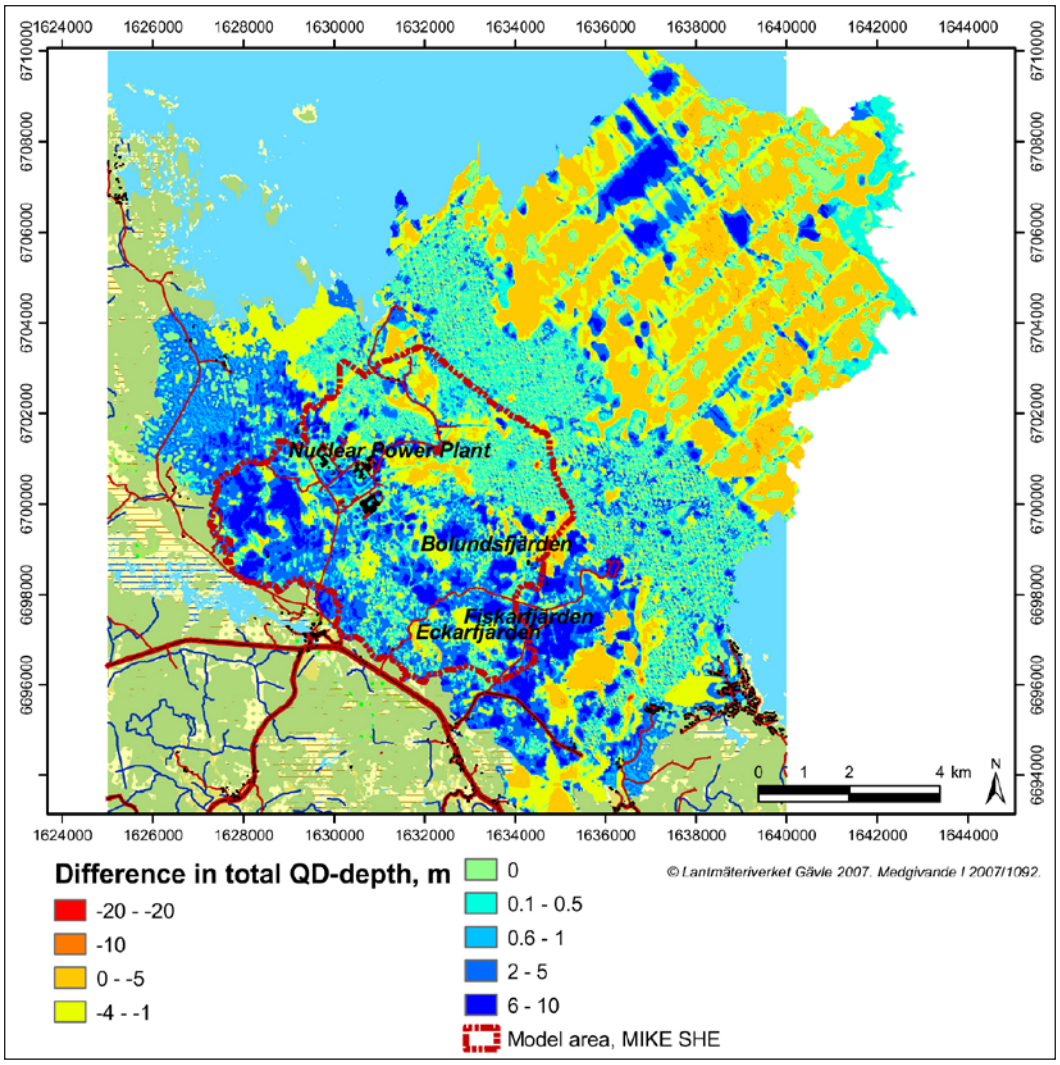

Figure 5-52. *Difference in total QD depth between the 2.2 and 2.3 versions of the Forsmark QD geometry model /Hedenström et al. 2008/.*

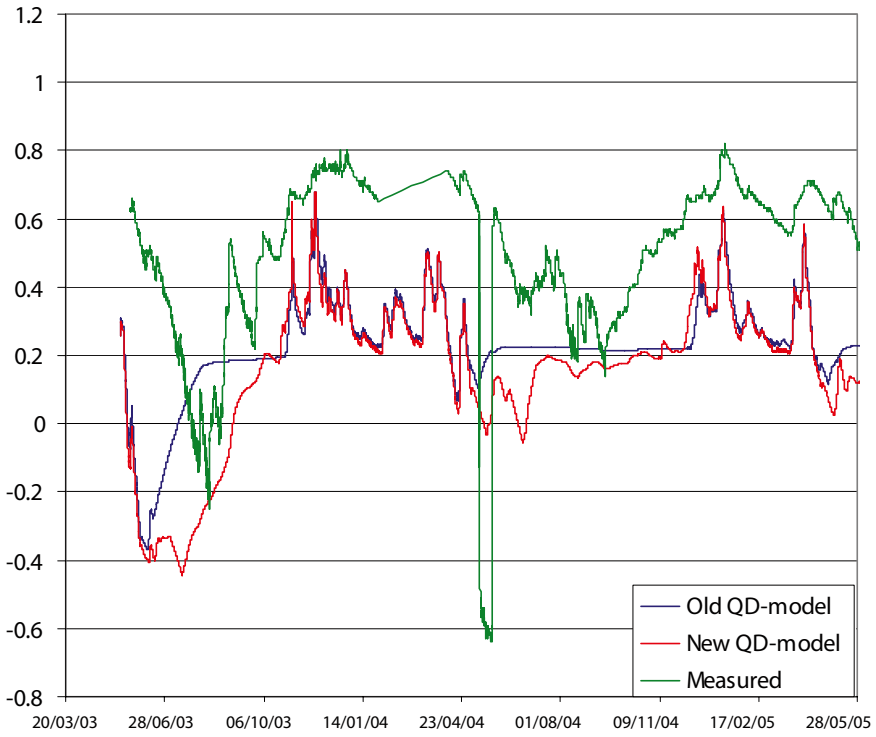

Figure 5-53. *Comparison between measured and calculated groundwater heads in SFM0033 for the old (2.2) and new (2.3) QD geometry models.*

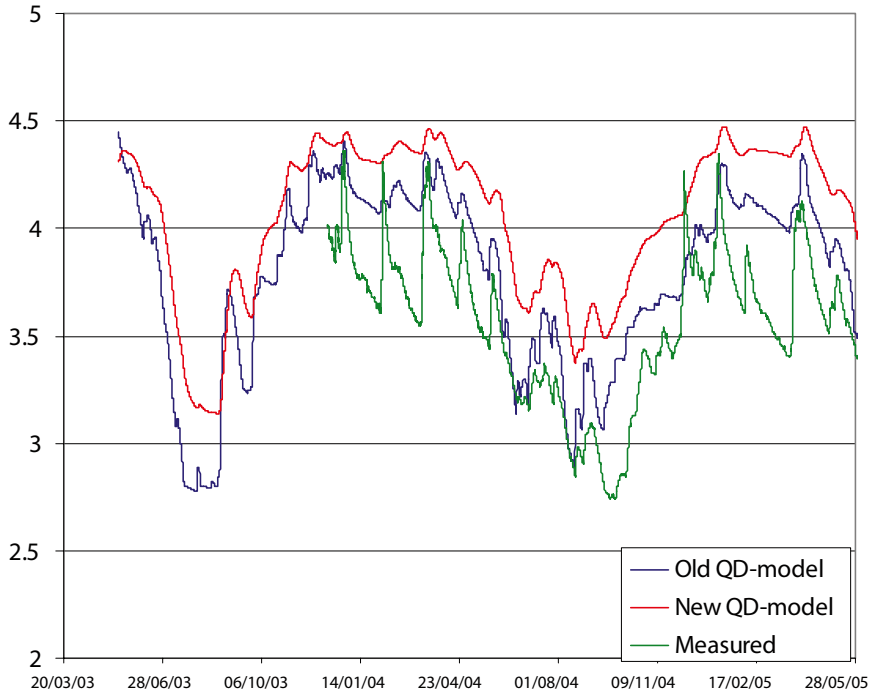

Figure 5-54. *Comparison between measured and calculated groundwater heads in SFM0057 for the old (2.2) and new (2.3) QD geometry models.*

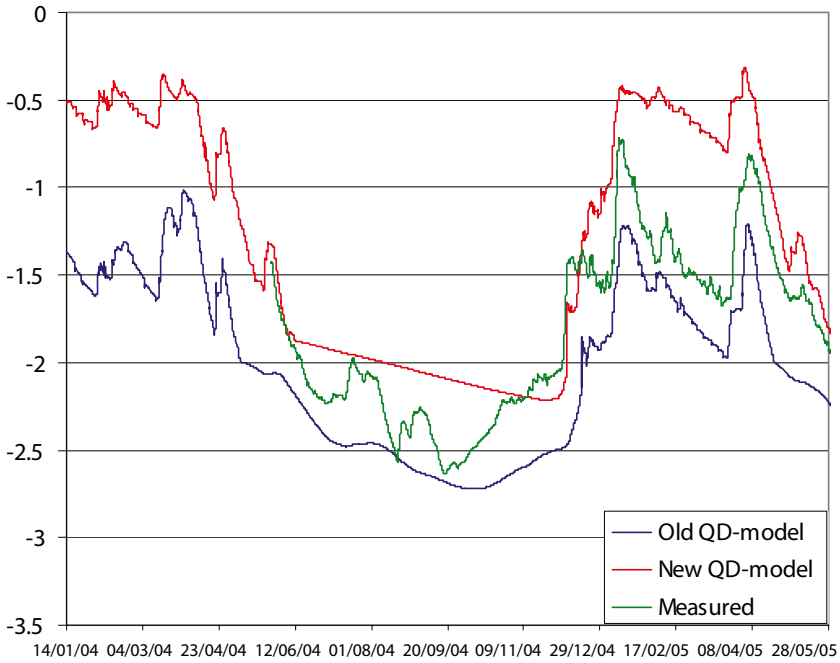

Figure 5-55. *Comparison between measured and calculated depths to the groundwater surface in SFM0058 for the old (2.2) and new (2.3) QD models.*

5.4.3 Results of particle tracking simulations

No major differences were found between the particle tracking results obtained with the old and new QD models. The case where one particle in each cell was released at c. 140 m depth was repeated with the updated QD-model, see summary of results in Table 5-7. The patterns of the exit points are the same for the two cases and the distribution of the sinks to which the particles have gone are almost the same. There is a slight increase of the sink "particles removed by drain to river" with 1%. The number of particles reaching the model boundary and the number of particles left in the model at the end of the simulation have also increased by c. 1%. A decrease with 1% can be noticed for the particles that have gone to the sea.

Figure 5-56 shows the locations where the particles have left the saturated zone from the simulations with the old and the new QD models. All the sinks for each QD model (unsaturated zone, overland water, the sea, etc) are marked with the same colour. The "exit points" obtained with the new QD model are marked in red and the "exit points" based on the old QD model are marked in blue. The overall pattern is the same for the two simulations. Figure 5-57 shows the exit points from the two models close to the nuclear power plant where the difference in total QD depth is significant. However, it is seen that the exit points also here are almost the same for the two QD models. The spreading of the exit points in the area shown in Figure 5-57 is somewhat smaller for the new QD-model than for the old one.

The case where particles were released only in the area of the planned repository was repeated with the new QD geometry model. There is only a slight difference between the exit points from the two models. The particles show up in the same sea basin for the two cases and no major differences can be seen. The exit points from this simulation performed with the old and the new QD model is shown in Figure 5-58.

Table 5-7. Distribution of particles on different sinks in a model based on the updated QD geometry model with injection of particles at a depth of c. 140 m.

Sink	Number of particles	%
Particles removed to OL-UZ*	8,878	39
Particles removed directly to streams	1,004	4
Particles removed by drain to streams	876	4
Particles gone to model boundary	440	2
Particles gone to the sea	2,403	11
Particles left in the model	9,266	41
Sum	22,867	100

*OL-UZ is the combined Overland flow-Unsaturated zone sink

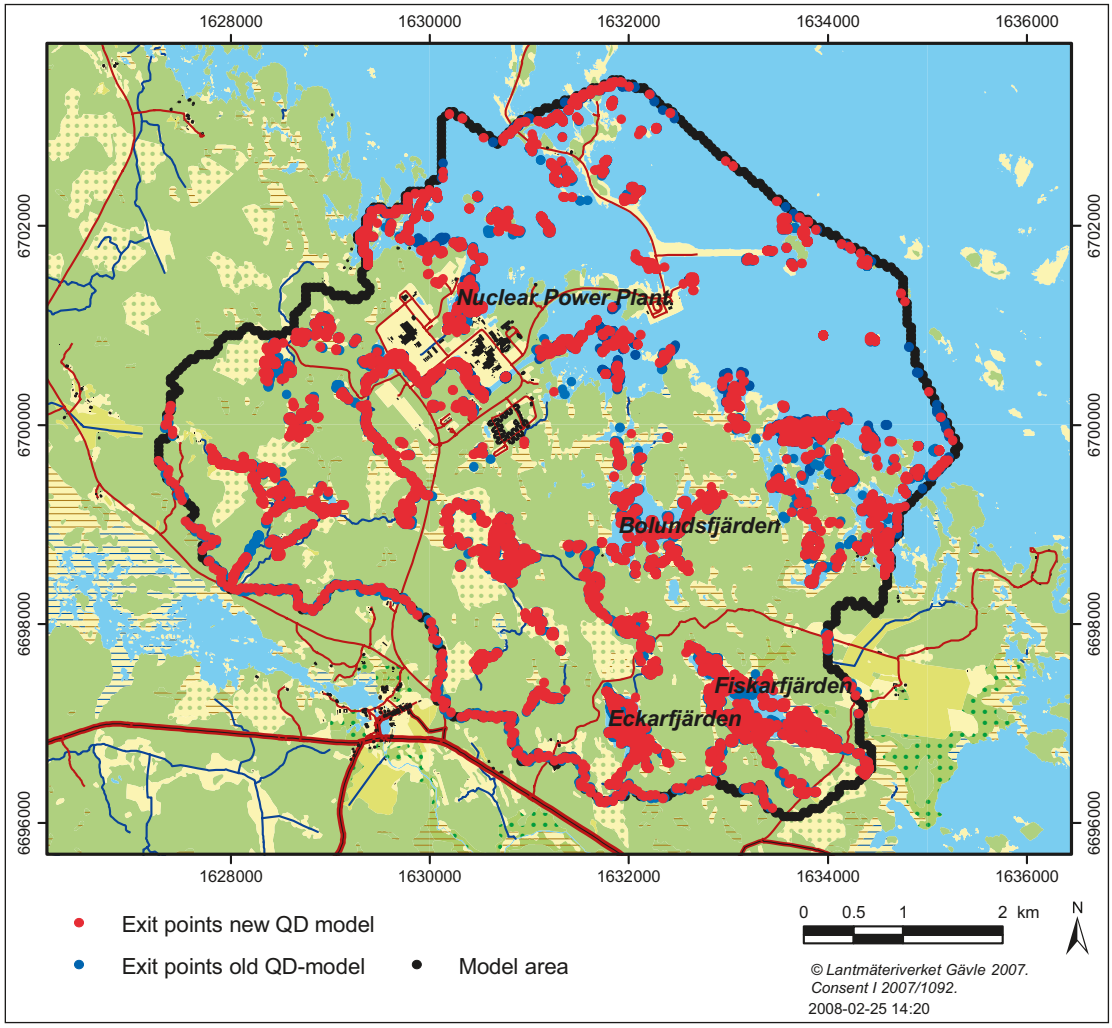

Figure 5-56. *Locations where the particles left the saturated zone. The blue points represent particles traced in the old QD model and the red points particles traced in the new QD model.*

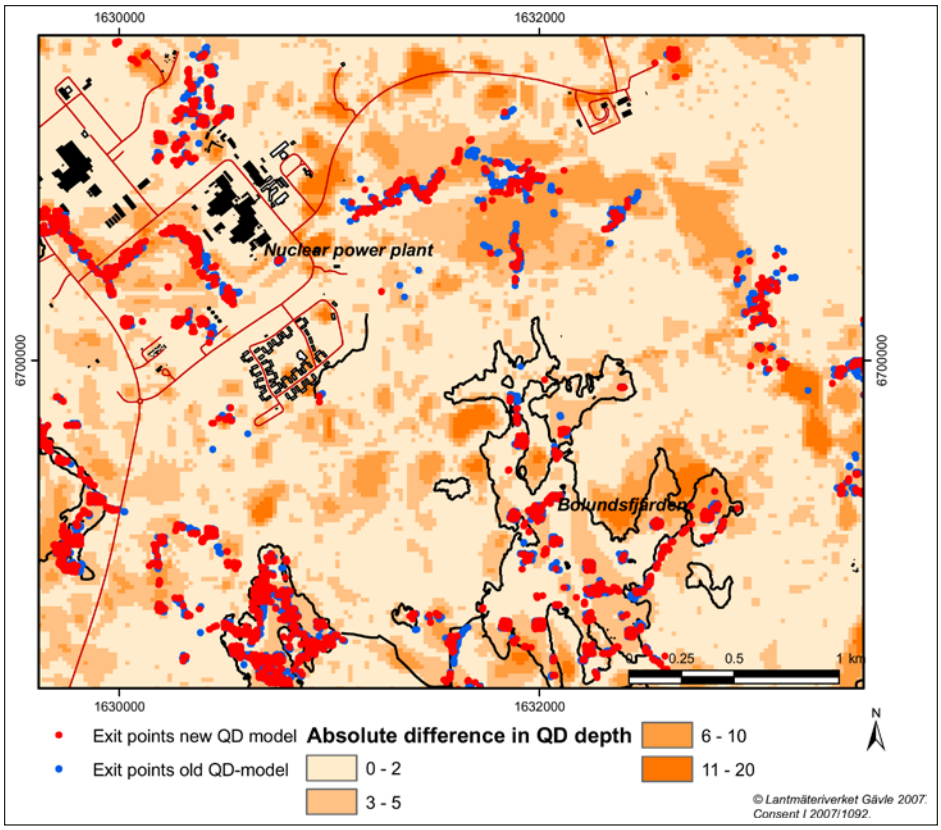

Figure 5-57. *Detailed map of locations where the particles left the saturated zone. The blue points represent particles traced in the old QD model and the red points particles traced in the new QD-model. The absolute difference in QD depth between the old and the new models is shown in the figure.*

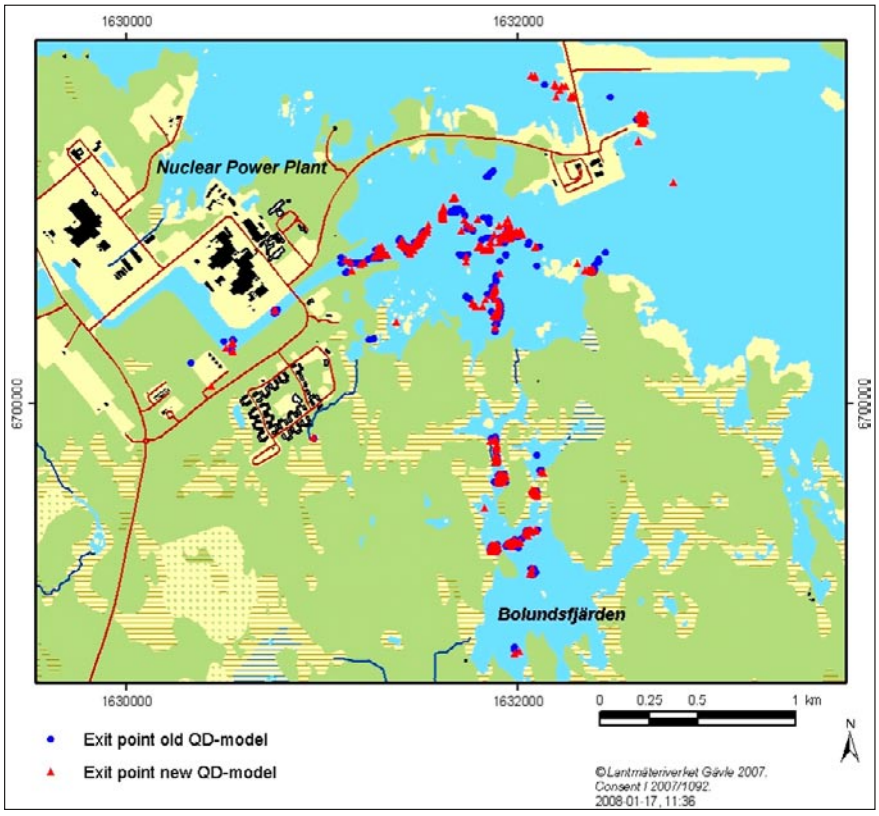

Figure 5-58. *Exit points of particles released in the area of the planned repository. The blue points are exit points calculated with the old QD model and the red points are exit points obtained using the new QD model.*

5.5 Conclusions on model performance

According to /Sonnenborg and Henriksen 2005/ a model is classified as good if the water balance error, here defined as the relative volumetric error, is lower than 20%. The relative volumetric error obtained for the Lake Bolundsfjärden station is 16%. In the same report, an R2-value of 0.50–0.65 is classified as "good" and R2 in the range 0.65–0.85 as "very good". The R2-value for Lake Bolundsfjärden, for the entire calibration and validation period, is 0.60, and the correlation coefficient (R) is 0.79 for the same period.

The performance of the groundwater model can be analysed in many ways, as discussed in Chapter 4. One of the recommended criteria in /Sonnenborg and Henriksen 2005/, β_1, is defined as the average of all mean errors (ME) in all observation points relative to the total gradient in the model area:

$\beta_1 = ME/\Delta h_{max}$,

where Δh_{max} is the difference between the maximum and the minimum groundwater heads in the area.

A model classified as "high fidelity" should have a value of β_1 less then 0.01, according to /Sonnenborg and Henriksen 2005/. In the present case, the average mean error for the SFM-wells is 0.02 m for the validation period and 0.01m for the calibration period. The maximum observed head difference between the different bore holes is approximately 12 m. This gives a $\beta_1 = 0.002$ for the validation period, which is well below the "high fidelity" limit.

For dynamic modelling, however, it can be argued that it is not sufficient to evaluate model performance based on the mean error only. In such cases, the root mean square error (RMS) or the mean absolute error (MAE) could be more relevant to compare with the total gradient in the model area. For the present model, the average mean absolute error (MAE) for the SFM-wells is 0.24 m for the validation period (and 0.23 m for the calibration period). This gives a relation between MAE and Δh_{max} of approximately 0.02. According to /Sonnenborg and Henriksen 2005/ a model classified as "high fidelity" should have a value of less then 0.05 (which, however, in /Sonnenborg and Henriksen 2005/ is defined using the RMS). The above comparisons indicate that the performance of the calibrated MIKE SHE model of the Forsmark area is satisfactory, and also equally good for the calibration and validation periods.

The performance evaluation presented above considers only the groundwater head elevations in the QD. The performance of the bedrock part of the model is not included. The reason is that the calibration of the groundwater model was only performed for the QD (the SFM-wells), whereas the observed head elevations in the bedrock (the HFM-wells) were used for comparison only without changing the bedrock parameters. For the continued groundwater modelling, it is strongly recommended to include also observed conditions in the bedrock in the calibration of the MIKE SHE model. Actually, a pre-calibration phase focusing on the bedrock conditions, before final calibration of the QD parameters, would be a proper order of actions. This is an important conclusion to bring on to the continued site modelling.

The particle tracking results indicated a very fast transport dominated of the upward component. In the model all lakes act as discharge areas, which is not always what is observed in the field data from the site. For example, Lake Bolundsfjärden is a recharge area according to measurements. For some areas, the small mean error in the SFM-wells, implying that the mean groundwater situation in the QD is well described by the model, generates incorrect gradients between the QD and the bedrock when combined with the overestimated modelled heads in the bedrock.

6 Complementary calibration and sensitivity analysis

6.1 Overview of modelling process

Although the tests and evaluations of models performance presented in Chapter 5 showed good results, there are still some discrepancies between field observations and the calculated flow dynamics. Based on the results for the validation period, four main problems were identified

1) The surface water flow dynamics during the spring 2006 discharge peak were not well represented by the model.
2) The surface water flow during autumn 2006, i.e. after the dry summer that year, also showed large deviations between model and field data.
3) The patterns of the groundwater head time series calculated for some SFM-wells for the dry summer of 2006 did not reproduce the corresponding measured time series.
4) The high calculated groundwater head elevations in the bedrock.

The high modelled head elevations in the bedrock were identified already during the calibration period. The other two problems were not observed during the calibration and were first identified when the validation period simulations were run.

The head elevations in the bedrock for the combined calibration-validation period are consistently too high. The mean absolute error, MAE, obtained when comparing measured and observed levels for all the HFM-wells included in the comparison was 0.75 m. The mean error, ME, was –0.75 m, which shows that all the calculated values were higher than the observed values. This implies that the hydraulic contact between the bedrock and the Quaternary deposits is not represented correctly in the model. In some areas, the head gradient is turned upside down and the vertical water flow is in the wrong direction.

The calculated groundwater fluxes in the bedrock also deviate too much from the observed flow situation. Therefore, an additional calibration and sensitivity analysis was decided to be performed for the bedrock properties. The complementary calibration and sensitivity analysis was carried out as described in Figure 6-1. The first part focused on the surface water dynamics and the SFM-wells, and the second part was a sensitivity analysis focused on investigating of the head elevations in the bedrock.

6.2 Further calibration and sensitivity analysis

6.2.1 Surface hydrology

During the model validation procedure, three main problems were identified with regard to the surface hydrology. The first problem was the lack of surface discharge during the fast and distinct snow-melt in the spring 2006, see Figure 6-2. During the snowmelt in April 2006, approximately 30% of the observed run-off is not captured by the model. Furthermore, in the autumn after the dry summer of 2006 the model does not reflect the first run-off event. The response of the surface water dynamics in the model is somewhat slow and the first run-off in the autumn is only captured by 50%. The same pattern is shown in all discharge stations. An example from PFM005764 upstream Lake Bolundsfjärden is given in Figure 6-2.

The third observed problem was that in the dry summer of 2006 the head elevation in some areas reached the bottom of the uppermost calculation layer. Since the transpiration processes, which are very important during this summer period, only are fully active in the uppermost calculation layer, the time series for the SFM wells situated in these areas showed “rectangular” patterns. An example of these flat calculated head curves is given in Figure 6-3.

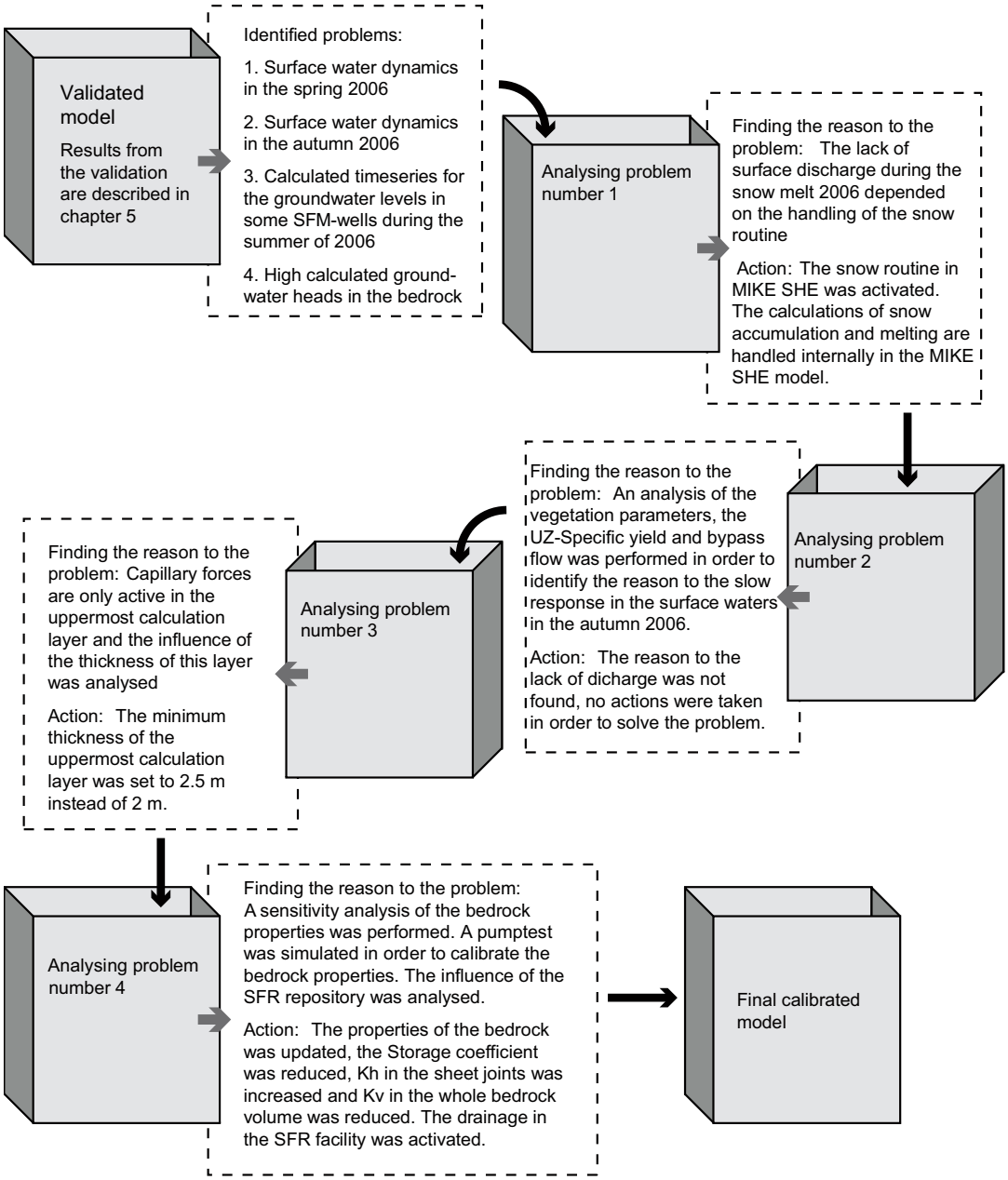

Figure 6-1. *Summary of the additional sensitivity analysis and calibration performed after the testing of the model (see Chapter 5).*

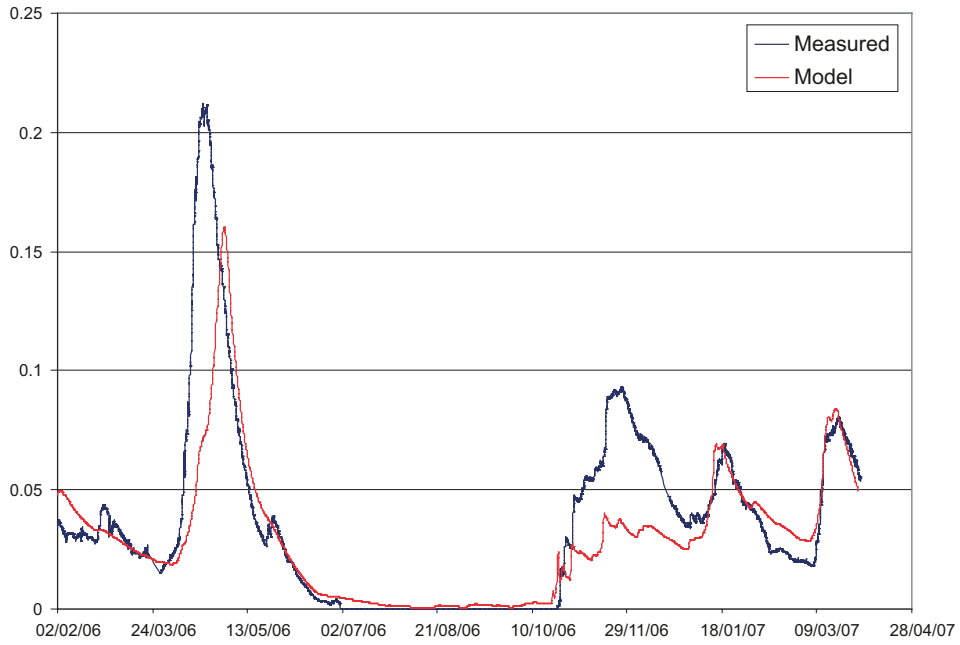

Figure 6-2. *Discrepancy between measured and calculated discharges (m^3/s) in PFM005764 upstream Lake Bolundsfjärden during snow melt and summer 2006.*

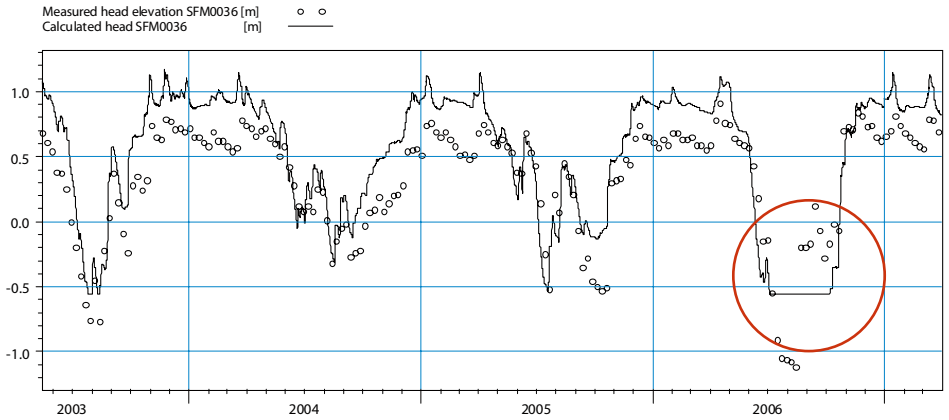

Figure 6-3. *Example of a time series where the calculated head reaches the bottom of the uppermost calculation layer.*

Discharge during spring 2006

The description of snow accumulation and melting has in previous simulations been managed outside the MIKE SHE model code, by a simple degree-day approach, in which accumulation and melting start at certain temperature thresholds and a certain melting intensity (the degree-day-coefficient) is applied, see /DHI Software 2007/ The output from this snow routine has been used as precipitation input in MIKE SHE. In MIKE SHE, precipitation passes through the vegetation as a first step, where a certain interception loss in canopy storage is calculated. This loss depends on the active leaf-area index, which varies in time with larger values during summer and values equal to zero during winter.

The combination of this principle and the simple handling of snow dynamics outside MIKE SHE according to the procedure outlined above can create problems. If the snow is falling during winter months with no evaporation processes and later melts during spring, there will be no interception losses in reality, because the snow is already on the ground when it melts. However, when handling the snow dynamics outside MIKE SHE, the model code will assume that any precipitation input is rain, although in reality it is melted water from snow on the ground, and interception losses will be calculated.

To resolve this problem, the approach for snow handling was changed to be included and managed fully by the MIKE SHE code. The input to the model is in this case the precipitation (rain volume or water content of snow when it falls) and temperature. The snow routine inside MIKE SHE is also based on the degree-day method, but melted water from the internal snow routine will go directly to the ground in the model, without passing the canopy storage, and consequently without interception losses.

The original method with snow handling outside MIKE SHE, according to /Aneljung and Gustafsson 2007/, was compared with two alternative parameter sets activating the internal snow model within MIKE SHE. One alternative used a melting threshold of 0.5°C and a degree-day coefficient of 1.5 mm/(°C day), and the second a melting threshold of –0.6°C and a degree-day coefficient of 0.837 mm/(°C day).

The results are shown in Figure 6-4 as time series of discharge and in Figure 6-5 as accumulated discharges, both showing the results at for the station just upstream Lake Bolundsfjärden (PFM5764). The method where the internal snow routine in MIKE SHE is used gives a better agreement with the measured total flow volume and a much better volumetric balance for the snow melt period during spring 2006, as compared to the original modelling approach. The alternative with a melting threshold of 0.5°C and a degree-day coefficient of 1.5 mm/(°C day) gives a slightly better description of the snow melting peak than the alternative parameter set.

Another advantage of using the internal snow routine in MIKE SHE is that the new 2008 version of the code also includes the possibility of describing the melt water storage capacity of the snow pack, and any refreezing of wet snow during colder periods. For example, in the new model version it is possible to set a maximum wet snow fraction. The wet snow fraction is the amount of wet snow divided by the total amount of snow storage. When the maximum wet snow fraction is exceeded, any excess melted snow will be converted to ponded water. The ponded water is then available for infiltration, evapotranspiration, or overland runoff.

When implementing the model in the new MIKE SHE version 2008, the maximum wet snow fraction was set to 0.1. This further increased the runoff during the snow melt event in the spring of 2006. Figure 6-6 shows a comparison between simulations with and without the snowfraction parameter for the station just upstream Lake Bolundsfjärden. Since the handling of the snow routine in version 2008 had a positive influence on the results and did not affect the processes in any other compartement of the model it was decided to use the this version in the remaining simulations.

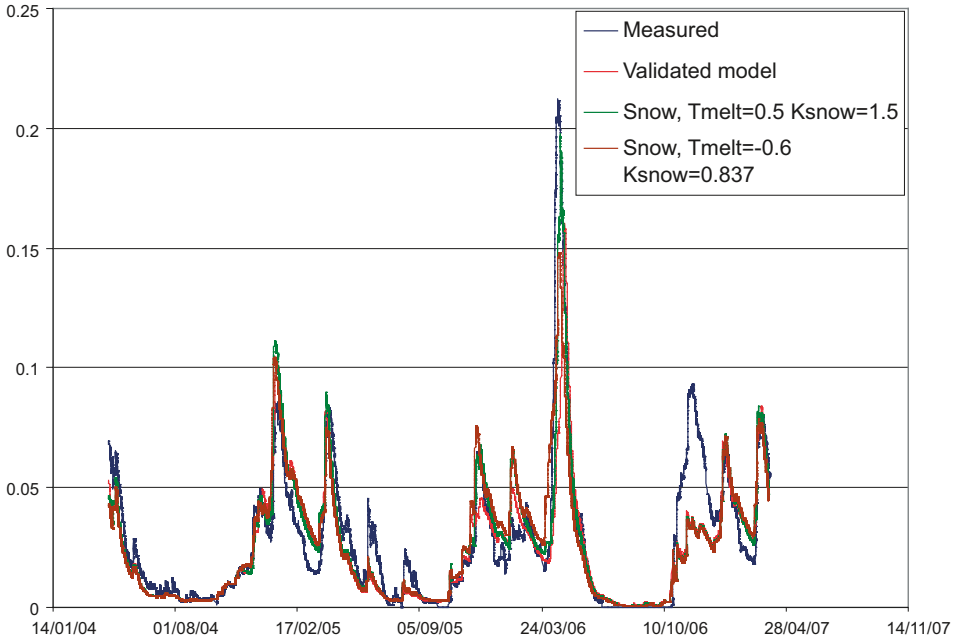

Figure 6-4. *Calculated and measured surface water discharges (m^3/s) time series upstream Lake Bolundsfjärden. Results from the "validation model" tested in Chapter 5 and two different sets of snow routine parameters (with parameter values given in the legend) are shown in the figure.*

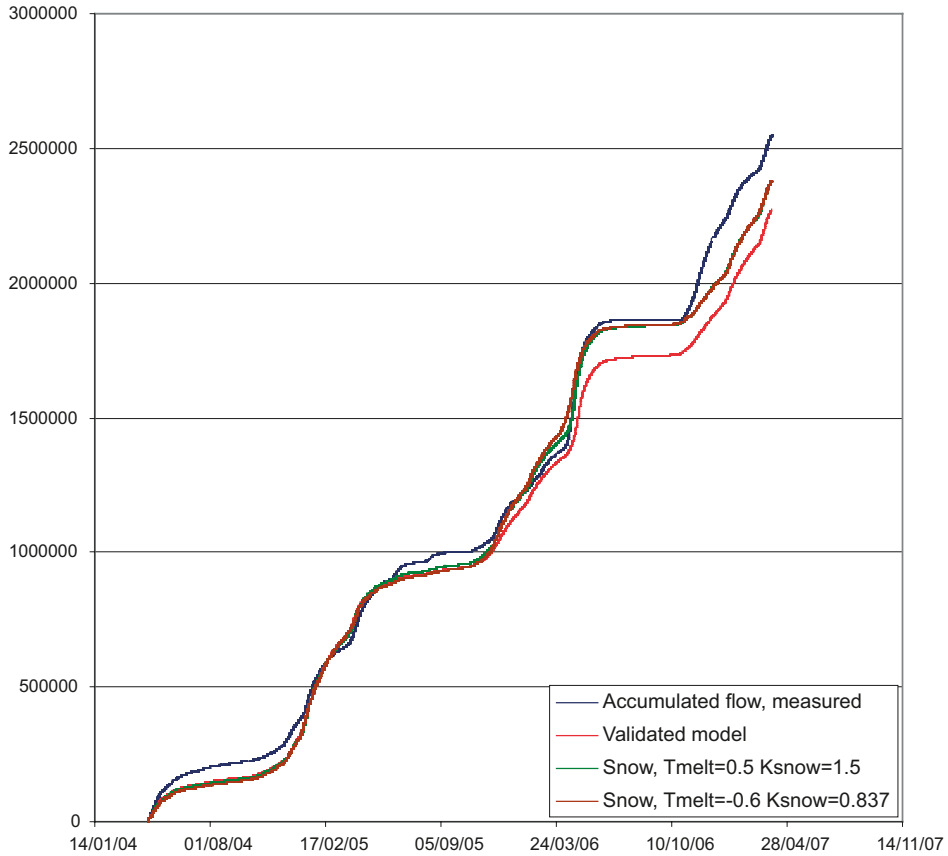

Figure 6-5. *Calculated and measured accumulated surface water discharges (m^3) upstream Lake Bolundsfjärden. Results from the "validation model" tested in Chapter 5 and two different sets of snow routine parameters (with parameter values given in the legend) are shown in the figure.*

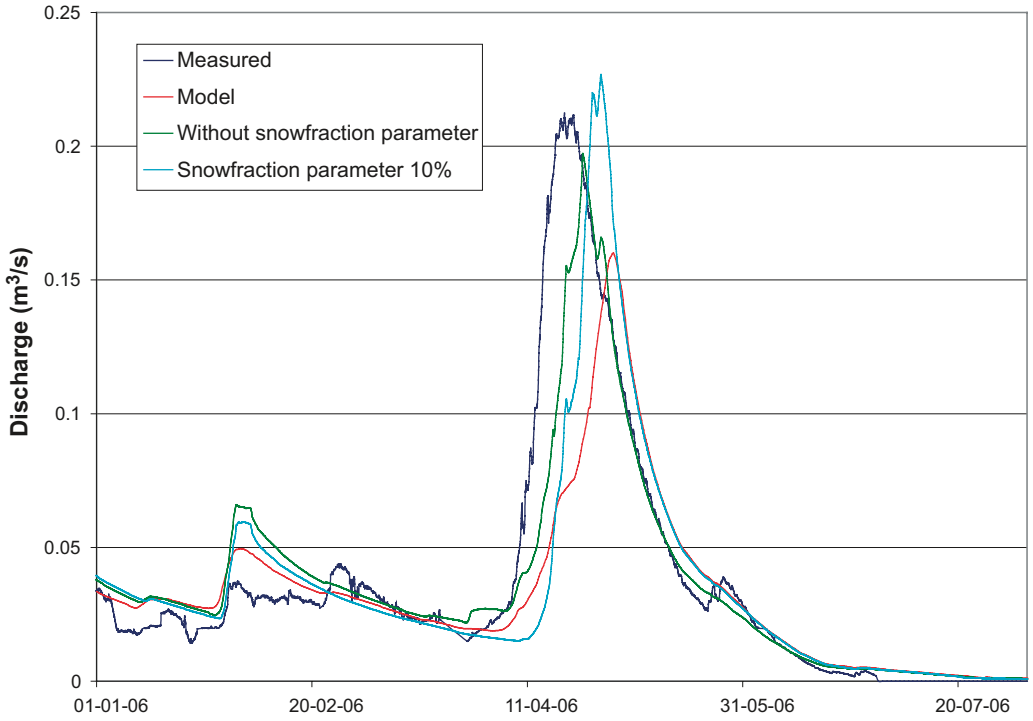

Figure 6-6. *Results of simulations with and without the snowfraction parameter for the discharge station upstream Lake Bolundsfjärden.*

Discharge during autumn 2006

After the very dry summer 2006, the model does not respond fast enough to the first rain event and shows a lack of surface discharge. The first discharge peak after the summer is only captured by about 50%. The pattern was the same for all discharge stations. After the dry summer the model response to the rain seems to be too slow with regard to the surface water discharge. Several sensitivity simulations were performed in order to try to increase the modelled discharge after the summer.

The first attempt was to include bypass flow, which is a simplified macropore flow. Flow through macropores in unsaturated soil is important for many soil types. In the model, the infiltration water is divided into one part that flows through the soil matrix and another part that is being routed directly to the groundwater table. The bypass flow is calculated as a fraction of the net rainfall for each time step. Two different bypass simulations were made. However, none of the simulations resulted in any significant improvement of the surface discharge peak after the summer 2006.

Therefore, simulations with changed LAI (leaf area index) values for the coniferous forest were made. Initially, the LAI-value was 7. In the complemetary sensitivity analysis, simulations with LAI equal to 6, 5 and 4 were made. However, no significant effect on the surface discharge peak was observed. Furthermore, simulations with the unsaturated zone specific yield, S_y, decreased by a factor of 2 were made. Also, the interception coefficient, C_{int}, was decreased by a factor of 2. None of these two simulations showed any effect on the first flow peak after the summer. Figure 6-7 shows the results from the sensitivity analysis for the discharge station just upstream Lake Bolundsfjärden. All the stations showed similar patterns.

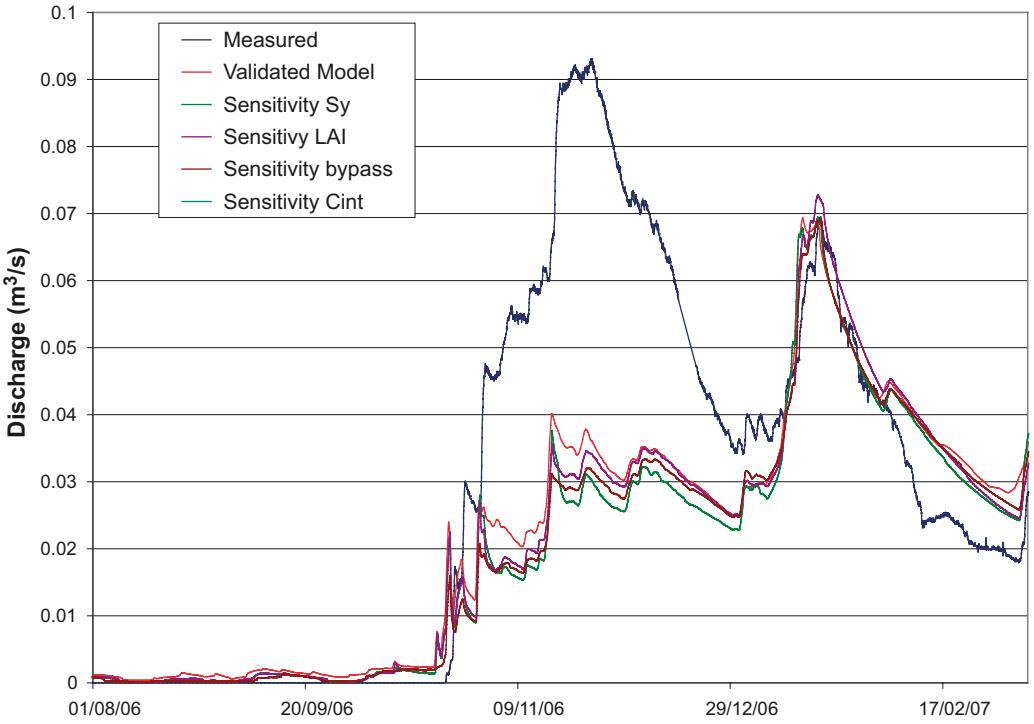

Figure 6-7. *Results from the sensitivity analysis of vegetation parameters and unsaturated zone parameters for the station upstream Lake Bolundsfjärden.*

Groundwater elevations during summer 2006

For some of the SFM monitoring wells, it was noted that the calculated head elevation time series for the dry summer of 2006 were flat during periods of very low heads. The reason was found to be that the head elevation reached the bottom of the calculation layer and then did not decrease further. Also, in the model the capillary forces, and therefore also transpiration, are limited to the uppermost calculation layer. This implies that the drawdown of the groundwater table due to transpiration processes is deactivated when the head elevation reaches the bottom of calculation layer 1.

In an attempt to solve this problem, the upper calculation layer thickness was increased from 2 m to 2.5 m. It turned out that this correction of the numerical description resulted in more realistic shapes of the groundwater head curves during the dry summer period. No effect on accumulated discharges of the increased calculation layer thickness was observed.

6.2.2 Bedrock hydraulics

In order to further test and analyse the model presented in Chapter 5, a simulation of an interference (pumping) test was performed. The interference test was performed in July 2006, with extraction of groundwater from HFM14 (Figure 2-16). Pumping started on July 4 and was terminated on July 25 the test and its results are described in /Gokall-Norman and Ludvigson 2006/. Hydraulic responses were monitored in a large number of borehole sections in rock, and also in some wells in QD.

The response of the original (Chapter 5) model to the pumping in HFM14 was too slow and the calculated drawdowns in most of the HFM-wells were more than 50% lower than the observed ones. An example of a typical calculated drawdown curve from this simulation is given in Figure 6-8. The evaluation of the modelling of the interference test resulted in a change in the storage coefficient of the bedrock. Thus far, the storage coefficient, S, had been described as a function of the hydraulic conductivity of the bedrock /Rehn et al. 1997/. This gave S-values in the range 10^{-7} to 10^{-5} m^{-1}.

The same pumping test was modelled also by the ConnectFlow modelling team, see /Follin et al. 2008/. To reach the observed response the storage coefficient of the bedrock had to be lowered. The results of the ConnectFlow simulations of the pumping test were that the storage coefficient parameterisation was changed to a homogenous value of $5 \cdot 10^{-9}$ m^{-1}. The same value was used to update the MIKE SHE model. With this lower *S*-value, the fast response to the pumping was better captured by the MIKE SHE model, but still the drawdown was too small. The drawdown curve for this simulation is showed in Figure 6-8.

Since the calculated drawdown in the pumping test was too low and the problem with the high groundwater heads in the bedrock still was a problem, an additional sensitivity analysis of the hydraulic properties of the bedrock was performed. Eight cases were defined, as listed in Table 6-1. In all cases, the storage coefficient of the bedrock was set to $5 \cdot 10^{-9}$ m^{-1}.

The upper 200 m of the bedrock within the so-called "target area" are characterised by a set of horizontal structures, referred to as fractures/sheet joints, which in some cases have high hydraulic conductivities. In the model, the high-conductive fractures/sheet joints are implemented as high-conductive areas in three geological layers at 30 m.b.s.l., 70 m.b.s.l. and 110 m.b.s.l. In cases 1–6 in Table 6-1, the horizontal hydraulic conductivities, K_h, in the fractures/sheet joints were modified in combination with different modifications of vertical conductivities, K_v, in bedrock, lake sediments and the QD layer that is in direct contact with the bedrock (Z6).

Whereas K_h in cases 1–6 was modified in the part of the model describing the sheet joints only, the bedrock K_v changes were made in the upper 200 m of the whole model. However, in cases 7 and 8 also K_h was modified in the whole bedrock model above 200 m (not just in the sheet joints). The simulations were run for the whole period for which data are available, i.e. from May 2005 to the end of March 2007. In addition, modelling of the pumping test in HFM14 was performed for cases 2, 5 and 6.

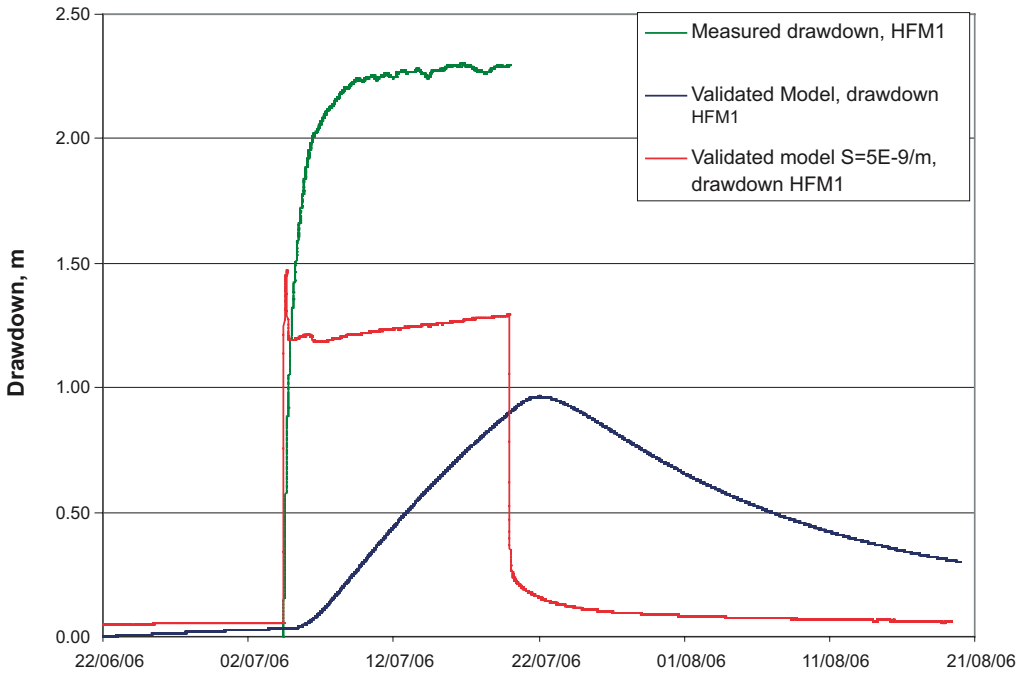

Figure 6-8. *Calculated and measured drawdowns in HFM1. Simulation results from the "validation model" tested in Chapter 5 and an updated model with a lower, uniform S-value are shown in the figure.*

Table 6-1. Definition of hydraulic properties sensitivity cases 1–8.

Case	Bedrock Kh	Bedrock Kv	QD
1	Kh sheet joints · 10		Unchanged
2	Kh sheet joints · 10		Kv lake sediments/100 and Kv Z6/100
3	Kh sheet joints · 10	Kv/10 for bedrock >–200m	Kv lake sediments/100 and Kv Z6/100
4	Kh sheet joints · 10	Kv/100 for bedrock >–200m	Kv lake sediments/100 and Kv Z6/100
5	Kh sheet joints · 10	Kv/10 for bedrock >–200m	Unchanged
6	Kh sheet joints · 10	Kv/100 for bedrock >–200m	Unchanged
7	Kh · 50 for bedrock >–200m	Kv/10 for bedrock >–200m	Unchanged
8	Kh · 50 for bedrock >–200m	Kv/100 for bedrock >–200m	Unchanged

The MAE and the ME for each SFM-well and HFM-well are listed in Tables 6-2 to 6-5. The average groundwater elevation in the QD is not strongly affected in any of the cases, as shown by the mean of the MAE- and ME-values. However, cases 2–4, where the vertical hydraulic conductivities of the lake sediments and the contact layer between bedrock and QD were reduced by a factor of 100, have a negative influence on the contact between the lake surface water and the underlying till in some lakes. In particular, the groundwater levels in the till under Lake Eckarfjärden (SFM0015) and Lake Gällsboträket (SFM0012) become too high when the vertical hydraulic conductivity is reduced.

The MAE for SFM0012, installed below Lake Gällsboträsket, is approximately 8 cm for the validation (Chapter 5) model and around 15 cm for cases 2–4. The MAE for SFM0015, below Lake Eckarfjärden, is approximately 9 cm for the validation model, whereas for cases 2–4 it is around 35 cm. Even at Lake Fiskarfjärden the groundwater elevation in the till under the lake becomes too high; the MAE is increased from 5 cm for the validated model to around 10 cm for case 2–4. The reduction of K_v in the lake sediments and Z6 also has a negative influence on SFM0001, SFM0002, SFM0013, SFM0014 and SFM0057. This effect becomes even larger in cases 3 and 4, where K_v in the bedrock also has been reduced.

Multiplying K_h in the sheet joints by a factor of 10 has a positive influence on the modelled groundwater head elevations in the bedrock. The mean of the MAE is reduced by 25% in case 1 compared to the validation model. However, all the calculated heads are still higher than the corresponding observed heads. In cases 2–6, where the vertical hydraulic conductivity was reduced either in the bedrock and the QD or in the bedrock only, a small negative influence on the HFM-wells was observed. In case 6 this counteracts the positive effect caused by an increase of K_h in the sheet joints, such that the mean MAE in case 6 is almost the same as for the validation model.

The MAE in the majority of the HFM-wells decreased in cases 2–6. In cases 7 and 8, where K_h in the bedrock was multiplied by a factor of 100 in combination with different reductions of K_v in the bedrock, the mean MAE increased. However, the ME is reduced, meaning that the calculated head in some wells is below the measured values.

The surface water dynamics are also affected by the parameter variations in cases 1–8. In terms of accumulated volume, sensitivity case 1 produced the best fit to the measured discharge. The rest of the cases generate somewhat lower accumulated discharge. The cases with high K_h in the bedrock, cases 7 and 8, and the those with reduced K_v, cases 2–4, show lower discharges from the bedrock to the surface waters, and the discharge in the water courses is reduced. Cases 5 and 6 generate acceptable accumulated discharges. The accumulated discharges in the station upstream Lake Bolundsfjärden for cases 1–8 are presented in Figure 6-9.

Table 6-2. MAE and ME for the SFM-wells for sensitivity cases 1-4 (specified in Table 6-1).

ID code SFM-well	Validated model		Case 1		Case2		Case 3		Case 4	
	MAE	ME	MAE	ME	MAE	ME	MAE	ME	MAE	ME
Heads										
SFM0003	0.21	–0.199	0.168	–0.099	0.195	–0.100	0.212	–0.096	0.208	–0.073
SFM0004	0.231	–0.122	0.255	0.190	0.299	0.248	0.213	0.066	0.223	–0.010
SFM0005	0.210	–0.11	0.202	–0.155	0.205	–0.147	0.212	–0.141	0.213	–0.131
SFM0012	0.078	–0.05	0.072	0.005	0.182	–0.138	0.159	–0.093	0.133	–0.020
SFM0013			0.278	–0.017	0.336	–0.128	0.327	–0.087	0.320	–0.079
SFM0014	0.24	–0.24	0.343	–0.343	0.882	–0.882	0.866	–0.866	0.854	–0.854
SFM0015	0.088	–0.079	0.086	–0.078	0.353	–0.349	0.347	0.343	0.336	–0.331
SFM0016	0.146	–0.146	0.138	–0.138	0.172	–0.172	0.163	–0.163	0.152	–0.152
SFM0017	0.370	0.372	0.377	–0.365	0.431	–0.395	0.652	–0.648	1.062	–1.061
SFM0019	0.512	0.512	0.529	0.529	0.550	0.550	0.558	0.558	0.556	0.556
SFM0022	0.054	–0.024	0.058	–0.028	0.101	–0.081	0.092	–0.055	0.098	–0.060
SFM0023	0.072	–0.059	0.072	–0.056	0.122	–0.120	0.084	–0.075	0.080	–0.069
SFM0026	0.335	–0.041	0.335	–0.043	0.325	–0.035	0.311	–0.092	0.456	–0.422
SFM0030	0.742	–0.742	0.825	–0.825	0.753	–0.749	0.717	–0.709	0.712	–0.702
SFM0033	0.317	0.243	0.335	0.314	0.248	0.221	0.277	0.254	0.274	0.252
SFM0034	0.284	–0.249	0.320	–0.211	0.331	–0.234	0.288	–0.078	0.285	–0.045
SFM0036	0.264	–0.216	0.245	–0.174	0.250	–0.160	0.247	–0.143	0.245	–0.141
SFM0039	0.043	–0.031	0.043	–0.031	0.041	–0.027	0.041	–0.025	0.043	–0.027
SFM0057	0.306	–0.273	0.498	–0.483	0.465	–0.439	0.615	–0.568	0.682	–0.620
SFM0062	0.106	0.044	0.103	0.047	0.105	0.081	0.124	0.106	0.124	0.107
SFM0065	0.199	–0.066	0.212	–0.084	0.188	–0.067	0.185	–0.019	0.188	–0.030
SFM0066	0.113	0.017	0.113	0.019	0.114	0.024	0.114	0.027	0.115	0.029
Depths to phreatic surface										
SFM0001	0.157	0.076	0.188	0.133	0.212	0.165	0.235	0.190	0.238	0.191
SFM0002	0.281	0.271	0.408	0.407	0.391	0.389	0.382	0.380	0.375	0.373
SFM0009	0.375	0.359	0.363	0.355	0.370	0.362	0.368	0.354	0.371	0.358
SFM0010	0.389	0.374	0.342	0.316	0.366	0.347	0.331	0.309	0.306	0.280
SFM0011	0.110	–0.109	0.098	–0.088	0.097	–0.084	0.095	–0.082	0.094	–0.082
SFM0018	0.172	–0.050	0.167	–0.050	0.170	–0.042	0.176	–0.037	0.178	–0.033
SFM0019	0.320	–0.309	0.319	–0.293	0.315	–0.280	0.310	–0.276	0.314	–0.280
SFM0020	0.220	–0.220	0.278	–0.276	0.274	–0.272	0.258	–0.257	0.258	–0.257
SFM0021	0.530	0.530	0.541	0.541	0.547	0.547	0.506	0.506	0.491	0.490
SFM0028	0.155	–0.053	0.154	–0.050	0.146	–0.046	0.145	–0.043	0.144	–0.033
SFM0030	0.612	0.522	0.591	0.560	0.612	0.586	0.635	0.616	0.640	0.624
SFM0049	0.187	–0.030	0.203	–0.057	0.212	0.001	0.222	0.042	0.223	0.007
SMF0058	0.567	0.577	0.403	–0.016	0.389	–0.008	0.427	–0.278	0.509	–0.431
Mean SFM	**0.265**	**0.014**	**0.276**	**–0.016**	**0.307**	**–0.041**	**0.311**	**–0.031**	**0.329**	**–0.076**

Table 6-3. MAE and ME for the SFM-wells for sensitivity cases 5-8 (specified in Table 6-1).

ID code SFM-well	Validated model		Case 5		Case 6		Case 7		Case 8	
	MAE	ME	MAE	ME	MAE	ME	MAE	ME	MAE	ME
Heads										
SFM0003	0.21	–0.199	0.187	–0.088	0.186	–0.044	0.149	–0.085	0.173	–0.081
SFM0004	0.231	–0.122	0.210	–0.006	0.232	–0.061	0.203	0.097	0.230	–0.057
SFM0005	0.210	–0.11	0.209	–0.146	0.213	–0.135	0.215	–0.118	0.214	–0.125
SFM0012	0.078	–0.05	0.076	0.012	0.078	0.018	0.080	–0.067	0.072	0.006
SFM0013			0.275	0.001	0.269	0.001	0.287	–0.042	0.272	–0.009
SFM0014	0.24	–0.24	0.338	–0.338	0.335	–0.335	0.369	–0.369	0.334	–0.334
SFM0015	0.088	–0.079	0.086	–0.077	0.086	–0.077	0.094	–0.088	0.084	–0.075
SFM0016	0.146	–0.146	0.137	–0.136	0.135	–0.135	0.141	–0.140	0.132	–0.132
SFM0017	0.370	0.372	0.632	–0.630	1.052	–1.052	1.013	–1.013	0.404	–0.378
SFM0019	0.512	0.512	0.531	0.531	0.534	0.534	0.511	0.511	0.525	0.525
SFM0022	0.054	–0.024	0.058	–0.021	0.058	–0.020	0.055	–0.029	0.057	–0.020
SFM0023	0.072	–0.059	0.071	–0.053	0.070	–0.052	0.070	–0.052	0.070	–0.051
SFM0026	0.335	–0.041	0.316	–0.092	0.456	–0.422	0.886	–0.883	1.420	–1.420
SFM0030	0.742	–0.742	0.758	–0.757	0.749	–0.748	0.777	–0.776	0.743	–0.742
SFM0033	0.317	0.243	0.350	0.322	0.353	0.335	0.351	0.334	0.353	0.335
SFM0034	0.284	–0.249	0.293	–0.104	0.295	–0.073	0.292	–0.121	0.295	–0.078
SFM0036	0.264	–0.216	0.242	–0.154	0.243	–0.150	0.248	–0.158	0.246	–0.152
SFM0039	0.043	–0.031	0.046	–0.028	0.043	–0.027	0.041	–0.027	0.042	–0.026
SFM0057	0.306	–0.273	0.630	–0.590	0.689	–0.633	0.517	–0.451	0.333	0.124
SFM0062	0.106	0.044	0.106	0.053	0.107	0.054	0.105	0.050	0.108	0.055
SFM0065	0.199	–0.066	0.208	–0.076	0.206	–0.072	0.211	–0.083	0.206	–0.073
SFM0066	0.113	0.017	0.115	0.027	0.116	0.030	0.114	0.021	0.116	0.030
Depths to phreatic surface										
SFM0001	0.157	0.076	0.212	0.162	0.221	0.172	0.221	0.194	0.225	0.186
SFM0002	0.281	0.271	0.369	0.367	0.364	0.362	0.339	0.336	0.332	0.329
SFM0009	0.375	0.359	0.364	0.349	0.368	0.354	0.387	0.378	0.376	0.364
SFM0010	0.389	0.374	0.313	0.287	0.297	0.268	0.428	0.418	0.302	0.278
SFM0011	0.110	–0.109	0.096	–0.085	0.095	–0.084	0.098	–0.089	0.095	–0.084
SFM0018	0.172	–0.050	0.174	–0.043	0.176	–0.038	0.177	–0.059	0.177	–0.034
SFM0019	0.320	–0.309	0.317	–0.289	0.316	–0.285	0.322	–0.307	0.315	–0.291
SFM0020	0.220	–0.220	0.259	–0.257	0.256	–0.254	0.270	–0.267	0.250	–0.248
SFM0021	0.530	0.530	0.478	0.476	0.478	0.477	0.506	0.506	0.483	0.483
SFM0028	0.155	–0.053	0.150	–0.042	0.144	–0.035	0.156	–0.051	0.146	–0.036
SFM0030	0.612	0.522	0.629	0.608	0.636	0.618	0.618	0.593	0.641	0.623
SFM0049	0.187	–0.030	0.202	0.013	0.214	0.052	0.194	0.035	0.210	0.051
SMF0058	0.567	0.577	0.432	–0.281	0.492	–0.408	0.421	–0.191	0.488	–0.404
Mean SFM	**0.265**	**0.014**	**0.282**	**–0.031**	**0.302**	**–0.053**	**0.310**	**–0.057**	**0.299**	**–0.042**

Table 6-4. MAE and ME for the HFM-wells for sensitivity cases 1-4 (specified in Table 6-1).

ID code HFM-well	Validated model		Case 1		Case2		Case 3		Case 4	
	MAE	ME	MAE	ME	MAE	ME	MAE	ME	MAE	ME
HFM01_1	0.80		0.830	–0.830	0.869	–0.869	0.850	–0.850	0.892	–0.892
HFM01_2	0.95		0.845	–0.845	0.877	–0.877	0.918	–0.918	1.002	–1.002
HFM02_1	1.12		0.696	–0.696	0.717	–0.717	0.834	–0.834	0.926	–0.926
HFM02_2	1.10		0.705	–0.705	0.718	–0.718	0.795	–0.795	0.959	–0.959
HFM02_3	1.12		0.725	–0.725	0.738	–0.738	0.816	–0.816	0.980	–0.980
HFM03_1	1.06		0.659	–0.659	0.664	–0.664	0.754	–0.754	0.908	–0.908
HFM03_2	1.05		0.646	–0.646	0.652	–0.652	0.742	–0.742	0.896	–0.896
HFM04_1	0.30		0.323	–0.323	0.411	–0.411	0.092	–0.043	0.084	–0.005
HFM04_2	0.41		0.410	–0.410	0.481	–0.481	0.181	–0.161	0.070	0.000
HFM04_3	0.16		0.144	–0.103	0.201	–0.179	0.134	0.127	0.289	0.289
HFM10_1	0.87		0.820	–0.820	0.817	–0.817	0.396	–0.396	0.092	0.008
HFM10_2	0.44		0.363	–0.343	0.403	–0.376	0.298	–0.249	0.304	0.187
HFM11_1	0.09		0.108	0.052	0.273	–0.177	0.408	–0.384	0.233	0.205
HFM11_2	0.33		0.227	–0.170	0.262	–0.210	0.324	–0.281	0.298	–0.217
HFM15_1	1.00		0.684	–0.684	0.718	–0.718	0.698	–0.698	0.719	–0.719
HFM15_2	0.97		0.641	–0.641	0.682	–0.681	0.643	–0.643	0.650	–0.650
HFM16_1	0.44		0.257	–0.249	0.316	–0.294	0.411	–0.411	0.629	–0.629
HFM16_2	0.47		0.283	–0.280	0.337	–0.323	0.478	–0.478	0.670	–0.670
HFM16_3	0.50		0.320	–0.319	0.369	–0.361	0.572	–0.572	0.678	–0.678
HFM20_2	0.54		0.347	–0.346	0.370	–0.361	0.518	–0.518	0.670	–0.670
HFM20_3	0.58		0.347	–0.345	0.369	–0.358	0.472	–0.471	0.594	–0.594
HFM20_4	0.98		0.579	–0.568	0.568	–0.544	0.776	–0.776	0.964	–0.964
HFM32_1	1.10		1.157	–1.157	1.200	–1.200	1.383	–1.383	1.495	–1.495
HFM32_2	1.10		1.200	–1.200	1.268	–1.268	1.438	–1.438	1.565	–1.565
HFM32_3	0.96		1.002	–1.002	1.121	–1.121	1.365	–1.365	1.450	–1.450
HFM32_4	0.92		1.047	–1.047	1.096	–1.096	1.349	–1.349	1.498	–1.498
HFM34_2			3.436	–3.436	3.305	–3.305	3.702	–3.702	4.210	–4.210
HFM34_3	0.81		0.856	–0.856	0.754	–0.754	0.973	–0.973	1.624	–1.624
HFM13_2			0.396	–0.362	0.422	–0.038	0.294	–0.248	0.256	–0.197
HFM13_3			0.458	0.412	0.468	0.417	0.314	–0.139	0.284	–0.145
HFM19_3			0.415	–0.406	0.449	–0.431	0.491	–0.485	0.616	–0.615
HFM19_2			0.615	–0.615	0.644	–0.644	0.580	–0.580	0.581	–0.581
HFM9			0.276	–0.275	0.239	–0.219	0.175	–0.130	0.160	0.153
HFM30			0.256	–0.045	0.279	0.168	0.214	0.091	0.381	–0.345
HFM12_1			0.253	0.159	0.270	0.187	0.249	–0.032	0.440	–0.412
HFM12_2			0.192	0.162	0.196	0.165	0.190	–0.043	0.224	–0.122
HFM26			0.761	–0.761	0.581	–0.581	0.340	–0.338	0.169	0.159
HFM14			0.729	–0.729	0.791	–0.791	0.738	–0.738	0.738	–0.738
HFM24			0.410	0.378	0.384	0.371	0.242	–0.082	0.475	–0.449
Mean HFM	**0.747**		**0.626**	**–0.550**	**0.648**	**–0.556**	**0.670**	**–0.631**	**0.761**	**–0.687**

Table 6-5. MAE and ME for the HFM-wells for sensitivity cases 5-8 (specified in Table 6-1).

ID code HFM-well	Validated model		Case 5		Case 6		Case 7		Case 8	
	MAE	ME	MAE	ME	MAE	ME	MAE	ME	MAE	ME
HFM01_1	0.80		0.824	–0.824	0.892	–0.892	0.791	–0.791	0.075	–0.075
HFM01_2	0.95		0.896	–0.896	1.001	–1.001	1.019	–1.019	0.924	–0.924
HFM02_1	1.12		0.822	–0.822	0.930	–0.930	0.992	–0.992	0.464	–0.464
HFM02_2	1.10		0.786	–0.786	0.964	–0.964	0.934	–0.934	0.895	–0.895
HFM02_3	1.12		0.806	–0.806	0.985	–0.985	0.955	–0.955	0.917	–0.917
HFM03_1	1.06		0.748	–0.748	0.915	–0.915	0.803	–0.803	0.915	–0.915
HFM03_2	1.05		0.736	–0.736	0.903	–0.903	0.791	–0.791	0.903	–0.903
HFM04_1	0.30		0.082	0.007	0.086	0.008	0.123	0.040	0.529	0.529
HFM04_2	0.41		0.146	–0.117	0.069	0.017	0.183	0.178	0.320	0.317
HFM04_3	0.16		0.174	0.171	0.305	0.305	0.466	0.466	0.604	0.604
HFM10_1	0.87		0.391	–0.391	0.091	0.010	0.294	0.293	1.631	1.631
HFM10_2	0.44		0.269	–0.219	0.314	0.187	0.451	0.401	1.470	1.470
HFM11_1	0.09		0.289	–0.277	0.255	0.252	1.798	1.798	4.216	4.216
HFM11_2	0.33		0.254	–0.220	0.227	–0.149	0.671	0.671	3.277	3.277
HFM15_1	1.00		0.681	–0.681	0.718	–0.718	0.601	–0.601	0.297	–0.290
HFM15_2	0.97		0.622	–0.622	0.645	–0.645	0.527	–0.527	0.231	–0.194
HFM16_1	0.44		0.405	–0.405	0.625	–0.625	0.429	–0.429	0.155	0.117
HFM16_2	0.47		0.472	–0.472	0.667	–0.667	0.447	–0.447	0.274	–0.274
HFM16_3	0.50		0.563	–0.563	0.672	–0.672	0.351	–0.351	0.380	–0.380
HFM20_2	0.54		0.483	–0.483	0.665	–0.665	0.446	–0.446	0.269	0.254
HFM20_3	0.58		0.437	–0.437	0.588	–0.588	0.376	–0.376	0.235	0.217
HFM20_4	0.98		0.791	–0.791	0.970	–0.970	0.916	–0.916	0.794	–0.794
HFM32_1	1.10		1.391	–1.391	1.492	–1.492	1.431	–1.431	0.555	–0.555
HFM32_2	1.10		1.432	–1.432	1.561	–1.561	1.499	–1.499	0.773	–0.773
HFM32_3	0.96		1.322	–1.322	1.441	–1.441	1.056	–1.056	1.222	–1.222
HFM32_4	0.92		1.366	–1.366	1.488	–1.488	1.118	–1.118	1.280	–1.280
HFM34_2			3.883	–3.883	4.213	–4.213	3.987	–3.987	3.634	–3.634
HFM34_3	0.81		1.088	–1.088	1.625	–1.625	1.244	–1.244	1.525	–1.525
HFM13_2			0.279	–0.239	0.248	–0.197	0.245	–0.215	0.288	0.250
HFM13_3			0.322	–0.167	0.294	–0.164	0.599	0.582	0.953	0.950
HFM19_3			0.473	–0.471	0.615	–0.615	0.471	–0.471	0.569	–0.569
HFM19_2			0.566	–0.566	0.581	–0.581	0.599	–0.599	0.155	–0.075
HFM9			0.183	–0.157	0.154	0.148	0.348	0.348	0.807	0.807
HFM30			0.233	–0.079	0.367	–0.353	0.303	–0.274	0.566	0.566
HFM12_1			0.243	–0.036	0.379	–0.358	0.222	–0.070	1.925	1.925
HFM12_2			0.167	–0.014	0.167	–0.067	0.789	0.789	3.319	3.319
HFM26			0.507	–0.507	0.168	0.164	0.547	0.547	0.728	0.728
HFM14			0.710	–0.710	0.730	–0.730	0.616	–0.615	0.272	–0.267
HFM24			0.226	–0.076	0.471	–0.457	0.308	–0.262	0.426	–0.415
Mean HFM	**0.747**		**0.668**	**–0.631**	**0.756**	**–0.680**	**0.763**	**–0.439**	**0.994**	**0.098**

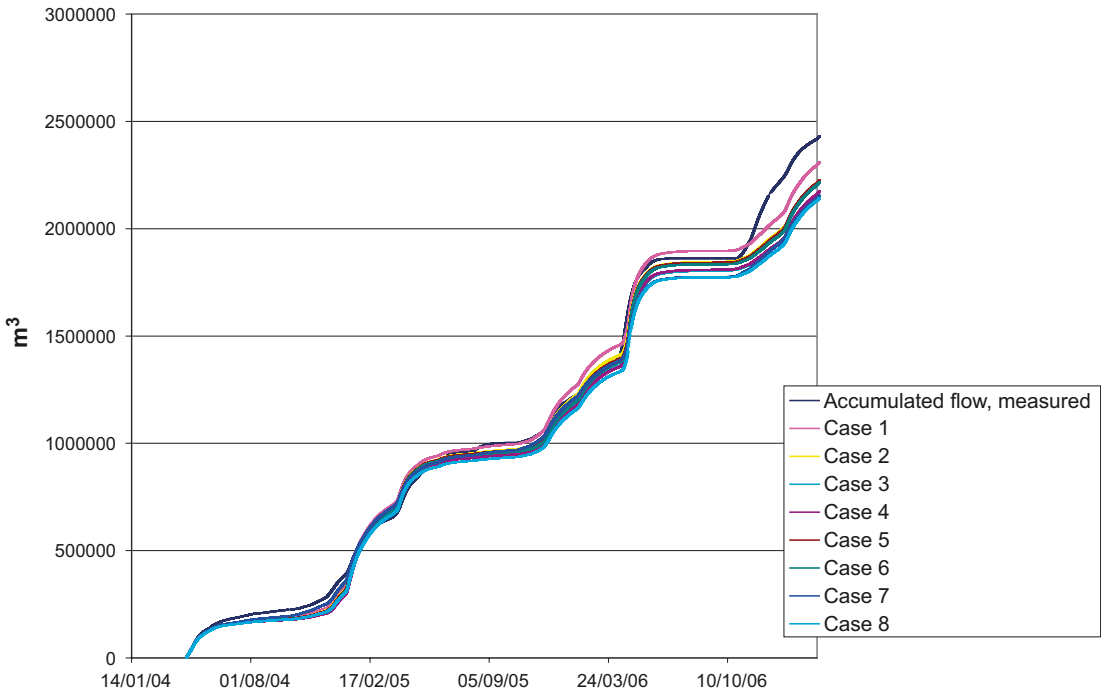

Figure 6-9. *Accumulated discharges in Lake Bolundsfjärden for sensitivity cases 1–8.*

Modelling of the pumping test in HFM14 was performed for cases 2, 5 and 6. The calculated drawdown for each case is listed in Table 6-6. Case 2 yields almost the same results as the Chapter 5 validation model. However, the pattern of the drawdown is better described in case 2 than for the original model, which is a result of the storage coefficient reduction. When reducing the vertical hydraulic conductivity, the drawdown increases. Dividing K_v by a factor of 10, i.e. case 5, produces the best agreement between measured and calculated drawdowns. When K_v is divided by a factor of 100, the calculated drawdown becomes too large; in case 6 the calculated drawdowns are several orders of magnitudes larger than the observed ones. Figures 6-10 and 6-11 give some examples of the resulting curves for case 5.

Summarising the results for the SFM-wells, HFM-wells, the surface water dynamics and the pumping test drawdowns, case 5 gives the best results. For each case, Table 6-7 lists the mean MAE and mean ME for all the SFM– and HFM-wells. It also presents the mean difference between observed and measured drawdowns for the cases where also the pumping test was modelled, and the accumulated calculated discharge in relation to the observed accumulated discharge.

Case 1 gives somewhat better results for the SFM-wells, but the drawdown in the pumping test is too small. Also the MAE and ME for the HFM-wells are a little larger in case 5 than in case 1, but also here the good results from the pumping test modelling for case 5 are considered more important. The accumulated discharge is 4% lower in case 5 than in case 1 but it is still an acceptable result; 92% of the measured accumulated discharge is captured by the model in case 5. Therefore, case 5 is selected as the final version of the MIKE SHE model. With this model, the head elevation in the bedrock is still constantly higher than the observed values. This will be further discussed in the following section.

Table 6-6. Calculated drawdowns for cases 2, 5 and 6. The measured values and the calculated drawdown for the Chapter 5 validation model are also listed. In the model, HFM15 is situated in the same cell as HFM14 where the pumping is performed. Therefore, the values HFM15 results are marked in yellow.

	Drawdown, m				
HFM-well nr	Validated model	Case 2	Case 5	Case 6	Measured
HFM1_1	1.3	1	2.8	11.4	2.3
HFM1-2	1.3	0.95	3	9.7	2.3
HFM1_3	1.3	0.7	2.5	8.4	2.3
HFM2_1	0.9	0.7	2.9	12.44	2.5
HFM2_2	0.75	0.85	2.35	9.3	2.5
HFM2_3	0.75	0.85	2.35	9.2	2.5
HFM3_1	0.8	0.8	2.45	8.35	2.5
HFM3_2	0.8	0.8	2.45	8.25	2.4
HFM4_1	0	0	0.1	1.95	0.2
HFM4_2	0	0	0.05–0.1	1.2	0.25
HFM4_3	0	0	0.05–0.1	1.2	0.1
HFM10_1	0.1	0.15	0.6	5.6	0.2
HFM10_2	0.1	0.15	0.4	5.1	0.2
HFM15_1	2.2	2.3	4.7	13.3	7.3
HFM15_2	2.6	2.8	4.9	13.7	8
HFM16_1	0.25	0.3	1.7	11.9	1.3
HFM16_2	0.25	0.3	1.6	10.3	1.3
HFM16_3	0.2	0.25	1.2	7.7	1.2
HFM20_2	0.3	0.4	1.4	9	1.3
HFM20_3	0.3	0.35	1.45	10.1	1.2
HFM20_4	0.3	0.2	0.9	7.2	0.8
HFM24_1	0.3	0.4	1.6	8.1	?
HFM24_2	0.05	0.1	0.4	4.1	?
HFM24_3	?	0.05	0.1	2.4	?
HFM32_1	0.5	0.6	1.85	6.55	2
HFM32_2	0.4	0.45	2.15	12.45	2
HFM32-3	0.2	0.25	0.86	6.16	0.15
HFM32_4	0.2	0.25	0.85	6.15	0.15
HFM34_2	0.1	0.15	1.4	10.6	?
HFM34_3	0.05	0.1	0.6	5.4	?
HFM13-2	1.8	1.8	1.2	4.42	1.9
HFM13_3	1.15	1	4.2	13.9	4.4
HFM19_2	2.3	2.3	3.15	9.65	6
HFM19_3	2.5	2.5	2.65	14.35	6
HFM9	0.25	0.35	0.8	5.1	0.25
HFM30	0	0	0	0	0
HFM12	0	0	0	0	0

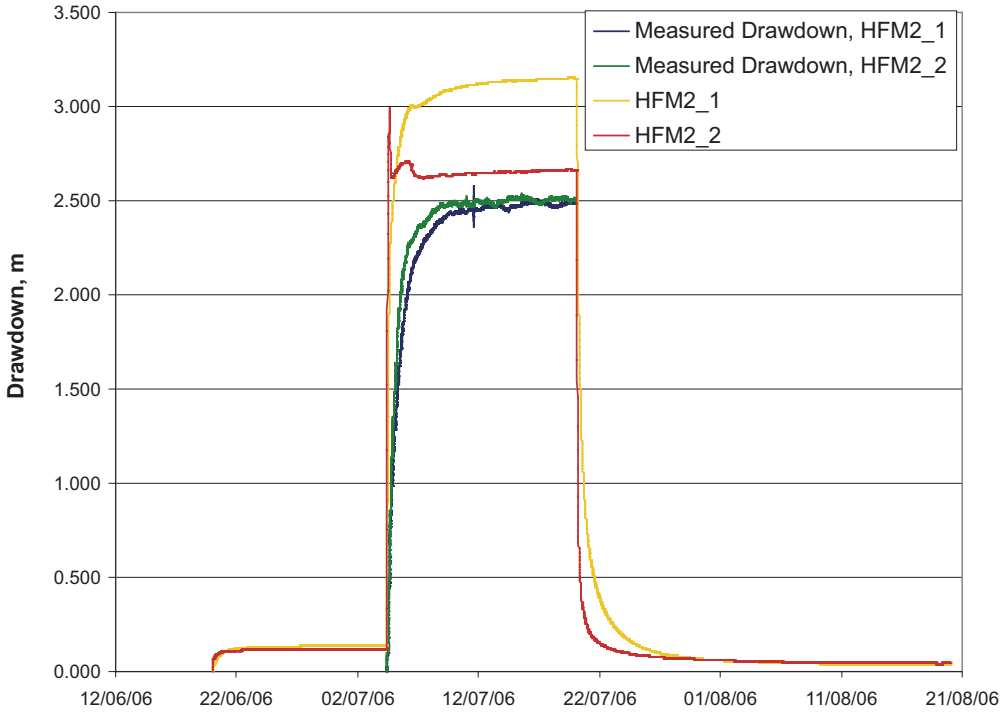

Figure 6-10. *Measured and calculated drawdowns in HFM2, section 1 and 2; the calculated values represent the case 5 pumping test results.*

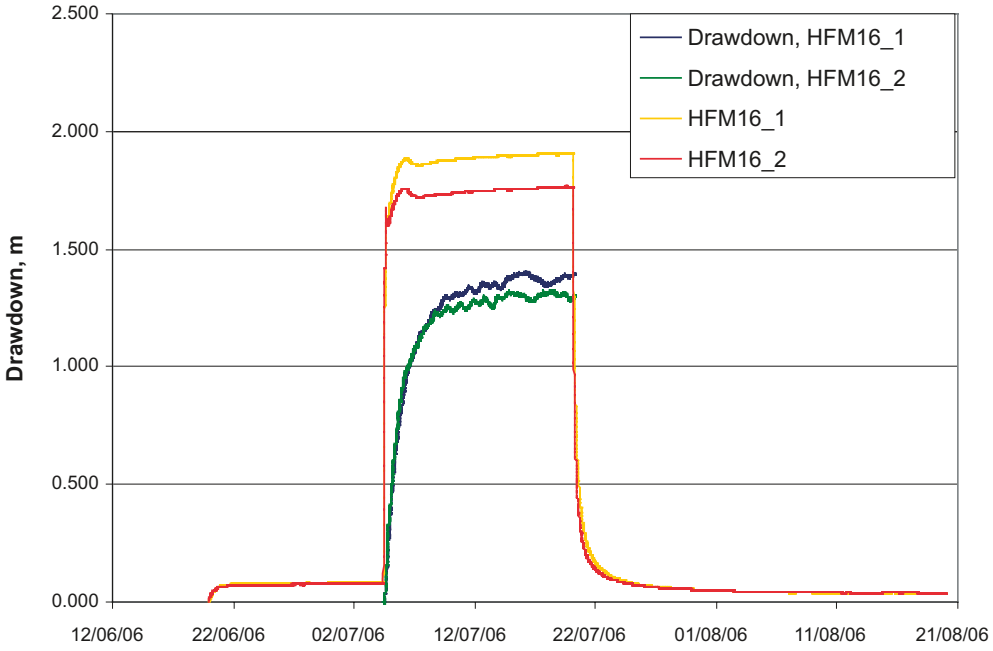

Figure 6-11. *Measured and calculated drawdowns in HFM16, section 1 and 2; the calculated values represent the case 5 pumping test results.*

Table 6-7. Summary of MAE and ME for the SFM- and HFM-wells, mean differences between observed and calculated drawdowns in the pumping test, and the accumulated discharges expressed in % of the measured accumulated discharges, for cases 1–8. An X indicates that the pump test has not been performed for that specific case.

Case	SFM-wells		HFM-wells		Drawdown pumping test, m	Accumulated calculated discharge downstream Lake Bolundsfjärden, % of measured values
	MAE	ME	MAE	ME	Mean (measured-calculated drawdown)	
1	0.28	–0.04	0.63	–0.55	X	96
2	0.31	–0.04	0.65	–0.56	1.32	79
3	0.31	–0.03	0.67	–0.63	X	77
4	0.33	–0.08	0.76	–0.69	X	91
5	0.28	–0.03	0.67	–0.63	0.25	92
6	0.30	–0.05	0.76	–0.68	–5.89	92
7	0.31	–0.06	0.76	–0.44	X	86
8	0.30	–0.04	1.00	0.10	X	89

6.2.3 Influence of the SFR repository drainage

For drainage of the SFR repository located below the sea in Forsmark Harbour, a pumping of approximately 6 L/s is necessary. The pumping is conducted from two sumps at two different levels, 88 and 140 m below the sea level. The pumping from the two levels are approximately, 1.2 and 4.8 L/s, respectively /Jakob Levén, pers. comm./. In /Follin et al. 2007/ it is discussed if one hypothesis to explain the observed downward gradient under Lake Bolundsfjärden could be the SFR drainage. To investigate whether the drainage of the SFR facility influences the hydrogeology of the site investigation area an additional simulation with case 5 was performed.

A pumping well was placed at SFR, Figure 2-18, a pumping rate of 6 L/s was applied to the well and the water extraction was active from 40 to 140 m b sl. The model was run for the same period as cases 1–8 analysed above. The introduction of the pumping at SFR in the model caused numerical instabilities. Therefore, the storage coefficient of the rock, which as described above had been reduced significantly to improve the fit to the interference test responses, was multiplied with a factor of ten. This correction of the storage coefficient resulted in a numerically stable model. To check whether the responses to the pumping test were influenced by the higher storage coefficient the pumping test was run for this parameterisation. It was found that the increased storage coefficient resulted in the same response as the pumping test for case 5. Therefore the SFR pumping simulation was run with a storage coefficient of $5 \cdot 10^{-8}$ m^{-1}.

The simulation results indicated that the drainage in the SFR facility could have a relatively strong influence on the groundwater head elevation in the bedrock. The MAE and ME for each HFM-well are listed in Table 6-8 and the radius of influence at 50 m.b.s.l. and at 110 m.b.s.l. are shown in Figures 6-12 and 6-13, respectively. The SFM-wells are not affected by the pumping; therefore, the MAE and ME for the SFM-wells are not listed in this chapter. The results from case 5 with and without SFR are presented in detail in Section 6.3.

Table 6-8. MAE and ME for the HFM-wells in case 5, with and without pumping at SFR.

ID code HFM-well	Case 5		Case 5 with SFR	
	MAE	ME	MAE	ME
HFM01_1	0.81	–0.81	0.28	0.28
HFM01_2	0.89	–0.89	0.26	–0.26
HFM02_1	0.82	–0.82	0.25	0.19
HFM02_2	0.78	–0.78	0.22	–0.14
HFM02_3	0.81	–0.81	0.21	–0.16
HFM03_1	0.75	–0.75	0.39	–0.39
HFM03_2	0.74	–0.74	0.38	–0.38
HFM04_1	0.08	–0.01	0.09	0.06
HFM04_2	0.15	–0.12	0.13	–0.09
HFM9	0.18	–0.16	0.13	0.07
HFM10_1	0.39	–0.39	0.23	–0.22
HFM10_2	0.27	–0.22	0.22	–0.09
HFM11_1	0.28	–0.28	0.28	–0.27
HFM11_2	0.26	–0.22	0.25	–0.22
HFM12_1	0.24	–0.04	0.24	–0.04
HFM12_2	0.17	–0.01	0.17	–0.01
HFM13_2	0.28	–0.24	0.66	0.66
HFM13_3	0.32	–0.17	0.38	0.28
HFM14	0.71	–0.71	0.21	0.19
HFM15_1	0.68	–0.68	0.25	0.23
HFM15_2	0.62	–0.62	0.30	0.28
HFM16_1	0.40	–0.40	1.02	1.02
HFM16_2	0.47	–0.47	0.54	0.54
HFM16_3	0.56	–0.56	0.22	0.16
HFM19_2	0.57	–0.57	0.37	0.37
HFM19_3	0.47	–0.47	0.24	–0.11
HFM20_2	0.48	–0.48	0.71	0.71
HFM20_3	0.44	–0.44	0.76	0.76
HFM20_4	0.79	–0.79	0.43	–0.34
HFM24	0.23	–0.07	0.25	0.14
HFM26	0.50	–0.50	0.50	–0.50
HFM30	0.23	–0.07	0.23	–0.07
HFM32_1	1.38	–1.38	0.78	–0.78
HFM32_2	1.43	–1.43	0.94	–0.94
HFM32_3	1.32	–1.32	0.98	–0.98
HFM32_4	1.37	–1.37	0.77	–0.77
HFM34_2	3.89	–3.89	0.77	–0.77
HFM34_3	1.09	–1.09	0.45	–0.45
Mean HFM	**0.68**	**–0.65**	**0.41**	**–0.05**

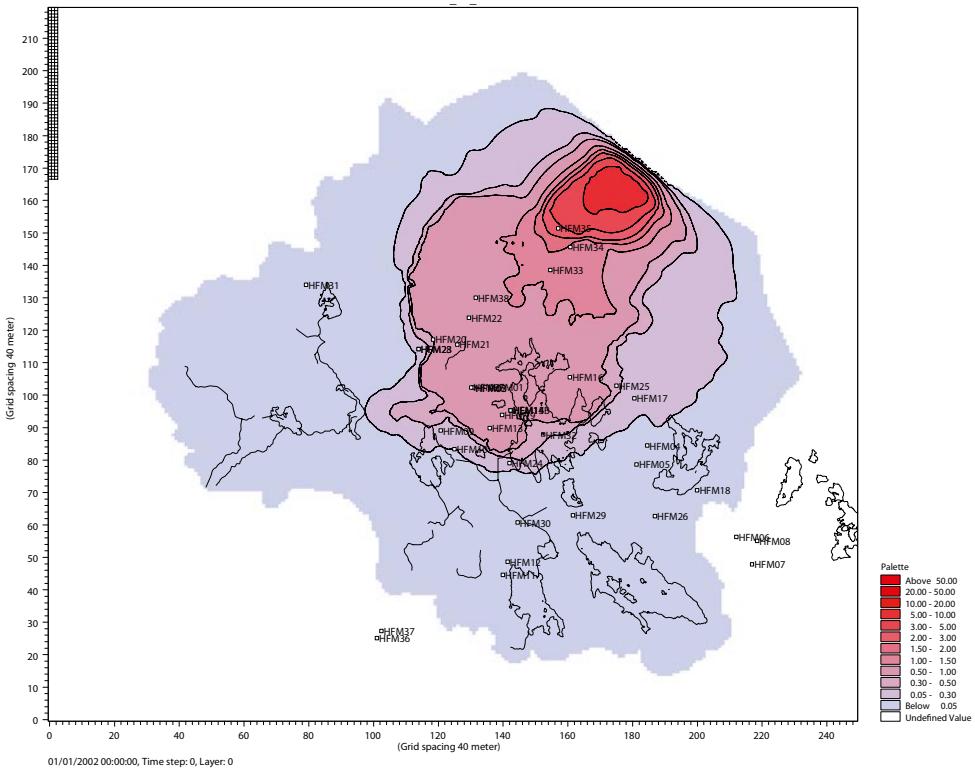

Figure 6-12. *Drawdown at 50 m.b.s.l. caused by the SFR-pumping The HFM-wells and the lakes and streams in the area are also marked in the figure.*

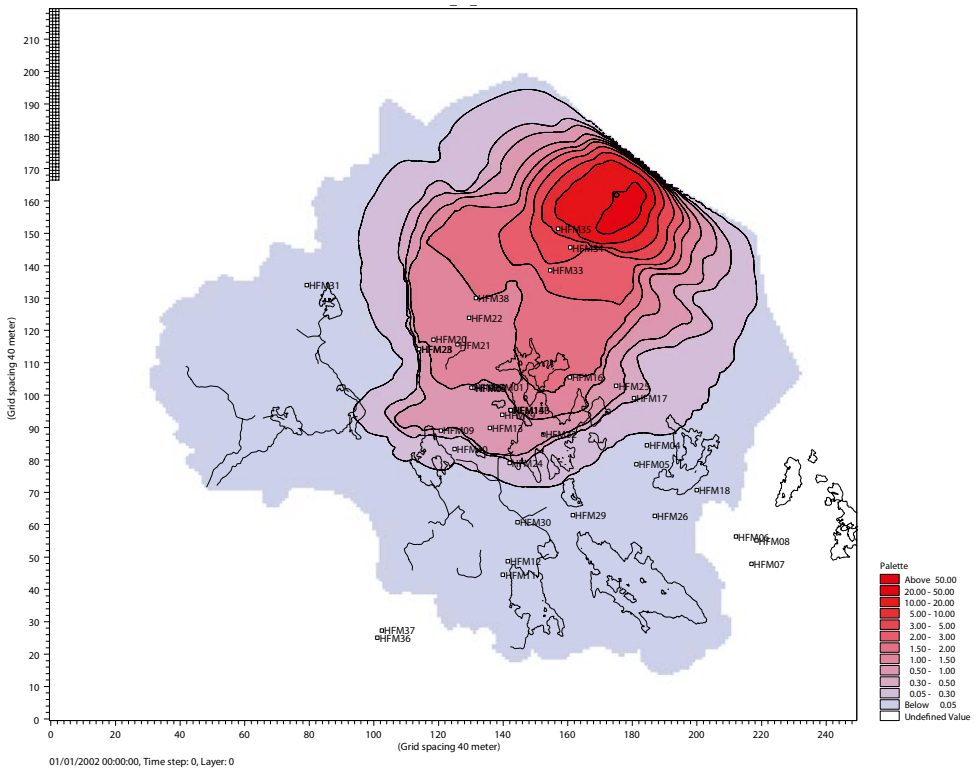

Figure 6-13. *Drawdown at 110 m.b.s.l. caused by the SFR-pumping The HFM-wells and the lakes and streams in the area are also marked in the figure.*

6.3 Results from the re-calibrated flow model

6.3.1 Surface water

As described in Section 6.2, case 5 was selected as the best case of the eight final calibration cases. For case 5, simulations were made both with and without the drainage pumping at SFR in the model. The results from the simulations are presented in detail in this section.

For the surface water discharge stations, the differences in results between simulations with and without the SFR drainage were small. Figures 6-14 to 6-17 illustrate results from the final simulations for the four surface discharge stations compared to measurements and to results from the previous validation model tested in Chapter 5. Figures 6-18 to 6-21 show the accumulated discharges. The figures show that the differences between case 5 and case 5 with SFR are very small with regard to surface water discharges. The complementary simulations showed no effect on the surface water levels, and therefore no new figures with water levels are presented in this section. For calculated surface water levels, see Chapter 5 (Figures 5-2 to 5-5.)

Table 6-9 illustrates the difference between measurements and calculations. The numbers are given in terms of accumulated surface water discharges and defined as the amount of calculated flow compared to measurements. In all four stations, the calculated values are still smaller than the measured although slightly increased compared to the previous validation model. Furthermore, it is seen that there is no effect of the SFR pump with regard to surface water discharges.

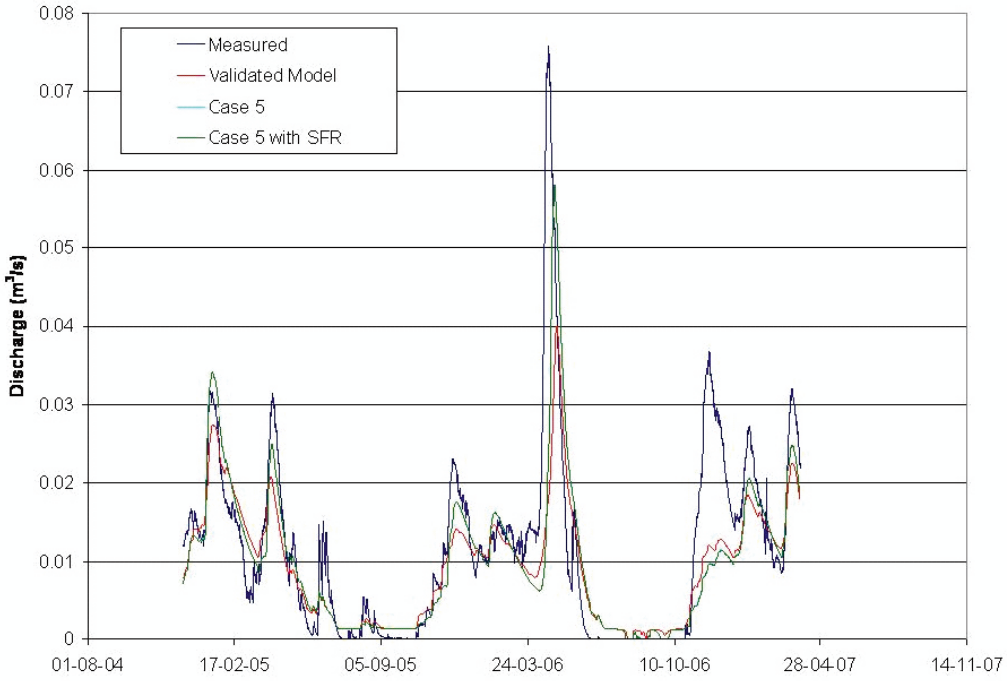

Figure 6-14. *Calculated surface water discharges compared to measurements at station PFM002668 (Lake Eckarfjärden); the simulation results include the validation model presented in Chapter 5 and sensitivity case 5 (this chapter) with and without pumping at SFR.*

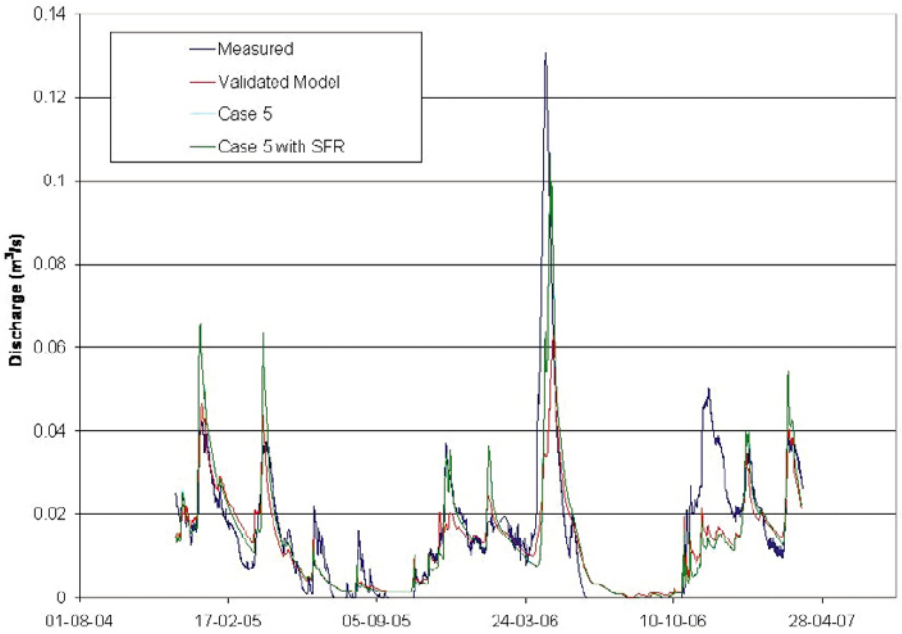

Figure 6-15. *Calculated surface water discharges compared to measurements at station PFM002667 (Lake Stocksjön); the simulation results include the validation model presented in Chapter 5 and sensitivity case 5 (this chapter) with and without pumping at SFR.*

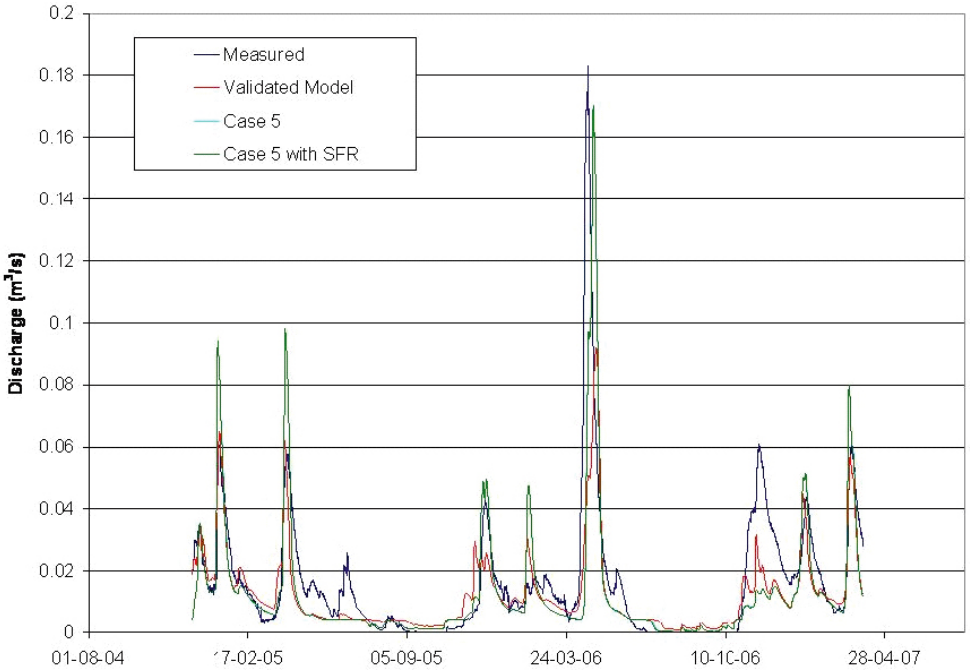

Figure 6-16. *Calculated surface water discharges compared to measurements at station PFM002669 (Lake Gunnarsboträsket); the simulation results include the validation model presented in Chapter 5 and sensitivity case 5 (this chapter) with and without pumping at SFR.*

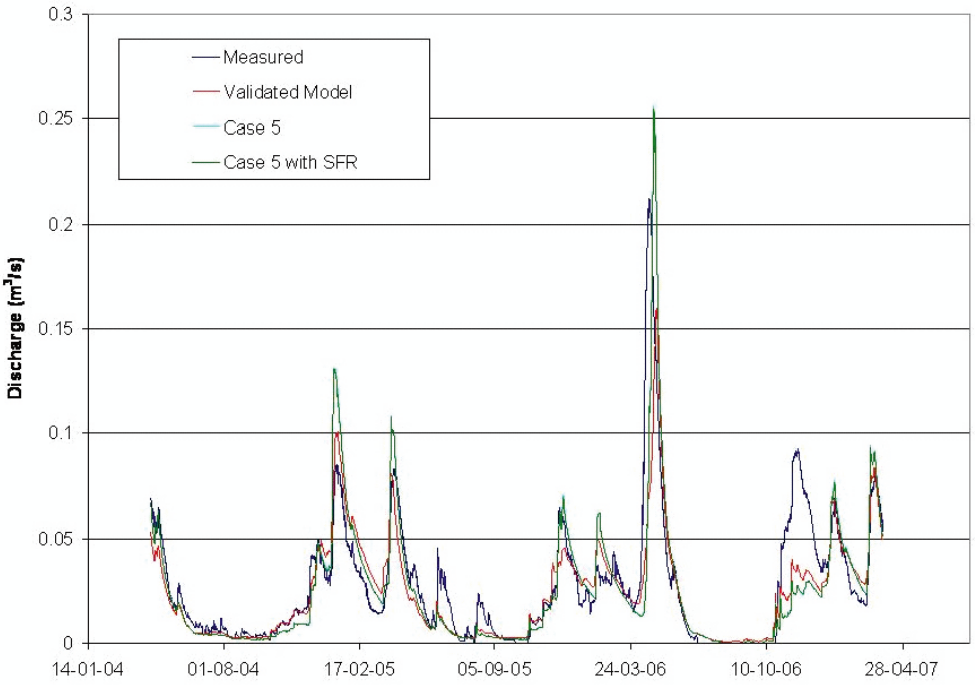

Figure 6-17. *Calculated surface water discharges compared to measurements at station PFM005764 (Lake Bolundsfjärden); the simulation results include the validation model presented in Chapter 5 and sensitivity case 5 (this chapter) with and without pumping at SFR.*

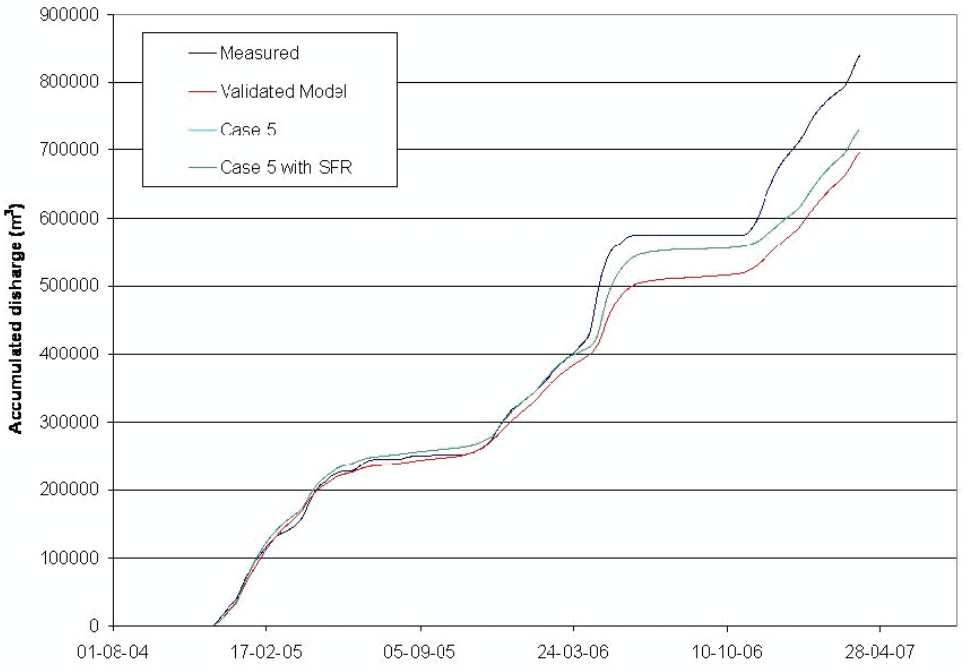

Figure 6-18. *Calculated accumulated discharges compared to measurements at station PFM002668 (Lake Eckarfjärden); the simulation results include the validation model presented in Chapter 5 and sensitivity case 5 (this chapter) with and without pumping at SFR.*

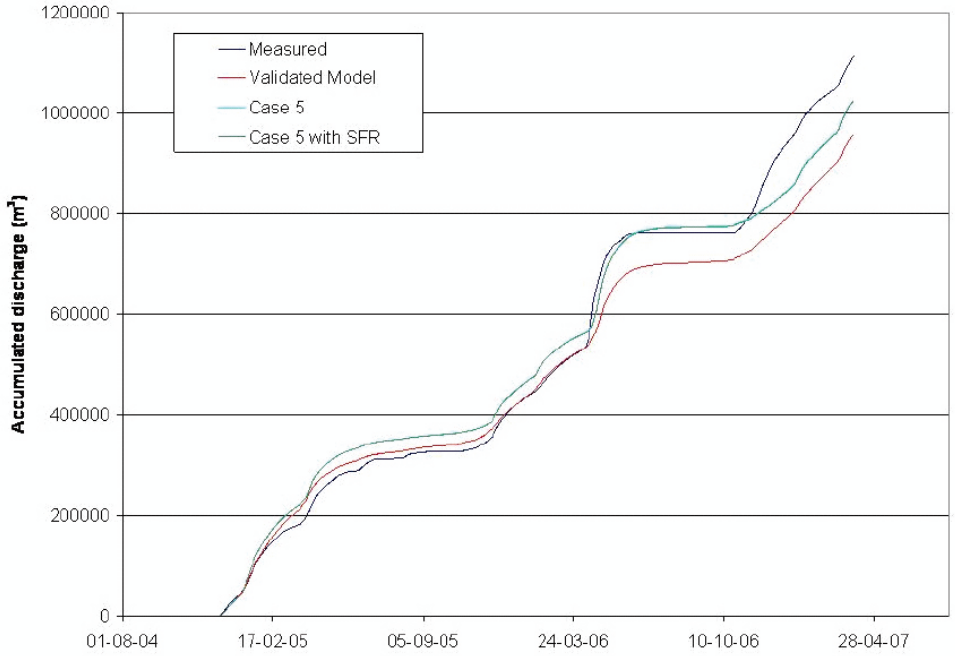

Figure 6-19. *Calculated accumulated discharges compared to measurements at station PFM002667 (Lake Stocksjön); the simulation results include the validation model presented in Chapter 5 and sensitivity case 5 (this chapter) with and without pumping at SFR.*

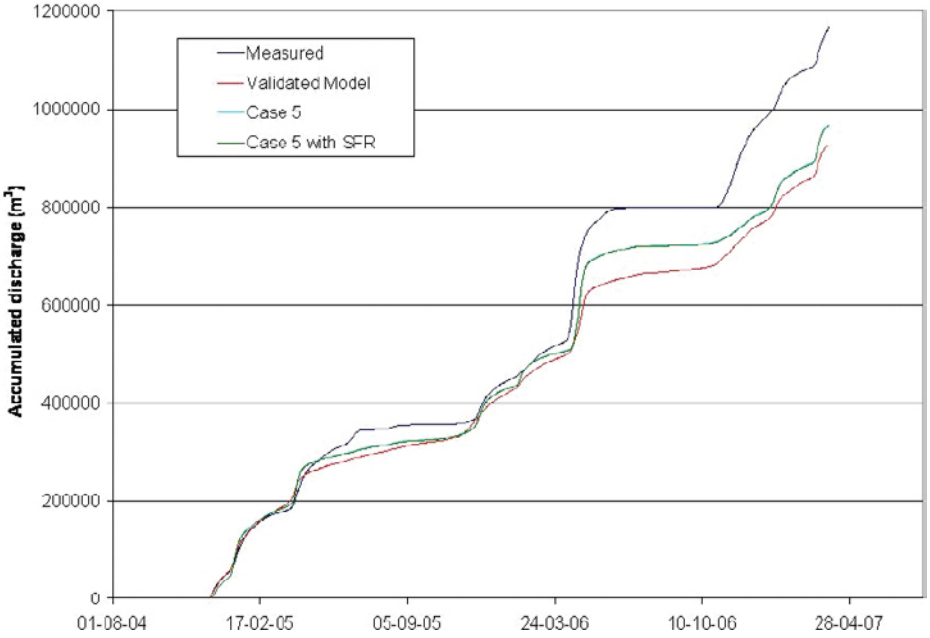

Figure 6-20. *Calculated accumulated discharges compared to measurements at station PFM002669 (Lake Gunnarsbofjärden); the simulation results include the validation model presented in Chapter 5 and sensitivity case 5 (this chapter) with and without pumping at SFR.*

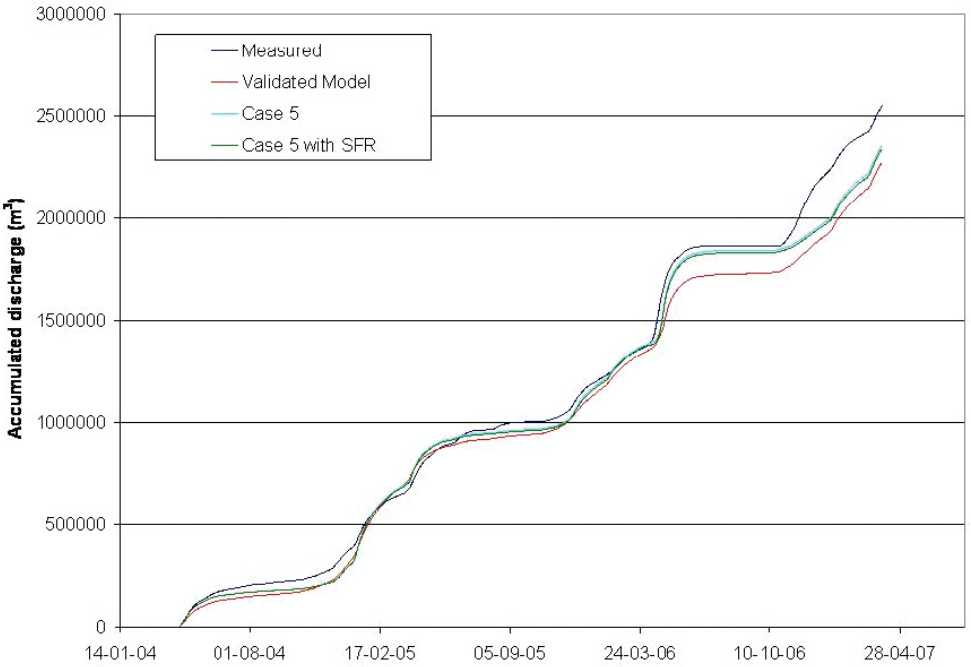

Figure 6-21. *Calculated accumulated discharges compared to measurements at station PFM005764 (Lake Bolundsfjärden); the simulation results include the validation model presented in Chapter 5 and sensitivity case 5 (this chapter) with and without pumping at SFR.*

Table 6-9. Comparison between calculated and measured accumulated discharges.

		Amount of calculated accumulated surface discharge compared to measurements in (in % of measured accumulated discharge)		
Station	**Period for comparison**	**Validation model**	**Case5**	**Case5 with SFR**
PFM002668 (Lake Eckarfjärden)	8/12 2004 to 31/3 2007	83	87	87
PFM002667 (Lake Stocksjön)	8/12 2004 to 31/3 2007	86	92	92
PFM002669 (Lake Gunnarsboträsket)	8/12 2004 to 31/3 2007	79	83	83
PFM005764 (Lake Bolundsfjärden)	14/4 2004 to 31/3 2007	89	92	92

6.3.2 Groundwater head elevation in QD and bedrock

When the calibrated model was tested to independent time series data, two problems were identified regarding the groundwater head elevation; the pattern of the calculated time series for some SFM-wells during the summer 2006 and the high calculated groundwater heads in the bedrock. The results of the complementary simulations performed to improve the model in these respects are discussed in the following.

During the dry summer of 2006 the head elevation in some areas reached the bottom of the calculation layer where the filter of the SFM-well is placed. Since the transpiration processes are fully active in the uppermost calculation layer only, it is important that the lower level of the uppermost calculation layer is deep enough. Otherwise, the effects of transpiration on the groundwater fluctuations may be underestimated (see Section 6.2.1). Therefore, simulations with a calculation layer that was increased from 2 m to 2.5 m were made. Since no negative effects of this were found, the 2.5 m calculation layer was used in all further calculations.

For the groundwater monitoring points in which the calculated head elevations reached the bottom of the uppermost layer, the results were improved. Figures 6-22 to 6-25 show examples of monitoring points for which the deeper calculation layer leads to improvement. In Figure 6-24, however, it is seen that the layer is still not deep enough; the flat curve in the summer of 2006 indicates that the bottom of the calculation layer is reached. Figures 6-22 to 6-25 show results from the simulation without the SFR-drainage activated. A comparison between MAE- and ME-values from the validated model and the case 5 model (described in Section 6.2) shows that some monitoring points are improved while others are not. However, the average effect of the model changes on MAE is small, see Table 6-3.

As discussed in Section 6.2.2, case 5 is the final version of the MIKE SHE model.
The case was modelled both without and with the SFR pumping. Since the main focus of the complementary calibration was to make improvements with regard to the bedrock, more monitoring points in bedrock were included in the model evaluation compared to the previous calibration (Chapter 4).

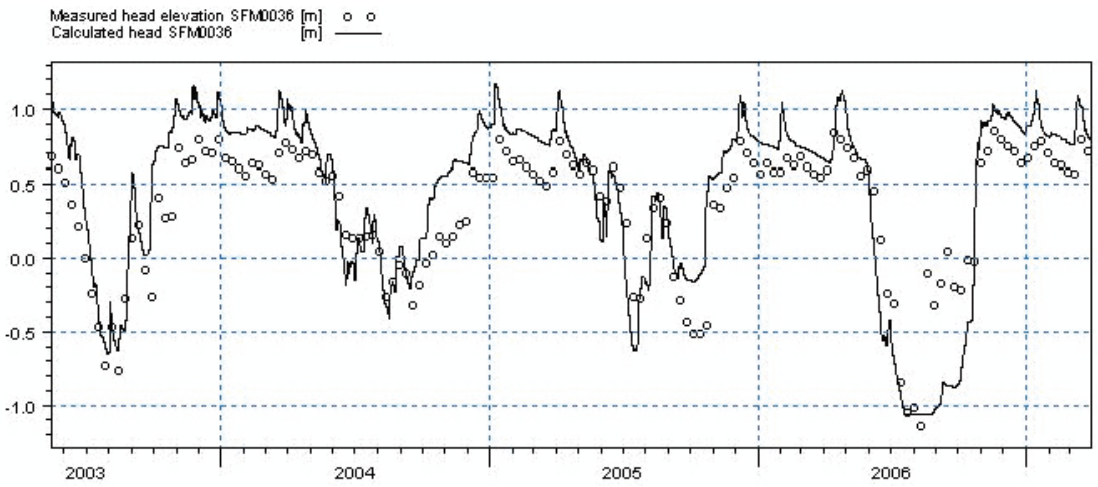

Figure 6-22. *Calculated and observed groundwater head elevations in SFM0036.*

Figure 6-23. *Calculated and observed depth to the groundwater table in SFM0001.*

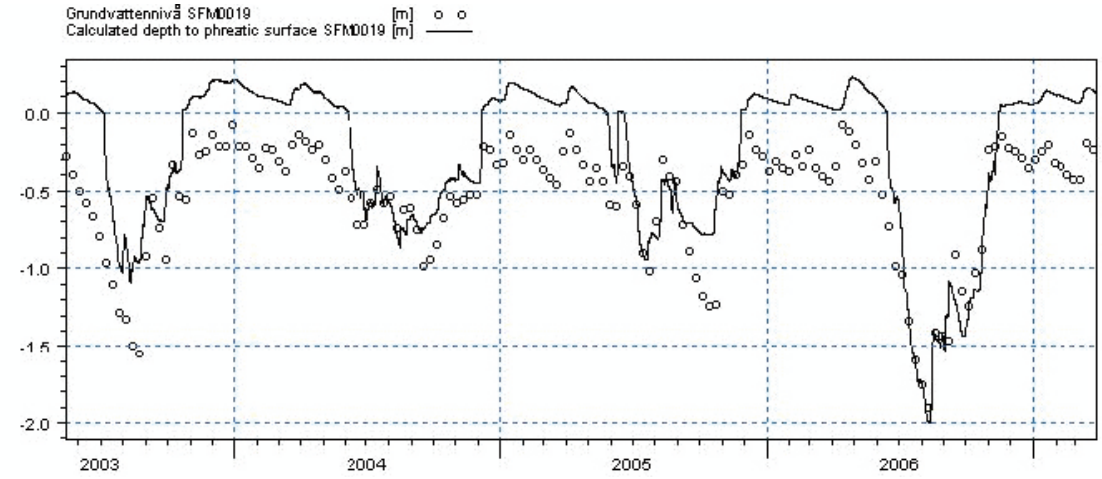

Figure 6-24. *Calculated and observed depth to the groundwater table in SFM0019.*

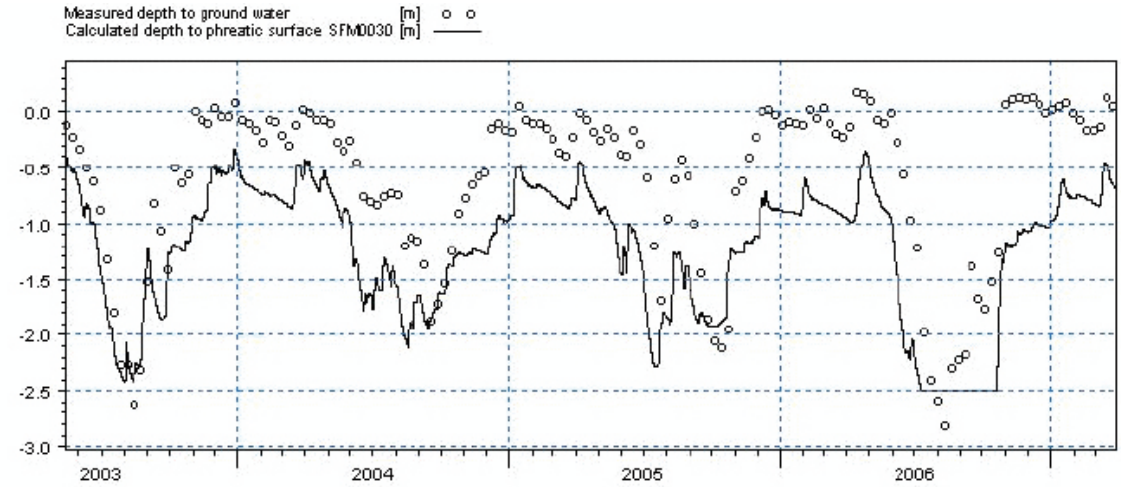

Figure 6-25. *Calculated and observed depth to the groundwater table in SFM0030.*

Table 6-8 in Section 6.2.3 illustrates that the MAE– and ME-values of the HFM boreholes in bedrock were improved when the SFR pumping was included. Figures 6-26 to 6-28 show the resulting graphs for some HFM monitoring sections included in the model, both with and without the SFR pumping activated in the model. Figures for all the HFM-sections are presented in Appendix 3. In several of monitoring points, the improvement is significant when the SFR pumping is included. Especially in HFM34_2 the improvement is remarkable. Only a few sections (HFM13_2, HFM16_1. HFM20_2 and HFM20_3) show larger errors when including the SFR pumping.

Correlation plots for head elevation in the final model, case 5, with and without the SFR pumping included in the model were made in the same way as in Section 5.2 (Figure 5-15). In the plot, also the new bedrock monitoring points are included. Figure 6-29 shows the resulting correlation plot for the case with no SFR pumping, blue dots, and when SFR pumping is included, red dots. The correlation is clearly better when the pumping is included.

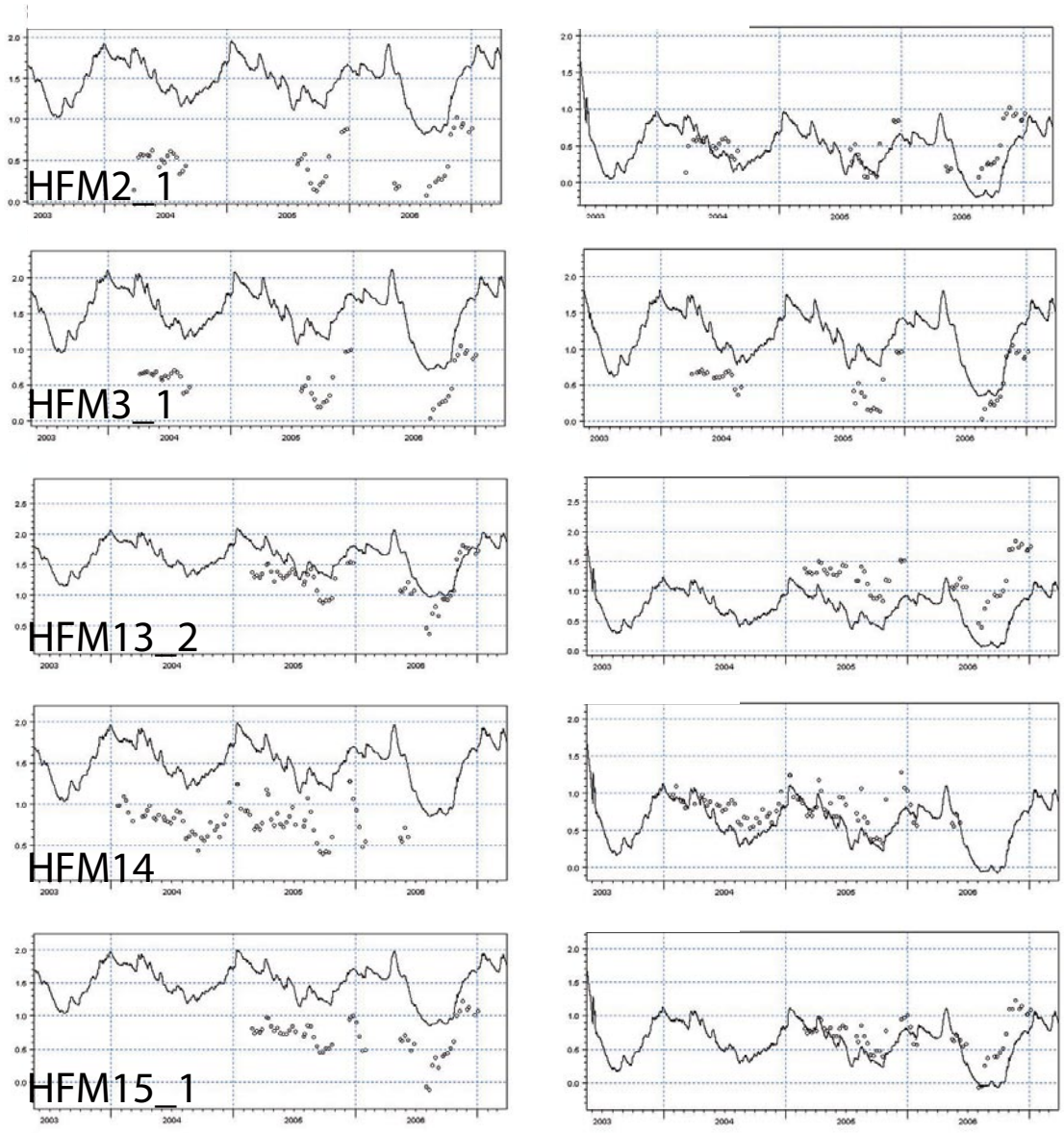

Figure 6-26. *Comparisons of measured and calculated groundwater head elevations in HFM02_1, HFM03_1, HFM13_2, HFM14 and HFM15_1. For each HFM section, the figures to the left and right are from simulations without and with the SFR drainage included in the model, respectively.*

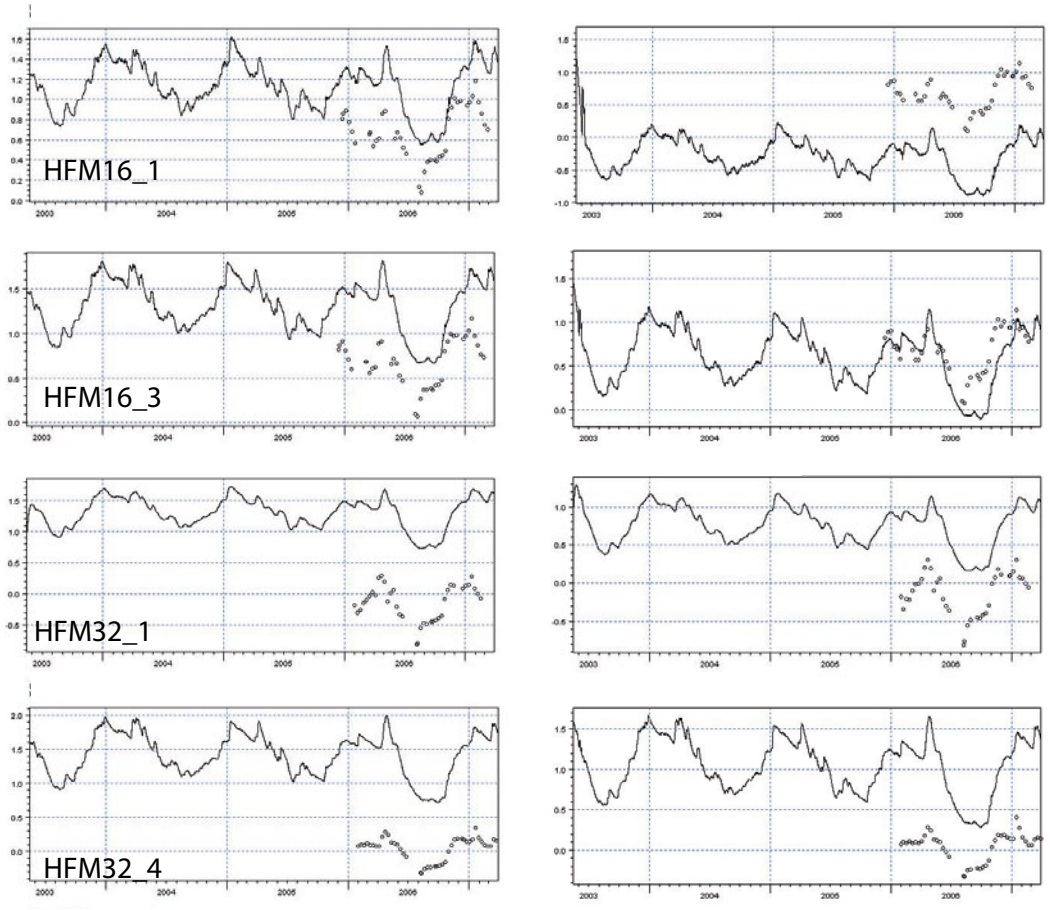

Figure 6-27. *Comparisons of measured and calculated groundwater head elevations in HFM16_1, HFM16_3, HFM32_1 and HFM32_2. For each HFM section, the figures to the left and right are from simulations without and with the SFR drainage included in the model, respectively.*

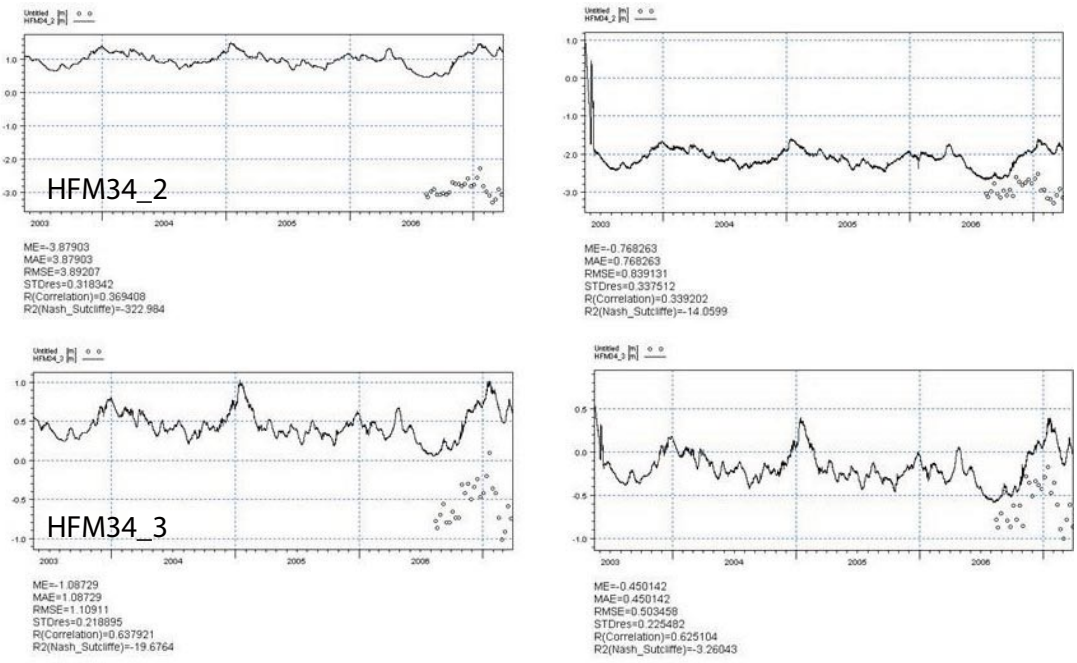

Figure 6-28. *Comparisons of measured and calculated groundwater head elevations in in HFM34_2 and 34_3. For each HFM section, the figures to the left and right are from simulations without and with the SFR drainage included in the model, respectively.*

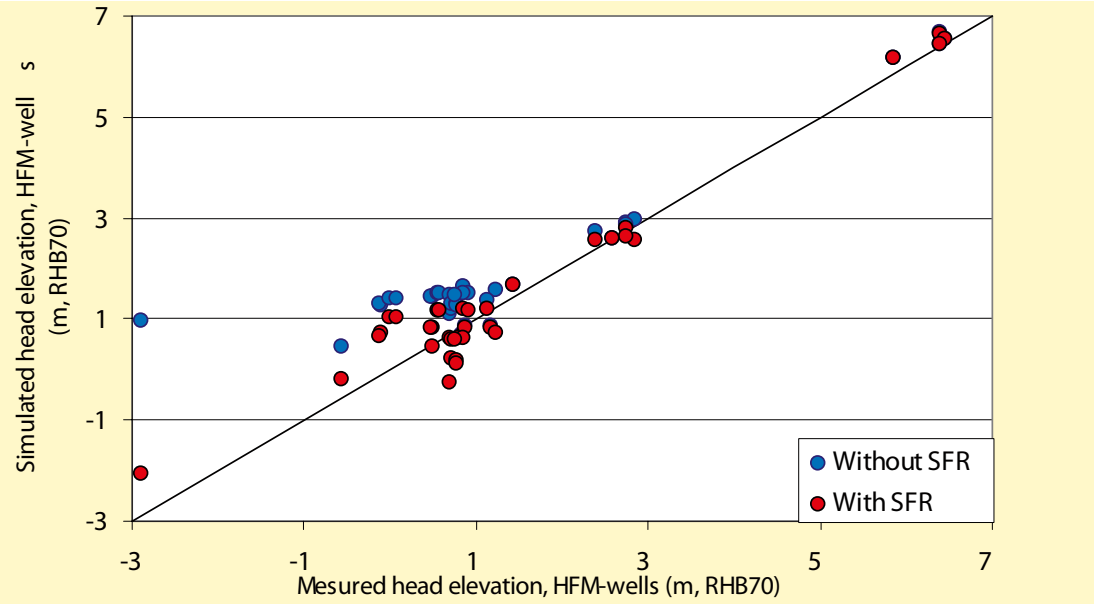

Figure 6-29. *Correlation plot for mean head elevation for case 5 with and without drainage of the SFR repository included in the model.*

6.3.3 Water balance

The calculated water balance for three years during the simulation period is shown in Figure 6-30; the numbers are annual mean values for the period 1/9 2003 to 1/9 2006 (i.e. average values for this three-year period, expressed in mm/year). The water balance is calculated for the land part of the model area, including the littoral zone. The red figures represent the values calculated without the SFR drainage activated and the blue figures are from the calculation where the SFR drainage is included in the model. It is seen that the SFR drainage does not have a strong influence on the overall water balance; therefore, the following text considers the case without the SFR drainage only.

The average annual precipitation is 533 mm and the total annual evapotranspiration is 405 mm. In the remainder of the discussion on the water balance, all quantities given in mm are average annual amounts (i.e. mm/year) for the simulation period. The total evapotranspiration is the sum of the different evaporation components. The transpiration from plants is 169 mm, the evaporation from soil is 56 mm and the evaporation from flooded areas is 28 mm. The amount of water intercepted by plant leaves is calculated to 122 mm and the evaporation from the saturated zone is 30 mm. The total discharge via the streams is calculated to 144 mm (74 + 70 mm).

In the model, the water in saturated areas is classified as “overland water”. Therefore a large amount of water, 74 mm, is transported from overland to the streams (MIKE 11). This should not be interpreted as direct run-off on the ground surface. Most of the water is transported in the saturated zone towards the “river links” in MIKE SHE. The cells in direct contact with MIKE 11 are often saturated or flooded. In the water balance calculation MIKE SHE does not take this into consideration and the water that is transported from the saturated zone to the streams via overland water is classified as flow from “overland to streams”. The infiltration from the overland compartment to the unsaturated zone is 351 mm and the groundwater recharge, defined as the water flow from the unsaturated to the saturated zone, is 124.5 mm.

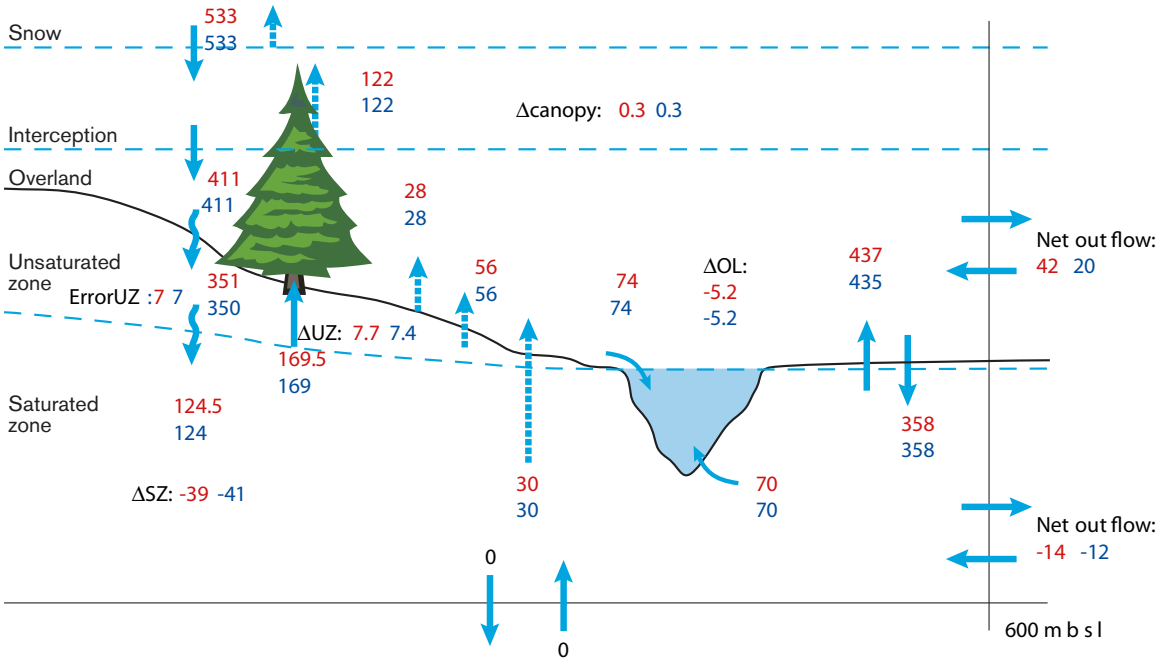

Figure 6-30. *Water balance in mm/year, showing the annual mean values for the three-year period from September 1, 2003, to September 1, 2006. Red figures represent the calculation results obtained without the pumping at SFR, and blue figures are the results from the simulation with the SFR drainage activated.*

The net outflow of water from the overland compartment and the exchange of water between the overland compartment and the saturated zone is an effect of the boundary condition at the sea. In the model, the sea is described as a high-conductive layer of gravel. The upper level of this layer is equal to the minimum sea level during the simulation period, 0.68 m.b.s.l.. The boundary condition in this layer is given by a time series describing the sea level during the simulation period. Thus, when the sea level rises over the minimum level, overland water is generated and water is transported from the saturated zone to the overland compartment. When the sea level drops, water is transported from the overland compartment to the saturated zone. Since the water balance is calculated for the land part of the model area, the outflow from the overland should be seen as internal fluxes in the littoral zone.

The water balance shown in Figure 6-30 is made for the areas at higher altitude than the minimum sea level during the simulation, i.e. the land parts and the littoral zone of the model area. Due to the boundary condition in the sea, overland water is produced in the littoral zone and the depth of this water is varying with the sea water level. This causes a water exchange between the overland compartment and the saturated zone and also a net outflow of water to the sea. Thus the numbers 437 mm from saturated zone to overland, 358 mm from overland to saturated zone, and 42 mm, the net outflow to the sea, are water fluxes due to the boundary condition.

The storage in the saturated zone decreases with approximately 40 mm. This is due to the very dry summer 2006. In 2003, an amount of 184 mm is added to the model between the 1st of June and the 1st of September. During the short period from the 15th of August to the 1st of September, some 100 mm are added to the model. In 2006, 101 mm of precipitation was added to the model between the 1st of June and the 1st of September; 47 mm was added during the last 15 days of August.

The water balance for each layer in the saturated zone is presented in Figure 6-31. All the flows outside the saturated zone except from the infiltration to the unsaturated zone are removed from the picture. The vertical flow in the bedrock decreases with depth. Below layer 10 the flow is insignificant (< 0.5 mm/year). The groundwater recharge from the unsaturated zone to the uppermost calculation layer containing the Quaternary deposits is 124 mm. The pumping at

SFR does not influence the recharge. The recharge to the lowest QD-layer (layer 2) is 44.7 mm. There are many local recharge and discharge areas in this layer; the figures by the upward arrows show that 41 mm is transported up to the above layer. Thus, the average annual net flux is only c. 4 mm.

According to the results in Figure 6-31, only 10.6 mm is flowing down to the bedrock, i.e. from layer 2 to layer 3. Since the vertical hydraulic conductivity has been reduced compared to the original setup of bedrock properties, the vertical groundwater fluxes are very low. When the pumping at the SFR facility is included in the model, the downward flow increases in the upper bedrock layers. The pumping is active down to 140 m.b.s.l. Below this level the influence of the SFR pumping is insignificant. Figure 6-31 represents the land part of the model area only. The SFR pumping has a stronger impact in the bedrock below the sea, which is shown in Figures 6-12 and 6-13 that illustrate the drawdown caused by SFR.

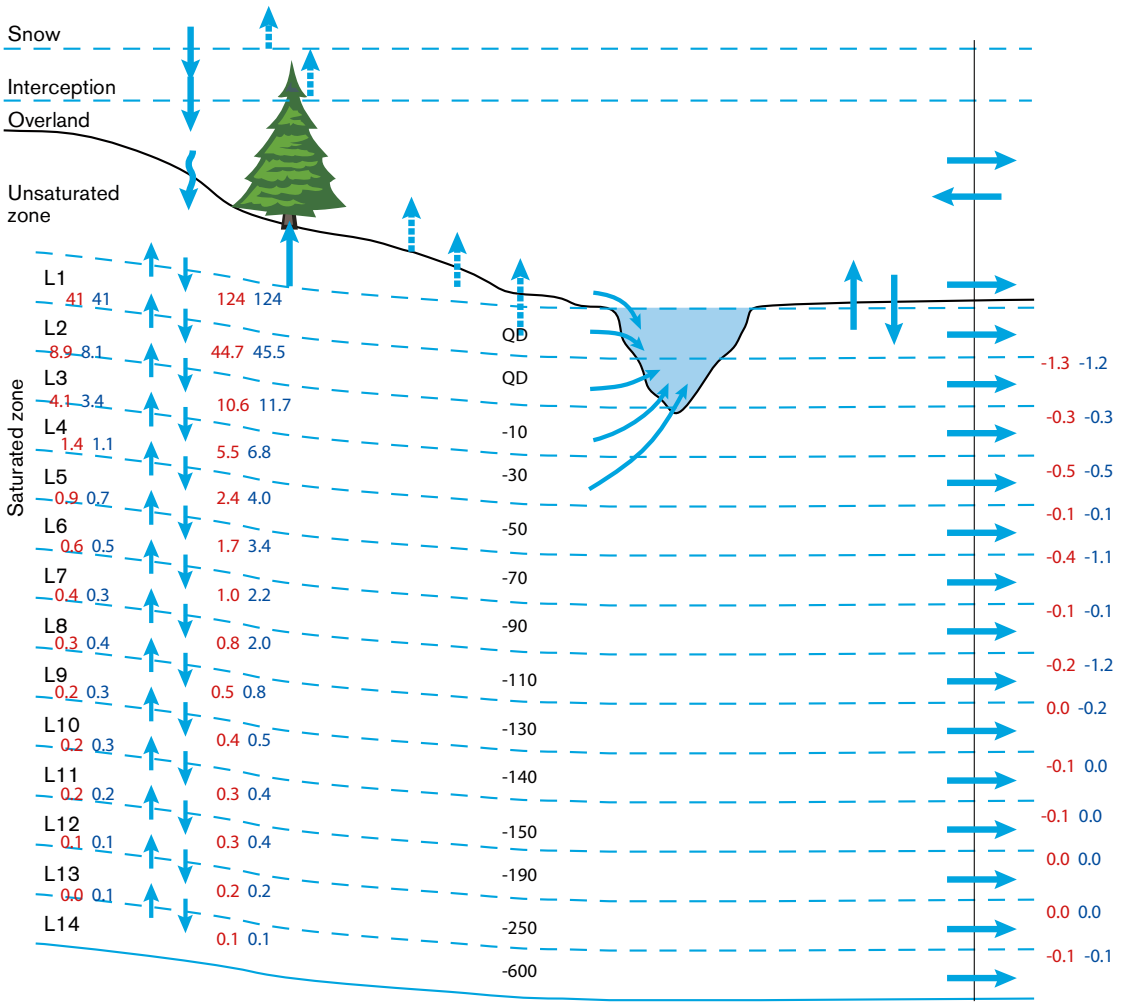

Figure 6-31. *The water balance for each layer in the saturated zone, expressed as annual vertical fluxes (mm/year) from layer to layer. Red figures represent the calculation without SFR, blue figures are results from the simulation with SFR drainage activated. Note that only the net flux is given for the recharge into the saturated zone (124 mm/year), whereas upward and downward components are reported for the saturated zone layers (e.g. 8.9/8.1 and 10.6/11.7 belong to the same layer interface). The mean lower level of each calculation layer is marked in the middle of the figure.*

6.3.4 Recharge and discharge areas

The results presented in this section are taken from the simulation without the drainage of the SFR repository. The influence of SFR on recharge and discharge patterns will be further discussed in Section 6.3.6.

The model results indicate that, as expected, lakes and stream valleys are discharge areas and the high altitude areas are recharge areas. However, the recharge and discharge areas are varying with the weather conditions. The mean situation during the period from September 2003 to September 2006 is presented in Figures 6-32 and 6-33. Figure 6-32 shows the head difference between layer 1 and 2, i.e. the local recharge and discharge areas in the Quaternary deposits. Figure 6-33 shows the head difference between layers 4 and 5 (about 40 m below ground), i.e. the recharge and discharge in the upper bedrock.

The sea, stream valleys and lakes in the model area are discharge areas both in the Quaternary deposits and in the upper bedrock. However, the pattern of recharge and discharge areas is more diffuse in the QD, where the local topography creates a varying pattern of recharge and discharge areas. In the bedrock the discharge areas are concentrated to the areas close to and under the lakes. Also, the depressions around the streams are reflected as discharge areas in the bedrock. In the upper bedrock, Figure 6-33, Lake Bolundsfjärden is deviating concerning the overall pattern of recharge and discharge areas. The main part of the area under the lake is a recharge area, as indicated by the downward gradient below the lake. The sheet joints short circuit the vertical flow and water is transported towards the sea. The model results indicating that Lake Bolundfjärden acts mainly as a recharge area are supported by local measurements in HFM32, a borehole in rock drilled from a small island is the lake.

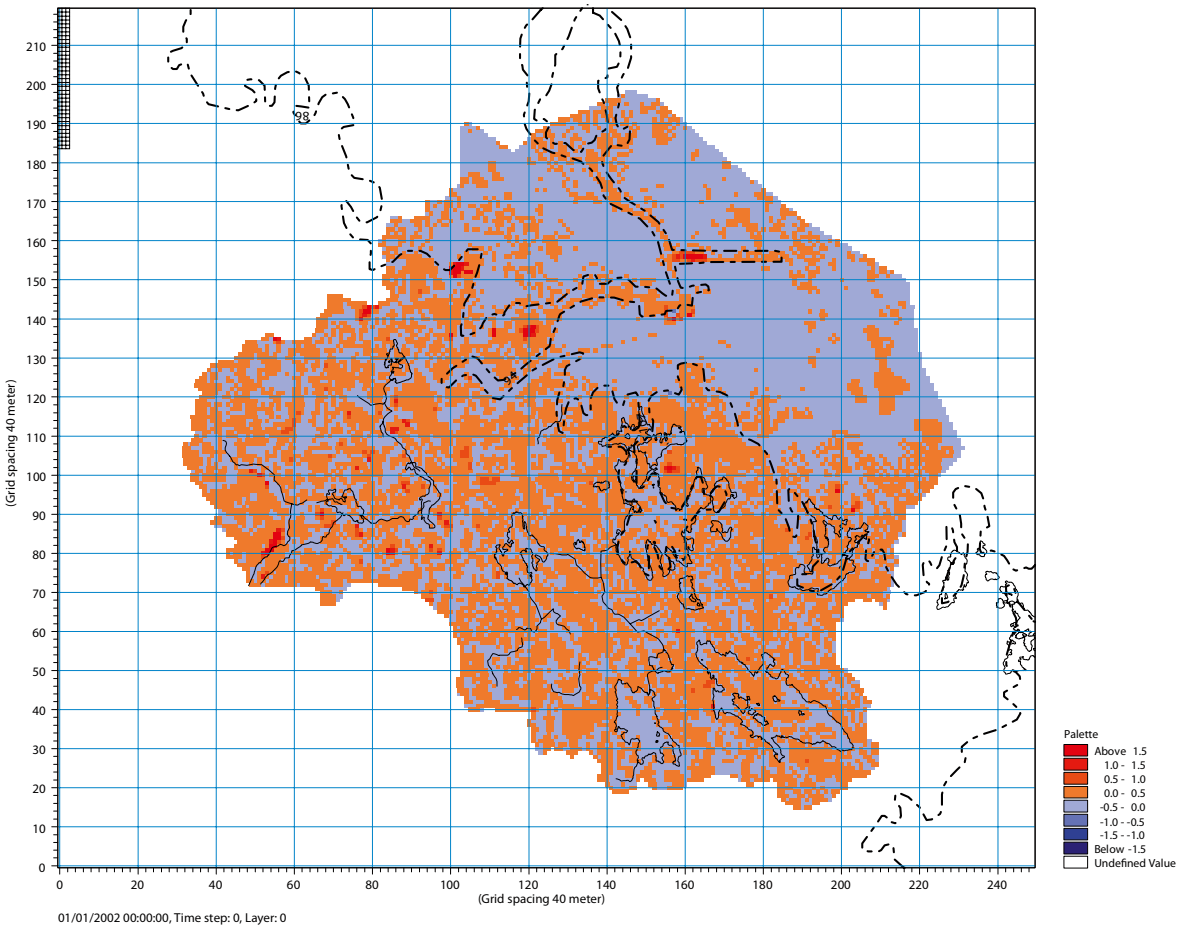

Figure 6-32. *The mean head difference, m, between calculation layers 1 and 2, i.e. recharge and discharge areas in the Quaternary deposits. As an orientation, the lakes and streams in the area and the coastline are marked in the figure.*

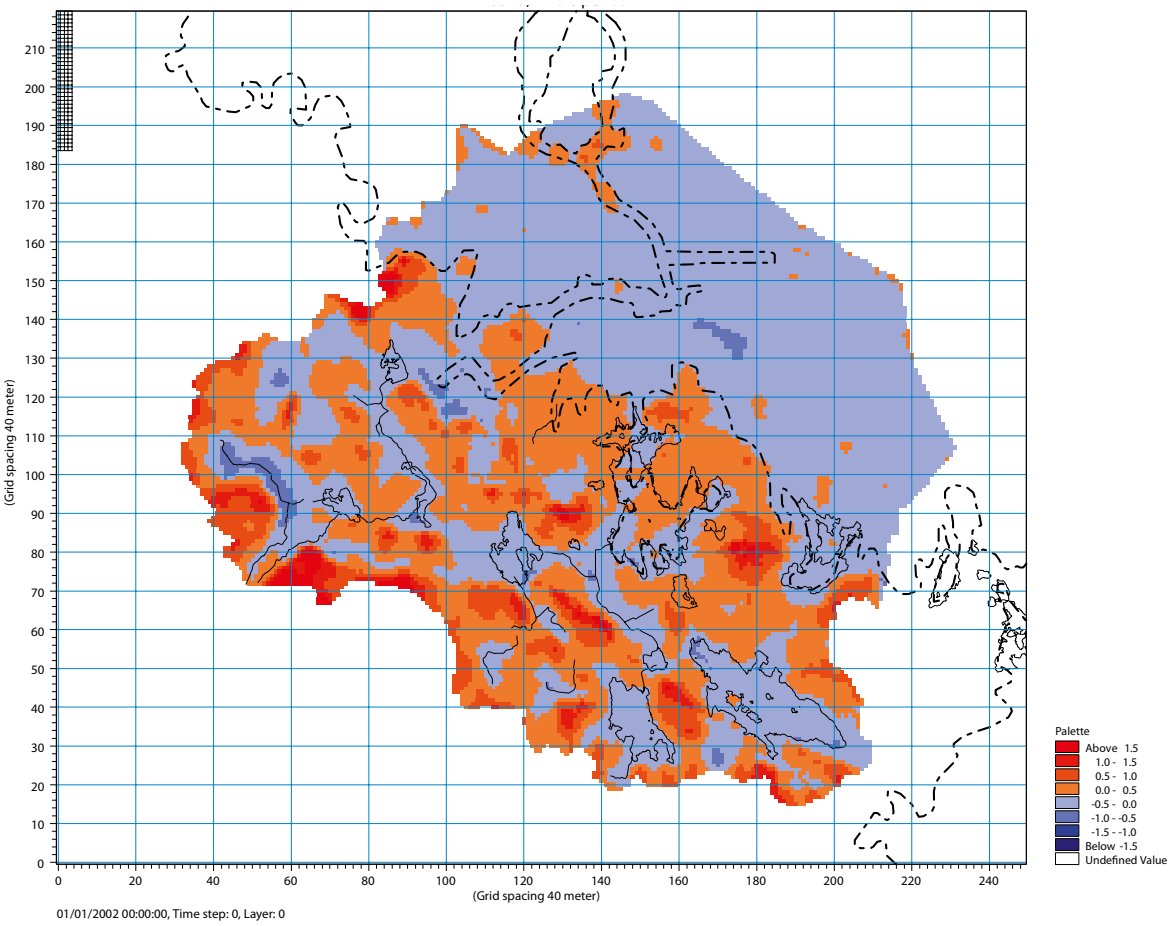

Figure 6-33. *The mean head difference, m, between layers 4 and 5, i.e. recharge and discharge areas in the upper bedrock. As an orientation, the lakes and streams in the area and the coastline are marked in the figure.*

The head differences in the Quaternary deposits are somewhat weaker than the head gradient between the two layers in the upper bedrock. The mean head difference in the recharge areas is 0.05 m between layers 1 and 2, and 0.34 m between layers 4 and 5. The mean head gradient in the discharge areas is –0.01 m between layers 1 and 2, and the corresponding value between layers 4 and 5 is –0.14 m.

In order to evaluate the changes in recharge and discharge areas between dry and wet conditions, the distribution has also been evaluated during two different periods. The dry conditions are represented by the mean head gradient between the 10th of July and the 25th of July, 2006, and the wet condition by the mean head gradient between the 15th of March and the 30th of March, 2004.

The overall pattern of recharge and discharge areas in the Quaternary deposits during a dry period is almost the same as the average values presented in Figure 6-32, with one exception. The total area of discharge areas increases in the QD during dry conditions. The biggest difference is found in the Lake Fiskarfjärden area. The recharge areas in the littoral zone in Lake Eckarfjärden are somewhat larger under dry conditions. The area in the south-western part of the lake turns into a recharge area due to the influence of evapotranspiration during the dry summer period. In the bedrock, the pattern under dry conditions is very similar to the mean situation. However, the area to the west of Lake Bolundsfjärden turns into a discharge area during the dry period.

During the wet period many discharge areas in the Quaternary deposits turn into recharge areas. The water levels in the lakes become higher than the groundwater heads in the underlying till, and the lakes become recharge areas. This pattern cannot be seen in the head difference between layers 4 and 5. In the upper bedrock, the lakes are discharge areas even during the period of wet conditions. The results are shown in Figures 6-34 to 6-37.

Tables 6-10 and 6-11 summarise the results in Figures 6-34 to 6-37. The results show how the distribution of recharge and discharge areas are varying with the weather conditions. Since most of the off-shore area is a discharge area, results are shown both for the whole model area and for the land part of the model area. The differences between recharge and discharge areas among the three cases are most obvious for the QD during the dry period. The size of the discharge areas in the Quaternary deposits increases with 30% during a dry period when considering the whole model area; when only the land part is taken into account the increase is 44%. Under wet conditions the recharge areas increase by 8% in the land part of the model area. Taking the whole model area into consideration, the recharge areas decrease during the wet period. This is likely due to an increase of the discharge areas in the littoral zone of the sea.

For the bedrock, the difference between the different weather situations is much smaller. There is a slight increase in the recharge areas, by 6%, during the wet period both for the whole model area and for the land part of the model area. The difference in the pattern of recharge and discharge areas under dry conditions is similar to the mean situation.

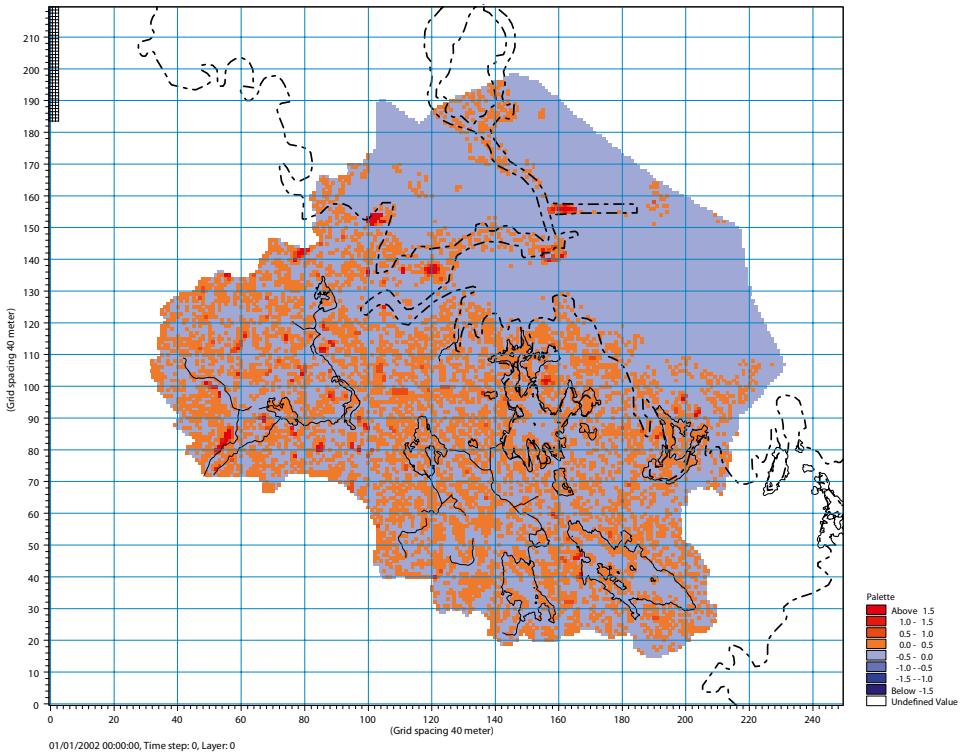

Figure 6-34. *The mean head difference, m, between layers 1 and 2 under dry conditions (July, 2006), i.e. recharge and discharge areas in the Quaternary deposits. As an orientation, the lakes and streams in the area and the coastline are marked in the figure.*

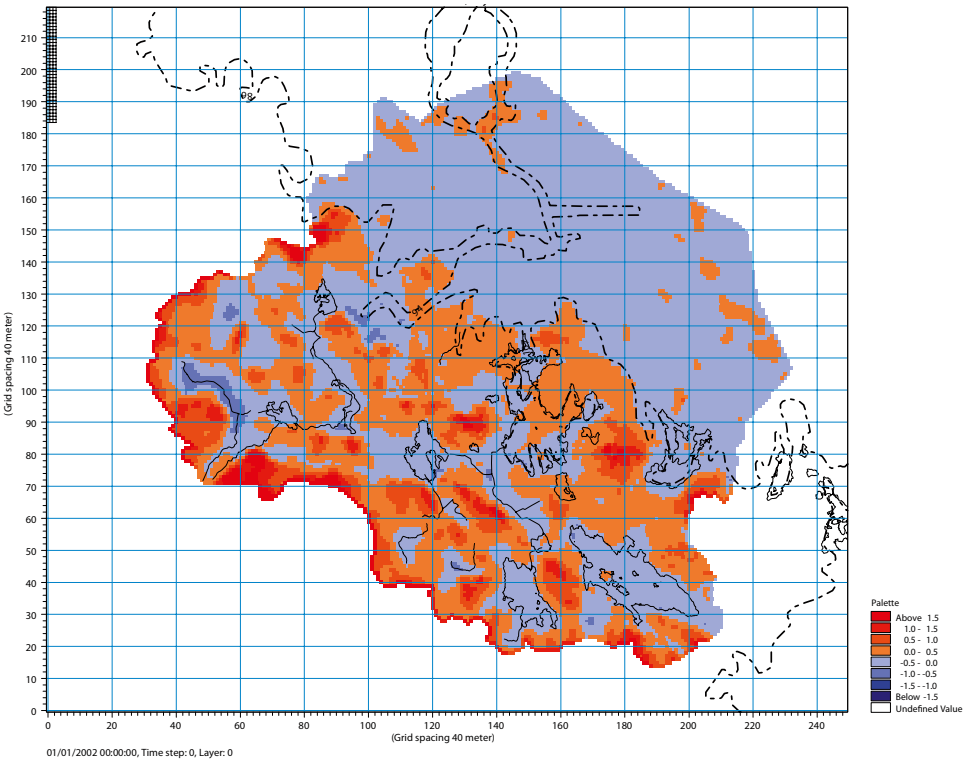

Figure 6-35. *The mean head difference, m, between layers 4 and 5 under dry conditions(July, 2006), i.e. recharge and discharge areas in the upper bedrock. As an orientation, the lakes and streams in the area and the coastline are marked in the figure.*

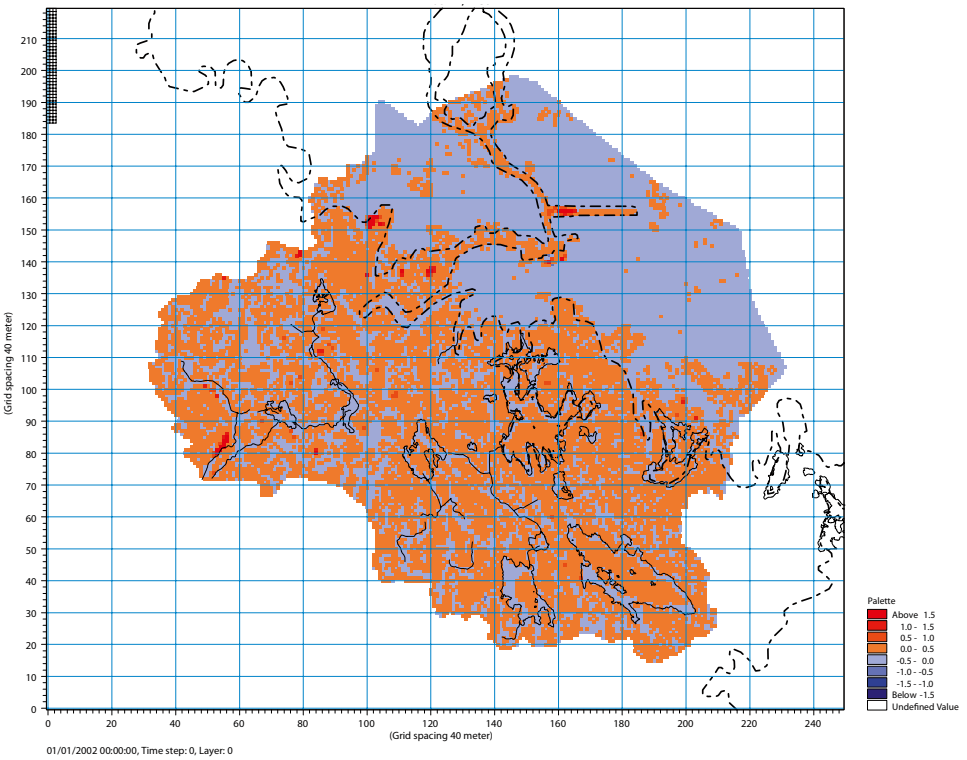

Figure 6-36. *The mean head difference, m, between layers 1 and 2 under wet conditions (March, 2004), i.e. recharge and discharge areas in the Quaternary deposits. As an orientation, the lakes and streams in the area and the coastline are marked in the figure.*

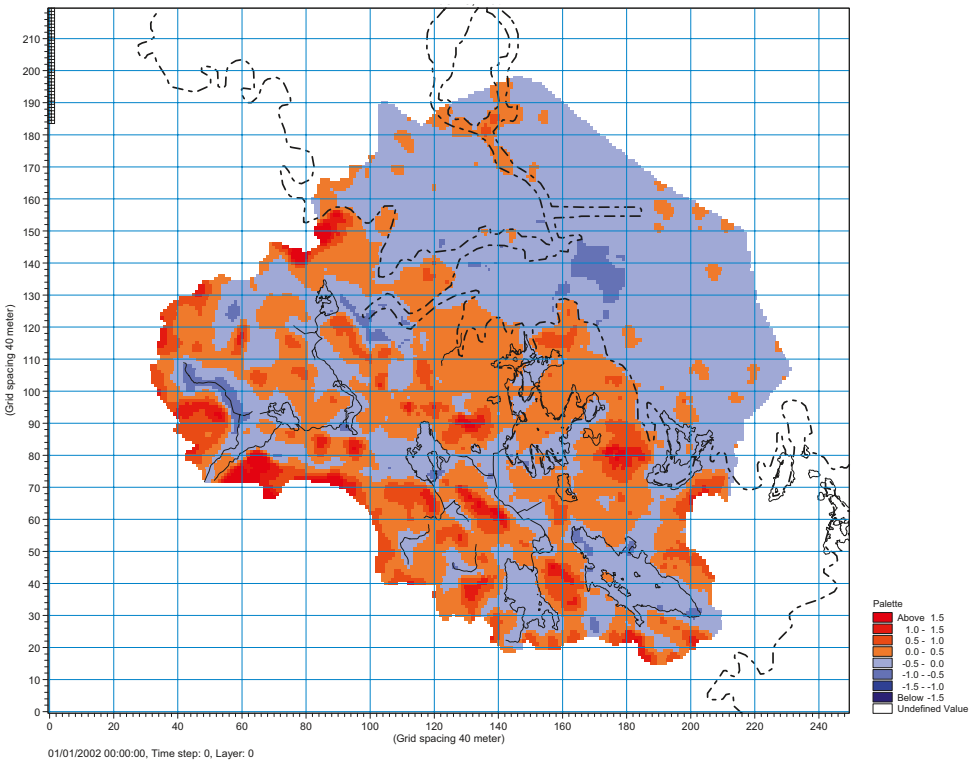

Figure 6-37. *The mean head difference, m, between layers 4 and 5 under wet conditions (March, 2004), i.e. recharge and discharge areas in the upper bedrock. As an orientation, the lakes and streams in the area and the coastline are marked in the figure.*

Table 6-10. The distribution of recharge and discharge areas in the Quaternary deposits under average, wet and dry conditions.

	Recharge, km²		Discharge, km²	
	Whole model area	Land part	Whole model area	Land part
Average	16.91	14.91	19.10	9.90
Wet	16.79	16.16	19.17	8.64
Dry	11.26	10.54	24.71	14.26

Table 6-11. The distribution of recharge and discharge areas in the upper bedrock under mean, wet and dry conditions.

	Recharge, km²		Discharge, km²	
	Whole model area	Land part	Whole model area	Land part
Average	14.48	14.21	21.49	10.6
Wet	15.39	15.01	20.58	9.8
Dry	14.21	13.60	21.76	11.21

6.3.5 Gradients between different model compartments

The gradients between different model compartments in the flow model are crucial for any kind of transport analyses with the flow model. The conditions around the lakes are of specific interest, because these areas may serve as discharge areas, either locally in the QD or on larger scales including the bedrock. The spatial and temporal distributions in the vertical flow direction, in the deeper bedrock and up to the QD, are important, but also the horizontal gradients around the lakes in the QD, and the upper bedrock, are of interest. All of the simulated results in this section are with the SFR pumping included in the model. Figure 6-38 shows the calculated and observed groundwater head elevations around Lake Eckarfjärden and Lake Bolundsfjärden.

In the Eckarfärden area, two of the boreholes are located on each side of the lake in the littoral zone (SFM0014 on the west side and SFM0016 on the east side), and one in the centre of the lake, SFM0015. The modelled horizontal gradient directions coincide with those observed most of the year, with a gradient from the west side of the lake to the centre and further from the centre to the east side.

Near Lake Bolundsfjärden, one borehole is located on the western side of the lake in the littoral zone (SFM0033), one borehole in till below the lake c. 100 m from the shoreline (SFM0062), and one borehole in till below the central part of the lake (SFM0023). During wet periods, the observed gradient direction in the till is from the littoral zone to the centre of the lake, whereas it is in the opposite direction under dry conditions. The calculated gradients have in principle the same directions, but the periods with a gradient from the littoral zone are shorter, and the difference between the two boreholes in the lake is much smaller than observed during the whole simulation period.

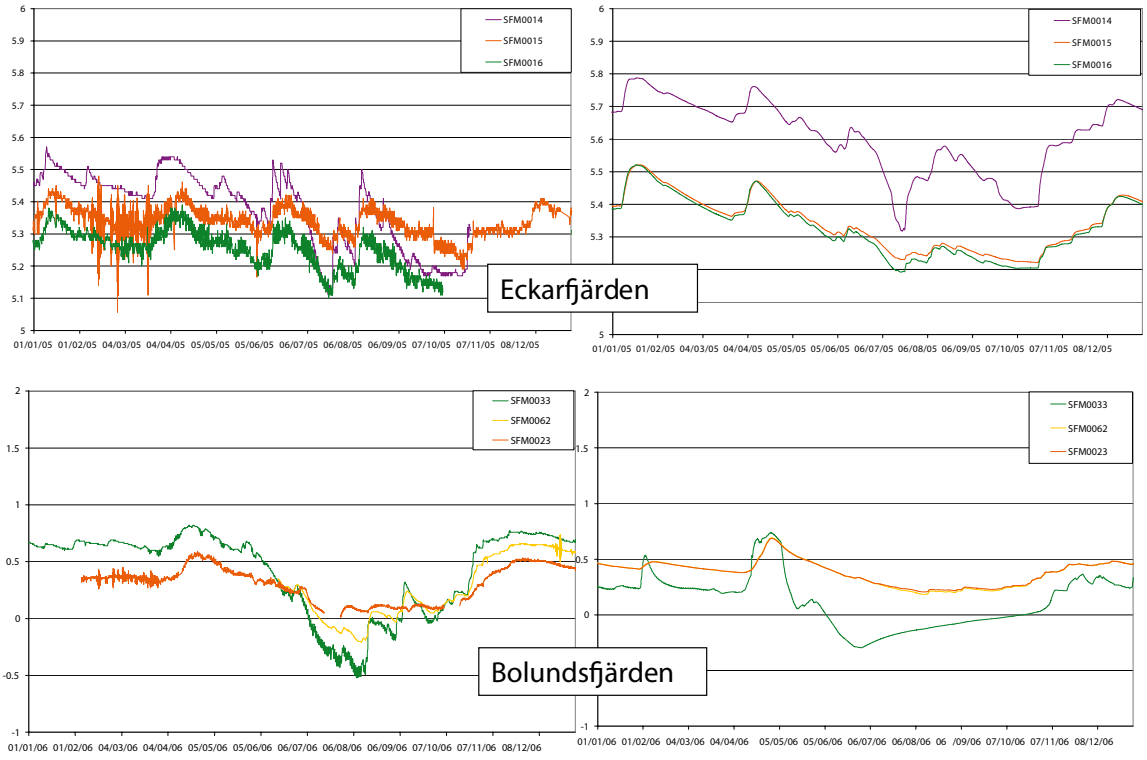

Figure 6-38. *Calculated and measured groundwater levels around Lake Eckarfjärden (top) and Lake Bolundsfjärden (bottom).*

Figure 6-39 shows the modelled and observed vertical gradients under Lake Eckarfjärden and Lake Bolundsfjärden, i.e. the surface water elevations in the lakes and the groundwater head elevations in the QD and the bedrock below the lakes. The observed surface water elevation in Lake Eckarfjärden and the groundwater head elevation under the lake show an upward gradient during all seasons. The same pattern can be seen in the model results, only with a few short exceptions during the fast rise in peaks due to a slightly faster response in the simulated surface water compared to the simulated groundwater. No HFM-wells are located under Lake Eckarfjärden; therefore, the only gradient that can be evaluated is that between the groundwater in QD and the lake water.

For the gradient between the surface water in Lake Bolundsfjärden and the groundwater in the QD below the lake, the opposite conditions are shown in the observed values compared to Lake Eckarfjärden. This implies a downward gradient from the surface water. In the simulated values, no difference can be seen between the surface water elevation and the groundwater head elevation in the QD under Lake Bolundsfjärden

In the observed groundwater head elevations in the bedrock under Lake Bolundsfjärden, the downward gradient continuous all the way down to 150 m.b.s.l., although the gradient over the last 50 m is small. This could be due to the SFR pumping, but although this sink is included in the simulation this downward gradient is not fully developed in the flow model. The modelled gradient in the bedrock under Lake Bolundsfjärden is downwards at some depths, but in the uppermost bedrock the gradient direction is still upwards according to the model. A slightly larger effect of the SFR pumping in the model would most likely turn this to a downward gradient in the whole profile, which would give a better fit to the observed gradient conditions.

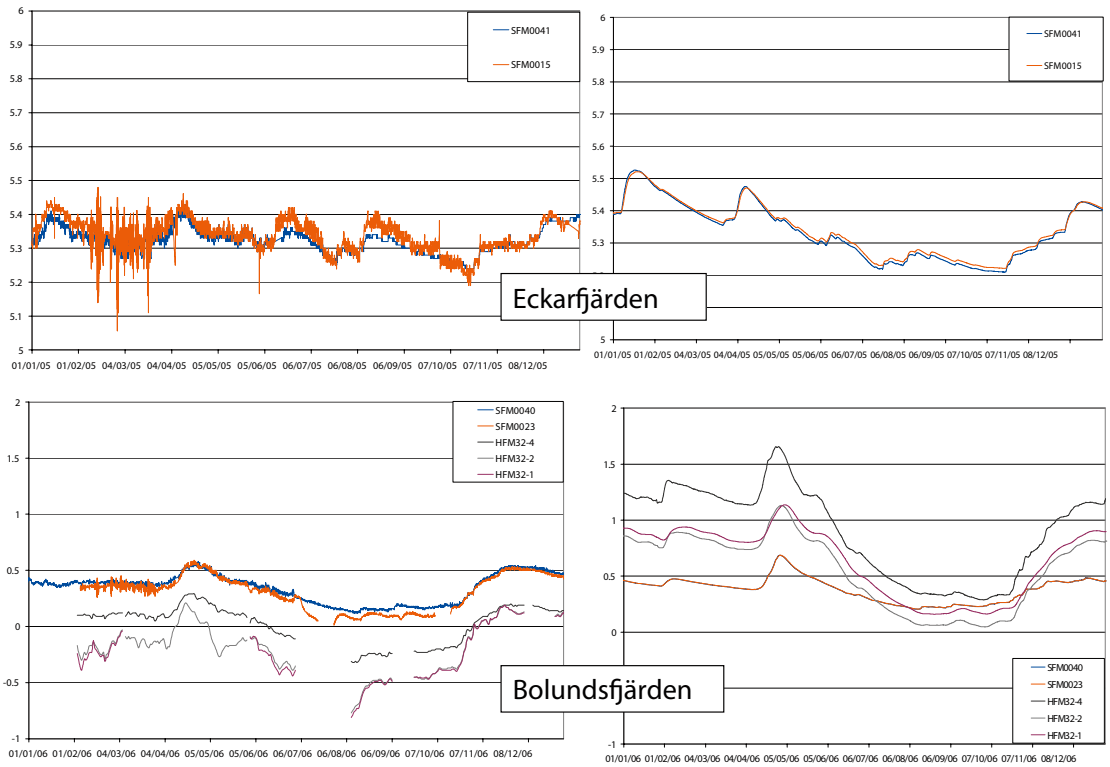

Figure 6-39. *Calculated and observed vertical gradients under Lake Eckarfjärden (top) and Lake Bolundsfjärden (bottom).*

Figure 6-40 shows the modelled and observed vertical gradients in two HFM boreholes in the vicinity of Lake Bolundsfjärden, HFM15 (and SFM0058) c. 100 m west of the lake and HFM04 (and SFM0004) c. 1,000 m to the east of the lake. At both locations (HFM15 and HFM04), a clear downward gradient can be seen from the QD, both in observed data and in modelled head elevations, and the downward gradient continues in the bedrock.

The observed head elevations indicate a smaller gradient between the QD and the bedrock during the dry summer months. This seems to be an effect by deep transpiration through capillary forces in the QD. The present version of the MIKE SHE model code supports these processes in the upper saturated zone layer only, why the response from these phenomena cannot be fully reproduced by the model. Because of this, the drawdown in the QD during extremely dry periods, such as the summer of 2006, may be underestimated in the model.

Figures 6-41 and 6-42 show a summary of the modelled and observed vertical gradients at four HFM-wells: HFM32, HFM16, HFM15 and HFM04, all in the vicinity of Lake Bolundsfjärden. In Figure 6-41 the conditions in April 2006, i.e. during a wet period, are shown. The simulated gradients have the same directions as the observed, except between the upper part of HFM32 and SFM0023, where the head elevations in the bedrock are too high.

In Figure 6-42 the conditions in August 2006, which was a dry period, are shown. The simulated gradients at HFM04 are still in agreement with measured data, whereas the agreement is not as good for the other wells. The head elevations in the bedrock at HFM32 are still too high.

Notable is that the observed head at 140 m.b.s.l. is lower than those measured higher up in the borehole, which is not the case in the model. This indicates a stronger hydraulic connection between the borehole and the SFR pumping than that in the model at this level.

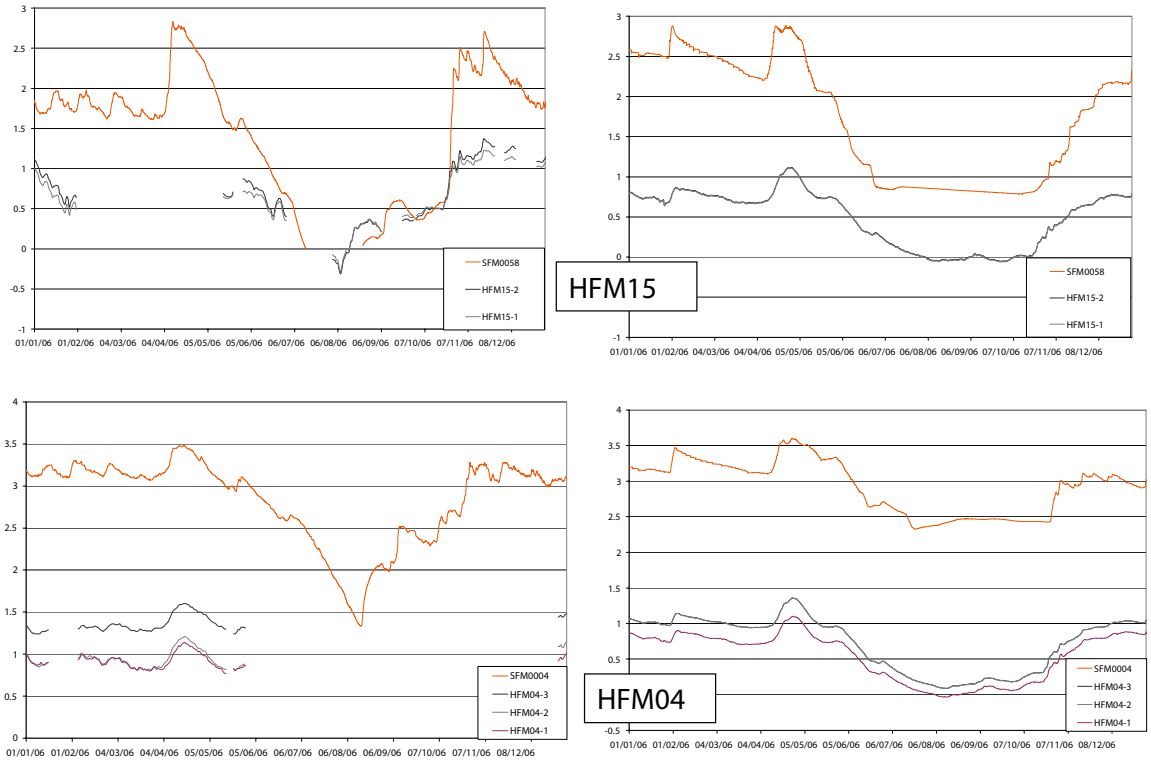

Figure 6-40. *Calculated and observed vertical gradients at two HFM borehole locations in the vicinity of Lake Bolundsfjärden; HFM15 is situated c. 100m west of the lake and HFM04 c. 1000m east of the lake.*

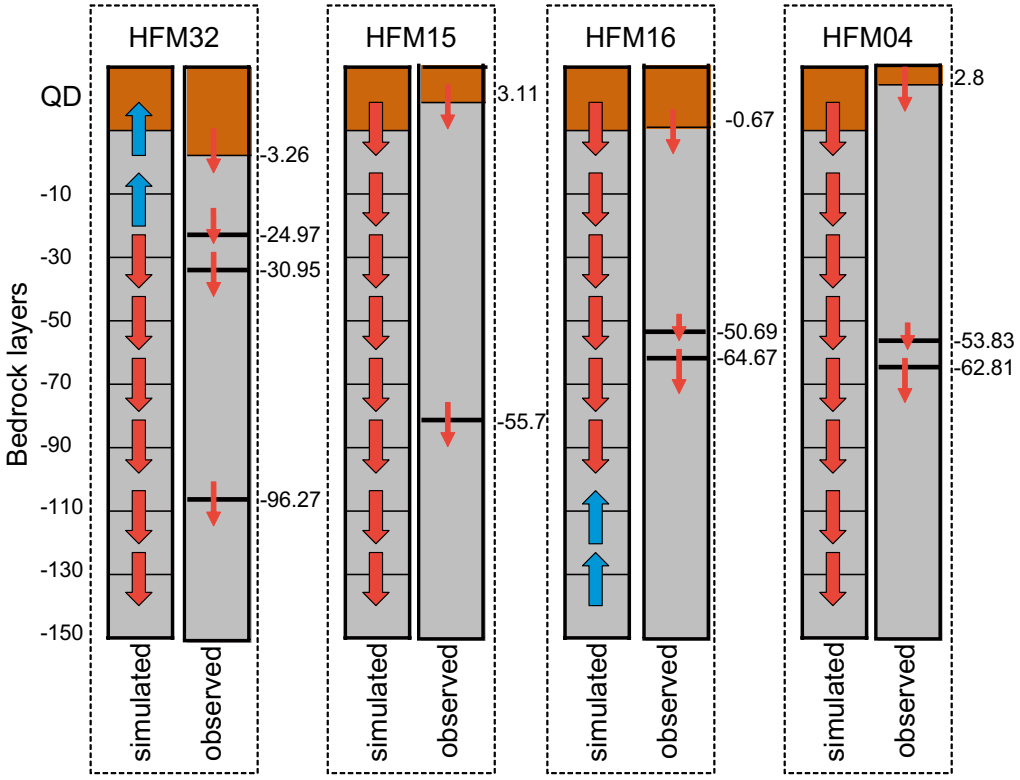

Figure 6-41. *Comparison of simulated (left column for each borehole) and observed (right column) vertical flow directions in HFM boreholes in the Lake Bolundsfjärden area during a wet period (April 2006); the SFR pumping is included in the model.*

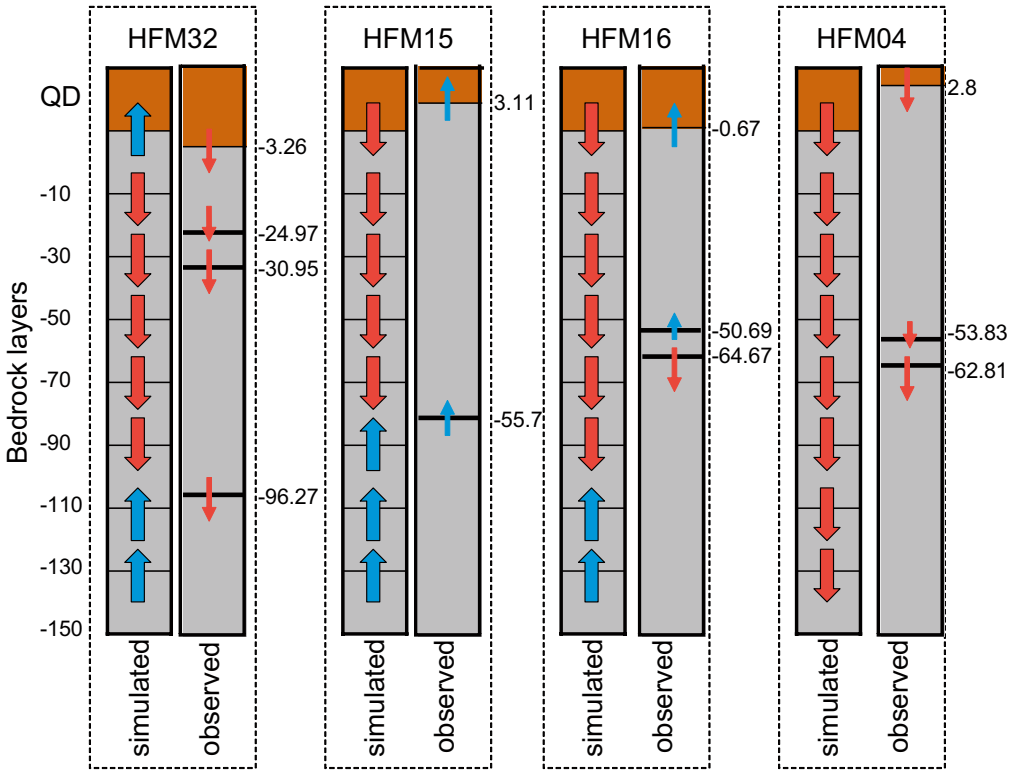

Figure 6-42. *Comparison of simulated (left column for each borehole) and observed (right column) vertical flow directions in HFM boreholes in the Lake Bolundsfjärden area during a dry period (August 2006); the SFR pumping is included in the model.*

At HFM15 and HFM16, the gradients are switched from downward in April to upward in August, according to observed gradients in Figures 6-41 and 6-42. This is most likely due to transpiration processes through deep capillary forces in the QD. In the model, these processes are limited to the upper layer of the saturated zone, which is 2.5 m thick in most parts of the model. Because of this, groundwater depths larger than 2.5 m due to capillary rise and transpiration only, can not be simulated. This is probably the reason why the simulated gradients are still downward in August at these two locations.

Figure 6-43 shows calculated groundwater head elevations in a west-east profile through Lake Eckarfjärden (through SFM0015). In the upper graph, the conditions during April 2006 (a wet period) are shown, and in the lower graph the conditions during August 2006 (a dry period). The red arrows in the figures indicate the prevailing flow directions.

During periods of wet conditions, Lake Eckarfjärden acts as discharge area for the upper parts of the profile, although relatively weak with higher gradients in the horizontal direction. Deeper down in the profile, a downward gradient to the east can be seen. Under dry conditions, the principal flow directions are more or less the same as under wet conditions, but gradients are somewhat weaker. An interesting phenomenon that shows up during the dry period is the effect of transpiration on the gradients in the littoral zones where a clear upward gradient can be observed.

Figure 6-44 shows simulated groundwater head elevations in a west-east profile through Lake Bolundsfjärden (through SFM0023). Under wet conditions, also Lake Bolundsfjärden acts as a discharge area for the upper parts of the profile, according to the model. However, the comments to Figures 6-39, 6-41 and 6-42 above mean that observed data do not support this, because the head elevations in the bedrock should be lower than those obtained from the model. Nevertheless, the simulated gradients in the upper part of Figure 6-44 show that layer 4 (c. 30 m.b.s.l.), being part of the high-conductive fractures/sheet joints in this area, transports the water from the higher areas, around the lake, in under the lake.

During periods of dry conditions, the effects of transpiration on the gradients in the littoral zones is even more obvious at Lake Bolundsfjärden than at Lake Eckarfjärden, at least on the east side of the lake where a significant upward gradient is obtained in the model. The following conclusions can be drawn based on the discussion in this section:

- In the model, the effect of the SFR pumping is clear and possibly the contact between Lake Bolundsfjärden and SFR should be even better than described in the model (see also next section).
- The transpiration processes together with the capillary forces are very important sinks, not only for the QD but also for the upper bedrock. In particular, this is the case for the littoral zone around the lakes. Since the model code allows transpiration processes being active in the uppermost calculation layer only, these effects may not be properly described in the model. Further development of the code to overcome this limitation is desirable. However, the only short term “solution” is to test the sensitivity to increasing the thickness of the upper layer even more, e.g. to 3.5 m instead of 2.5 m.

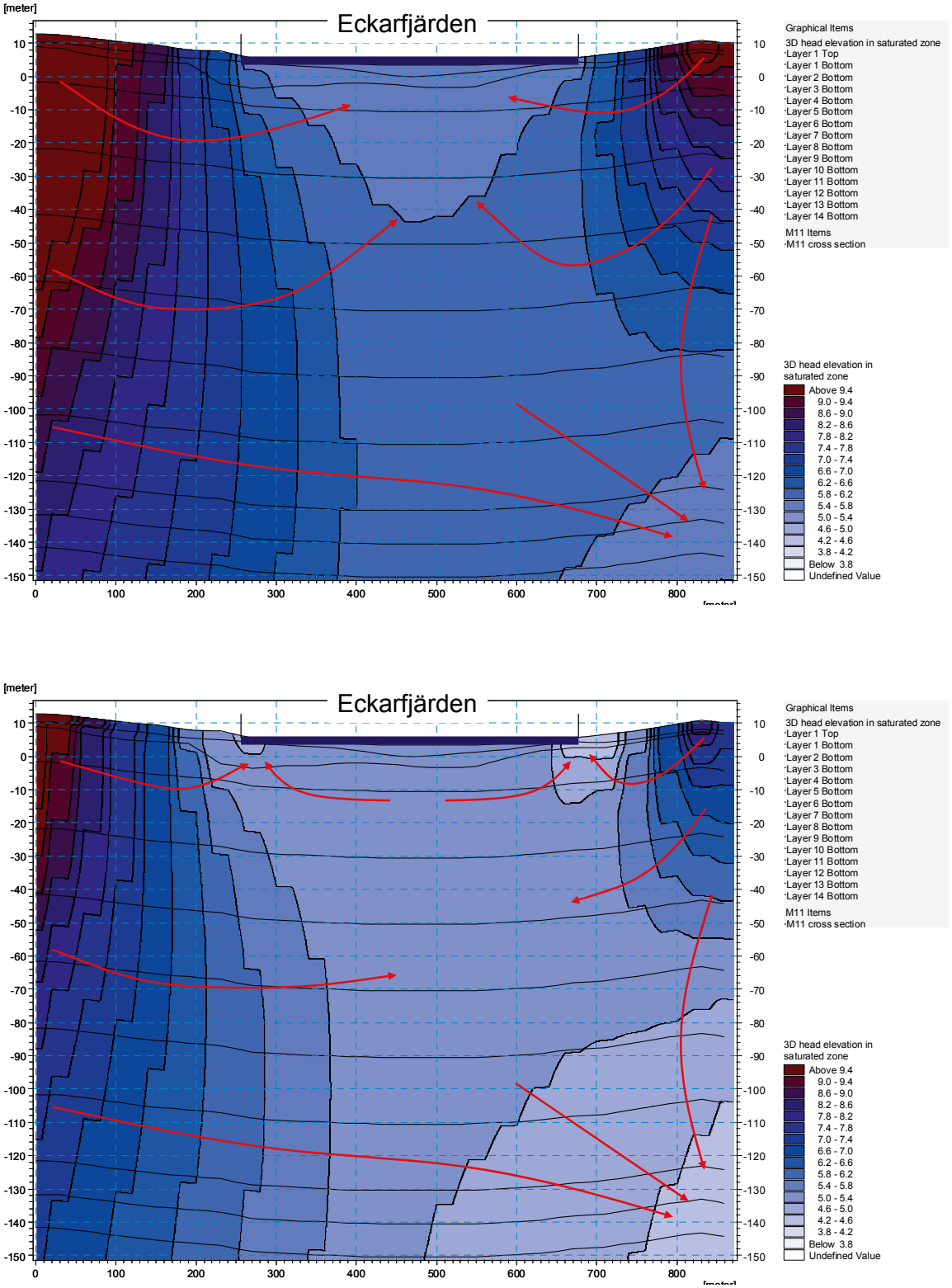

Figure 6-43. *Modelled groundwater heads and flow directions below Lake Eckarfjärden under wet (April 2006; top) and dry (August 2006; bottom) conditions.*

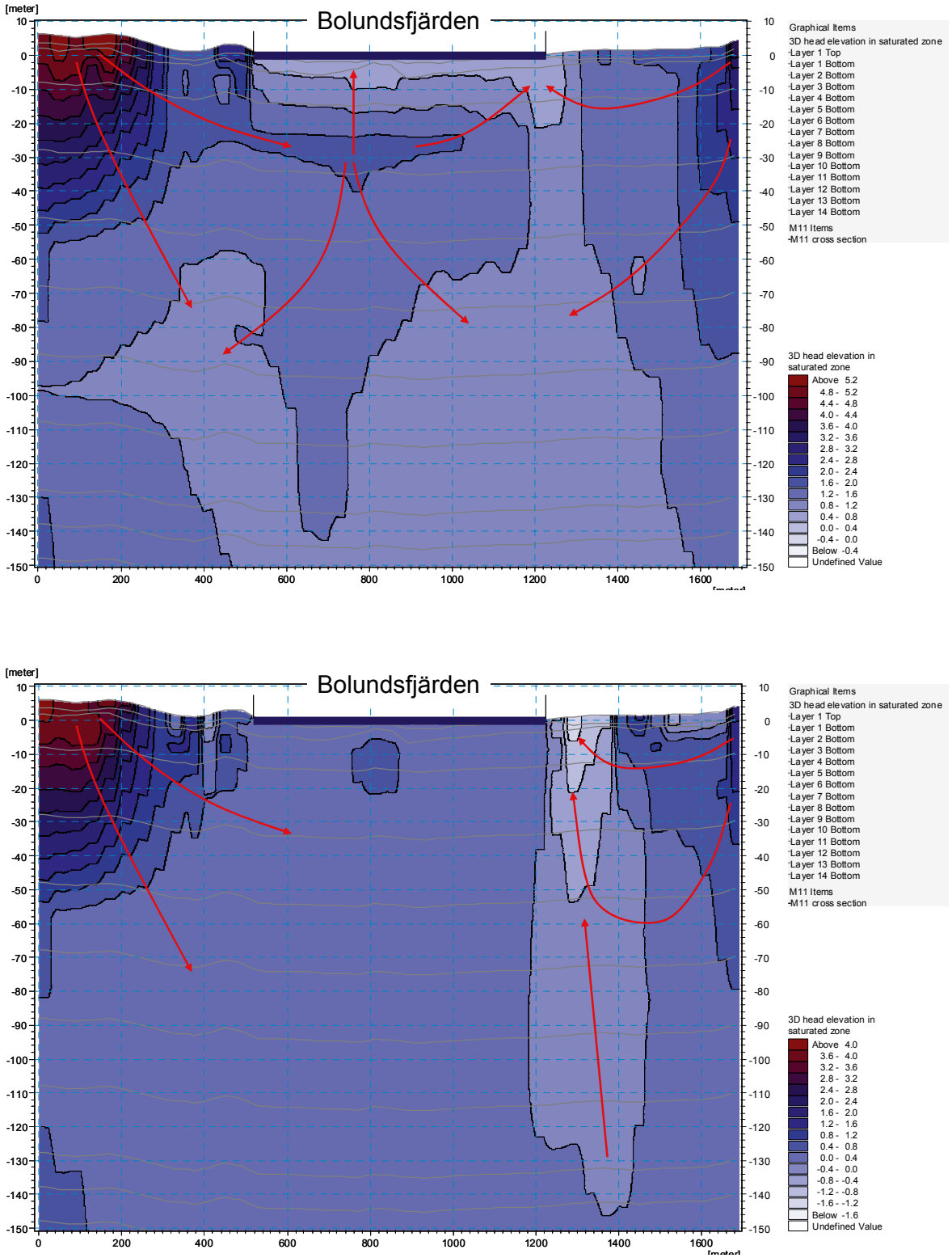

Figure 6-44. *Modelled groundwater heads and flow directions below Lake Bolundsfjärden under wet (April 2006; top) and dry (August 2006; bottom) conditions.*

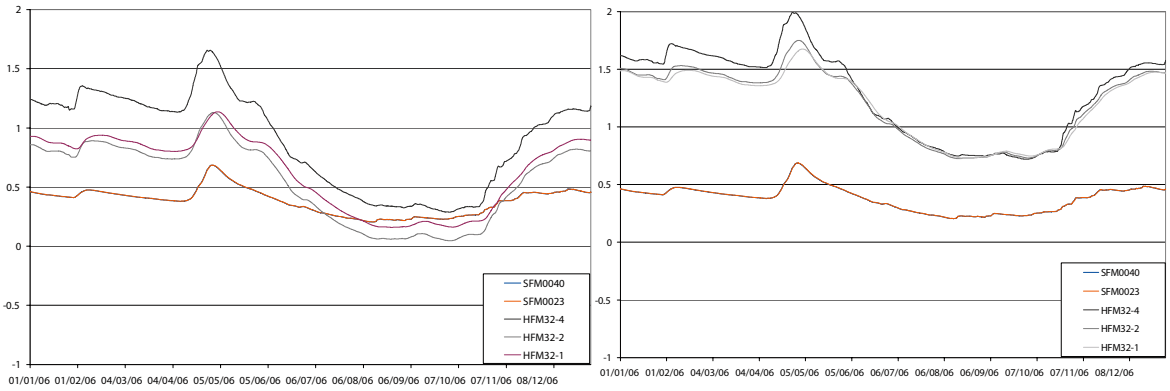

Figure 6-45. *Modelled effect of SFR on groundwater head elevations below Lake Bolundsfjärden.*

6.3.6 Influence of the drainage of the SFR facility

The importance of the drainage at the SFR facility for the groundwater head elevations in the bedrock has already been stated several times in this chapter. This can be exemplified by the effect on the head elevation conditions under Lake Bolundsfjärden, shown in Figure 6-45 below. In this section, the spatial and temporal effects of the SFR pumping are summarised. Figure 6-46 shows the simulated drawdown from SFR in March 2005 in the horizontal plane at approximately 50 m.b.s.l. (upper part of the figure) and at approximately 110 m.b.s.l. (lower part of the figure).

Naturally, the drawdown is larger, and covers a larger area, in the deeper plane at 110 m.b.s.l. compared to higher up, but the difference is not very large. The influence area includes most parts of Lake Bolundsfjärden, but referring to the concluding remarks in the section above, the observations indicate that this influence area should be slightly increased to the south at Lake Bolundsfjärden.

Figures 6-47 and 6-48 summarise the effect of the SFR pumping on the vertical gradient conditions in four HFM-wells (HFM32, HFM16, HFM15 and HFM04), all in the vicinity of Lake Bolundsfjärden. The flow directions during wet periods, like in April 2006 shown in Figure 6-47, are not much influenced by SFR; only minor changes can be seen. It is interesting to notice the change from downward to upward direction in HFM16 when SFR is included. This is because the upper layer, at 110 m.b.s.l., is influenced more than the ones below due to the high conductive sheet joints present in this layer.

The flow directions during dry periods, here exemplified by August 2006 shown in Figure 6-48, are influenced much more than those under wet conditions. The only borehole that is unchanged is HFM04, where the gradients are downwards already without SFR. The overall pattern in the other boreholes is a switch to downward direction down to the layer where the deepest sheet joints are located (at 110 m.b.s.l.), and a switch to an upward direction to the same layer from the deeper bedrock layers below the sheet joints.

Figures 6-49 and 6-50 show simulated groundwater head elevations with and without SFR in a south-north profile from the location of HFM32 in Lake Bolundsfjärden, through Lake Puttan, and to the location of HFM34 on the peninsula where SFR is located. In Figure 6-49 the modelled conditions in April 2006 are shown. The upper graph shows the conditions without the SFR pumping and the lower graph the conditions with the SFR pumping included in the model.

It is seen that the lakes and the sea act as strong discharge areas when SFR is not taken into account. When the SFR pumping is included, a pronounced downward and north going gradient is created, leaving very weak, or no, discharge areas. The same holds for the conditions in August 2006, shown in Figure 6-50, but here even more pronounced, with no upward directed gradients when SFR is included.

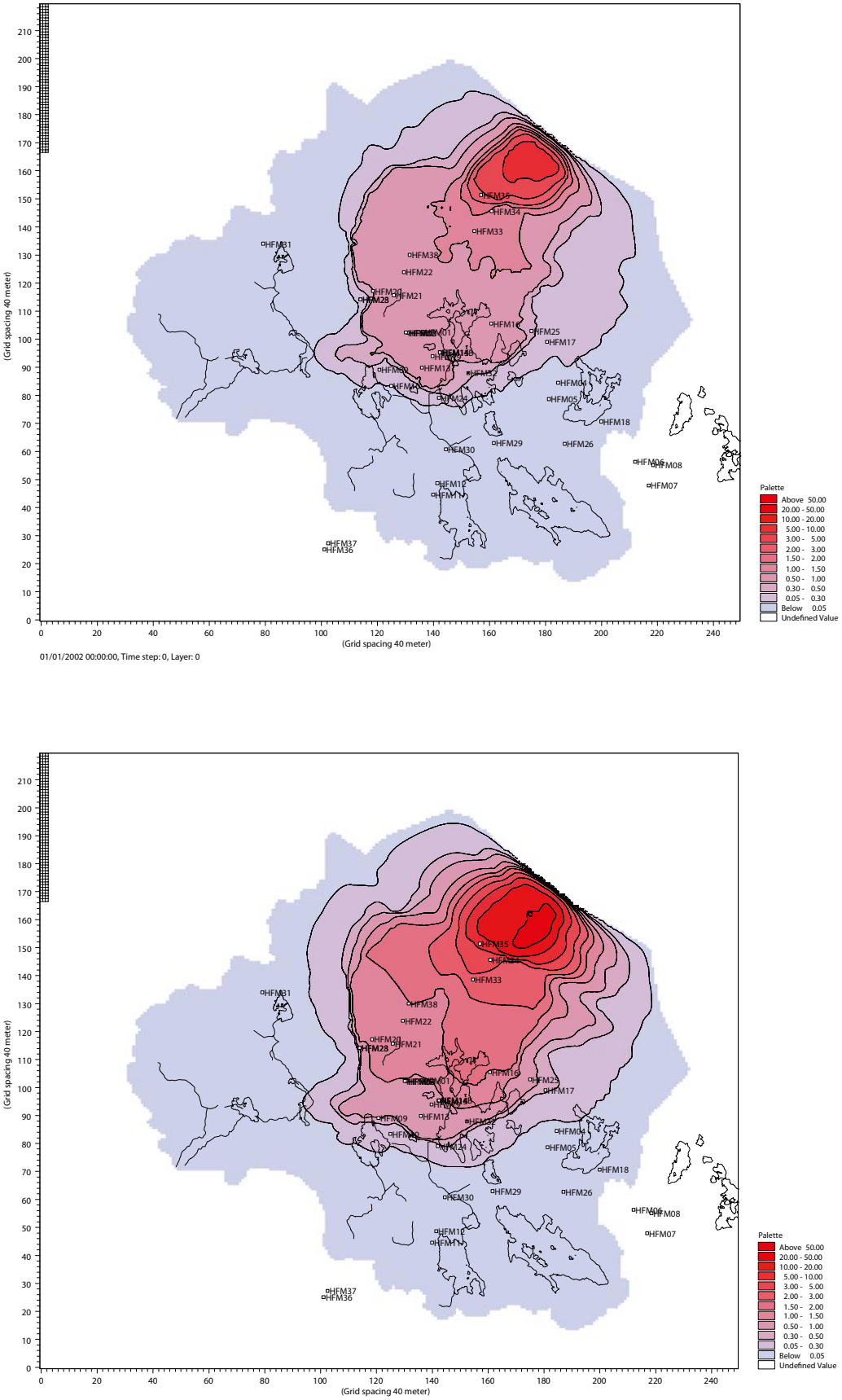

Figure 6-46. *Modelled drawdown caused by SFR, layer 5 (top) and layer 8 (bottom).*

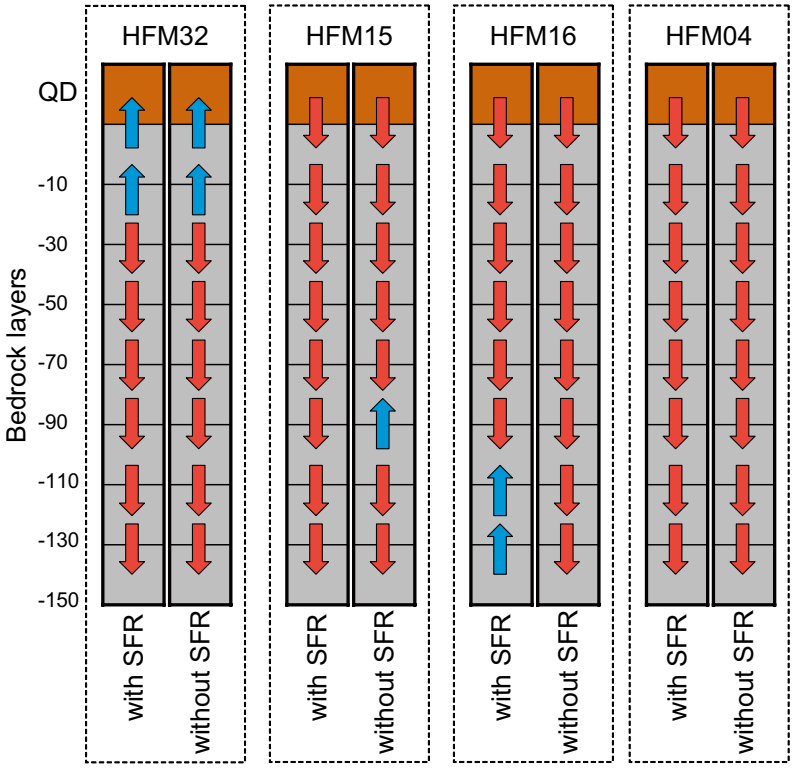

Figure 6-47. *Modelled vertical flow directions in HFM boreholes in the Lake Bolundsfjärden area with (left column for each borehole) and without (right column) SFR during a wet period (April 2006).*

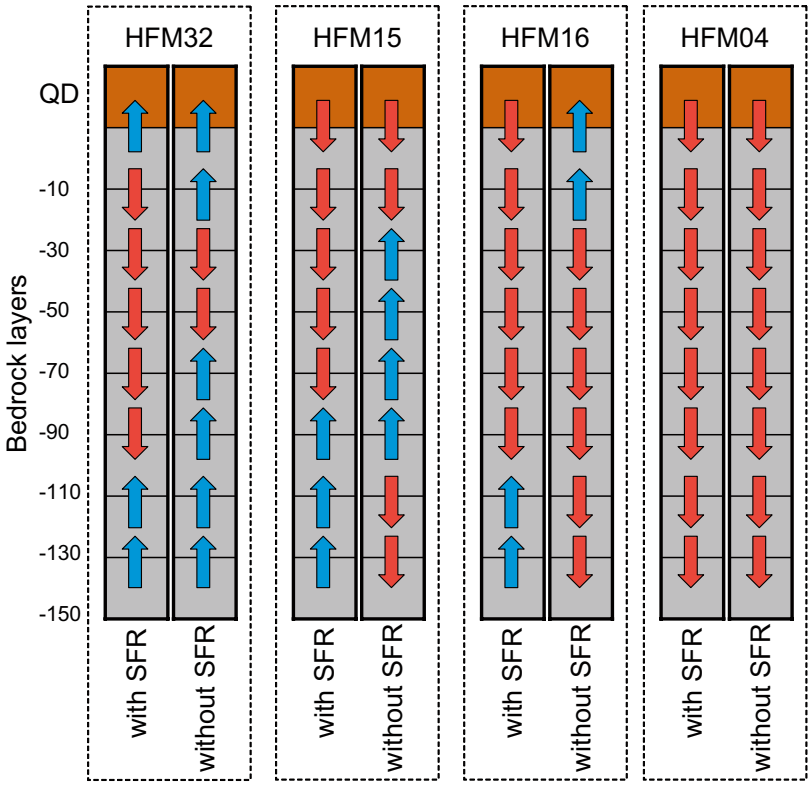

Figure 6-48. *Modelled vertical flow directions in HFM boreholes in the Lake Bolundsfjärden area with (left column for each borehole) and without (right column) SFR during a dry period (August 2006).*

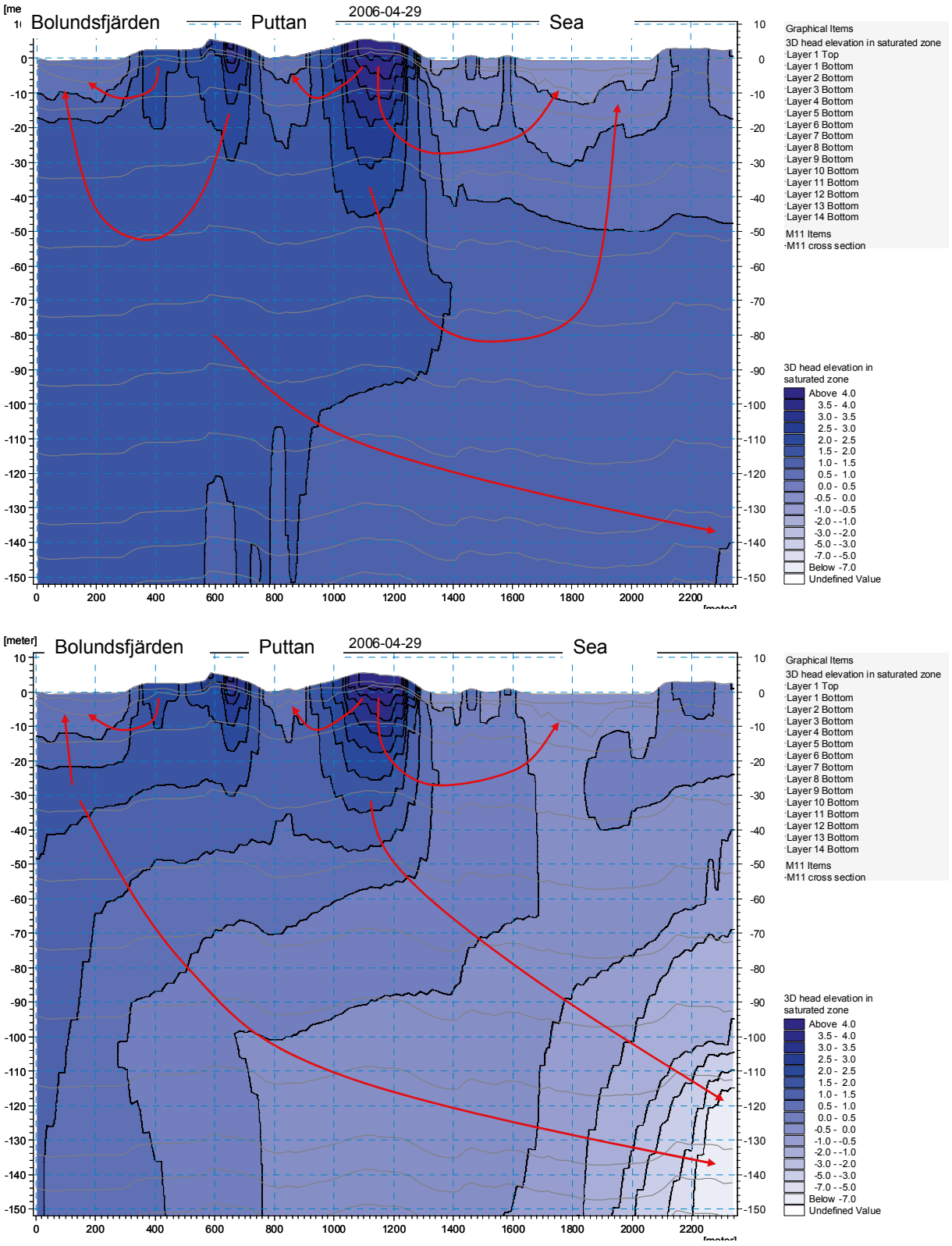

Figure 6-49. *Modelled groundwater heads below Lake Bolundsfjärden in April 2006 without (top) and with (bottom) the SFR drainage pumping in the model.*

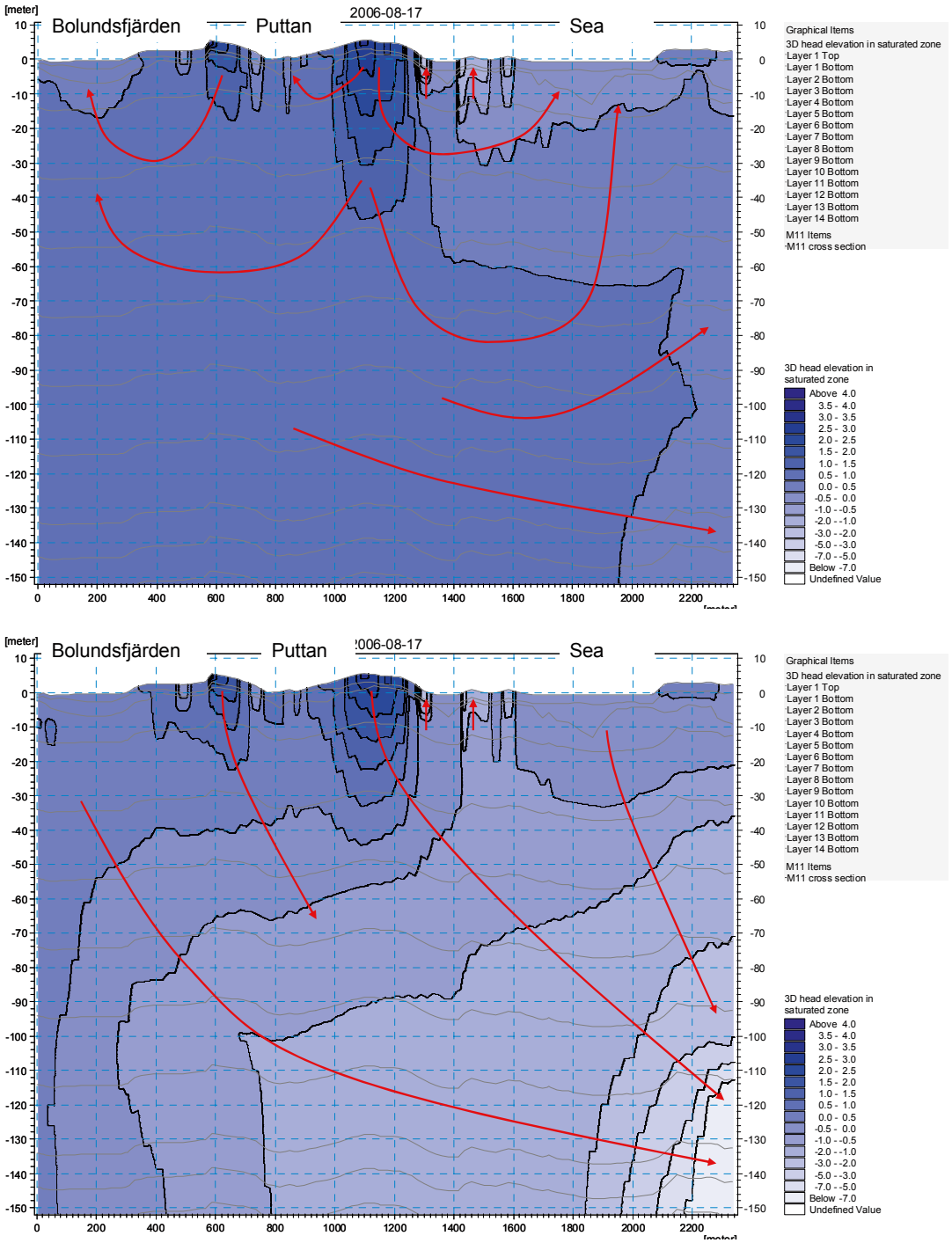

Figure 6-50. *Modelled groundwater heads below Lake Bolundsfjärden in August 2006 without (top) and with (bottom) the SFR drainage pumping in the model.*

6.4 Transport modelling

6.4.1 Particle tracking results

Similar to the modelling presented in Chapter 5, the transport modelling discussed in this section has been performed with the purpose of supporting the hydrogeological description. This means that it is used to investigate and illustrate important hydrogeological characteristics such as recharge and discharge areas and flow paths from bedrock to surface and vice versa. The transport modelling performed with MIKE SHE and associated transport modules includes particle tracking simulations and modelling with a tool based on the advection-dispersion equation. A more detailed description of the transport modelling is given in /Gustafsson et al. 2008/.

Particle tracking simulations have been run for sensitivity case 5 (cf. above) with and without pumping at the SFR facility. The following cases were considered:

- *PT5-allover:* One particle was introduced in each cell at 140 m.b.s.l.; the particle injection scenario was the same as in the *PT0-bedrock* case discussed in Chapter 5.
- *PT5-repository:* One particle was introduced in each cell within the area corresponding to the planned repository. Also is this case, the particles were introduced at 140 m.b.s.l. (even though the repository is planned to be built at c. 500 m.b.s.l.).

The simulation period was 300 years in all four simulations, using the calculated transient flow modelling results obtained for the simulated one-year period from October 2003 to October 2004 as input. This means that the model results from the transient MIKE SHE Water movement calculation for this one-year period were cycled 300 times. A similar 5,000-year simulation was also performed with the *PT5-repository* model.

The present results show that many particles are still left in the model after 300 years compared to the Chapter 5 results. This is an effect of the changes in the hydraulic parameters of the rock relative to the previous model, primarily the reduction of the hydraulic conductivity of the upper 200 m of the bedrock. Also, the horizontal hydraulic conductivities have been increased by a factor of ten in the area corresponding to the fractures/sheet joints in the upper rock. This has an effect on the horizontal transport of particles in these specific layers, i.e. horizontal transport distances tend to increase. The results for *PT5-allover* with and without pumping in the SFR facility are summarised in Table 6-12. Again, they are expressed in terms of where the particles left the saturated zone, i.e. to which other model compartments or boundaries they went.

The dominating sink without the SFR pumping is the combined Overland flow-Unsaturated zone compartment. It is not possible to separate these two sinks. A large fraction, 65%, of the particles are still left in the model volume at the end of the simulation, which implies that it takes less than 300 years for 35% of the flow paths to reach the ground surface from 140 m depth. When pumping at SFR, the sink “particles removed by wells” is the dominating sink. Specifically, 15% of the particles left the model volume through the drainage in SFR. Only 5% of the particles moves to the sea when pumping in SFR, compared to 14% when the SFR pump is not activated. When pumping in the SFR facility 66% of the particles are left in the model volume after 300 years. However, it should also be noted that the travel times are longer than the time SFR will be in operation, implying that this is not a realistic case to assess.

Illustrations of the numbers in Table 6-12 are shown in Figures 6-51 and 6-52. The figures show the position of each particle where it left the saturated zone and moved to a specific sink; results are shown both for the case with and for that without SFR. The different sinks are marked with different colours. The blue dots represent the particles that moved to the combined Overland flow-Unsaturated zone sink. Since the majority of the blue dots are situated in the lakes and close to water courses, i.e. in water-saturated areas, it is concluded the majority of the particles registered in this sink have moved to the Overland flow compartment. When pumping at SFR, the majority of the particles that have gone to sinks outside the land part of the model area have been removed by the pump in SFR.

Table 6-12. Distribution of particles on different sinks for particle tracking in the case 5 model with and without pumping in the SFR facility.

Sink	PT5-allover, no SFR Number of particles	%	PT5-allover, SFR Number of particles	%
Particles removed to OL-UZ*	3,460	15	2,480	11
Particles removed directly to streams	817	4	468	2
Particles removed by drain to streams	415	2	352	1
Particles gone to the sea	3,349	14	1,149	5
Particles removed by wells	0	0	3,404	15
Particles left in model	14,826	65	15,014	66
Sum	22,867	100	22,867	100

*OL-UZ is the combined Overland flow-Unsaturated zone sink

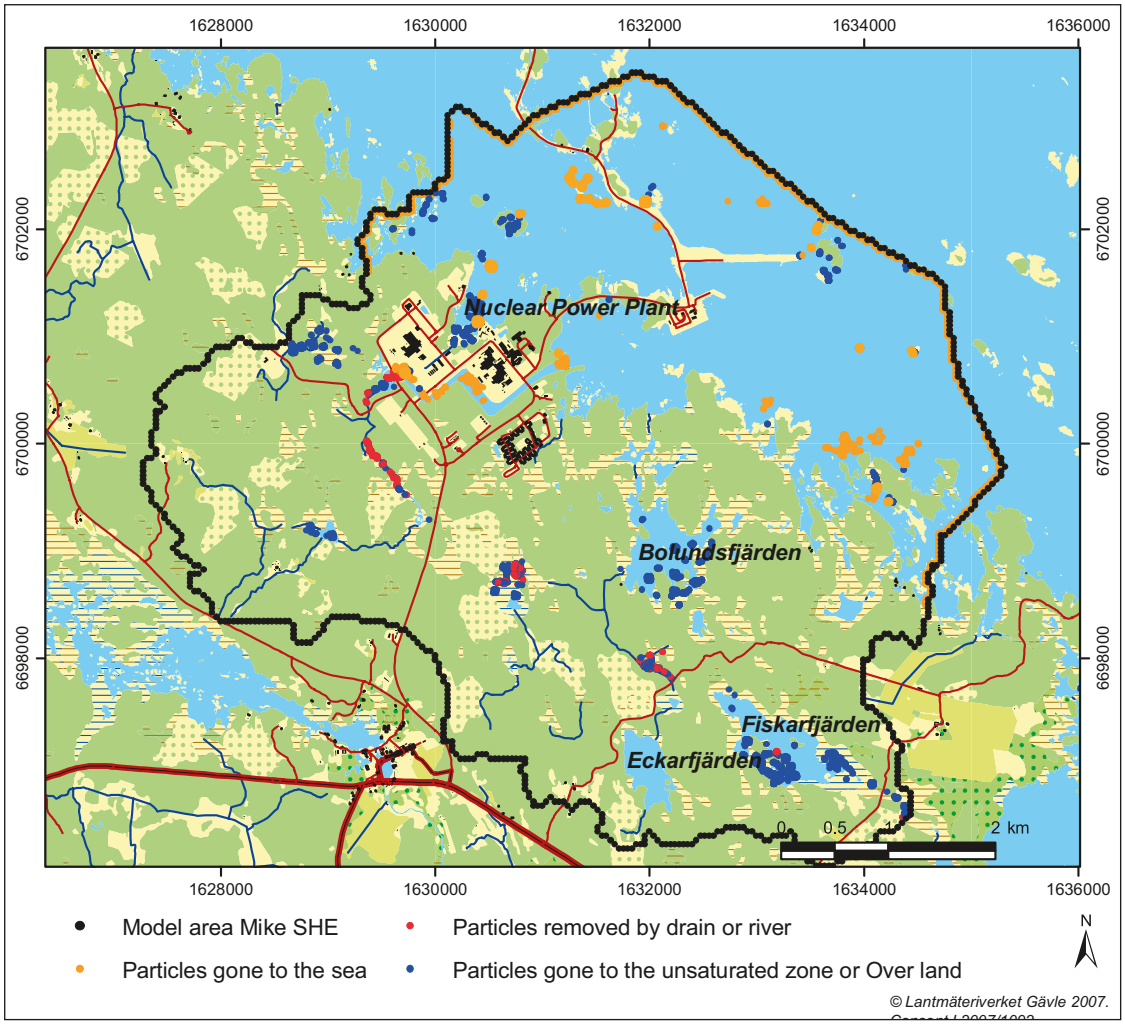

Figure 6-51. *Sinks for the particles in case PT5-allover. The figure presents the results obtained without the SFR drainage in the model.*

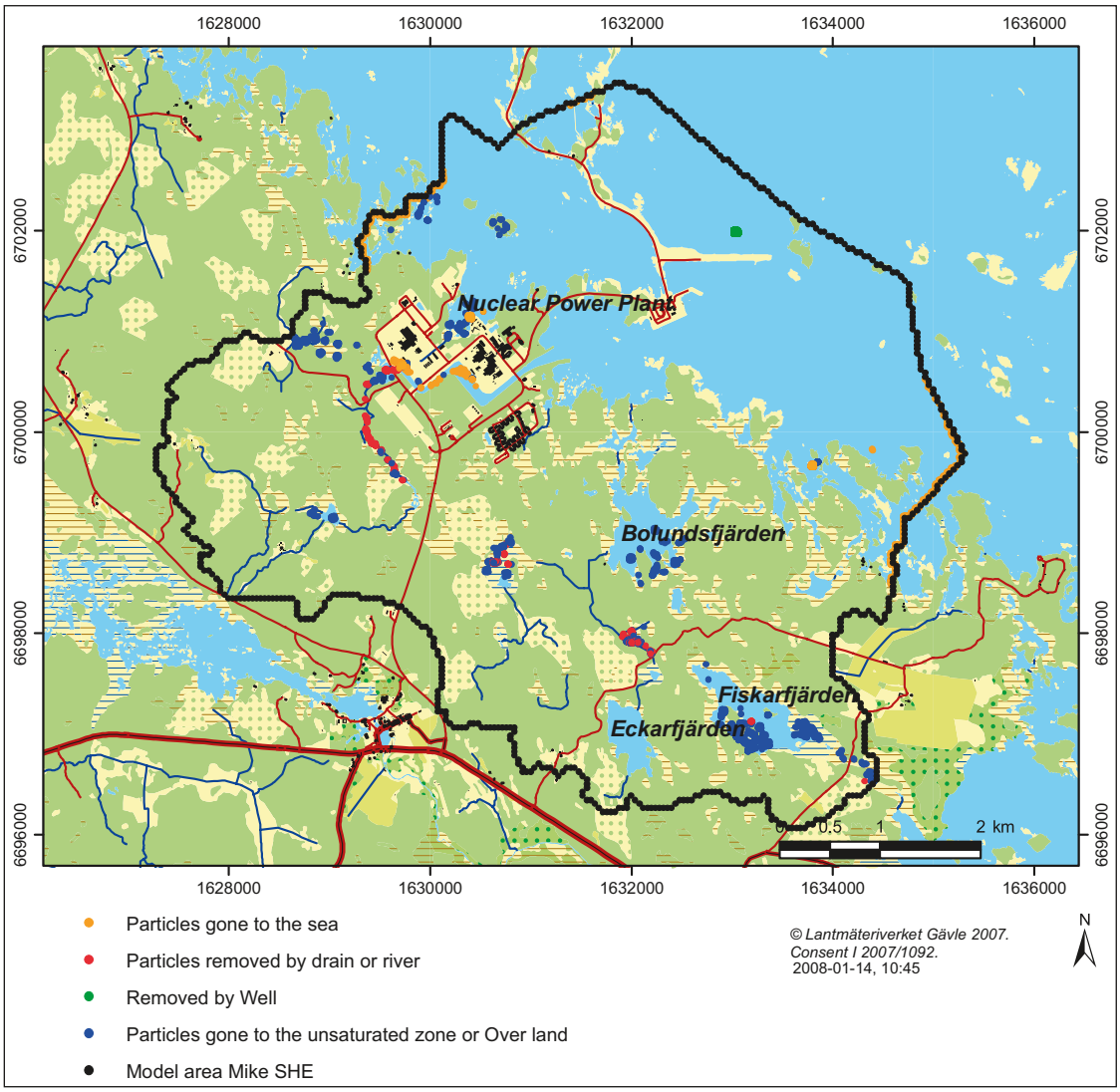

Figure 6-52. *Sinks for the particles in case PT5-allover. The figure presents the results obtained with the SFR drainage activated in the model.*

Figure 6-53 shows the accumulated particle counts for each cell at 150, 130, 110 and 90 m.b.s.l. at the end of the simulation. To the left the case without the SFR drainage is presented and the case with the SFR drainage is presented to the right. The accumulated particle count is a way to present the density of the flow paths. Each time a particle passes a cell the accumulated particle count of that cell is increased by one. This means that the higher value for a cell the more particles have travelled along flow paths going through that specific cell. The particle count reflects both horizontal and vertical transport, and since flow is transient a particle can pass the same cell several times.

The particles were introduced at 140 m.b.s.l.; since one particle has been introduced in each cell at this level, the minimum accumulated particle count in this layer is 1. Pink colour indicates cells where no particles have passed. As shown in Figure 6-53, the flow paths concentrate to specific areas on their way towards the surface. At 110 m.b.s.l. one layer of horizontal fractures sheet joints are represented in the model. It is seen that the particles concentrates there, as indicated by the red areas in the figure. The same pattern is seen for both cases, with and without the SFR facility included. When pumping at SFR, particles released in the north-eastern part of the model area move towards SFR. The majority of the particles moves towards SFR in the layer at 110 m.b.s.l. Above this level only 40% of the cells that received a particle at 110 m.b.s.l. are hit by a particle.

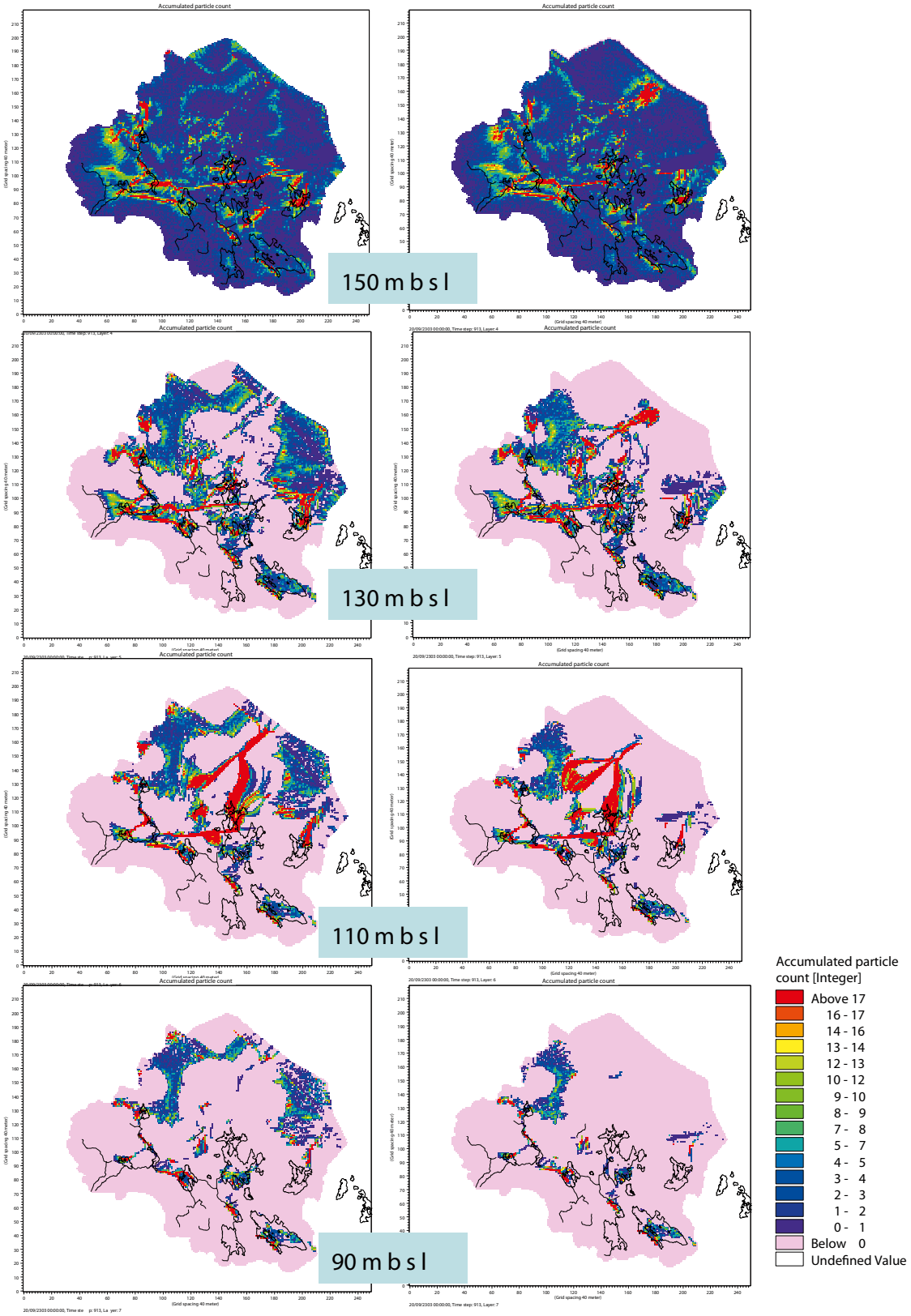

Figure 6-53. *Accumulated particle counts at 150 m.b.s.l., 130 m.b.s.l., 110 m.b.s.l. and 90 m.b.s.l. The particles move towards the fractures/sheet joints in the layer at 110 m.b.s.l. The figure to the left presents the PT5-allover results without the SFR drainage, and the figure to the right the results from the PT5-allover case with the SFR drainage was activated.*

In case *PT5-repository*, 1,501 particles were released at 140 m.b.s.l. inside the area corresponding to the planned repository. After the 300-years simulation period only 10% of the particles have left the model volume; all the particles that have left the model volume have gone to the sea. When pumping at SFR, 18% have left the model volume through the pumping in SFR.

The remaining 82% of the particles are still left in the model volume. For both cases, with and without SFR, the major part of the particles moves toward the sea at 110 m.b.s.l., see Figures 6-54 and 6-55. The particles concentrate to the sheet joint areas and the horizontal transport is dominating. Above this level only a few cells are passed by a particle. When pumping in SFR, no particles reach higher than 70 m.b.s.l. Thus, there are no exit points at the surface after 300 years simulation time when pumping at SFR. In the case where the pumping in SFR is not activated, a few particles reach the sea. These exit points are located close to the shoreline.

Since so many particles were still left in the model volume after 300 years, an additional longer simulation was run using the *PT5-repository*. This particle tracking simulation was run for a period of 5,000 years. The exit points at the surface after 5,000 years are shown in Figure 6-56. As a comparison the exit points after 300 years are also shown in the same figure. The transport times are very long and even after 5,000 years the majority, 81%, of the particles are still left in the model volume. Still no exit points are found in the land part of the model area. All the particles exit the model volume to the sea. The results show that 79 particles, 5% of the total number of particles introduced, are stuck in the marine sediments. Apart from them, no particles are found in the upper calculation layers. All the other particles that are left in the model after 5,000 years are found in the deeper bedrock between layer 8 at 110 m.b.s.l. and layer 14 at 600 m.b.s.l.

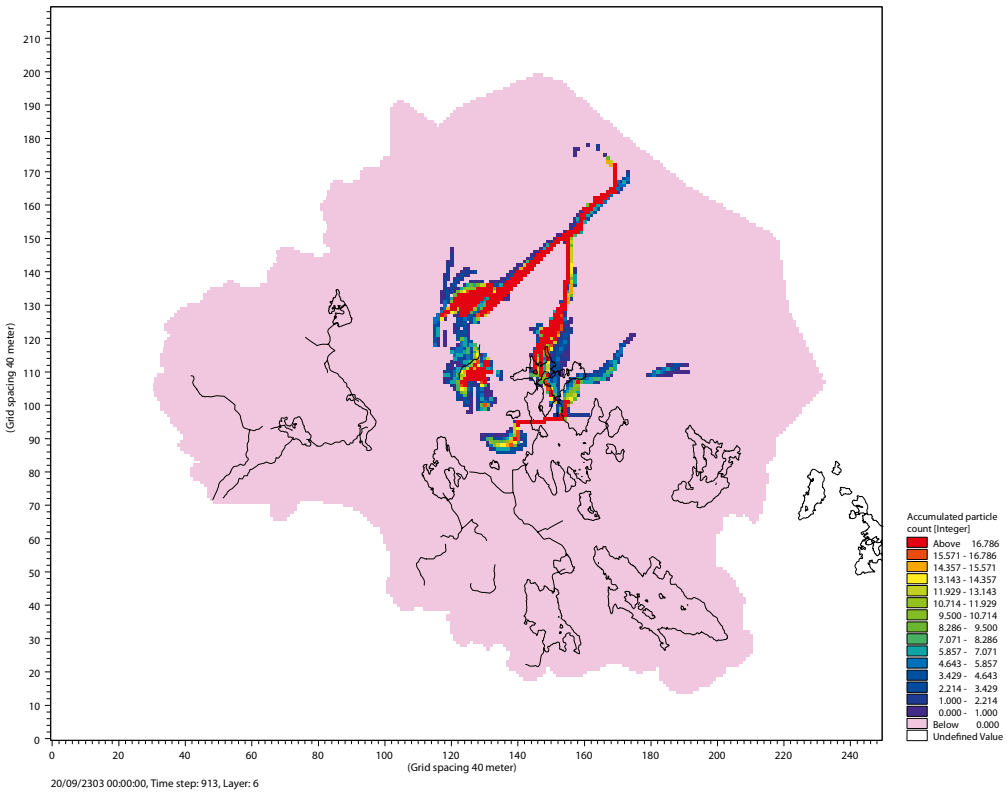

Figure 6-54. *Accumulated particle count at 110 m.b.s.l. for the PT5-repository model without the SFR pumping included in the model.*

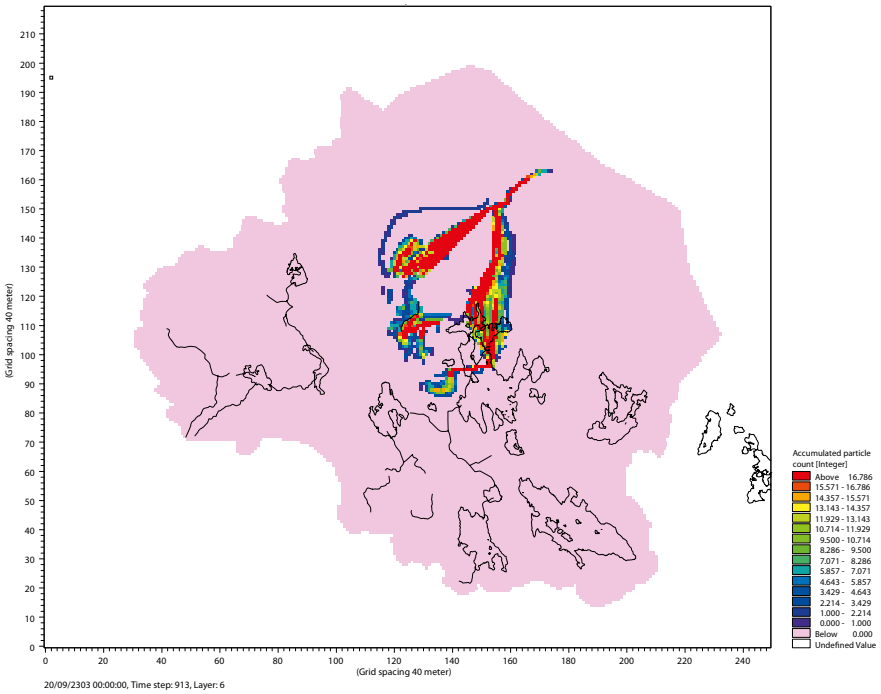

Figure 6-55. *Accumulated particle count at 110 m.b.s.l. for the PT5-repository model with the SFR pumping included in the model.*

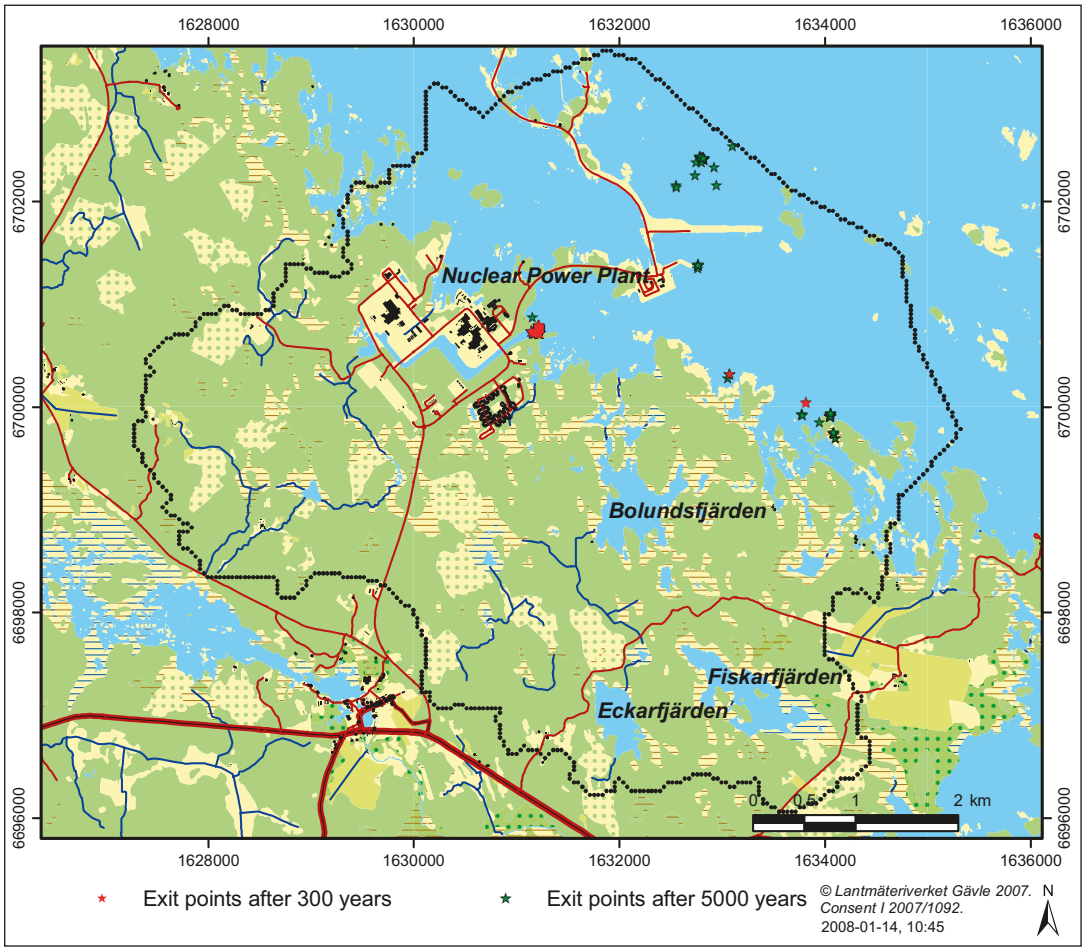

Figure 6-56. *Exit points at the surface or sea bottom after 5000 years. As a comparison, the exit points after 300 years are also marked in the figure.*

6.4.2 Advection-dispersion modelling results

Two different solute transport analyses were performed with the MIKE SHE advection-dispersion (AD) module. In both of the simulations, only solute transport in the saturated zone was considered. The advective transport was modelled by use of the flow field from the "case 5" simulation where SFR was not included. The results from the MIKE SHE Water movement calculations are used by cycling the calculated flow for one year, from May 2004 to May 2005; see /Gustafsson et al. 2008/ for a detailed description of the advection-dispersion module in MIKE SHE. In the first simulation, the solute source is located in a bedrock layer at a depth of approximately 140 m.b.s.l.

The source is applied all over the model area with a concentration of 1 g/m^3. The initial concentration in the model is 0 g/m^3. The source is applied for one month, starting at the time of the simulation. The solute dispersion is anisotropic with a longitudinal dispersivity of 0.2 m and a transversal dispersivity of 0.01 m. The dispersion coefficients correspond to a very low solute dispersion.

Figures 6-57 to 6-59 show simulation results for three different layers at six different times each. Two of the layers are bedrock layers and one is a layer in the Quaternary deposits. The figures show concentrations after 2 months, 2, 10, 20, 100 and 200 years of simulation time. The scale of the solute concentration is the same in all figures. Figure 6-57 shows concentration plots from a bedrock layer at a depth of approximately 130 m.b.s.l.. The layer is situated just above the layer with the hypothetical solute source. The figure illustrates that the solute concentration is high in the beginning of the simulation but then decreases as the pollution is transported away from the layer. It is also seen that the concentration initially is high in connection to the more conductive zones in the bedrock. As time progresses, the concentration in the conductive zones decreases and instead the concentration is higher in connection to the sea.

Figure 6-58 shows concentration plots from a bedrock layer at an elevation of approximately 70 m.b.s.l., containing areas with high horizontal hydraulic conductivities north west of the Lake Bolundsfjärden and towards the sea. The figure illustrates that initially the concentration is high in the fracture zones under the lakes and watercourses. After 20 years the concentrations in the most conductive zones have decreased, whereas concentrations have increased in areas covered by the sea. After 200 years, the concentration pattern is concentrated to the sea areas.

Figure 6-59 show concentration plots from calculation layer 2, which is the lower layer in the Quaternary deposits containing sea bottom sediments. The figure shows that after two months almost no solute has yet reached the Quaternary deposits. It can be seen that the solute has reached the upper part of the model after two years. The figure shows that the solute is mainly transported upwards through the fracture zones that are connected to the lakes and water courses. This is further established in the plots showing concentrations after 10 and 20 years, where it is also seen that the lake areas are solute recipients. After 100 years the concentrations are decreasing.

A comparison between results from simulations with the PT module and the AD module shows that the overall pattern is the same for both modules. In Figure 6-53 the accumulated particle count is illustrated at a depth of 130 m.b.s.l.. The left figure is based on the flow results without the SFR drainage included. Figure 6-57 show results from the AD simulation based on the same flow results and at approximately the same depth. The figures illustrate that the patterns are very similar.

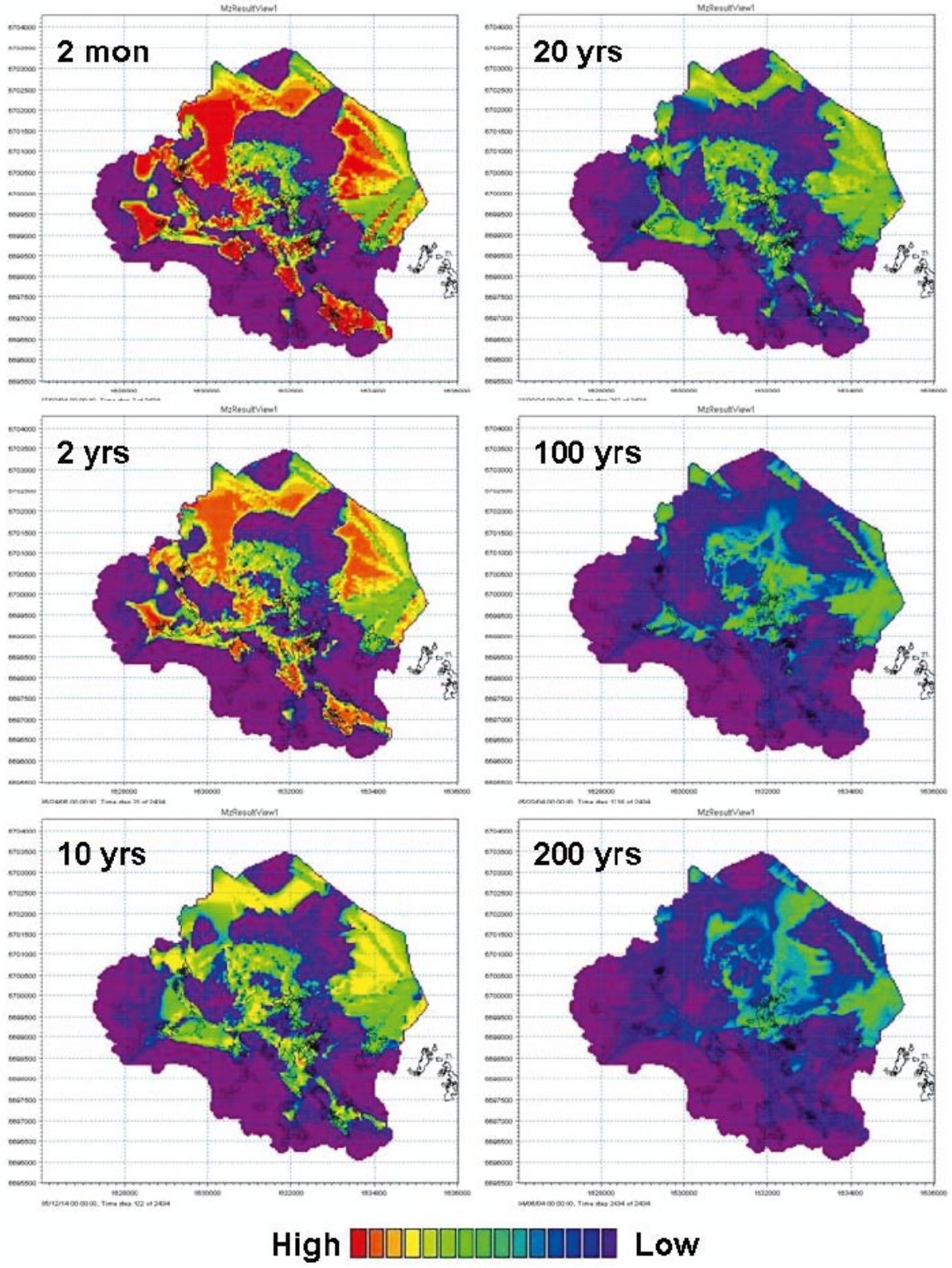

Figure 6-57. *Results of advection-dispersion simulation with a uniform pulse solute source in the bedrock showing concentrations in the bedrock at approximately 130 m.b.s.l. at different times after solute injection.*

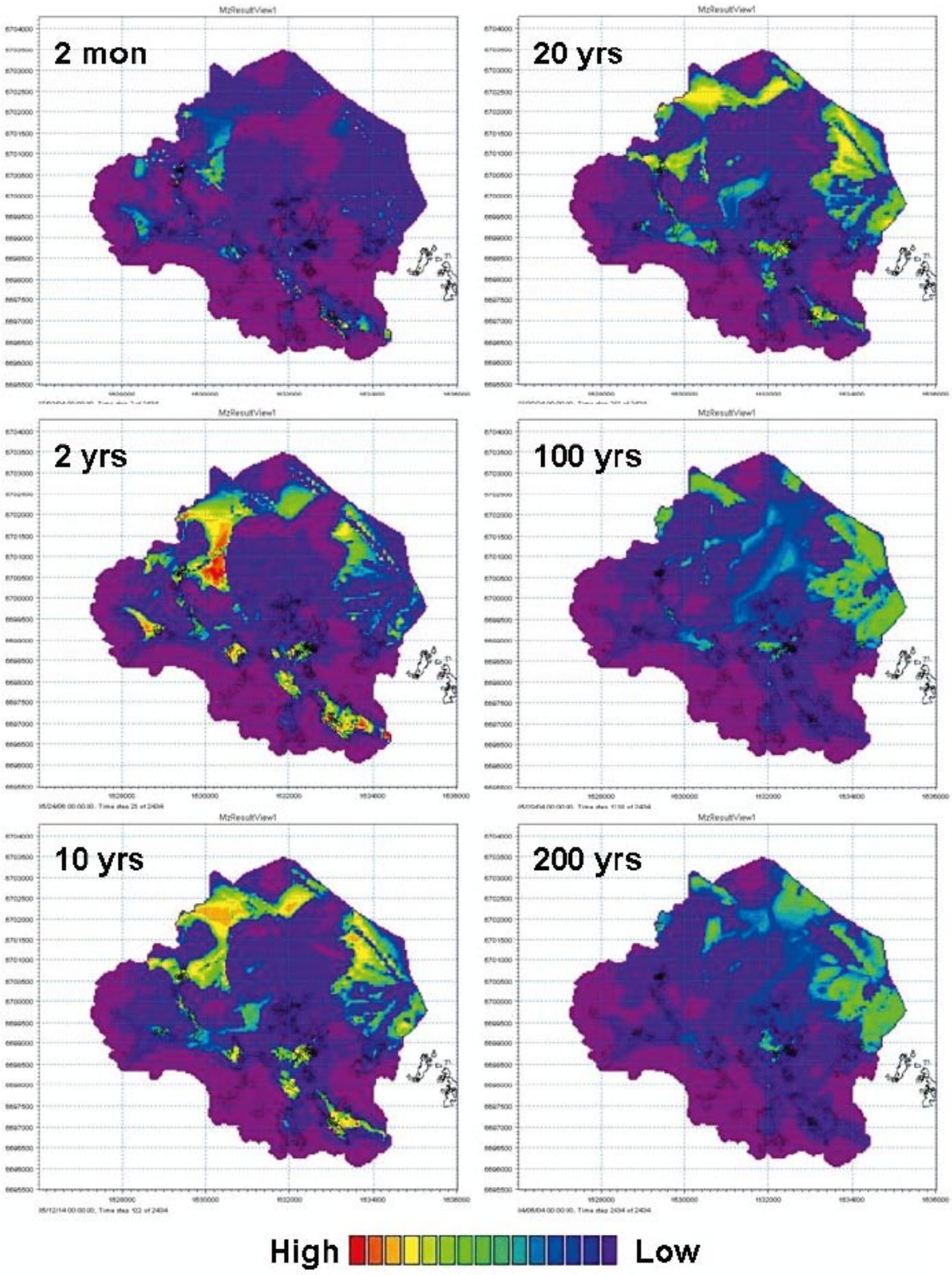

Figure 6-58. *Results of advection-dispersion simulation with a uniform pulse solute source in the bedrock showing concentrations in the bedrock at approximately 70 m.b.s.l. at different times after solute injection.*

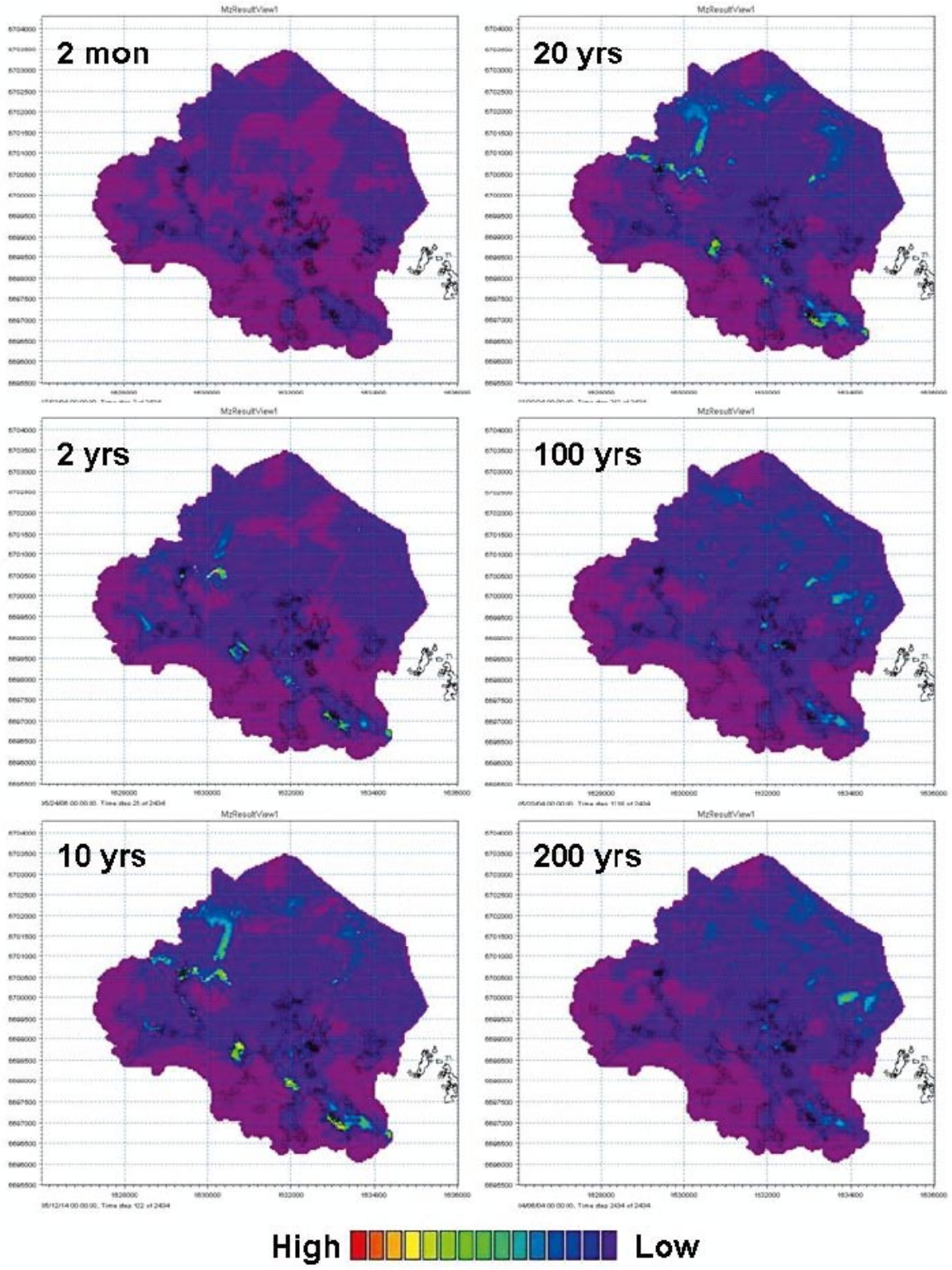

Figure 6-59. *Results of advection-dispersion simulation with a uniform pulse solute source in the bedrock showing concentrations in the Quaternary deposits at different times after solute injection. The purple colour is zero concentration and the dark blue colour indicates a low concentration, 0–1 g/m³.*

To further illustrate the solute transport pattern, a vertical concentration profile through the model area is analysed. The profile is taken according to Figure 6-60. Figure 6-61 shows the vertical profile at six different time steps, i.e. 2 months and 2, 10, 20, 100 and 200 years. The white area at a depth of about 140 m.b.s.l. is the layer in which the solute source is applied. It illustrated in the figure that parts of the applied solute mass are transported downwards. The areas in which the solute is transported downwards are located in topographically relatively higher areas, which act as recharge areas. The solute mass moving upwards is mainly transported towards the sea and the lake areas.

Figure 6-62 is the same figure as Figure 6-61 but looking only at the upper part of the model, above the pollution source. The figure further shows that the solute transport mainly takes place towards the sea and the lake areas. It also illustrates that some solute is transported rapidly while some is moving slowly, which reflects the heterogeneity of the flow field.

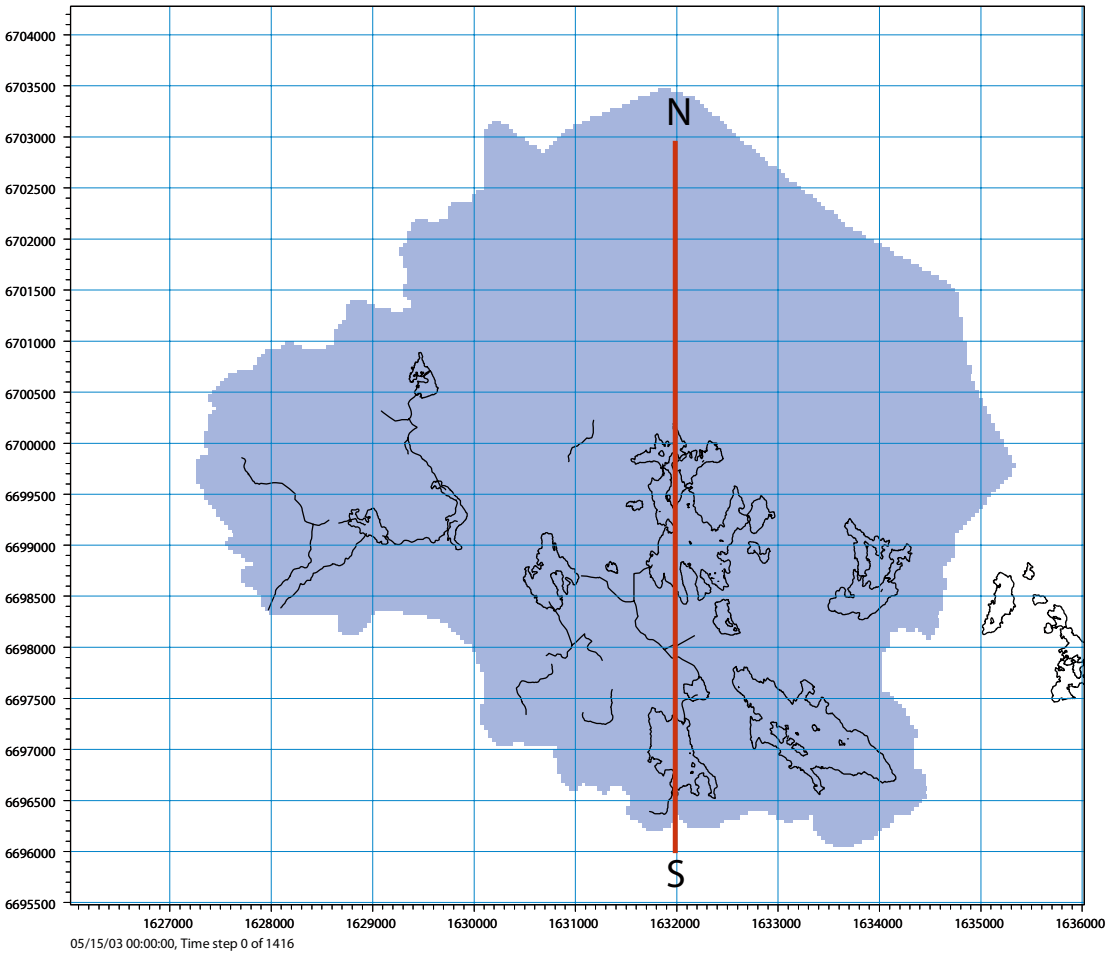

Figure 6-60. *Position of profile through the model area, in the north-south (N-S) direction.*

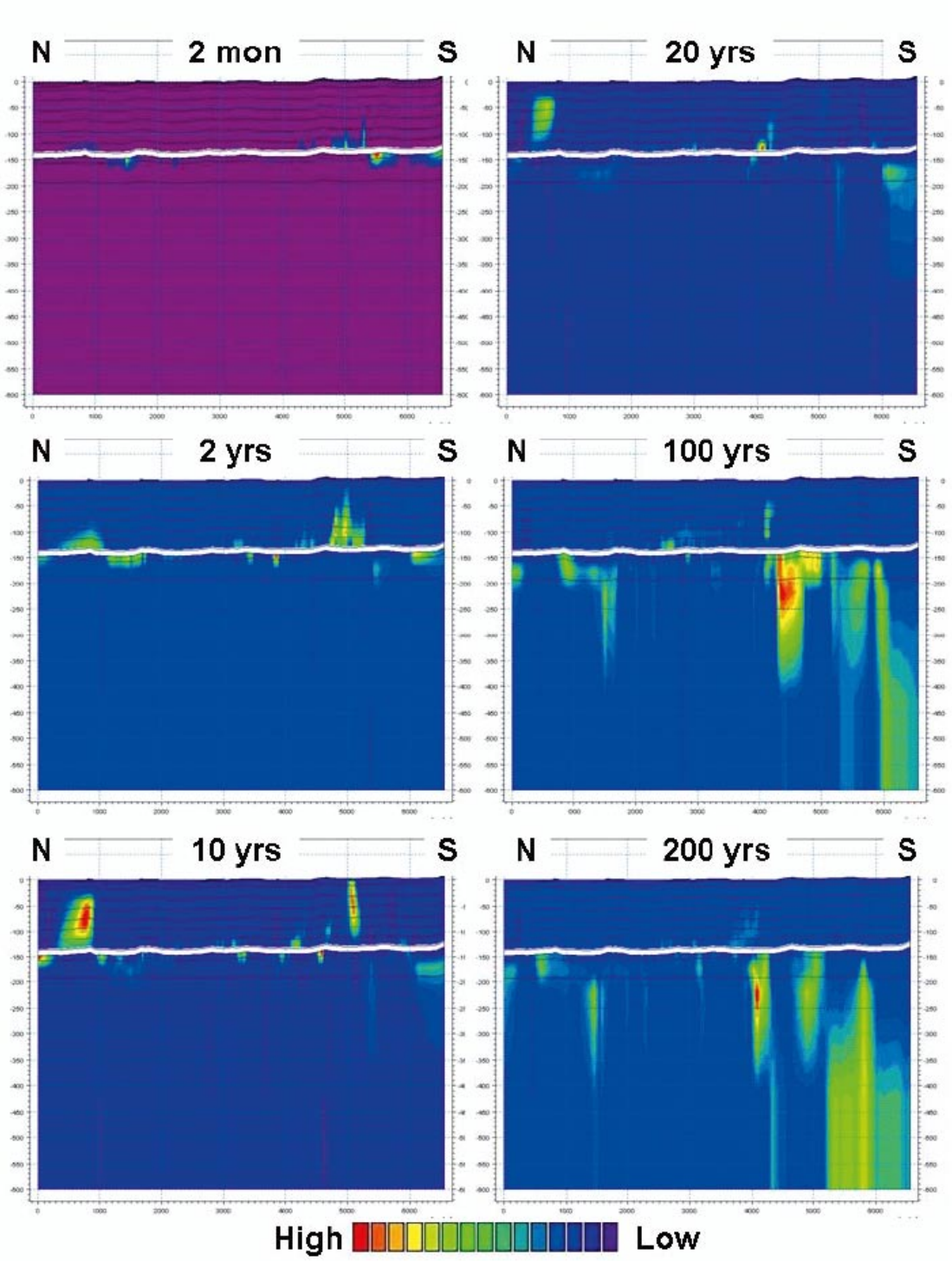

Figure 6-61. *Profile through the model area (location indicated in Figure 6-60) showing the advection-dispersion solute concentrations at six different times during the simulation.*

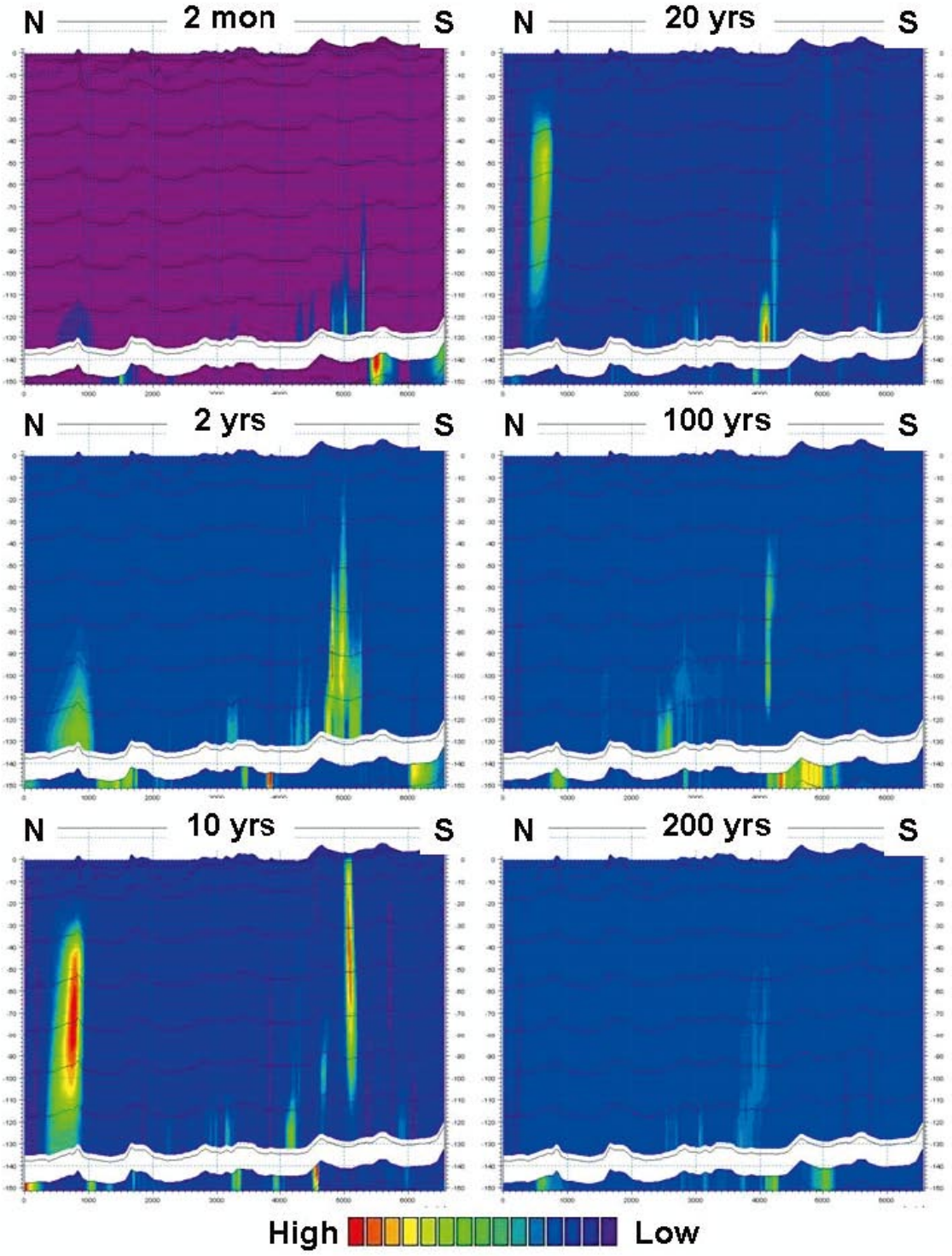

Figure 6-62. *Profile through the model area (location indicated in Figure 6-60) showing the advection-dispersion solute concentrations in the upper 150 m at six different times during the simulation.*

As discussed in Section 3.2.1 and illustrated in Figure 3-5, zones with high horizontal hydraulic conductivities in the bedrock exist within the model area. In these areas, solute transport is mainly directed in the horizontal direction towards the sea. Figure 6-63 shows the position of the profile for which concentrations are displayed in Figure 6-64. In this profile, there are zones with high horizontal conductivities at depths of approximately 70 and 100 m.b.s.l. In Figure 6-64, concentrations along the profile are illustrated for simulation times 10, 20, 50, 100, 150 and 200 years. The horizontal transport towards the sea is clearly seen in the results.

The figures illustrate that solute is moving mainly in the vertical direction until it reaches the area with the higher horizontal conductivity, located at a depth of approximately 100 m.b.s.l.. The solute is then transported mainly in the horizontal direction. After about 100 years, parts of the solute mass are transported to the upper layer with high horizontal conductivity, located at a depth of approximately 70 m.b.s.l., and at that level it starts moving towards the sea.

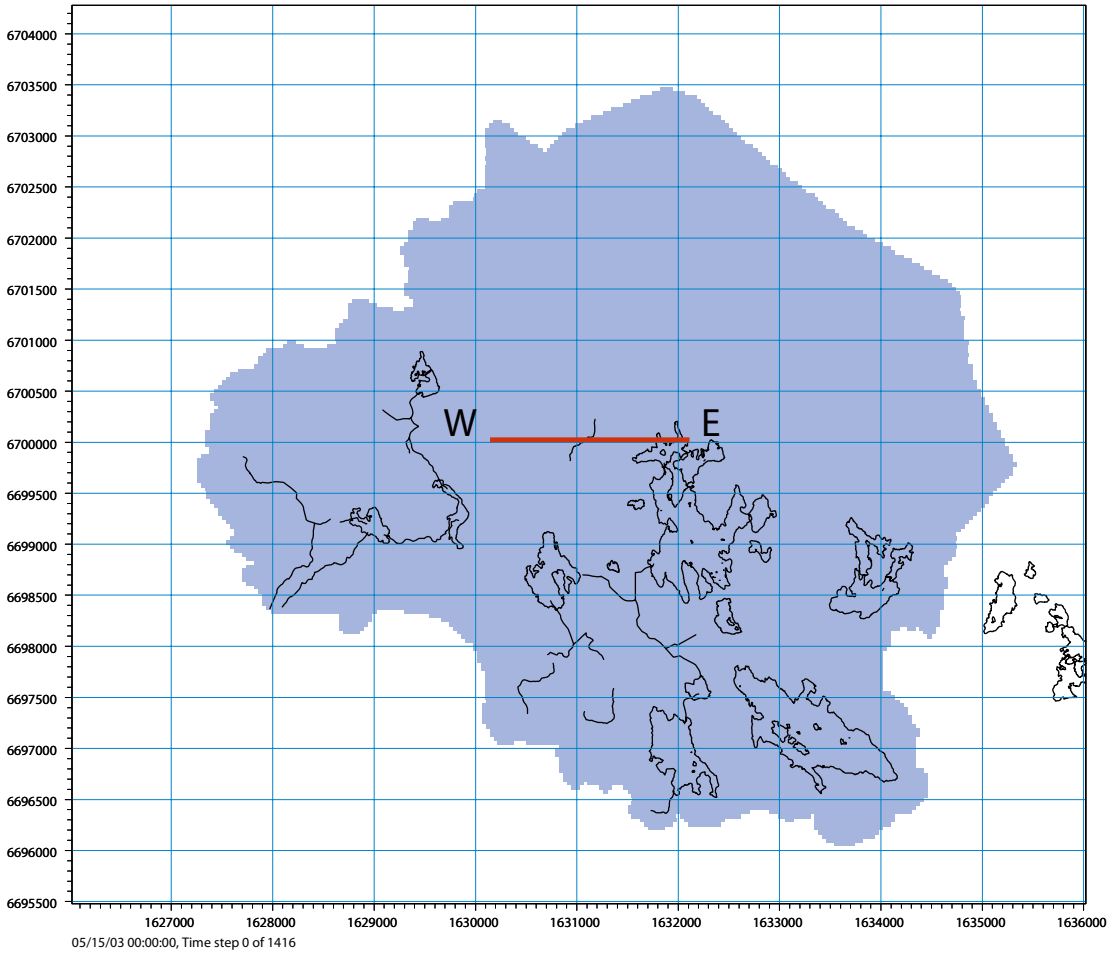

Figure 6-63. *Position of profile through an area of high horizontal conductivity, in the west-east (W-E) direction.*

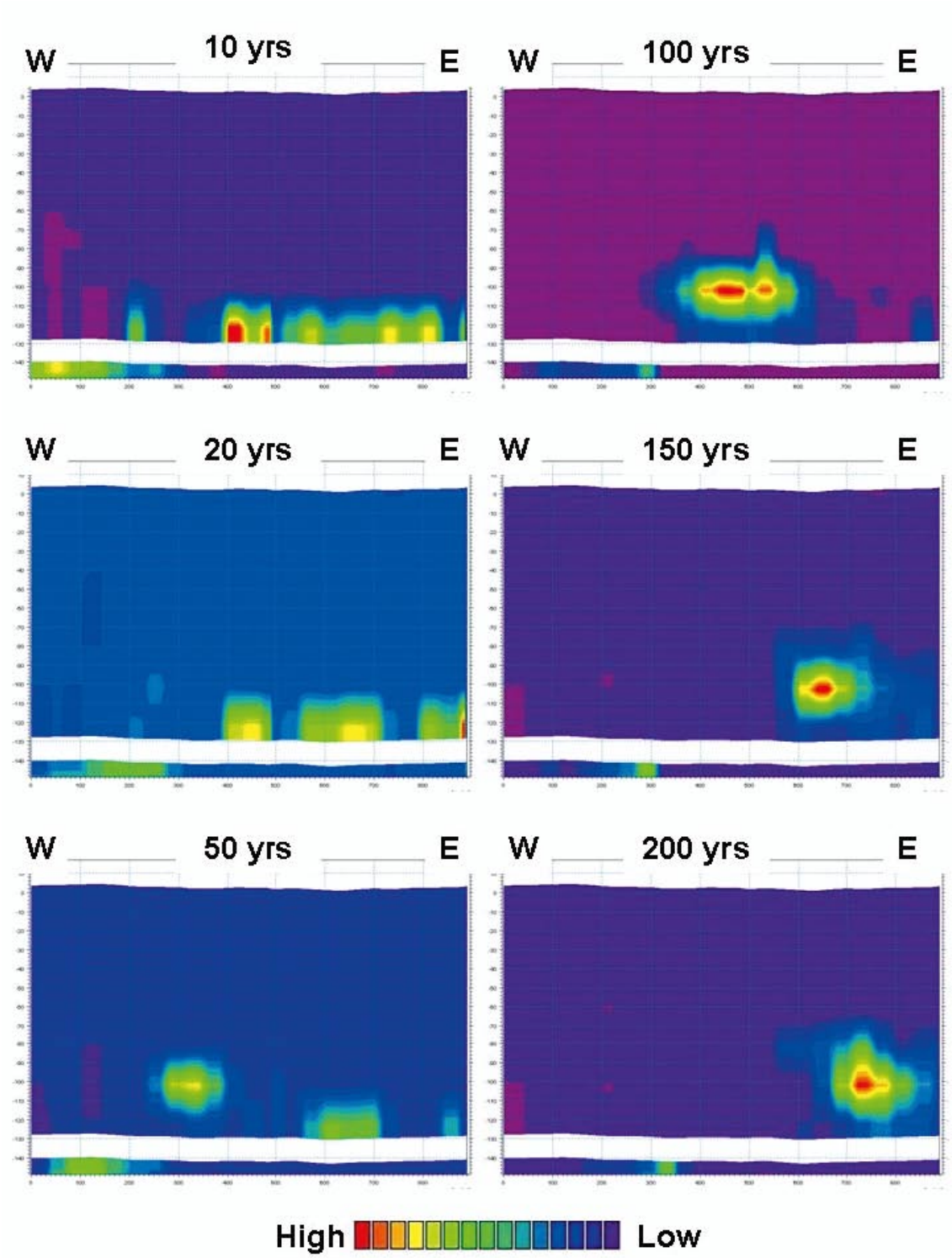

Figure 6-64. *Profile through the model area (location indicated in Figure 6-63) showing the advection-dispersion solute concentrations at six different times during the simulation.*

The difference in transport velocity between different subareas within the model area is illustrated by examples of time series in Figures 6-66 and 6-67. Figure 6-65 shows the positions of the four points for which time series are illustrated. Each figure presents time series in seven different calculation layers in the model. The uppermost layer is situated in the Quaternary deposits while the other layers are in the bedrock. Cell (107,147) is situated close to the coastline in the northern part of the model area, cell (104,128) is situated in the cooling water intake channel of the power plant, cell (176, 121) is in the sea close to the coastline, and cell (155, 87) is situated in Lake Bolundsfjärden.

Figure 6-66 shows the time series in cell (107,147) and cell (104,128). Both figures show a relatively fast solute breakthrough; the maximum concentration is reached within a few years in all layers. Furthermore, in both figures it is seen that the concentrations in the upper layers are affected by seasonal variations, especially in cell (107,147).

Figure 6-67 illustrates time series from a point in the sea area, cell (176,121). The solute transport is slower than for the previous two points; maximum concentrations are reached after about 10 years in the lower layer and after about 20 years in the upper layers. Furthermore, in all layers the solute concentration decreases for about 70–80 years after the maximum value but then increases to a new maximum which is reached after approximately 100 years of simulation. The reason for this is probably that a part of the solute mass is moving in areas with higher transport velocity, whereas the rest travels in parts where lower velocities prevail.

In the fourth time series figure, also in Figure 6-67, the solute transport is significantly slower. The maximum concentration is reached after approximately 150 years. The cell is situated under Lake Bolundsfjärden, where also measurements indicate that water movement is slow.
In Section 6.3, a discussion concerning flow gradients under Lake Bolundsfjärden is presented.

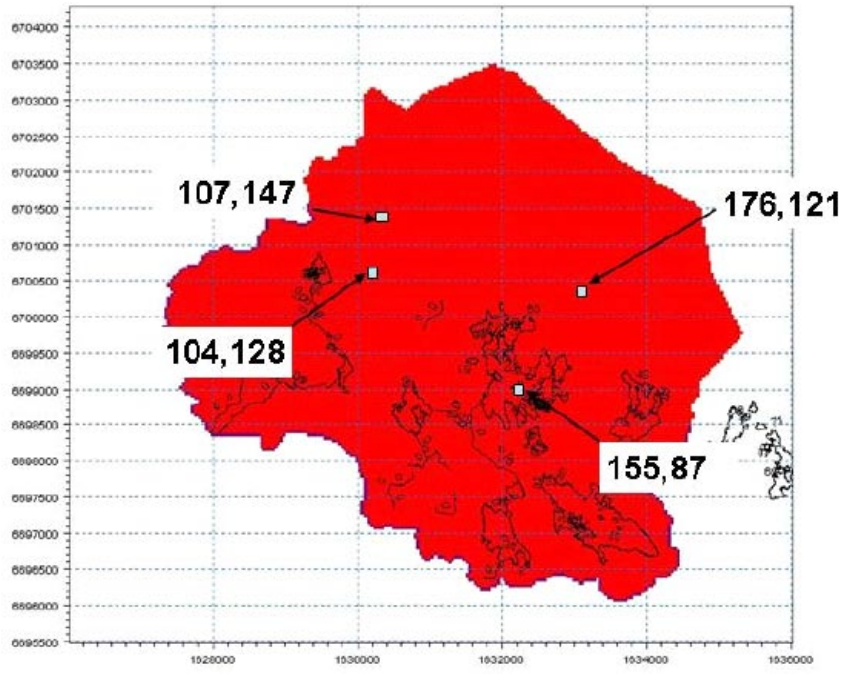

Figure 6-65. *Cells for which time series are illustrated in Figures 6-66 and 6-67.*

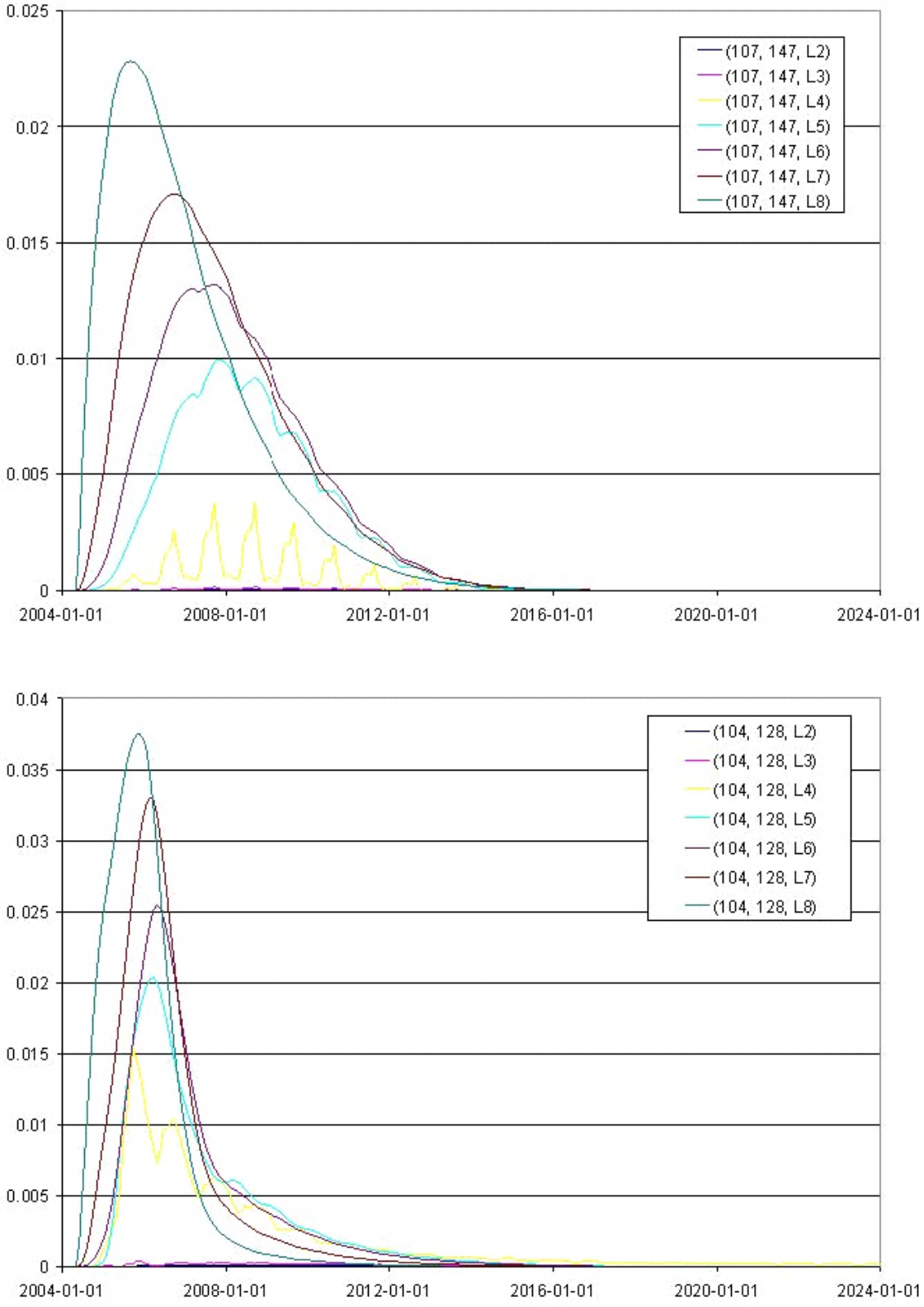

Figure 6-66. *Solute concentrations in different layers (L2 is layer 2, L3 layer 3, etc), in the upper figure from cell (107,147) and in the lower figure from cell (104,128).*

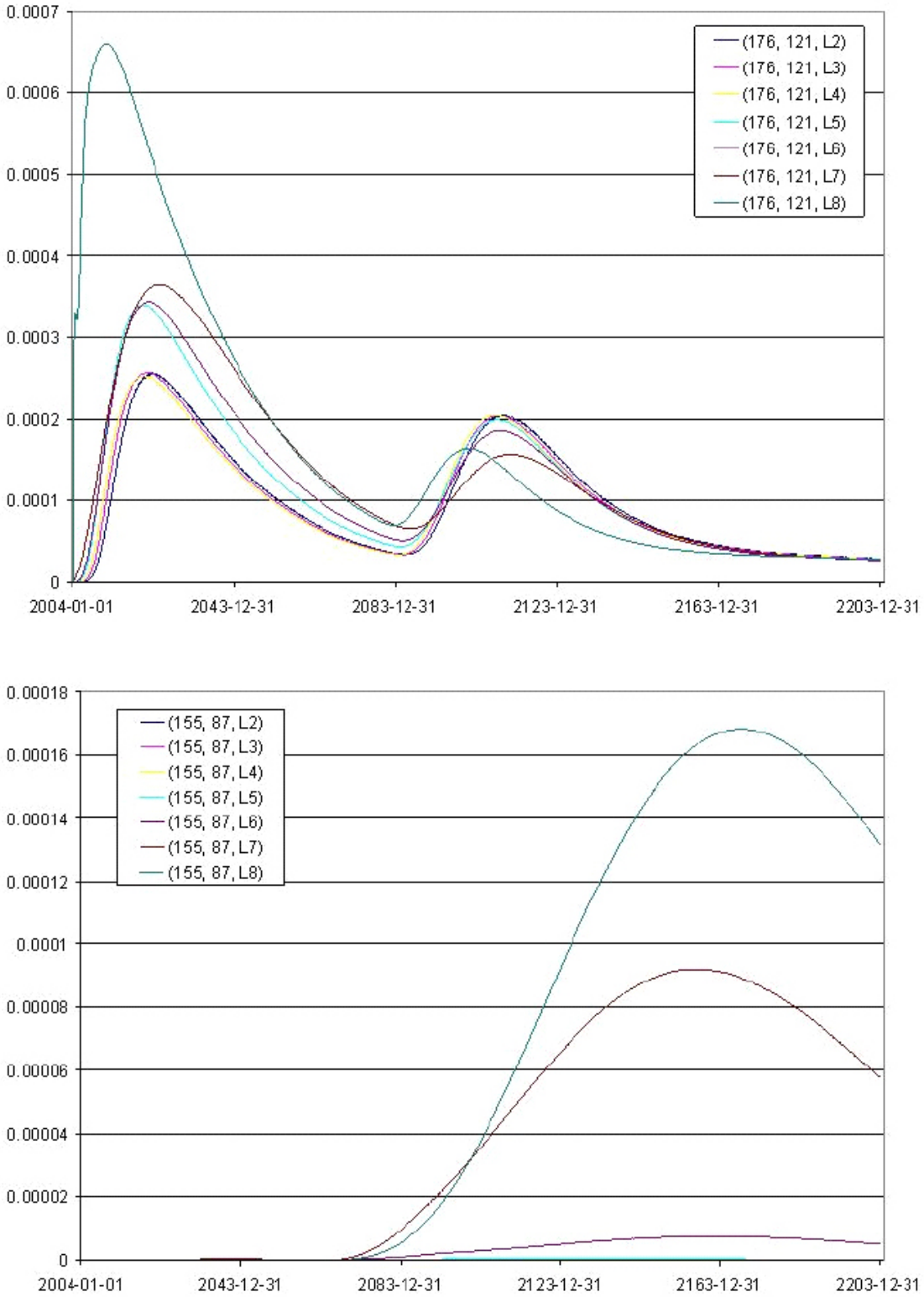

Figure 6-67. *Solute concentrations in different layers (L2 is layer 2, L3 layer 3, etc), in the upper figure from cell (176,121) and in the lower figure from cell 155, 87).*

A profile is drawn between the two cells (176,121) and (155, 87), in order to further illustrate the flow pattern from Lake Bolundsfjärden and the sea, see Figure 6-68. In the bedrock layers along the profile, layers with high horisontal conductivities are present at depths of approximately 70 m.b.s.l and 110 m.b.s.l. Figure 6-69 shows the concentrations along the profile at six different times. The figures show that after 20 years only the fast transport close to cell (176,121) has reached the upper layers. As time goes, solute starts spreading upwards also closer to cell (155,87), and after 40 years it is seen that solute that has reached a level of 110 m.b.s.l starts moving horisontally towards the sea. After 50 years, solute has also reached the layer at a depth of 70 m.b.s.l and the figures show that the solute transport at that level is also towards the sea.

Table 6-13 shows a summary of model sinks where the solute left the saturated zone; see /Gustafsson et al. 2008/ for a description of this and other simulation cases. The amount in each sink is compared to the total amount applied in the source. After 200 years, almost half of the applied source (48.9%) is still left in the saturated zone. The major part of the applied mass that has left the saturated zone goes to the sea. Also, a large amount of the applied mass goes to the unsaturated zone.

In the second simulation, the pollution source is applied as a continuous infiltration source, i.e. the source is infiltrated to the model by the precipitation. As a consequence, the amount of solute infiltrated to the model depends on the amount of precipitation. The source is continuous with a concentration of 1 g/m^3. The initial concentration is zero and the dispersion coefficients are the same as in the case with a bedrock source. In cells with a fixed head the concentration is always zero.

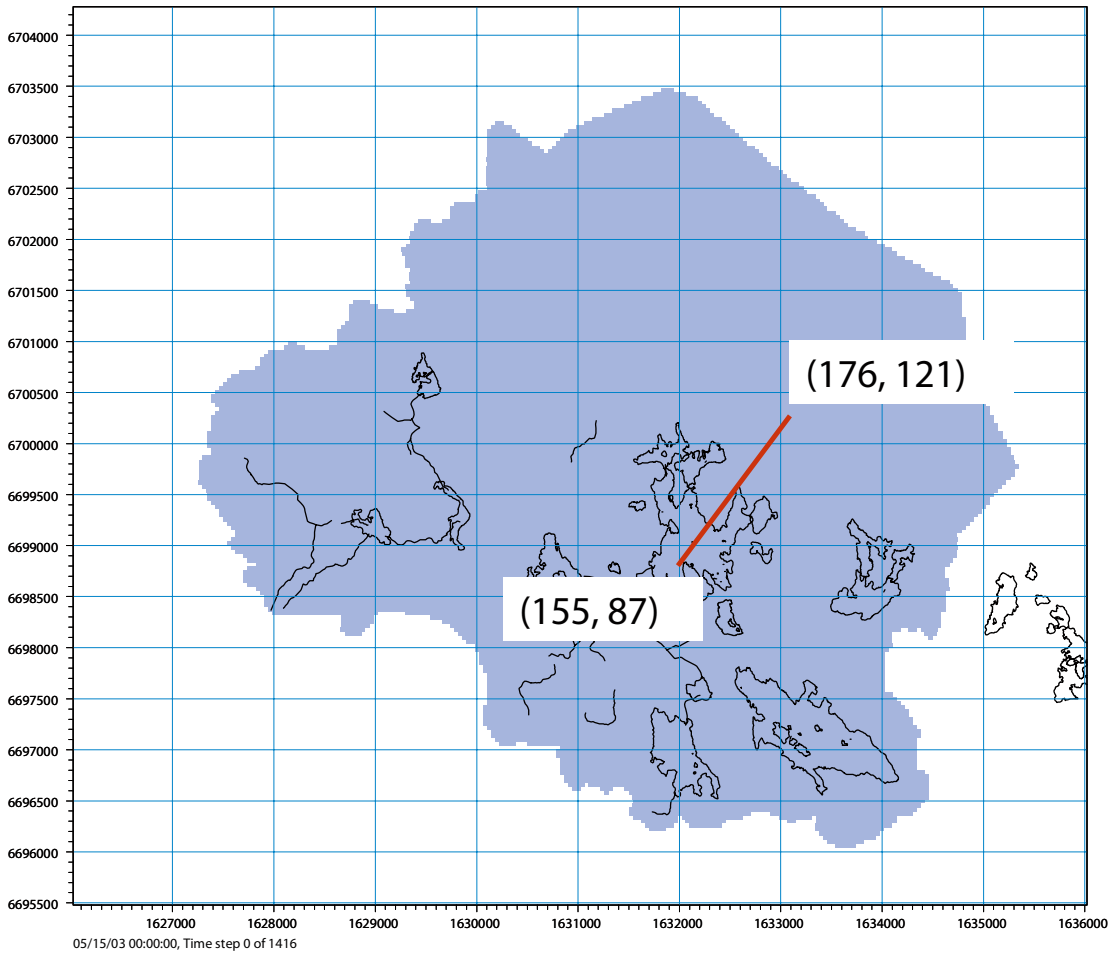

Figure 6-68. *Position of profile between cells (176,121) and (155, 87).*

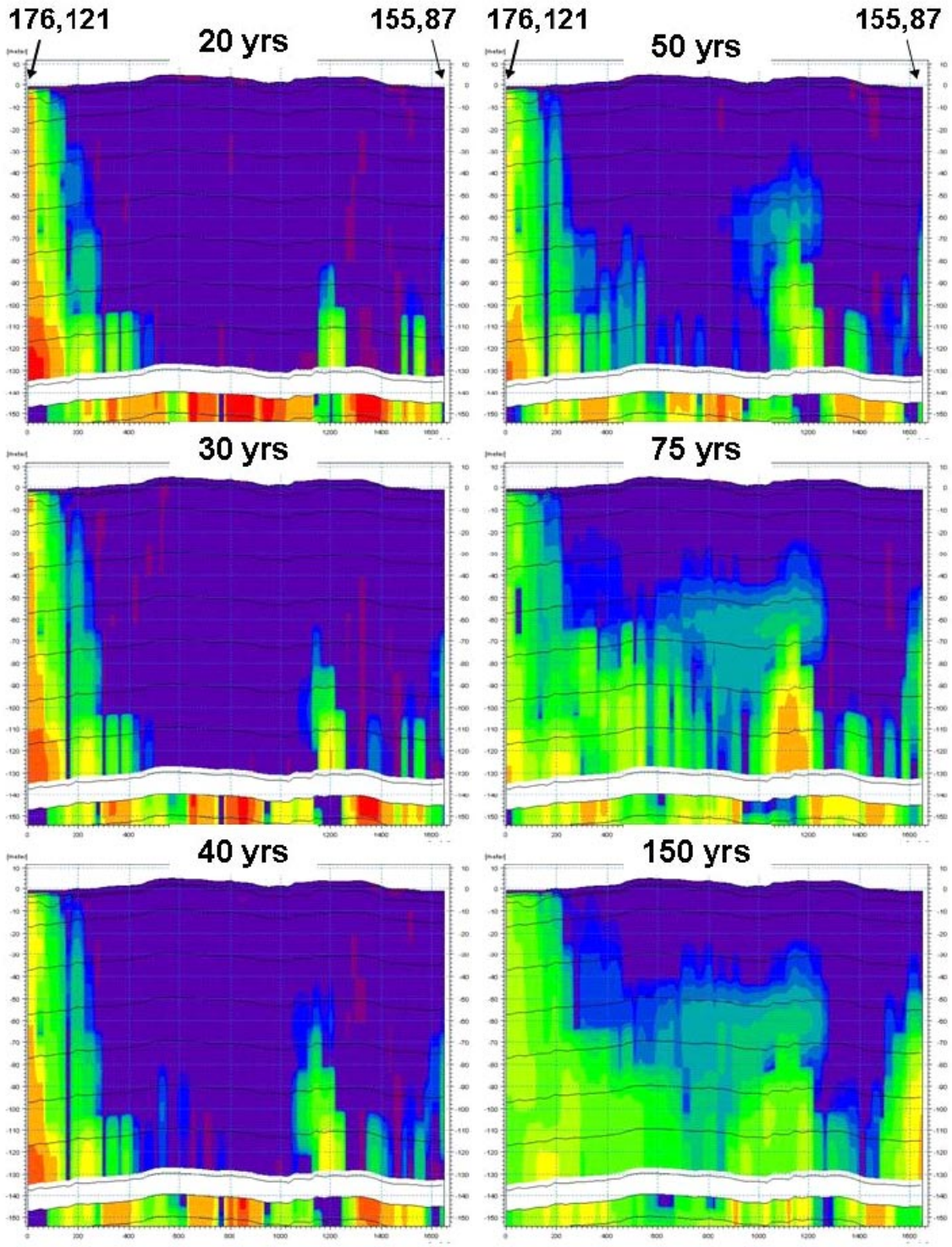

Figure 6-69. *Solute concentrations in a profile between cells (176,121) and (155, 87) for six different times during the advection-dispersion simulation.*

Table 6-13. Summary of model sinks after 200 years advection-dispersion simulation with a source at a depth of 130 m.b.s.l.

	Accumulated mass in % of total applied source mass after 200 years
Saturated zone storage	48.9
Saturated zone to unsaturated zone	16.9
Saturated zone baseflow to streams	1.2
Saturated zone drain to streams	1.8
Saturated zone to the sea	19.7
Saturated zone flow to boundaries	10.6
Saturated zone drain to boundaries	0.9
Total source to saturated zone	100.0

Figure 6-70 shows simulation results in three different layers after 5 years. The upper figure is from the Quaternary deposits. Whereas the source is an infiltration source, discharge areas with no infiltration have no external source. This is the case with, for example, the lake areas. Areas with larger amount of infiltration, being recharge areas over the whole year, consequently act as larger infiltration sources.

The middle figure is from a bedrock layer at 70 m.b.s.l. and indicates this pattern even clearer, with the solute concentration concentrated to recharge areas. Furthermore, in the figure it may be noted that because of the sheet joints that are located in bedrock layers further up under Lake Bolundsfjärden, the solute is transported horizontally towards the sea.

The lower figure, which is from a lower bedrock layer at 130 m.b.s.l., further indicates that the solute concentration is mainly concentrated to recharge areas. Furthermore, both in the middle and in the lower figure, the effect of the regional fracture zone in connection to Lake Eckarfjärden (see Figure 3-2) is clearly illustrated. The low concentrations in the fracture zones indicate that they are recharge areas from the deeper bedrock.

Results for the vertical profile in Figure 6-60 are illustrated in Figure 6-71 for the case with the infiltration source. The figure shows the solute concentration along the profile after 10 years of simulation. The figure confirms what is said above about the pattern of the source strengths. However, a horizontal solute transport from higher recharge areas to lower discharge areas (i.e. lakes etc) would be expected, but it seems like the littoral zones act as hydraulic barriers around some of the lakes, as exemplified by Lake Eckarfjärden in Figure 6-73. This effect is not so clear around Lake Bolundsfjärden, see Figure 6-72, where the horizontal transport seems to spread the solute also under some parts of the lake. In both cases however, the spreading through horizontal transport in the upper layers is much smaller than the effects from vertical flow directions. The flow patterns of Lake Eckarfjärden and Lake Bolundsfjärden are further discussed in Section 6.3.5.

Table 6-14 shows a summary of sinks where the solute leaves the saturated zone. Each sink parameter is compared to the total saturated zone output at the end of the simulation. The major part of the applied mass goes to the unsaturated zone, which is expected with an infiltration source. Finally, a large part of the applied source mass goes to the sea, which was also noted in the simulation with the bedrock source.

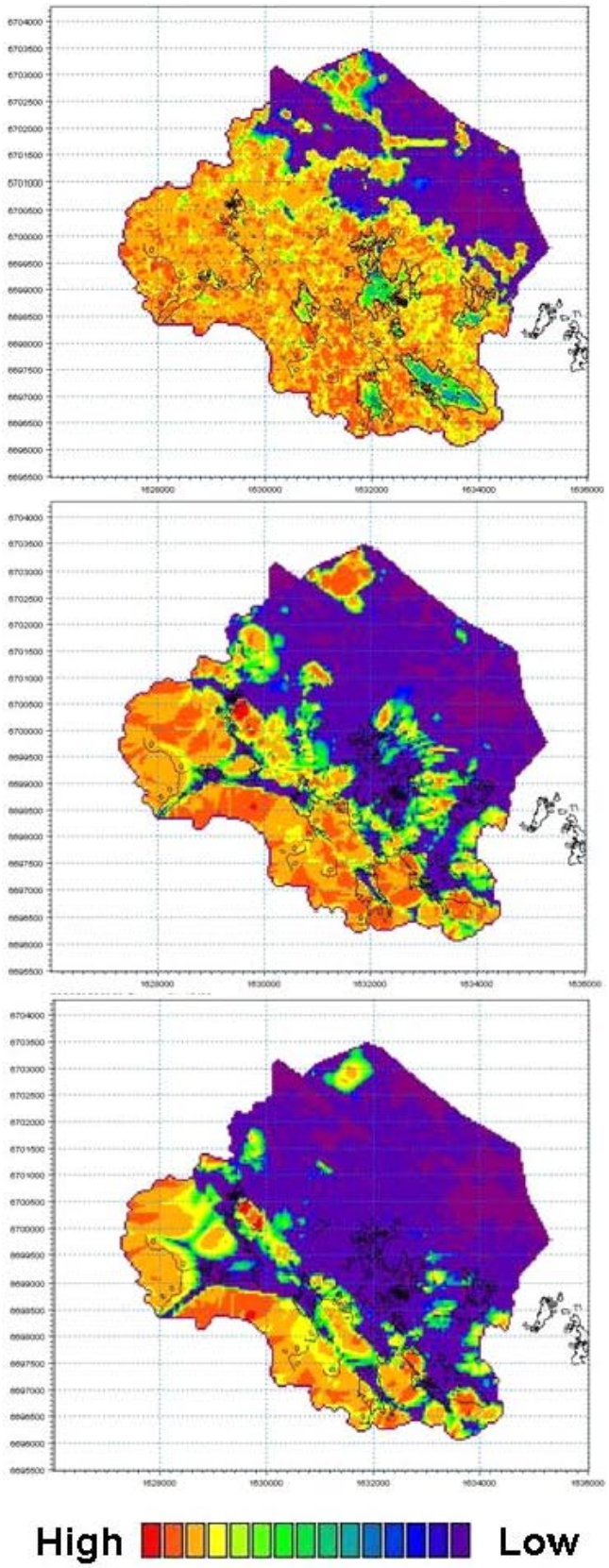

Figure 6-70. *Advection-dispersion simulation results after five years for three different layers, from top to bottom: layer 2 (in Quaternary deposits), layer 6 and layer 9.*

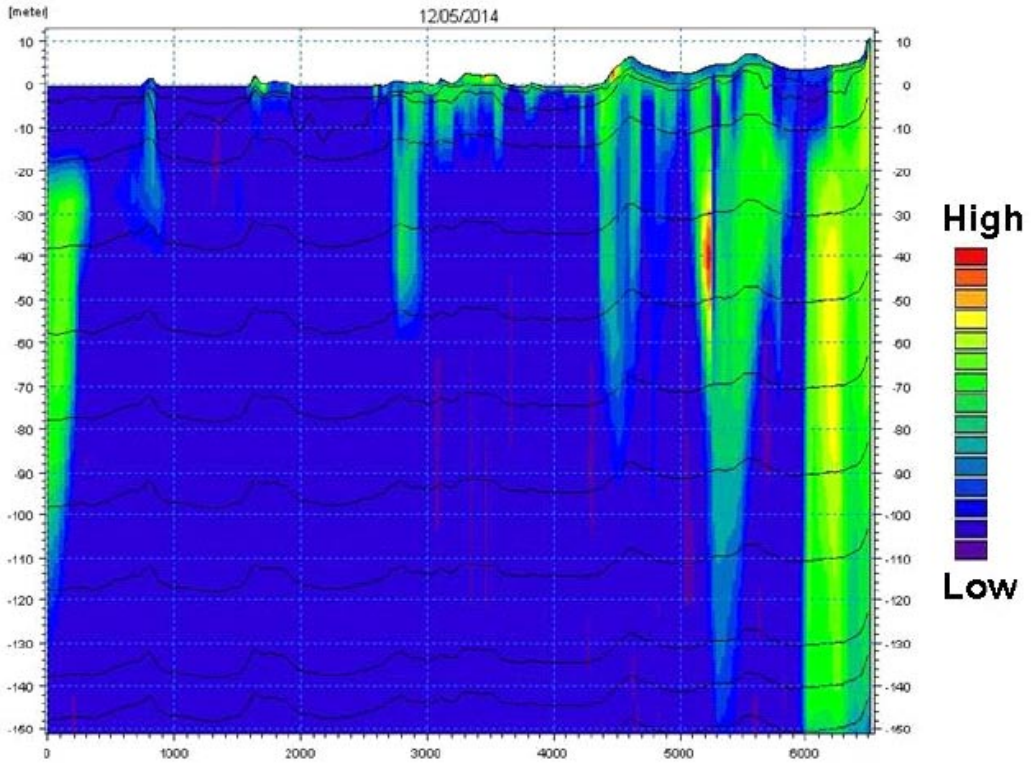

Figure 6-71. *Solute concentrations after 10 years in the profile shown in Figure 6-60 from advection-dispersion modelling of transport from a continuous infiltration source.*

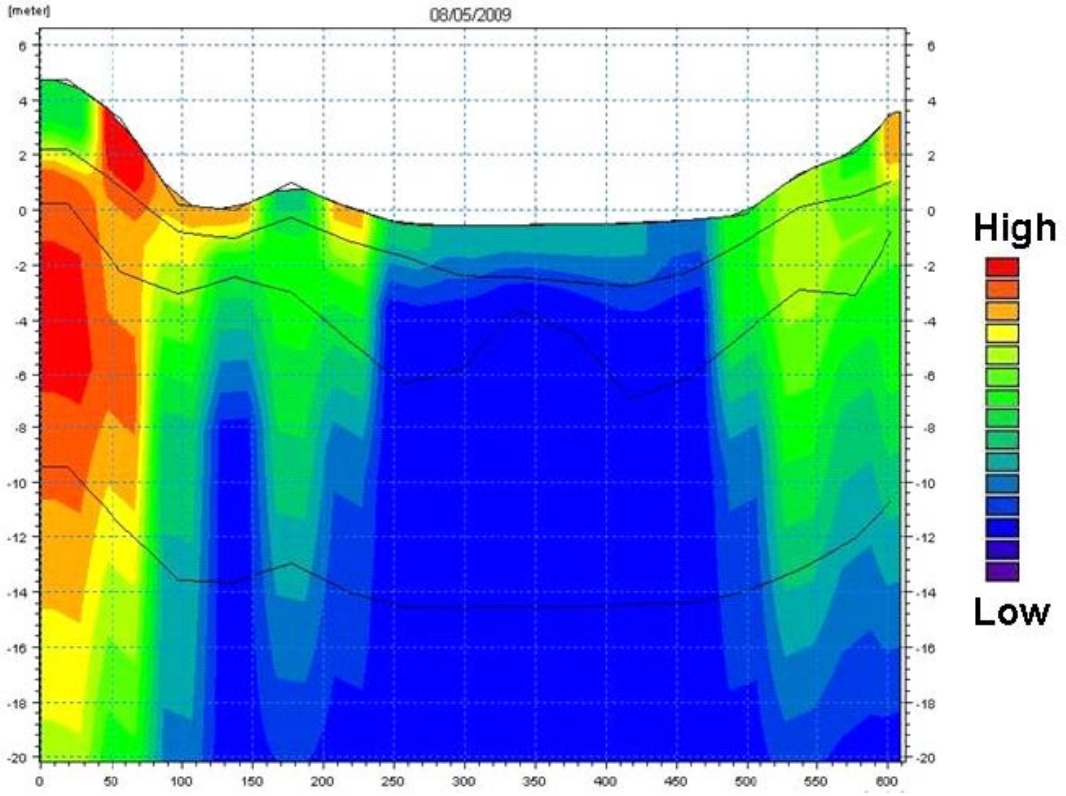

Figure 6-72. *Solute concentrations after 5 years in a profile in the west-east direction through Lake Bolundsfjärden, from advection-dispersion modelling of transport from a continuous infiltration source.*

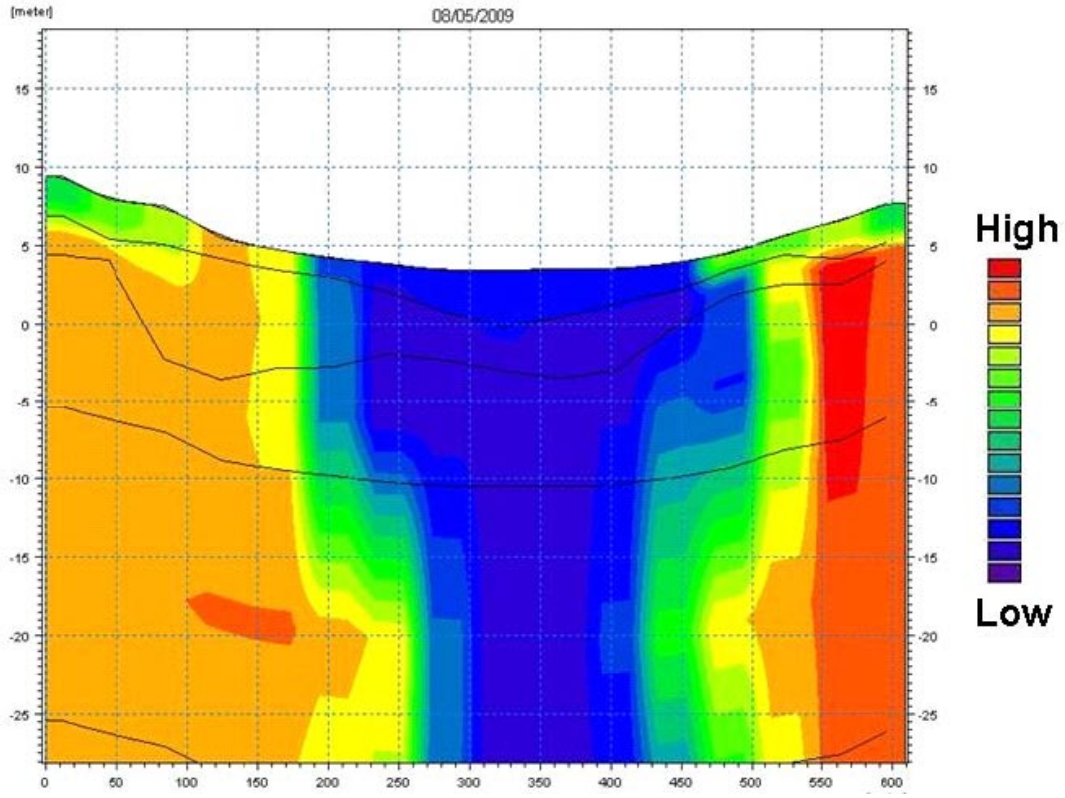

Figure 6-73. *Solute concentrations after 5 years in a profile in the west-east direction through Lake Eckarfjärden, from advection-dispersion modelling of transport from a continuous infiltration source.*

Table 6-14. Summary of model sinks after 200 years advection-dispersion simulation with a continuous infiltration source.

	Accumulated mass in % of total applied source mass after 200 years
Saturated zone to unsaturated zone	56.4
Saturated zone baseflow to streams	1.2
Saturated zone drain to streams	2.4
Saturated zone to the sea	36.4
Saturated zone flow to boundaries	0.4
Saturated zone drain to boundaries	3.2
Total saturated zone output	100.0

7 Conclusions of flow and transport modelling

7.1 Flow modelling

The sensitivity analysis and calibration process are summarised in Section 4.6. The validation and testing of the model performance is presented in Chapter 5. Due to discrepancies between the conceptual model and the tested numerical model complementary sensitivity analysis and calibration were performed. This work is presented in Chapter 6. The main conclusions of the modelling are summarised as follows:

- The observed fast response in the water courses after a rain or snow melt event indicates that the uppermost soil layer is very high conductive. The fast response was not captured by the model and the calculated accumulated discharge was too low with the original data set up. A drainage function had to be activated to reach an acceptable agreement with the observed surface water flow dynamics.
- To reach an appropriate accumulated discharge the potential evapotranspiration had to be reduced. Previous analyses have shown that the only way to reach a considerable increase of the surface water discharge was to decrease the potential evapotranspiration. The main reason for this is the fact that wetlands dominate the area, where the actual evaporation is to large extent controlled by the potential evaporation.
- Measurements have indicated a low degree of contact between the lake and the underlying till. The hydraulic conductivity of the clay layer in the lake sediments were set to 10^{-8} m/s. It was not necessary to correct the conductivity values for the lake sediments during the calibration process. The initial low values have been kept and the results show very good agreement between measured and calculated head elevations in the till under the lakes in the model area.
- To reach a good agreement between measured and calculated head elevation in the Quaternary deposits the original values of the hydraulic parameters had to be corrected for the till layers in the geological model. The best results were achieved when anisotropy was applied. Sensitivity analysis showed that the case where the horizontal conductivity was multiplied by 5 and the vertical conductivity was divided by 2 resulted in the best agreement between measured and calculated groundwater head elevations.
- One important discovery in the calibration process was the outcome of the analysis of the bottom boundary condition. This analysis showed that the bottom boundary condition used in the base model setup of the model generated water to the model, resulting in too high vertical groundwater fluxes and too high groundwater elevations in the bedrock. After this analysis the model was extended to 600 m depth and a no-flow boundary was used at the bottom of the model. The prescribed head at the bottom boundary in the original model "pushed" water up to the surface system resulting in too high discharges in some water courses. This resulted in a large variation in specific discharge between different catchment areas.
- MIKE SHE does not handle density driven flow, which could be a problem when extending the vertical extent of the model. The salt content increases with depth, which means that the model results are less reliable for the deep bedrock. The extension of the model is primarily made to generate an appropriate flow field in the upper bedrock. Thus, the results under 200 m depth are not used to describe the hydrogeological situation at the site. Hydrogeological models able to describe density driven flow are used to describe the details of the deeper parts of the bedrock. The coupling and agreement between the "near-surface hydrological model", i.e. the MIKE SHE model, and the "deep rock hydrogeological model", the ConnectFlow model, were evaluated by comparing groundwater flow in the bedrock. It was found that the MIKE SHE-calculated groundwater flow at 150 m.b.s.l. was in the same range as the corresponding groundwater flow in the ConnectFlow model.

- No major differences were found between the simulations with models based on different versions of the geometric Quaternary deposits (QD) model. The shape of the groundwater table, the mean absolute error between calculated and observed values in the SFM- and HFM-wells and the overall water balance were almost the same for the simulations performed with the two different QD-models.
- The surface water system generally shows a good agreement between measured and calculated water levels and discharges. The main difference with regard to surface water discharges is that the model does not manage to accurately simulate the surface water response to precipitation after the dry summer of 2006.
- It was found important to introduce the melted water from snow on the ground instead of adding it as precipitation. Adding snow melt water as precipitation causes unrealistic interception losses. This implies that the calculation of snow accumulation and melting should be handled inside the MIKE SHE model.
- The dry conditions during the spring and summer of 2006 were "extreme" relative to the corresponding events taking place during the calibration period. The effects of the extremely dry summer are not fully described by the model in all bore holes measuring the groundwater head elevation. A reason for this is the fact that the transpiration cannot reach deeper than to the bottom of the upper saturated zone calculation layer, which is often only 2.5 m deep.
- In order to accurately describe the gradients between the bedrock and the QD it is crucial to reach the same accuracy in measurements and model results in both the bedrock and the QD. In the model, the drainage of the SFR repository had to be included if a good agreement should be reached between measurements and calculations. The overall pattern of recharge and discharge areas between the bedrock and QD observed in measurements is then reproduced by the model. However, there is still some discrepancy in the area around Lake Bolundsfjärden.
- The calculated head elevation in the bedrock is coherently higher than measured values when the drainage of the SFR repository is not activated. Correct reproduction of site measurements demand the drainage of the SFR repository to be included in the model.
- Local topography has a strong impact on the pattern of recharge and discharge areas in the QD. In the bedrock, the discharge areas are concentrated to lakes and depressions connected to the streams. However, the main part of Lake Bolundsfjärden act as a recharge area in the bedrock. The groundwater flow towards the sea in the fractures/sheet joints generates a downward gradient under the lake. Discharge areas are generally weaker than recharge areas, i.e. discharge areas more easily turn into recharge areas than vice versa. The weather conditions have a stronger impact on the recharge and discharge areas in the QD than in the bedrock.

7.2 Transport modelling

The transport simulations are presented and discussed in Chapter 6. A detailed and more extensive analysis of the sensitivity to different transport properties is presented in /Gustafsson et al. 2008/. The main conclusions from the transport simulations presented in this report are:

- The particle tracking results indicates a relative slow transport from sources att c. 140 m depth in the bedrock up to the ground surface. After 300 years, the majority of the introduced particles are still left in the model volume. The areas with high horizontal hydraulic conductivity, the areas with horizontal fractures/sheet joints, short circuit the flow paths of particles released in the area where these structures are represented.
- The particles reaching ground surface when introducing particles all over the model area, are concentrated to lake areas, the depressions around the streams, and the sea. When activating the drainage at the SFR repository no particles discharge to the sea; instead, the particles are removed by the well in SFR. Otherwise, the pattern of the exit points at the ground surface is the same.
- When introducing particles inside the planned repository area, all particle exit points are in the sea, provided that the drainage in the SFR repository is not included in the model. With the SFR pumping in the model, SFR is an additional sink for particles injected within the planned repository area. No particles discharge within the land part of the model area. The overall pattern of exit points after 300 years does not change when running the model for 5,000 years, but the exit points move further out in the sea.
- The advection-dispersion modelling results for a case where the solute is introduced at 140 m.b.s.l. show that the transport is directed both upwards and downwards. The upward transport in the bedrock is mainly directed towards the sea and the lake areas. When the solute reaches a layer where the sheet joints are represented in the model, the horizontal component of transport is dominating. As a result, only a minor fraction of the solute appears above the areas with high hydraulic conductivity.
- Vertical profiles confirm the importance of the sheet joints for the overall pattern of the transport. Each time the solute reaches a layer with sheet joints, which are represented at three different levels, a spreading towards the sea can be noticed.
- Discharge from the bedrock to the QD is small. Only areas above the Eckarfjärden regional deformation zone receive solute from the bedrock to the QD.
- When applying an infiltration source only producing solutes in recharge areas, a horizontal solute transport from higher recharge areas to lower discharge areas (e.g. lakes) is expected. However, it appears that the littoral zones acts as hydraulic barriers around some of the lakes. This means that the spreading through horizontal transport in the upper layers is much smaller than the effects from vertical flow directions.

8 References

Aneljung M, Gustafsson L-G, 2007. Sensitivity analysis and development of calibration methodology for near-surface hydrogeology model of Forsmark. SKB R-07-27, Svensk Kärnbränslehantering AB.

Aneljung M, Sassner M, Gustafsson L-G, 2007. Sensitivity analysis and development of calibration methodology for near-surface hydrogeology model of Laxemar. SKB R-07-52, Svensk Kärnbränslehantering AB.

Bosson E, Berglund S, 2006. Near-surface hydrogeological model of Forsmark. Open repository and solute transport applications – Forsmark 1.2. SKB R-06-52, Svensk Kärnbränslehantering AB.

Brunberg A-K, Carlsson T, Blomqvist P, Brydsten L, Strömgren M, 2004. Forsmark site investigation. Identification of catchments, lake-related drainage parameters and lake habitats. SKB P-04-25, Svensk Kärnbränslehantering AB. (Revised December 2007.)

DHI Software, 2007. MIKE SHE – User Manual. DHI Water & Environment, Hørsholm, Denmark.

DHI Software, 2008. MIKE SHE – User Manual. DHI Water & Environment, Hørsholm, Denmark.

Eriksson B, 1981. Den potentiella evapotranspirationen i Sverige. SMHI Rapport RMK 28. (In Swedish.)

Follin S, Johansson P-O, Hartley L, Jackson P, Roberts D, Marsic N, 2007. Hydrogeological conceptual model development and numerical modelling using CONNECTFLOW, Forsmark modelling stage 2.2. SKB R-07-49, Svensk Kärnbränslehantering AB.

Follin S, Hartley L, Jackson P, Roberts D, Marsic N, 2008. Hydrogeological conceptual model development and numerical modelling using CONNECTFLOW, Forsmark modelling stage 2.3. SKB R-08-23, Svensk Kärnbränslehantering AB.

Gokall-Norman K, Ludvigson J-E, 2006. Forsmark site investigation. Hydraulic interference test in borehole HFM14. SKB P-06-196, Svensk Kärnbränslehantering AB.

Gustafsson L-G, Sassner M, Bosson E, 2008. Numerical modelling of solute transport at Forsmark with MIKE SHE. Site descriptive modelling, SDM-Site Forsmark. SKB R-08-106, Svensk Kärnbränslehantering AB.

Hedenström A, Sohlenius G, 2008. Description of the regolith at Forsmark. Site descriptive modelling, SDM-Site Forsmark. SKB R-08-04, Svensk Kärnbränslehantering AB.

Hedenström A, Sohlenius G, Strömgren M, Brydsten L, Nyman H, 2008. Depth and stratigraphy of regolith at Forsmark. Site descriptive modelling, SDM-Site Forsmark. SKB R-08-07, Svensk Kärnbränslehantering AB.

Johansson P-O, 2008. Description of surface hydrology and near-surface hydrogeology at Forsmark. Site descriptive modelling, SDM-Site Forsmark. SKB R-08-08**,** Svensk Kärnbränslehantering AB.

Johansson P-O, Öhman J, 2008. Presentation of meteorological, hydrological and hydrogeological monitoring data from Forsmark. Site descriptive modelling, SDM-Site Forsmark. SKB R-08-10, Svensk Kärnbränslehantering AB.

Johansson P-O, Werner K, Bosson E, Berglund S, Juston J, 2005. Description of climate, surface hydrology, and near-surface hydrogeology. Preliminary site description, Forsmark area – version 1.2. SKB R-05-06, Svensk Kärnbränslehantering AB.

Juston J, Johansson P-O, Levén J, Tröjbom M, Follin S, 2007. Analysis of meteorological, hydrological and hydrogeological monitoring data. Forsmark – stage 2.1. SKB R-06-49, Svensk Kärnbränslehantering AB.

Knutsson G, Morfeldt C-O, 2002. Grundvatten teori och tillämpning. AB Svensk Byggtjänst. (In Swedish.)

Kristensen K J, Jensen S E, 1975. A model for estimating actual evapotransipration from potential evapotranspiration. Nordic Hydrology, vol. 6, pp. 170–188.

Lindborg T (ed.), 2008. Surface system Forsmark. Site descriptive modelling, SDM-Site Forsmark. SKB R-08-11, Svensk Kärnbränslehantering AB.

Lundin L, Stendahl J, Lode E, 2005. Forsmark site investigation. Soils in two large trenches. SKB P-05-166, Svensk Kärnbränslehantering AB.

Rhén I (ed.), Gustafson G, Stanfors R, Wikberg P, 1997. Äspö HRL – Geoscientific evaluation 1997/5. Models based on site characterization 1986–1995. SKB TR-97-06, Svensk Kärnbränslehantering AB.

SKB, 2005. Preliminary site description. Forsmark area – version 1.2. SKB R-05-18, Svensk Kärnbränslehantering AB.

SKB, 2008. Site description of Forsmark at completion of the site investigation phase. SKB TR-08-05, Svensk Kärnbränslehantering AB.

Sonnenborg T O, Henriksen H J (eds.), 2005. Håndbog i grundvandsmodellering. GEUS rapport 2005/80, GEUS, Copenhagen, Denmark. (In Danish.)

Werner K, Bosson E, Berglund S, 2005. Description of climate, surface hydrology, and near-surface hydrogeology. Simpevarp 1.2. SKB R-05-04, Svensk Kärnbränslehantering AB.

Werner K, Johansson P-O, 2003. Forsmark site investigation. Slug tests in groundwater monitoring wells in soil. SKB P-03-65, Svensk Kärnbränslehantering AB.

Appendix 1

Time series for all SFM-wells in the calibration

Comparison of measured and calculated groundwater levels (elevations or depths) in all groundwater monitoring wells used in the calibration of the flow model.

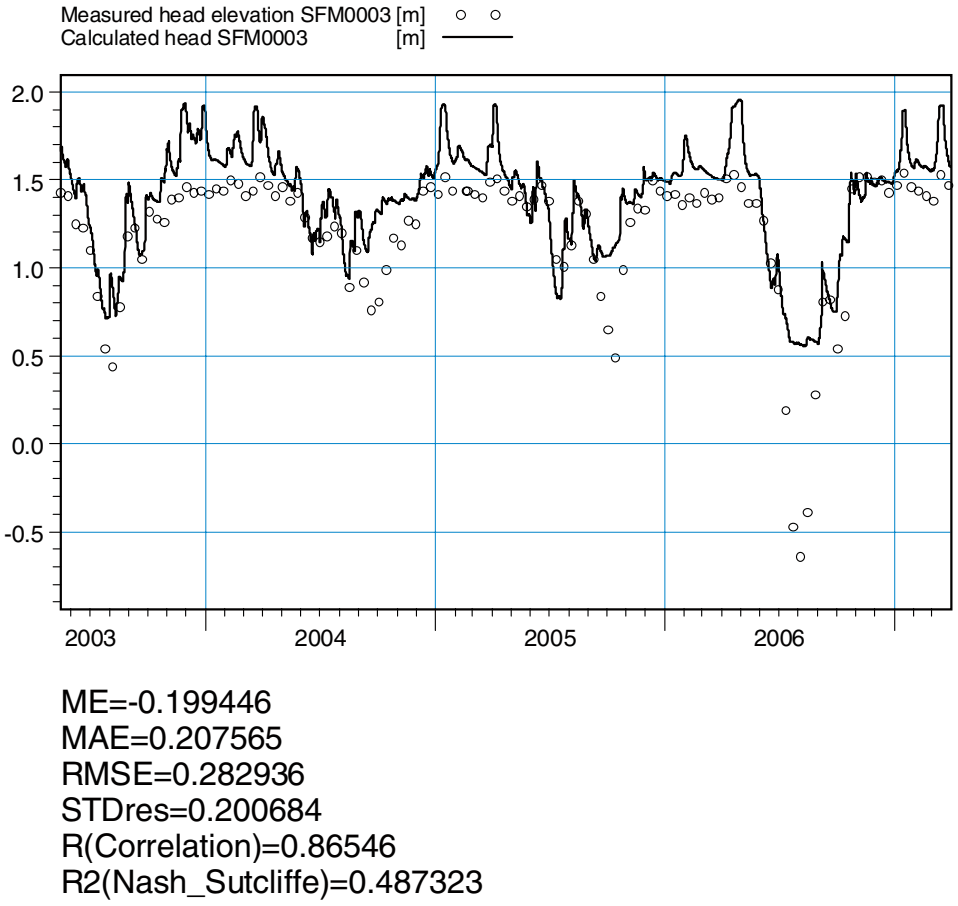

Figure A1-1. *Measured and calculated head elevation in SFM0003*

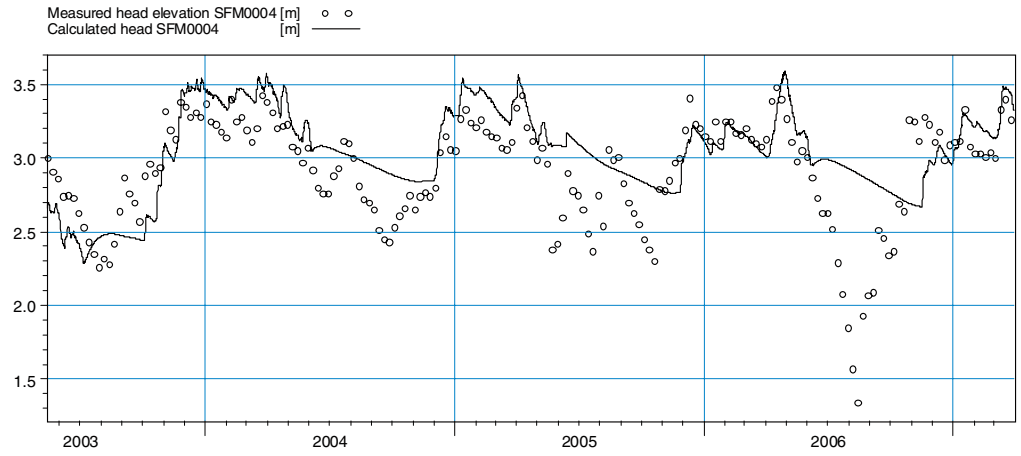

ME=-0.122342
MAE=0.230899
RMSE=0.310915
STDres=0.285833
R(Correlation)=0.65446
R2(Nash_Sutcliffe)=0.280701

Figure A1-2. *Measured and calculated head elevation in SFM0004.*

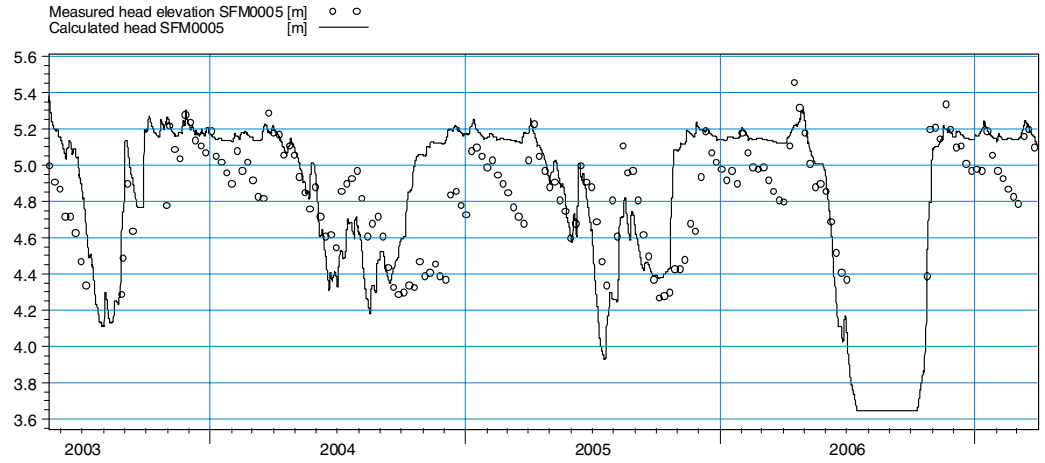

ME=-0.109538
MAE=0.209007
RMSE=0.269024
STDres=0.245715
R(Correlation)=0.64487
R2(Nash_Sutcliffe)=0.000287347

Figure A1-3. *Measured and calculated head elevation in SFM0005*

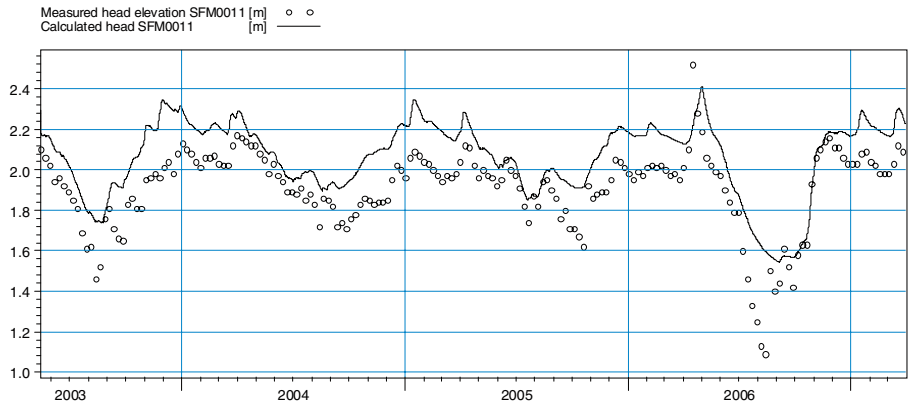

ME=-0.162495
MAE=0.165149
RMSE=0.182602
STDres=0.0833013
R(Correlation)=0.896632
R2(Nash_Sutcliffe)=0.031702

Figure A1-4. *Measured and calculated head elevation in SFM00011*

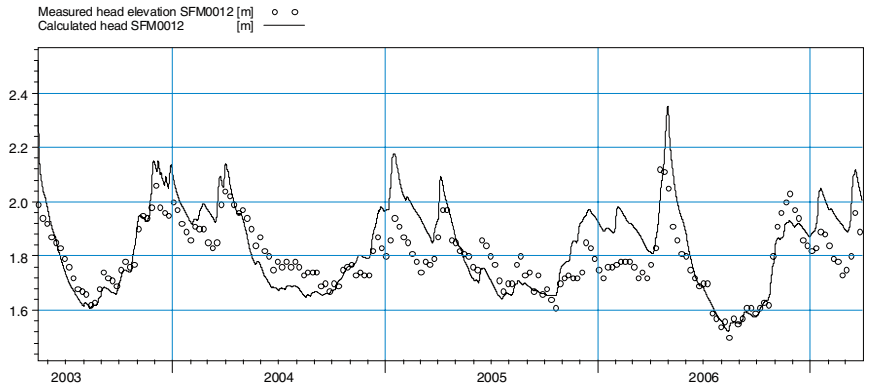

ME=-0.0476403
MAE=0.0783763
RMSE=0.0948149
STDres=0.0819772
R(Correlation)=0.877628
R2(Nash_Sutcliffe)=0.384091

Figure A1-5. *Measured and calculated head elevation in SFM00012.*

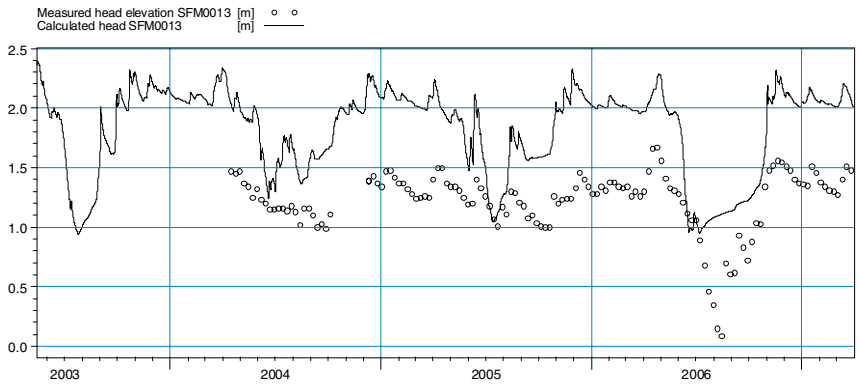

ME=-0.560515
MAE=0.562575
RMSE=0.597516
STDres=0.206998
R(Correlation)=0.82503

Figure A1-6. *Measured and calculated head elevation in SFM0013*

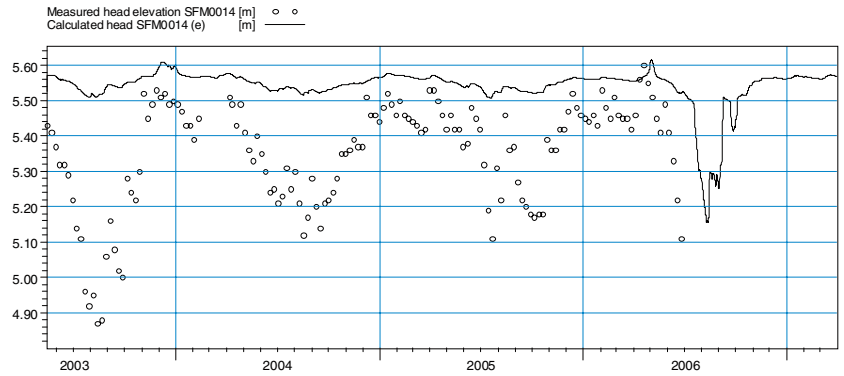

ME=-0.242097
MAE=0.242373
RMSE=0.295058
STDres=0.168666
R(Correlation)=0.844842
R2(Nash_Sutcliffe)=-1.46388

Figure A1-7. *Measured and calculated head elevation in SFM0014*

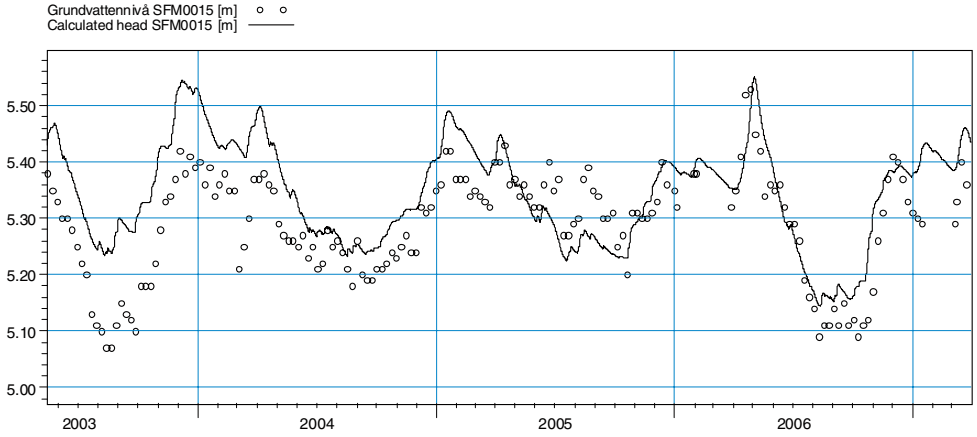

ME=-0.0792843
MAE=0.0877464
RMSE=0.0992607
STDres=0.0597218
R(Correlation)=0.770746
R2(Nash_Sutcliffe)=-0.453664

Figure A1-8. *Measured and calculated head elevation in SFM0015.*

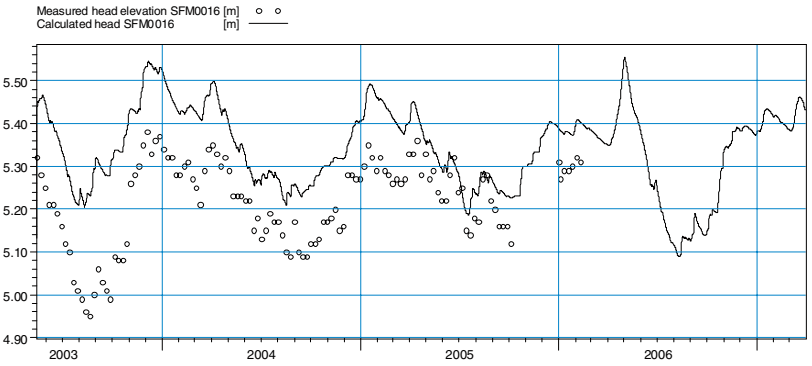

ME=-0.145964
MAE=0.14628
RMSE=0.156967
STDres=0.0577324
R(Correlation)=0.828952
R2(Nash_Sutcliffe)=-1.38542

Figure A1-9. *Measured and calculated head elevation in SFM0016.*

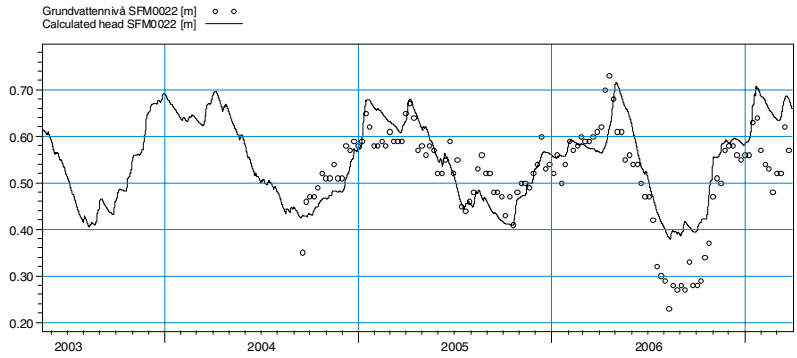

ME=-0.0241239
MAE=0.0536042
RMSE=0.0663902
STDres=0.0618522
R(Correlation)=0.785439
R2(Nash_Sutcliffe)=0.538296

Figure A1-10. *Measured and calculated head elevation in SFM00022.*

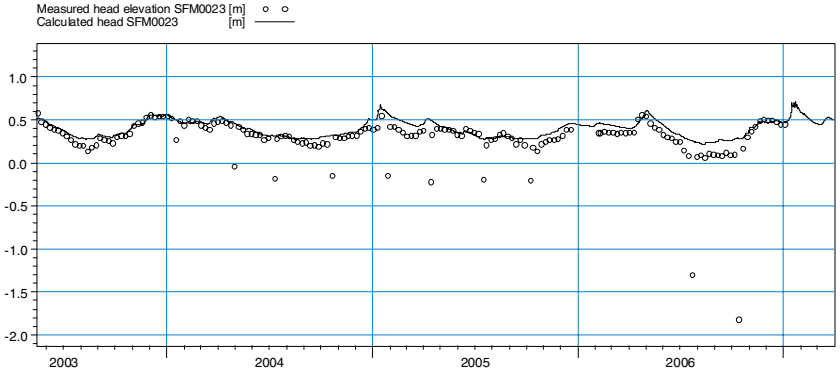

ME=-0.0593063
MAE=0.0722972
RMSE=0.192031
STDres=0.182644
R(Correlation)=0.61371
R2(Nash_Sutcliffe)=0.25892

Figure A1-11. *Measured and calculated head elevation in SFM0023.*

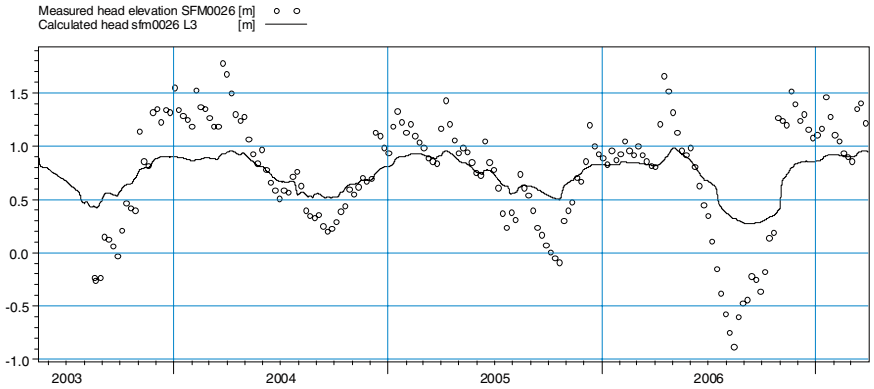

ME=-0.0414774
MAE=0.334824
RMSE=0.404533
STDres=0.402401
R(Correlation)=0.922634
R2(Nash_Sutcliffe)=0.462951

Figure A1-12. *Measured and calculated head elevation in SFM0026.*

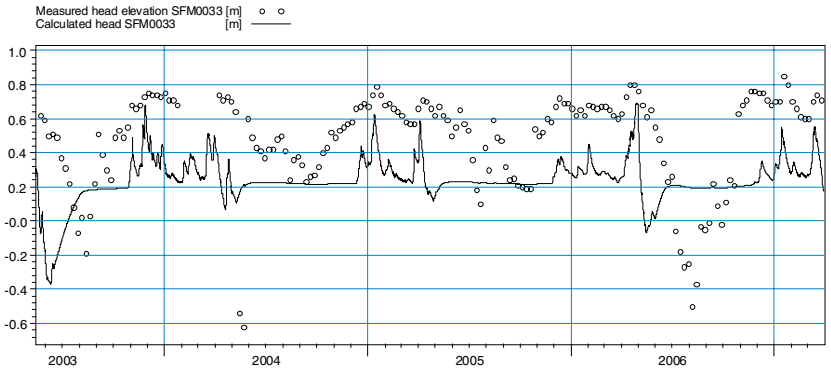

ME=0.243233
MAE=0.316535
RMSE=0.359776
STDres=0.265097
R(Correlation)=0.366063
R2(Nash_Sutcliffe)=-0.617949

Figure A1-13. *Measured and calculated head elevation in SFM0033.*

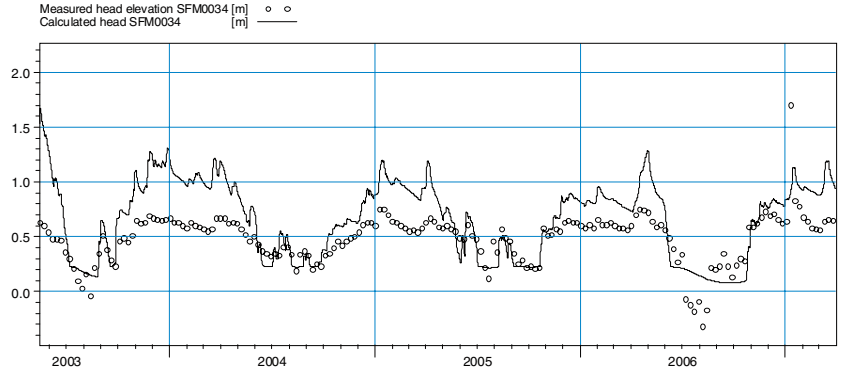

ME=-0.248614
MAE=0.284416
RMSE=0.337684
STDres=0.22852
R(Correlation)=0.8087
R2(Nash_Sutcliffe)=-1.65794

Figure A1-14. *Measured and calculated head elevation in SFM0034.*

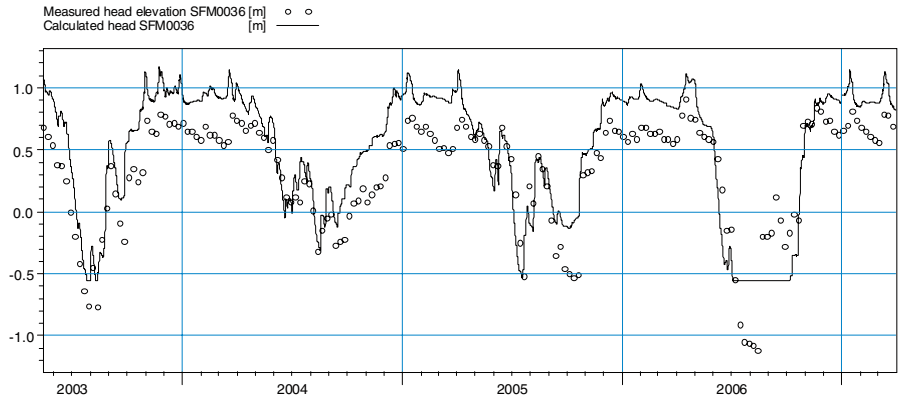

ME=-0.215606
MAE=0.264227
RMSE=0.289797
STDres=0.19364
R(Correlation)=0.918319
R2(Nash_Sutcliffe)=0.524591

Figure A1-15. *Measured and calculated head elevation in SFM0036.*

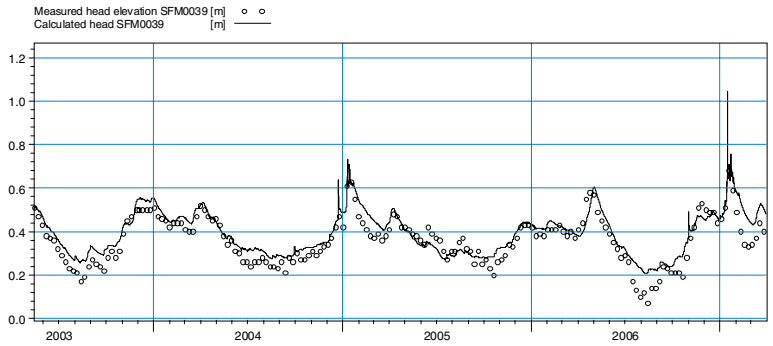

ME=-0.0312626
MAE=0.0425485
RMSE=0.051654
STDres=0.0411192
R(Correlation)=0.928724
R2(Nash_Sutcliffe)=0.780996

Figure A1-16. *Measured and calculated head elevation in SFM0039.*

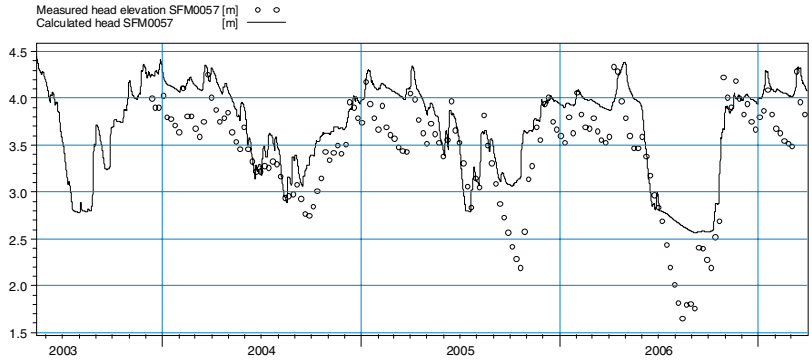

ME=-0.273222
MAE=0.305685
RMSE=0.365558
STDres=0.242863
R(Correlation)=0.90355
R2(Nash_Sutcliffe)=0.580875

Figure A1-17. *Measured and calculated head elevation in SFM0057*

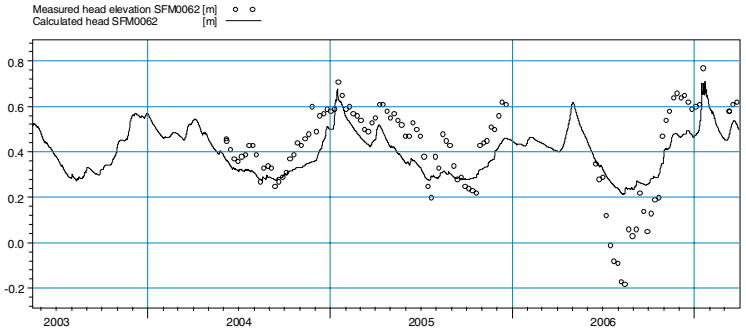

ME=0.0436248
MAE=0.106126
RMSE=0.12819
STDres=0.120538
R(Correlation)=0.840339
R2(Nash_Sutcliffe)=0.570225

Figure A1-18. *Measured and calculated head elevation in SFM0062.*

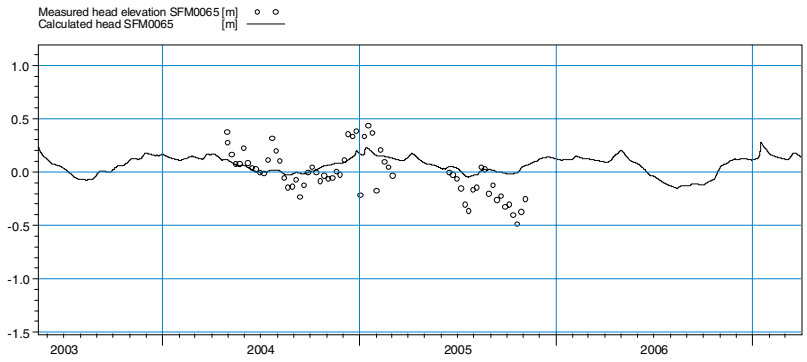

ME=-0.0655039
MAE=0.199311
RMSE=0.281871
STDres=0.274154
R(Correlation)=0.403547
R2(Nash_Sutcliffe)=0.0939502

Figure A1-19. *Measured and calculated head elevation in SFM0065.*

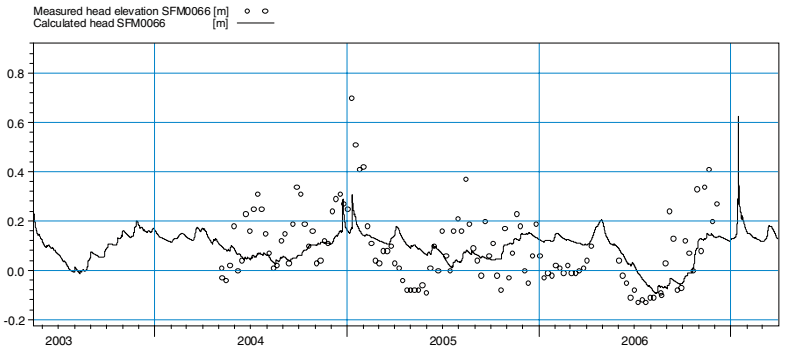

ME=0.0170079
MAE=0.113022
RMSE=0.144908
STDres=0.143906
R(Correlation)=0.428131
R2(Nash_Sutcliffe)=0.170631

Figure A1-20. *Measured and calculated head elevation in SFM0066.*

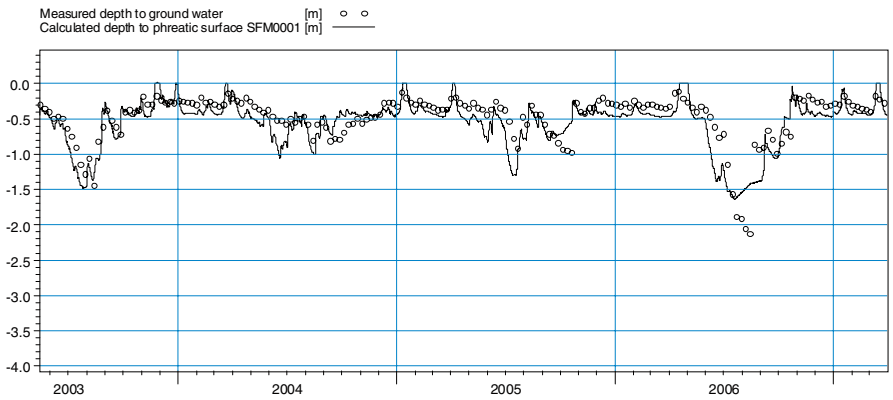

ME=0.0763
MAE=0.157913
RMSE=0.21426
STDres=0.200214
R(Correlation)=0.827232
R2(Nash_Sutcliffe)=0.605896

Figure A1-21. *Measured and calculated depth to phreatic surface in SFM0001.*

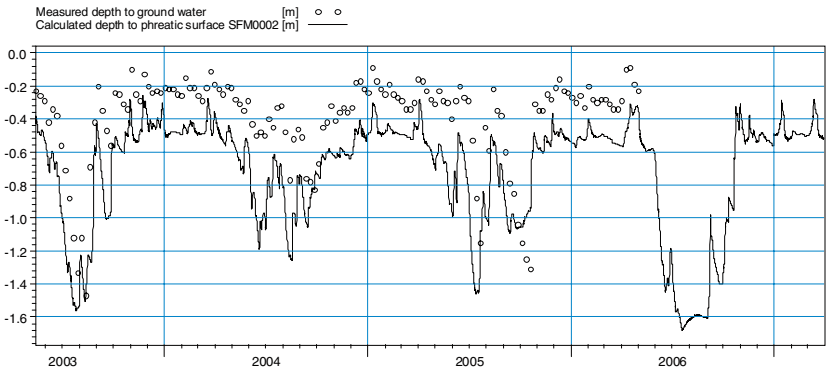

ME=0.270895
MAE=0.281047
RMSE=0.30316
STDres=0.136096
R(Correlation)=0.880535
R2(Nash_Sutcliffe)=-0.223788

Figure A1-22. *Measured and calculated depth to phreatic surface in SFM0002.*

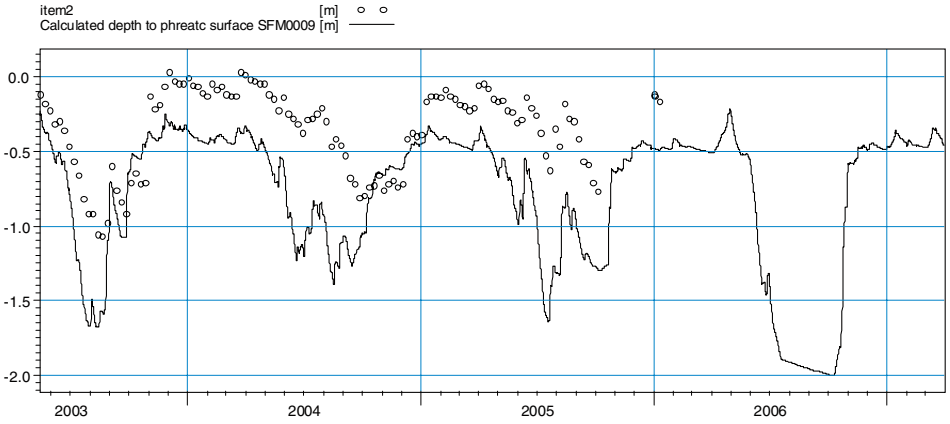

ME=0.359121
MAE=0.374505
RMSE=0.419798
STDres=0.217399
R(Correlation)=0.777564
R2(Nash_Sutcliffe)=-1.19581

Figure A1-23. *Measured and calculated depth to phreatic surface in SFM0009.*

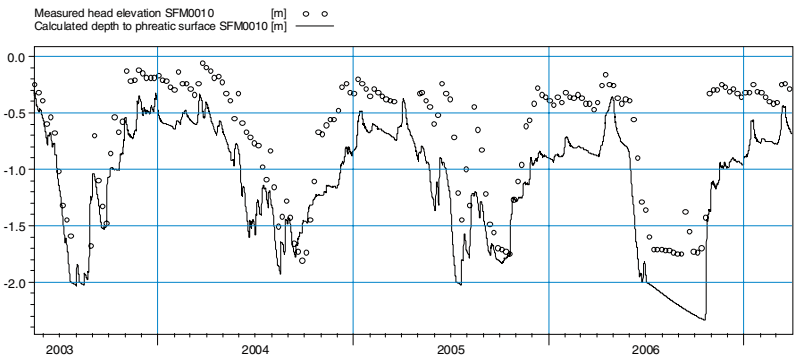

ME=0.374439
MAE=0.389225
RMSE=0.430721
STDres=0.212875
R(Correlation)=0.91161
R2(Nash_Sutcliffe)=0.286576

Figure A1-24. *Measured and calculated depth to phreatic surface in SFM0010.*

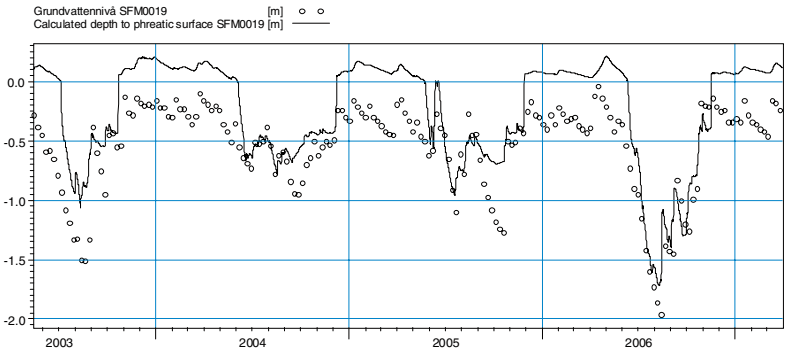

ME=-0.309941
MAE=0.324969
RMSE=0.366982
STDres=0.1965
R(Correlation)=0.887692
R2(Nash_Sutcliffe)=0.0578039

Figure A1-25. *Measured and calculated depth to phreatic surface in SFM0019.*

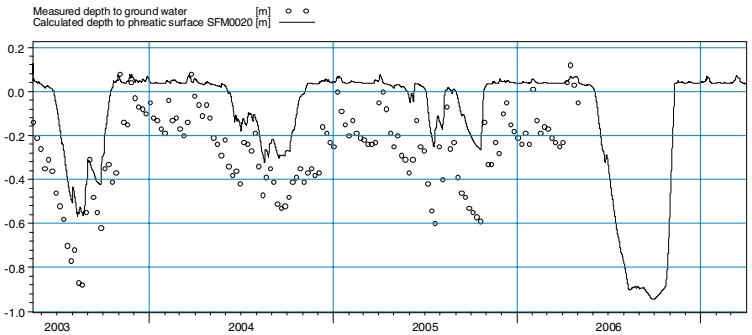

ME=-0.217507
MAE=0.220905
RMSE=0.243617
STDres=0.109728
R(Correlation)=0.837754
R2(Nash_Sutcliffe)=-0.490981

Figure A1-26. *Measured and calculated depth to phreatic surface in SFM0020.*

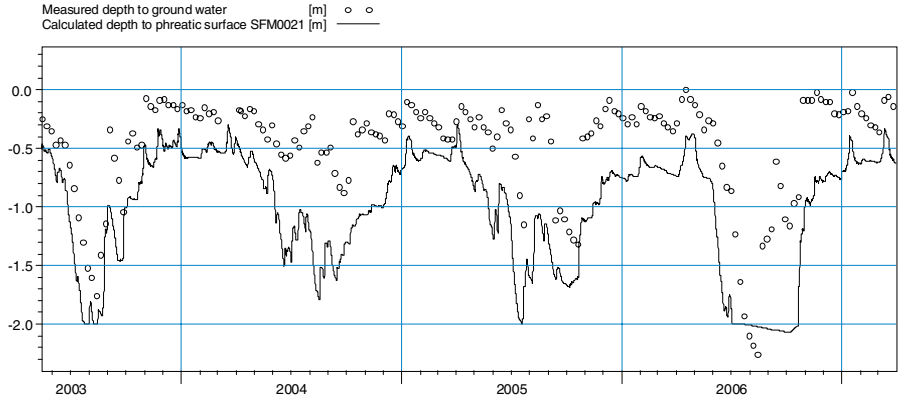

ME=0.52745
MAE=0.532137
RMSE=0.589872
STDres=0.264095
R(Correlation)=0.84811
R2(Nash_Sutcliffe)=-0.791636

Figure A1-27. *Measured and calculated depth to phreatic surface in SFM0021.*

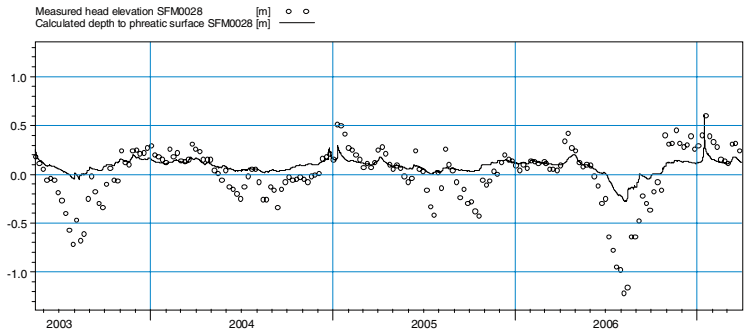

ME=-0.0525009
MAE=0.154917
RMSE=0.229738
STDres=0.223659
R(Correlation)=0.913331
R2(Nash_Sutcliffe)=0.363946

Figure A1-28. *Measured and calculated depth to phreatic surface in SFM0028.*

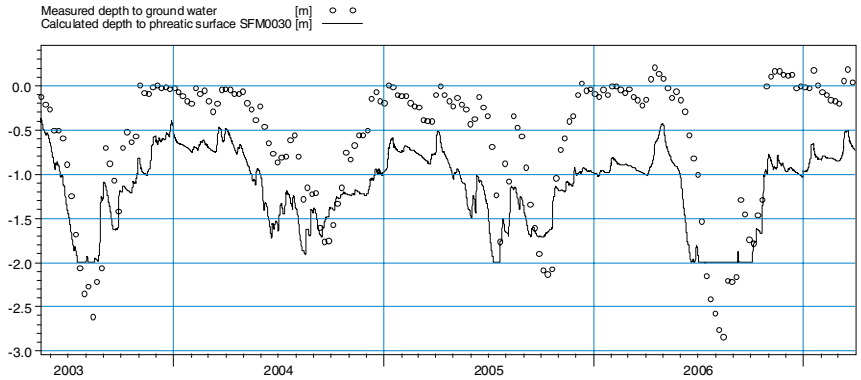

ME=0.522848
MAE=0.612491
RMSE=0.663675
STDres=0.408772
R(Correlation)=0.871104
R2(Nash_Sutcliffe)=0.184956

Figure A1-29. *Measured and calculated depth to phreatic surface in SFM0030.*

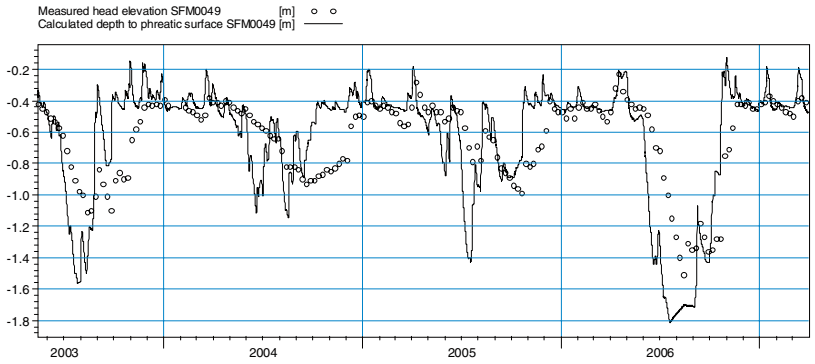

ME=-0.025235
MAE=0.186908
RMSE=0.265096
STDres=0.263892
R(Correlation)=0.708358
R2(Nash_Sutcliffe)=0.00278572

Figure A1-30. *Measured and calculated depth to phreatic surface in SFM0049.*

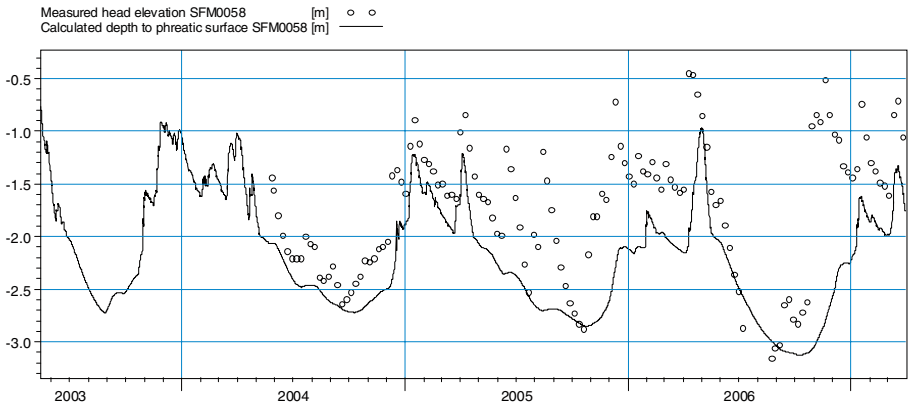

ME=0.557082
MAE=0.566843
RMSE=0.71889
STDres=0.454381
R(Correlation)=0.674601
R2(Nash_Sutcliffe)=-0.389444

Figure A1-31. *Measured and calculated depth to phreatic surface in SFM0058.*

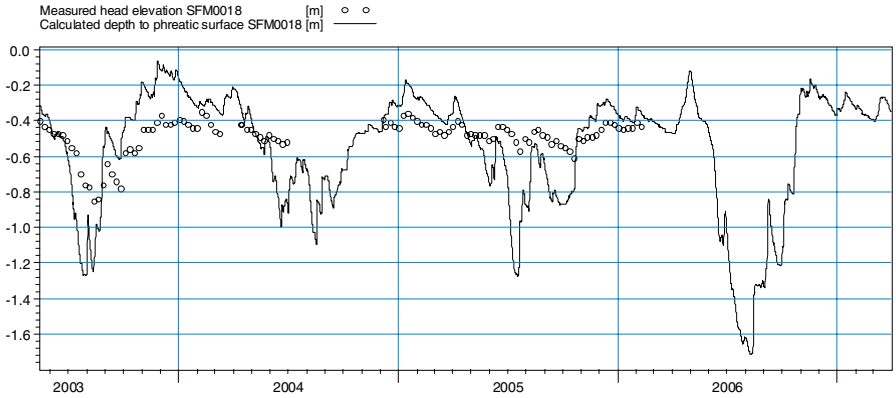

ME=-0.0508991
MAE=0.172071
RMSE=0.209336
STDres=0.203053
R(Correlation)=0.697206
R2(Nash_Sutcliffe)=-3.32795

Figure A1-32. *Measured and calculated depth to phreatic surface in SFM0018.*

Appendix 2

Comparison of results obtained with F2.2 and F2.3 QD models

Mean absolute errors (MAE) and mean errors (ME) for SFM- and HFM- wells and surface water level stations from simulations based on the "old" (Forsmark 2.2) and new (Forsmark 2.3) QD-models.

Table A2-1. MAE and ME for SFM-wells from the simulations with the old, F2.2, QD-model and the new, F2.3, QD-model.

ID Code SFM-well	Validation period		New QD-model	
	MAE	ME	MAE	ME
Heads				
SFM0003	0.21	–0.2	0.2	–0.18
SFM0004	0.23	–0.12	0.24	–0.08
SFM0005	0.21	–0.11	0.2	–0.16
SFM0011	0.17	–0.16	0.18	–0.17
SFM0012	0.08	–0.05	0.07	0
SFM0013	0.23	–0.07	0.26	–0.07
SFM0014	0.24	–0.24	0.31	–0.31
SFM0015	0.09	–0.08	0.08	–0.08
SFM0016	0.15	–0.15	0.14	–0.14
SFM0017	0.37	0.37	0.39	–0.38
SFM0022	0.05	–0.02	0.06	–0.02
SFM0023	0.07	–0.06	0.07	–0.06
SFM0026	0.34	–0.04	0.35	–0.07
SFM0033	0.32	0.24	0.35	0.33
SFM0034	0.28	–0.25	0.29	–0.1
SFM0036	0.26	–0.22	0.27	–0.22
SFM0039	0.04	–0.03	0.04	–0.02
SFM0057	0.31	–0.27	0.58	–0.56
SFM0062	0.11	0.04	0.1	0.05
SFM0065	0.2	–0.07	0.21	–0.09
SFM0066	0.11	0.02	0.11	0.02
Depths to phreatic surface				
SFM0001	0.16	0.08	0.17	0.1
SFM0002	0.28	0.27	0.29	0.28
SFM0009	0.38	0.36	0.36	0.35
SFM0010	0.39	0.37	0.33	0.31
SFM0011	0.11	–0.11	0.11	–0.1
SFM0018	0.17	–0.05	0.16	–0.04
SFM0019	0.32	–0.31	0.32	–0.31
SFM0020	0.22	–0.22	0.28	–0.28
SFM0021	0.53	0.53	0.51	0.51
SFM0028	0.16	–0.05	0.15	–0.05
SFM0030	0.61	0.52	0.6	0.51
SFM0049	0.19	-0.03	0.18	-0.05
SMF0058	0.57	0.58	0.45	-0.23
Mean SFM	**0.24**	**0.01**	**0.25**	**-0.04**

Table A2-2. MAE and ME for HFM-wells from the simulations with the old, F2.2, QD-model and the new, F2.3, QD-model.

ID CODE HFM-well	Old QD-model		New QD-model	
	MAE	ME	MAE	ME
HFM01_1	0.80	–0.80	0.79	–0.79
HFM01_2	0.95	–0.95	0.97	–0.97
HFM02_1	1.12	–1.12	1.06	–1.06
HFM02_2	1.10	–1.10	1.03	–1.03
HFM02_3	1.12	–1.12	1.05	–1.05
HFM03_1	1.06	–1.06	0.98	–0.98
HFM03_2	1.05	–1.05	0.97	–0.97
HFM04_1	0.30	–0.30	0.28	–0.28
HFM04_2	0.41	–0.41	0.40	–0.40
HFM04_3	0.16	–0.16	0.14	–0.14
HFM10_1	0.87	–0.87	0.84	–0.84
HFM10_2	0.44	–0.44	0.42	–0.42
HFM11_1	0.09	–0.09	0.08	–0.08
HFM11_2	0.33	–0.33	0.21	–0.21
HFM15_1	1.00	–1.00	0.95	–0.95
HFM15_2	0.97	–0.97	0.92	–0.92
HFM16_1	0.44	–0.44	0.45	–0.45
HFM16_2	0.47	–0.47	0.49	–0.49
HFM16_3	0.50	–0.50	0.51	–0.51
HFM20_2	0.54	–0.54	0.55	–0.55
HFM20_3	0.58	–0.58	0.58	–0.58
HFM20_4	0.98	–0.98	0.96	–0.96
HFM32_1	1.10	–1.10	1.12	–1.12
HFM32_2	1.10	–1.10	1.13	–1.13
HFM32_3	0.96	–0.96	0.99	–0.99
HFM32_4	0.92	–0.92	0.95	–0.95
HFM34_3	0.81	–0.81	0.76	–0.76
Mean HFM	**0.75**	**–0.75**	**0.73**	**–0.73**

Table A2-3. MAE and ME for the surface water levels from the simulations with the old, F2.2, QD-model and the new, F2.3, QD-model.

ID CODE SFM-well	Old QD-model		New QD-model	
M11 – Water Level				
SFM0041	0.07	–0.03	0.07	–0.02
SFM0042	0.05	0.01	0.05	0.02
SFM0040	0.03	–0.03	0.03	–0.02
SFM0064	0.10	0.09	0.11	0.10
Mean M11, level	**0.06**	**0.01**	**0.07**	**0.02**

Appendix 3

Calculated and measured head elevations in the HFM-wells

Results from sensitivity case 5 with and without the SFR-drainage activated in the model.

Without SFR ***With SFR***

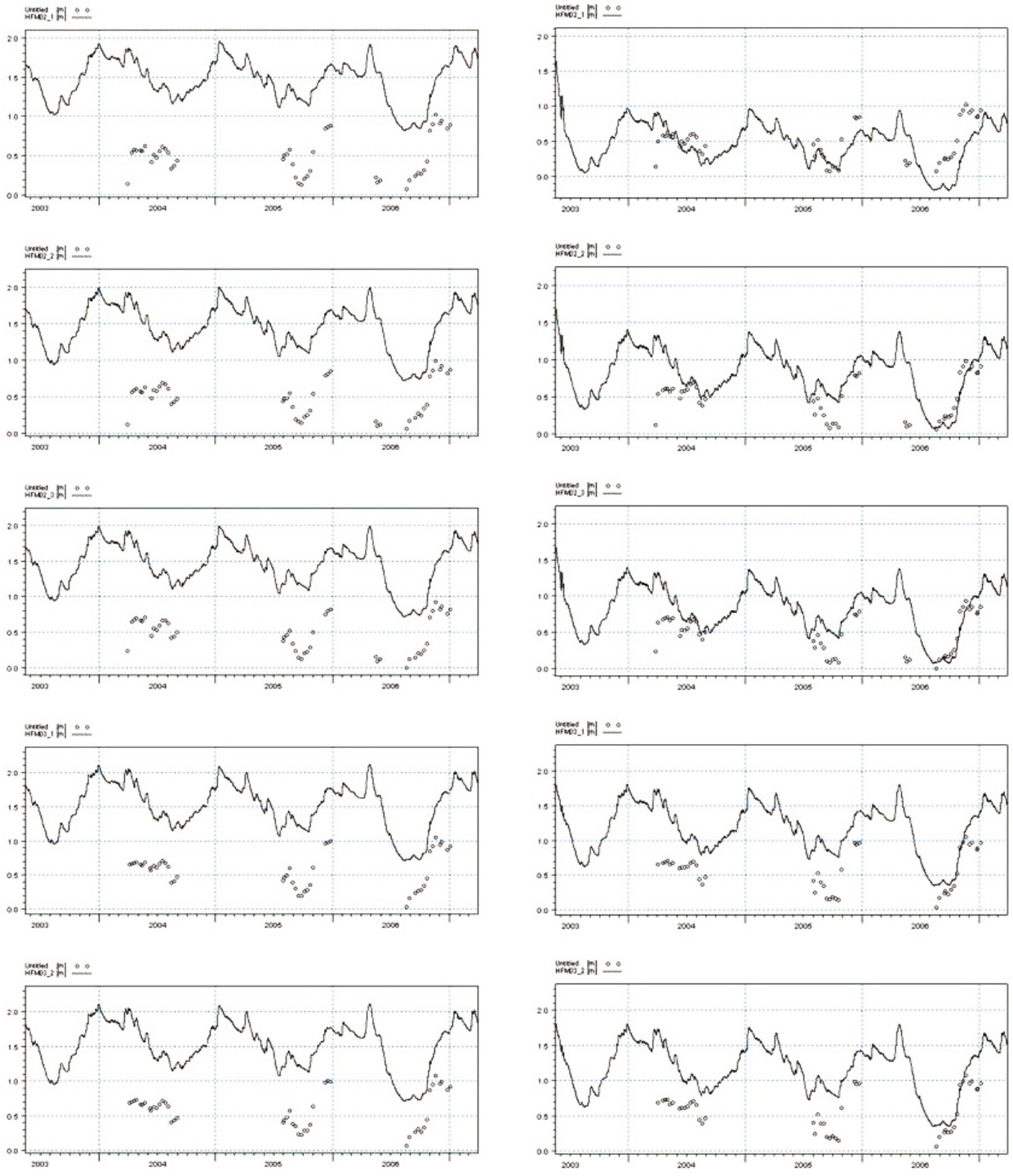

Figure A3-1. *Comparison between measured and calculated head from a simulation with and without the SFR-drainage fo*

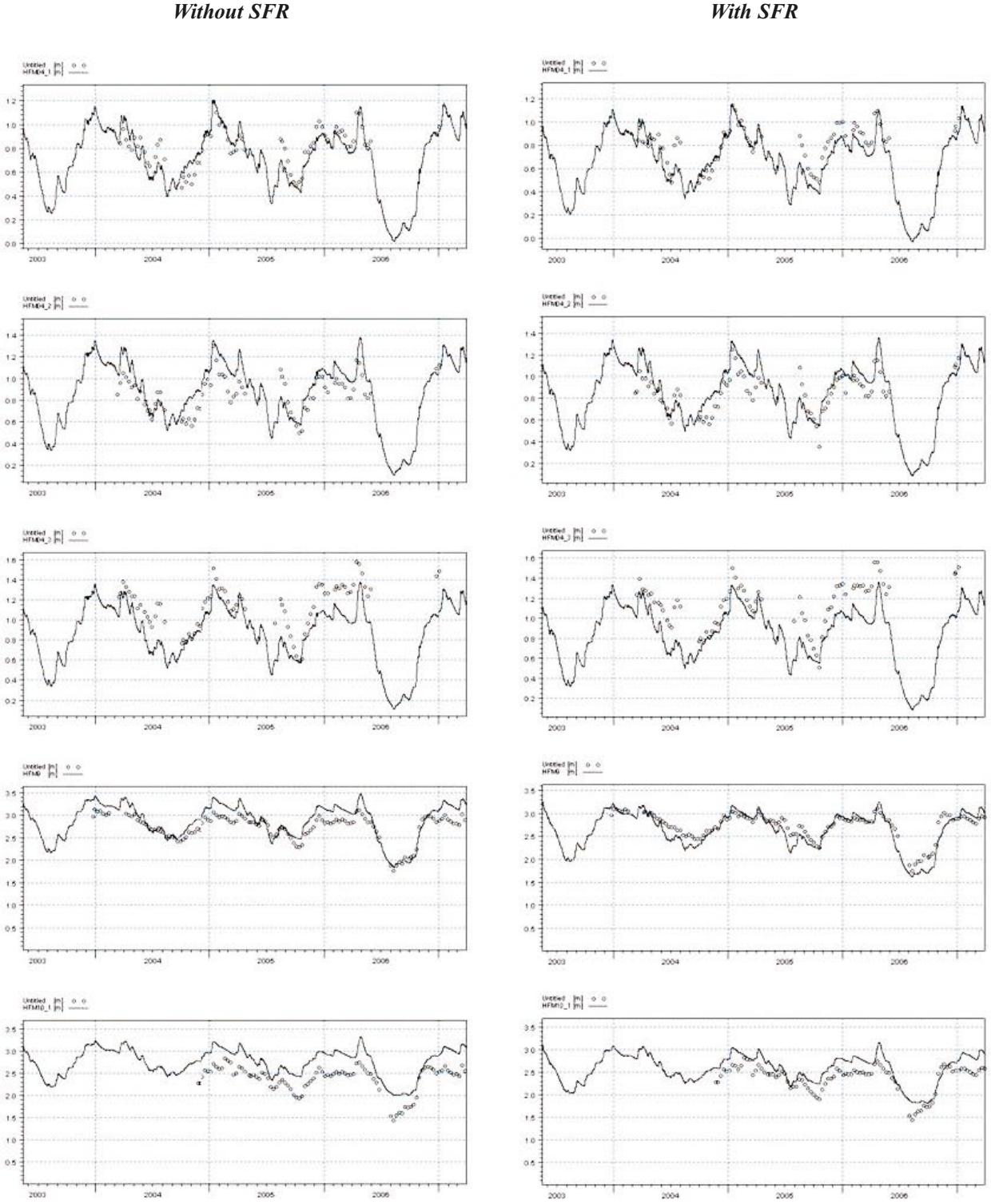

Figure A3-2. *Comparison between measured and calculated head from a simulation with and without the SR-drainage for HFM04_1, HFM04_2, HFM04_3, HFM09, HFM10_1.*

Without SFR ***With SFR***

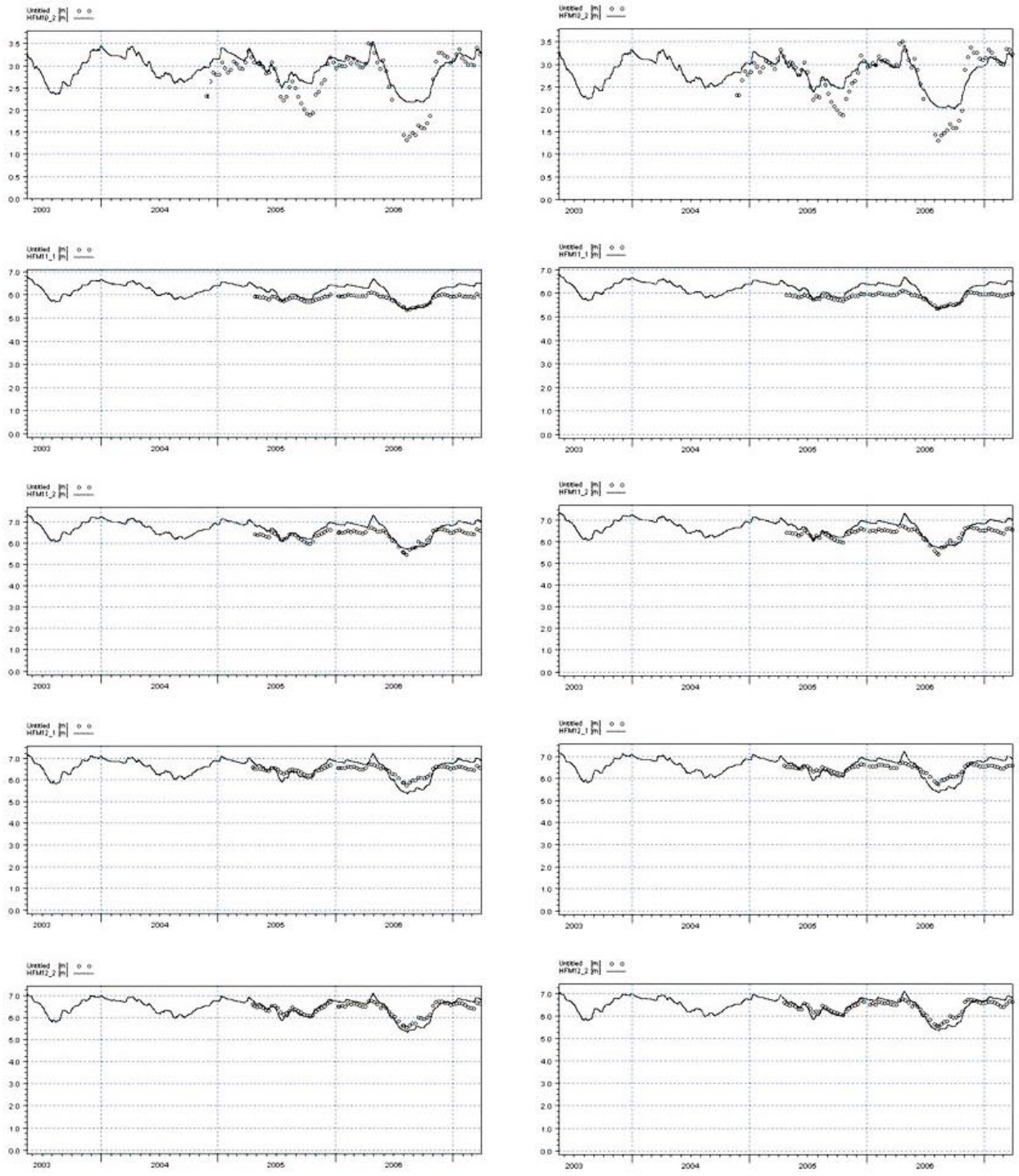

Figure A3-3. *Comparison between measured and calculated head from a simulation with and without the SFR-drainage for HFM10_2, HFM11_1, HFM11_2, HFM12_1, HFM12_2.*

Without SFR ***With SFR***

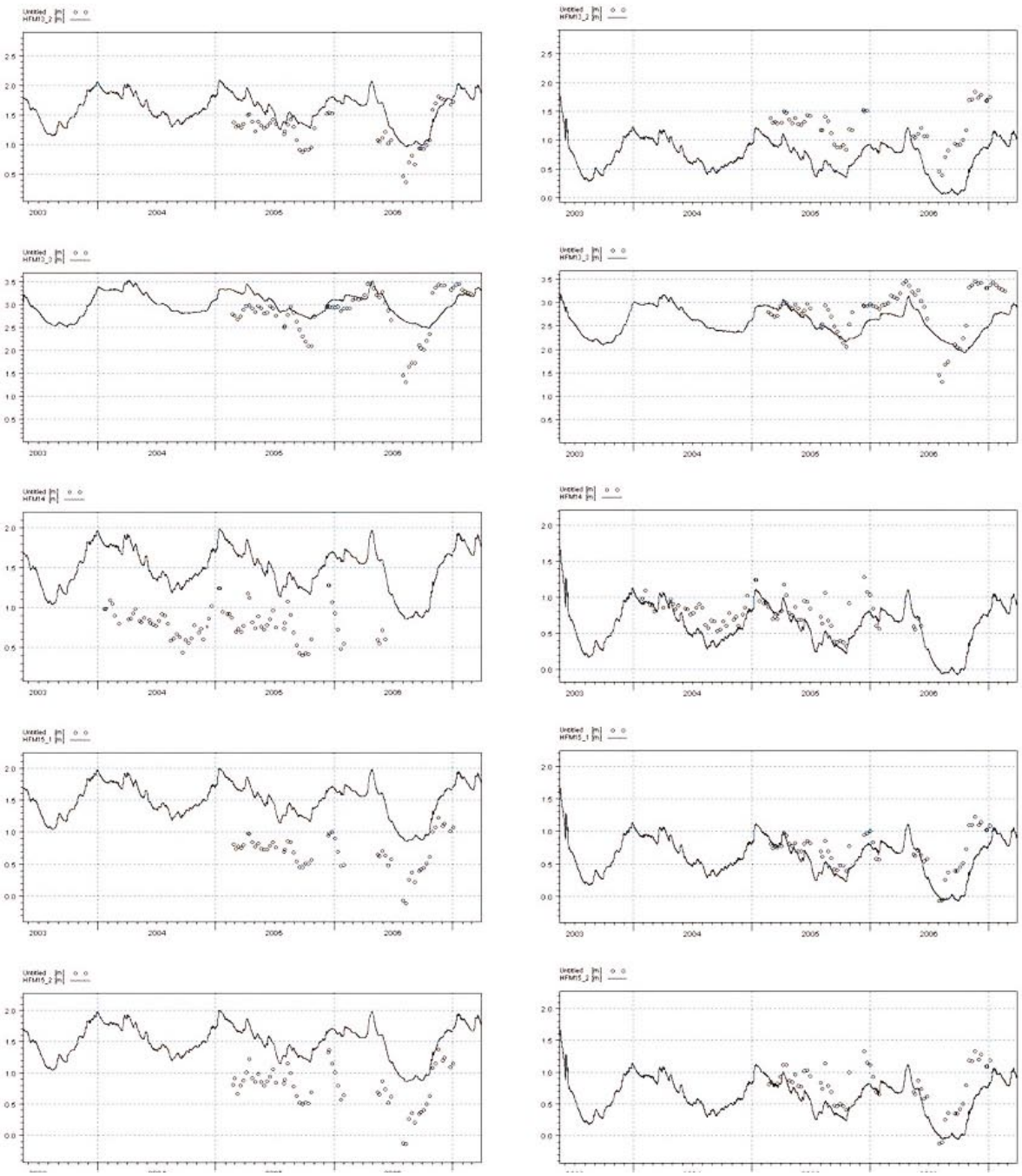

Figure A3-4. *Comparison between measured and calculated head from a simulation with and without the SFR-drainage for HFM13_2, HFM13_3, HFM14, HFM15_1, HFM15_2.*

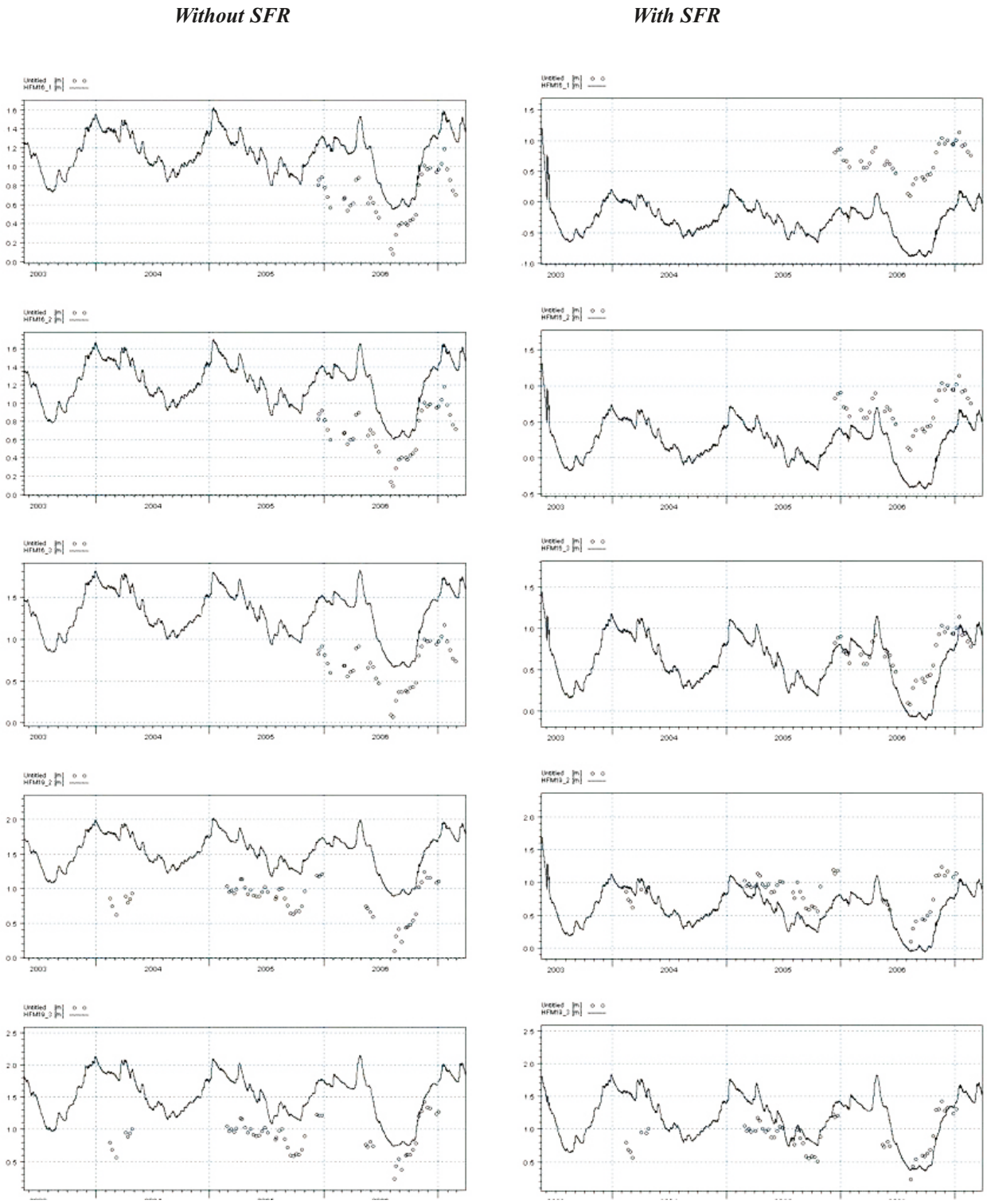

Figure A3-5. *Comparison between measured and calculated head from a simulation with and without the SFR-drainage for HFM16_1, HFM16_2, HFM16_3, HFM19_2, HFM19_3.*

Without SFR ***With SFR***

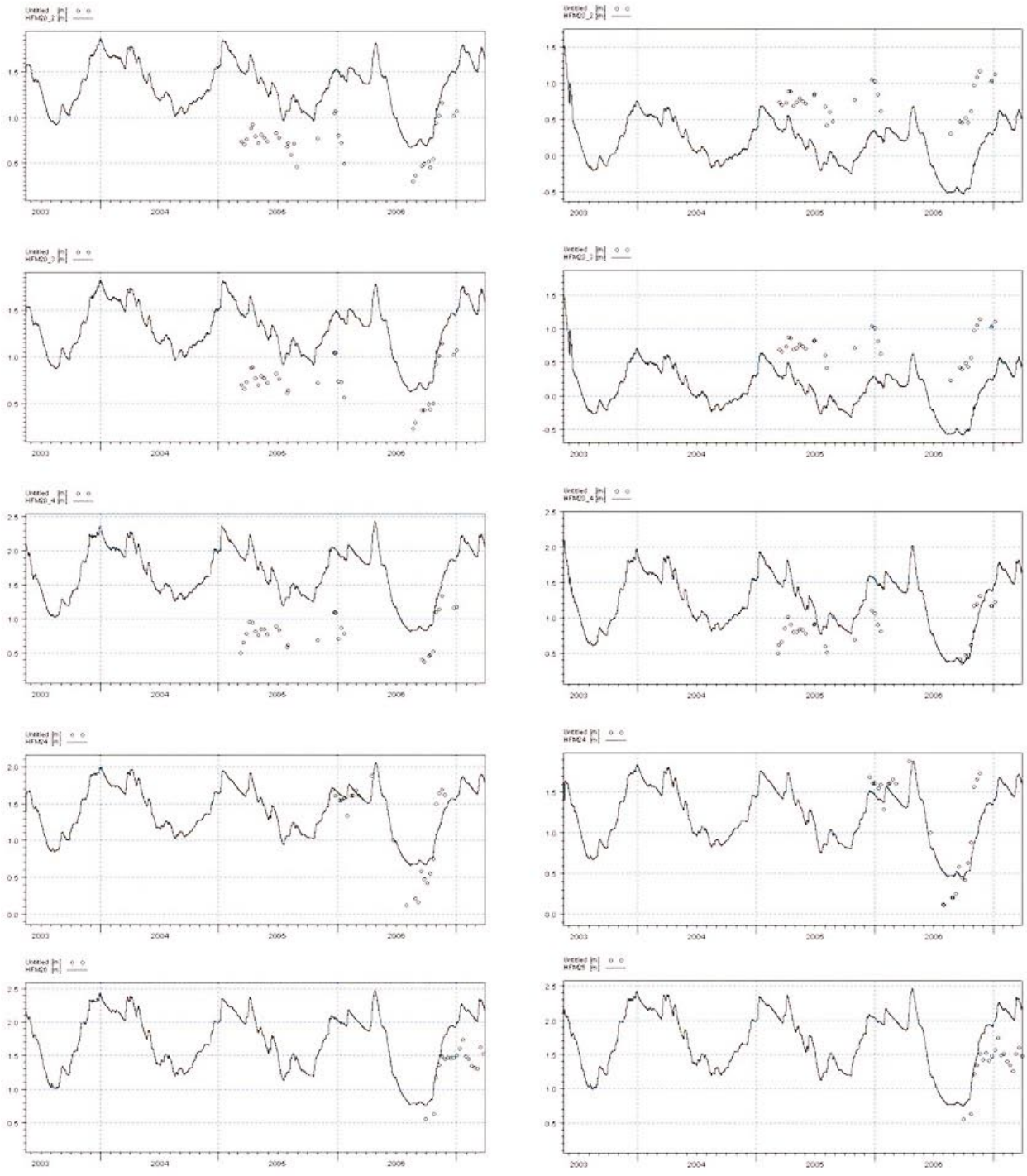

Figure A3-6. *Comparison between measured and calculated head from a simulation with and without the SFR-drainage for HFM20_2, HFM20_3, HFM20_4, HFM24, HFM26.*

Without SFR ***With SFR***

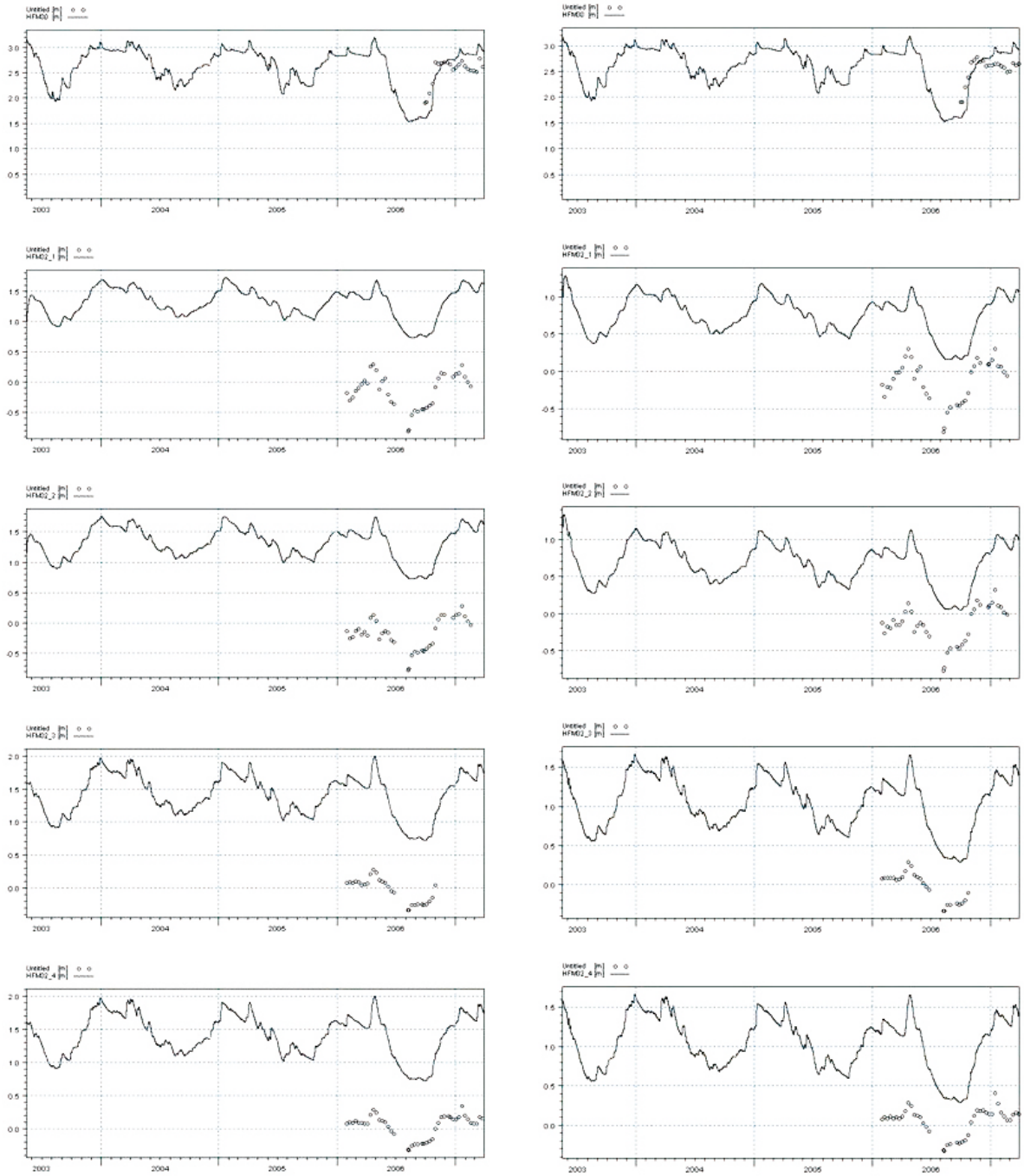

Figure A3-7. *Comparison between measured and calculated head from a simulation with and without the SFR-drainage for HFM30, HFM32_1, HFM32_2, HFM32_3, HFM32_4.*

Without SFR ***With SFR***

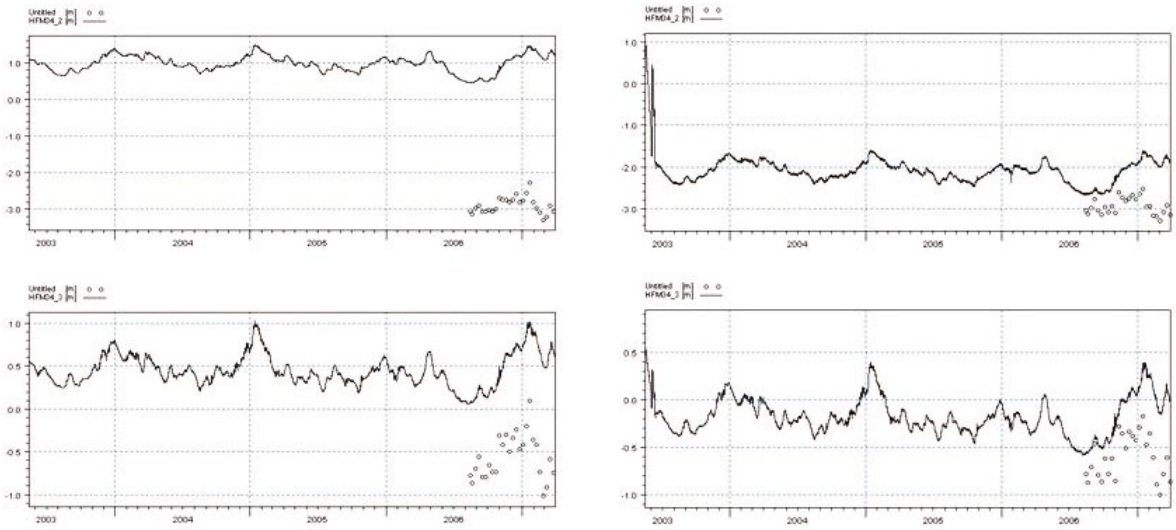

Figure A3-8. *Comparison between measured and calculated head from a simulation with and without the SFR-drainage for HFM34_2, HFM34_3.*